UNIVERSIDADE DE LISBOA

FACULDADE DE MEDICINA

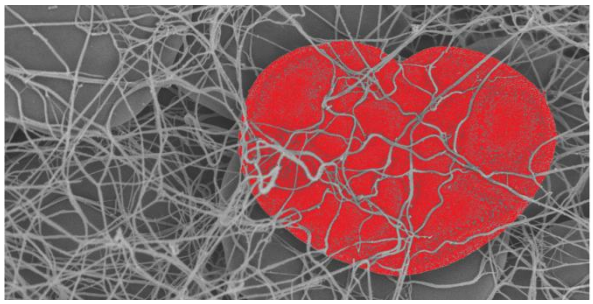

Molecular characterization of the fibrinogen-erythrocyte interaction as a cardiovascular risk

Ana Filipa Barata Duarte Guedes

Orientadores: Prof. Doutor Nuno Fernando Duarte Cordeiro Correia dos Santos

Prof[a]. Doutora Filomena Maria Dias Almeida Carvalho Arede

Tese especialmente elaborada para obtenção do grau de

Doutor em Ciências Biomédicas, especialidade de Bioquímica Médica.

2018

UNIVERSIDADE DE LISBOA

FACULDADE DE MEDICINA

Molecular characterization of the fibrinogen-erythrocyte interaction as a cardiovascular risk

Ana Filipa Barata Duarte Guedes

Orientadores: Prof. Doutor Nuno Fernando Duarte Cordeiro Correia dos Santos

Prof[a]. Doutora Filomena Maria Dias Almeida Carvalho Arede

Tese especialmente elaborada para obtenção do grau de

Doutor em Ciências Biomédicas, especialidade de Bioquímica Médica.

Júri: **Presidente:** Doutor José Luís Bliebernicht Ducla Soares, Professor Catedrático em regime de *tenure* e Vice-Presidente do Conselho Científico da Faculdade de Medicina da Universidade de Lisboa;

Vogais: Doutor Martin Guthold, *Associate* Professor da Wake Forest University, Winston-Salem, Carolina do Norte, EUA;

Doutor Henrique Manuel Paixão dos Santos Girão, Investigador Auxiliar da Faculdade de Medicina da Universidade de Coimbra;

Doutor Francisco Jorge Fernandes Caldeira, Professor Associado do Instituto Universitário Egas Moniz da Cooperativa de Ensino Superior Egas Moniz;

Doutor Miguel Augusto Rico Botas Castanho, Professor Catedrático da Faculdade de Medicina da Universidade de Lisboa;

Doutor Nuno Fernando Duarte Cordeiro Correia dos Santos, Professor Associado com Agregação da Faculdade de Medicina da Universidade de Lisboa – (*Orientador*);

Doutor Luís Alberto da Cunha Mendes Pedro, Professor Associado com Agregação da Faculdade de Medicina da Universidade de Lisboa.

Bolsa de Doutoramento SFHR/BD/84414/2012 financiada pela

Fundação para a Ciência e a Tecnologia (FCT, Portugal).

2018

A impressão desta tese foi aprovada pelo Conselho Científico da Faculdade de Medicina de Lisboa em reunião de 24 de Outubro de 2017.

As opiniões expressas nesta publicação são

da exclusiva responsabilidade do autor

- Aos meus queridos pais, ***Fernanda e Orlando*** *-*

"Porque grandes e sublimes são as investigações científicas que têm por fim conservar a saúde e a vida de todos os seres"

Maimónides

(Médico judeu, nascido em Córdoba durante o período mulçumano, século XII)

Table of contents

Preface ..... **xvii**

Acknowledgments ..... **xxiii**

Abstract ..... **xxix**

Resumo ..... **xxxi**

Keywords ..... **xxxv**

Palavras-chave ..... **xxxv**

Symbols and abbreviations ..... **xxxvi**

Chapter I ▫ Introduction ***Fibrinogen: from the interaction with erythrocytes to its influence on cardiovascular disease*** **1**

Overview 2

Human fibrinogen biology and structure 3

Alternatively spliced fibrinogen variant γ' 6

Clot formation, structure and stability 9

Clotting *versus* Bleeding 11

Abnormal architecture of fibrin clots in disease 13

Erythrocytes biology and structure 14

Rheological properties of erythrocytes 16

Effects of erythrocytes on fibrin clot formation, structure and stability 18

Ligand-receptor binding: interactions between erythrocytes and fibrinogen 19

Cardiovascular diseases 22

Heart Failure 25

Essential arterial hypertension 26

Cerebrovascular diseases 27

Stroke 28

New biomarkers for CVDs 29

Atomic Force Microscopy – a powerful Nanomedicine tool 31

Key elements and basic principles of AFM 34

Single-molecule force spectroscopy 35

Protein-cell interactions 38

Cantilevers functionalization for protein-cell interaction measurements 38

Single-cell force spectroscopy: cell-cell adhesion 39

Cantilevers functionalization for cell-cell adhesion 42
Indentation – cell elasticity 43
Applications of AFM in Medicine 44
References of Chapter I 46
Aims of the project 80
Chapter II ▫ Impact of heterodimer γ' fibrinogen on fibrin clot 83
Overview 84
Declaration of authorship 85
Abstract 88
Introduction 89
Methods 92
Results 95
Discussion 105
References of Chapter II 110
Supplementary information of Chapter II 115
Chapter III ▫ Influence of homodimer γ' fibrinogen on fibrin clot 125
Overview 126
Declaration of authorship 127
Abstract 130
Introduction 131
Methods 133
Results 139
Discussion 148
References of Chapter III 153
Supplementary information of Chapter III 160
Chapter IV ▫ Erythrocyte binding sites on the fibrinogen molecule 167
Overview 168
Declaration of authorship 169
Abstract 172
Introduction 174
Methods 176
Results and discussion 179
References of Chapter IV 188
Chapter V ▫ Fibrinogen-erythrocyte binding in chronic heart failure 191

Overview 192
Declaration of authorship 193
Abstract 196
Introduction 197
Results and discussion 198
Methods 209
References of Chapter V 215
Supplementary information of Chapter V 219
Chapter VI ▫ Fibrinogen-erythrocyte binding in essential arterial hypertension 233
Overview 234
Declaration of authorship 235
Abstract 238
Introduction 239
Methods 242
Results 247
Discussion 256
References of Chapter VI 261
Supplementary information of Chapter VI 270
Chapter VII ▫ Erythrocyte adhesion in healthy and pathological conditions 275
Overview 276
Declaration of authorship 277
Abstract 280
Introduction 281
Methods 284
Results 288
Discussion 296
References of Chapter VII 301
Supplementary information of Chapter VII 306
Chapter VIII ▫ Adhesion of erythrocytes in stroke disease *Preliminary results* 309
Overview 310
Introduction 311
Methods 314
Preliminary results 315
Discussion 321

References of Chapter VIII 323
Chapter IX ▫ Integrated discussion and final remarks 329
Integrated discussion 330
Final remarks and future directions 339
References of Chapter IX 342
Annexes ▫ Published articles 347
Article 1 349
Article 2 371
Article 3 381
Article 4 403

Preface

The work presented in this Thesis arises from the research done during my doctoral studies, made possible by Fundação para a Ciência e a Tecnologia (FCT), Ministério da Ciência, Tecnologia e Ensino Superior (MCTES), Portugal, which provided me the PhD fellowship SFRH/BD/84414/2012. This project was developed between 2013 and 2017. It was a great honor for me to belong to the Doctoral Programme of Centro Académico de Medicina de Lisboa (CAML), shared between Instituto de Medicina Molecular (iMM, Lisbon, Portugal), Faculdade de Medicina da Universidade de Lisboa (FMUL, Lisbon, Portugal) and Centro Hospitalar Lisboa Norte (CHLN, Lisbon, Portugal). I am gladly part of Nuno C. Santos' Lab team, where most of this PhD Thesis work took place, under the supervision of Prof. Nuno C. Santos and co-supervision of Prof. Filomena A. Carvalho. Part of this work was also carried out on the Thrombosis and Tissue Repair Group, headed by Prof. Robert Ariëns, at the Division of Cardiovascular and Diabetes Research, Leeds Institute of Cardiovascular and Metabolic Medicine and Multidisciplinary Cardiovascular Centre, Faculty of Medicine and Health, University of Leeds, United Kingdom.

This study is a direct follow-up of one of the research lines that was ongoing at the iMM Lab when I started my PhD project, in 2013. Before that, I started my research at Nuno C. Santos' Lab with a 6 months fellowship. It was in a different research field, but for me it was an excellent opportunity to learn completely new methodologies.

Until that moment, the fibrinogen-erythrocyte binding had been studied in our Lab only in healthy donors and Glanzmann thrombasthenia patients. Prof. Nuno C. Santos proposed me to follow these interactions in different cardiovascular pathologies. To perform this, I had the opportunity to closely collaborate with clinicians from different services of two different hospitals in Lisbon: Hospital Pulido Valente and Hospital de Santa Maria. I could learn from them the complications associated to those pathologies, as well as the patients' suffering. This encouraged me to work hard every day as a challenge to learn and help in some way. Two of the main outcomes of this study were the following articles and one manuscript:

- **Guedes AF**, Carvalho FA, Malho I, Lousada N, Sargento L, Santos NC. **(2016)** Atomic force microscopy as a tool to evaluate the risk of cardiovascular diseases in patients. **Nature Nanotechnology** 11(8): 687-92. doi: 10.1038/nnano.2016.52. **Impact Factor 2016: 38.986;**

- **Guedes AF***, Carvalho FA*, Moreira C, Nogueira JB, Santos NC. **(2017)** Essential arterial hypertension patients present higher cell adhesion forces, contributing for fibrinogen-dependent cardiovascular risk. **Nanoscale** 9: 14897-14906. doi: 10.1039/c7nr03891g. **Impact Factor 2016: 7.367** (*co-first authors)**;**

- **Guedes AF**, Moreira C, Nogueira JB, Santos NC, Carvalho FA. Fibrinogen-erythrocyte binding and hemorheology measurements on the assessment of essential arterial hypertension patients (submitted).

A better understanding of a scientific topic usually raises new questions, doubts and hypotheses to be answered. This way, I went to Leeds during 4 months to improve the knowledge regarding the fibrin clot structure and its properties. It was also our aim to produce several fibrinogen mutants (either recombinants or isolated from commercial plasma) to better understand the specific binding sites of fibrinogen to interact with erythrocytes. The impact of the presence of different fibrinogen variants and erythrocytes on blood clots was also studied. To reach these goals, I learned and applied new methodologies and techniques, which were not available at iMM. Prof. Robert Ariëns and his team gave me the best conditions for developing our research goals. Moreover, we tried to find out which could be the receptor for fibrinogen on the membrane of erythrocytes and understand its binding mechanism, in order to overcome erythrocyte hyperaggregation that could lead to cardiovascular complications. The results from these research lines are now included in articles or manuscripts. Some of them were already published and others submitted or ready to be submitted (here included as Chapters of this Thesis). All of them are the result from collaborative work. The authors of each article/manuscript and their contributions are listed on each Chapter.

- **Guedes AF**, Carvalho, FA, Domingues M, Macrae FL, McPherson H, Santos NC, Ariëns R. **(2018)** Sensing adhesion forces between erythrocytes and γ' fibrinogen, modulating fibrin clot architecture and function. **Nanomedicine: Nanotechnology, Biology and Medicine** 14(3):909-918. doi: 10.1016/j.nano.2018.01.006. **Impact Factor 2016: 5.720;**

- **Guedes AF**, Carvalho, FA, Domingues M, Macrae FL, McPherson H, Martins IC, Duval C, Santos NC, Ariëns R. Impact of γ'γ' fibrinogen interaction with red blood cells on fibrin clots (submitted).

- Carvalho FA*, **Guedes AF***, Duval C, Macrae FL, Swithenbank L, Farrell D, Robert A, Santos NC. **(2018)** The $_{95}$RGD$_{97}$ sequence on the Aα chain of fibrinogen is essential for binding to its erythrocyte receptor. **International Journal of Nanomedicine** 13:1985-1992. doi: 10.2147/IJN.S154523. **Impact factor 2016: 4.300** (*co-first authors).

It is worth mentioning that, during these years, I have learned and applied several biophysical and molecular biology approaches to reach our goals. I would like to emphasize the work done and the results we obtained with a powerful and versatile nanotool – Atomic Force Microscopy (AFM) – but others are also mentioned throughout this Thesis. Some of these methodologies were completely new for me, since my basic formation is in the Genetics field. In fact, this knowledge provided me a great awareness of the importance of these studies and it had a big impact on my personal scientific growth.

Another advantage of my work is that, over these years, I had the opportunity of travelling all over the world. I had the privileged of participating in 15 international and 10 national scientific conferences, as well as 18 advanced courses or workshops, doing 12 oral communications (one of them receiving the best oral communication award) and presenting 13 posters (one of them receiving the best poster award). To enable the participation on some of these conferences, I received several grants from different scientific societies or international associations: European Foundation for Clinical

Nanomedicine, International Fibrinogen Research Society, Sociedade Portuguesa de Biofísica, Sociedade de Biofísica de España, Sociedade Portuguesa de Bioquímica, Sociedade Brasileira de Bioquímica e Biologia Molecular, Federation of European Biochemical Societies, International Union for Pure and Applied Biophysics, Biophysical Society (USA) and European Cooperation in Science and Technology. The participation on those scientific events allowed me to be updated on the most recent advances on different research fields and to contact with scientists from other countries, with different backgrounds and interests. The participation on these congresses was an opportunity to present and discuss our work and share opinions with other researchers. Other presentations related to this work were also held by my supervisors and our collaborators. Further information on this is detailed on my Curriculum Vitae. I also received the "Prémio Jovem Biofísico 2016" from the Sociedade Portuguesa de Biofísica and "Prémio Pulido Valente Ciência 2017" from Fundação para a Ciência e Tecnologia and Fundação Professor Francisco Pulido Valente.

During my PhD studies, I have also collaborated with other groups, from iMM (Dr. Luisa Figueiredo's Lab, on a project of Dr. João Rodrigues, and with Prof. João Eurico Fonseca's Lab, on a project of Dr. Bruno Vidal) and from other institutions, namely, Instituto de Patologia Molecular e Imunologia – IPATIMUP / I3S (with Dr. Joana Paredes), Instituto de Higiene e Medicina Tropical – IHMT (with Dr. Ana Paula Arez). I was also involved in other international collaborations, namely with the Department of Medical Physics, M. Smoluchowski Institute of Physics, Jagiellonian University, Krakow, Poland (with Prof. Ewa Stępień) and with the Departament of Pathology and Laboratory Medicine, University of North Carolina School of Medicine, Chapel Hill, North Carolina, USA (with Prof. Alisa Wolberg). However, as the results obtained under the framework of these collaborations are not part of my PhD project, they were not included in this Thesis. Nevertheless, one of them, on the impact of P-cadherin and SFK activation on cell-cell biomechanical properties, done in collaboration with IPATIMUP, University of Porto, lead already to an article published on *Nanoscale*. On those projects, I was involved on the application of atomic force microscopy, namely, force spectroscopy and imaging, and on AFM data treatment.

During my PhD, I was also involved on the writing of research funding applications. Additionally, I had the opportunity to co-supervise two Medical doctor students and

monitor three Master students in our Lab, which was very challenging and rewarding for me.

The main results obtained during my PhD are compiled in this Thesis, composed by six central chapters, which are based on the inclusion of the content of the above mentioned articles or manuscripts, preceded by an overview explaining their context and declarations of authorship. In each chapter, I considered the manuscripts autonomous units, as they have their own sections, figure numbering and references. The work conducted is presented sequentially, but not in a chronological order. Three more chapters complete this Thesis: one with the state of the art, another with preliminary results from an ongoing project in the lab and the last one with the general conclusions.

Chapter I is an introductory section focusing on the current state-of the art on the most relevant topics related with the main aims of this Thesis. The following chapters contain the original research manuscripts. Chapter II is focused on the molecular mechanisms underpinning the effects of the γ' fibrinogen heterodimer together with erythrocytes on fibrin clot structure, in terms of biophysical, viscoelastic and permeability properties that can modulate its function. Most of this work was developed abroad, during my stay at the University of Leeds (UK). This paper was published in *Nanomedicine: Nanotechnology, Biology and Medicine*. In Chapter III, we wanted to assess the impact of homodimeric γ' fibrinogen on erythrocyte binding, as well as, on blood clot structure. Most of this work was also developed at the University of Leeds. Chapter IV reports mainly our new advances on the study of the protein binding sites involved on the interaction between fibrinogen and erythrocytes. This paper was published in *International Journal of Nanomedicine*. Chapter V details the use of atomic force microscopy as a tool to evaluate the risk for cardiovascular diseases in chronic heart failure patients, the focus of our study. This paper was also already published in *Nature Nanotechnology*. The following Chapter VI is centered on the assessment of the binding between fibrinogen and the erythrocyte receptor as cardiovascular risk factor in essential arterial hypertension patients. Chapter VII addresses the influence of fibrinogen molecules on erythrocyte aggregation in cardiovascular diseases. Here, we also evaluated how γ' fibrinogen is altered in these pathologies and whether this variant could be considered a new marker for cardiovascular risk. This paper was already published in *Nanoscale*. Chapter VIII contains our preliminary results on the interactions between

fibrinogen and erythrocytes and changes on hemorheological parameters in patients who suffered a stroke. Finally, Chapter IX discusses the major findings of this Thesis, generating new hypotheses and opening new future directions for the research in this field.

I hope the results described in my PhD Thesis could be a good contribution to the advances on the research in cardiovascular medicine and could help clinicians to improve patients' life.

Acknowledgments

The limited space in this section of acknowledgments, surely, does not allow me, at the end of this journey, to thank, as it should be, to all the people who, throughout my PhD project helped and guided me. Their encouragement and belief on me were so important to fulfill my objectives and accomplish this stage of my academic formation! Though this is a personal project many people really contributed for it.

So, firstly, I wish to express my deep gratitude to Prof. Nuno Santos, my PhD supervisor and Prof. Filomena Carvalho, my co-supervisor. From my heart.. Sincerely many, many thanks to them! I have met here so wonderful people and had so good conditions that it makes me believe this was the best place I could have ever found to carry out my PhD project. They always gave me excellent expertise, guiding, advising and friendship, supporting my ideas and decisions. To highlight, they always encouraged me to participate in scientific conferences, courses and workshops, to apply for fellowships and awards, and to go abroad for receiving training. They also stimulated me to belong to or seek for new projects. Especially, I would like to thank my co-supervisor, Filomena Carvalho for having shared her experience and expertise on teaching me how to work with the atomic force microscope. This marked my entrance in a new and challenging world – that of the biophysics fields. Her wisdom and guidance were essential to reach the end of this work with an enormous sense of self-satisfaction. Many thanks to give me a continuous day-to-day support and help. Thank you both for this unforgettable experience that allowed me to grow professionally and personally!

I thank Instituto de Medicina Molecular, Faculdade de Medicina da Universidade de Lisboa and the Doctoral Programm of Centro Académico de Medicina de Lisboa (CAML) for the excellent conditions of work as well as the opportunity of being part of the PhD students group. I loved to belong to the PhD commission, which often allowed me to organize meetings, workshops and seminars. It was a privilege and a great honor to take part in so many challenges!

I would like to thank my Thesis Committee members, Prof. Miguel Castanho, Prof. Jorge Caldeira and Prof. Teresa Pacheco, who followed the progression of my work, giving me some important pieces of advice, scientific input and valuable discussions.

I sincerely thank Prof. Robert Ariëns, in collaboration with Prof. Helen Philippou, for kindly accepting me in their Labs, in the University of Leeds. They helped, taught and supported me, always with a very big smile! I was so lucky to meet and work with them! Some grateful words too to my lab mates who, accompanying me during 4 months, especially, Helen McPherson, Fraser Macrae, Lewis Hardy, Allan Sabban and Cédric Duval helped me to use different methodologies and approaches. I sincerely appreciated their good hospitality, as well as the good and funny moments I shared with them in Leeds.

I am very grateful to our clinical collaborators, Prof. Carlos Moreira, Dr. Eduardo Infante de Oliveira, Dr. Alice Tavares, Prof. Ana Catarina Fonseca and all the nursing staff, who provided us the samples from patients. Their collaboration made possible to achieve some of the clinical results and fruitful discussions for this Thesis and with them, I have learnt a lot! I must highlight and give a special thank you to Dr. Luís Sargento, who was a reference for me both as a clinician and as a researcher. His willing, wisdom and support was remarkable!

I also express my gratitude and solidarity to all Patients who, although anonymously, gave a fundamental contribution to make this study possible. Their samples were a great help for the advances in scientific research of this area of knowledge.

I would like to mention that this work was mostly funded by Fundação para a Ciência e a Tecnologia (FCT) through my PhD fellowship (SFRH/BD/84414/2012) and the projects PTDC/QUI-BIQ/119509/2010 and PTDC/BBB-BMD/6307/2014. Moreover, I am also grateful to several scientific organizations for their grants and awards, which allowed me to participate in several meetings, courses and workshops. They are: Sociedade Portuguesa de Biofísica, European Foundation for Clinical Nanomedicine, International Fibrinogen Research Society, European Cooperation in Science and Technology, Sociedade Brasileira de Bioquímica e Biologia Molecular, Federation of European Biochemical Societies, Sociedad de Biofísica de España, International Union for Pure and

Applied Biophysics, and Biophysical Society (USA). My participation in all these activities was really an important and enthusiastic step in my scientific formation.

I am indebted to all colleagues from my Lab Group. I have all of them in my heart and memory. Thank you so much for maintaining a healthy and friendly working-atmosphere, listening, laughing and helping me. In their presence, I could learn and grow every single day and even the time spent outside the working lab increased our affection and relationships. I would like to give a special thank to: Teresa Freitas, who always helped and accompanied me in the lab; Marco Domingues, for his friendship and all insightful discussions of the work and for being always ready to help and give advice in Portugal and in Leeds; and, André Faustino because, since the beginning, he was someone I always could rely on. My gratitude to other friends I made here, Ana Martins, Bárbara Gomes, Mário Felício, Ivo Martins, Sónia Abreu, Marcelo Augusto, Susana Gregório, and many others. I would also like to thank "my students" who helped me to develop this Thesis, increasing my responsibility and defining my mission, Catarina Lopes, Joana Monteiro, Inês Malho and Eduardo Bento. I will remember so funny and delicious moments with them.

I would like to thank Miguel Castanho's Lab mates for being good collaborators and friends, specially, Vera Neves and Antónia Pinto, for their kindness and friendship. No doubt, I will never forget them.

Thank you to all people from iMM, from the different Labs or Services, I met here and with whom I had the opportunity to share ideas, learn and laugh!

A huge thank to Rita Vaz-Drago, my iMM unforgettable friend who I luckily met during this journey. Actually, I do not have enough words to thank her for all her affection, friendship and care of me. Both in good and not so good moments, she always stayed with me and gave me inspiration, even when her life was not so easy. Thank you so much!

I am also thankful to all my old and new friends, from each part of the world. I do not have enough space to enumerate all of them but I cannot forget them. Even so, an

individual thank to Joana Oliveira, Maria João Ribeiro, Ana Pissarra and Cristiana Macedo, for all their comfort words and encouragement every time, being always close to me.

A warm heart-felt thank to Tiago for his unconditional love, comforting words and patience with me. Thank you for always being here and be proud of me. It is so easy to make me laugh!

I would also give a BIG thank you to ALL my Family, particularly my brother, Luís, and my grandparents, Maria and António, Carminha and Domingos, for all the times they made my life so special, for their dreams and for having always believed in me.

And finally but still more important, to my Parents, Fernanda and Orlando, for their love, for the tranquility and good energies that always transmitted me, for all their sacrifices and support in all moments of my life. Their principles and values will always be a reference for me. Thank you for allowing me that this dream of mine will become true today!

All my efforts and this Thesis, I especially dedicate to them...

The work presented in this Thesis was mainly done in Instituto de Medicina Molecular, Faculdade de Medicina, Universidade de Lisboa, but also in the Leeds Institute of Cardiovascular and Metabolic Medicine and Multidisciplinary Cardiovascular Centre, at University of Leeds. The candidate belong to a Doctoral Programme of Centro Académico de Medicina de Lisboa. The project was also carried out in collaboration with Centro Hospitalar Lisboa Norte (Hospital Santa Maria and Hospital Pulido Valente) and Insituto Português do Sangue e Transplantação. It was funded by Fundação para Ciência e Tecnologia (FCT) with the projects PTDC/QUI-BIQ/119509/2010 and PTDC/BBB-BMD/6307/2014 and British Heart Foundation. The candidate preformed the experimental work supported with the FCT PhD fellowship SFRH/BD/84414/2012.

Abstract

Cardiovascular diseases (CVD) are the major cause of death worldwide. The evaluation of new risk factors can help to identify individuals at higher risk. Erythrocyte aggregation is one of the indicators of cardiovascular risk, which seems to be influenced by high plasma fibrinogen levels. This acute plasma protein has an alternatively spliced γ-chain variant (γ' fibrinogen) that has been particularly associated with altered structure or properties of the clots and with increased cardiovascular risk. However, this association has been controversial and the molecular mechanisms are not clear. Based on these findings, we studied how fibrinogen and its variants interact with erythrocytes, and how this binding influences erythrocyte aggregation and fibrin clot properties. After the evaluation and characterization of the fibrinogen-erythrocyte binding in healthy subjects, the main goal of this Thesis was the study of fibrinogen-erythrocyte binding in patients with different cardiovascular and cerebrovascular diseases, as a clinical risk factor, trying to understand the impact of the presence of fibrinogen on erythrocyte aggregation. Clinical and hemorheological profiles, and the changes on γ' fibrinogen levels associated to CVDs were also evaluated.

To reach our goals, different experimental approaches were performed, including atomic force microscopy-based force spectroscopy, magnetic tweezers, ELISA assays, confocal and scanning electron microscopy, hemorheological methodologies and clot permeability studies. Patients with chronic heart failure (CHF), essential arterial hypertension (EAH) and stroke were enrolled in this study. Results were correlated with patient's clinical profile.

Our conclusions are that erythrocytes triggered variability in the fibrin network structure, in the individual fiber characteristics and overall clot properties. The presence of γ' chain on the fibrinogen molecule, even combined with γA chain, altered the clot structure. Thus, clots with γAγ' fibrinogen might interact differently with erythrocytes, potentially increasing the risk of thrombosis.

Addressing our main goal, we found, at the single-molecule level, that fibrinogen-erythrocyte binding forces were higher in EAH, CHF and stroke patients, when compared with the control group, despite of a lower binding frequency. This transient binding is not

enough to form a clot, but it could lead to changes on whole blood flow, representing a cardiovascular risk factor. Moreover, a 12-month clinical follow-up showed that CHF patients with higher fibrinogen-erythrocyte binding forces had a significantly higher probability of being hospitalized due to cardiovascular complications in the following year, pointing out the value of this approach for clinical prognosis. Importantly, we also showed that erythrocytes from EAH patients adhere more than those from the control group. Upon increasing fibrinogen concentration, there was an increase in the work and force necessary for cell-cell detachment, both on healthy donors and EAH patients, showing the importance of this plasma protein on the adhesion between these cells. Changes on hemorheological profiles were found in patients compared to the control group. γ' fibrinogen levels were higher in patients than in healthy donors, which is indicative of an increased cardiovascular risk. Thus, these results are relevant to conclude on the degree of pathophysiological relevance of fibrinogen and erythrocyte aggregation, since an increment on both might induce a state of microcirculatory slower flow, increasing the probability of cardiovascular complications. Moreover, it was concluded that the specific receptor of fibrinogen on erythrocyte membrane is the integrin $\alpha_v\beta_3$ and the $_{94}$RGD$_{97}$ sequence on the Aα-chain of the fibrinogen is one of the essential binding sites.

These results, together with future studies, will be important to discover therapeutic drugs in order to overcome the erythrocyte aggregation promoted by the fibrinogen-erythrocyte binding and, thus, reduce the possibility of cardiovascular events.

Resumo

As doenças cardiovasculares (CVDs) representam a principal causa de morte a nível mundial. Estudos longitudinais têm evidenciado o papel de novos fatores de risco cardiovascular, cuja avaliação a curto ou longo prazo poderá contribuir para a identificação de indivíduos com risco elevado, prevenindo eventos cardiovasculares. Facilitará também a identificação de indivíduos que melhor poderão beneficiar de futuras intervenções terapêuticas. O controlo de doenças cardiovasculares está direcionado para a identificação e gestão de fatores de risco, tanto a nível individual como populacional, através da prevenção primária e secundária. Apesar dos avanços científicos e clínicos nesta área, a mortalidade e morbilidade permanecem, no entanto, com elevadas taxas.

O fibrinogénio é a terceira proteína mais abundante no plasma humano, cujos níveis, em condições normais podem variar entre 1.5 e 4.0 g/L. É uma glicoproteína com 340 kDa, constituída por dois domínios idênticos, cada um constituído por três polipéptidos (cadeias Aα-alfa, Bβ-beta e γ-gama). Elevados níveis plasmáticos de fibrinogénio têm sido associados a alterações das propriedades reológicas do sangue, tais como, a viscosidade sanguínea, a agregação e a deformabilidade eritrocitária, que poderão ser a causa ou o efeito do desenvolvimento e/ou progressão das doenças cardiovasculares e cerebrovasculares. O papel dos eritrócitos na hemostase e trombose tem atraído recentemente nova atenção, uma vez que a agregação eritrocitária parece ser um indicador importante de risco cardiovascular. Assim, a relação entre o fibrinogénio e o aumento da agregação eritrócitária poderá ser um importante biomarcador de avaliação do risco de eventos cérebro-cardiovasculares.

O plasma sanguíneo contém diferentes variantes do fibrinogénio, merecendo destaque o fibrinogénio γ'. As mutações do fibrinogénio γ' ocorrem com maior frequência apenas numa das cadeias gama da estrutura proteica, formando o heterodímero γA/γ', correspondente a 8-15% do fibrinogénio total circulante *in vivo*. A variante de fibrinogénio γ' surge de uma alteração de *splicing* da cadeia gama do RNA mensageiro, resultando na substituição dos últimos 4 resíduos de aminoácidos (AGDV) da cadeia γA por uma sequência de resíduos de 20 aminoácidos (VRPEHPAETEYDSLYPEDDL), que inclui uma elevada proporção de resíduos carregados negativamente. Níveis elevados desta variante de fibrinogénio têm sido associados a alterações na estrutura e propriedades dos

coágulos de fibrina. No entanto, a sua interação com os eritrócitos assim como os mecanismos moleculares associados ao risco cardiovascular são ainda assuntos controversos.

O trabalho descrito nesta tese inicia-se com o estudo das variantes de fibrinogénio em termos de interação com os eritrócitos, estrutura e propriedades dos coágulos. Pretendeu-se também avaliar os locais de ligação entre a molécula de fibrinogénio e os eritrócitos e definir qual o recetor na membrana dos eritrócitos responsável por esta ligação. Estudos anteriores publicados no grupo tinham demonstrado que o recetor do fibrinogénio no eritrócito é uma integrina com uma subunidade β_3. Após a avaliação da ligação fibrinogénio-eritrócito em dadores saudáveis, o principal objetivo desta tese centrou-se no estudo detalhado das interações fibrinogénio-eritrócito em doentes com patologia cardíaca ou cerebrovascular. A avaliação da adesão eritrócito-eritrócito, de modo a compreender a influência do fibrinogénio na agregação eritrocitária e a possível alteração desta adesão em condições patológicas, foi também um dos principais objetivos desta tese. Desta forma, diferentes doenças foram estudadas no decorrer deste projeto, tais como a insuficiência cardíaca crónica (CHF), hipertensão arterial essencial (EAH) e o acidente vascular cerebral. Avaliou-se a interação molecular entre o fibrinogénio e os eritrócitos como fator de risco de doença, fazendo também um estudo com base no seguimento e avaliação clínica dos doentes (*follow-up*), em estreita colaboração com clínicos de diferentes especialidades e hospitais. Os parâmetros hemoreológicos do sangue, assim como os perfis clínicos, foram igualmente avaliados. Adicionalmente, procedeu-se à avaliação das propriedades viscoelásticas dos eritrócitos de doentes, comparando-as com as de dadores saudáveis. A avaliação da concentração de fibrinogénio γ' no plasma sanguíneo, em doentes e dadores saudáveis, foi também objeto de estudo.

Durante o desenvolvimento desta tese, foram aplicadas diferentes técnicas e metodologias, de forma a alcançar os objetivos propostos. Salienta-se o uso da microscopia de força atómica (AFM), essencialmente através de metodologias de espectroscopia de força, que permitiu avaliar a ligação fibrinogénio-eritrócito e a adesão eritrócito-eritrócito. Também foram utilizadas outras técnicas biofísicas, hemoreológicas e de biologia molecular, entre outras.

Os resultados mostraram que a presença de eritrócitos e da variante do fibrinogénio γ', mesmo combinada com a variante mais comum, γA, promove alterações na ligação aos eritrócitos e na estrutura e propriedades dos coágulos. Em particular, observou-se que era necessária maior força para a completa separação entre dois eritrócitos quando na presença do fibrinogénio γAγ' do que na presença do fibrinogénio γAγA. Esta interação entre os eritrócitos e o fibrinogénio γAγ' conduziu a alterações na estrutura e propriedades da fibrina, formando uma estrutura heterogénea, com áreas muito densas e ramificadas, o que poderá conduzir ao aumento do risco de doença cardiovascular e/ou à sua progressão. A presença dos eritrócitos em coágulos com fibrinogénio γAγ' alterou também as propriedades viscoelásticas do coágulo, apresentando-se com maior rigidez, menor permeabilidade e maior resistência à sua lise. Também a fibrinólise nos coágulos com o fibrinogénio recombinante γ'γ', quando na presença de eritrócitos, demorou significativamente mais tempo do que na ausência destas células.

Sendo o principal objetivo desta tese, a avaliação da interação fibrinogénio-eritrócito em diferentes patologias, fez-se um estudo a nível de molécula única, concluindo-se que há um aumento da força necessária para quebrar a ligação entre a proteína (fibrinogénio) e as células (eritrócitos) nas várias CVDs estudadas comparativamente ao grupo de controlo. Nos doentes com insuficiência cardíaca, fez-se um estudo de seguimento clínico durante 12 meses e observou-se que os doentes que apresentaram no início do estudo uma maior força de interação entre o fibrinogénio e os eritrócitos, tiveram maior probabilidade de serem hospitalizados devido a complicações cardiovasculares, ao longo do ano seguinte. A ligação transiente entre esta proteína e eritrócitos não é suficiente para a formação de um coágulo, mas poderá conduzir à agregação eritrocitária induzindo uma alteração no fluxo, tornando-o mais lento e aumentando assim o possível risco de eventos cardiovasculares. Concluindo, a ligação fibrinogénio-eritrócito representa um possível fator de risco para a ocorrência de eventos cardiovasculares e para um mau prognóstico da doença.

Considera-se que um estudo mais alargado de doentes, assim como a avaliação de outras patologias cardiovasculares, poderá contribuir para uma melhor definição da aplicabilidade e impacto desta metodologia ao nível clínico.

Os resultados de adesão célula-célula mostraram que os eritrócitos dos doentes com hipertensão arterial essencial têm uma maior força de ligação intercélula que os dos dadores saudáveis, sendo esta adesão progressivamente maior com o aumento da concentração do fibrinogénio plasmático. Alterações nos parâmetros hemoreológicos (viscosidade total do sangue, agregação eritrocitária, hematócrito ou deformabilidade eritrocitária) foram também observadas nos vários grupos de doentes estudados. Especificamente, verificou-se que os doentes com insuficiência cardíaca apresentam uma maior viscosidade sanguínea, comparativamente ao grupo de controlo. Estes doentes mostraram também maior deformabilidade eritrocitária que os dadores saudáveis em baixas tensões de cisalhamento e menor deformabilidade a elevadas tensões de cisalhamento, o que poderá comprometer a microcirculação. A elasticidade dos eritrócitos foi também avaliada, observando-se diferenças estatisticamente significativas em doentes (CHF, EAH e acidente vascular cerebral) comparativamente aos dadores saudáveis. A quantificação do fibrinogénio γ' no plasma de doentes com patologia cardíaca (EAH) ou cerebrovascular (acidente vascular cerebral) mostrou-se também relevante, dado o incremento observado dos valores nestes doentes comparativamente aos dadores saudáveis, revelando-se um potencial fator de risco a ser futuramente ponderado ao nível clínico. A identificação do recetor específico para o fibrinogénio na membrana eritrocitária (a integrina $\alpha_v\beta_3$), assim como a caracterização da sequência $_{94}RGD_{97}$ como um possível local de ligação entre a proteína e a célula, poderão abrir novas portas para o futuro desenvolvimento de fármacos que impeçam a ligação fibrinogénio-eritrócito, associada ao aumento da agregação eritrocitária. Esta estratégia poderá ter um grande impacto na redução ou prevenção de doenças cardiovasculares, com consequente impacto no aumento da esperança de vida.

Keywords

Fibrinogen

Erythrocyte

γ’ fibrinogen

Fibrin clot

Cardiovascular diseases

Atomic force microscopy

Palavras-chave

Fibrinogénio

Eritrócito

Fibrinogénio γ’

Coágulo de fibrina

Doenças cardiovasculares

Microscopia de força atómica

Symbols and abbreviations

The acronyms used are described on first usage and whenever seemed necessary to improve clarity. Common acronyms, scientific or not (such as “UK”) are not expanded. Amino acid residues are generally indicated using the one-letter code.

ACE | Angiotensin-converting enzyme

AFM | Atomic force microscopy

AHA | American Heart Association

APTES | 3-aminopropyl-triethoxysilane

BHK | Baby hamster kidney cell line

BP | Blood pressure

BSGC | Buffered saline glucose citrate

CAML | Centro Académico de Medicina de Lisboa

CHF | Chronic heart failure

CHLN |Centro Hospitalar Lisboa Norte

CHO | Chinese hamster ovary cells

ConA | Concanavalin A

CVD | Cardiovascular diseases

DBP | Diastolic blood pressure

DVT | Deep vein thrombosis

EA | Erythrocyte aggregation

EAH | Essential arterial hypertension

EDTA | Ethylenediaminetetraacetic acid

EEIs | Erythrocyte elongation indexes

EF | Ejection fraction

ELISA | Enzyme-linked immunosorbent assay

ESC | European Society of Cardiology

FCT | Fundação para a Ciência e Tecnologia

FMUL | Faculdade de Medicina da Universidade de Lisboa

G' | Storage modulus

G'' | Loss modulus

HR | Hazard ratio

iMM | Instituto de Medicina Molecular

IPST | Instituto Português do Sangue e da Transplantação

ISTH | International Society on Thrombosis and Hemostasis

I-TASSER | Iterative threading ASSEmbly refinement (server for protein structure and function prediction)

K_s | Darcy constant

LDH | Lactate dehydrogenase

LSCM | Laser scanning confocal microscopy

LV | Left ventricular

MCTES | Ministério da Ciência, Tecnologia e Ensino Superior

NHYA | New york heart association functional classification

NT-ProBNP | N-terminal pro-brain natriuretic peptide

OR | Odds-ratio

PBS | Phosphate-buffered saline

PDB | Protein data bank

PLL | Poly-L-lysine

PNH | Paroxysmal nocturnal hemoglobinuria

PTX3 | Acute-phase include pentraxin 3

PMSF | Phenylmethylsulfonyl fluoride

RBC | Red blood cell

RDW | Red blood cell distribution width

RGD | Arginine-glycine-aspartate sequence

Rh | Recombinant human fibrinogen

SBP | Systolic blood pressure

SD | Standard deviation

SEM | Scanning electron microscopy

SEM | Standard error of mean: SD/$\sqrt{n}$

SPM | Scanning probe microscopy

STM | Scanning tunneling microscopy

Tan δ | Loss tangent or damping factor

TBS | Tris buffered saline

tPA | Tissue-type plasminogen activator

UCSF | University of Califórnia at San Francisco

WHO | World Health Organization

WT | Wild-type

Chapter I ▫

Introduction

Fibrinogen: from the interaction with erythrocytes to its influence on cardiovascular disease

Overview

Fibrinogen and fibrin are essential for hemostasis, but they are also major factors in thrombosis, wound healing and several other biological functions and pathological conditions. Little is known about mechanisms regulating the interaction between fibrinogen and erythrocyte and how this protein-cell interaction contributes to a state of slower microcirculatory flow, increasing the probability of cardiovascular complications. This Chapter reviews the state of the art about the role of fibrinogen and its properties, as well as its protein variants, on the structure of the blood clot, and also on the development and progression of cardiovascular pathologies. The concepts about the binding between the erythrocyte receptor and fibrinogen are also a relevant key point in order to find strategies to inhibit it. Here, we also want to focus on the importance of emerging biomarkers, having in mind to encourage healthcare services to improve laboratory methodologies in early diagnosis as well as to implement a more precise evaluation of the patients' risk in order to establish a successful prognosis (Figure 1).

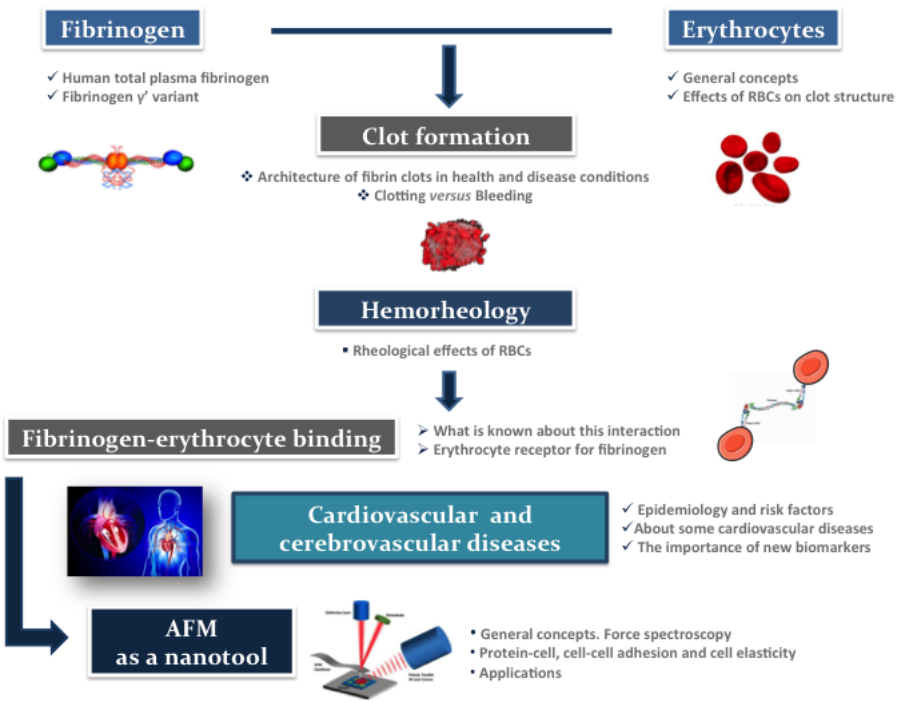

Figure 1 | Flowchart of the introduction. Schematic representation of the main topics addressed in the state of the art.

Human fibrinogen biology and structure

Being an essential protein for hemostasis, fibrinogen is also the third most abundant of all human plasma proteins (after albumin and the immunoglobulins). In healthy individuals, fibrinogen circulates in plasma at concentration between 1.5–4 g/L[1-3], being the liver the primary source of this protein[3]. However, its concentration can exceed 7 g/L during acute inflammation in response to injury. Due to interleukin-6 and other cytokines, fibrinogen gene promoters rapidly increase gene transcription, leading to higher circulating fibrinogen levels[4, 5]. Therefore, fibrinogen is considered as an acute phase protein[6]. It is important to note that its concentration can also be influenced both by environmental and genetic factors[7-9]. The levels are also known to differ between Caucasian and African-Americans, as well as with Africans, being higher levels observed in the Black ethnicities[10, 11].

Three quarters of this protein is present in plasma, but it is also present in lymph, interstitial fluid and platelets. The normal half-life of fibrinogen is around 3-5 days[12]. In hepatocytes, in the rough endoplasmic reticulum, its chains are synthesized and, after being properly assembled, fibrinogen is secreted into the blood stream[13] (Figure 2).

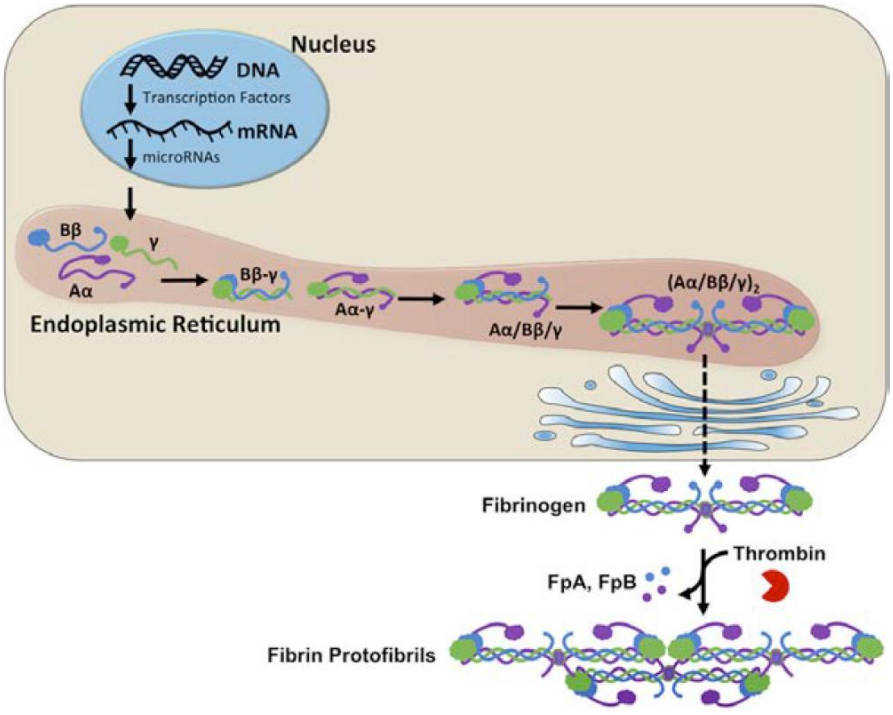

Figure 2 | Schematic diagram of the synthesis and expression of fibrinogen. Fibrinogen synthesis, which occurs primarily in hepatocytes, is regulated by

transcriptional and translational mechanisms. After the six chains are translated, the assembly takes place in a stepwise manner in which single chains assemble first into Aα-γ and Bβ-γ complexes, then into Aα/Bβ/γ half molecules and finally into hexameric complexes Aα/Bβ/γ_2. Once fibrinogen is released into blood, it circulates until thrombin cleaves fibrinopeptides from Aα and Bβ chains to form fibrin monomers[14]. Detailed information about this process is described on the following pages.

Fibrinogen, as a particular and large protein, has a length when stretched of about 80 nm[15], 4 nm in diameter and a molecular mass of 340 kDa[16]. It is composed of three globular regions, namely, a central region, E, connected by a coiled-coil segment to two identical terminal regions, D, as shown in Figure 3. They are grouped in a pair of three polypeptide chains linked by several disulfide bridges, to form two symmetrical half-molecule. The chains are composed by 2 Aα, 2 Bβ and 2 γ polypeptide chains. All these 6 fibrinogen chains are assembled with their N-termini located in a central E region[17-19]. The Bβ and γ chains terminate in globular regions known as βC and γC modulus, respectively. These domains collectively comprise the D regions. The Aα chains are the largest. At the end of the coiled-coil region, each chain extends into a highly flexible series of repeats, followed by globular αC regions[20].

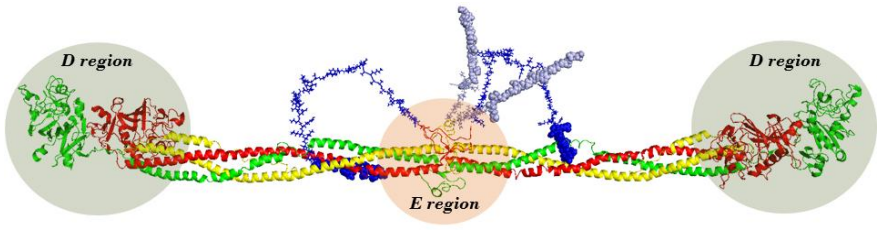

Figure 3 | Representation of the human fibrinogen molecule. Fibrinogen occurs as a symmetric dimer, where each monomer is constituted of three non-identical polypeptide chains, Aα, Bβ and γ, linked together by a total of 29 disulphide bonds. The domain is constituted by: D-coil-E-coil-D. The C-terminal of the Aα chain extends, at each end, beyond the D region as an extend protuberance that is important for cross-linking the molecule. Modified from PyMOL: 3GHG[20, 21].

The Aα chains contain fibrinopeptides A and the Bβ chains have fibrinopeptides B. The γ chain does not have any kind of fibrinopeptides. Concerning these chains, Aα chain has 610 amino acid residues and 70 kDa, Bβ chain has 461 amino acid residues and 56 kDa and γ chain has 411 amino acid residues and 48 kDa. These same chains are encoded by distinct closely linked genes, namely, FGA, FGB, and FGG, clustered on human chromosome 4 (4q31.3)[22, 23].

The structure of fibrinogen could be changed even after it has been secreted into the blood, once fibrinogen undergoes a number of co-translational and pos-translational modifications (such as, glycosylation and proteolysis)[24]. Additionally, since fibrinogen is a six-chain molecule containing two copies each of the Aα, Bβ, and γ chains, several combinations of altered chains can be assembled resulting from heterozygous polymorphisms or mutations. Polymorphic variations in both Aα and Bβ chains have been described, suggesting that there are more than a million non-identical forms in a healthy individual as a result of the different combinations of modified or inherently polymorphic sites[25, 26]. Single nucleotide polymorphisms on fibrinogen have been shown to account for approximately 1.4–3.8% and 2% of variance in total fibrinogen levels in African-Americans[27, 28] and non-Hispanic blacks[29], respectively, which tend to be mostly lower[27, 28] when compared to the contribution in white populations, which range is 1-6 to 15%[27, 28]. Genetic polymorphisms do not only affect the concentration of fibrinogen, but can also change their functionality leading to an altered blood clot[30].

Due to important role of fibrinogen in the coagulation process, it is perhaps surprising that patients with deficiencies on this protein, either quantitatively (hypo- and a-fibrinogenemia) or qualitatively (dysfibrinogenemia) can be symptomless, but they also can present bleeding or even thrombosis[31-34]. It was reported that around 30% of patients with fibrinogen deficiency present thrombosis, and this percentage may even be higher in patients with afibrinogenemia[33]. As the causes for this variable clinical phenotype of fibrinogen deficiency remain unclear[35], a better understanding of the structure and function of the molecule, especially in pathological processes is still necessary.

Alternatively spliced fibrinogen variant γ'

In the plasma, a highly heterogeneous mixture of fibrinogen variants can be detected. Alternative mRNA processing and post-translational modifications give rise to different fibrinogen isoforms with widely varying features[36]. Particularly, the fibrinogen γ chain has two different isoforms, the γA (or simply γ) isoform and the γ' (or γB) isoform[37]. In 1972, Mosesson *et al.* discovered a variant of the γ-chain with a higher molecular weight, which recently received more attention[37]. They also showed that fibrinogen's heterogeneity in size and charge was due to this minor variant of the γ chain[37]. γ' fibrinogen is a variant that arises from altered splicing of the γ-chain mRNA, leading to a bulky structure[38, 39]. The splice variation is caused by alternative polyadenylation, which leads to the inclusion of intron 9 in the transcript. The open reading frame from intron 9 introduces 20 new residues (VRPEHPAETEYDSLYPEDDL) at the γ chain C-terminus, replacing 4 residues (AGDV) encoded by exon 10 (the 'normal' γA sequence), followed by a stop codon[39, 40] (Figure 4).

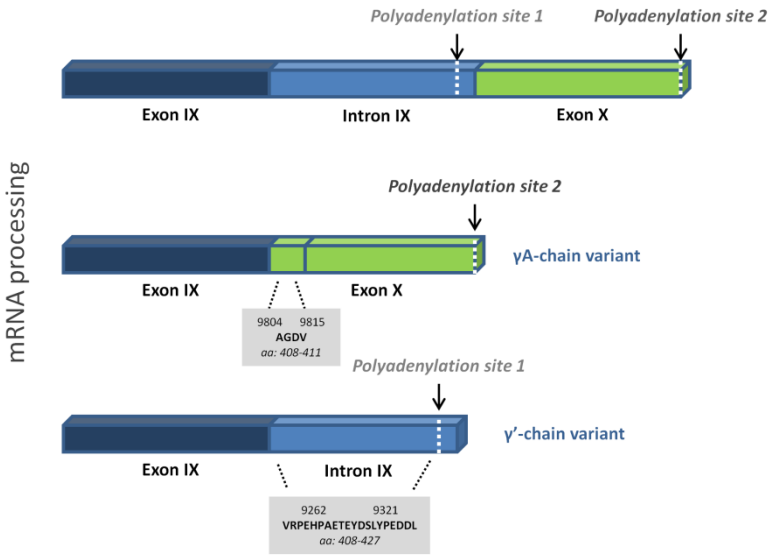

Figure 4 | **Alternative mRNA processing**. The common γA chain is formed when the polyadenylation occurs downstream of exon 10, at the polyadenylation site 2. On the other hand, the γ' chain is formed when an alternative polyadenylation occurs in the intron 9 (polyadenylation site 1). This precursor molecule matures into the mRNA that codes for the 20 unique amino acids at the terminal end of the γ' chain, substituting the 4 γA amino acids of exon 10. Adapted from[41].

The C-terminal sequence of γ', containing several Asp and Glu residues, adds substantial negative charge to the region and two sulphated tyrosine residues[40]. The majority of γ' fibrinogen exists in the form of a heterodimer with γA, γ'/γA (therefore, only one of the two γ-chains at one end of the dimeric fibrinogen molecule contains the γ' sequence) and constitutes around 8–15% of total fibrinogen. The γ'/γ' homodimer represents only a small fraction (<1%) of total fibrinogen, and most (~80-85%) of total fibrinogen is constituted by the γA/γA homodimer in healthy conditions[39, 42]. γ' fibrinogen is also genetically regulated and genetic factors are considered to explain 30–40% of the variation in fibrinogen concentration in white populations[43, 44].

The γ' chain contains unique properties having biochemical and biophysical features that distinguish it from the more common γA chain. γA/γ' clots have different structure and behavior when compared with γA/γA clots. However, the exact mechanisms underpinning these differences remain largely unknown[45-47]. The γ' chain, when incorporated into a mature fibrinogen molecule, can produce clots with altered architecture that are also more resistant to breakdown[48]. In the presence of factor XIII (zymogen of the transglutaminase FXIIIa that exerts its enzymatic activity to stabilize blood clots), the clots become highly resistant to fibrinolysis[45, 48-50]. Moreover, studies demonstrated that the γ' chain binds to thrombin with high affinity through exosite II[50-52]. Actually, the effects of γ' fibrinogen was also named antithrombin I, due to its inhibitory effect on thrombin[53]. It is likely that the antithrombin I activity of γ' fibrinogen is largely due to sequestering of thrombin via γ' into the forming fibrin clot, leading to a reduction of the thrombin available in the remaining plasma. Interestingly, thrombin when bound to γ' in the clot is also relatively protected from inhibition by antithrombin and heparin[54]. Moreover, *in vitro* studies showed that clots made with purified γA/γ' fibrinogen polymerize at a slower rate compared to clots made with purified γA/γA fibrinogen[46]. This may lead to a different clot formation rate and different characteristics of the fibrin network, and may therefore contribute to the pathological conditions detailed in the following pages.

Possibly as a result of these properties, recent studies suggest that γ' fibrinogen is a newly-emerging risk factor for cardiovascular diseases. Studies have associated γ' fibrinogen concentrations with coronary diseases[55], myocardial infarction[56] and ischemic stroke[57]. In particular, the finding that some patients have an increased γ' fibrinogen to

total fibrinogen ratio[57-60] indicates that γA/γ′ fibrinogen is not merely a biomarker of increased total fibrinogen in plasma and suggests a specific role for γA/γ′ variant in arterial thrombosis[61]. However, these studies do not and cannot demonstrate causality of γ′ chain–containing fibrinogen in thrombosis. Walton *et al*. (2014) showed in mice that both γA/γA and γA/γ′ fibrinogen increased the fibrin formation rate in plasma, but γA/γA fibrinogen accelerated the rate to a greater extent than γA/γ′ fibrinogen[62]. They showed the independent roles of γA/γA and γA/γ′ fibrinogen in arterial thrombosis and suggested that γA/γA fibrinogen promotes thrombosis, whereas γA/γ′ binds thrombin *in vivo* and limits thrombin activity[62]. A recent report by Appiah *et al.* showed that γ' fibrinogen does not add much to CVD prediction beyond traditional risk factors and total plasma fibrinogen level[63]. Pieters *et al.* showed that γ′ fibrinogen levels increase as total fibrinogen increases, although with a less extent, resulting in a decrease in γ′/total fibrinogen ratio at high fibrinogen concentrations in the apparently healthy black African population[64]. Increases in both γ′ fibrinogen and total fibrinogen were associated with increased maximum absorbance, in agreement with the formation of clots composed of increased fibrin material. However, the γ′/total fibrinogen ratio was associated with decreased maximum absorbance, in agreement with clots made of thinner fibrin fibers. Increased γ′ fibrinogen levels were associated with prolonged clot lysis. Traditional cardiovascular risk factors (excluding fibrinogen) explained 20% and 3%, respectively, of the variance in γ′ fibrinogen and γ′/total fibrinogen ratio, with C-reactive protein making the largest contribution. These data show that physiological levels of γ′ fibrinogen influence fibrin clot structure in plasma[64]. Unfortunately, studies on the clinical significance of γ' fibrinogen and thrombotic diseases have been hampered by the lack of a standardized assay with well-described analytical parameters.

Additionally, until now, most of the studies used commercial plasma fibrinogen to evaluate the clots, containing just the γAγA and γAγ′ variants[46, 49, 65]. Just a couple of studies used synthesized recombinant fibrinogen, comparing the homodimeric molecules[47, 48].

Prof. David H. Farrell and his collaborators, in Gamma Terapeutics, considered that there are a several novel biomarkers emerging, and not all of them have held up to closer scrutiny or correlated with existing risk factors. The group believes, however, that the

measurement of γ' fibrinogen could help to bridge the residual-risk gap in patients with normal cholesterol levels and help to identify patients with high cardiovascular risk[66].

Clot formation, structure and stability

"If you enjoy a pretty sight, examine the clotted blood with a microscope. You will see a fibrous texture and a network of nerve-like threads"

Marcello Malpigh, 1666[67]

Although the Koran, on the 7th century, said that humans were created from clots of blood, it was only on the 20th century that Marcello Malpighi described the structural component of blood clots as a white fibrous substance that we know as fibrin[67].

Fibrinogen, a soluble macromolecule, provides the main building block of the blood clot, responding rapidly to tissue damage, being converted to the insoluble fibrin by thrombin during the final steps of coagulation[22, 68]. This is activated by a cascade of enzymatic reactions triggered by vessel wall injury, activated blood cells or a foreign surface[24]. Its thrombin-catalized transformation into fibrin, the fundamental component of blood clots, has intrigued protein scientists for more than a century[22, 68]. Its function is to break the bonds of the fibrinopeptides in the molecule of fibrinogen, in order to release them from the former structure[16, 69]. Thus, fibrinogen is converted to fibrin by thrombin cleavage of two fibrinopeptides A and two fibrinopeptides B from the Aα- and Bβ-chains, respectively[69, 70]. The cleavage of these short, acidic N-terminal peptides exposes polymerization sites, and results in a change in solubility, causing the molecules to polymerize and form fibrin fibers. At the molecular level, thrombin cleaves faster the fibrinopeptide A, between Arg16 and Gly17[71, 72], than the fibrinopeptide B, exposing a binding site on the fibrin E-region specific for a binding pocket in the D-region. This is sufficient to initiate fibrin polymerization. By this mechanism, one fibrin molecule can bind to two other fibrin molecules, which in turn can bind to another one, and so on, producing a fibrin polymer, or protofibril, comprised of staggered and overlapping fibrin molecules[34, 70-72], as shown in Figure 5.

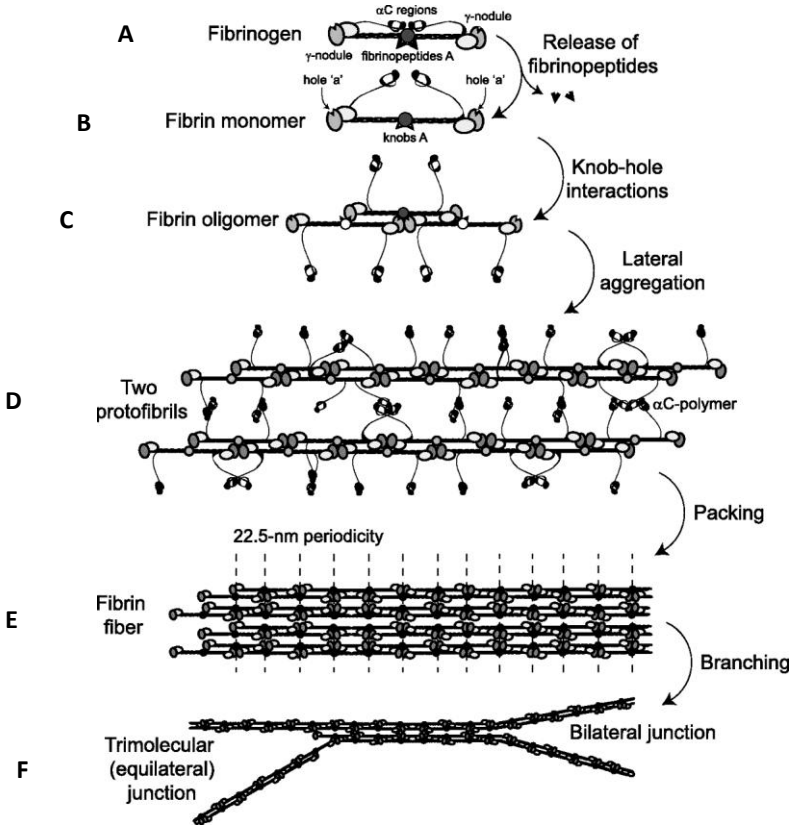

Figure 5 | **Schematic representation of the major steps of fibrin polymerization.** The consecutive steps are shown: (A) release of fibrinopeptides from fibrinogen; (B) formation of monomeric fibrin containing exposed knobs and partial dissociation of the αC regions; (C) self-assembly of monomeric fibrin via knob-hole interactions and formation of half-staggered 2-stranded fibrin oligomers; (D) lateral aggregation of protofibrils (fibrin oligomers made of 20 to 25 monomers) promoted by homophilic αC-αC-interactions within and between protofibrils, including the formation of αC-polymers; (E) packing of protofibrils into a fiber; and, (F) fibrin network formation due to the branching of fibers[24, 73, 74].

This subsequent aggregation of protofibrils into fibers yields a fibrin meshwork that is essential for blood clot stability. Finally, the fibrin polymer is stabilized via covalent crosslinking by factor XIIIa (plasma transglutaminase) to form a mechanically and chemically more stable mature fibrin clot[24, 61, 72, 75].

During fibrin generation, several conditions may strongly influence clot formation, structure and stability. These include the concentrations of procoagulants,

anticoagulants, fibrin(ogen)-binding proteins[76-78] and metal ions[79] as well as contributions from blood and vascular cells, cell-derived microvesicles[80, 81] and the presence of blood flow[82, 83]. Alterations on fibrin(ogen) structure and stability may lead to several diseases[14] (Figure 6).

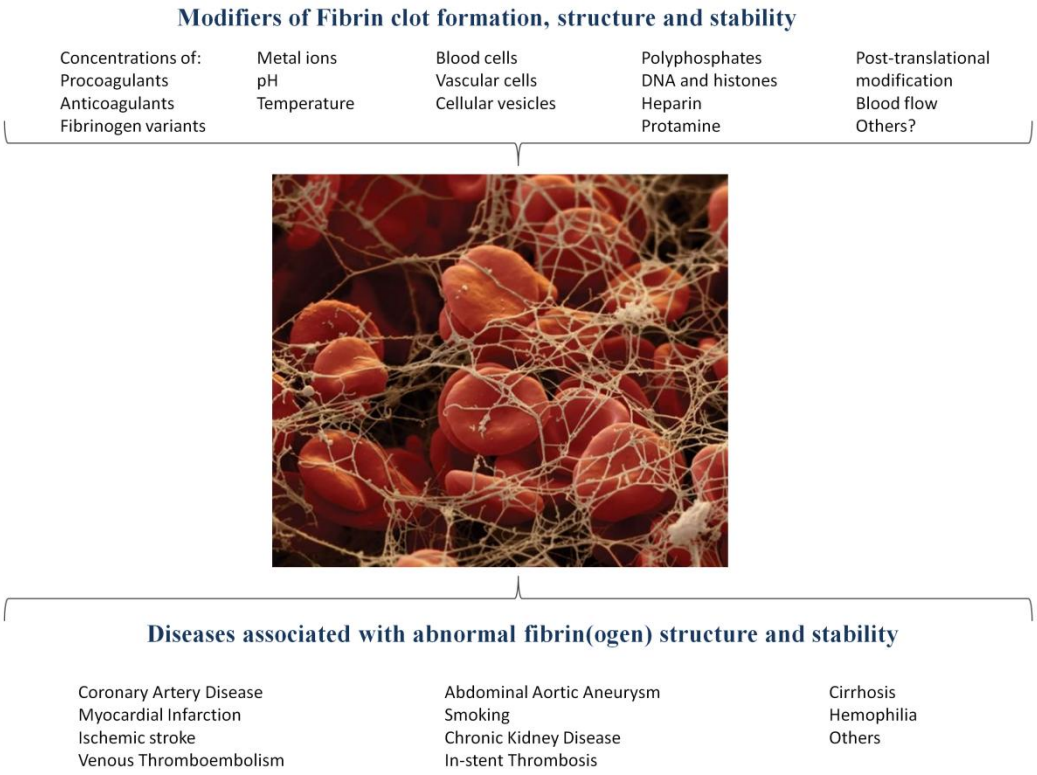

Figure 6 | **Contributers to changes on fibrin clot formation, structure and stability and association with different diseases**. During fibrin generation, several conditions may influence clot formation, structure and stability, creating abnormal clots, which are associated with the development of diseases (Adapted from[14]).

Clotting *versus* Bleeding

As previously mentioned, the clot is formed through a cascade of enzymatic reactions that activate prothrombin to thrombin, which converts soluble fibrinogen into insoluble fibrin in a process named blood clotting, preventing blood loss. Afterwards, the fibrin clot is dissolved through fibrinolysis or cleavage by plasmin, resulting in fibrin degradation products. Plasmin is formed on the fibrin surface, from the zymogen

plasminogen, by plasminogen activators. There is a careful balance *in vivo* between clotting and fibrinolysis, the proteolytic dissolution of the clot. Imbalance in one direction, such as, the prevalence of fibrinolysis, can lead to bleeding. The opposite imbalance, the prevalence of clotting, can cause thrombosis or formation of a clot that blocks the blood flow through a vessel or artery, creating a thrombus (Figure 7). This way, thrombosis is the most common cause of myocardial infarction, ischemic stroke, deep vein thrombosis and other cardiovascular diseases[24].

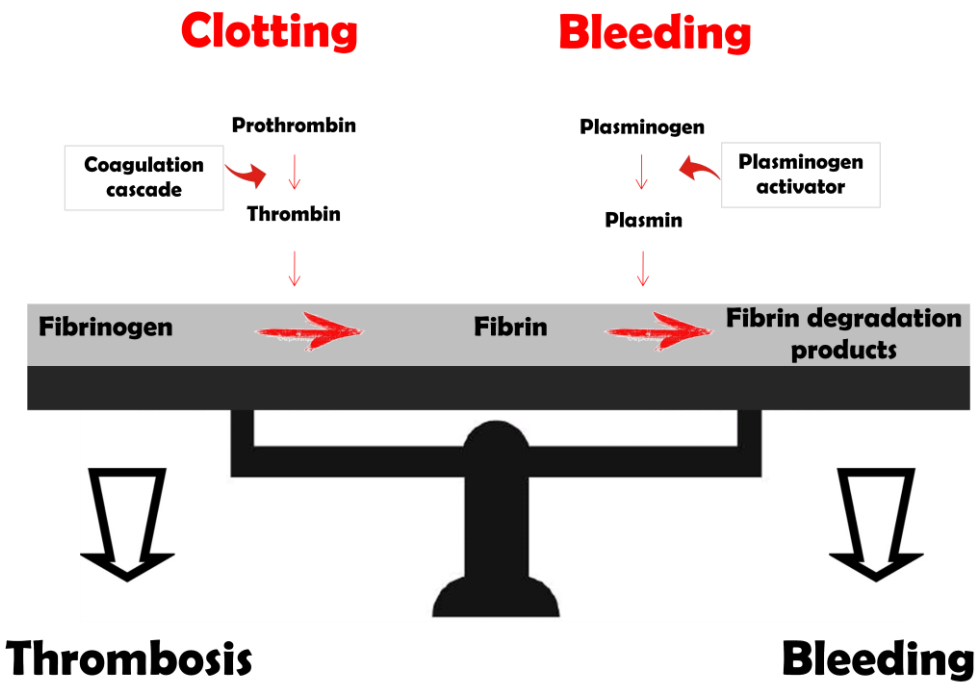

Figure 7 | **Schematic representation of the balance between the fibrin clot formation and fibrinolysis processes**. A balance between clotting and fibrinolysis should exist, otherwise excess clotting can promote thrombosis, while excess fibrinolysis can lead to bleeding (Adapted from[24]).

Despite its recognition as a key component of blood clotting, the role of fibrinogen and fibrin in hemostasis and thrombosis are not fully understood[14].

Abnormal architecture of fibrin clots in disease

Alterations on fibrin clot architecture have been shown to be associated with atherosclerosis or cardiovascular diseases and are thought to contribute to their pathogenesis and progression[84-86]. The production of clots with abnormal structure and stability has been demonstrated in plasma samples from patients with high cardiovascular disease risk[84-86]. The association of fibrin clot structural parameters with clinical pathologies such as dense networks of thinner/compact fibers with increased thrombotic risk[85, 86] and coarse networks of thicker/less compact fibers with increased bleeding risk[86, 87], suggests that fibrin structure is a critical determinant for hemostasis and thrombosis.

Changes in clot structure have been found in patients with different CVDs[85, 88-90]. Fatah *et al.* reported that patients with myocardial infarction formed clot structures denser and less permeable than those from healthy individuals[88, 89]. Patients who developed in-stent thrombosis after percutaneous coronary intervention, showed abnormal plasma clot characteristics, namely, permeability, turbidity and lysis time, compared with patients who did not develop in-stent thrombosis[91]. Collet *et al*. found increased stiffness, higher fiber density and increased resistance to fibrinolysis in young survivors of myocardial infarction[92]. The first-degree relatives of patients with coronary artery disease also showed altered fibrin structure with denser clots, suggesting a familial predisposition to altered fibrin structure and disease[84]. Fibrin clots in patients with diabetes show a denser structure with smaller pores and increased resistance to fibrinolysis[93].

It remains unclear whether these fibrin clot abnormalities are the consequence or the cause of the disease and what is the impact of erythrocytes on a fibrin clot.

Erythrocytes biology and structure

"Thus blood, for all its raw physicality, its heat, color and smell, remains first and foremost a powerfully symbolic substance—capable of representing the most primeval forces of life, and of death"

James Bradburne, 2002[94]

Blood can be basically divided into two parts, the plasma and the blood cells. Plasma constitutes about 55% of the total blood volume and roughly 92% of it is water. Blood cells can be divided into three major types, white blood cells or leucocytes, platelets and red blood cells or erythrocytes, being the latter the most abundant cell type in the blood.

The potential involvement of erythrocytes in hemostasis and thrombosis is being recognized. In the past, most scientists and clinicians have assumed that they play a largely passive and relatively unimportant role. However, there has been increasing evidence that erythrocytes have a variety of active functions in hemostasis and thrombosis that are significant and need to be taken into account upon assessing health and disease[95].

Erythrocytes are anucleated cells with a cytoplasm rich in hemoglobin. Erythrocytes are highly specialized O_2 carrier system in the body[96, 97]. For the erythrocyte to transport hemoglobin and consequently oxygen to all cells, it must travel through the circulatory system, including the microcirculation, where it encounters small capillary spaces and high shear stresses. In order for the cell to be able to survive this, a highly deformable yet robust membrane is required[98, 99]. These cells are very flexible, biconcave and derived from bone marrow. Typically, mature erythrocytes have approximately 8 µm diameter, a thickness of 2 µm, a surface area of 132 μm^2 and a volume of 90 fL. They circulate at 4.2-6.1×10^9 cells/mL in humans, having an *in* vivo life span of approximately 120 days. They are selectively removed from circulation via phagocytosis[100].

Erythrocytes have a relatively simple structure, being easy to isolate from the blood, and they have the most extensively studied cell membranes[98]. The membrane comprises an overlaying asymmetric phospolipid bilayer, as shown in Figure 8[101].

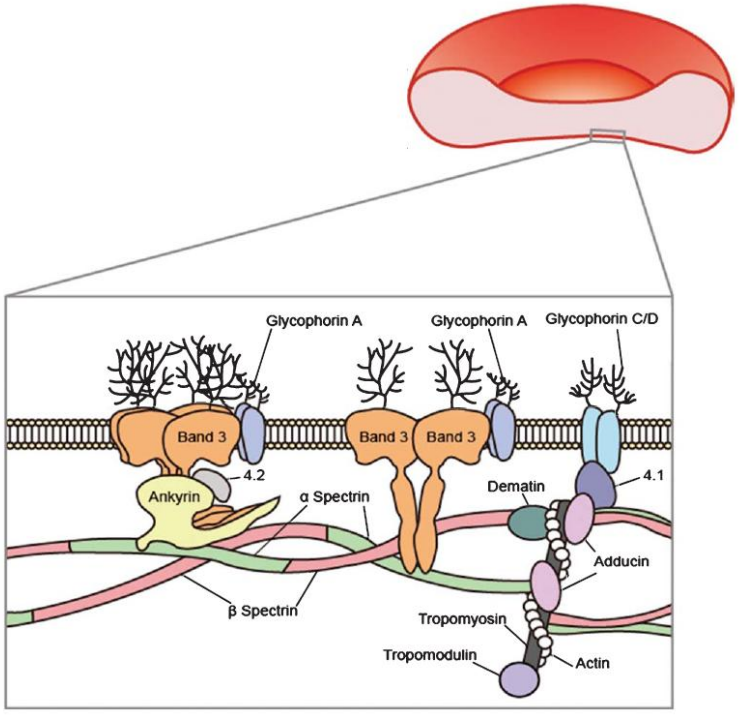

Figure 8 | Erythrocyte membrane composition: lipid bilayer, transmembrane proteins and filamentous meshwork of proteins, forming the cytoskeleton. The membrane proteins are asymmetrically oriented and with three main functions: structural, catalytic and receptor proteins[102].

The proteins of the cytoskeleton of the erythrocytes have been identified using sodium dodecyl sulphate polyacrylamide gel electrophoresis. Its main components are: spectrin, ankyrin, band 3, glycophorin C, band 4.1 and actin, in descending order of molecular weight[103, 104]. However, other molecules are also present but at lower concentrations. The plasma membrane, together with its cytoskeleton support, is responsible for the maintenance of the shape and stability of erythrocytes, thereby retaining their normal biconcave shape, and it also allows extensive deformations when needed[105]. The biconcave shape and corresponding deformability is an essential feature for proper biological functioning of human erythrocytes. Furthermore, the roughness of the cell membrane is a very interesting indicator of cell's health state[106]. During its life span, the erythrocyte undergoes progressive physical and chemical changes altering their macrostructure[107], such as, the decrease on cell volume with cell aging. This could be caused by the loss of potassium and the loss of membrane patches by microvesiculation,

resulting in an increase on cell density[108]. Changes in their membrane skeletal proteins, shape, rheological and mechanical properties or integrity of the erythrocytes may result in several diseases and dysfunctions[109].

Rheological properties of erythrocytes

Blood rheology is a complex field, mainly determined by variables such as hematocrit, blood viscosity, erythrocyte aggregation and deformability[110]. Hemorheological factors, due to their effects on microcirculation, have long been implicated in the pathogenesis of cardiovascular diseases. Overall, a significant shift in the erythrocyte microrheology could have physiological relevance on changes of blood flow, affecting the ability of erythrocytes to cross capillaries, modulating the distribution of blood in the vascular territories and, this way, impairing tissue oxygenation[111, 112].

In recent years, numerous advances in the setting of clinical hemorheology have been reported[113-116], contributing to the deeper understanding of the role of blood flow behavior [97, 117, 118]. Therefore, the behavior of blood flow is influenced by its viscosity, a macrorheological parameter, which in turn is dependent on the hematocrit, the erythrocyte aggregation and deformability properties (microrheological parameters)[119]. Shape and elasticity of erythrocytes are also apparently important to the pathogenesis of certain vascular diseases[120].

Cardiovascular illness[121], essential hypertension[122] and alcoholic liver disease[123] have been previously associated with abnormal hemorheological profiles. Additionally, pathological alterations in erythrocyte deformability have been associated with different diseases[124], such as, malaria[125], sickle cell anemia[126], diabetes[96], hereditary disorders[117], myocardial infarction[127], essential hypertension[128] and paroxysmal nocturnal hemoglobinuria (PNH)[129]. Some diseases, such as diabetes, hypertension, lower limb vein thrombosis and coronary heart disease, can secondarily alter the properties of erythrocytes, making them stiffer and prothrombotic[130]. Several diseases of the heart and circulatory system have been linked with insufficient deformability and increased aggregability of erythrocytes[131]. Also, changes in erythrocyte membrane parameters,

particularly in phospholipids, can produce serious metabolic disorders and influences the rheological properties of erythrocytes[132].

Erythrocyte aggregation is one of the important hemorheological determinants that may create problems at the level of microcirculation[133]. Pathological erythrocyte aggregation can stimulate abnormal processes by itself and intensify some abnormalities of blood coagulation. It has a direct effect in thrombosis pathogenesis[134]. Vessel injury in a vein with slowed or arrested blood flow will usually lead to a thrombus that is rich in fibrin and red blood cells (red thrombus). Conversely, a thrombus formed in the arterial circulation, where flow is relatively undisturbed, will consist primarily of platelets and some stabilizing fibrin (white thrombus)[135]. Erythrocyte aggregation has been shown to be elevated in patients with coronary heart disease[136]. Other authors showed that erythrocyte aggregation was elevated in patients with diabetic nephropathy[137]. Glacet-Bernard *et al.* have also found that elevated erythrocyte aggregation was an independent risk factor for central retinal vein occlusion[138]. Pharmacological approaches to the elevated erythrocyte aggregation have been a subject of investigation in recent years. Beta-blockers, calcium channel blockers, and ticlopidine are only a few drugs shown to decrease elevated erythrocyte aggregation[139-141]. However, the exact mechanism(s) of elevated erythrocyte aggregation in the pathogenesis of thrombotic disorders have not been fully established yet and further studies are required to elucidate them. The strength of erythrocyte aggregation can be influenced by fibrinogen binding to a previously unknown erythrocyte receptor, and platelets may contribute to increasing the force of the erythrocyte aggregation in normal conditions[142].

High hematocrit results in an increase in blood viscosity that impairs normal blood flow[143]. It can be a strong prothrombotic factor. The hematocrit-related blood viscosity may have physical effects on the interaction between platelets and blood vessel surfaces. Under flow conditions, platelet adhesion increases greatly with hematocrit. Thus, the volume fraction of erythrocytes may have a significant impact on hemostasis and thrombosis, with the nature of the effect related to the flow conditions[144].

Erythrocytes are remarkably deformable, which is important to minimize their resistance to flow and to allow them to fit through blood vessels smaller than their size. More rigid erythrocytes may be less able to squeeze through the capillaries, increasing the susceptibility to thrombosis[145]. Decreased erythrocyte deformability reduces

permeability of blood clots and thrombi, which may also have implications for the penetration of fibrinolytic agents[146].

Effects of erythrocytes on fibrin clot formation, structure and stability

Blood flow is one of the most important physical factors that affect profoundly the formation of the fibrin network, its structure and *in vivo* properties[147]. Particularly, fibrin structure and properties are greatly influenced by the presence of blood cells, namely activated platelets and erythrocytes[148] that form a natural and very active environment for clot formation. Clot quality is heavily influenced by these cells and cell-derived components are present at the injury site[80, 81, 149].

The presence of erythrocyte during clot formation seems to induce heterogeneity in the fibrin network, displaying densely packed fibers alongside regions with few fibers[149]. But whether erythrocytes increase or decrease fibrin fiber thickness is unclear. At the site of clot formation, erythrocytes can support thrombin generation[150-152] and alter procoagulant activity. It has been shown that the effects of erythrocytes on fibrin structure are reduced in the presence of eptifibatide, suggesting that these effects are modulated in part by an interaction between fibrin(ogen) and a cell surface integrins. We already reported that fibrinogen binds erythrocytes via a β_3-containing integrin on the erythrocyte surface[153], although neither the binding site on fibrin(ogen) nor the putative erythrocyte receptor has been completely identified until now.

Recent findings about contracted whole blood clots showed profound compression of resident erythrocytes into structures called polyhedrocytes[154, 155]. This tight packing arrangement reduces the permeability of the clot and may justify the resistance of older, compact clots to thrombolysis[154].

Intact or damaged erythrocytes seem to induce variability in the fibrin network structure, individual fiber features and viscoelasticity properties of the clots. These changes may have important implications for *in vivo* clot formation, maturation, stability, embolization and the efficacy of prophylactic anticoagulation and therapeutic fibrinolysis[149].

Ligand-receptor binding: interactions between erythrocytes and fibrinogen

Proteins perform their functions through dynamic structural changes and dynamic interactions with other molecules or cells[156]. Thus, interaction between ligands and proteins are crucial for the proper function of living organisms[157]. Fibrinogen can mediate diverse biological responses due to its ability to affect different cell types by binding to unique cellular receptors[158] (Figure 9).

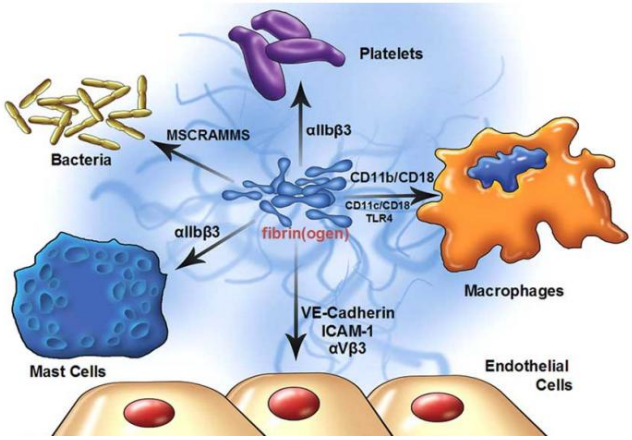

Figure 9 | Cellular receptors and target cells for fibrinogen. Fibrinogen mediates different biological responses by binding to integrin and non-integrin receptors, expressed on different target cells. For instance, fibrinogen binds to the integrin $\alpha_{IIb}\beta_3$ on platelets, leading to platelet aggregation necessary for blood coagulation[158].

An increase in fibrinogen concentration may lead to greater erythrocyte aggregation. This transient aggregation may promote cardiovascular and cerebrovascular diseases[159]. It may be induced when macromolecules interact with the surface of the erythrocytes by promoting the formation of bridges between these cells. Some physicochemical properties, such as ligand molecular mass, charge and concentration of the interacting molecules, are essential to enable the aggregation of erythrocytes[160]. However, little is known about how erythrocytes can interact with fibrinogen.

As described, the increase on erythrocyte aggregation associated with a higher incidence of cardiovascular pathologies is based on an increase on plasma adhesion proteins concentration[160, 161]. Fibrinogen has a greater effect than other plasma proteins

on erythrocyte aggregation[162-164]. This process has generally been considered to be caused by the nonspecific binding of fibrinogen to the erythrocyte membrane[160, 165]. In contrast, platelets are known to have a fibrinogen integrin receptor expressed on the membrane surface (the membrane glycoprotein complex $\alpha_{IIb}\beta_3$) necessary for blood coagulation [166]. Lominadze *et al.* suggested that fibrinogen can also specifically interact with erythrocyte membranes[161]. Erythrocytes have been shown to interact specifically with fibrin(ogen), with approximately 20 000 binding sites/erythrocytes and with a dissociation constant (K_d) of 1.3 μM[161]. In hypertensive rats, the erythrocytes aggregation was associated with hypertension, by changes of the composition of the erythrocyte membrane[163]. This may suggest that specific fibrinogen receptors on the erythrocyte membrane may be altered in hypertension. It was also reported that the binding is inhibited by the integrin receptor antagonist Arg-Gly-Asp-Ser (RGDS)[161].

There were several reports showing the existence of various (integrin or non-integrin) glycoproteins that are involved in the adhesion of erythrocytes or endothelial cells[167-169]. The presence of the integrin $\alpha_{IIb}\beta_3$ and non-integrin glycoprotein Ib on erythrocytes[169], which was reported by a group of researchers, was completely contradicted by the results from another group[170]. Another study reported the presence of integrin $\alpha_4\beta_1$ on the surface of reticulocytes, but not on mature erythrocytes from sickle cell patients[170, 171]. In addition, a low level of non-integrin glycoprotein IV (CD36) on the surface of normal erythrocytes has been found to be involved in adhesion of malaria-infected cells, suggesting that CD36 mediates an yet unidentified physiological process in healthy humans[172]. Other two potential receptors on erythrocytes have been implicated in fibrin(ogen)-erythrocyte interactions: an integrin with a β_3 subunit[153] and the integrin-associated protein CD47[173]. Since CD47 was originally identified for its interaction with $\alpha_v\beta_3$, $\alpha_{IIb}\beta_3$, and $\alpha_2\beta_1$ integrins, it is possible that the fibrinogen-binding site on erythrocytes consists of a complex of both of these molecules[148].

The discovery of the structural basis of the recognition between integrins and their natural ligands is very important for mechanisms elucidation. Some studies have shown that, on the fibrinogen molecule, the interaction with erythrocytes involves the Aα chain[174]. By the cleavage of the near terminal domain of the Aα chain (Aα-(1-206)), most of the carboxy-terminal extensions are removed (approximately 70% of the native chain). After this cleavage, erythrocyte aggregation is decreased, suggesting that the fibrinogen

binding site to the erythrocyte membrane was lost[174]. On the other hand, the Aα (207-303) region was found to be one of the possible erythrocyte-binding sites in fibrinogen, since the velocity of rouleaux using the fibrinogen fragment is preserved[174]. The fibrinopeptide-containing region in the central domain (including the Aα and Bβ chains) were shown to be repulsive to the negatively charged erythrocyte membrane[160]. The contribution of the carboxy-terminus of the fibrinogen γ-chain for erythrocyte binding must also be taken into consideration, as for the fibrinogen-platelet binding, but this is not yet clear[160]. The recognition of the fibrinogen molecule by the activated platelet $\alpha_{IIb}\beta_3$ receptor occurs through the two Arg-Gly-Asp (RGD) sequences at the fibrinogen Aα chains and the C-terminal domain of the γ chain. RGD is a consensus binding sequence for integrins and was identified using synthetic peptides[175] (Figure 10). The Aα chain of fibrinogen contains both RGD sequences, at residues 95-97 (arginine-glycine-aspartate-phenylalaline, RGDF) and 572-574 (arginine-glycine-aspartate-serine, RGDS)[176-178]. RGD peptides are also well known to bind to the $\alpha_V\beta_3$ integrin[179].

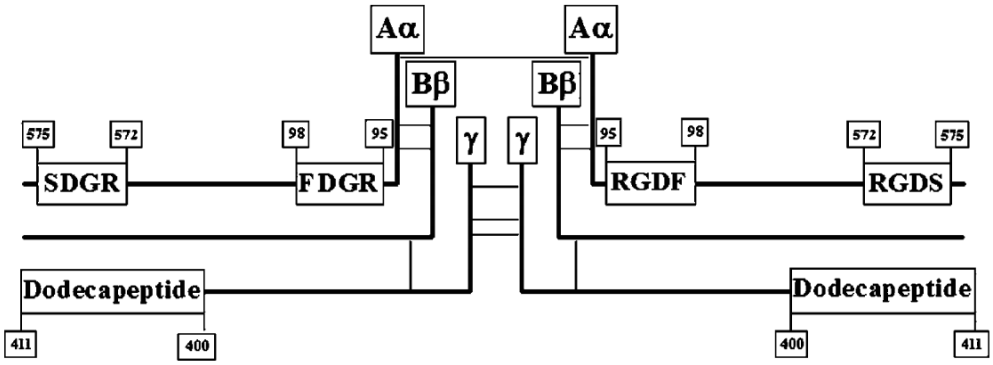

Figure 10 | Structure of fibrinogen molecule containing the 2 Aα, 2 Bβ and 2 γ chain. The two Aα chain RGD motifs and the $\gamma^{400-411}$ dodecapeptide sequence are represented. The interchain connections represent the disulfite bonds[180].

The residues 118-131 of the receptor β_3 chain were identified as the sequence of recognition of the RGD peptides[181]. The fibrinogen-platelet receptor interaction can also occur through a non-RGD sequence, the dodecapeptide (HHLGGAKQAGDV) sequence in the γ chain carboxy-terminal region (residues 400-411), which binds to $\alpha_{IIb}\beta_3$ through the amino acid residues 294 to 314 on the α_{IIb} chain of the receptor. Carvalho *et al*., demonstrated by force spectroscopy using atomic force microscopy (AFM) the existence

of a single molecule interaction between fibrinogen and an unknown receptor on the erythrocyte membrane, with a lower but comparable affinity relative to platelet binding. This receptor was not as strongly influenced by calcium ions and eptifibatide (an $\alpha_{IIb}\beta_3$ specific inhibitor) as the platelet receptor. However, its inhibition by eptifibatide indicated that it is an $\alpha_{IIb}\beta_3$-related integrin. They also studied a patient with Glanzmann thrombastenia (a rare hereditary bleeding disease caused by $\alpha_{IIb}\beta_3$ deficiency) and they showed (for the first time) an impaired fibrinogen-erythrocyte interaction[153]. Genetic analysis showed that one of the units of the fibrinogen receptor on erythrocytes was a product of the expression of the β_3 gene, found to be mutated in this patient[153]. Therefore, this suggested the possible existence of an unidentified integrin-type receptor on the surface of erythrocytes.

Thus, there are some pieces of evidence of the specific fibrinogen-erythrocyte binding during the erythrocyte aggregation process. It will be relevant to identify the fibrinogen receptor on erythrocytes and to know which are the recognition binding sites of fibrinogen, aiming to discover a pharmacological strategy to inhibit it in order to decrease erythrocyte aggregation.

Cardiovascular diseases

Cardiovascular diseases (CVDs) are the leading cause of death and disability worldwide. In 2012, it was estimated that 17.5 million people died due to CVDs, representing 31% of all global deaths. Of these deaths, an estimated 6.7 million were due to stroke and 7.4 million were due to coronary heart disease. Over three quarters of CVD deaths take place in low- and middle-income countries[182, 183] (Figure 11).

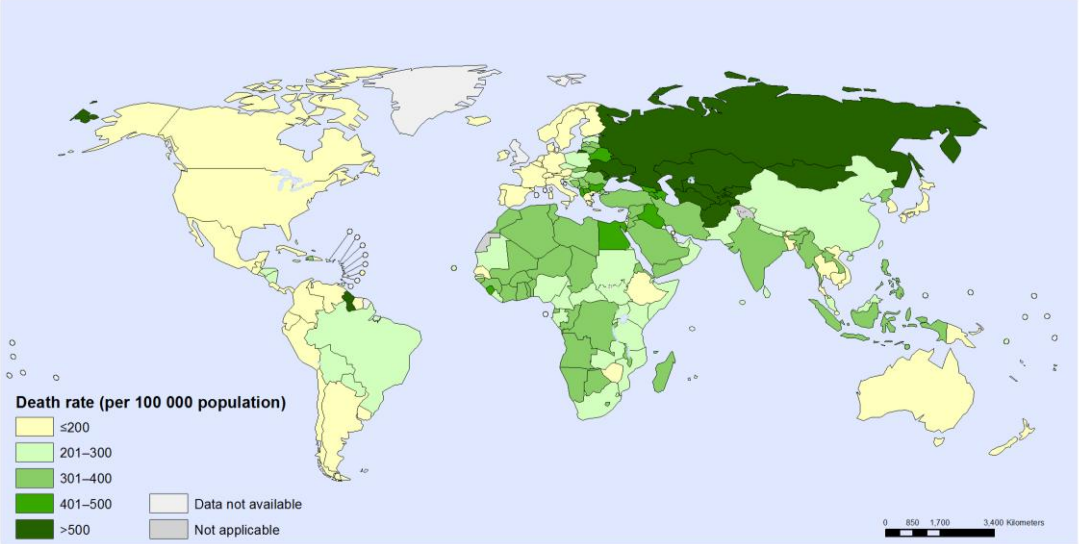

Figure 11 | **Cardiovascular diseases mortality in the world**. Age-standardized death rate per 100 000 population, both sexes, 2000-2012[183].

In Portugal, cardiovascular diseases are also the leading cause of death. In 2012, 32 859 people died from CVD and, from those, 14 393 were male and 18 466 female[184].

By 2030, when the world population is expected to reach 8.2 billion, 33% of all deaths are expected to be of CVD[185].

Cardiovascular diseases encompass different atherosclerotic vascular diseases such as coronary heart disease, cerebrovascular disease, as well as peripheral arterial diseases[159]. To address total cardiovascular risk, the World Health Organization (WHO) recommended to integrate the management of hypertension, diabetes and other cardiovascular risk factors in primary care, and target available resources at individuals most likely to develop diabetes complications, heart attacks and strokes[186]. In addition to first attacks, recurrent heart attacks and strokes also need to be prevented in those with established disease (secondary prevention). These individuals face considerably greater risk of recurrent vascular events and are much more likely to die in a recurrent event[187].

Some agents, like aspirin, beta-blockers and angiotensin-converting enzyme inhibitors, together with smoking cessation, could prevent up to three quarters of recurrent heart attack and stroke[188]. However, a sole focus on secondary prevention is

insufficient to attain this target, as a considerable number of heart attack and stroke deaths are at first event[188].

The medicine field has made a drastic progress in diagnosis, prevention and treatment of CVD over the past three decades; however, it is necessary to go on and look for new emerging risk factors to decrease the associated high morbility and mortality. Predominantly, there are five existing modifiable risk factors, namely, high blood pressure, high blood cholesterol, tobacco use (chewing/smoking), diabetes mellitus and obesity, which constitute approximately one-third of all the causes of CVD cases. In developing countries, in addition to these five existing modifiable risk factors, low vegetable and fruit intake, as well as, alcohol abuse ranks first in the list of risk factors[189] (Figure 12).

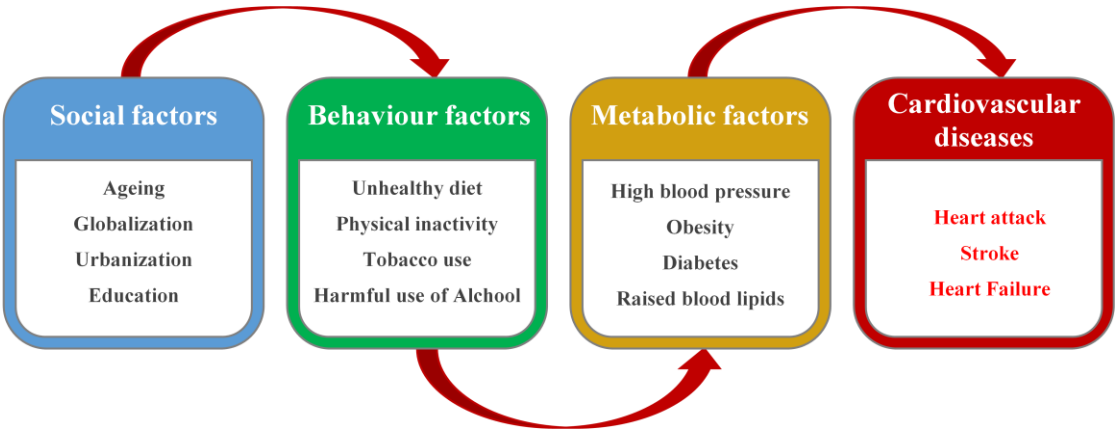

Figure 12 | Great contributory risk factors to high blood pressure and its complications associated with developing of cardiovascular diseases. Different risk factors have been reported in progression and development of cardiovascular diseases. Adapted from[187].

It is important to note that the literature well documented the association between serum concentrations of acute phase proteins and the onset of coronary heart disease and myocardial infarction[190, 191]. The emerging inflammatory markers in the acute-phase include pentraxin 3 (PTX3), amyloid A and fibrinogen[192-194]. Although the role of fibrinogen as inflammatory marker of risk is still discussed, many studies indicated an association of hyperfibrinogenemia with atherothrombosis[195].

In the next pages, there is a detailed description of the cardiovascular diseases studied on this Thesis.

Heart Failure

Heart failure (HF), is a complex clinical syndrome that can result from any structural or functional cardiac disorder that impairs the ability of the ventricle to fill or eject enough blood around the body in the right pressure[196, 197]. HF usually occurs because the heart muscle has become too weak or stiff to work properly[198]. It may be considered as the fatal finishing line of all cardiovascular disorders, causing high hospitalization and high mortality rates. In industrialized countries, the most common cause of heart failure is ischemic cardiomyopathy. Ischemic heart disease is a chronic condition in which there is a lack of blood supply to tissues, leading to a shortage of oxygen and glucose needed for normal cellular metabolism[199]. In epidemiological surveys and in large-scale therapeutic trials, the prognosis of patients with ischemic heart failure is worse than in patients with a non-ischemic etiology[200]. Even heart transplant candidates may respond better to intensifying therapy if they have non-ischemic heart failure. Non-ischemic heart disease includes different subgroups, such as hypertensive heart disease, myocarditis, alcoholic cardiomyopathy and cardiac dysfunction due to rapid atrial fibrillation (which could be reversible)[200]. The therapeutic effect of essential drugs, such as angiotensin-converting enzyme inhibitors, beta-blockers and diuretics, in general, does not significantly differ between ischemic and non-ischemic patients. However, in some clinical trials, response to certain drugs (such as digoxin, tumor necrosis factor-α and amiodarone) was found to be better in non-ischemic patients. As referred, due to distinct prognostics of the disease and possible therapeutic differences, the etiology of heart failure should be determined routinely for all patients[200]. Further studies to clarify the effects of etiology of HF on the response of treatment or prognosis could be particularly important for preventing progression to more advanced stages, in which any type of drug therapy may have limited value in prolonging survival. An individual therapeutic approach, based on etiology of HF could result in major progress in treating HF patients[201].

The prevalence of HF disease has been growing, affecting 23 million people worldwide[202-205]. Half of those affected have reduced ejection fraction (EF < 40%); the remaining have HF with preserved EF (EF > 50%) or borderline HF (EF 40–50%)[206]. Despite significant advances in the management of HF, survival remains poor, with a 50%

mortality within 5 years of diagnosis[202]. According to the American Heart Association (AHA) / American College of Cardiology guidelines[196, 197], "it is largely a clinical diagnosis that is based on a careful history and physical examination". Thus, HF diagnosis can be challenging, as symptoms are often non-specific and the physical exam can be misleading. In light of the staggering costs, morbidity and mortality associated with HF, the emergence of biomarkers for both diagnosis and prognosis provides important objectivity in its assessment. A few biomarkers have been reported that have led to diagnostic, prognostic and therapeutic developments, such as natriuretic peptides[207], soluble toll-like receptor 2[208], galectin-3[209] and copeptin[210] (Figure 13).

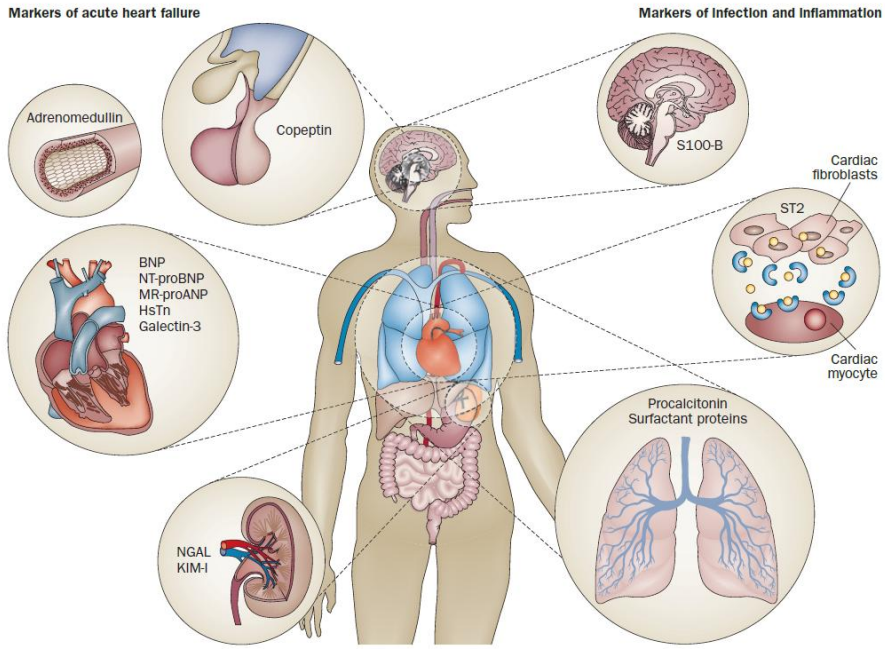

Figure 13 | **Biomarkers and their organ-specific release sites in the body in response to stress or injury**. On the left-hand side are shown the various organs affected in acute heart failure, and on the right-hand side are displayed the organs affected in the settings of infection and inflammation[211].

Essential arterial hypertension

Recently, a report categorizes individuals as hypertensive "when they persistently cross the blood pressure threshold above which there is robust scientific evidence that antihypertensive treatment will improve their prognosis"[212]. Thus, hypertension is

defined as a persistently elevated blood pressure equal or above 140 for the systolic blood pressure (SBP) or 90 mm Hg for the diastolic blood pressure (DBP). It is the major risk factor for premature cardiovascular disease (CVD), morbidity and mortality[213].

Essential arterial hypertension is often referred to as "the silent killer" once frequently displaying no overt symptomatology. Approximately half of patients with hypertension remain undiagnosed[214]. In most patients with hypertension, no clear etiology is identified. This is considered as essential, primary or idiopathic hypertension. Essential hypertension is a diagnosis of exclusion and accounts for ~ 90–95% of all cases of hypertension. It appears to be caused by a complex interaction between genetic predisposition and environmental factors[215, 216]. Secondary hypertension refers to arterial hypertension due to an identifiable cause and affects ~5–10% of the general hypertensive population[217]. The prevalence and potential etiologies of secondary hypertension vary by age. The most common identifiable causes in children are renal parenchymal disease and coarctation of the aorta. In adults 65 years and older, atherosclerotic renal artery stenosis, renal failure, and hypothyroidism are common causes[218].

Cerebrovascular diseases

Cerebrovascular diseases are all diseases in which the blood vessels of the brain are primarily involved[219]. They often lead to serious symptoms. However, cerebrovascular abnormalities can be present without any acute symptoms as well. Silent brain infarcts, white-matter lesions and microbleeds are examples of such subclinical cerebrovascular disease[220]. There are a number of ways in which cerebrovascular disease can develop, being atherosclerosis one of the most common.

Atherosclerosis is where high cholesterol levels, coupled with inflammation in the arteries of the brain, cause cholesterol to build up in the vessel as a thick, waxy plaque. This plaque can limit or completely obstruct blood flow to the brain, causing a stroke or a transient ischemic attack, which may lead to cognitive impairment and dementia[221].

Stroke

Stroke is the most common manifestation of cerebrovascular disease and a major global health problem[222, 223]. Epidemiologic studies have played an essential role in assessing this burden and in detecting the risk factors for stroke. Primary prevention of these risk factors, essential hypertension, smoking, diabetes, and atrial fibrillation, has reduced the incidence in high-income countries. However, stroke remains a major cause of death and disability, and therefore research should be increased.

The traditional definition of stroke is clinical and based on the sudden onset of focal neurological function if an artery supplying the brain, retina or spinal cord is occluded or ruptures, leading to tissue death and neurologic deficits. This can be due to atherosclerosis, cardioembolism or small-vessel disease[224]. It can be a consequence of bleeding (hemorrhagic stroke) or ischemia (ischemic stroke). Different symptoms of stroke can be reported, including sudden unilateral weakness, numbness or visual loss, diplopia, altered speech, ataxia and non-orthostatic vertigo[225]. The diagnosis of stroke is most difficult in the initial hours, particularly if the onset is uncertain, the features are atypical or changing, the patient is unwell or agitated, access to imaging is delayed or brain imaging is normal[226]. The benefits of aspirin in preventing early recurrent stroke are greater than previously recognized[227]. Other strategies to prevent recurrent stroke now include oral anticoagulants as an alternative to warfarin for atrial fibrillation and carotid stenting as an alternative to endarterectomy for symptomatic carotid stenosis[226].

Neurological and medical complications after stroke are a major cause of morbidity and mortality if they are not anticipated, prevented and managed appropriately. Patients with acute stroke need assessment for the nature and severity of their neurological deficits and the prognosis, goals and rehabilitation requirements for recovery[226]. The case fatality rates after stroke are about 15% at 1 month, 25% at 1 year and 50% at 5 years[228]. After an event, the risk of recurrent stroke without treatment is about 10% at 1 week, 15% at 1 month and 18% at 3 months[229]. The long-term risk of recurrent stroke is about 10% at 1 year, 25% at 5 years and 40% at 10 years[230]. Thus, stroke requires rapid assessment and treatment. Biomonitoring and multimarker strategies can improve patient outcomes, decrease length of hospital admission and reduce hospitalization costs.

New biomarkers for CVDs

More than 100 new or emerging risk factors have been discovered for their ability to improve global risk assessment[231]. These biomarkers were referred as emerging risk factors since they were directly associated with increased risk of CVD but their causative, quantitative and independent contributions to CVD were not fully elucidated with respect to conventional risk factors[232]. These emerging risk factors helped to reclassify intermediate patients' risk for major cardiovascular events, requiring more aggressive risk reduction[232, 233].

The ideal biomarker must have the following five features: 1) to be highly sensitive or specific; 2) to provide clinically relevant and meaningful information; 3) to demonstrate the ability to guide therapy; 4) to be cost effective; and 5) to be easily monitored during therapy[234]. At present, no single biomarker meets all these criteria for HF, for instance[234].

The role of an ideal biomarker has evolved over the past decade (Figure 14), owing to the growing need for risk stratification strategies to mitigate the adverse outcomes associated with each pathology[211].

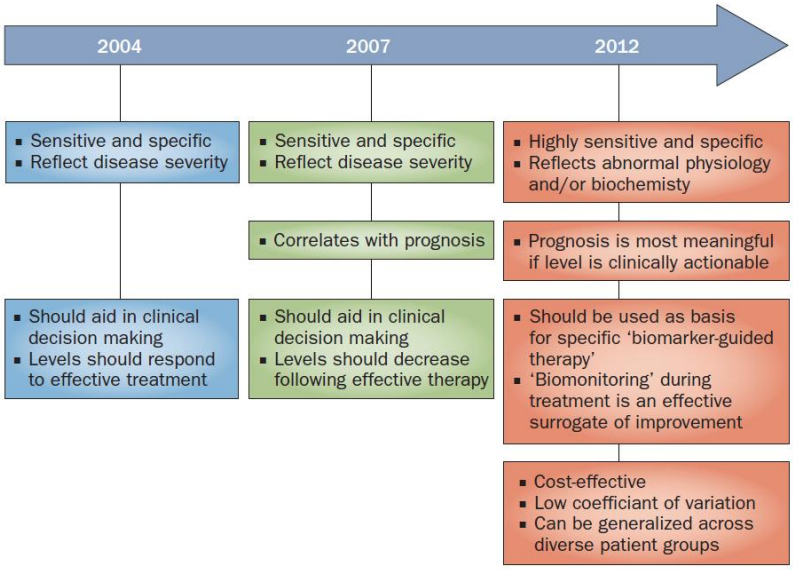

Figure 14 | The CVDs biomarker timeline. The progression of an ideal biomarker for cardiovascular diseases in the past decades[211, 235].

Biomarkers could be proteins secreted from specific sites in the body in response to stress or injury and can be defined as a feature that is objectively measured and evaluated as an indicator of normal biologic processes pathogenic processes or the response to a therapeutic intervention[236]. Currently, biomarkers are defined as any clinical feature, imaging quantification or laboratory-based test markers that characterize disease activity, which are useful for diagnosing, monitoring disease processes or response to therapy[237]. Identifying individuals with CVD who are at higher risk of disease progression would enable more personalized management, in order to slow down this progression. However, providing reliable evidence to validate biomarkers before clinical implementation remains an important challenge. Issues to be addressed include the accuracy and reliability of biomarkers for the clinical state of interest, as well as, the evaluation of clinical utility and cost-effectiveness compared to other biomarkers[238].

In the past years numerous biomarkers, such as C reactive protein, cytokines and adhesion molecules, have been observed to be related to adverse cardiovascular prognosis[239-241]. More recently, several studies found an association among inflammatory biomarkers and cardiovascular diseases, suggesting their utility to identify the risk of an acute ischemic event and the detection of vulnerable plaques. The emerging inflammatory markers are well divided for diagnosis and prognosis and plaque instability of coronary artery disease[194].

The Emerging Risk Factors Collaboration showed that the measurement of fibrinogen level in patients at risk for coronary artery disease could prevent an additional event of the disease in the next 10 years for every 400-500 people studied[242]. Additionally, recent studies show that the evaluation of fibrinogen during myocardial infarction may be useful in identifying patients at high risks for future acute events[193]. Epidemiological data have shown the important predictive role of fibrinogen in CVD[243-245]. However, it is not known why fibrinogen is not systematically measured in patients to evaluate the risk of thrombosis, either before the event or to evaluate the short and long-term outcome of a thromboembolic event such as stroke[246]. The main arguments that explain why fibrinogen plasma concentration has not attracted more attention as a predictor of thrombotic risk are detailed on Table 1.

Table 1 | The main reasons for not considering fibrinogen plasma concentration as a thrombotic risk factor[32]

○ Problems of standardization of the assays
○ What is the normal value for a given individual?
○ Frequent variations (acute-phase protein)
○ Ongoing debate on whether fibrinogen is the cause or consequence of thrombosis
○ No approved specific treatment to lower fibrinogen levels

However, most of the studies showed that high fibrinogen levels are a relevant cardiovascular risk factor, but the biological mechanisms associated with pathologic alterations are not totally clear. Recent studies have demonstrated the influence of fibrinogen in erythrocyte hyperaggregation and this interaction could be an important evaluation in the future[218]. Koster *et al*. found, in a case-control study, that individuals with a plasma fibrinogen >5 g/L had an almost fourfold increase of thrombosis risk compared with reference category (3 g/L). These high levels were present in 3% of thrombosis patients and 1% of the controls[247]. The identification of biomarkers would therefore minimize the exposure of a relevant patient population to investigational medicines prior to at least some determination of their safety and effectiveness[248]. Establishing the diagnostic, extent and severity of cardiovascular diseases, as well as determining the potential risk of cardiovascular events, are crucial steps toward improving patient outcomes.

Imaging technologies, such as Doppler ultrasound or computed tomography show vascular abnormalities and flow disturbances around the thrombus, but do not reveal information about thrombus composition[249]. Thus, the development of technologies to detect the thrombus composition and to measure the binding force between protein and ligands could also be useful on the clinical setting.

Atomic Force Microscopy – a powerful Nanomedicine tool

New and powerful nanotechnologies integrated with population studies for medical applications have been growing and continuously updated. This increases the selectivity and efficacy to treat and prevent diseases in the coming decades[250, 251]. Particularly,

atomic force microscopy (AFM) may play an important role on the nanomedicine knowledge necessary for fruitful developments in diagnostics, prognostics and therapeutics. Thus, the use of AFM could be highly relevant for the improvement of health care processes, namely on the cardiovascular area.

The basic principles of AFM are outlined in the next pages, followed by the description of different AFM applications.

Atomic force microscopy or scanning force microscopy belongs to a wider group of techniques named scanning probe microscopies (SPM)[252]. As a common feature, all these techniques aim at obtaining the topography of a sample, with nanometer resolution, line by line, measuring the interaction between a sharp tip and a sample's surface[253, 254]. A fundamental component of SPM is a probe and all techniques of this family evolved from the invention of the scanning tunneling microscopy (STM) in 1982[252]. For the first time it was possible to visualize matter at the level of single atoms. In STM, a sharp tip is raster scanned over a surface and its distance is controlled using the tunneling current from tip to surface as a control signal. Normally, this is performed in vacuum and at low temperatures, which limits applications in biology. Scanning probe imaging of biomolecules at a nanometer scale became possible with the invention of AFM (a variation of STM) in 1986, by Gerd Binnig, Calvin Quate and Christopher Gerber[253]. With the AFM, the requisite that the surface must be conductive was overcome.

AFM has several properties that make it a well suited tool that allows imaging and force probing biological samples with nanometer (nm) topographical and pico-Newton (pN) force resolution, measuring forces at the single molecule level[254]. The AFM was originally designed as an imaging tool, but was later modified to be operated in the force scan mode[253] (Figure 15).

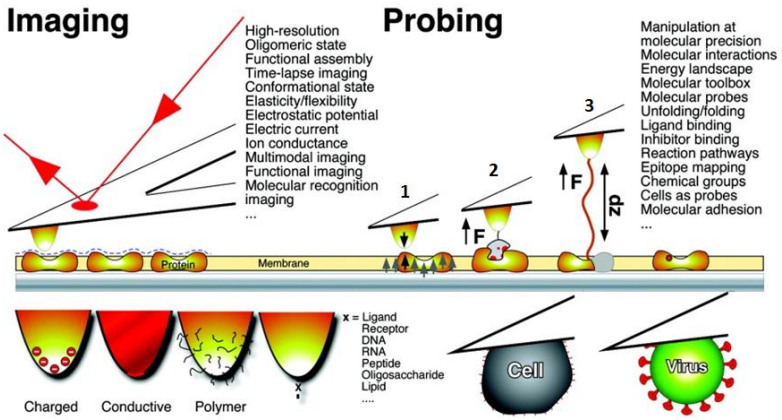

Figure 15 | AFM-based nanotools for imaging and probing in living cells at the molecular level. In the imaging mode, the topography of the cell surface under near physiological conditions is evaluated using a sharp tip. Applications and imaging modes are listed at the right of "Imaging". Functionalized AFM cantilevers can be used for detecting biological, chemical and physical interactions. Applications and probing modes are listed at the right of "Probing". Examples developed for biological characterization using functionalized probes are represented in this Figure: 1) an atomic force microscope probing the local elasticity of a biological membrane; 2) the AFM probe measures the interaction between a receptor and ligand; and, 3) an AFM probe unfolding a membrane protein (top right panel). In the bottom panel, from left to right, are shown ways to functionalize the cantilever to specifically probe chemical, biological, cellular or viral interactions[255].

The atomic force microscope has become a true enabling platform in Life Sciences that allows visualization, probing and manipulation across the length scales from single molecules to living cells in non-aqueous, aqueous or dry conditions[101]. Therefore, the sample may remain under conditions close to its natural environment, which is critical for biological applications[256]. Thus, high sensitivity, high resolution and no sample processing, makes AFM versatile in terms of the large variety of experiments that can be done[257]. Employing AFM, physical, chemical and biological properties of erythrocytes can be studied even under near physiological conditions[258, 259].

Key elements and basic principles of AFM

Due to their global simplicity, atomic force microscopes are small and compact equipments[254]. They are mainly composed by sample stage, the controller of the electronics and a computer (Figure 16).

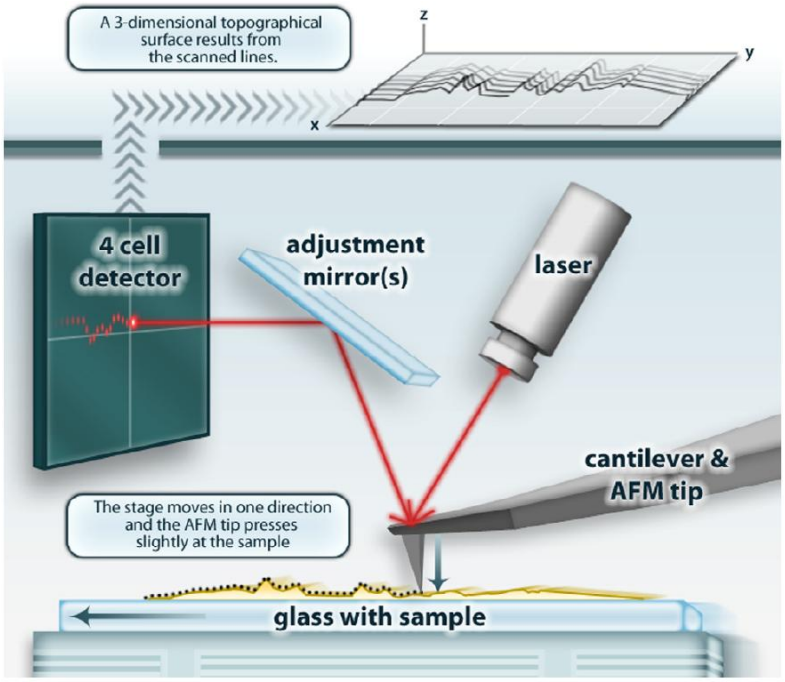

Figure 16 | Main components of a typical atomic force microscope. The stage is typically moved in the x-y axis, while the cantilever is moved on the z-plan. The movement of the reflected laser on the detector is caused by the movement of the cantilever through sample scanning. As the cantilever can be viewed as a spring, the cantilever deflection can be used to calculate the force applied[257].

The heart of the AFM is the cantilever and the tip is considered the most important part of the cantilever. The probe is made by triangular or rectangular cantilever, at which end there is a sharp tip used to probe the sample[260]. On one hand, the cantilevers are microscopic with tens to hundreds of micrometers length and width. On the other hand, the chip is macroscopic and can be firmly attached to piezo electric holder, which allows the vertical movement of the cantilever (z-axis)[261]. AFM uses this tip (probe) attached to a flexible cantilever of a specific spring constant, which is responsible for signal transduction. This technique is based on the detection of repulsive and/or attractive surface forces between the atoms of the sample and those of the tip, which scans the

surface of the sample. During tip scanning of the sample surface, the cantilever deflects in the z-direction due to the surface topography, while a small laser detects any bending or twisting of the cantilever[262, 263]. Thus, the cantilever movement is detected by shinning a laser off the back of the cantilever onto a detector. This photodiode commonly has four quadrants, with the laser initially pointed at the center of them (Figure 16). Upon the scanning of the sample, any small deflection of the cantilever will change the position of the reflected laser. It is the variation of the point of incidence of the reflected beam on the photodiode that measures any minimal bending or twisting of the cantilever and thus, the interaction of the tip with the sample. In such manner, the cantilever deflections, corresponding to the applied force can be detected. The quantitative concept of AFM is based on the Hooke's law of elasticity, which consists in a simple equation expressing the force generated within a spring when compressed in terms of known "spring constant" and the length of the deflection of the spring (displacement of the z-piezo, z). Cantilevers are like springs and the deflection of the spring can be converted in measurements of force by the following equation.

$$F = - k\Delta x \quad (1)$$

where F is the force acting on the cantilever, k the spring constant of the cantilever and Δx the length of its deflection[264-266].

Attending to the AFM potentialities in terms of its reduced dimensions and high resolution, it would be expectable that its isolation from any external vibration would be a major difficulty. However, this trouble can easily overcome by placing the microscope in an isolated noise room and on a small solid surface[254]. This way, the vibrations are reduced and do not interfere with the measurements[254, 263].

Single-molecule force spectroscopy

Taking advantage of the pico-Newton sensivity of the method, this approach is usually termed "force spectroscopy" (but actually it is not a spectroscopy, as it is not based on the interaction of radiation with matter)[267]. Among force spectroscopy methodologies, the most commonly used are optical tweezers, magnetic tweezers and atomic force microscopy[268, 269]. Thus, in addition of AFM use in imaging mode, this

technique can also be used to quantify the interaction between the tip and a specific point of the sample, detecting and localizing single molecular recognition events[268, 270].

AFM-based force spectroscopy allows the measurement of the inter- and intramolecular interaction forces necessary to separate the tip from the sample. When performing force spectroscopy measurements, it is not mandatory for the tip to scan the sample surface, as it may be just be brought into contact with the surface and then retracted[267]. The principle of this methodology is represented on the typical force-distance curve shown in Figure 17.

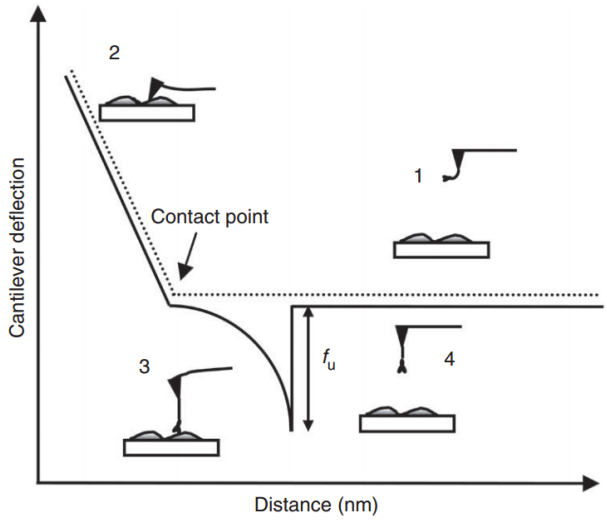

Figure 17 | Schematic representation of a typical force-distance curve, according to the movement of the cantilever. Firstly, the tip is moved towards the cell surface (dotted line, 1, 2), where there is a contact point and subsequently retracted (solid line). During tip approach, adhesion between the cantilever and the sample may occur, leading to a force signal (3) during tip retraction. The force increases until dissociation occurs (4) at an unbinding force (f_u)[271].

To conduct a force spectroscopy measurement, the cantilever is approached to and retracted from a surface using a piezo, which controls movement in the z direction. At the beginning, when the tip is far away from the surface, no interaction is observed (non-contact). After the tip-sample contact, if the approach continues, the cantilever will deflect. A feedback system stops the piezo movement when a given deflection, and therefore force, is reached. The cantilever deflection can be recorded as a function of the vertical displacement of the piezo scanner, during the procedure. The result is a cantilever

deflection *versus* scanner displacement curve, which can be converted into a force-distance curve after applying the Hookes´ law of elasticity, as mentioned before[267, 272, 273]. A possible strategy is to bind ligands to the AFM tips and receptors to the sample surface, or vice versa. The ligand can be a specific antibody, protein of interest, a substrate or, for instance, an inhibitor. The surface (*e.g.*, mica, glass or silicon) can have immobilized proteins, or the proteins expressed at the substrate of living cell[271]. If there is any kind of interaction between the cantilever and the surface, it will be pulled down toward the surface until the force required to break the interaction between probe and surface is reached. Through this methodology, multiple interactions or multiple unbinding events can be detected[274].

As mentioned above, the tip is attached to a very flexible cantilever, which bends toward or away from the sample when attractive or repulsive forces are present, respectively. Thus, different types of forces can be studied. The main type of force presents upon the approaching of two hard surfaces in the absence of long-range interaction is Van der Waals interactions[275]. Moreover, electrostatic or polymer-brush forces may also be present, if the approach curve has smooth and exponentially increasing repulsive forces[272, 273]. On the retraction curve, it is common to observe an adhesion force profile. The central basis of adhesion forces is the development of capillary bridge between the tip and the sample[275]. Thus, the nature of ligand-receptor specific binding forces comes generally from the combination of non-covalent weak bonds, such as Van der Walls, electrostatic, hydrophobic, dipole-dipole interactions and hydrogen bonds, which binding forces depend on the different conditions (*e.g.*, pH and ionic strength). The force-distance curve is influenced by the tip, sample and medium composition[267]. A complete force curves set consists of successive approach and retraction curves, which are rich in information. From single-cell force spectroscopy, it is possible to get more information than just absolute force values, enabling to quantify the underlying molecular interactions of cell surface receptors with their respective substrates[276].

AFM can particularly be used in force spectroscopy mode to observe changes in cell stiffness, protein-cell interactions and cell-cell adhesion.

Protein-cell interactions

In single-molecule force spectroscopy recognition studies, tips are generally functionalized with one or a small amount of probe molecules. They can recognize a specific target molecule on the samples surface[267]. The biochemical modification of the cantilever tip[277-279] enables the detection of ligand-membrane protein interactions at the single-molecule level, thereby providing fundamental insights into the molecular dynamics of biological processes (*e.g.*, the inter- and intramolecular interactions of biomolecules)[280].

Cantilevers functionalization for protein-cell interaction measurements

Usually, in this methodology, a cell of interest is attached to the sample surface and the protein is anchored to the AFM tip. This demands several requirements for tip and sample functionalization, as a proper functionalization of the tip and sample is crucial for force spectroscopy experiments, in order to measure specific and strong interactions. Thus, the attachment should be firm enough to avoid reallocations but, at the same time, it should maintain some autonomy of the molecule, to have enough mobility and to allow change its conformations during or before the interaction[281, 282].

Many different approaches have been used to attach proteins to AFM probes. More details about these methods can be found in some reviews[281, 282]. Before selecting the best functionalization method, some considerations need to be taken into account about the appropriate cantilever, the composition of the ligand molecule, as well as some experimental conditions, such as temperature, buffer composition or pH[283]. A silicon nitride (Si_3N_4) or silicon (Si) tip on a cantilever is commonly used for functionalization. Firstly, it is generally recommended to introduce linker molecules. One of the most common approaches is the amination of the tip by silanization, using APTES (3-aminopropyltriethoxysilane)[284]. Its main purpose is to introduce amine groups to the cantilevers. These terminal amino functions have been used to anchor different biological

ligands, such as proteins[153], antigens or antibodies[283]. After functionalization of the AFM probe, specific interactions can be detected.

Single-cell force spectroscopy: cell-cell adhesion

Atomic force microscopy based single cell force spectroscopy is widely used to study complex cell mechanisms and cell adhesion[285]. Adhesion is a common and fundamental process in all multicellular organisms; however, the adhesion of cells to surfaces or the adhesion between cells is a complex process, not well clarified. Cells interact with their environment via their surfaces. Therefore, cell surfaces play essential roles in basic cellular processes such as signaling, communication, adhesion, sensing, transport, energy generation, embryonic and tissue development, tumor metastasis, and viral or bacterial infection[286-290]. Every process of the cell surface relies on molecular forces that are a complex interplay of chemical, biological and physical interactions[290, 291]. Typical interactions occurring at biological surfaces include hydrophobic, hydrophilic, electrostatic, van der Waals and hydrogen bond interactions, and the force measured for a specific biological interaction reflects the sum of all its contributing components.

Research on this field is a great challenge, due to different factors. Using a living cell as a probe ensures that the receptors are on their native conformation and, moreover, the mechanisms by which they are regulated can be examined[276]. First and foremost, the single-molecule interactions recorded should be predominantly, if not exclusively, between the receptor and ligand of interest. To this end, recombinant substrates are often used and cells may be genetically modified to limit the number of receptors expressed. Control experiments demonstrating the specificity of the observed interactions must be performed[255]. AFM, as an advanced technique, enables to quantify forces involved in cell adhesion, using cells immobilized on an AFM cantilever. Particularly, force spectroscopy is capable of resolving individual detachment events, as well as the overall force required to detach a cell from another cell[292-294]. The great advantages of using AFM in cell adhesion studies are specificity and the wealth of data that is obtained. This technique is particularly useful to probe adhesive properties of

suspended cells, such as erythrocytes or leukocytes, allowing the characterization of multiple and single-molecule rupture events[295].

The CellHesion is an additional module of the AFM Nanowizard IV (JPK Instruments, Berlin), which is installed on an inverted microscope, allowing a 100 µm pulling range. This range is necessary for the complete detachment of two adhered cells, including the jumps and membrane tethers between cells, as well as, the elongation and elasticity of the cells. If this pulling distance is not enough, the cells will not be completely separated on the acquisitions of consecutive force-distance curves. When conducting single-cell force spectroscopy experiments, a number of critical parameters need to be considered, such as pulling distance, contact force, time and speed of approach to and retraction from the surface. Like in single-molecule force spectroscopy, in single-cell force spectroscopy, the cell is attached to the cantilever and brought into contact with the other cell, adhered to the substrate[276] as it can be seen on Figure 18. A tipless cantilever is positioned above the center of a cell and carefully lowered onto it for a set contact time and force. Thereafter, the cantilever-bound cell is retracted, the bonds between the cells cause the cantilever deflection[157, 296].

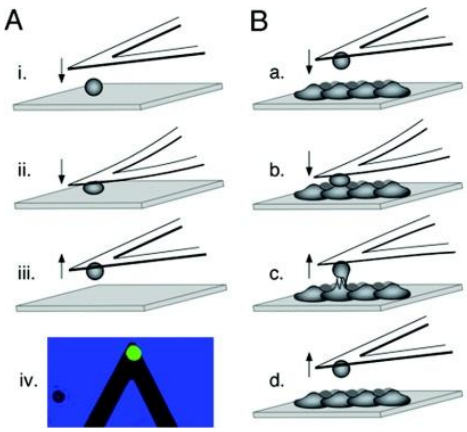

Figure 18 | AFM-based single-cell force spectroscopy using a cell attached to the cantilever to probe cellular interactions. (A) Binding of the cell to the cantilever: i) the AFM cantilever is positioned above a cell; (ii) the cantilever is pushed onto the cell and allowed to adhere; (iii) separating the cantilever from the support detaches the cell from the solid substrate and allows the bound cell to establish firm adhesion to the cantilever; and (iv) a cell (green) bound to a tipless cantilever. (B) Adhesion measurements using AFM: (a) the cantilever functionalized with the living cell is positioned over other cells; (b)

the cell is brought into contact with a cell of interest for a preset contact time; (c) the cantilever is retracted to separate the cells; and (d) the complete unbinding between cells is reached[255].

The AFM force-distance curves provide information about the individual bond strengths as well as the force and work that is required to separate the entire complex[157, 296]. Combining single-molecule and multiple-bond data enable to describe the thermodynamic model of separation of a complex, as well as the mechanism of its action on the cellular scale[297, 298]. The force-distance curve describes the separation of a cell from a substrate and can be split into different phases (Figure 19).

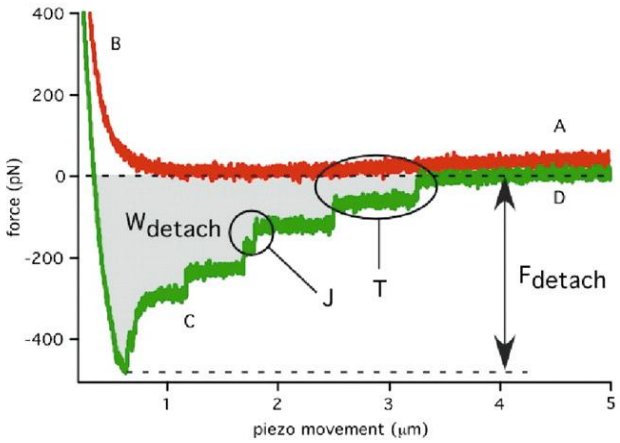

Figure 19 | Cell-cell adhesion force-distance curve. The resulting force-distance curve provides a signature of the cell adhesion and can be separated into several processes. The red line represents the approach curve and the green line the retraction curve. The cantilever/cell is moved towards the surface and no force is detected (A). When the cell is pressed onto the sample (contact point), the force increases until it reaches a preset level (B). After a given contact time, the cantilever/cell is moved away from the surface and the bonds that have been formed break sequentially (C), until the cell is completely separated from the surface (D). The maximum force measured is termed the detachment force (F_{detach}). During separation, membrane tethers (T) can be pulled out of the cell. Tethers are characterized by long *plateaus* at constant force. The separation curve also includes the breaking of individual bonds, named jumps (J). The shaded area under the approach curve represents the work required to detach one cell from the other[293].

Cantilevers functionalization for cell-cell adhesion

The success of the cell force spectroscopy measurements depends on the binding of the cell to the cantilever. This important step means that the cantilever must be coated with a molecule that will allow the binding of the cell with bond strength higher than the force of the bonds that will be formed between the cantilever-bound cell and the second cell on the substrate. Several methods have been developed to attach cells to cantilevers. The most common is the use of concanavalin A[276], a lectin that binds D-glucose and α-D-mannose sugar moieties at the cell surface glycoproteins. Concanavalin A can be adsorbed onto plasma-cleaned cantilevers or attached via a streptavidin-biotin linker[297, 299]. In more detail, this functionalization include different steps, as shown in Figure 20.

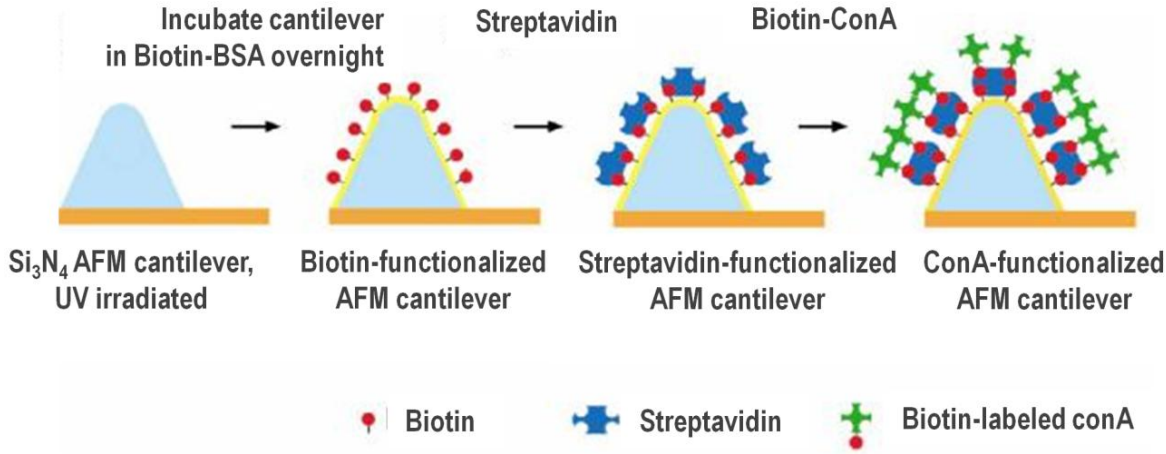

Figure 20 | **Functionalization of an AFM cantilever with concanavalin A**. This is a multi-step process, where the cantilever should be initially activated and well-cleaned by UV treatment. Then, the cantilever is successively coated with biotinylated-bovine serum albumin (BSA) overnight, followed by the binding to streptavidin and, at the end, with biotinylated concanavalin A. Adapted from[157].

Alternatively, another lectin (wheat germ agglutinin[300]) or extracellular matrix proteins (such as collagen and fibronectin[301]) can be used to functionalize the cantilever for cell attachment[302].

Indentation – cell elasticity

The AFM can also be used as a microindenter, in order to obtain data about the biomechanical properties of the cell. Thus, cell elasticity can be measured by using the tip to indent the cell. The Hertzian theory of elastic contact is the most common used approach to estimate the elastic properties of cells from force indentation curves, using the depth of indentation to assess elasticity in terms of the Young's elastic modulus. After the contact, the tip exerts a force against the cell that is proportional to the deflection of the cantilever. This is recorded as a function of the piezoelectric translator position during the approach and withdrawal of the AFM tip. The force-indentation curves of the cells are derived from these records and from measurements on a glass surface to calibrate the deflection of the cantilever. Estimates of the Young's modulus are made. In the application of Hertz model of indentation, the relationship between the depth of indentation and the force applied to the indenter is experimentally determined[303].

This is a very powerful tool for *in situ* characterization of interfaces of heterogeneous polymer systems and measurements of the elasticity of biological structures, on different types of cells and organelles[272, 295, 304] (Figure 21). Alterations on cell mechanical properties can be visualized during cell division, or on adding different drugs to the cell, such as, cytochalasin, which disrupts the cytoskeleton[305].

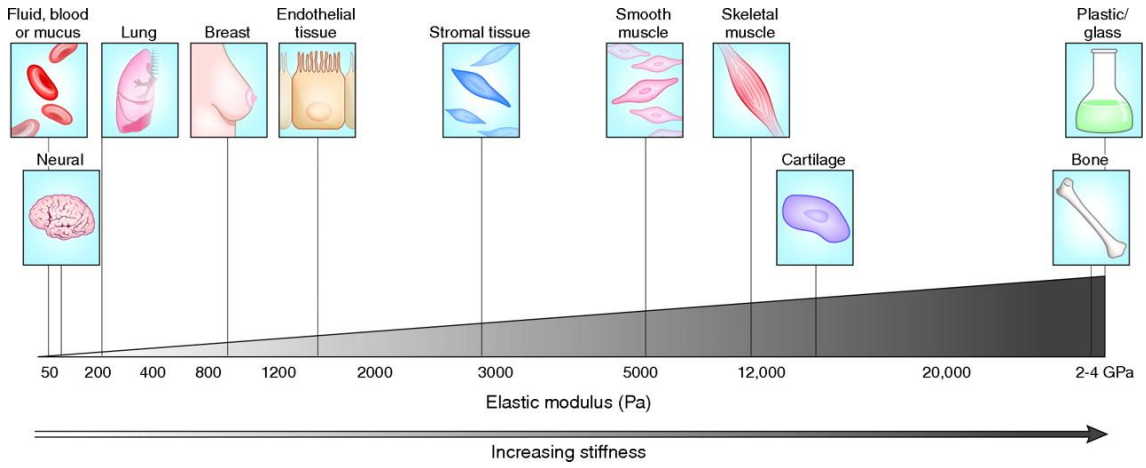

Figure 21 | **Changes on stiffness according to different cells/tissues**. Differences on elastic modulus (in Pa) for cells, organs and tissues are shown, displaying distinct biomechanical properties[306, 307].

Applications of AFM in Medicine

There is an increasing number of reports using AFM as a nanomedicine tool[182, 267, 308]. AFM has been widely applied on the imaging of biological samples under native conditions. However, probably the most remarkable advances are being achieved on the use of AFM to measure inter- and intramolecular interaction forces with pico-Newton resolution, not only to demonstrate this ability but also actually to solve biological and biomedical relevant raising questions. The potentialities of the atomic force microscopy as a tool with undeniable value for the study of biological samples are clear, becoming progressively a benchtop technique[254]. In general, its potential includes measuring local chemical, physical and mechanical properties of surfaces (charge density, rigidity, viscosity and elasticity) and intermolecular forces, as well as to manipulate single molecules[254].

Different applications have been reported in the last years to study the unfolding and folding of individual proteins[309, 310], to be used in adhesion studies involving whole cells[311], to be served as a microindenter to probe the cells reveling information about their mechanical properties, estimating the Young's modulus of cells[297], to observe the structural variability of native membrane proteins[312, 313], to detect and locate ligand and inhibitor binding to membrane proteins[314, 315], to probe specific interactions of cellular membranes[316], among other[255]. Carvalho *et al*. implemented the AFM-based force spectroscopy technique as a highly sensitive, rapid and low operation cost nanotool for the diagnostic and unbiased functional evaluation of the severity of hematological diseases[267]. Cross *et al.* showed that cancer cells from patients have a significant decrease of their cell stiffness, when compared with healthy cells[182]. Another report used AFM to detect early stages of cartilage degeneration on osteoarthritis that could not be detected by the most common available techniques[308]. Our group also used AFM to understand the molecular determinants and identify the ligand for the dengue virus capsid protein on intracellular lipid droplets[317] and very low density lipoproteins[318]. In another study, using different AFM modes, we showed that P-cadherin/Src family kinase signaling induces changes on the morphological and viscoelastic properties of breast cancer cells[319]. These cells revealed differences on their biomechanical properties and cell-cell adhesion, which are associated with a more invasive breast cancer cell phenotype.

Several studies have characterized the mechanical behavior of cells under healthy and pathological conditions, most of them using AFM[182, 320, 321]. It has been reported that many diseases have their cause at the molecular level, sometimes resulting in a malfunctioning of molecular recognition and directly impacting cell behavior. Thus, understanding the specific molecular forces between individual receptors and ligands can be of great relevance for the biomedical research community. The application of AFM-based force spectroscopy as a diagnostic or prognostic tool is a very promising field for the near future. A detailed understanding of the molecular mechanisms involved on the development and progression of a disease will be essential for the future development of new treatments for it. AFM-based force spectroscopy measurements can surely contribute at this level.

References of Chapter I

1. Collen, D., Tytgat, G.N., Claeys, H. & Piessens, R. Metabolism and distribution of fibrinogen. I. Fibrinogen turnover in physiological conditions in humans. *Br J Haematol* **22**, 681-700 (1972).
2. Hantgan, R.R., Lord, S.T. Fibrinogen structure and physiology´ in: Hemostasis and Thrombosis. *Basic Principles and Clinical Practive (5th Ed.)*, 285-316 (2006).
3. Takeda, Y. Studies of the metabolism and distribution of fibrinogen in healthy men with autologous 125-I-labeled fibrinogen. *J Clin Invest* **45**, 103-11 (1966).
4. Lane, A., Graham, L., Cook, M., Chantry, D., Green, F., Nigon, F. & Humphries, S.E. Cytokine production by cholesterol-loaded human peripheral monocyte-macrophages: the effect on fibrinogen mRNA levels in a hepatoma cell-line (HepG2). *Biochim Biophys Acta* **1097**, 161-5 (1991).
5. Dalmon, J., Laurent, M. & Courtois, G. The human beta fibrinogen promoter contains a hepatocyte nuclear factor 1-dependent interleukin-6-responsive element. *Mol Cell Biol* **13**, 1183-93 (1993).
6. Ritchie, D.G. & Fuller, G.M. Hepatocyte-stimulating factor: a monocyte-derived acute-phase regulatory protein. *Ann N Y Acad Sci* **408**, 490-502 (1983).
7. Kamath, S. & Lip, G.Y. Fibrinogen: biochemistry, epidemiology and determinants. *QJM* **96**, 711-29 (2003).
8. Ajjan, R. & Grant, P.J. Coagulation and atherothrombotic disease. *Atherosclerosis* **186**, 240-59 (2006).
9. Jobse, A., Pieters, M., Nienaber-Rousseau, C., Boshuizen, H., Hoekstra, T. & de Maat, M.P. The contribution of genetic and environmental factors to changes in total and gamma' fibrinogen over 5 years. *Thromb Res* (2015).
10. Folsom, A.R., Wu, K.K., Conlan, M.G., Finch, A., Davis, C.E., Marcucci, G., Sorlie, P.D. & Szklo, M. Distributions of hemostatic variables in blacks and whites: population reference values from the Atherosclerosis Risk in Communities (ARIC) Study. *Ethn Dis* **2**, 35-46 (1992).
11. Pieters, M. & Vorster, H.H. Nutrition and hemostasis: a focus on urbanization in South Africa. *Mol Nutr Food Res* **52**, 164-72 (2008).

12. Parry, D.A.D. & Squire, J.M. Fibrous proteins: Structures and Mechanisms. *Subcell Biochem* **82**, 409-412 (2017).
13. Redman, C.M. & Xia, H. Fibrinogen biosynthesis. Assembly, intracellular degradation, and association with lipid synthesis and secretion. *Ann N Y Acad Sci* **936**, 480-95 (2001).
14. Kattula, S., Byrnes, J.R. & Wolberg, A.S. Fibrinogen and Fibrin in Hemostasis and Thrombosis. *Arterioscler Thromb Vasc Biol* **37**, e13-e21 (2017).
15. Di Stasio, E., Nagaswami, C., Weisel, J.W. & Di Cera, E. Cl- regulates the structure of the fibrin clot. *Biophys J* **75**, 1973-9 (1998).
16. Weisel, J.W., Stauffacher, C.V., Bullitt, E. & Cohen, C. A model for fibrinogen: domains and sequence. *Science* **230**, 1388-91 (1985).
17. Blomback, B., Hessel, B. & Hogg, D. Disulfide bridges in nh2 -terminal part of human fibrinogen. *Thromb Res* **8**, 639-58 (1976).
18. Henschen, A., Lottspeich, F., Kehl, M. & Southan, C. Covalent structure of fibrinogen. *Ann N Y Acad Sci* **408**, 28-43 (1983).
19. Huang, S., Cao, Z. & Davie, E.W. The role of amino-terminal disulfide bonds in the structure and assembly of human fibrinogen. *Biochem Biophys Res Commun* **190**, 488-95 (1993).
20. Mosesson, M.W., Siebenlist, K.R. & Meh, D.A. The structure and biological features of fibrinogen and fibrin. *Ann N Y Acad Sci* **936**, 11-30 (2001).
21. InterPro. Fibrinogen, alpha/beta/gamma chain, C-terminal globular domain (IPR002181).
22. Weisel, J.W. Fibrinogen and fibrin. *Adv Protein Chem* **70**, 247-99 (2005).
23. Asselta, R., Duga, S. & Tenchini, M.L. The molecular basis of quantitative fibrinogen disorders. *J Thromb Haemost* **4**, 2115-29 (2006).
24. Weisel, J.W. & Litvinov, R.I. Fibrin Formation, Structure and Properties. *Subcell Biochem* **82**, 405-456 (2017).
25. Baumann, R.E. & Henschen, A.H. Human fibrinogen polymorphic site analysis by restriction endonuclease digestion and allele-specific polymerase chain reaction amplification: identification of polymorphisms at positions A alpha 312 and B beta 448. *Blood* **82**, 2117-24 (1993).

26. Henschen-Edman, A.H. Fibrinogen non-inherited heterogeneity and its relationship to function in health and disease. *Ann N Y Acad Sci* **936**, 580-93 (2001).

27. Reiner, A.P., Carty, C.L., Carlson, C.S., Wan, J.Y., Rieder, M.J., Smith, J.D., Rice, K., Fornage, M., Jaquish, C.E., Williams, O.D., Tracy, R.P., Lewis, C.E., Siscovick, D.S., Boerwinkle, E. & Nickerson, D.A. Association between patterns of nucleotide variation across the three fibrinogen genes and plasma fibrinogen levels: the Coronary Artery Risk Development in Young Adults (CARDIA) study. *J Thromb Haemost* **4**, 1279-87 (2006).

28. Wassel, C.L., Lange, L.A., Keating, B.J., Taylor, K.C., Johnson, A.D., Palmer, C., Ho, L.A., Smith, N.L., Lange, E.M., Li, Y., Yang, Q., Delaney, J.A., Tang, W., Tofler, G., Redline, S., Taylor, H.A., Jr., Wilson, J.G., Tracy, R.P., Jacobs, D.R., Jr., Folsom, A.R., Green, D., O'Donnell, C.J. & Reiner, A.P. Association of genomic loci from a cardiovascular gene SNP array with fibrinogen levels in European Americans and African-Americans from six cohort studies: the Candidate Gene Association Resource (CARe). *Blood* **117**, 268-75 (2011).

29. Jeff, J.M., Brown-Gentry, K. & Crawford, D.C. Replication and characterisation of genetic variants in the fibrinogen gene cluster with plasma fibrinogen levels and haematological traits in the Third National Health and Nutrition Examination Survey. *Thromb Haemost* **107**, 458-67 (2012).

30. Mannila, M.N., Eriksson, P., Ericsson, C.G., Hamsten, A. & Silveira, A. Epistatic and pleiotropic effects of polymorphisms in the fibrinogen and coagulation factor XIII genes on plasma fibrinogen concentration, fibrin gel structure and risk of myocardial infarction. *Thromb Haemost* **95**, 420-7 (2006).

31. Hill, M. & Dolan, G. Diagnosis, clinical features and molecular assessment of the dysfibrinogenaemias. *Haemophilia* **14**, 889-97 (2008).

32. de Moerloose, P., Boehlen, F. & Neerman-Arbez, M. Fibrinogen and the risk of thrombosis. *Semin Thromb Hemost* **36**, 7-17 (2010).

33. Bornikova, L., Peyvandi, F., Allen, G., Bernstein, J. & Manco-Johnson, M.J. Fibrinogen replacement therapy for congenital fibrinogen deficiency. *J Thromb Haemost* **9**, 1687-704 (2011).

34. Ariëns, R.A. Fibrin(ogen) and thrombotic disease. *J Thromb Haemost* **11**, 294-305 (2013).
35. Riedelova-Reicheltova, Z., Kotlin, R., Suttnar, J., Geierova, V., Riedel, T., Majek, P. & Dyr, J.E. A novel natural mutation AalphaPhe98Ile in the fibrinogen coiled-coil affects fibrinogen function. *Thromb Haemost* **111**, 79-87 (2014).
36. Lord, S.T. Fibrinogen and fibrin: scaffold proteins in hemostasis. *Curr Opin Hematol* **14**, 236-41 (2007).
37. Mosesson, M.W., Finlayson, J.S. & Umfleet, R.A. Human fibrinogen heterogeneities. 3. Identification of chain variants. *J Biol Chem* **247**, 5223-7 (1972).
38. Chung, D.W. & Davie, E.W. gamma and gamma' chains of human fibrinogen are produced by alternative mRNA processing. *Biochemistry* **23**, 4232-6 (1984).
39. Wolfenstein-Todel, C. & Mosesson, M.W. Human plasma fibrinogen heterogeneity: evidence for an extended carboxyl-terminal sequence in a normal gamma chain variant (gamma'). *Proc Natl Acad Sci U S A* **77**, 5069-73 (1980).
40. Wolfenstein-Todel, C. & Mosesson, M.W. Carboxy-terminal amino acid sequence of a human fibrinogen gamma-chain variant (gamma'). *Biochemistry* **20**, 6146-9 (1981).
41. Macrae, F.L., Domingues, M.M., Casini, A. & Ariëns, R.A. The (Patho)physiology of Fibrinogen gamma'. *Semin Thromb Hemost* **42**, 344-55 (2016).
42. Uitte de Willige, S., Standeven, K.F., Philippou, H. & Ariëns, R.A. The pleiotropic role of the fibrinogen gamma' chain in hemostasis. *Blood* **114**, 3994-4001 (2009).
43. Reed, T., Tracy, R.P. & Fabsitz, R.R. Minimal genetic influences on plasma fibrinogen level in adult males in the NHLBI twin study. *Clin Genet* **45**, 71-7 (1994).
44. Friedlander, Y., Elkana, Y., Sinnreich, R. & Kark, J.D. Genetic and environmental sources of fibrinogen variability in Israeli families: the Kibbutzim Family Study. *Am J Hum Genet* **56**, 1194-206 (1995).
45. Siebenlist, K.R., Mosesson, M.W., Hernandez, I., Bush, L.A., Di Cera, E., Shainoff, J.R., Di Orio, J.P. & Stojanovic, L. Studies on the basis for the properties of fibrin produced from fibrinogen-containing gamma' chains. *Blood* **106**, 2730-6 (2005).
46. Cooper, A.V., Standeven, K.F. & Ariëns, R.A. Fibrinogen gamma-chain splice variant gamma' alters fibrin formation and structure. *Blood* **102**, 535-40 (2003).

47. Gersh, K.C., Nagaswami, C., Weisel, J.W. & Lord, S.T. The presence of gamma' chain impairs fibrin polymerization. *Thromb Res* **124**, 356-63 (2009).

48. Collet, J.P., Nagaswami, C., Farrell, D.H., Montalescot, G. & Weisel, J.W. Influence of gamma' fibrinogen splice variant on fibrin physical properties and fibrinolysis rate. *Arterioscler Thromb Vasc Biol* **24**, 382-6 (2004).

49. Falls, L.A. & Farrell, D.H. Resistance of gammaA/gamma' fibrin clots to fibrinolysis. *J Biol Chem* **272**, 14251-6 (1997).

50. Pineda, A.O., Chen, Z.W., Marino, F., Mathews, F.S., Mosesson, M.W. & Di Cera, E. Crystal structure of thrombin in complex with fibrinogen gamma' peptide. *Biophys Chem* **125**, 556-9 (2007).

51. Meh, D.A., Siebenlist, K.R. & Mosesson, M.W. Identification and characterization of the thrombin binding sites on fibrin. *J Biol Chem* **271**, 23121-5 (1996).

52. Lovely, R.S., Moaddel, M. & Farrell, D.H. Fibrinogen gamma' chain binds thrombin exosite II. *J Thromb Haemost* **1**, 124-31 (2003).

53. de Bosch, N.B., Mosesson, M.W., Ruiz-Saez, A., Echenagucia, M. & Rodriguez-Lemoin, A. Inhibition of thrombin generation in plasma by fibrin formation (Antithrombin I). *Thromb Haemost* **88**, 253-8 (2002).

54. Fredenburgh, J.C., Stafford, A.R., Leslie, B.A. & Weitz, J.I. Bivalent binding to gammaA/gamma'-fibrin engages both exosites of thrombin and protects it from inhibition by the antithrombin-heparin complex. *J Biol Chem* **283**, 2470-7 (2008).

55. Lovely, R.S., Falls, L.A., Al-Mondhiry, H.A., Chambers, C.E., Sexton, G.J., Ni, H. & Farrell, D.H. Association of gammaA/gamma' fibrinogen levels and coronary artery disease. *Thromb Haemost* **88**, 26-31 (2002).

56. Mannila, M.N., Lovely, R.S., Kazmierczak, S.C., Eriksson, P., Samnegard, A., Farrell, D.H., Hamsten, A. & Silveira, A. Elevated plasma fibrinogen gamma' concentration is associated with myocardial infarction: effects of variation in fibrinogen genes and environmental factors. *J Thromb Haemost* **5**, 766-73 (2007).

57. Cheung, E.Y., Uitte de Willige, S., Vos, H.L., Leebeek, F.W., Dippel, D.W., Bertina, R.M. & de Maat, M.P. Fibrinogen gamma' in ischemic stroke: a case-control study. *Stroke* **39**, 1033-5 (2008).

58. Drouet, L., Paolucci, F., Pasqualini, N., Laprade, M., Ripoll, L., Mazoyer, E., Bal dit Sollier, C. & Vanhove, N. Plasma gamma'/gamma fibrinogen ratio, a marker of

arterial thrombotic activity: a new potential cardiovascular risk factor? *Blood Coagul Fibrinolysis* **10**, S35-9 (1999).

59. Cheung, E.Y., Vos, H.L., Kruip, M.J., den Hertog, H.M., Jukema, J.W. & de Maat, M.P. Elevated fibrinogen gamma' ratio is associated with cardiovascular diseases and acute phase reaction but not with clinical outcome. *Blood* **114**, 4603-4; 4604-5 (2009).
60. van den Herik, E.G., Cheung, E.Y., de Lau, L.M., den Hertog, H.M., Leebeek, F.W., Dippel, D.W., Koudstaal, P.J. & de Maat, M.P. gamma'/total fibrinogen ratio is associated with short-term outcome in ischaemic stroke. *Thromb Haemost* **105**, 430-4 (2011).
61. Bridge, K.I., Philippou, H. & Ariëns, R. Clot properties and cardiovascular disease. *Thromb Haemost* **112**, 901-8 (2014).
62. Walton, B.L., Getz, T.M., Bergmeier, W., Lin, F.C., Uitte de Willige, S. & Wolberg, A.S. The fibrinogen gammaA/gamma' isoform does not promote acute arterial thrombosis in mice. *J Thromb Haemost* **12**, 680-9 (2014).
63. Appiah, D., Heckbert, S.R., Cushman, M., Psaty, B.M. & Folsom, A.R. Lack of association of plasma gamma prime (gamma') fibrinogen with incident cardiovascular disease. *Thromb Res* **143**, 50-2 (2016).
64. Pieters, M., de Maat, M.P., Jerling, J.C., Hoekstra, T. & Kruger, A. Fibrinogen concentration and its role in CVD risk in black South Africans-effect of urbanisation. *Thromb Haemost* **106**, 448-56 (2011).
65. Allan, P., Uitte de Willige, S., Abou-Saleh, R.H., Connell, S.D. & Ariëns, R.A. Evidence that fibrinogen gamma' directly interferes with protofibril growth: implications for fibrin structure and clot stiffness. *J Thromb Haemost* **10**, 1072-80 (2012).
66. Lovely, R.S., Kazmierczak, S.C., Massaro, J.M., D'Agostino, R.B., O'Donnell, C.J. & Farrell, D.H. Gamma' fibrinogen: evaluation of a new assay for study of associations with cardiovascular disease. *Clin Chem* **56**, 781-8 (2010).
67. Forrester, J.M. Malpighi's De polypo cordis: an annotated translation. *Med Hist* **39**, 477-92 (1995).
68. Doolittle, R.F. Structural aspects of the fibrinogen to fibrin conversion. *Adv Protein Chem* **27**, 1-109 (1973).

69. Yang, Z., Mochalkin, I. & Doolittle, R.F. A model of fibrin formation based on crystal structures of fibrinogen and fibrin fragments complexed with synthetic peptides. *Proc Natl Acad Sci USA* **97**, 14156-61 (2000).

70. Cilia La Corte, A.L., Philippou, H. & Ariëns, R.A. Role of fibrin structure in thrombosis and vascular disease. *Adv Protein Chem Struct Biol* **83**, 75-127 (2011).

71. Blomback, B., Hessel, B., Hogg, D. & Therkildsen, L. A two-step fibrinogen--fibrin transition in blood coagulation. *Nature* **275**, 501-5 (1978).

72. Weisel, J.W. Fibrin assembly. Lateral aggregation and the role of the two pairs of fibrinopeptides. *Biophys J* **50**, 1079-93 (1986).

73. Weisel, J.W. & Litvinov, R.I. Mechanisms of fibrin polymerization and clinical implications. *Blood* **121**, 1712-9 (2013).

74. Weisel, J.W. & Dempfle, C.E.H. Fibrinogen structure and Function. In Hemostasis and thrombosis: basic principles and clinical practice. *Lippincott Willians and Wilkins, Philadelphia* (2013).

75. Mullin, J.L., Gorkun, O.V., Binnie, C.G. & Lord, S.T. Recombinant fibrinogen studies reveal that thrombin specificity dictates order of fibrinopeptide release. *J Biol Chem* **275**, 25239-46 (2000).

76. Blomback, B., Carlsson, K., Fatah, K., Hessel, B. & Procyk, R. Fibrin in human plasma: gel architectures governed by rate and nature of fibrinogen activation. *Thromb Res* **75**, 521-38 (1994).

77. Ryan, E.A., Mockros, L.F., Weisel, J.W. & Lorand, L. Structural origins of fibrin clot rheology. *Biophys J* **77**, 2813-26 (1999).

78. Smith, S.A. & Morrissey, J.H. Polyphosphate enhances fibrin clot structure. *Blood* **112**, 2810-6 (2008).

79. Henderson, S.J., Xia, J., Wu, H., Stafford, A.R., Leslie, B.A., Fredenburgh, J.C., Weitz, D.A. & Weitz, J.I. Zinc promotes clot stability by accelerating clot formation and modifying fibrin structure. *Thromb Haemost* **115**, 533-42 (2016).

80. Aleman, M.M., Gardiner, C., Harrison, P. & Wolberg, A.S. Differential contributions of monocyte- and platelet-derived microparticles towards thrombin generation and fibrin formation and stability. *J Thromb Haemost* **9**, 2251-61 (2011).

81. Campbell, R.A., Overmyer, K.A., Selzman, C.H., Sheridan, B.C. & Wolberg, A.S. Contributions of extravascular and intravascular cells to fibrin network formation, structure, and stability. *Blood* **114**, 4886-96 (2009).

82. Campbell, R.A., Aleman, M., Gray, L.D., Falvo, M.R. & Wolberg, A.S. Flow profoundly influences fibrin network structure: implications for fibrin formation and clot stability in haemostasis. *Thromb Haemost* **104**, 1281-4 (2010).

83. Gersh, K.C., Edmondson, K.E. & Weisel, J.W. Flow rate and fibrin fiber alignment. *J Thromb Haemost* **8**, 2826-8 (2010).

84. Mills, J.D., Ariëns, R.A., Mansfield, M.W. & Grant, P.J. Altered fibrin clot structure in the healthy relatives of patients with premature coronary artery disease. *Circulation* **106**, 1938-42 (2002).

85. Undas, A., Zawilska, K., Ciesla-Dul, M., Lehmann-Kopydlowska, A., Skubiszak, A., Ciepluch, K. & Tracz, W. Altered fibrin clot structure/function in patients with idiopathic venous thromboembolism and in their relatives. *Blood* **114**, 4272-8 (2009).

86. Zabczyk, M., Plens, K., Wojtowicz, W. & Undas, A. Prothrombotic Fibrin Clot Phenotype Is Associated With Recurrent Pulmonary Embolism After Discontinuation of Anticoagulant Therapy. *Arterioscler Thromb Vasc Biol* **37**, 365-373 (2017).

87. Wolberg, A.S., Allen, G.A., Monroe, D.M., Hedner, U., Roberts, H.R. & Hoffman, M. High dose factor VIIa improves clot structure and stability in a model of haemophilia B. *Br J Haematol* **131**, 645-55 (2005).

88. Fatah, K., Hamsten, A., Blomback, B. & Blomback, M. Fibrin gel network characteristics and coronary heart disease: relations to plasma fibrinogen concentration, acute phase protein, serum lipoproteins and coronary atherosclerosis. *Thromb Haemost* **68**, 130-5 (1992).

89. Fatah, K., Silveira, A., Tornvall, P., Karpe, F., Blomback, M. & Hamsten, A. Proneness to formation of tight and rigid fibrin gel structures in men with myocardial infarction at a young age. *Thromb Haemost* **76**, 535-40 (1996).

90. Undas, A., Podolec, P., Zawilska, K., Pieculewicz, M., Jedlinski, I., Stepien, E., Konarska-Kuszewska, E., Weglarz, P., Duszynska, M., Hanschke, E., Przewlocki, T. &

Tracz, W. Altered fibrin clot structure/function in patients with cryptogenic ischemic stroke. *Stroke* **40**, 1499-501 (2009).

91. Undas, A., Zalewski, J., Krochin, M., Siudak, Z., Sadowski, M., Pregowski, J., Dudek, D., Janion, M., Witkowski, A. & Zmudka, K. Altered plasma fibrin clot properties are associated with in-stent thrombosis. *Arterioscler Thromb Vasc Biol* **30**, 276-82 (2010).
92. Collet, J.P., Allali, Y., Lesty, C., Tanguy, M.L., Silvain, J., Ankri, A., Blanchet, B., Dumaine, R., Gianetti, J., Payot, L., Weisel, J.W. & Montalescot, G. Altered fibrin architecture is associated with hypofibrinolysis and premature coronary atherothrombosis. *Arterioscler Thromb Vasc Biol* **26**, 2567-73 (2006).
93. Jorneskog, G., Egberg, N., Fagrell, B., Fatah, K., Hessel, B., Johnsson, H., Brismar, K. & Blomback, M. Altered properties of the fibrin gel structure in patients with IDDM. *Diabetologia* **39**, 1519-23 (1996).
94. Bradburne JM, G.M. Blood and magic in classical antiquity. *Blood: Art, Power, Politics and Pathology*, 33-39 (2002).
95. Litvinov, R.I. & Weisel, J.W. Role of red blood cells in haemostasis and thrombosis *ISBT Science Series* (2016).
96. Buys, A.V., Van Rooy, M.J., Soma, P., Van Papendorp, D., Lipinski, B. & Pretorius, E. Changes in red blood cell membrane structure in type 2 diabetes: a scanning electron and atomic force microscopy study. *Cardiovasc Diabetol* **12**, 25 (2013).
97. Baskurt, O.K. & Meiselman, H.J. Blood rheology and hemodynamics. *Semin Thromb Hemost* **29**, 435-50 (2003).
98. Kozlova, E.K., Chernysh, A.M., Moroz, V.V. & Kuzovlev, A.N. Analysis of nanostructure of red blood cells membranes by space Fourier transform of AFM images. *Micron* **44**, 218-27 (2013).
99. Girasole, M., Dinarelli, S. & Boumis, G. Structure and function in native and pathological erythrocytes: a quantitative view from the nanoscale. *Micron* **43**, 1273-86 (2012).
100. Danon, D. & Marikovsky, Y. The aging of the red blood cell. A multifactor process. *Blood Cells* **14**, 7-18 (1988).
101. Mukherjee, R., Chaudhury, K. & Chakraborty, C. Topological features of erythrocytes in thalassemic patients: quantitative characterization by scanning

electron and atomic force microscopy. *Anal Quant Cytopathol Histpathol* **36**, 91-9 (2014).

102. Kim J, L.H., Shin S. Advances in the measurement of red blood cell deformability: A brief review. *J Cell Biotech* **1**, 63-79 (2015).
103. Steck, T.L. & Yu, J. Selective solubilization of proteins from red blood cell membranes by protein perturbants. *J Supramol Struct* **1**, 220-32 (1973).
104. Yu, J., Fischman, D.A. & Steck, T.L. Selective solubilization of proteins and phospholipids from red blood cell membranes by nonionic detergents. *J Supramol Struct* **1**, 233-48 (1973).
105. Betz, T., Bakowsky, U., Muller, M.R., Lehr, C.M. & Bernhardt, I. Conformational change of membrane proteins leads to shape changes of red blood cells. *Bioelectrochemistry* **70**, 122-6 (2007).
106. Antonio, P.D., Lasalvia, M., Perna, G. & Capozzi, V. Scale-independent roughness value of cell membranes studied by means of AFM technique. *Biochim Biophys Acta* **1818**, 3141-8 (2012).
107. Moroz, V.V., Chernysh, A.M., Kozlova, E.K., Borshegovskaya, P.Y., Bliznjuk, U.A., Rysaeva, R.M. & Gudkova, O.Y. Comparison of red blood cell membrane microstructure after different physicochemical influences: atomic force microscope research. *J Crit Care* **25**, 539 e1-12 (2010).
108. Kosower, N.S. Altered properties of erythrocytes in the aged. *Am J Hematol* **42**, 241-7 (1993).
109. Girasole, M., Pompeo, G., Cricenti, A., Congiu-Castellano, A., Andreola, F., Serafino, A., Frazer, B.H., Boumis, G. & Amiconi, G. Roughness of the plasma membrane as an independent morphological parameter to study RBCs: a quantitative atomic force microscopy investigation. *Biochim Biophys Acta* **1768**, 1268-76 (2007).
110. Resch, KL, Ernest, E., Matrai, A., Buhl, M., Schlosser, P., Paulsen, H.F. Can rheologic variables be of prognostic relevance in arteriosclerotic diseases? *Angiology* **42**, 963-970 (1991).
111. Schmid-Schönbein, H. Blood rheology and physiology of microcirculation. *Ric Clin Lab* **11**, 13-33 (1981).

112. Stoltz, J.F. Red blood cell microrheology (clinical and pharmacological applications). *Ric Clin Lab* **13**, 53-70 (1983).

113. Dintenfass, L. Methods and instrumentation used in practice of clinical haemorheology. *Biorheology Suppl* **1**, 63-9 (1984).

114. Dormandy, J.A. The clinical relevance of the flow properties of blood cells. *Wien Med Wochenschr* **136**, 41-3 (1986).

115. Gori, T., Di Stolfo, G., Sicuro, S., Dragoni, S., Parker, J.D. & Forconi, S. The effect of ischemia and reperfusion on microvascular function: a human in vivo comparative study with conduit arteries. *Clin Hemorheol Microcirc* **35**, 169-73 (2006).

116. Stoltz, J.F., Muller, S., Kadi, A., Decot, V., Menu, P. & Bensoussan, D. Introduction to endothelial cell biology. *Clin Hemorheol Microcirc* **37**, 5-8 (2007).

117. Da Costa, L., Galimand, J., Fenneteau, O. & Mohandas, N. Hereditary spherocytosis, elliptocytosis, and other red cell membrane disorders. *Blood Rev* **27**, 167-78 (2013).

118. Delamaire, M. & Durand, F. Erythrocyte aggregation and vascular pathology. *J Mal Vasc* **15**, 344-5 (1990).

119. Boisseau, M.R. Roles of mechanical blood forces in vascular diseases. A clinical overview. *Clin Hemorheol Microcirc* **33**, 201-7 (2005).

120. Tomaiuolo, G. Biomechanical properties of red blood cells in health and disease towards microfluidics. *Biomicrofluidics* **8**, 051501 (2014).

121. Lowe, G., Rumley, A., Norrie, J., Ford, I., Shepherd, J., Cobbe, S., Macfarlane, P. & Packard, C. Blood rheology, cardiovascular risk factors, and cardiovascular disease: the West of Scotland Coronary Prevention Study. *Thromb Haemost* **84**, 553-8 (2000).

122. Freitas, J., Braz-Nogueira, J., Nogueira da Costa, J., Martins-Silva, J. Whole blood filterability and blood oxygen transport in human hypertension. *Clin Hemorheol* **3**, 367-373 (1983).

123. Shiraishi, K., Matsuzaki, S., Ishida, H. & Nakazawa, H. Impaired erythrocyte deformability and membrane fluidity in alcoholic liver disease: participation in disturbed hepatic microcirculation. *Alcohol Alcohol Suppl* **1A**, 59-64 (1993).

124. Shattil S., F.B., Cohen H., Silverstein L., Glave P., and Strauss M. Hematology: Basic Principles and Practice. *Churchill Livingstone, Philadelphia* (2000).

125. Hosseini, S.M. & Feng, J.J. How Malaria Parasites Reduce the Deformability of Infected Red Blood Cells. *Biophys J* **103**, 1-10 (2012).

126. Barabino, G.A., Platt, M.O. & Kaul, D.K. Sickle cell biomechanics. *Annu Rev Biomed Eng* **12**, 345-67 (2010).

127. Vaya, A., Rivera, L., de la Espriella, R., Sanchez, F., Suescun, M., Hernandez, J.L. & Facila, L. Red blood cell distribution width and erythrocyte deformability in patients with acute myocardial infarction. *Clin Hemorheol Microcirc* **59**, 107-14 (2015).

128. Sandhagen, B. Red cell fluidity in hypertension. *Clin Hemorheol Microcirc* **21**, 179-81 (1999).

129. Smith, B.D. Abnormal erythrocyte fragmentation and membrane deformability in paroxysmal nocturnal hemoglobinuria. *Am J Hematol* **20**, 337-43 (1985).

130. Symeonidis, A., Athanassiou, G., Psiroyannis, A., Kyriazopoulou, V., Kapatais-Zoumbos, K., Missirlis, Y. & Zoumbos, N. Impairment of erythrocyte viscoelasticity is correlated with levels of glycosylated haemoglobin in diabetic patients. *Clin Lab Haematol* **23**, 103-9 (2001).

131. Starzyk, D., Korbut, R. & Gryglewski, R.J. Effects of nitric oxide and prostacyclin on deformability and aggregability of red blood cells of rats ex vivo and in vitro. *J Physiol Pharmacol* **50**, 629-37 (1999).

132. Chen, C.F., Jia, H.Y., Ma, H.W., Wang, D.Y., Guo, S.S. & Qu, S. Rheologic determinant changes of erythrocytes in Binswanger's disease. *Zhonghua Yi Xue Za Zhi* **62**, 76-85 (1999).

133. Puniyani, R.R., Ajmani, R. & Kale, P.A. Risk factors evaluation in some cardiovascular diseases. *J Biomed Eng* **13**, 441-3 (1991).

134. Stoltz J.F., Donner, M. Hemorheology: Importance of erythrocyte aggregation. *Clin Hemorheol* **7**, 15 (1987).

135. Kroll, M.H., Hellums, J.D., McIntire, L.V., Schafer, A.I. & Moake, J.L. Platelets and shear stress. *Blood* **88**, 1525-41 (1996).

136. Demiroglu H, B.I., Dündar S. Erythrocyte aggregability in patients with coronary heart disease. *Clin Hemorheol* **16**, 313 (1996).

137. Demiroglu, H. & Gurlek, A. Altered red blood cell rheology as a predisposing factor for diabetic nephropathy. *Nephron* **79**, 121-2 (1998).

138. Glacet-Bernard, A., Chabanel, A., Lelong, F., Samama, M.M. & Coscas, G. Elevated erythrocyte aggregation in patients with central retinal vein occlusion and without conventional risk factors. *Ophthalmology* **101**, 1483-7 (1994).

139. Boogaerts, M.A., Roelant, C., Temmerman, J., Goossens, W. & Verwilghen, R.L. Effect of beta-blocking drugs on red cell adhesive and rheological properties. *J Lab Clin Med* **102**, 899-908 (1983).

140. Hayakawa, M. & Kuzuya, F. Effects of ticlopidine on erythrocyte aggregation in thrombotic disorders. *Angiology* **42**, 747-53 (1991).

141. Koenig W, E.E. The effect of calcium channel blockers on blood fluidity. *J Cardiovasc Pharmacol* **6**, 40 (1990).

142. Gafarova, M.E., Rykova, S.Y., , Khokhlova, M.D., Lubinb E.V., Skryabinab, M.V., Fedyaninb, A.A. & Sokolova, I.A. Red blood cell (dis)aggregation: effect of inhibition of fibrinogen binding. *Ser Biomech* **27**, 69-73 (2012).

143. Andrews, D.A. & Low, P.S. Role of red blood cells in thrombosis. *Curr Opin Hematol* **6**, 76-82 (1999).

144. Turitto, V.T. & Weiss, H.J. Red blood cells: their dual role in thrombus formation. *Science* **207**, 541-3 (1980).

145. Aarts, P.A., Banga, J.D., van Houwelingen, H.C., Heethaar, R.M. & Sixma, J.J. Increased red blood cell deformability due to isoxsuprine administration decreases platelet adherence in a perfusion chamber: a double-blind cross-over study in patients with intermittent claudication. *Blood* **67**, 1474-81 (1986).

146. van Gelder, J.M., Nair, C.H. & Dhall, D.P. Erythrocyte aggregation and erythrocyte deformability modify the permeability of erythrocyte enriched fibrin network. *Thromb Res* **82**, 33-42 (1996).

147. Swieringa, F., Baaten, C.C., Verdoold, R., Mastenbroek, T.G., Rijnveld, N., van der Laan, K.O., Breel, E.J., Collins, P.W., Lance, M.D., Henskens, Y.M., Cosemans, J.M., Heemskerk, J.W. & van der Meijden, P.E. Platelet Control of Fibrin Distribution and Microelasticity in Thrombus Formation Under Flow. *Arterioscler Thromb Vasc Biol* **36**, 692-9 (2016).

148. Aleman, M.M., Walton, B.L., Byrnes, J.R. & Wolberg, A.S. Fibrinogen and red blood cells in venous thrombosis. *Thromb Res* **133**, S38-40 (2014).

149. Gersh, K.C., Nagaswami, C. & Weisel, J.W. Fibrin network structure and clot mechanical properties are altered by incorporation of erythrocytes. *Thromb Haemost* **102**, 1169-75 (2009).

150. Horne, M.K., Cullinane, A.M., Merryman, P.K. & Hoddeson, E.K. The effect of red blood cells on thrombin generation. *Br J Haematol* **133**, 403-8 (2006).

151. Peyrou, V., Lormeau, J.C., Herault, J.P., Gaich, C., Pfliegger, A.M. & Herbert, J.M. Contribution of erythrocytes to thrombin generation in whole blood. *Thromb Haemost* **81**, 400-6 (1999).

152. Whelihan, M.F., Zachary, V., Orfeo, T. & Mann, K.G. Prothrombin activation in blood coagulation: the erythrocyte contribution to thrombin generation. *Blood* **120**, 3837-45 (2012).

153. Carvalho, F.A., Connell, S., Miltenberger-Miltenyi, G., Pereira, S.V., Tavares, A., Ariëns, R.A. & Santos, N.C. Atomic force microscopy-based molecular recognition of a fibrinogen receptor on human erythrocytes. *ACS Nano* **4**, 4609-20 (2010).

154. Cines, D.B., Lebedeva, T., Nagaswami, C., Hayes, V., Massefski, W., Litvinov, R.I., Rauova, L., Lowery, T.J. & Weisel, J.W. Clot contraction: compression of erythrocytes into tightly packed polyhedra and redistribution of platelets and fibrin. *Blood* **123**, 1596-603 (2014).

155. Tutwiler, V., Peshkova, A.D., Andrianova, I.A., Khasanova, D.R., Weisel, J.W. & Litvinov, R.I. Contraction of Blood Clots Is Impaired in Acute Ischemic Stroke. *Arterioscler Thromb Vasc Biol* **37**, 271-279 (2017).

156. Uchihashi, T., Kodera, N. & Ando, T. Guide to video recording of structure dynamics and dynamic processes of proteins by high-speed atomic force microscopy. *Nat Protoc* **7**, 1193-206 (2012).

157. Wojcikiewicz, E.P., Zhang, X. & Moy, V.T. Force and Compliance Measurements on Living Cells Using Atomic Force Microscopy (AFM). *Biol Proced Online* **6**, 1-9 (2004).

158. Adams, R.A., Schachtrup, C., Davalos, D., Tsigelny, I. & Akassoglou, K. Fibrinogen signal transduction as a mediator and therapeutic target in inflammation: lessons from multiple sclerosis. *Curr Med Chem* **14**, 2925-36 (2007).

159. Murray, C.J. & Lopez, A.D. Alternative projections of mortality and disability by cause 1990-2020: Global Burden of Disease Study. *Lancet* **349**, 1498-504 (1997).

160. Maeda, N., Seike, M., Kume, S., Takaku, T. & Shiga, T. Fibrinogen-induced erythrocyte aggregation: erythrocyte-binding site in the fibrinogen molecule. *Biochim Biophys Acta* **904**, 81-91 (1987).

161. Lominadze, D. & Dean, W.L. Involvement of fibrinogen specific binding in erythrocyte aggregation. *FEBS Lett* **517**, 41-4 (2002).

162. Game, L., Voegel, J.C., Schaaf, P. & Stoltz, J.F. Do physiological concentrations of IgG induce a direct aggregation of red blood cells: comparison with fibrinogen. *Biochim Biophys Acta* **1291**, 138-42 (1996).

163. Lominadze, D., Joshua, I.G. & Schuschke, D.A. Increased erythrocyte aggregation in spontaneously hypertensive rats. *Am J Hypertens* **11**, 784-9 (1998).

164. Weng, X., Cloutier, G., Beaulieu, R. & Roederer, G.O. Influence of acute-phase proteins on erythrocyte aggregation. *Am J Physiol* **271**, H2346-52 (1996).

165. Chien, S. & Jan, K. Ultrastructural basis of the mechanism of rouleaux formation. *Microvasc Res* **5**, 155-66 (1973).

166. Parise, L.V. & Phillips, D.R. Reconstitution of the purified platelet fibrinogen receptor. Fibrinogen binding properties of the glycoprotein IIb-IIIa complex. *J Biol Chem* **260**, 10698-707 (1985).

167. Manodori, A.B. Sickle erythrocytes adhere to fibronectin-thrombospondin-integrin complexes exposed by thrombin-induced endothelial cell contraction. *Microvasc Res* **61**, 263-74 (2001).

168. Sugihara, K., Sugihara, T., Mohandas, N. & Hebbel, R.P. Thrombospondin mediates adherence of CD36+ sickle reticulocytes to endothelial cells. *Blood* **80**, 2634-42 (1992).

169. Wick, T.M., Moake, J.L., Udden, M.M. & McIntire, L.V. Unusually large von Willebrand factor multimers preferentially promote young sickle and nonsickle erythrocyte adhesion to endothelial cells. *Am J Hematol* **42**, 284-92 (1993).

170. Joneckis, C.C., Ackley, R.L., Orringer, E.P., Wayner, E.A. & Parise, L.V. Integrin alpha 4 beta 1 and glycoprotein IV (CD36) are expressed on circulating reticulocytes in sickle cell anemia. *Blood* **82**, 3548-55 (1993).

171. Joneckis, C.C., Shock, D.D., Cunningham, M.L., Orringer, E.P. & Parise, L.V. Glycoprotein IV-independent adhesion of sickle red blood cells to immobilized thrombospondin under flow conditions. *Blood* **87**, 4862-70 (1996).

172. van Schravendijk, M.R., Handunnetti, S.M., Barnwell, J.W. & Howard, R.J. Normal human erythrocytes express CD36, an adhesion molecule of monocytes, platelets, and endothelial cells. *Blood* **80**, 2105-14 (1992).

173. De Oliveira, S., Vitorino de Almeida, V., Calado, A., Rosario, H.S. & Saldanha, C. Integrin-associated protein (CD47) is a putative mediator for soluble fibrinogen interaction with human red blood cells membrane. *Biochim Biophys Acta* **1818**, 481-90 (2012).

174. Rampling, M.W. The binding of fibrinogen and fibrinogen degradation products to the erythrocyte membrane and its relationship to haemorheology. *Acta Biol Med Ger* **40**, 373-8 (1981).

175. Ruoslahti, E. & Pierschbacher, M.D. New perspectives in cell adhesion: RGD and integrins. *Science* **238**, 491-7 (1987).

176. Doolittle, R.F., Watt, K.W., Cottrell, B.A., Strong, D.D. & Riley, M. The amino acid sequence of the alpha-chain of human fibrinogen. *Nature* **280**, 464-8 (1979).

177. Bennett, J.S. Structure and function of the platelet integrin $\alpha_{IIb}\beta_3$. *J Clin Invest* **115**, 3363-9 (2005).

178. Phillips, D.R., Charo, I.F., Parise, L.V. & Fitzgerald, L.A. The platelet membrane glycoprotein IIb-IIIa complex. *Blood* **71**, 831-43 (1988).

179. Danhier, F., Le Breton, A. & Preat, V. RGD-based strategies to target $\alpha_V\beta_3$ integrin in cancer therapy and diagnosis. *Mol Pharm* **9**, 2961-73 (2012).

180. Salsmann, A., Schaffner-Reckinger, E. & Kieffer, N. RGD, the Rho'd to cell spreading. *Eur J Cell Biol* **85**, 249-54 (2006).

181. Cieutat, A.M., Lobel, P., August, J.T., Kjeldsen, L., Sengelov, H., Borregaard, N. & Bainton, D.F. Azurophilic granules of human neutrophilic leukocytes are deficient in lysosome-associated membrane proteins but retain the mannose 6-phosphate recognition marker. *Blood* **91**, 1044-58 (1998).

182. Cross, S.E., Jin, Y.S., Rao, J. & Gimzewski, J.K. Nanomechanical analysis of cells from cancer patients. *Nat Nanotechnol* **2**, 780-3 (2007).

183. WHO. Cardiovascular diseases (CVD). (2016). http://www.who.int/cardiovascular_diseases/en/

184. SPCardiologia. Prevenção Cardiovascular: Ideias e Números. *Revista Factores de Risco* **36**, 1-58 (2015).

185. Mackay, J.M., G. Atlas of Heart Disease and Stroke. *World Health Organization* (2004).

186. Zhang, X.H., Lisheng, L., Campbell, N.R., Niebylski, M.L., Nilsson, P., Lackland, D.T. & World Hypertension, L. Implementation of World Health Organization Package of Essential Noncommunicable Disease Interventions (WHO PEN) for Primary Health Care in Low-Resource Settings: A Policy Statement From the World Hypertension League. *J Clin Hypertens* **18**, 5-6 (2016).

187. WHO. Prevention of cardiovascular disease: guidelines for assessment and management of total cardiovascular risk. (2007). http://www.who.int/cardiovascular_diseases/publications/Prevention_of_Cardiovascular_Disease/en/

188. WHO. Prevention of recurrent heart attacks and strokes in low and middle income populations. (2013). http://www.who.int/cardiovascular_diseases/resources/pub0402/en/

189. Gupta, S., Gudapati, R., Gaurav, K. & Bhise, M. Emerging risk factors for cardiovascular diseases: Indian context. *Indian J Endocrinol Metab* **17**, 806-14 (2013).

190. Lindahl, B., Toss, H., Siegbahn, A., Venge, P. & Wallentin, L. Markers of myocardial damage and inflammation in relation to long-term mortality in unstable coronary artery disease. FRISC Study Group. Fragmin during Instability in Coronary Artery Disease. *N Engl J Med* **343**, 1139-47 (2000).

191. Biasucci, L.M., Liuzzo, G., Grillo, R.L., Caligiuri, G., Rebuzzi, A.G., Buffon, A., Summaria, F., Ginnetti, F., Fadda, G. & Maseri, A. Elevated levels of C-reactive protein at discharge in patients with unstable angina predict recurrent instability. *Circulation* **99**, 855-60 (1999).

192. Reinhart, W.H. Fibrinogen-marker or mediator of vascular disease? *Vasc Med* **8**, 211-6 (2003).

193. Coppola, G., Rizzo, M., Abrignani, M.G., Corrado, E., Di Girolamo, A., Braschi, A., Braschi, G. & Novo, S. Fibrinogen as a predictor of mortality after acute myocardial infarction: a forty-two-month follow-up study. *Ital Heart J* **6**, 315-22 (2005).

194. Lubrano, V. & Balzan, S. Consolidated and emerging inflammatory markers in coronary artery disease. *World J Exp Med* **5**, 21-32 (2015).

195. Maresca, G., Di Blasio, A., Marchioli, R. & Di Minno, G. Measuring plasma fibrinogen to predict stroke and myocardial infarction: an update. *Arterioscler Thromb Vasc Biol* **19**, 1368-77 (1999).

196. Hunt, S.A., American College of, C. & American Heart Association Task Force on Practice, G. ACC/AHA 2005 guideline update for the diagnosis and management of chronic heart failure in the adult: a report of the American College of Cardiology/American Heart Association Task Force on Practice Guidelines (Writing Committee to Update the 2001 Guidelines for the Evaluation and Management of Heart Failure). *J Am Coll Cardiol* **46**, e1-82 (2005).

197. Jessup, M., Abraham, W.T., Casey, D.E., Feldman, A.M., Francis, G.S., Ganiats, T.G., Konstam, M.A., Mancini, D.M., Rahko, P.S., Silver, M.A., Stevenson, L.W. & Yancy, C.W. 2009 focused update: ACCF/AHA Guidelines for the Diagnosis and Management of Heart Failure in Adults: a report of the American College of Cardiology Foundation/American Heart Association Task Force on Practice Guidelines: developed in collaboration with the International Society for Heart and Lung Transplantation. *Circulation* **119**, 1977-2016 (2009).

198. Mann, D.L. & Bristow, M.R. Mechanisms and models in heart failure: the biomechanical model and beyond. *Circulation* **111**, 2837-49 (2005).

199. Colluci, W.B. Textbook of cardiovascular Medicine. *Philadelphia: WB Saunders*, 394-420 (1997).

200. Follath, F. Ischemic versus non-ischemic heart failure: should the etiology be determined? *Heart Fail Monit* **1**, 122-5 (2001).

201. Follath, F., Cleland, J.G., Klein, W. & Murphy, R. Etiology and response to drug treatment in heart failure. *J Am Coll Cardiol* **32**, 1167-72 (1998).

202. Bui, A.L., Horwich, T.B. & Fonarow, G.C. Epidemiology and risk profile of heart failure. *Nat Rev Cardiol* **8**, 30-41 (2011).

203. McMurray, J.J., Petrie, M.C., Murdoch, D.R. & Davie, A.P. Clinical epidemiology of heart failure: public and private health burden. *Eur Heart J* **19**, P9-16 (1998).

204. Mozaffarian, D., Benjamin, E.J., Go, A.S., Arnett, D.K., Blaha, M.J., Cushman, M., Das, S.R., de Ferranti, S., Despres, J.P., Fullerton, H.J., Howard, V.J., Huffman, M.D., Isasi, C.R., Jimenez, M.C., Judd, S.E., Kissela, B.M., Lichtman, J.H., Lisabeth, L.D., Liu, S., Mackey, R.H., Magid, D.J., McGuire, D.K., Mohler, E.R., Moy, C.S., Muntner,

P., Mussolino, M.E., Nasir, K., Neumar, R.W., Nichol, G., Palaniappan, L., Pandey, D.K., Reeves, M.J., Rodriguez, C.J., Rosamond, W., Sorlie, P.D., Stein, J., Towfighi, A., Turan, T.N., Virani, S.S., Woo, D., Yeh, R.W., Turner, M.B., American Heart Association Statistics, C. & Stroke Statistics, S. Heart Disease and Stroke Statistics-2016 Update: A Report From the American Heart Association. *Circulation* **133**, e38-360 (2016).

205. Roger, V.L. Epidemiology of heart failure. *Circ Res* **113**, 646-59 (2013).

206. Yancy, C.W., Jessup, M., Bozkurt, B., Butler, J., Casey, D.E., Jr., Drazner, M.H., Fonarow, G.C., Geraci, S.A., Horwich, T., Januzzi, J.L., Johnson, M.R., Kasper, E.K., Levy, W.C., Masoudi, F.A., McBride, P.E., McMurray, J.J., Mitchell, J.E., Peterson, P.N., Riegel, B., Sam, F., Stevenson, L.W., Tang, W.H., Tsai, E.J. & Wilkoff, B.L. 2013 ACCF/AHA guideline for the management of heart failure: executive summary: a report of the American College of Cardiology Foundation/American Heart Association Task Force on practice guidelines. *Circulation* **128**, 1810-52 (2013).

207. Yancy, C.W., Jessup, M., Bozkurt, B., Butler, J., Casey, D.E., Jr., Drazner, M.H., Fonarow, G.C., Geraci, S.A., Horwich, T., Januzzi, J.L., Johnson, M.R., Kasper, E.K., Levy, W.C., Masoudi, F.A., McBride, P.E., McMurray, J.J., Mitchell, J.E., Peterson, P.N., Riegel, B., Sam, F., Stevenson, L.W., Tang, W.H., Tsai, E.J., Wilkoff, B.L., American College of Cardiology, F. & American Heart Association Task Force on Practice, G. 2013 ACCF/AHA guideline for the management of heart failure: a report of the American College of Cardiology Foundation/American Heart Association Task Force on Practice Guidelines. *J Am Coll Cardiol* **62**, e147-239 (2013).

208. Dieplinger, B. & Mueller, T. Soluble ST2 in heart failure. *Clin Chim Acta* **443**, 57-70 (2015).

209. Medvedeva, E.A., Berezin, II, Surkova, E.A., Yaranov, D.M. & Shchukin, Y.V. Galectin-3 in patients with chronic heart failure: association with oxidative stress, inflammation, renal dysfunction and prognosis. *Minerva Cardioangiol* **64**, 595-602 (2016).

210. Stoiser, B., Mortl, D., Hulsmann, M., Berger, R., Struck, J., Morgenthaler, N.G., Bergmann, A. & Pacher, R. Copeptin, a fragment of the vasopressin precursor, as a novel predictor of outcome in heart failure. *Eur J Clin Invest* **36**, 771-8 (2006).

211. Maisel, A.S. & Choudhary, R. Biomarkers in acute heart failure-state of the art. *Nat Rev Cardiol* **9**, 478-90 (2012).

212. Olsen, M.H., Angell, S.Y., Asma, S., Boutouyrie, P., Burger, D., Chirinos, J.A., Damasceno, A., Delles, C., Gimenez-Roqueplo, A.P., Hering, D., Lopez-Jaramillo, P., Martinez, F., Perkovic, V., Rietzschel, E.R., Schillaci, G., Schutte, A.E., Scuteri, A., Sharman, J.E., Wachtell, K. & Wang, J.G. A call to action and a lifecourse strategy to address the global burden of raised blood pressure on current and future generations: the Lancet Commission on hypertension. *Lancet* **388**, 2665-2712 (2016).

213. Lim, S.S., Vos, T., Flaxman, A.D., Danaei, G., Shibuya, K., Adair-Rohani, H., Amann, M., Anderson, H.R., Andrews, K.G., Aryee, M., Atkinson, C., Bacchus, L.J., Bahalim, A.N., Balakrishnan, K., Balmes, J., Barker-Collo, S., Baxter, A., Bell, M.L., Blore, J.D., Blyth, F., Bonner, C., Borges, G., Bourne, R., Boussinesq, M., Brauer, M., Brooks, P., Bruce, N.G., Brunekreef, B., Bryan-Hancock, C., Bucello, C., Buchbinder, R., Bull, F., Burnett, R.T., Byers, T.E., Calabria, B., Carapetis, J., Carnahan, E., Chafe, Z., Charlson, F., Chen, H., Chen, J.S., Cheng, A.T., Child, J.C., Cohen, A., Colson, K.E., Cowie, B.C., Darby, S., Darling, S., Davis, A., Degenhardt, L., Dentener, F., Des Jarlais, D.C., Devries, K., Dherani, M., Ding, E.L., Dorsey, E.R., Driscoll, T., Edmond, K., Ali, S.E., Engell, R.E., Erwin, P.J., Fahimi, S., Falder, G., Farzadfar, F., Ferrari, A., Finucane, M.M., Flaxman, S., Fowkes, F.G., Freedman, G., Freeman, M.K., Gakidou, E., Ghosh, S., Giovannucci, E., Gmel, G., Graham, K., Grainger, R., Grant, B., Gunnell, D., Gutierrez, H.R., Hall, W., Hoek, H.W., Hogan, A., Hosgood, H.D., 3rd, Hoy, D., Hu, H., Hubbell, B.J., Hutchings, S.J., Ibeanusi, S.E., Jacklyn, G.L., Jasrasaria, R., Jonas, J.B., Kan, H., Kanis, J.A., Kassebaum, N., Kawakami, N., Khang, Y.H., Khatibzadeh, S., Khoo, J.P., Kok, C., Laden, F., Lalloo, R., Lan, Q., Lathlean, T., Leasher, J.L., Leigh, J., Li, Y., Lin, J.K., Lipshultz, S.E., London, S., Lozano, R., Lu, Y., Mak, J., Malekzadeh, R., Mallinger, L., Marcenes, W., March, L., Marks, R., Martin, R., McGale, P., McGrath, J., Mehta, S., Mensah, G.A., Merriman, T.R., Micha, R., Michaud, C., Mishra, V., Mohd Hanafiah, K., Mokdad, A.A., Morawska, L., Mozaffarian, D., Murphy, T., Naghavi, M., Neal, B., Nelson, P.K., Nolla, J.M., Norman, R., Olives, C., Omer, S.B., Orchard, J., Osborne, R., Ostro, B., Page, A., Pandey, K.D., Parry, C.D., Passmore, E., Patra, J., Pearce, N., Pelizzari, P.M.,

Petzold, M., Phillips, M.R., Pope, D., Pope, C.A., 3rd, Powles, J., Rao, M., Razavi, H., Rehfuess, E.A., Rehm, J.T., Ritz, B., Rivara, F.P., Roberts, T., Robinson, C., Rodriguez-Portales, J.A., Romieu, I., Room, R., Rosenfeld, L.C., Roy, A., Rushton, L., Salomon, J.A., Sampson, U., Sanchez-Riera, L., Sanman, E., Sapkota, A., Seedat, S., Shi, P., Shield, K., Shivakoti, R., Singh, G.M., Sleet, D.A., Smith, E., Smith, K.R., Stapelberg, N.J., Steenland, K., Stockl, H., Stovner, L.J., Straif, K., Straney, L., Thurston, G.D., Tran, J.H., Van Dingenen, R., van Donkelaar, A., Veerman, J.L., Vijayakumar, L., Weintraub, R., Weissman, M.M., White, R.A., Whiteford, H., Wiersma, S.T., Wilkinson, J.D., Williams, H.C., Williams, W., Wilson, N., Woolf, A.D., Yip, P., Zielinski, J.M., Lopez, A.D., Murray, C.J., Ezzati, M., AlMazroa, M.A. & Memish, Z.A. A comparative risk assessment of burden of disease and injury attributable to 67 risk factors and risk factor clusters in 21 regions, 1990-2010: a systematic analysis for the Global Burden of Disease Study 2010. *Lancet* **380**, 2224-60 (2012).

214. Kearney, P.M., Whelton, M., Reynolds, K., Whelton, P.K. & He, J. Worldwide prevalence of hypertension: a systematic review. *J Hypertens* **22**, 11-9 (2004).

215. Bussemaker, E., Hillebrand, U., Hausberg, M., Pavenstadt, H. & Oberleithner, H. Pathogenesis of hypertension: interactions among sodium, potassium, and aldosterone. *Am J Kidney Dis* **55**, 1111-20 (2010).

216. Carretero, O.A. & Oparil, S. Essential hypertension. Part I: definition and etiology. *Circulation* **101**, 329-35 (2000).

217. Rimoldi, S.F., Scherrer, U. & Messerli, F.H. Secondary arterial hypertension: when, who, and how to screen? *Eur Heart J* **35**, 1245-54 (2014).

218. Charles, L., Triscott, J. & Dobbs, B. Secondary Hypertension: Discovering the Underlying Cause. *Am Fam Physician* **96**, 453-461 (2017).

219. Capildeo, R., Haberman, S. & Rose, F.C. The definition and classification of stroke. A new approach. *QJM* **47**, 177-96 (1978).

220. Portegies, M.L., Koudstaal, P.J. & Ikram, M.A. Cerebrovascular disease. *Handb Clin Neurol* **138**, 239-61 (2016).

221. Zhuhai Luda Medical Group. Cerebrovascular treatment. (2017). http://www.zhluda.net/diseases/81.html

222. Lozano, R., Naghavi, M., Foreman, K., Lim, S., Shibuya, K., Aboyans, V., Abraham, J., Adair, T., Aggarwal, R., Ahn, S.Y., Alvarado, M., Anderson, H.R., Anderson, L.M., Andrews, K.G., Atkinson, C., Baddour, L.M., Barker-Collo, S., Bartels, D.H., Bell, M.L., Benjamin, E.J., Bennett, D., Bhalla, K., Bikbov, B., Bin Abdulhak, A., Birbeck, G., Blyth, F., Bolliger, I., Boufous, S., Bucello, C., Burch, M., Burney, P., Carapetis, J., Chen, H., Chou, D., Chugh, S.S., Coffeng, L.E., Colan, S.D., Colquhoun, S., Colson, K.E., Condon, J., Connor, M.D., Cooper, L.T., Corriere, M., Cortinovis, M., de Vaccaro, K.C., Couser, W., Cowie, B.C., Criqui, M.H., Cross, M., Dabhadkar, K.C., Dahodwala, N., De Leo, D., Degenhardt, L., Delossantos, A., Denenberg, J., Des Jarlais, D.C., Dharmaratne, S.D., Dorsey, E.R., Driscoll, T., Duber, H., Ebel, B., Erwin, P.J., Espindola, P., Ezzati, M., Feigin, V., Flaxman, A.D., Forouzanfar, M.H., Fowkes, F.G., Franklin, R., Fransen, M., Freeman, M.K., Gabriel, S.E., Gakidou, E., Gaspari, F., Gillum, R.F., Gonzalez-Medina, D., Halasa, Y.A., Haring, D., Harrison, J.E., Havmoeller, R., Hay, R.J., Hoen, B., Hotez, P.J., Hoy, D., Jacobsen, K.H., James, S.L., Jasrasaria, R., Jayaraman, S., Johns, N., Karthikeyan, G., Kassebaum, N., Keren, A., Khoo, J.P., Knowlton, L.M., Kobusingye, O., Koranteng, A., Krishnamurthi, R., Lipnick, M., Lipshultz, S.E., Ohno, S.L., Mabweijano, J., MacIntyre, M.F., Mallinger, L., March, L., Marks, G.B., Marks, R., Matsumori, A., Matzopoulos, R., Mayosi, B.M., McAnulty, J.H., McDermott, M.M., McGrath, J., Mensah, G.A., Merriman, T.R., Michaud, C., Miller, M., Miller, T.R., Mock, C., Mocumbi, A.O., Mokdad, A.A., Moran, A., Mulholland, K., Nair, M.N., Naldi, L., Narayan, K.M., Nasseri, K., Norman, P., O'Donnell, M., Omer, S.B., Ortblad, K., Osborne, R., Ozgediz, D., Pahari, B., Pandian, J.D., Rivero, A.P., Padilla, R.P., Perez-Ruiz, F., Perico, N., Phillips, D., Pierce, K., Pope, C.A., 3rd, Porrini, E., Pourmalek, F., Raju, M., Ranganathan, D., Rehm, J.T., Rein, D.B., Remuzzi, G., Rivara, F.P., Roberts, T., De Leon, F.R., Rosenfeld, L.C., Rushton, L., Sacco, R.L., Salomon, J.A., Sampson, U., Sanman, E., Schwebel, D.C., Segui-Gomez, M., Shepard, D.S., Singh, D., Singleton, J., Sliwa, K., Smith, E., Steer, A., Taylor, J.A., Thomas, B., Tleyjeh, I.M., Towbin, J.A., Truelsen, T., Undurraga, E.A., Venketasubramanian, N., Vijayakumar, L., Vos, T., Wagner, G.R., Wang, M., Wang, W., Watt, K., Weinstock, M.A., Weintraub, R., Wilkinson, J.D., Woolf, A.D., Wulf, S., Yeh, P.H., Yip, P., Zabetian, A., Zheng, Z.J., Lopez, A.D., Murray, C.J., AlMazroa, M.A. & Memish, Z.A. Global and regional

mortality from 235 causes of death for 20 age groups in 1990 and 2010: a systematic analysis for the Global Burden of Disease Study 2010. *Lancet* **380**, 2095-128 (2012).

223. Murray, C.J., Vos, T., Lozano, R., Naghavi, M., Flaxman, A.D., Michaud, C., Ezzati, M., Shibuya, K., Salomon, J.A., Abdalla, S., Aboyans, V., Abraham, J., Ackerman, I., Aggarwal, R., Ahn, S.Y., Ali, M.K., Alvarado, M., Anderson, H.R., Anderson, L.M., Andrews, K.G., Atkinson, C., Baddour, L.M., Bahalim, A.N., Barker-Collo, S., Barrero, L.H., Bartels, D.H., Basanez, M.G., Baxter, A., Bell, M.L., Benjamin, E.J., Bennett, D., Bernabe, E., Bhalla, K., Bhandari, B., Bikbov, B., Bin Abdulhak, A., Birbeck, G., Black, J.A., Blencowe, H., Blore, J.D., Blyth, F., Bolliger, I., Bonaventure, A., Boufous, S., Bourne, R., Boussinesq, M., Braithwaite, T., Brayne, C., Bridgett, L., Brooker, S., Brooks, P., Brugha, T.S., Bryan-Hancock, C., Bucello, C., Buchbinder, R., Buckle, G., Budke, C.M., Burch, M., Burney, P., Burstein, R., Calabria, B., Campbell, B., Canter, C.E., Carabin, H., Carapetis, J., Carmona, L., Cella, C., Charlson, F., Chen, H., Cheng, A.T., Chou, D., Chugh, S.S., Coffeng, L.E., Colan, S.D., Colquhoun, S., Colson, K.E., Condon, J., Connor, M.D., Cooper, L.T., Corriere, M., Cortinovis, M., de Vaccaro, K.C., Couser, W., Cowie, B.C., Criqui, M.H., Cross, M., Dabhadkar, K.C., Dahiya, M., Dahodwala, N., Damsere-Derry, J., Danaei, G., Davis, A., De Leo, D., Degenhardt, L., Dellavalle, R., Delossantos, A., Denenberg, J., Derrett, S., Des Jarlais, D.C., Dharmaratne, S.D., Dherani, M., Diaz-Torne, C., Dolk, H., Dorsey, E.R., Driscoll, T., Duber, H., Ebel, B., Edmond, K., Elbaz, A., Ali, S.E., Erskine, H., Erwin, P.J., Espindola, P., Ewoigbokhan, S.E., Farzadfar, F., Feigin, V., Felson, D.T., Ferrari, A., Ferri, C.P., Fevre, E.M., Finucane, M.M., Flaxman, S., Flood, L., Foreman, K., Forouzanfar, M.H., Fowkes, F.G., Fransen, M., Freeman, M.K., Gabbe, B.J., Gabriel, S.E., Gakidou, E., Ganatra, H.A., Garcia, B., Gaspari, F., Gillum, R.F., Gmel, G., Gonzalez-Medina, D., Gosselin, R., Grainger, R., Grant, B., Groeger, J., Guillemin, F., Gunnell, D., Gupta, R., Haagsma, J., Hagan, H., Halasa, Y.A., Hall, W., Haring, D., Haro, J.M., Harrison, J.E., Havmoeller, R., Hay, R.J., Higashi, H., Hill, C., Hoen, B., Hoffman, H., Hotez, P.J., Hoy, D., Huang, J.J., Ibeanusi, S.E., Jacobsen, K.H., James, S.L., Jarvis, D., Jasrasaria, R., Jayaraman, S., Johns, N., Jonas, J.B., Karthikeyan, G., Kassebaum, N., Kawakami, N., Keren, A., Khoo, J.P., King, C.H., Knowlton, L.M., Kobusingye, O., Koranteng, A., Krishnamurthi, R., Laden, F., Lalloo, R., Laslett, L.L.,

Lathlean, T., Leasher, J.L., Lee, Y.Y., Leigh, J., Levinson, D., Lim, S.S., Limb, E., Lin, J.K., Lipnick, M., Lipshultz, S.E., Liu, W., Loane, M., Ohno, S.L., Lyons, R., Mabweijano, J., MacIntyre, M.F., Malekzadeh, R., Mallinger, L., Manivannan, S., Marcenes, W., March, L., Margolis, D.J., Marks, G.B., Marks, R., Matsumori, A., Matzopoulos, R., Mayosi, B.M., McAnulty, J.H., McDermott, M.M., McGill, N., McGrath, J., Medina-Mora, M.E., Meltzer, M., Mensah, G.A., Merriman, T.R., Meyer, A.C., Miglioli, V., Miller, M., Miller, T.R., Mitchell, P.B., Mock, C., Mocumbi, A.O., Moffitt, T.E., Mokdad, A.A., Monasta, L., Montico, M., Moradi-Lakeh, M., Moran, A., Morawska, L., Mori, R., Murdoch, M.E., Mwaniki, M.K., Naidoo, K., Nair, M.N., Naldi, L., Narayan, K.M., Nelson, P.K., Nelson, R.G., Nevitt, M.C., Newton, C.R., Nolte, S., Norman, P., Norman, R., O'Donnell, M., O'Hanlon, S., Olives, C., Omer, S.B., Ortblad, K., Osborne, R., Ozgediz, D., Page, A., Pahari, B., Pandian, J.D., Rivero, A.P., Patten, S.B., Pearce, N., Padilla, R.P., Perez-Ruiz, F., Perico, N., Pesudovs, K., Phillips, D., Phillips, M.R., Pierce, K., Pion, S., Polanczyk, G.V., Polinder, S., Pope, C.A., 3rd, Popova, S., Porrini, E., Pourmalek, F., Prince, M., Pullan, R.L., Ramaiah, K.D., Ranganathan, D., Razavi, H., Regan, M., Rehm, J.T., Rein, D.B., Remuzzi, G., Richardson, K., Rivara, F.P., Roberts, T., Robinson, C., De Leon, F.R., Ronfani, L., Room, R., Rosenfeld, L.C., Rushton, L., Sacco, R.L., Saha, S., Sampson, U., Sanchez-Riera, L., Sanman, E., Schwebel, D.C., Scott, J.G., Segui-Gomez, M., Shahraz, S., Shepard, D.S., Shin, H., Shivakoti, R., Singh, D., Singh, G.M., Singh, J.A., Singleton, J., Sleet, D.A., Sliwa, K., Smith, E., Smith, J.L., Stapelberg, N.J., Steer, A., Steiner, T., Stolk, W.A., Stovner, L.J., Sudfeld, C., Syed, S., Tamburlini, G., Tavakkoli, M., Taylor, H.R., Taylor, J.A., Taylor, W.J., Thomas, B., Thomson, W.M., Thurston, G.D., Tleyjeh, I.M., Tonelli, M., Towbin, J.A., Truelsen, T., Tsilimbaris, M.K., Ubeda, C., Undurraga, E.A., van der Werf, M.J., van Os, J., Vavilala, M.S., Venketasubramanian, N., Wang, M., Wang, W., Watt, K., Weatherall, D.J., Weinstock, M.A., Weintraub, R., Weisskopf, M.G., Weissman, M.M., White, R.A., Whiteford, H., Wiebe, N., Wiersma, S.T., Wilkinson, J.D., Williams, H.C., Williams, S.R., Witt, E., Wolfe, F., Woolf, A.D., Wulf, S., Yeh, P.H., Zaidi, A.K., Zheng, Z.J., Zonies, D., Lopez, A.D., AlMazroa, M.A. & Memish, Z.A. Disability-adjusted life years (DALYs) for 291 diseases and injuries in 21 regions,

1990-2010: a systematic analysis for the Global Burden of Disease Study 2010. *Lancet* **380**, 2197-223 (2012).

224. Mohr, J.P., Albers, G.W., Amarenco, P., Babikian, V.L., Biller, J., Brey, R.L., Coull, B., Easton, J.D., Gomez, C.R., Helgason, C.M., Kase, C.S., Pullicino, P.M. & Turpie, A.G. American Heart Association Prevention Conference. IV. Prevention and Rehabilitation of Stroke. Etiology of stroke. *Stroke* **28**, 1501-6 (1997).
225. Hankey, G.J. & Blacker, D.J. Is it a stroke? *BMJ* **350**, h56-h62 (2015).
226. Hankey, G.J. Stroke. *Lancet* **389**, 641-654 (2017).
227. Hankey, G.J. The benefits of aspirin in early secondary stroke prevention. *Lancet* **388**, 312-314 (2016).
228. Luengo-Fernandez, R., Paul, N.L., Gray, A.M., Pendlebury, S.T., Bull, L.M., Welch, S.J., Cuthbertson, F.C., Rothwell, P.M. & Oxford Vascular, S. Population-based study of disability and institutionalization after transient ischemic attack and stroke: 10-year results of the Oxford Vascular Study. *Stroke* **44**, 2854-61 (2013).
229. Coull, A.J., Lovett, J.K. & Rothwell, P.M. Population based study of early risk of stroke after transient ischaemic attack or minor stroke: implications for public education and organisation of services. *BMJ* **328**, 326 (2004).
230. Mohan, K.M., Wolfe, C.D., Rudd, A.G., Heuschmann, P.U., Kolominsky-Rabas, P.L. & Grieve, A.P. Risk and cumulative risk of stroke recurrence: a systematic review and meta-analysis. *Stroke* **42**, 1489-94 (2011).
231. Brotman, D.J., Walker, E., Lauer, M.S. & O'Brien, R.G. In search of fewer independent risk factors. *Arch Intern Med* **165**, 138-45 (2005).
232. Hackam, D.G. & Anand, S.S. Emerging risk factors for atherosclerotic vascular disease: a critical review of the evidence. *JAMA* **290**, 932-40 (2003).
233. Helfand, M., Buckley, D.I., Freeman, M., Fu, R., Rogers, K., Fleming, C. & Humphrey, L.L. Emerging risk factors for coronary heart disease: a summary of systematic reviews conducted for the U.S. Preventive Services Task Force. *Ann Intern Med* **151**, 496-507 (2009).
234. Wettersten, N. & Maisel, A.S. Biomarkers for Heart Failure: An Update for Practitioners of Internal Medicine. *Am J Med* **129**, 560-7 (2016).
235. Maisel, A. Biomonitoring and biomarker-guided therapy: the next step in heart failure and biomarker research. *J Am Coll Cardiol* **58**, 1890-2 (2011).

236. Biomarkers Definitions Working group. Biomarkers and surrogate endpoints: preferred definitions and conceptual framework. *Clin Pharmacol Ther* **69**, 89-95 (2001).

237. Shaw, J.G., Vaughan, A., Dent, A.G., O'Hare, P.E., Goh, F., Bowman, R.V., Fong, K.M. & Yang, I.A. Biomarkers of progression of chronic obstructive pulmonary disease (COPD). *J Thorac Dis* **6**, 1532-47 (2014).

238. Woodcock, J. Assessing the clinical utility of diagnostics used in drug therapy. *Clin Pharmacol Ther* **88**, 765-73 (2010).

239. Blankenberg, S., Rupprecht, H.J., Bickel, C., Peetz, D., Hafner, G., Tiret, L. & Meyer, J. Circulating cell adhesion molecules and death in patients with coronary artery disease. *Circulation* **104**, 1336-42 (2001).

240. Heeschen, C., Dimmeler, S., Hamm, C.W., Fichtlscherer, S., Boersma, E., Simoons, M.L., Zeiher, A.M. & Investigators, C.S. Serum level of the antiinflammatory cytokine interleukin-10 is an important prognostic determinant in patients with acute coronary syndromes. *Circulation* **107**, 2109-14 (2003).

241. Ridker, P.M., Rifai, N., Rose, L., Buring, J.E. & Cook, N.R. Comparison of C-reactive protein and low-density lipoprotein cholesterol levels in the prediction of first cardiovascular events. *N Engl J Med* **347**, 1557-65 (2002).

242. Kaptoge, S., Di Angelantonio, E., Pennells, L., Wood, A.M., White, I.R., Gao, P., Walker, M., Thompson, A., Sarwar, N., Caslake, M., Butterworth, A.S., Amouyel, P., Assmann, G., Bakker, S.J., Barr, E.L., Barrett-Connor, E., Benjamin, E.J., Bjorkelund, C., Brenner, H., Brunner, E., Clarke, R., Cooper, J.A., Cremer, P., Cushman, M., Dagenais, G.R., D'Agostino, R.B., Sr., Dankner, R., Davey-Smith, G., Deeg, D., Dekker, J.M., Engstrom, G., Folsom, A.R., Fowkes, F.G., Gallacher, J., Gaziano, J.M., Giampaoli, S., Gillum, R.F., Hofman, A., Howard, B.V., Ingelsson, E., Iso, H., Jorgensen, T., Kiechl, S., Kitamura, A., Kiyohara, Y., Koenig, W., Kromhout, D., Kuller, L.H., Lawlor, D.A., Meade, T.W., Nissinen, A., Nordestgaard, B.G., Onat, A., Panagiotakos, D.B., Psaty, B.M., Rodriguez, B., Rosengren, A., Salomaa, V., Kauhanen, J., Salonen, J.T., Shaffer, J.A., Shea, S., Ford, I., Stehouwer, C.D., Strandberg, T.E., Tipping, R.W., Tosetto, A., Wassertheil-Smoller, S., Wennberg, P., Westendorp, R.G., Whincup, P.H., Wilhelmsen, L., Woodward, M., Lowe, G.D., Wareham, N.J., Khaw, K.T., Sattar, N., Packard, C.J., Gudnason, V., Ridker, P.M.,

Pepys, M.B., Thompson, S.G. & Danesh, J. C-reactive protein, fibrinogen, and cardiovascular disease prediction. *N Engl J Med* **367**, 1310-20 (2012).

243. Lowe, G.D. & Rumley, A. Fibrinogen and its degradation products as thrombotic risk factors. *Ann N Y Acad Sci* **936**, 560-5 (2001).

244. Danesh, J., Lewington, S., Thompson, S.G., Lowe, G.D., Collins, R., Kostis, J.B., Wilson, A.C., Folsom, A.R., Wu, K., Benderly, M., Goldbourt, U., Willeit, J., Kiechl, S., Yarnell, J.W., Sweetnam, P.M., Elwood, P.C., Cushman, M., Psaty, B.M., Tracy, R.P., Tybjaerg-Hansen, A., Haverkate, F., de Maat, M.P., Fowkes, F.G., Lee, A.J., Smith, F.B., Salomaa, V., Harald, K., Rasi, R., Vahtera, E., Jousilahti, P., Pekkanen, J., D'Agostino, R., Kannel, W.B., Wilson, P.W., Tofler, G., Arocha-Pinango, C.L., Rodriguez-Larralde, A., Nagy, E., Mijares, M., Espinosa, R., Rodriquez-Roa, E., Ryder, E., Diez-Ewald, M.P., Campos, G., Fernandez, V., Torres, E., Marchioli, R., Valagussa, F., Rosengren, A., Wilhelmsen, L., Lappas, G., Eriksson, H., Cremer, P., Nagel, D., Curb, J.D., Rodriguez, B., Yano, K., Salonen, J.T., Nyyssonen, K., Tuomainen, T.P., Hedblad, B., Lind, P., Loewel, H., Koenig, W., Meade, T.W., Cooper, J.A., De Stavola, B., Knottenbelt, C., Miller, G.J., Cooper, J.A., Bauer, K.A., Rosenberg, R.D., Sato, S., Kitamura, A., Naito, Y., Palosuo, T., Ducimetiere, P., Amouyel, P., Arveiler, D., Evans, A.E., Ferrieres, J., Juhan-Vague, I., Bingham, A., Schulte, H., Assmann, G., Cantin, B., Lamarche, B., Despres, J.P., Dagenais, G.R., Tunstall-Pedoe, H., Woodward, M., Ben-Shlomo, Y., Davey Smith, G., Palmieri, V., Yeh, J.L., Rudnicka, A., Ridker, P., Rodeghiero, F., Tosetto, A., Shepherd, J., Ford, I., Robertson, M., Brunner, E., Shipley, M., Feskens, E.J., Kromhout, D., Dickinson, A., Ireland, B., Juzwishin, K., Kaptoge, S., Lewington, S., Memon, A., Sarwar, N., Walker, M., Wheeler, J., White, I. & Wood, A. Plasma fibrinogen level and the risk of major cardiovascular diseases and nonvascular mortality: an individual participant meta-analysis. *JAMA* **294**, 1799-809 (2005).

245. Kannel, W.B., Wolf, P.A., Castelli, W.P. & D'Agostino, R.B. Fibrinogen and risk of cardiovascular disease. The Framingham Study. *JAMA* **258**, 1183-6 (1987).

246. Di Napoli, M.S., P. Is plasma fibrinogen useful in evaluating ischemic stroke patients? Why, How and When. *Stroke* **40**, 1549-52 (2009).

247. Koster, T., Rosendaal, F.R., Reitsma, P.H., van der Velden, P.A., Briet, E. & Vandenbroucke, J.P. Factor VII and fibrinogen levels as risk factors for venous

thrombosis. A case-control study of plasma levels and DNA polymorphisms-the Leiden Thrombophilia Study (LETS). *Thromb Haemost* **71**, 719-22 (1994).

248. Mannino, D.M., Tal-Singer, R., Lomas, D.A., Vestbo, J., Graham Barr, R., Tetzlaff, K., Lowings, M., Rennard, S.I., Snyder, J., Goldman, M., Martin, U.J., Merrill, D., Martin, A.L., Simeone, J.C., Fahrbach, K., Murphy, B., Leidy, N. & Miller, B. Plasma Fibrinogen as a Biomarker for Mortality and Hospitalized Exacerbations in People with COPD. *Chronic Obstr Pulm Dis* **2**, 23-34 (2015).
249. Mulligan, P.R., Prajapati, H.J., Martin, L.G. & Patel, T.H. Vascular anomalies: classification, imaging characteristics and implications for interventional radiology treatment approaches. *Br J Radiol* **87**, 20130392 (2014).
250. Weisenhorn, A.L., Drake, B., Prater, C.B., Gould, S.A., Hansma, P.K., Ohnesorge, F., Egger, M., Heyn, S.P. & Gaub, H.E. Immobilized proteins in buffer imaged at molecular resolution by atomic force microscopy. *Biophys J* **58**, 1251-8 (1990).
251. Zhang, Y., Hu, X., Sun, J., Shen, Y., Hu, J., Xu, X. & Shao, Z. High-resolution imaging and nano-manipulation of biological structures on surface. *Microsc Res Tech* **74**, 614-26 (2011).
252. Binnig, G., Rohrer, H., Gerber, Ch., Weibel, E. Surface studies by scanning tunneling microscopy. *Phys. Rev. Lett.* **49**, 57-61 (1982).
253. Binnig, G., Quate, C.F., Gerber, Ch. Atomic Force Microscope. *Phys. Rev. Lett.* **56**, 930-933 (1986).
254. Santos, N.C. & Castanho, M.A. An overview of the biophysical applications of atomic force microscopy. *Biophys Chem* **107**, 133-49 (2004).
255. Muller, D.J. AFM: a nanotool in membrane biology. *Biochemistry* **47**, 7986-98 (2008).
256. Mukherjee, R., Chaudhury, K., Das, S., Sengupta, S. & Biswas, P. Posterior capsular opacification and intraocular lens surface micro-roughness characteristics: an atomic force microscopy study. *Micron* **43**, 937-47 (2012).
257. Schon, P. Imaging and force probing RNA by atomic force microscopy. *Methods* **103**, 25-33 (2016).
258. Dulinska, I., Targosz, M., Strojny, W., Lekka, M., Czuba, P., Balwierz, W. & Szymonski, M. Stiffness of normal and pathological erythrocytes studied by means of atomic force microscopy. *J Biochem Biophys Methods* **66**, 1-11 (2006).

259. Ebner, A., Schillers, H. & Hinterdorfer, P. Normal and pathological erythrocytes studied by atomic force microscopy. *Methods Mol Biol* **736**, 223-41 (2011).

260. Eaton, P., West, P. Atomic Force Microscopy. *Oxford University Press* (2010).

261. Gavara, N. A beginner's guide to atomic force microscopy probing for cell mechanics. *Microsc Res Tech* **80**, 75-84 (2017).

262. Muller, D.A., Kurt. Biomolecular imaging using atomic force microscopy. *Trends in Biotechnology* **20**, S45-S49 (2002).

263. Garcia, R. & Herruzo, E.T. The emergence of multifrequency force microscopy. *Nat Nanotechnol* **7**, 217-26 (2012).

264. Cleveland, J.P., Manne, S. A nondestructive method for determining the spring constant of cantilevers for scanning force microscopy *Rev Sci Instrum* **64**, 403 (1993).

265. Hutter, J.L., Bechhoefer, J. Calibration of atomic-force microscope tips. *Rev Sci Instrum* **64** (1993).

266. Senden, T., Ducker, W. Experimental Determination of Spring Constants in Atomic Force Microscopy. *Langmuir* **10**, 1003-1004 (1994).

267. Carvalho, F.A. & Santos, N.C. Atomic force microscopy-based force spectroscopy-biological and biomedical applications. *IUBMB Life* **64**, 465-72 (2012).

268. Cluzel, P., Lebrun, A., Heller, C., Lavery, R., Viovy, J.L., Chatenay, D. & Caron, F. DNA: an extensible molecule. *Science* **271**, 792-4 (1996).

269. Neuman, K.C. & Nagy, A. Single-molecule force spectroscopy: optical tweezers, magnetic tweezers and atomic force microscopy. *Nat Methods* **5**, 491-505 (2008).

270. Willemsen, O.H., Snel, M.M., Cambi, A., Greve, J., De Grooth, B.G. & Figdor, C.G. Biomolecular interactions measured by atomic force microscopy. *Biophys J* **79**, 3267-81 (2000).

271. Puntheeranurak, T., Neundlinger, I., Kinne, R.K. & Hinterdorfer, P. Single-molecule recognition force spectroscopy of transmembrane transporters on living cells. *Nat Protoc* **6**, 1443-52 (2011).

272. Heinz, W.F. & Hoh, J.H. Spatially resolved force spectroscopy of biological surfaces using the atomic force microscope. *Trends Biotechnol* **17**, 143-50 (1999).

273. Zlatanova, J., Lindsay, S.M. & Leuba, S.H. Single molecule force spectroscopy in biology using the atomic force microscope. *Prog Biophys Mol Biol* **74**, 37-61 (2000).

274. JPK Instruments. Nanowizard AFM. Handbook Version 2.2.5-5-57. (2009).

275. Israelachvili, J.N. & McGuiggan, P.M. Forces between surfaces in liquids. *Science* **241**, 795-800 (1988).

276. Helenius, J., Heisenberg, C.P., Gaub, H.E. & Muller, D.J. Single-cell force spectroscopy. *J Cell Sci* **121**, 1785-91 (2008).

277. Ebner, A., Wildling, L., Zhu, R., Rankl, C., Haselgrubler, T., Hinterdorfer, P. & Gruber, H.J. Functionalization of probe tips and supports for single-molecule recognition force microscopy. *Top Curr Chem* **285**, 29-76 (2008).

278. Kamruzzahan, A.S., Ebner, A., Wildling, L., Kienberger, F., Riener, C.K., Hahn, C.D., Pollheimer, P.D., Winklehner, P., Holzl, M., Lackner, B., Schorkl, D.M., Hinterdorfer, P. & Gruber, H.J. Antibody linking to atomic force microscope tips via disulfide bond formation. *Bioconjug Chem* **17**, 1473-81 (2006).

279. Verbelen, C., Gruber, H.J. & Dufrene, Y.F. The NTA-His6 bond is strong enough for AFM single-molecular recognition studies. *J Mol Recognit* **20**, 490-4 (2007).

280. Harder, A., Walhorn, V., Dierks, T., Fernandez-Busquets, X. & Anselmetti, D. Single-molecule force spectroscopy of cartilage aggrecan self-adhesion. *Biophys J* **99**, 3498-504 (2010).

281. Barattin, R. & Voyer, N. Chemical modifications of AFM tips for the study of molecular recognition events. *Chem Commun*, 1513-32 (2008).

282. Barattin, R. & Voyer, N. Chemical modifications of atomic force microscopy tips. *Methods Mol Biol* **736**, 457-83 (2011).

283. Ebner, A., Hinterdorfer, P. & Gruber, H.J. Comparison of different aminofunctionalization strategies for attachment of single antibodies to AFM cantilevers. *Ultramicroscopy* **107**, 922-7 (2007).

284. Christian K. Rienera, C.M.S., Andreas Ebnera, Christian Klampflb, Alex A. Gallc, Christoph Romanina, Yuri L. Lyubchenkod, Peter Hinterdorfera, Hermann J. Grubera,. Simple test system for single molecule recognition force microscopy. *Anal Chim Acta* **479**, 59-75 (2003).

285. Taubenberger, A.V., Hutmacher, D.W. & Muller, D.J. Single-cell force spectroscopy, an emerging tool to quantify cell adhesion to biomaterials. *Tissue Eng Part B Rev* **20**, 40-55 (2014).

286. Discher, D.E., Janmey, P. & Wang, Y.L. Tissue cells feel and respond to the stiffness of their substrate. *Science* **310**, 1139-43 (2005).

287. Gumbiner, B.M. Regulation of cadherin-mediated adhesion in morphogenesis. *Nat Rev Mol Cell Biol* **6**, 622-34 (2005).

288. Lecuit, T. & Lenne, P.F. Cell surface mechanics and the control of cell shape, tissue patterns and morphogenesis. *Nat Rev Mol Cell Biol* **8**, 633-44 (2007).

289. Sheetz, M.P. Cell control by membrane-cytoskeleton adhesion. *Nat Rev Mol Cell Biol* **2**, 392-6 (2001).

290. Vogel, V. & Sheetz, M. Local force and geometry sensing regulate cell functions. *Nat Rev Mol Cell Biol* **7**, 265-75 (2006).

291. Bustamante, C., Chemla, Y.R., Forde, N.R. & Izhaky, D. Mechanical processes in biochemistry. *Annu Rev Biochem* **73**, 705-48 (2004).

292. Benoit, M. & Gaub, H.E. Measuring cell adhesion forces with the atomic force microscope at the molecular level. *Cells Tissues Organs* **172**, 174-89 (2002).

293. Puech, P.H., Taubenberger, A., Ulrich, F., Krieg, M., Muller, D.J. & Heisenberg, C.P. Measuring cell adhesion forces of primary gastrulating cells from zebrafish using atomic force microscopy. *J Cell Sci* **118**, 4199-206 (2005).

294. Zhang, X., Chen, A., De Leon, D., Li, H., Noiri, E., Moy, V.T. & Goligorsky, M.S. Atomic force microscopy measurement of leukocyte-endothelial interaction. *Am J Physiol Heart Circ Physiol* **286**, H359-67 (2004).

295. Casuso, I., Rico, F. & Scheuring, S. Biological AFM: where we come from--where we are--where we may go. *J Mol Recognit* **24**, 406-13 (2011).

296. JPK Instruments. Unsing the CellHesion module - a pratical guide. 1-8 (2015).

297. Wojcikiewicz, E.P., Zhang, X., Chen, A. & Moy, V.T. Contributions of molecular binding events and cellular compliance to the modulation of leukocyte adhesion. *J Cell Sci* **116**, 2531-9 (2003).

298. Zhang, X., Wojcikiewicz, E. & Moy, V.T. Force spectroscopy of the leukocyte function-associated antigen-1/intercellular adhesion molecule-1 interaction. *Biophys J* **83**, 2270-9 (2002).

299. Friedrichs, J., Torkko, J.M., Helenius, J., Teravainen, T.P., Fullekrug, J., Muller, D.J., Simons, K. & Manninen, A. Contributions of galectin-3 and -9 to epithelial cell adhesion analyzed by single cell force spectroscopy. *J Biol Chem* **282**, 29375-83 (2007).

300. Benoit, M., Gabriel, D., Gerisch, G. & Gaub, H.E. Discrete interactions in cell adhesion measured by single-molecule force spectroscopy. *Nat Cell Biol* **2**, 313-7 (2000).

301. Lehenkari, P.P. & Horton, M.A. Single integrin molecule adhesion forces in intact cells measured by atomic force microscopy. *Biochem Biophys Res Commun* **259**, 645-50 (1999).

302. Thie, M., Rospel, R., Dettmann, W., Benoit, M., Ludwig, M., Gaub, H.E. & Denker, H.W. Interactions between trophoblast and uterine epithelium: monitoring of adhesive forces. *Hum Reprod* **13**, 3211-9 (1998).

303. Ikai, A. & Afrin, R. Toward mechanical manipulations of cell membranes and membrane proteins using an atomic force microscope: an invited review. *Cell Biochem Biophys* **39**, 257-77 (2003).

304. Vinckier, A. & Semenza, G. Measuring elasticity of biological materials by atomic force microscopy. *FEBS Lett* **430**, 12-6 (1998).

305. Rotsch, C. & Radmacher, M. Drug-induced changes of cytoskeletal structure and mechanics in fibroblasts: an atomic force microscopy study. *Biophys J* **78**, 520-35 (2000).

306. Butcher, D.T., Alliston, T. & Weaver, V.M. A tense situation: forcing tumour progression. *Nat Rev Cancer* **9**, 108-22 (2009).

307. Cox, T.R. & Erler, J.T. Remodeling and homeostasis of the extracellular matrix: implications for fibrotic diseases and cancer. *Dis Model Mech* **4**, 165-78 (2011).

308. Aigner, T., Schmitz, N. & Haag, J. Nanomedicine: AFM tackles osteoarthritis. *Nat Nanotechnol* **4**, 144-5 (2009).

309. Oesterhelt, F., Oesterhelt, D., Pfeiffer, M., Engel, A., Gaub, H.E. & Muller, D.J. Unfolding pathways of individual bacteriorhodopsins. *Science* **288**, 143-6 (2000).

310. Rief, M., Gautel, M., Oesterhelt, F., Fernandez, J.M. & Gaub, H.E. Reversible unfolding of individual titin immunoglobulin domains by AFM. *Science* **276**, 1109-12 (1997).

311. Yuan, C., Chen, A., Kolb, P. & Moy, V.T. Energy landscape of streptavidin-biotin complexes measured by atomic force microscopy. *Biochemistry* **39**, 10219-23 (2000).

312. Engel, A. & Muller, D.J. Observing single biomolecules at work with the atomic force microscope. *Nat Struct Biol* **7**, 715-8 (2000).

313. Scheuring, S., Muller, D.J., Stahlberg, H., Engel, H.A. & Engel, A. Sampling the conformational space of membrane protein surfaces with the AFM. *Eur Biophys J* **31**, 172-8 (2002).

314. Kedrov, A., Wegmann, S., Smits, S.H., Goswami, P., Baumann, H. & Muller, D.J. Detecting molecular interactions that stabilize, activate and guide ligand-binding of the sodium/proton antiporter MjNhaP1 from Methanococcus jannaschii. *J Struct Biol* **159**, 290-301 (2007).

315. Kedrov, A., Ziegler, C. & Muller, D.J. Differentiating ligand and inhibitor interactions of a single antiporter. *J Mol Biol* **362**, 925-32 (2006).

316. Hinterdorfer, P. & Dufrene, Y.F. Detection and localization of single molecular recognition events using atomic force microscopy. *Nat Methods* **3**, 347-55 (2006).

317. Carvalho, F.A., Carneiro, F.A., Martins, I.C., Assuncao-Miranda, I., Faustino, A.F., Pereira, R.M., Bozza, P.T., Castanho, M.A., Mohana-Borges, R., Da Poian, A.T. & Santos, N.C. Dengue virus capsid protein binding to hepatic lipid droplets (LD) is potassium ion dependent and is mediated by LD surface proteins. *J Virol* **86**, 2096-108 (2012).

318. Faustino, A.F., Carvalho, F.A., Martins, I.C., Castanho, M.A., Mohana-Borges, R., Almeida, F.C., Da Poian, A.T. & Santos, N.C. Dengue virus capsid protein interacts specifically with very low-density lipoproteins. *Nanomedicine* **10**, 247-55 (2014).

319. Ribeiro, A.S., Carvalho, F.A., Figueiredo, J., Carvalho, R., Mestre, T., Monteiro, J., Guedes, A.F., Fonseca, M., Sanches, J., Seruca, R., Santos, N.C. & Paredes, J. Atomic force microscopy and graph analysis to study the P-cadherin/SFK mechanotransduction signalling in breast cancer cells. *Nanoscale* **8**, 19390-19401 (2016).

320. Lekka, M., Gil, D., Pogoda, K., Dulinska-Litewka, J., Jach, R., Gostek, J., Klymenko, O., Prauzner-Bechcicki, S., Stachura, Z., Wiltowska-Zuber, J., Okon, K. & Laidler, P.

Cancer cell detection in tissue sections using AFM. *Arch Biochem Biophys* **518**, 151-6 (2012).

321. Li, Q.S., Lee, G.Y., Ong, C.N. & Lim, C.T. AFM indentation study of breast cancer cells. *Biochem Biophys Res Commun* **374**, 609-13 (2008).

Aims of the project

Cardiovascular diseases are the leading cause of death and disability worldwide. Despite the progress on its prevention, diagnosis, prognosis and treatment, the molecular interactions of the blood components underlying these diseases are not well understood. With this in mind, the major objective of this Thesis was to understand the interaction between fibrinogen and erythrocytes in healthy and pathological conditions, pinpointing patients with increased cardiovascular risk. To achieve this main objective, we proposed to reach more specific goals:

- ✓ To understand the effect of human plasma fibrinogen variants (namely the heterodimer and homodimer γ' fibrinogen) on clot structure and network with erythrocytes.
- ✓ To finish the identification of the fibrinogen receptor on the erythrocyte membrane (one of its units had already been identified before the beginning of this work, but not the other subunit).
- ✓ To identify the binding sites on the fibrinogen molecule for its interaction with the erythrocyte membrane receptor.
- ✓ To understand the influence of fibrinogen on erythrocyte-erythrocyte adhesion.
- ✓ To evaluate the binding between fibrinogen and erythrocytes in different cardiovascular pathologies: chronic heart failure (ischemic and non-ischemic), essential arterial hypertension and stroke.

The information achieved on the final aim will be useful to the development of new fibrinogen-erythrocyte binding inhibition strategies that could improve blood flow and microcirculation.

To achieve those goals, a combination of *in vitro* and *in silico* approaches was applied. Several techniques and methodologies were used, namely, atomic force microscopy (AFM)-based force spectroscopy, laser confocal microscopy, magnetic tweezers, permeability analysis, scanning electron microscopy, enzyme-linked immunosorbent assay (ELISA), cell culture, site-directed mutagenesis, protein purification, whole blood viscosity, erythrocyte deformability and erythrocyte aggregation analysis. To

complement the molecular level information gathered, protein computational analysis was also applied.

The work done on each of the topics indicated above is discussed in the following Chapters. At the beginning of each Chapter, there is an overview of the work motivation, key findings and main conclusions described on it.

The published results will be displayed in agreement to the journal's formatting rules, as the version published. Unpublished results will be added in the other Chapters.

Chapter II ▫

Impact of heterodimer γ’ fibrinogen on fibrin clot

Overview

The work described in this Chapter was focused on the study of the interaction between the heterodimer γAγ' fibrinogen and erythrocytes, as well as its influence on blood clot structure, properties and function. The rational for this study was that the total plasma fibrinogen contains an alternatively spliced γ-chain variant (γ'), which mainly exists as a heterodimer (γAγ') that has recently received the most attention. Elevated γAγ' levels have been associated with alterations in risk for bleeding or thrombosis. Different studies using isolated fibrin clots have been performed but there are scarce *in vitro* studies using fibrin clots containing erythrocytes. We found that the presence of erythrcoytes triggered variability in the fibrin network structure, individual fiber characteristics and overall clot properties. The presence of the γ' chain, even combined with γA, altered the clot structure, becoming heterogeneous, and conditioned erythrocyte adhesion. Our data also enabled to hypothesize that clots with γAγ' fibrinogen might interact differently with erythrocytes and, thereby, alter the risk for thrombosis. Further details are described on the Supplementary Information of this article.

This work was mainly conducted on the Leeds Institute of Cardiovascular and Metabolic Medicine and Multidisciplinary Cardiovascular Centre, at Faculty of Medicine and Health, University of Leeds, United Kingdom, with the supervision of Prof. Robert Ariëns.

Declaration of authorship

I, Ana Filipa Guedes, declare that most of the laboratory work, data analysis and writing of the manuscript initial draft were done by me. Particularly, AFM-based force spectroscopy data analysis and discussion were done under the supervision of Prof. Filomena A. Carvalho and Prof. Nuno C. Santos. The purification of fibrinogen variants was carried out by me with the help and supervision of Dr. Marco M. Domingues. Magnetic tweezers experiments were mainly conducted by Dr. Marco M. Domingues, with my help on the experiments and my input on data analysis and discussion. Fraser L. Macrae conducted with me the measurements and helped me on the optimization of the scanning electron microscopy procedure. Helen R. McPherson helped me on laser scanning confocal microscopy optimization and permeability studies. Magnetic tweezers, scanning electron microscopy, laser scanning confocal microscopy and permeability measurements were carried out by me under supervision of Prof. Robert A. S. Ariëns, in Leeds. All authors revised and improved the manuscript.

I, Filomena A. Carvalho, as co-supervisor of Ana Filipa Guedes and co-author of the manuscript, hereby declare that the information above is correct.

I, Nuno C. Santos, as supervisor of Ana Filipa Guedes and co-corresponding author of the manuscript, hereby declare that the information above is correct.

Lisbon, April 6, 2018

Ana Filipa Guedes | Filomena A. Carvalho | Nuno C. Santos

Article information (annexes, article 1, start in page 349):

Sensing adhesion forces between erythrocytes and γ' fibrinogen, modulating fibrin clot architecture and function.

Ana Filipa Guedes[1,2], Filomena A. Carvalho[1], Marco M. Domingues[1,2], Fraser L. Macrae[2], Helen R. McPherson[2], Nuno C. Santos[1,*#], Robert A. S. Ariëns[2,*#]

Status: Published online on February 2, 2018

***Journal* (year) volume, pages:** *Nanomedicine:* Nanotechnology, Biology and Medicine (2018) 14:909-918

DOI: 10.1016/j.nano.2018.01.006

JCR Impact factor 2016, quartile and field: 5.720, Q1 in Nanoscience and Nanotechnology and Biophysics

Sensing adhesion forces between erythrocytes and γ' fibrinogen, modulating fibrin clot architecture and function

Ana Filipa Guedes[1,2], Filomena A. Carvalho[1], Marco M. Domingues[1,2], Fraser L. Macrae[2], Helen R. McPherson[2], Nuno C. Santos[1,*#], Robert A. S. Ariëns[2,*#]

[1]Instituto de Medicina Molecular, Faculdade de Medicina, Universidade de Lisboa, Lisboa, Portugal; [2]Thrombosis and Tissue Repair Group, Division of Cardiovascular and Diabetes Research, Leeds Institute of Cardiovascular and Metabolic Medicine and Multidisciplinary Cardiovascular Centre, Faculty of Medicine and Health, University of Leeds, Leeds, United Kingdom.

[#]To whom correspondence should be addressed:

* Equal contribution

Robert Ariëns, Thrombosis and Tissue Repair Group, Division of Cardiovascular and Diabetes Research, Leeds Institute of Cardiovascular and Metabolic Medicine and Multidisciplinary Cardiovascular Centre, Faculty of Medicine and Health, University of Leeds, Leeds, Clarendon Way, Leeds LS2 9JT, United Kingdom; Tel: (+44)1133437734, Fax: (+44) 1133437738; Email: r.a.s.ariens@leeds.ac.uk.

Nuno C. Santos, Instituto de Medicina Molecular, Faculdade de Medicina, Universidade de Lisboa, Av. Prof. Egas Moniz, 1649-028 Lisboa, Portugal; Tel.: (+351)217999480; Fax: (+351) 217999477; E-mail: nsantos@medicina.ulisboa.pt

Abstract

Plasma fibrinogen includes an alternatively spliced γ-chain variant (γ'), which mainly exists as a heterodimer (γAγ') and has been associated with thrombosis. We tested γAγ' fibrinogen-red blood cells (RBCs) interaction using atomic force microscopy-based force spectroscopy, magnetic tweezers, fibrin clot permeability, scanning electron microscopy and laser scanning confocal microscopy. Data reveal higher work necessary for RBC-RBC detachment in the presence of γAγ' rather than γAγA fibrinogen. γAγ' fibrinogen-RBCs interaction is followed by changes in fibrin network structure, which forms an heterogeneous clot structure with areas of denser and highly branched fibrin fibers. The presence of RBCs also increased the stiffness of γAγ' fibrin clots which are less permeable and more resistant to lysis than γAγA clots. The modifications on clots promoted by RBCs-γAγ' fibrinogen interaction could alter the risk of thrombotic disorders.

Keywords: cell adhesion, atomic force microscopy, magnetic tweezers, fibrin clot, γ' fibrinogen.

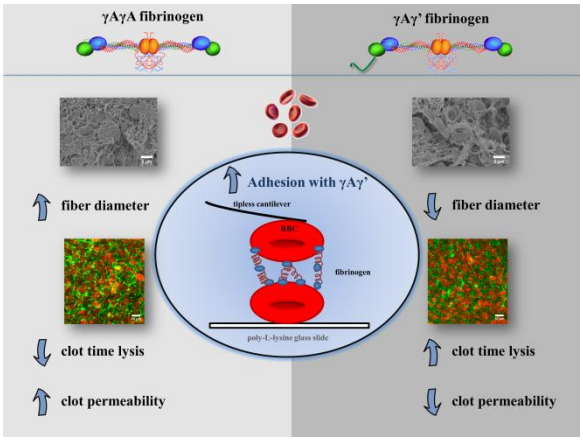

Graphical abstract description

Comparison of the interaction between red blood cells (RBCs) and γAγA or γAγ' fibrinogen. Schematic representation of the adhesion forces between two RBCs in the presence of γAγ' fibrinogen, which affects clot properties and function. Changes on fibrin network structure, decreased fiber diameter, increased fibrinolysis and decreased permeability by γAγ' fibrinogen-RBC interactions were encountered. The nanotechnology-based approach was essential to understand that the RBCs interact differently with clots made with γ' chain fibrinogen splice variant instead of the common variant, γA. This may explain some of the cardiovascular clinical associations that have been reported for γ' fibrinogen.

Introduction

Fibrinogen is a 340 kDa homodimeric plasma glycoprotein, composed of three pairs of polypeptide chains, denoted Aα, Bβ and γ, linked together by 29 disulphide bonds[1]. A common variant of the fibrinogen is produced by alternative splicing of mRNA of the γ-chain, called γ' fibrinogen[2]. The γ' isoform has a substitution of the final 4 carboxyl-terminal amino acid residues (AGDV) of the prevalent γA-chain with a different 20-amino acid residue sequence (VRPEHPAETEYDSLYPEDDL), which includes a high proportion of negatively charged residues and two sulfated tyrosines. This variant accounts for 8-15% of all plasma fibrinogen, largely in the form of the heterodimer γAγ', while the homodimer γ'γ' accounts for less than 1% of total plasma fibrinogen[3]. γ' fibrinogen has distinct biochemical and biophysical properties that distinguish it from the more common γA isoform[4-6]. Studies have highlighted that abnormal plasma levels of γAγ' fibrinogen are associated with thrombotic diseases, such as coronary artery disease[7], myocardial infarction[8] and stroke[9]. Elevated levels of γ' fibrinogen in patients with cardiovascular disease (CVD) were independent of the total plasma fibrinogen concentration[7]. This could indicate that the proportion of γ' variant in plasma may be a risk factor for cardiovascular pathologies. However, reduced concentrations have been associated with microangiopathy syndrome[10] and deep vein thrombosis[11]. Studies by Appiah *et al*. did not support the hypothesis that γ' fibrinogen influences CVD events through its prothrombotic properties. Rather, γ' fibrinogen concentrations seem to reflect general inflammation that accompanies and may contribute to atherosclerotic CVD, instead of γ' fibrinogen being a causal risk factor[12]. In addition to this, Walton *et al*. found that elevated levels of γAγA fibrinogen promoted arterial thrombosis *in vivo*, whereas γAγ' fibrinogen did not[13]. Nevertheless, as γ' chain modulates clot formation *in vitro*, further studies are required to elucidate its functional properties and its possible relationship with bleeding disorders or thrombosis.

The formation of a thrombus and subsequent impairment of blood flow to vital organs are the immediate cause of CVD events[14]. The architecture of the clot network affects clot stability, particularly its viscoelastic or mechanical properties and fibrinolytic characteristics[15, 16]. These aspects can determine if the clot is broken down by fibrinolysis

or if it will lead to occlusion or embolization[17]. Other studies have indicated the clinical relevance of fibrin clot structure. It has been shown that tightly packed and rigid clots with thinner fibers and low porosity are less susceptible to the action of thrombolytic agents[18, 19], and a prolonged clot lysis time has been associated with CVD events[20]. Several studies have shown that clots produced from γAγ' fibrinogen have a different structure and behave differently from γAγA clots[4-6]. Fibrin clots formed in the presence of the fibrinogen γ' variant are more resistant to fibrinolysis, due to reduced binding of plasminogen and tissue plasminogen activator, leading to reduced plasmin generation[21]. Fibrinogen γ' variant is associated with a heterogeneous, non-uniform clot structure, with more branch points than clots formed by γA chains[6, 22, 23]. In addition, γ' fibrinogen binds to thrombin exosite II[24]. The binding of thrombin to the γ' chain has been reported to modulate thrombin activity, particularly towards substrates that require exosite II interaction such as coagulation factors FV and FVIII (but not those dependent on exosite I interactions, e.g. fibrinogen and factor FXIII), which may influence clot structure[6]. However, some of the effects of γ' fibrinogen on clot structure have been shown to be independent of thrombin, as clots produced with snake venom enzyme ancrod, which cleaves fibrinopeptide A from fibrinogen but not fibrinopeptide B, show similar structural abnormalities as those produced with thrombin[22]. On the other hand, it has been shown that the high affinity binding of thrombin to γAγ'-fibrin protects thrombin from inhibition by antithrombin, raising the possibility that γAγ'-fibrin serves as a scavenger and reservoir for thrombin in the clot[25].

Fibrinogen is thought to contribute to CVD, not only through altering the fibrin network structure, but also through several other mechanisms, such as promoting red blood cell (RBC) aggregation[26]. Although several studies on isolated fibrin clots have been performed, *in vitro* experiments using fibrin blood clots containing RBCs are scarce in the literature. RBCs play a role in blood coagulation by increasing blood viscosity, which is associated with propensity for clot formation[27]. RBCs have been shown to interact specifically with fibrinogen, with *ca.* 20,000 binding sites *per* RBC and a dissociation constant, K_d, of approximately 1.3 μM[28]. We have identified a specific receptor for fibrinogen on the surface of RBCs[29-31].

Despite their significance in thrombosis and hemostasis, relatively few studies have been conducted to describe the effects of RBCs on blood clot structure, particularly with

different fibrinogen variants. One complication of studying RBC-rich thrombi is that incorporation of RBCs into a thrombus seems uncontrolled and variable. This scarcity may also be, in part, due to the fact that the presence of RBCs in a clot often interferes with the techniques available to monitor clot structure[32].

The present study aimed to investigate, through atomic force microscopy-based force spectroscopy, the adhesion of RBCs in the presence of γAγA or γAγ' fibrinogen variants. Moreover, we aimed to understand the effect of RBC-γAγ' fibrinogen interactions on fibrin clot structure, properties and function through scanning electron microscopy, laser scanning confocal microscopy, magnetic tweezers and permeability studies.

Methods

Purification of γAγA and γAγ' fibrinogen

The γAγA and γAγ' fibrinogen variants were purified from human plasminogen-depleted fibrinogen using anion-exchange chromatography (Millipore, Billerica, MA) as previously described[22,23]. Detailed description of the method can be found in Supplementary Material.

Human RBCs isolation

Blood from healthy donors was obtained, with written informed consent, at the Instituto Português do Sangue e da Transplantação (IPST, Lisbon) and at the University of Leeds. This study was approved by the joint Ethics Committee of Faculdade de Medicina da Universidade de Lisboa and Centro Hospitalar Lisboa Norte, and by the University of Leeds Medical School Ethical Committee. RBCs were isolated through standard procedures[29-31].

Atomic Force Microscopy (AFM) – *Cell-Cell adhesion*

AFM studies were performed on a NanoWizard II atomic force microscope with a CellHesion 200 module (JPK Instruments, Berlin, Germany), mounted on an Axiovert200 inverted optical microscope (Zeiss, Jena, Germany). RBCs were attached to tipless cantilevers through concanavalin A functionalization process (for details see Supplementary Material). RBCs on the substrate were adhered to poly-L-lysine coated glass slides. RBC-RBC adhesion was measured in the presence of different fibrinogen variants concentrations, from 0 to 1.0 mg/ml. Detailed description of the method can be found in Supplementary Material.

Magnetic tweezers

To examine the viscoelastic properties of the fibrin clots, magnetic tweezers were used. The magnetic microrheometer operates by applying a force of 40 pN to a 4.5 μm superparamagnetic bead (Dynabeads M-450 Epoxy, Invitrogen, Paisley, UK) using a

magnetic field gradient generated by four electromagnets in 2D directions. The device was used coupled with an Olympus IX71 inverted microscope (Olympus, UK) incorporating an ultralong working objective (40× magnification) and a CCD camera. Particle tracking, electromagnet control and image analysis were performed in real time using custom written Labview 7.1 software (National Instruments, Newbury, UK). Fibrin clots were formed with and without RBCs. The viscoelastic properties were measured using the procedure of Evans *et al*.[33]. The parameters G', G'' and Tan δ were calculated at a frequency of 0.1 Hz. The displacement of 8 random magnetic beads was measured *per* sample, and each sample was studied at least in triplicate. Please find detailed description in Supplementary Material.

Fibrin clot permeability

To study the clot permeability, samples were prepared in triplicate, according to the standardized protocol published by the Fibrinogen and FXIII Subcommittee of the International Society on Thrombosis and Hemostasis (ISTH)[34]. Purified fibrinogen samples (final concentration of 1 mg/ml) were incubated with 1 U/ml human thrombin (Calbiochem, Nottingham, UK) and 2.5 mM $CaCl_2$. Samples were placed in mechanically scratched open clotting tips for 120 min, at room temperature, in a humidity chamber. A detailed description of the method can be seen in Supplementary Material.

Scanning electron microscopy

Scanning electron microscopy (SEM) was used to further investigate the structure of clots formed with γAγA and γAγ' fibrinogen in the presence or in the absence of RBCs.

Clots were generated by adding 100 µl of γAγA or γAγ' fibrinogen variants (final concentration of 1 mg/ml) to 10 µl of activation mixture (human thrombin 1 U/ml and 10 mM $CaCl_2$, final concentrations, in TBS (50 mM Tris, 100 mM NaCl, pH 7.5)). All details of the procedure are described in Supplementary Material.

Laser scanning confocal microscopy

Fibrin clots were prepared according to the procedure described in Supplementary Material. Three random areas of the clot were visualized under higher magnification. 20 μm optical z-stacks were obtained and projected into 2D images. In order to obtain 3D images of the fibrin clots, 40 μm z-stacks were also performed. Confocal microscopy was also used to assess, in real time, the rate of fibrinolysis following the procedure also described in Supplementary Material.

Statistical Analysis

Descriptive statistics are given as mean ± standard error of mean (SEM). Unpaired Student's *t*-test was used for statistical analysis of comparisons between two groups. Non-parametric analysis was also performed in cell-cell adhesion data, applying the Mann Whitney U test. *P*-values below 0.05 were considered to indicate statistical significance. Statistical analyses were performed using GraphPad Prism 5 (La Jolla, CA, USA).

Results

RBC-RBC adhesion is altered in the presence of fibrinogen variants

Atomic force microscopy (AFM) experiments were performed to investigate RBC cell-cell adhesion and the influence of γAγ' and γAγA fibrinogen variants in the cells adhesion. We evaluated the interaction between RBCs, in the presence of different concentrations of γAγA and γAγ' fibrinogen variants, up to 1.0 mg/ml, by force-distance retract curves (Figure 1).

Force spectroscopy data showed that, in the presence of low concentrations of γAγ' fibrinogen, the work (thermodynamic parameter corresponding to the area under the curve on a force × distance plot, Figure 1B) required to detach one RBC from another was higher than in the presence of the same concentration of γAγA fibrinogen (0.87 ± 0.07 fJ *vs.* 0.55 ± 0.04 fJ, $p = 0.0275$, for 0.1 mg/ml fibrinogen, and 1.03 ± 0.06 fJ *vs.* 0.65 ± 0.07 fJ, $p < 0.0001$, for 0.4 mg/ml fibrinogen) (Figure 1C). At higher concentrations of fibrinogen variants, statistically significant differences between both variants were not observed (for 1.0 mg/ml fibrinogen, 0.71 ± 0.05 fJ for γAγ' *vs.* 1.10 ± 0.13 fJ for γAγA, $p = 0.144$; for 0.7 mg/ml fibrinogen, 0.57 ± 0.07 fJ for γAγ' *vs.* 0.86 ± 0.04 fJ for γAγA, $p = 0.248$). γAγA fibrinogen concentrations showed a clear dose-response for interactions with RBCs, whereas γAγ' had a dual effect at low and high concentrations (Figure 1C). Values of the maximum detachment force (schematically explained in Figure 1B) were also calculated. As shown on Figure 1D, statistically significant differences between the values of maximum RBC-RBC detachment force in the presence of γAγ' or γAγA fibrinogen were found at all fibrinogen concentrations: for 0.1 mg/ml fibrinogen, 141.8 ± 17.2 pN for γAγA *vs.* 173.6 ± 0.85 pN for γAγ', $p = 0.0279$; for 0.4 mg/ml fibrinogen, 246.3 ± 5.64 pN for γAγA *vs.* 203.7 ± 0.70 pN for γAγ', $p < 0.0001$; for 0.7 mg/ml fibrinogen, 141.2 ± 5.35 pN for γAγA *vs.* 170.3 ± 0.95 pN for γAγ', $p < 0.0001$; and, for 1 mg/ml fibrinogen, 182.9 ± 9.80 pN for γAγA *vs.* 205.5 ± 1.90 pN for γAγ', $p = 0.0054$). With the exception of the data obtained for 0.4 mg/ml fibrinogen, the values of maximum detachment force obtained for γAγA fibrinogen were always lower than those of γAγ' fibrinogen.

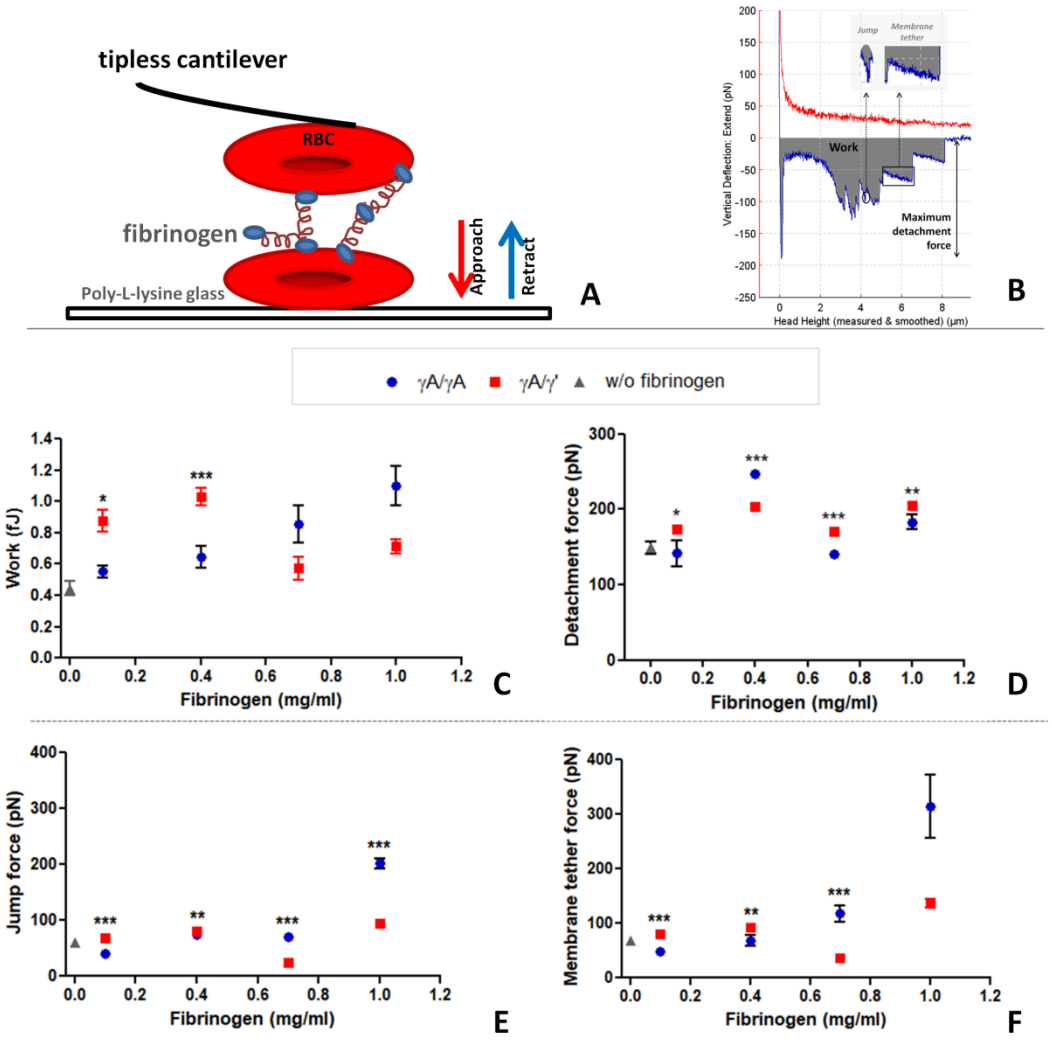

Figure 1 | **AFM cell-cell adhesion data**. A) Schematic representation of the adhesion between two RBCs (one chemically attached to the cantilever and the other on the poly-L-lysine-treated substrate) in the presence of fibrinogen variants. B) Representative force-distance curve with the relevant analyzed parameters, namely, work of cell-cell detachment (grey area), maximum detachment force, jumps and membrane tethers (insets magnify examples of a jump and a membrane tether event on the force-distance curve). C) Work necessary to overcome RBC-RBC adhesion in the presence of different concentrations of γAγA or γAγ' fibrinogen (*, $p = 0.0275$; ***, $p < 0.0001$). D) Maximum detachment force values to detach two RBCs (*, p = 0.0279; **, $p = 0.0054$; ***, $p < 0.0001$). E) Jumps and F) membrane tethers force data (**, $p \leq 0.0069$; ***, $p < 0.0001$) in the presence of each fibrinogen variant or in their absence. Values are presented as mean ± standard error of mean (SEM).

After the initial maximum detachment force, two types of jumps could be observed on the force curves (Figure 1B): jumps preceded by a ramp of force or jumps preceded by a force plateau. We considered a membrane tether as a step in force detected after a force plateau of 0.25 µm in distance. Jump events were assigned to the unbinding of membrane ligand-receptor interactions without a preceding membrane deformation, while membrane tether events corresponded to situations where a membrane tether was extruded before the unbinding of the ligand-receptor complex (Figure 1B)[35]. A combination of each of the parameters extracted from the force-distance curves (maximum detachment force, number of jumps events/curve × mean force of jumps and number of membrane tethers events × mean force of tethers) could be considered as the value of the work needed to detach one cell from another. Similarly to the values of work (Figure 1C), the same profile is observed for the values of force of jumps and membrane tethers events with increasing fibrinogen concentrations when comparing both fibrinogen variants. As depicted in Figure 1E, F, at lower fibrinogen concentrations, jumps and membrane tethers displayed higher forces for γAγ' fibrinogen, when compared to γAγA variant, both for 0.1 mg/ml fibrinogen (jumps, 68.52 ± 2.42 pN *vs.* 40.40 ± 0.80 pN, $p < 0.0001$; membrane tethers, 79.80 ± 7.06 pN *vs.* 47.56 ± 3.37 pN, $p < 0.0001$) and 0.4 mg/ml fibrinogen (jumps, 80.82 ± 3.45 pN *vs.* 74.94 ± 3.31 pN, $p = 0.0061$; membrane tethers, 91.91 ± 6.32 pN *vs.* 68.08 ± 9.69 pN, $p = 0.0069$). Figure 1E, F also shows that, at higher fibrinogen concentrations, similarly to the values of work, higher forces of jumps and membrane tethers were measured for γAγA fibrinogen, when compared to the γAγ' variant. This becomes evident at 0.7 mg/ml of fibrinogen (jumps, 70.94 ± 4.36 pN *vs.* 24.01 ± 0.77 pN, $p < 0.0001$; membrane tethers, 117.75 ± 14.64 pN *vs.* 36.47 ± 5.13 pN, $p < 0.0001$) and at 1.0 mg/ml of fibrinogen (jumps, 201.51 ± 8.54 pN *vs.* 93.41 ± 2.85 pN, $p < 0.0001$; membrane tethers, 313.95 ± 58.05 pN *vs.* 135.51 ± 7.98 pN, $p > 0.05$).

RBCs influence γAγ' fibrin clot mechanical properties

The viscoelastic properties of γAγA and γAγ' fibrin clots were examined using a magnetic microrheometer and the influence of RBCs was studied. In agreement with

previous findings[22], we observed that γAγA clots were stiffer than γAγ' (storage modulus G' 1.076 ± 0.065 Pa *vs.* 0.512 ± 0.051 Pa, respectively; $p < 0.0001$) (Figure 2).

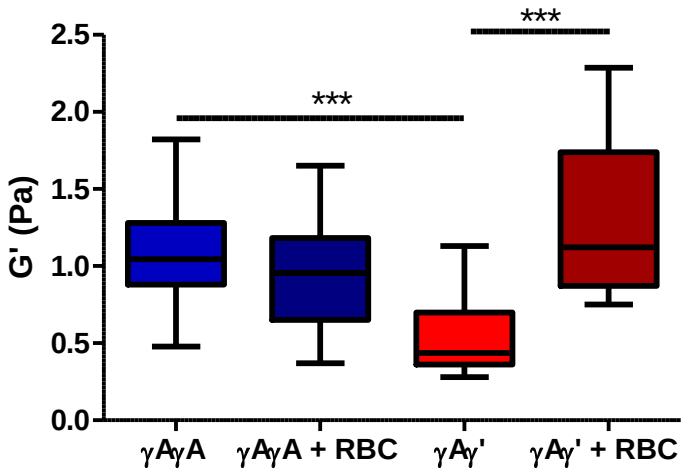

Figure 2 | **Viscoelastic properties of the purified γAγA and γAγ' fibrinogen clots**. Storage modulus G' (elastic modulus) data are presented in the presence of 0.5% RBCs and in the absence of RBCs (***, $p < 0.0001$ for γAγA *vs*. γAγ' and for γAγ' *vs.* γAγ' + RBC). Fibrinogen concentration was 0.5 mg/ml. Values are presented as mean ± SEM.

The presence of RBCs in the γAγA fibrin clots did not statistically change their stiffness. On the other hand, a significant increase in the stiffness of γAγ' clots was observed in clots with RBCs, when compared to those without RBCs (1.220 ± 0.104 Pa *vs.* 0.512 ± 0.051 Pa, respectively; $p < 0.0001$). There were no significant differences on storage modulus G' between γAγA and γAγ' clots in the presence of RBCs; however, there was a trend for the γAγ' clots to be stiffer than γAγA clots (Figure 2).

In addition, we observed a statistically significant change on loss tangent (Tan δ) comparing γAγA clots with RBCs and without RBCs (0.460 ± 0.066 *vs.* 1.013 ± 0.126, respectively; $p = 0.0008$), but only a trend for higher Tan δ in γAγ' with RBCs than for this variant in the absence of RBCs (data not shown).

RBCs reduce γAγ' fibrin clot permeability

To characterize the fibrin network of γAγA and γAγ' fibrin with and without RBCs, permeability experiments were performed. The results for the Darcy constant (K_s), which represent the pore size of the fibrin clot, are shown in Figure 3.

Importantly, in the presence of RBCs, normalized K_s was higher for γAγA fibrin clots with RBCs ((2.44 ± 0.31) × 10^{-9}cm^2) than for γAγ' fibrin clot with RBCs ((1.40 ± 0.10) × 10^{-9}cm^2) (p = 0.0001). Thus, when comparing clots of both fibrinogen variants with RBCs, the γAγ' clots were less porous.

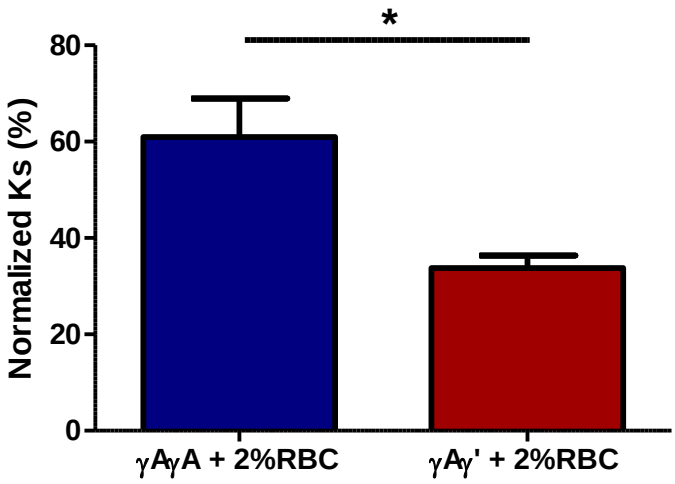

Figure 3 | **Normalized permeability data (normalized in percentage against K_s of each variant without RBCs) in the presence of RBCs for fibrin clots formed with purified γAγA or γAγ' fibrinogen**. Darcy constant, K_s, represents the average size of the pores within the clot (*, p = 0.0319). Values are presented as mean ± SEM.

RBCs influence γAγA and γAγ' fibrin clot structure

Scanning electron microscopy data showed differences between the structures of the fibers formed by γAγA or γAγ' fibrinogen (different magnification micrographs from each sample are shown in Figure S1 in the supplementary information).

We next investigated the structure of clots formed *in vitro* in the presence of RBCs to determine the effect that these cells might have on clot structure *in vivo*. RBCs tended to be heterogeneously spread throughout the sample, particularly in clots produced with

γAγ' fibrin (Figure 4). Upon the addition of 20% RBCs, the structure of the γAγ' clot became more heterogeneous, with densely packed fiber regions, as well as, large holes where more RBCs were located (Figure 4B, D, F). γAγ' fibrin fibers were thinner and the network of the clot showed more interconnections with RBCs compared to γAγA fibers. On the micrographs of Figure 4B, D and F, it can be noticed that γAγ' fibrin clots contained more free fiber ends and there were more fiber-to-RBC points of connections, when compared to γAγA fibrin clots (Figure 4A, C, E) resulting in "clustered" cell arrangements.

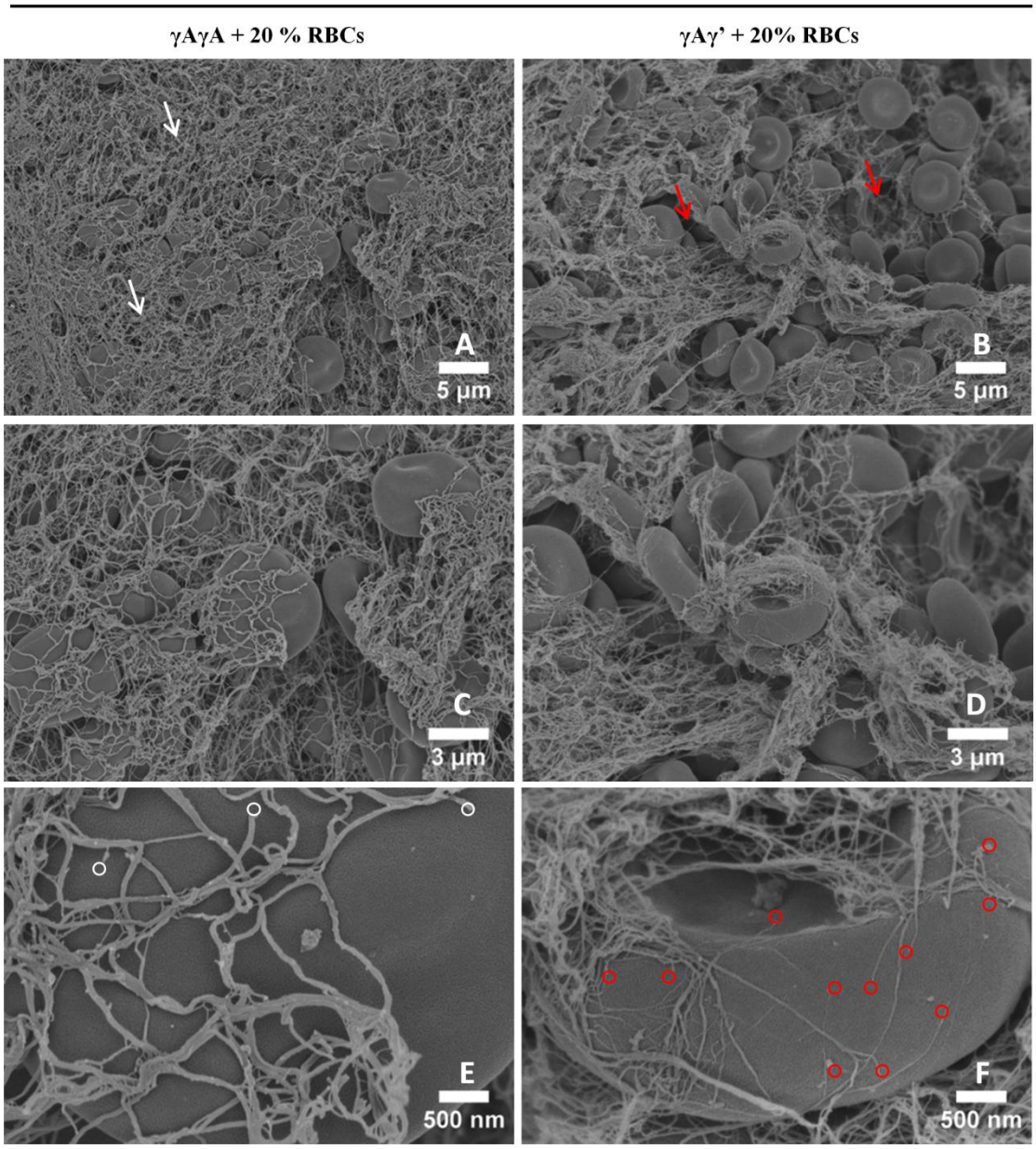

Figure 4 | Scanning electron micrographs of fibrin fiber clots with 20% of RBCs. Fibers were formed from 1.0 mg/ml fibrinogen variants γAγA (A, C and E) and γAγ' (B, D and F). White arrows in A indicate the more homogeneous structure in the γAγA clot

network, when compared with the areas of small and large holes, pinpointed by red arrows in B, associating a more heterogeneous structure to the γAγ' clots. The free fiber ends and the fiber-to-RBC points of connections are represented as small circles, being more frequent for γAγ' (red circles in F) than for γAγA (white circles in E). Magnifications: A and B, 2500×; C and D, 5000×; E and F, 25000×.

In order to measure the diameter of the fibers, twenty fibers from 50000× magnification images were assessed on 2 different clots from each condition and in 3 different zones of the clot. Average fiber diameters were smaller in γAγ' fibrin compared to the γAγA variant (18.29 ± 1.32 nm *vs.* 41.10 ± 1.58 nm; $p < 0.0001$) (Figure 5). The presence of RBCs in the fibrin clot caused a decrease of the γAγA fibers diameters compared to the clot without RBCs (41.10 ± 1.58 nm in the absence of RBCs *vs.* 35.39 ± 2.46 nm in the presence of RBCs; $p = 0.044$) (Figure 5). The presence of RBCs on clots with γAγ' fibers did not statistically change the diameter of the fibers compared to the clots without cells. However, clots with RBCs and prepared with γAγ' fibrinogen led to thinner fibers than those produced with γAγA fibrinogen and RBCs (35.39 ± 2.46 nm for γAγA*vs.*15.23 ± 0.98 nm for γAγ'; $p < 0.0001$) (Figure 5).

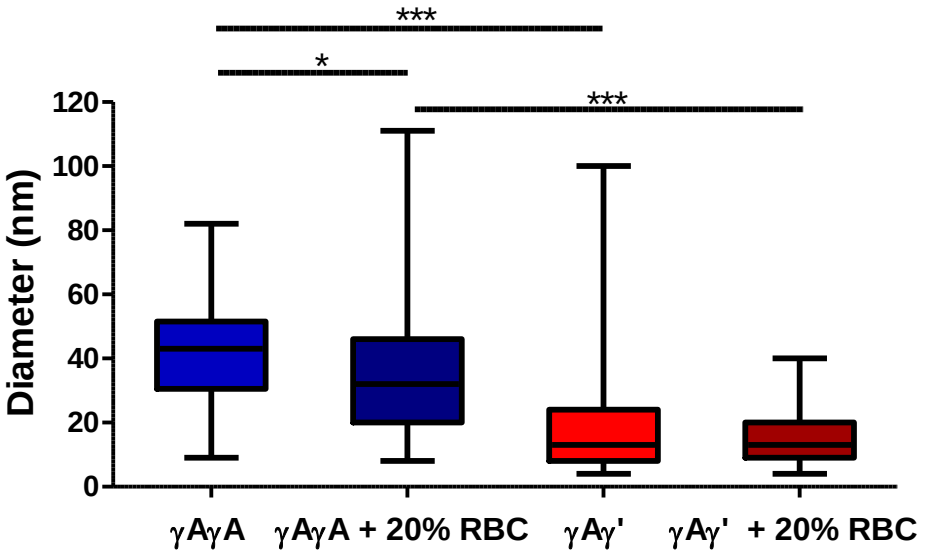

Figure 5 | Diameters of purified γAγA and γAγ' fibrin fibers in the absence or in the presence of 20% of RBCs. Fiber diameters were measured from 20 random fibers of each image using a 50000× magnification (*, $p = 0.0439$; ***, $p < 0.0001$).

Increased fibrinolytic resistance of γAγ' fibrin clots in the presence of RBCs

We used laser scanning confocal microscopy (LSCM) to study clot structure and resistance to fibrinolysis in the presence and absence of RBCs for each fibrin variant.

Figure 6 shows representative examples of the confocal micrographs obtained for fiber clots made with γAγA and γAγ' purified fibrinogen variants. In clots formed with γAγA fibrinogen, the area occupied by the fibers seems to be larger (Figure 6A) than for the clots with γAγ' fibrinogen (Figure 6B).

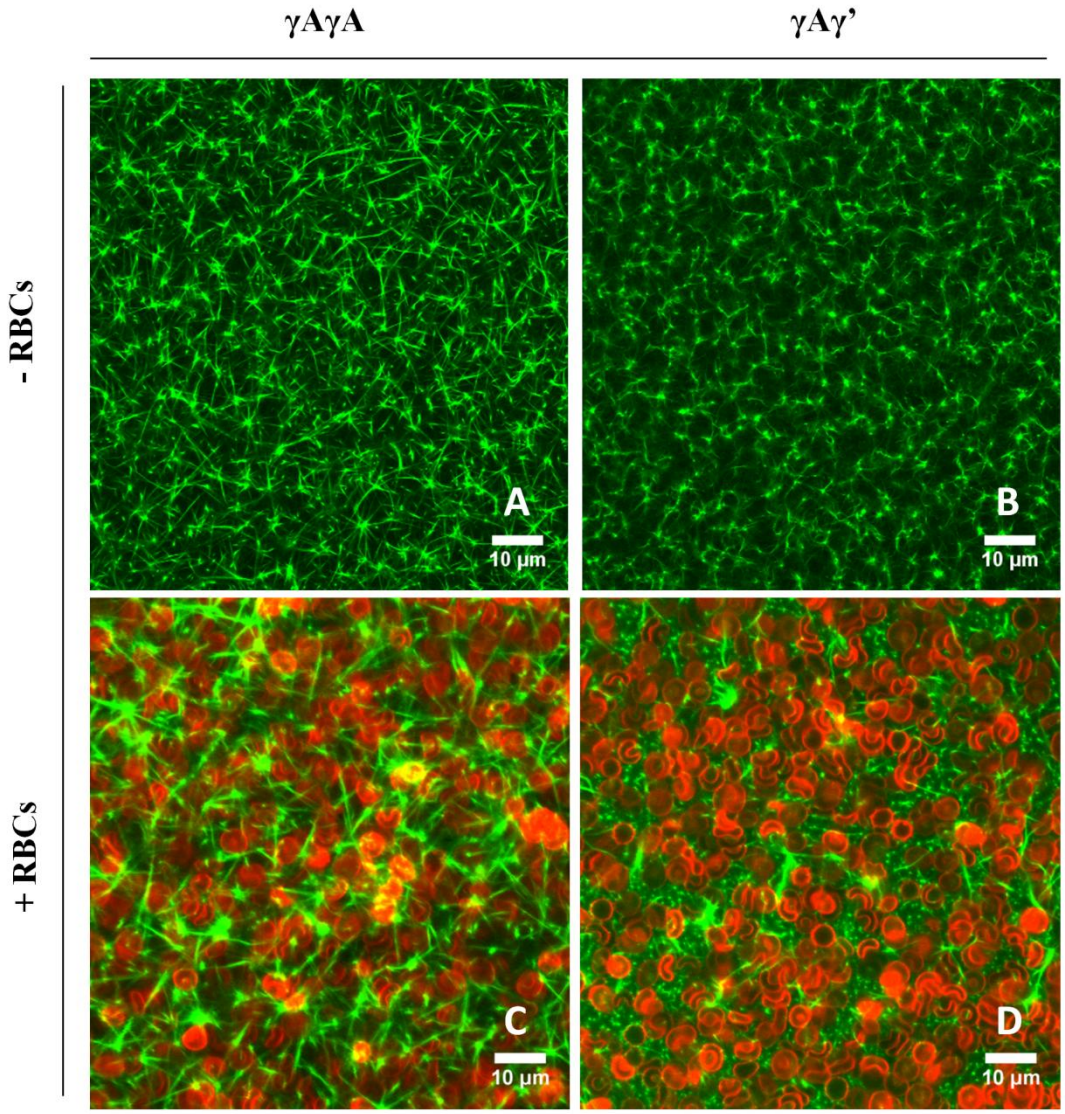

Figure 6 | Laser scanning confocal microscopy images of fiber clots formed with purified γAγA (A and C) and γAγ' (B and D) fibrinogen, at 1.0 mg/ml fibrinogen concentration. Alexa 488-labelled fibrin fibers are shown in green. Confocal micrographs of fiber clots with 2% of RBCs formed with 1.0 mg/ml of purified γAγA (C) and γAγ'

fibrinogen (D). RBCs were labeled with Vibrant DiD cell-labeling solution (red). Z-stack images at 40 µm and 63× magnification are shown in panel A and B and Z-stacks images at 20 µm, also with 63× magnification are shown in panel C and D.

However, these differences were not statistically significant. In agreement with SEM imaging and with previous studies[22], there was a clear difference between the structures of γAγA and γAγ' fibrin. The γAγA fibrin clots were composed of longer and straighter fibers than γAγ' fibrin clots. The later showed fibers that were shorter and clustered, producing larger pores. However, we did not find differences regarding the fiber density comparing γAγA with γAγ' fibrin clots (Figure S2 in Supplementary information).

Relevant was to study the micrographs of fibrin clots from γAγA and γAγ' fibrinogen variants in the presence of 2% of RBCs as shown on Figure 6 (C, D). In the presence of γAγA fibrinogen, the network of the fibers seemed straighter and denser. In clots with γAγ' fibers, we observed that the fibers were more clustered and the RBCs were more visible. We also studied fibrin clots in the presence of 5% and 10% of RBCs by LSCM; however, the high number of RBCs did not allow clearly differentiating fibrin fibers from RBCs. Thus, technical limitations restricted us to increase the amount of RBCs closer to the physiological range (the normal hematocrit is ~40% RBCs).

Finally, we studied fibrinolysis of clots made with both fibrinogen variants (Figure 7). In line with previous studies[21], a significant increase in lysis time was observed for γAγ' compared with γAγA fibrin clots (15.82 ± 1.48 min *vs.* 10.54 ± 0.44 min, respectively; p = 0.0267). During the experiment, we observed a non-uniform lysis of the γAγ' fibrin clot, taking more time to achieve complete lysis than the γAγA clot (videos in Supplementary information).

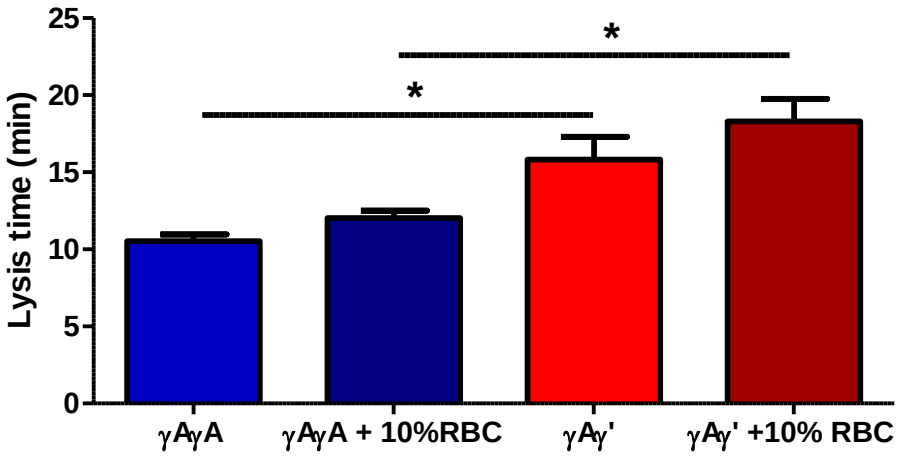

Figure 7 | **Fibrinolysis time were assessed by laser scanning confocal microscopy from clots formed with purified γAγA and γAγ' fibrinogen, in the absence and presence of RBCs (10%)**. The serial time scans were taken with 40× magnification. Values are shown as mean ± SEM (*, $p \leq 0.0476$).

We measured the lysis time for γAγA and γAγ' clots in the presence of 5% (data not shown) and 10% of RBCs. Under these conditions, there were no significant differences in fibrinolysis times in the presence of RBCs, when compared to the clots without RBCs. Statistical significance was observed in fibrinolysis times for γAγA *vs.* γAγ' fibrin clots in the presence of RBCs (12.03 ± 0.49 min *vs.* 18.30 ± 1.47 min; $p = 0.0476$).

Discussion

In this study, we evaluated the interaction of purified γAγ' and γAγA fibrinogen with RBCs, as well as their influence on the structure and function of clots formed with both variants. They show a discernible effect of the presence of RBCs on fibrin clot structure and function. To pursue this study further, we purified the main component of plasma fibrinogen, γAγA, and its splice-variant, γAγ'. Cell-cell adhesion studies were performed to evaluate the relative roles of both fibrinogen variants on the interaction between RBCs. We also evaluated the changes of biophysical properties of the clots, by studying their permeability and viscoelastic properties. By laser scanning confocal microscopy and scanning electron microscopy, we directly observed the effects of RBCs on the architecture of clots formed from γAγ' and γAγA fibrinogens.

AFM data showed that in the presence of low concentrations of γAγ' fibrinogen (≤ 0.4 mg/ml), the force of the binding between two RBCs was higher than with γAγA fibrinogen. Statistically significant differences between both fibrinogen variants at all fibrinogen concentrations were obtained for the values of force for the maximum cell-cell detachment, jumps and membrane tether events. Although these three parameters contribute to the values of the work necessary to completely detach two RBCs, no statistically significant variations were obtained for this parameter at fibrinogen concentrations ≥ 0.7 mg/mL.

Thus, at lower fibrinogen concentrations, γAγ' fibrinogen binds more promptly to RBCs, inducing higher RBC-RBC adhesion than γAγA fibrinogen. RBCs adhesion has a clear γAγA fibrinogen dose response curve, whereas γAγ' did not. This could be due to differences in fibrinogen variant molecular conformations and net protein electrostatic charge, which could lead to different binding affinities at different fibrinogen concentrations. It is known that RBCs present sialic acid residues on their surface, contributing to their negative surface charge, which induces repulsive electrostatic forces that minimize RBC aggregation under blood flow conditions[36]. The binding of the more negatively charged γ' fibrinogen to RBCs may increase the overall negative cell surface charge. This may overcome the strong RBC-RBC interactions observed at lower γAγ' fibrinogen concentration, by lowering cell-cell adhesion forces, due to increased electrostatic repulsion. On the other hand, γAγA fibrinogen lacks the negatively charged

sequence of the γ' chain, leading to an increase of RBC-RBC adhesion upon increasing its concentration.

Previous studies have shown that RBCs influence the viscoelastic properties of the clot[32, 37]. Our evaluation of the viscoelastic properties of the clots revealed that γAγA fibrin clots are stiffer than γAγ' fibrin clots in the absence of RBCs, in agreement with previous studies on the effect of γAγ' on clot stiffness[22]. Our data shows that γAγ' clots are inherently weaker. This is likely due to differences in fibrin fiber structure. We recently demonstrated that fibrinogen γ' influences intrafibrillar structure of fibrin and significantly reduces the average number of protofibrils packed within the fibrin fiber, thereby influencing clot stiffness[38]. In γAγA fibrin clots, more protofibrils are packed within fibrin fibers, which increases the rigidity and the viscosity of the clot, when compared to γAγ' fibrin clots. In this study, the presence of RBCs did not influence the stiffness of the γAγA fibrin clots. In γAγ' fibrin clots, the presence of RBCs resulted in a significant increase in stiffness. This indicates that the combination of γAγ' fibrinogen variant and RBCs may affect clot structure and mechanical properties. The stiffening of the γAγ' fibrin clots in the presence of RBCs may be related to rearrangements of protofibril packing or significant modifications in clot structure. The imaging by SEM of the clot structure in the presence of RBCs, compared to its absence, showed a looser structure in clots produced with γAγ' fibrinogen, which may be more prone to creep, as well as more fiber interconnections, which turn the clot more rigid. Our data indicates that RBCs are not a mere bystander in blood clot formation. Indeed, other studies have shown that RBCs influence fibrin network structure and pore size[39, 40]. A decrease in the permeability of fibrin clots after the addition of RBCs was shown to be proportional to the total RBC surface area and their total concentration[40]. Here, we show that the addition of RBCs promotes the decrease of permeability. Importantly, we show that the γAγ' clots with RBCs were less porous than γAγA clots with RBCs. This could potentially lead to pro-thrombotic clots, due to a higher resistance to fibrinolysis[41]. In agreement with this, we also found an increase in the lysis time of γAγ' clots with RBCs, when compared to γAγA clots with RBCs.

According with previous studies[22, 23], SEM and confocal microcopy showed that the clots formed by γAγA and γAγ' fibers have a different structure. The incorporation of RBCs has an important impact on fibrin fiber size and on its network structure. Regions of

higher and lower RBC density were clearly visible in the clots made with γ' fibrinogen. In the presence of RBCs, the γ' fibrin clots were more heterogeneous, seeming to form a looser structure when compared with the clots of γA fibrinogen. These findings are supported by our AFM data. At high γAγ' fibrinogen concentrations, the work necessary to detach two RBCs was the same that the one achieved in the presence of γAγA fibrinogen. In agreement with this, the clot might become looser, with a higher ability to deform and embolise, eventually blocking a downstream blood capillary.

The γAγ' fibrin clots contain a large number of free fiber ends. Fiber ends are normally found at low levels in scanning electron micrographs of fibrin clots, and have been suggested to arise from early truncation of protofibril formation or lateral aggregation[42, 43]. It was previously proposed that the negative charge of γAγ' fibrinogen on the D-D interface may disrupt oligomerization and, therefore, interrupt the continuous growth of the protofibril, leading to highly branched fibers[44, 45].

This study has shown that the incorporation of RBCs into the clot affects fibrin fiber formation. RBCs induced thinning of fibers in fibrin clots formed with γAγA, but not with γAγ' fibrinogen. However, in the presence of RBCs, γAγA fibers remained significantly thicker than γAγ' fibers. Here, we could conclude that thinner fibrin fibers (such as γAγ' fibrin fibers) form highly branched networks. We propose that growing fibers surround RBCs, interacting with them through an RBC surface receptor. We have already reported the existence of a receptor for fibrinogen on RBCs[29-31]: RBCs specifically bind fibrin(ogen) via an integrin receptor with a β_3 subunit[29], possibly $\alpha_v\beta_3$[31].

Previous studies indicated that fibrin clots with increased fiber branching and resistance to fibrinolysis are a risk factor for thrombosis[15]. Fibrinolysis data showed that the lysis time of a γAγ' fibrin clot is longer than for a γAγA clot, as already reported[4, 5]. The presence of RBCs seems to increase the lysis time. However these studies were conducted with a 10% hematocrit, due to technical limitations, considerably below the normal hematocrit of ~40% RBCs. Aleman *et al*. and Tutwiler *et al*. suggested that RBCs cause direct and complex effects on clot structure and stability[46, 47]. Furthermore, RBCs can support thrombin generation and decrease fibrinolysis, suggesting that RBCs may promote fibrin deposition during venous thrombosis[46]. Other authors reported the role of RBCs on stabilizing clots based on suppressed tissue plasminogen activator (tPA)-induced fibrinolysis in RBC-modified fibrin structures. They also observed, using eptifibatide

inhibition, that RBCs modulate fibrinolysis through a specific fibrinogen receptor[41]. Collet *et al.* demonstrated that fibrin clots with a tight fibrin conformation made of thinner fibers were lysed at a slower rate than those with a loose fibrin conformation made of thicker fibers, although the overall fibrin content remained constant[48]. The γAγ' clot is more heterogeneous than the γAγA clot. The densely packed areas with fibers and RBCs may impair the diffusion of fibrinolytic agents. However, at the same time, there are areas with large holes, where their diffusion may be increased. It was suggested that the slower lysis of γ' clots is due to delayed fibrinopeptide B release, leading to a delay of plasminogen binding and activation[21].

Some of these findings may provide a mechanism underpinning the epidemiological data suggesting that a high ratio between γAγ' and γAγA fibrinogen variants may be a risk factor for thrombotic disease[7-9]. Further studies on the prothrombotic nature of RBCs and on fibrinogen variants are necessary to fully understand the contribution of the γ' chain and RBCs to different etiologies of thrombotic diseases.

In conclusion, the incorporation of RBCs into a fibrin clot significantly affects the clot structure and its mechanical properties. RBCs interact differently with clots made with γ-chain fibrinogen splice variants, which may explain some of the cardiovascular clinical associations that have been reported with these fibrinogen variants.

Abbreviations

γ', gamma prime fibrinogen; AFM, atomic force microscopy; γA, the most common fibrinogen variant; RBCs, red blood cells; CVD, cardiovascular diseases; FXIII, factor XIII; SEM, scanning electron microscopy, LSCM, laser scanning confocal microscopy.

Funding

This work was supported by Fundação para a Ciência e a Tecnologia – Ministério da Ciência, Tecnologia e Ensino Superior (FCT-MCTES, Portugal; PTDC/QUI-BIQ/119509/2010, PTDC/BBB-BMD/6307/2014 and SFRH/BD/84414/2012), the British Heart Foundation (RG/13/3/30104) and the Garfield Weston Trust.

Conflicts of interest

The authors have no conflicts of interest to disclose.

References of Chapter II

1. Brown, J.H., Volkmann, N., Jun, G., Henschen-Edman, A.H. & Cohen, C. The crystal structure of modified bovine fibrinogen. *Proc Natl Acad Sci USA* **97**, 85-90 (2000).
2. Chung, D.W. & Davie, E.W. gamma and gamma' chains of human fibrinogen are produced by alternative mRNA processing. *Biochemistry* **23**, 4232-6 (1984).
3. Mosesson, M.W., Finlayson, J.S. & Umfleet, R.A. Human fibrinogen heterogeneities. 3. Identification of chain variants. *J Biol Chem* **247**, 5223-7 (1972).
4. Collet, J.P., Nagaswami, C., Farrell, D.H., Montalescot, G. & Weisel, J.W. Influence of gamma' fibrinogen splice variant on fibrin physical properties and fibrinolysis rate. *Arterioscler Thromb Vasc Biol* **24**, 382-6 (2004).
5. Falls, L.A. & Farrell, D.H. Resistance of gammaA/gamma' fibrin clots to fibrinolysis. *J Biol Chem* **272**, 14251-6 (1997).
6. Siebenlist, K.R., Mosesson, M.W., Hernandez, I., Bush, L.A., Di Cera, E., Shainoff, J.R., Di Orio, J.P. & Stojanovic, L. Studies on the basis for the properties of fibrin produced from fibrinogen-containing gamma' chains. *Blood* **106**, 2730-6 (2005).
7. Lovely, R.S., Falls, L.A., Al-Mondhiry, H.A., Chambers, C.E., Sexton, G.J., Ni, H. & Farrell, D.H. Association of gammaA/gamma' fibrinogen levels and coronary artery disease. *Thromb Haemost* **88**, 26-31 (2002).
8. Mannila, M.N., Lovely, R.S., Kazmierczak, S.C., Eriksson, P., Samnegard, A., Farrell, D.H., Hamsten, A. & Silveira, A. Elevated plasma fibrinogen gamma' concentration is associated with myocardial infarction: effects of variation in fibrinogen genes and environmental factors. *J Thromb Haemost* **5**, 766-73 (2007).
9. Cheung, E.Y., Uitte de Willige, S., Vos, H.L., Leebeek, F.W., Dippel, D.W., Bertina, R.M. & de Maat, M.P. Fibrinogen gamma' in ischemic stroke: a case-control study. *Stroke* **39**, 1033-5 (2008).
10. Mosesson, M.W., Hernandez, I., Raife, T.J., Medved, L., Yakovlev, S., Simpson-Haidaris, P.J., Uitte de Willige, S. & Bertina, R.M. Plasma fibrinogen gamma' chain content in the thrombotic microangiopathy syndrome. *J Thromb Haemost* **5**, 62-9 (2007).

11. Uitte de Willige, S., de Visser, M.C., Houwing-Duistermaat, J.J., Rosendaal, F.R., Vos, H.L. & Bertina, R.M. Genetic variation in the fibrinogen gamma gene increases the risk for deep venous thrombosis by reducing plasma fibrinogen gamma' levels. *Blood* **106**, 4176-83 (2005).
12. Appiah, D., Schreiner, P.J., MacLehose, R.F. & Folsom, A.R. Association of Plasma gamma' Fibrinogen With Incident Cardiovascular Disease: The Atherosclerosis Risk in Communities (ARIC) Study. *Arterioscler Thromb Vasc Biol* **35**, 2700-6 (2015).
13. Walton, B.L., Getz, T.M., Bergmeier, W., Lin, F.C., Uitte de Willige, S. & Wolberg, A.S. The fibrinogen gammaA/gamma' isoform does not promote acute arterial thrombosis in mice. *J Thromb Haemost* **12**, 680-9 (2014).
14. Fuster, V., Moreno, P.R., Fayad, Z.A., Corti, R. & Badimon, J.J. Atherothrombosis and high-risk plaque: part I: evolving concepts. *J Am Coll Cardiol* **46**, 937-54 (2005).
15. Undas, A. & Ariëns, R.A. Fibrin clot structure and function: a role in the pathophysiology of arterial and venous thromboembolic diseases. *Arterioscler Thromb Vasc Biol* **31**, e88-99 (2011).
16. Weisel, J.W. Structure of fibrin: impact on clot stability. *J Thromb Haemost* **5**, 116-24 (2007).
17. Weisel, J.W. The mechanical properties of fibrin for basic scientists and clinicians. *Biophys Chem* **112**, 267-76 (2004).
18. Collet, J.P., Soria, J., Mirshahi, M., Hirsch, M., Dagonnet, F.B., Caen, J. & Soria, C. Dusart syndrome: a new concept of the relationship between fibrin clot architecture and fibrin clot degradability: hypofibrinolysis related to an abnormal clot structure. *Blood* **82**, 2462-9 (1993).
19. Bridge, K.I., Philippou, H. & Ariëns, R. Clot properties and cardiovascular disease. *Thromb Haemost* **112**, 901-8 (2014).
20. Carter, A.M., Cymbalista, C.M., Spector, T.D. & Grant, P.J. Heritability of clot formation, morphology, and lysis: the EuroCLOT study. *Arterioscler Thromb Vasc Biol* **27**, 2783-9 (2007).
21. Kim, P.Y., Vu, T.T., Leslie, B.A., Stafford, A.R., Fredenburgh, J.C. & Weitz, J.I. Reduced plasminogen binding and delayed activation render gamma'-fibrin more resistant to lysis than gammaA-fibrin. *J Biol Chem* **289**, 27494-503 (2014).

22. Allan, P., Uitte de Willige, S., Abou-Saleh, R.H., Connell, S.D. & Ariëns, R.A. Evidence that fibrinogen gamma' directly interferes with protofibril growth: implications for fibrin structure and clot stiffness. *J Thromb Haemost* **10**, 1072-80 (2012).
23. Cooper, A.V., Standeven, K.F. & Ariëns, R.A. Fibrinogen gamma-chain splice variant gamma' alters fibrin formation and structure. *Blood* **102**, 535-40 (2003).
24. Lovely, R.S., Moaddel, M. & Farrell, D.H. Fibrinogen gamma' chain binds thrombin exosite II. *J Thromb Haemost* **1**, 124-31 (2003).
25. Fredenburgh, J.C., Stafford, A.R., Leslie, B.A. & Weitz, J.I. Bivalent binding to gammaA/gamma'-fibrin engages both exosites of thrombin and protects it from inhibition by the antithrombin-heparin complex. *J Biol Chem* **283**, 2470-7 (2008).
26. de Moerloose, P., Boehlen, F. & Neerman-Arbez, M. Fibrinogen and the risk of thrombosis. *Semin Thromb Hemost* **36**, 7-17 (2010).
27. Schmid-Schönbein, H., Wells, R. & Goldstone, J. Influence of deformability of human red cells upon blood viscosity. *Circ Res* **25**, 131-43 (1969).
28. Lominadze, D., Dean, W.L., Tyagi, S.C. & Roberts, A.M. Mechanisms of fibrinogen-induced microvascular dysfunction during cardiovascular disease. *Acta Physiol* **198**, 1-13 (2010).
29. Carvalho, F.A., Connell, S., Miltenberger-Miltenyi, G., Pereira, S.V., Tavares, A., Ariëns, R.A. & Santos, N.C. Atomic force microscopy-based molecular recognition of a fibrinogen receptor on human erythrocytes. *ACS Nano* **4**, 4609-20 (2010).
30. Carvalho, F.A., de Oliveira, S., Freitas, T., Gonçalves, S. & Santos, N.C. Variations on fibrinogen-erythrocyte interactions during cell aging. *PLoS One* **6**, e18167 (2011).
31. Guedes, A.F., Carvalho, F.A., Malho, I., Lousada, N., Sargento, L. & Santos, N.C. Atomic force microscopy as a tool to evaluate the risk of cardiovascular diseases in patients. *Nat Nanotechnol* **11**, 687-92 (2016).
32. Gersh, K.C., Nagaswami, C. & Weisel, J.W. Fibrin network structure and clot mechanical properties are altered by incorporation of erythrocytes. *Thromb Haemost* **102**, 1169-75 (2009).
33. Evans, R.M., Tassieri, M., Auhl, D. & Waigh, T.A. Direct conversion of rheological compliance measurements into storage and loss moduli. *Phys Rev E Stat Nonlin Soft Matter Phys* **80**, 012501 (2009).

34. Pieters, M., Undas, A., Marchi, R., De Maat, M.P., Weisel, J. & Ariëns, R.A. An international study on the standardization of fibrin clot permeability measurement: methodological considerations and implications for healthy control values. *J Thromb Haemost* **10**, 2179-81 (2012).

35. Ribeiro, A.S., Carvalho, F.A., Figueiredo, J., Carvalho, R., Mestre, T., Monteiro, J., Guedes, A.F., Fonseca, M., Sanches, J., Seruca, R., Santos, N.C. & Paredes, J. Atomic force microscopy and graph analysis to study the P-cadherin/SFK mechanotransduction signalling in breast cancer cells. *Nanoscale* **8**, 19390-19401 (2016).

36. Fernandes, H.P., Cesar, C.L. & Barjas-Castro Mde, L. Electrical properties of the red blood cell membrane and immunohematological investigation. *Rev Bras Hematol Hemoter* **33**, 297-301 (2011).

37. Carr, M.E. & Hardin, C.L. Fibrin has larger pores when formed in the presence of erythrocytes. *Am J Physiol* **253**, H1069-73 (1987).

38. Domingues, M.M., Macrae, F.L., Duval, C., McPherson, H.R., Bridge, K.I., Ajjan, R.A., Ridger, V.C., Connell, S.D., Philippou, H. & Ariëns, R.A. Thrombin and fibrinogen gamma' impact clot structure by marked effects on intrafibrillar structure and protofibril packing. *Blood* **127**, 487-95 (2016).

39. Cines, D.B., Lebedeva, T., Nagaswami, C., Hayes, V., Massefski, W., Litvinov, R.I., Rauova, L., Lowery, T.J. & Weisel, J.W. Clot contraction: compression of erythrocytes into tightly packed polyhedra and redistribution of platelets and fibrin. *Blood* **123**, 1596-603 (2014).

40. van Gelder, J.M., Nair, C.H. & Dhall, D.P. The significance of red cell surface area to the permeability of fibrin network. *Biorheology* **31**, 259-75 (1994).

41. Wohner, N., Sotonyi, P., Machovich, R., Szabo, L., Tenekedjiev, K., Silva, M.M., Longstaff, C. & Kolev, K. Lytic resistance of fibrin containing red blood cells. *Arterioscler Thromb Vasc Biol* **31**, 2306-13 (2011).

42. Woodhead, J.L., Nagaswami, C., Matsuda, M., Arocha-Pinango, C.L. & Weisel, J.W. The ultrastructure of fibrinogen Caracas II molecules, fibers, and clots. *J Biol Chem* **271**, 4946-53 (1996).

43. Hamano, A., Mimuro, J., Aoshima, M., Itoh, T., Kitamura, N., Nishinarita, S., Takano, K., Ishiwata, A., Kashiwakura, Y., Niwa, K., Ono, T., Madoiwa, S., Sugo, T.,

Matsuda, M. & Sakata, Y. Thrombophilic dysfibrinogen Tokyo V with the amino acid substitution of gammaAla327Thr: formation of fragile but fibrinolysis-resistant fibrin clots and its relevance to arterial thromboembolism. *Blood* **103**, 3045-50 (2004).

44. Macrae, F.L., Domingues, M.M., Casini, A. & Ariëns, R.A. The (Patho)physiology of Fibrinogen gamma'. *Semin Thromb Hemost* **42**, 344-55 (2016).
45. Gersh, K.C., Nagaswami, C., Weisel, J.W. & Lord, S.T. The presence of gamma' chain impairs fibrin polymerization. *Thromb Res* **124**, 356-63 (2009).
46. Aleman, M.M., Walton, B.L., Byrnes, J.R. & Wolberg, A.S. Fibrinogen and red blood cells in venous thrombosis. *Thromb Res* **133**, S38-40 (2014).
47. Tutwiler, V., Litvinov, R.I., Lozhkin, A.P., Peshkova, A.D., Lebedeva, T., Ataullakhanov, F.I., Spiller, K.L., Cines, D.B. & Weisel, J.W. Kinetics and mechanics of clot contraction are governed by the molecular and cellular composition of the blood. *Blood* **127**, 149-59 (2016).
48. Collet, J.P., Park, D., Lesty, C., Soria, J., Soria, C., Montalescot, G. & Weisel, J.W. Influence of fibrin network conformation and fibrin fiber diameter on fibrinolysis speed: dynamic and structural approaches by confocal microscopy. *Arterioscler Thromb Vasc Biol* **20**, 1354-61 (2000).

Supplementary information of Chapter II

Sensing adhesion forces between erythrocytes and γ' fibrinogen, modulating fibrin clot architecture and function

Ana Filipa Guedes[1,2], Filomena A. Carvalho[1], Marco M. Domingues[1,2], Fraser L. Macrae[2], Helen R. McPherson[2], Nuno C. Santos[1,*#], Robert A. S. Ariëns[2,*#]

Supplementary methods

Purification of γAγA and γAγ' fibrinogen

The variants were separated by chromatography on DE-52 resin using an AKTA Avant 25. Before chromatography, fibrinogen was dissolved in equilibration buffer (39 mM Tris, 5 mM H_3PO_4, 0.5 mM phenylmethylsulfonyl fluoride (PMSF), 1 mM benzamidine and 5 mM ε-aminocaproic acid, pH 8.6). Elution of the fibrinogen variants was established by a concave gradient from equilibration buffer to elution buffer (0.5 M Tris, 0.65 M H_3PO_4, 0.5 mM PMSF, 1 mM benzamidine and 5 mM ε-aminocaproic acid, pH 4.2). Fractions containing γAγA and γAγ' were concentrated using a Vivaspin centrifugal concentrator (Sartorius, Germany). Protein peaks were analyzed by 8%-12% SDS-PAGE electrophoresis and protein concentration was determined by spectrophotometry, using a molar extinction coefficient at 280 nm of 1.51 $mg^{-1}.ml.cm^{-1}$.

Atomic Force Microscopy (AFM) – Cell-Cell adhesion

For the cell-cell adhesion studies, RBCs were diluted to 0.1% hematocrit on BSGC with $CaCl_2$ and placed on a clean poly-L-lysine coated glass slide. Cells were firmly attached to poly-L-lysine according to our previous procedures[1,2,3].

RBCs were attached to tipless cantilevers (Arrow TL2, NanoWorld AG, Switzerland) using the lectin concanavalin A (ConA). Initially, the cantilever was UV-light treated and

then subsequently coated with biotinylated BSA (0.5 mg/ml, at 37ºC, overnight), streptavidin (0.5 mg/ml, for 30 min) and finally biotinylated ConA (0.4 mg/ml, for 30 min). This way, the cell could be attached to the flexible cantilever and brought into contact with the second cell, attached to poly-L-lysine coated glass slide (substrate). The applied force was adjusted to 300 pN before retraction. Data collection for each force-distance cycle was performed at 2 µm/s, with a z-length of 30 µm. Retraction and extension delays were set to 5 s. Force curves were analyzed using JPK image processing software v. 4.2.61 (JPK Instruments, Berlin, Germany).

Fibrinogen was added, at different concentrations, to BSCG with $CaCl_2$ and allowed to incubate for 15 min before starting the measurements. For each cell attached to the cantilever, approximately 40 force *vs.* distance curves were performed for each fibrinogen concentration (5 curves per RBC on the substrate). At least 3 cantilevers, with 6 different cells attached (2 cells/cantilever) were tested on each condition.

Magnetic tweezers

The fibrin clots were prepared using fibrinogen variants at 0.5 mg/ml, $CaCl_2$ at 5.0 mM and thrombin at 1 U/ml. Magnetic beads were added at 1:250 (v:v), just before the addition of $CaCl_2$ and thrombin. Immediately after thrombin addition, the mixture was transferred to a small capillary tube, which was sealed with vaseline on both ends to avoid sample dehydration. The magnetic beads are trapped within the polymerizing fibrin clot network. Viscoelastic properties of the blood clots after the addition of RBCs were also evaluated. For these experiments, 0.5% of RBCs were added for each condition. In each experiment, an isolated magnetic bead was selected (away from capillary walls) and tested.

The viscoelastic properties were measured, calculating the parameters of G', G'' and Tan δ. The storage modulus, G' (elastic modulus), is a measure of the elastic energy stored during deformation and relates to clot stiffness. The loss modulus G'' (viscous modulus), is a measure of the energy dissipated during deformation and relates to clot viscosity. The loss tangent (Tan δ) or damping factor (G''/G'), indicates the physical behavior of a system, thus showing the ratio of the viscous and the elastic portion of the viscoelastic deformation. For a viscous material, Tan δ>>1, *i.e.*, G''>>G', whereas for an

elastic solid, Tan δ<<1, *i.e.*, G''<<G'. For a viscoelastic material with Tan δ≈1, the amounts of energy dissipated and stored are similar.

Fibrin clot permeability

To study clot permeability, samples were prepared in triplicate, according to the standardized protocol published by the Fibrinogen and FXIII Subcommittee of the International Society on Thrombosis and Hemostasis (ISTH).

Briefly, purified fibrinogen samples (final concentration of 1 mg/ml) were incubated with 1 U/ml human thrombin (Calbiochem, Nottingham, UK) and 2.5 mM $CaCl_2$. Samples were incubated in mechanically scratched open clotting tips for 120 min, at room temperature, in a humidity chamber. The tubes with the fibrin clots were connected via a silicone tube to a reservoir containing TBS buffer (50 mM Tris, 100 mM NaCl, pH 7.5), with 4 cm of pressure drop. After the clot had been washed for 120 min, flow rates of buffer through the fibrin clots were calculated every 30 min for 120 min on each tube. For each 30 min time point, the eluted buffer solution was collected and the volume was analyzed by weight measurements using an analytical balance. The fibrin clot permeability was also evaluated with 2% of RBCs. From the extracted data, the Darcy constant, K_s, which represent the average pore size within the clot, was calculated as previously described, using the equation:

$$K_s = \frac{Q \cdot L \cdot \eta}{t \cdot A \cdot \Delta P} \quad (1)$$

Where Q is the volume of liquid (ml), with viscosity η (10^{-2} poise), flowing through a clot with length L (1.3 cm) and a cross-sectional area A (0.049 cm^2), in time t (s), under a pressure ΔP (dyn/cm^2). The unit of the resulting Darcy constant is cm^2. The mean value of K_s was calculated from triplicates for each sample.

Scanning electron microscopy

To prepare the clots of γAγA and γAγ' fibrinogen variants (100 µl, final concentration of 1 mg/ml) were added to the activation mixture (10 µl, human thrombin 1 U/ml and $CaCl_2$ 10 mM, final concentrations, in TBS). The mixtures were immediately transferred to pierced Eppendorf lids. Clots were formed in a humidity chamber at room

temperature for 120 min. Clots were washed with saline solution to remove excess salt and prepared for microscopy by fixation in 2% glutaraldehyde solution for at least 120 min. Clots were further washed with sodium cacodylate buffer and dehydrated in a series of increasing concentrations of acetone (30–100%). Clots were critical-point dried with CO_2, mounted onto stubs and sputter-coated with platinum using a Cressington 208 HR (Cressington Scientific Instruments, Watford, UK). Clots were also prepared in the presence of 20% RBCs. They were observed and photographed digitally in at least 3 different areas *per* clot, using a scanning electron microscope Hitachi SU8230 FE-SEM (Hitachi, Tokyo. Japan), at 5 different magnifications (2500 ×, 5000 ×, 10000 × (data not shown), 25000 × and 50000 ×). Clots were also formed in duplicate. Average fiber diameters were measured from 20 random fibers of each image in high magnification (50000 ×) using ImageJ software (National Institutes of Health, Bethesda, MD, USA). Each cross-section measurement was performed over a single fibrin fiber and values of the fibrin diameter were extracted and averaged. All cross-section measurements were performed away from the branching points, in order to avoid biased results.

Laser scanning electron microscopy

Fibrin clots were prepared by mixing purified fibrinogen variants (1.0 mg/ml) with $CaCl_2$ (5 mM), 5% AlexaFluor 488 fibrinogen (Invitrogen, Paisley, UK) and TBS buffer. RBCs were labeled with Vibrant DiD cell-labeling solution (Molecular Probes, Leiden, Netherlands) and washed with HEPES buffer (HEPES 10 mM, NaCl 150 mM, pH 7.4) supplemented with 0.05% Pluronic F-127 (Sigma, Saint Louis, MO, USA). Clots with labeled RBCs were performed at a final RBCs concentration (hematocrit) of 2% (just for images), 5% and 10%. After the addition of human thrombin (0.1 U/ml; Calbiochem, Nottingham, UK), the reaction components were gently mixed and immediately transferred into slides (µ-slide $VI^{0.4}$, Ibidi GmbH, Munich, Germany). Clots were incubated for 120 min in a humidity chamber, at room temperature, protected from the light. Laser scanning confocal microscopy (LSCM) was performed using an upright Zeiss LSM510 META (Axioplan 2 stand) microscope (Carl Zeiss, Welwyn Garden City, UK), with a 63× oil immersion objective, using a 488 nm Argon laser and 633 nm HeNe laser.

Confocal microscopy was also used to assess, in real time, the rate of fibrinolysis. Lysis of the fibrin clots was initiated by loading a mixture containing tissue-type plasminogen activator (tPA) at 5 ng/ml (Technoclone, Vienna, Austria) and 1.1 µM Glu-Plasminogen (Enzyme Research, Swansea, UK) in TBS buffer, to the edge of the thrombus in a uniform manner after which the slides were held in a vertical position for 1 min. The slide was next incubated in a flat position for 4 min before starting a time series of imaging under 40× magnification. The visual field was set and real time serial scans (every 1 s) were taken as the front of fibrinolysis proceeded across the visual field digesting the edge of the clot. The time of fibrin clot lysis was monitored. Fibrinolysis experiments were performed, at least, in triplicate.

Supplementary results

γAγ*A and* γAγ*' fibrin clot structure*

It could be observed that γAγA fibers (Figure S1, left column) were more uniformly spatially distributed than γAγ' fibers (Figure S1, right column). Fibers produced with γAγA fibrinogen were also straighter and showed less bending. Clots from γAγ' fibers were structured into tight interconnecting bundles, producing zones with more branches and larger pores. It is possible to observe areas with fibers that were very compacted, highly connected and with small pores (Figure S1, right column). Furthermore, γAγ' fibrin clots showed more branching than γAγA fibrin clots.

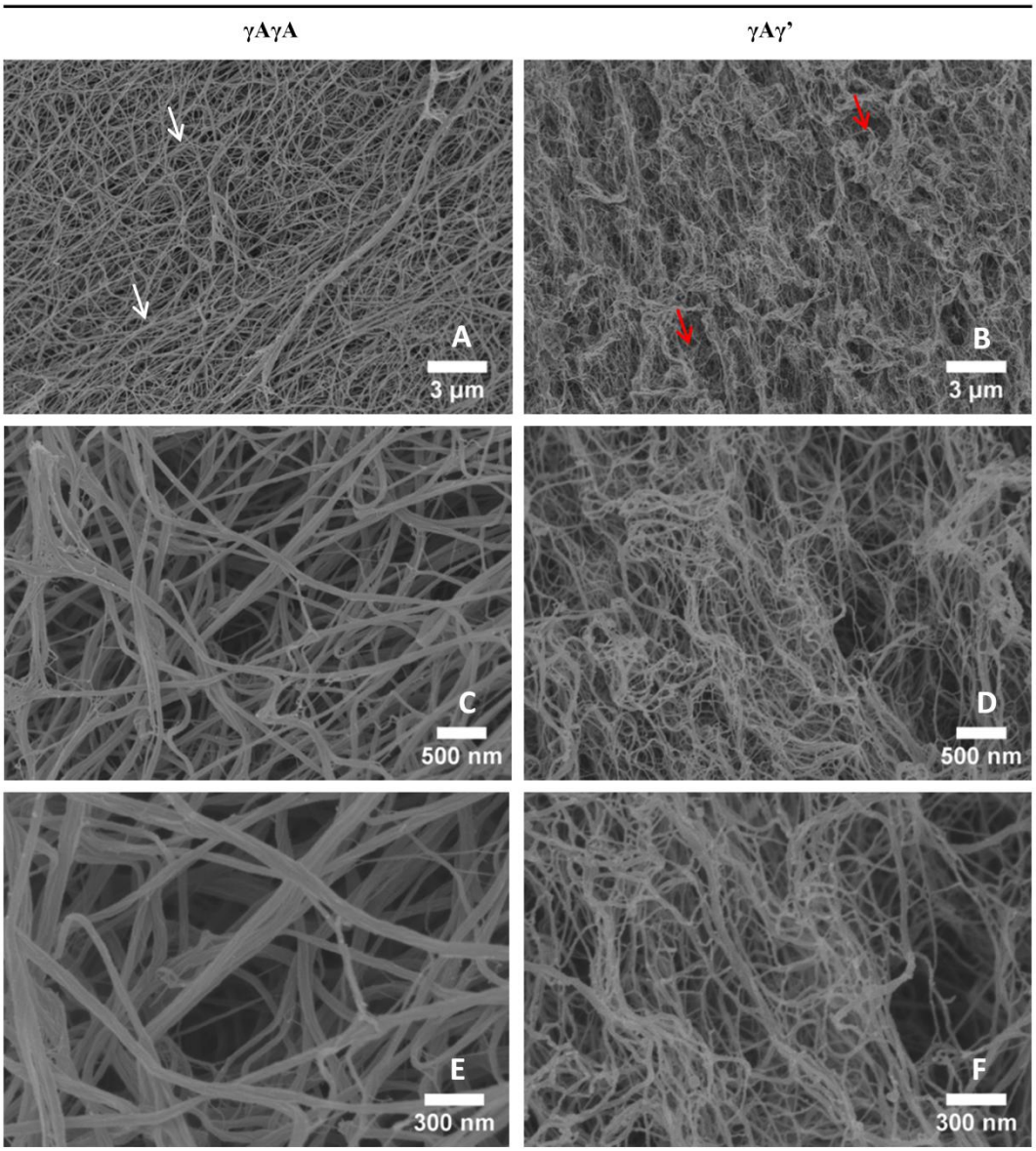

Figure S1 | Scanning electron micrographs of fibrin fiber clots (without RBCs) formed with 1.0 mg/ml of γAγA (A, C and E) or γAγ' (B, D and F) fibrinogen variants. White arrows in A highlight the more homogeneous structure of the γAγA clot network, while the red arrows in B indicate the areas with small or large holes, associating a more heterogeneous structure to the γAγ' clots. Images were obtained with a Cold Field Emission SEM, as detailed in the Methods section. Magnifications: A and B, 5000×; C and D, 25000×; E and F, 50000×.

Laser scanning confocal microscopy image analysis

Confocal microscopy images, shown on Figure 6 of the main manuscript, were analyzed to determine the fibrin fiber density (Figure S2). Fiber density was determined by counting the number of fibers crossing three arbitrary horizontal and vertical lines of 100 µm through each image. The analysis was done in three different micrographs per sample. The fiber density of the sample was taken as the average number of fibers per 100 µm of length. There were no statistical differences between fibrinogen variants regarding the number of fibers that cross the horizontal or vertical lines.

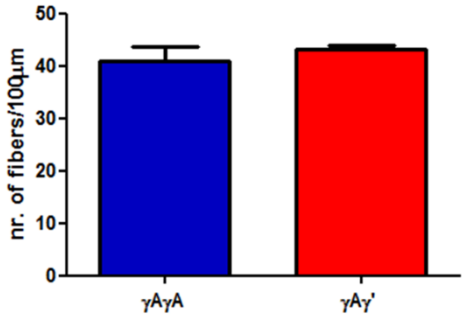

Figure S2 | **Fibrin fiber density analysis.** Data obtained from confocal images of γAγA and γAγ' fibrin clots. Values are presented as mean ± SEM.

It could be observed from confocal microscopy images that γAγ' fibrin clots have lower fiber density. This could be explained by the fact that γAγ' fibers are more compacted in some areas, producing large pores and not by the increase on the number of fibers (Figure S2)

Fibrinolysis data for fibrinogen variants

Fibrinolysis movies for γAγA (A) and γAγ' (B) fibrinogen variants were obtained, in real time by laser scanning confocal microscopy. The time serial scans were taken under 40× magnification. Clots were produced with 1.0 mg/ml fibrinogen, 5 mM $CaCl_2$ and 0.1 U/ml human thrombin final concentrations.

References

1. Carvalho, F.A., Connell, S., Miltenberger-Miltenyi, G., Pereira, S.V, Tavares, A., Ariëns, R.A., Santos, N.C. Atomic force microscopy-based molecular recognition of a fibrinogen receptor on human erythrocytes. *ACS Nano* **4,** 4609-20 (2010).
2. Carvalho, F.A., de Oliveira, S., Freitas, T., Gonçalves, S., Santos, N.C.. Variations on fibrinogen-erythrocyte interactions during cell aging. *PLoS One* **6,** e18167 (2011).
3. Guedes, A.F., Carvalho, F.A., Malho, I., Lousada, N., Sargento, L., Santos, N.C. Atomic force microscopy as a tool to evaluate the risk of cardiovascular diseases in patients. *Nat Nanotechnol* **11,** 687-92 (2016).
4. Pieters, M., Undas, A., Marchi, R., De Maat, M.P., Weisel, J., Ariëns, R.A. An international study on the standardization of fibrin clot permeability measurement: methodological considerations and implications for healthy control values. *J Thromb Haemost* **10,** 2179-81 (2012).
5. Ariëns, R.A., Philippou, H., Nagaswami, C., Weisel, J.W., Lane, D.A., Grant, P.J. The factor XIII V34L polymorphism accelerates thrombin activation of factor XIII and affects cross-linked fibrin structure. *Blood* **96**, 988-95 (2000).

Chapter III ▫

Influence of homodimer γ’ fibrinogen on fibrin clot

Overview

The clinical importance of the structural and functional properties of the clot in hemostasis and thrombosis is not clearly understood, particularly in the presence of plasma fibrinogen variants. Among the protein isoforms, γ' homodimer fibrinogen (γ'γ') is the least abundant variant. This variant is characterized by the negative charge extension on the C-terminus of both γ chains. In this Chapter, following our previous data, we wanted to study the influence of the clinically-relevant γ'γ' homodimer fibrinogen on the binding to its human erythrocyte receptor and on the structure and properties of the blood clot. Computational analyses, through which we developed a fibrin model, were also applied. In this study, we produced recombinant fibrinogen variants and we showed that the recombinant human (rh) γ'γ' fibrinogen increases the frequency of the binding to erythrocytess, promoting cell aggregation. Also, a particular structure and properties of rhγ'γ' clot were displayed. Computational predictions further reinforce these findings. The full length of γ' chain structure prediction allows an increased binding between γ' fibers (and eventually, with erythrocytes). Our results about how is the behavior of the homodimer γ' fibrinogen in blood clot shed new light to innovative therapeutic perspectives in order to control γ' fibrinogen activity. Additional information is presented on the supplementary data of this manuscript.

This work was mainly done, in Leeds Institute of Cardiovascular and Metabolic Medicine and Multidisciplinary Cardiovascular Centre, Faculty of Medicine and Health, University of Leeds, United Kingdom, with the supervision of Prof. Robert Ariëns.

Declaration of authorship

I, Ana Filipa Guedes, declare that most of the experimental work, data analysis and writing of the manuscript initial draft presented in this Chapter were done by me. However, different people have also contributed to this work. The construction of recombinant fibrinogen variants was shared between me and Helen R. McPherson. She also helped me to optimize the laser scanning confocal microscopy experiments. AFM-based force spectroscopy experiments data, analysis and discussion were shared by me and Prof. Filomena A. Carvalho. Computational predictions were done mainly by Dr. Ivo C. Martins and Dr. Marco M. Domingues. AFM and computational predictions were carried out under the supervision of Prof. Nuno C. Santos. Magnetic tweezers experiments were mainly conducted by Dr. Marco M. Domingues with my input on the preparation of samples, data analysis and discussion. Fraser L. Macrae helped me on the scanning electron microscopy experiments. Dr. Cédric Duval was also envolved in the expression of the recombinant fibrinogen. Magnetic tweezers, scanning electron microscopy and laser scanning confocal microscopy experiments were carried out under the supervision of Prof. Robert A. S. Ariëns. All authors revised and improved the manuscript.

I, Filomena A. Carvalho, as co-supervisor of Ana Filipa Guedes and co-author of the manuscript, hereby declare that the information above is correct.

I, Nuno C. Santos, as supervisor of Ana Filipa Guedes and co-corresponding author of the manuscript, hereby declare that the information above is correct.

Lisbon, April 6, 2018

Ana Filipa Guedes | Filomena A. Carvalho | Nuno C. Santos

Manuscript:

Impact of γ'γ' fibrinogen interaction with red blood cells on fibrin clots

Ana Filipa Guedes[1,2]; Filomena A. Carvalho[1]; Marco M. Domingues[1,2]; Fraser L. Macrae[2]; Helen R. McPherson[2]; Ivo C. Martins[1]; Cédric Duval[2]; Nuno C. Santos[1, *, #]; Robert A. S. Ariëns[2, *, #]

- Submitted -

Impact of γ'γ' fibrinogen interaction with red blood cells on fibrin clots

Ana Filipa Guedes[1,2]; Filomena A. Carvalho[1]; Marco M. Domingues[1,2]; Fraser L. Macrae[2]; Helen R. McPherson[2]; Ivo C. Martins[1]; Cédric Duval[2]; Nuno C. Santos[1, *, #]; Robert A. S. Ariëns[2, *, #]

[1]Instituto de Medicina Molecular, Faculdade de Medicina, Universidade de Lisboa. Av. Professor Egas Moniz, 1649-028, Lisboa, Portugal; [2]Thrombosis and Tissue Repair Group, Division of Cardiovascular and Diabetes Research, Leeds Institute of Cardiovascular and Metabolic Medicine and Multidisciplinary Cardiovascular Centre, Faculty of Medicine and Health, University of Leeds, Leeds, United Kingdom.

[#]To whom correspondence should be addressed:

* Equal contribution

Nuno C. Santos, Instituto de Medicina Molecular, Faculdade de Medicina, Universidade de Lisboa. Av. Prof. Egas Moniz, 1649-028, Lisboa, Portugal; Tel.: +351 217999480; Fax: +351 217999477; E-mail: nsantos@fm.ul.pt.

Robert Ariëns, Thrombosis and Tissue Repair Group, Division of Cardiovascular and Diabetes Research, Leeds Institute of Cardiovascular and Metabolic Medicine, Faculty of Medicine and Health, University of Leeds, Leeds, Clarendon Way, Leeds LS2 9JT, United Kingdom; Tel: +44 1133437734; Fax: +44 1133437738; E-mail: r.a.s.ariens@leeds.ac.uk.

Abstract

γ' fibrinogen has been associated with thrombosis. Here the interactions between γ'γ' or γAγA fibrinogen and red blood cells (RBCs), and their role on fibrin clot properties were studied. Atomic force microscopy shows that the recombinant human rhγ'γ' fibrinogen increases the binding force and the frequency of the binding to RBCs compared to rhAγA, promoting cell aggregation. Other microscopy approaches show structural changes in rhγ'γ' fibrin clots, displaying a non-uniform fibrin network. The presence of RBCs increases the fibrinolysis rate and viscosity of rhγ'γ' fibrin clots. The full length of γ' chain structure, revealed by computational analysis, occupies a much wider surface and is more flexible, allowing an increase of the binding between γ' fibers (and, eventually with RBCs).

Keywords: fibrin clot, γ' fibrinogen, red blood cell, thrombosis.

Summary points:

i) γ'γ' fibrinogen has increased binding force and frequency of the binding to RBCs compared to γAγA, promoting cell aggregation.

ii) A non-uniform fibrin network and changes on viscoelastic properties were observed for γ'γ' fibrin clot in presence of RBCs.

iii) With RBCs, rhγ'γ' fibrin clots are more viscous.

iv) Fibrinolysis of γ'γ' fibrin clots with RBCs took longer than without these cells.

v) Computational analyses of both fibrin models reinforce these findings.

vi) The production of a non-uniform fibrin clot may contribute to the association of γ' fibrinogen with thrombosis and increased risk of embolism.

vii) Our data shed light on the risk of increasing γ' fibrinogen plasma levels and the possible consequences on its interaction with RBCs and on the properties of the blood clot.

Introduction

The physiological process of blood clotting is an essential component of hemostasis. Fibrinogen is a blood plasma protein that plays a key role in this process, through fibrin clot formation and also partly through its interaction with blood cells [1]. Several cardiovascular and cerebrovascular disorders are associated with increased blood fibrinogen concentration [2, 3]. There is a growing number of reports showing that increasing fibrinogen plasma concentration results in changes in blood rheological properties, such as an increase in red blood cell (RBC) aggregation. This aggregation is one of the most important factors affecting blood flow and microcirculation, being a significant cardiovascular risk factor [4, 5].

Fibrinogen is a 340 kDa glycoprotein comprising six polypeptide chains, with two monomers of each of its three different chains, termed Aα, Bβ, and γ, which are connected by disulfide bonds. Fibrinogen occurs in plasma as a mixture of different isoforms [6]. Gamma prime (γ') fibrinogen arises from a splice variant of the γ chain mRNA, resulting from an alternative polyadenylation signal on intron 9 [7, 8]. This polyadenylation leads to the translation of C-terminal extension of 20-amino acid residues, encoded by intron 9 (^{408}VRPEHPAETEYDSLYPEDDL^{427}), which substitutes the last four residues of the most common γA chain (^{408}AGDV^{411}) of exon 10 [8-10]. Most of the plasma γ' fibrinogen occurs as a heterodimer with γA chain, *i.e.* γAγ' fibrinogen. This variant makes up approximately 8-15% of total circulating fibrinogen *in vivo*, although this value can diverge extensively between individuals [8, 11, 12]. A small fraction (<1%) of total plasma fibrinogen corresponds to the homodimer γ'γ' fibrinogen, while 85-90% of total plasma fibrinogen exist as the homodimer γAγA fibrinogen [8, 11, 12]. The unique sequence of the fibrinogen γ' chain contains a high affinity-binding site for thrombin [11, 13-15]. Clots formed with γ' fibrin are more resistant to fibrinolysis, [16, 17] and have thinner fibers and smaller pores when compared with γAγA fibrin clots [18-20]. Due to these characteristics, γ' fibrinogen has been associated with thrombosis [12, 21, 22]. In addition, coronary artery disease patients undergoing coronary angiography have, in average, higher γAγ' fibrinogen levels than patients without coronary artery disease [23]. This association was independent of total fibrinogen levels in plasma [23]. The increased

risk of thrombosis has been attributed to the aforementioned capacity of the γ' chain to modulate fibrin clot architecture [15]. However, the underlying mechanisms beyond structural and functional properties of the clot are still a matter of debate. Recently, prospective data from a large elderly cohort displayed a lack of association of plasma γ' fibrinogen with the incidence of cardiovascular disease [24]. These authors concluded that there was not a direct correlation between γ' fibrinogen and cardiovascular disease events [25].

It has been observed that γAγ' fibrinogen affects the structure and properties of fibrin clots *in vitro* [18, 26, 27], but it remains unclear which effect could cause the presence of γ'γ' homodimer fibrinogen on fibrin clots in the presence of RBCs. Until now, only studies using recombinant homodimer γ' fibrinogen in the absence of RBCs on the clot structure were performed [16, 19].

The main purpose of the present study was to evaluate the impact of the interaction between human γ'γ' fibrinogen and red blood cells on the formation and properties of a fibrin clot. For this, recombinant human rhγ'γ' fibrinogen and rhγAγA fibrinogen (the common variant) were synthesized and the mechanical, biophysical and morphological properties of fibrin blood clots in the presence of RBCs were characterized. Computational predictions of the protein structures for the γA and γ' chains on fibrin helped us to corroborate our results. This data can shed light on the risk of increasing γ' fibrinogen plasma levels and the possible consequences on its interaction with RBCs and on the properties of the blood clot. Knowledge of these aspects may lead to innovative perspectives on the development of new therapeutic drugs that can be successfully used to modulate γ' fibrinogen levels and overcome the risks of fibrinogen-driven RBCs hyperaggregation [28].

Methods

Fibrinogen variants expression

Recombinant fibrinogen isoforms were prepared as previously described [29-31]. To produce the fibrinogen variants, we performed DNA sequence analysis, constructed the expression vectors and conducted site-directed mutation analysis according to established procedures. Briefly, we used Chinese hamster ovary (CHO) cells engineered to express wild-type recombinant human fibrinogen (rhγAγA), or fibrinogen with a γ chain mutation (rhγ'γ'). On rhγ'γ' fibrinogen variant production, both γ chains were built with an extension of 20 amino acid residues (^{408}VRPEHPAETEYDSLYPEDDL^{427}) instead of the four C-terminal residues of the γA chain (^{408}AGDV^{411}). CHO cells expressing either rhγAγA or rhγ'γ' fibrinogen were grown in Petri dishes, and transferred into roller bottles containing adherent microcarrier beads. They were kept in serum-free DMEM/F12 supplemented with 2 mg/mL aprotinin and 5 mg/mL insulin-transferrin-sodium selenite (Roche, Burgess Hill, UK). The medium was harvested, replaced every 48 h and stored at –80°C in the presence of 150 µM phenylmethylsulfonyl fluoride (PMSF), for as long as fibrinogen was detectable by ELISA. Fibrinogen was precipitated overnight with 40% saturated ammonium sulfate (Fisher Scientific, Loughborough, UK) and purified through IF-1 affinity chromatography (immunoaffinity), as previously described [29-31]. Protein peaks were analyzed by 8%-12% SDS-PAGE electrophoresis and protein concentration was determined spectrophotometrically, at 280 nm, with a molar extinction coefficient (Ɛ) of 1.51 mg^{-1}.mL.cm^{-1}.

Red blood cells isolation and blood cell deposition

Blood was collect from healthy donors into K_3EDTA anticoagulant tubes, with their previous written informed consent, following a protocol with Instituto Português do Sangue e da Transplantação (IPST, Lisbon, Portugal), with the approval of the joint Ethics Committee of Faculdade de Medicina da Universidade de Lisboa and Centro Hospitalar Lisboa Norte. RBCs were isolated from the other blood components, according to established procedures [28, 32, 33]. Blood cells were centrifuged at 3000 rpm during 10 min and washed three times with buffered saline glucose citrate (BSGC: 1.6 mM KH_2PO_4,

8.6 mM Na_2HPO_4, 0.12 M NaCl, 13.6 mM sodium citrate, 11.1 mM glucose, pH 7.3) supplemented with 1 mM calcium chloride.

AFM tip functionalization

A previously optimized procedure was used for the covalent attachment of fibrinogen to the atomic force microscopy (AFM) tips (functionalization) [28, 32, 33]. Briefly, AFM silicon nitride tips (OMCL TR-400-type, Olympus, Tokyo, Japan) were cleaned under UV/ozone chamber for 15 min. Then, tips were silanized with 3-aminopropyl-triethoxysilane (APTES) for 1 h, in argon atmosphere. After that, the probes were immersed into a 2.5% (v/v) glutaraldehyde solution for 20 min. Finally, the tips were placed in a 0.5 mg/mL final concentration solution of rhγAγA or rhγ'γ' fibrinogen variants during 30 min, at room temperature. Functionalized tips were immediately mounted on the AFM and used for force spectroscopy experiments.

AFM-based force spectroscopy measurements

For the atomic force microscopy studies, RBCs were diluted to 0.1% hematocrit using BSGC buffer with $CaCl_2$. Five-hundred microliters of the 0.1% hematocrit RBCs suspension were placed on a clean poly-L-lysine-coated glass slide and allowed to deposit for 1 h. Non-adherent cells were removed by washing with BSGC + $CaCl_2$ buffer and allowed to equilibrate for 30 min before measurements.

Using a NanoWizard II atomic force microscope (JPK Instruments, Berlin, Germany), mounted on an Axiovert 200 inverted optical microscope (Zeiss, Jena, Germany), we performed force spectroscopy measurements with AFM tips previously functionalized with recombinant fibrinogen, as described before, with slight modifications [28, 32]. Different control experiments and $\alpha_V\beta_3$ integrin-antibody specific binding inhibition studies were already conducted by us, indicating the existence of a specific binding between fibrinogen and its RBC membrane receptor [28, 32]. Here, we used the softest triangular cantilevers, with a tip radius of 15 nm and a resonant frequency of 11 Hz. The spring constants of the tip were calibrated by the thermal fluctuation method [34], resulting in values of 0.019 ± 0.007 N/m. The applied force was adjusted to 0.8 nN before retraction. Molecular recognition was searched by intermittently pressing the cantilevers on each RBC adsorbed on the poly-L-lysine-coated glass slide. Force mapping was used to

select one point on each RBC adhered to the glass slide and to certify that all measurements were done close to the center of the RBC surface. Data collection for each force-distance cycle was performed at 2 μm/s, leading to a loading rate of 4 nN/s. Force curves were analyzed using the JPK image processing software v.4.2.61. For any given experiment, approximately 6000 force-distance curves were collected, analyzed and adjusted by polynomial fit [35]. Each experiment was performed at least three times, each time on a different blood sample and with different functionalized tips. For each blood donor, 15 RBCs were evaluated and 150 force-distance curves were performed on a defined point of each cell [28]. Histograms of the unbinding forces of each studied fibrinogen-cell complex were constructed choosing 5 pN as the ideal bin size to achieve the best Gaussian model fit. Rupture force values up to 10 pN were considered as noise, artifacts or nonspecific interactions, and were excluded from the data analysis.

Magnetic tweezers

Magnetic tweezers were used to study the viscoelastic properties of the clots. Briefly, the magnetic microrheometer acts by applying a force of 40 pN to a 4.5 μm superparamagnetic particle (Dynabeads M-450 Epoxy, Invitrogen, Paisley, UK) using a magnetic field gradient generated by four electromagnets. The electromagnets are mounted on top of an Olympus IX71 inverted microscope incorporating an ultra long working objective (40× magnification) and charged couple device camera. Particle tracking, electromagnet field and image analysis were controlled in real time through custom written Labview 7.1 software (National Instruments, Newbury, UK). We prepared fibrin clots using recombinant fibrinogen variants at 0.5 mg/mL, 5.0 mM calcium chloride and 1 U/mL thrombin, with embedded magnetic particles at 1:250 (v:v). The mixture was immediately transferred to a small capillary tube, then sealed with vaseline on both ends to avoid sample dehydration. In the presence of RBCs, clots were formed with 0.5% (v/v) RBCs to evaluate their effect on viscoelastic properties. In each experiment, a single magnetic particle was selected (located at the center of the capillary and away from other magnetic particles) and tested. The viscoelastic properties were measured using the procedure of Evans *et al*. [36]. The storage modulus, G' (elastic modulus), represents the elastic energy stored during deformation and relates to clot stiffness. The loss modulus, G'' (viscous modulus), is the energy dissipated during deformation and relates to clot

viscosity. The loss tangent (Tan δ) or damping factor (G''/G') indicates the physical behavior of a system; thus, showing the ratio of the viscous and the elastic portion of the viscoelastic deformation. The Tan δ was calculated and values of Tan δ>> 1 (*i.e.*, G''>>G') indicate viscous material, while Tan δ<<1 (*i.e.*, G'<<G'') is indicative of an elastic solid. For a viscoelastic material with Tan δ=1, the amounts of energy dissipated and stored are equal. The displacement of 8 random magnetic beads was measured per sample, and each sample was studied, at least, in triplicate. Results were obtained at a frequency of 0.1 Hz.

Scanning electron microscopy

Scanning electron microscopy (SEM) was applied in order to investigate the network structure of clots formed from rhγAγA or rhγ'γ' fibrinogen, in the presence and absence of RBCs. Fibrinogen variants rhγAγA or rhγ'γ' (1 mg/mL final concentration) and $CaCl_2$ (final concentration 10 mM) were diluted in TBS (50 mM Tris-HCl, 100 mM NaCl, pH 7.5) and premixed. Human α-thrombin (Calbiochem, Nottingham, UK, final concentration 1 U/mL) was then added to initiate clotting. The mixtures were transferred to Eppendorf lids, which were pierced with a syringe to assist solvent permeation. Clots were formed in a moist chamber, at room temperature, during 120 min. Then, clots were washed with saline solution to remove excess salt, followed by fixation in 2% glutaraldehyde (120 min). Extensive washes of the clots with sodium cacodylate buffer (67 mM $C_2H_6AsNaO_2$, pH 7.4) were done and their dehydration were performed in a series of increasing acetone concentrations (30-100%). Clots were critical-point dried with CO_2, mounted onto stubs and sputter-coated with platinum using a Cressington 208 HR (Cressington Scientific Instruments, Watford, UK). RBCs at a final concentration of 20% (v/v) were also included on the clots, on experiments carried out in duplicate. Images of two different clots were captured on different areas *per* clot (n=4), using a scanning electron microscope Hitachi SU8230 FESEM (Tokyo, Japan), at 5 different magnifications (2500× – data not shown, 5000×, 10000× – data not shown, 25000× and 50000×). The average fibrin fiber diameters were quantified using ImageJ software (National Institutes of Health, Bethesda, MD) on up to 80 random fibers of each image (n=4), at high magnification (50000×).

Laser scanning confocal microscopy

Fibrin clots were prepared in a total volume of 40 µl, by mixing recombinant human fibrinogen (final concentration of 1.0 mg/mL), $CaCl_2$ (final concentration of 5 mM), 5% AlexaFluor 488-fibrinogen conjugate (Invitrogen, Paisley, UK) and TBS buffer. Clots with labeled RBCs were also prepared, for final RBC concentrations of 2% (v/v; just for images) and 5% (v/v). The Vibrant DiD cell-labeling solution (Molecular Probes, Leiden, The Netherlands) was used to label RBCs. Before labeling, RBCs were washed with HEPES buffer (10 mM HEPES + 150 mM NaCl, pH7.4) supplemented with 0.05% Pluronic F-127 (Sigma, St. Louis, MO, UK). After addition of thrombin (Calbiochem, Nottingham, UK; final concentration 0.1 U/mL) the reaction components were gently mixed and immediately transferred into slides (µ-slide $VI^{0.4}$, Ibidi GmbH, Munich, Germany). Clots were formed for 2 h in a moist atmosphere, at room temperature, protected from the light. Laser scanning confocal microscopy (LSCM) was carried out using an upright Zeiss LSM-510 META Axioplan 2 microscope (Carl Zeiss, Welwyn Garden City, UK) with a 63× oil immersion objective, using a 488 nm Argon laser and a 633 nm HeNe laser. Three random areas of the clot were imaged. Images with 20 µm optical slice thickness were obtained and projected into single reconstructed images. These images were obtained in order to measure the fibrin fiber density (*vd.* Supplementary Information). However, some images were obtained performing z-stacks with 40 µm optical slice thickness in the middle of the clot, to better distinguish the fibers in the clots visually. Fiber density was determined by counting the number of fibers crossing 3 horizontal lines and 3 vertical lines across each image obtained, in order to calculate the average number of fibers. Three different micrographs per sample were analyzed (*vd.* Supplementary Information), using ImageJ software (National Institutes of Health, Bethesda, MD, USA).

Fibrinolysis rate was assessed by confocal microscopy. Fibrinolysis was initiated by loading a solution containing 5 ng/mL tissue-type plasminogen activator (tPA; Technoclone, Vienna, Austria) and 1.1 µM Glu-Plasminogen (Enzyme Research, Swansea, UK) to the edge of the clot, in a uniform manner. The slide was kept in a vertical position for 1 min and, after that, incubated on a flat position for 4 min before starting time series under 40× magnification. Real time serial scans were taken as the lysis front proceeded across the visual field digesting the edge of the clot, at least 2 times.

Computational analysis

Computational predictions were done for the full-length structure of the fibrinogen γA and γ' chains, in order to understand the differences between them. From the Protein Data Bank (PDB, www.pdb.org, file 3GHG), we accessed the partial experimental X-ray structure coordinates of human fibrinogen [37]. In this experimental structure, the N- and C-terminal elements of the γ-chain (in the N-terminus, from amino acid residue Y1 to E15, and in the C-terminus, from residue G395 to V411) are missing. We also obtained from PDB the experimental X-ray structure of the fibrinogen D-dimer (file 3H32) [38] to create a model of fibrin aggregation. Thus, 3GHG and 3H32 molecules were superimposed. Given our interest in the C-terminal section (involved in blood clotting and fibrin formation), we performed an *in silico* prediction of possible protein structures of the full-length γA and γ' chains using I-TASSER (http://zhanglab.ccmb.med.umich.edu/I-TASSER/), [39] a *de novo* protein structure prediction algorithm. Full details about the procedure followed on these computational predictions can be found in the Supplementary Information.

Statistical Analysis

Descriptive statistics are given as mean ± standard error of mean (SEM). Unpaired samples Student's *t*-test was used for statistical analysis. Differences were considered statistically significant for $p<0.05$. Statistical analyses were performed using GraphPad Prism 5 (La Jolla, USA).

Results

To unravel the impact of the γ' fibrinogen homodimer on RBC binding and on blood clot properties, human recombinant γ'γ' fibrinogen was used and studied through different biophysical and bioimaging approaches, as well as computationally. AFM based-force spectroscopy measurements were applied and force-distance curves acquired after the binding of rhγ'γ' fibrinogen variant or rhγAγA fibrinogen (covalently attached to the AFM tip) to the receptor on the RBC membrane. Well-defined and measurable (un)binding force curves were observed (Figure 1a). RBCs showed good adherence to poly-L-lysine and visually maintained their typical morphology.

Figure 1b shows the rupture force histogram of the (un)binding events between fibrinogen (rhγ'γ' or rhγAγA fibrinogen variants) and RBCs. It can be noticed that, in the presence of the rhγ'γ' fibrinogen, the histogram was slightly shifted to higher binding forces, when compared with the one obtained for rhγAγA fibrinogen. Accordingly, the average of force necessary to break the bond between rhγ'γ' fibrinogen and RBC receptors was 51.41 ± 0.37 pN (Figure 1c), slightly higher than observed for rhγAγA fibrinogen (48.0 ± 0.63 pN). This difference was statistically significant (p<0.0001). In addition, for the rhγ'γ' fibrinogen variant there was a 16 % increase on the frequency of RBC binding, relative to rhγAγA fibrinogen (18.5 ± 0.11 % *vs.* 15.9 ± 0.07 %, respectively).

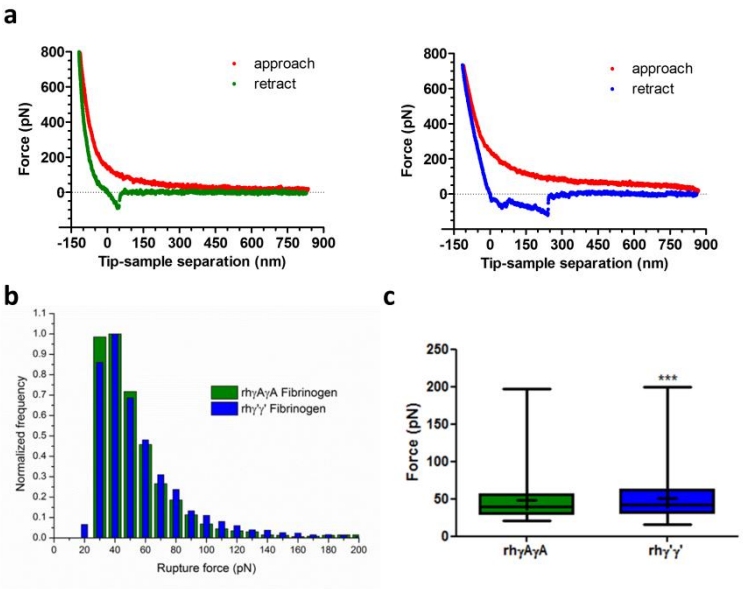

Figure 1 | Interaction force of rhγAγA and rhγ'γ' fibrinogen with red blood cells, measured using atomic force microscopy-based force spectroscopy. (a) Examples of

force-distance curves of the interaction between rhγAγA (left) or rhγ'γ' (right) fibrinogen with RBCs. (b) Rupture force histogram of the interactions between rhγAγA or rhγ'γ' fibrinogen with RBCs. On the rupture force histogram, each count represents the binding between a single fibrinogen molecule and one of its receptors on RBCs. (c) Average binding force of the interactions between the fibrinogen variants and RBCs. Values are presented as box with median value and whiskers with maximum and minimum values. The mean value is presented as '+'. *** indicates $p<0.0001$ (Student's *t*-test).

A magnetic rheometer was used to evaluate the effect of both rhγAγA and rhγ'γ' fibrinogen on clot rheological properties, in the absence and presence of RBCs (Figure 2). The loss tangent (Tan δ) of rhγAγA and rhγ'γ' fibrin clots was larger in the absence of RBCs than in their presence (for rhγAγA: 0.60 ± 0.03 without RBCs and 0.30 ± 0.08 with RBCs, $p=0.001$; for rhγ'γ': 0.70 ± 0.06 without RBCs and 0.47 ± 0.03 with RBCs, $p=0.003$). This suggests that the presence of RBCs in the clot have a significant effect on changing their viscoelastic properties. Regardless the type of fibrinogen used to form the clot, the presence of RBCs turns the overall clot structure less viscous. In the presence of RBCs, the difference between the rhγAγA and rhγ'γ' fibrin clots Tan δ values was statistically significant (0.30 ± 0.08 *vs.* 0.47 ± 0.03, respectively; $p=0.045$). This difference was not so evident in the absence of RBCs. These data show that, in the presence of RBCs, rhγ'γ' fibrin clots are more viscous than rhγAγA fibrin clots.

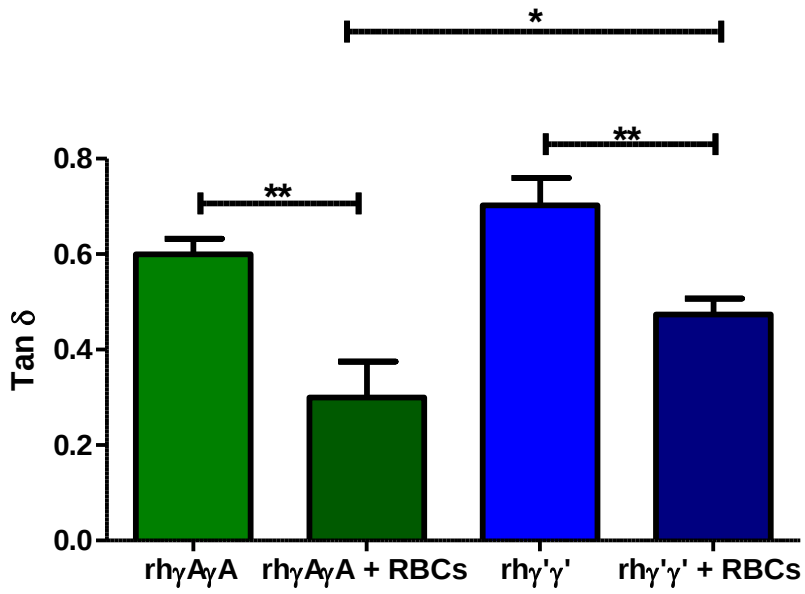

Figure 2 | Effect of RBCs on the viscoelastic properties of rhγAγA and rhγ'γ' fibrinogen variants clots. Comparison between the values of Tan δ (or loss tangent) of clots formed with each fibrinogen variant with and without RBCs. Values are shown as mean ± SEM. * p=0.045; ** $p \leq 0.003$.

To investigate the fibrin clot architecture, scanning electron microscopy was used to obtain high resolution images of the fibrin network and of the structure of fibers. These experiments were performed with both fibrinogen variants, in the presence or in the absence of RBCs. From Figure 3, it is possible to observe that RBCs tend to be heterogeneously dispersed throughout the fibrin clot, especially when rhγ'γ' fibers were present (Figure 3 b,d,f). In both sets of images, it is possible to observe clumps of RBCs interspersed between bundles of fibers. In rhγ'γ' fibrin clots, the fiber network seems to be less dense, with larger pores, in the presence of RBCs than in their absence (*vd.* Supplementary Figure 1). rhγ'γ' fibers are more branched and twisted compared to rhγAγA fibers, both in clots with and without RBCs (Figure 3 and Supplementary Figure 1).

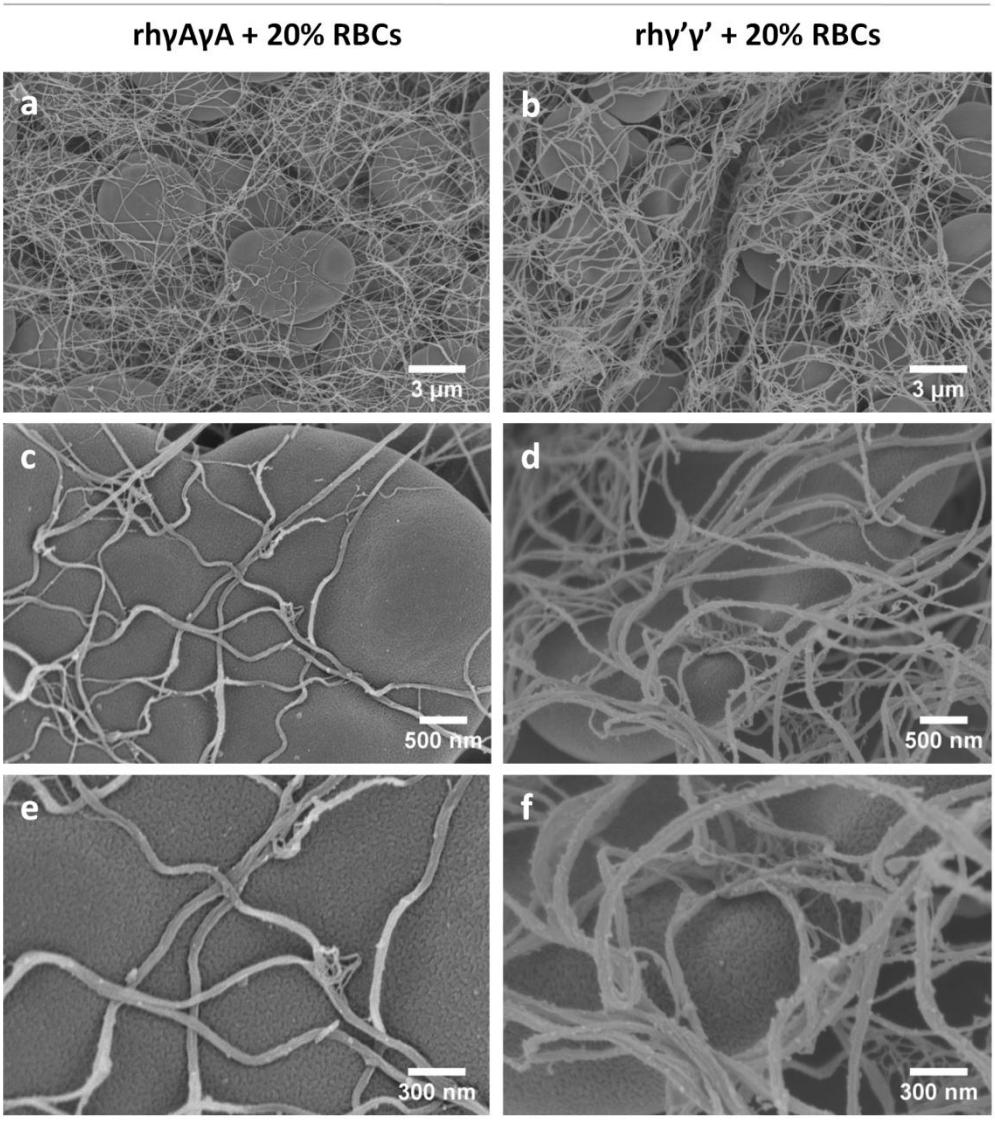

Figure 3 | Changes in the fibrin network structure caused by rhγ'γ' fibers and red blood cells. Scanning electron micrographs of fibers from recombinant rhγAγA (a, c, e) and rhγ'γ' (b, d, f) fibrin clots in the presence of 20% of RBCs. Both fibrinogen variants were at a concentration of 1 mg/mL. Images were obtained at 3 different magnifications (a, b – 5000×; c, d – 25000×; e, f – 50000×).

From the electron micrographs, it was possible to measure the average diameter of the rhγAγA and the rhγ'γ' fibrin fibers, in the presence and in the absence of RBCs (Figure 4). Our results show that rhγ'γ' clots present several zones composed of thinner fibers, when compared with the rhγAγA fibrin fibers (32.7 ± 1.2 nm *vs.* 39.2 ± 1.1 nm, respectively; $p<0.0001$). In accordance with the visual differences on the fibrin fibers

structure, statistically significant differences were found between the diameters of rhγAγA and rhγ'γ' fibrin fibers in the presence of RBCs (23.8 ± 0.7 nm *vs.* 30.4 ± 1.1 nm, respectively; $p<0.0001$). rhγ'γ' fibrin clots have more heterogeneous zones than rhγAγA fibrin clots, in the presence of RBCs. The presence of 20% of RBCs lead to a significant decrease of the rhγAγA fibrin fiber diameter (39.2 ± 1.1 nm without RBCs *vs.* 23.8 ± 0.7 nm in their presence; $p<0.0001$). No statistically significant differences were obtained for rhγ'γ' fibrin fibers diameters with or without the presence of RBCs (Figure 4).

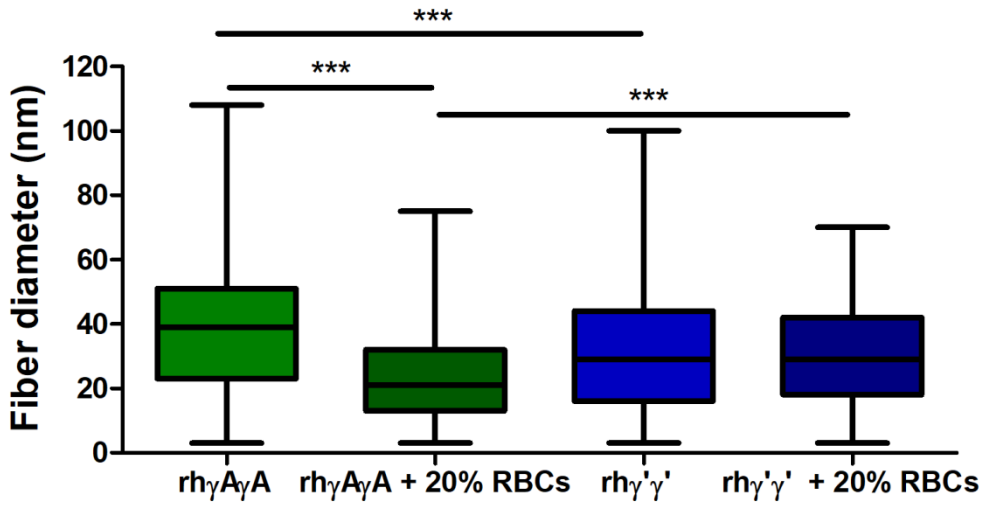

Figure 4 | **Diameter of rhγAγA and rhγ'γ' fibrin fibers in the absence and presence of RBCs**. Fiber diameters were measured at 50000× magnification on 4 images of two different clots (n=320 random rhγAγA fibrin fibers, with and without 20% of RBCs; n=261 random rhγ'γ' fibrin fibers; and n=180 random rhγ'γ' fibrin fibers with 20% of RBCs). Statistical values: *** $p\leq0.0001$.

To complement our results, confocal microscopy was applied, studying the fully hydrated, three-dimensional structure of rhγAγA and rhγ'γ' fibrin clots in the presence or in the absence of RBCs. Confocal images show that rhγAγA clots are composed of longer and straighter fibers, when compared with rhγ'γ' fibers, which are more bent and clustered (Figure 5 a,b). It can be noticed that the red-labeled RBCs are more visible in rhγ'γ' clots than for rhγAγA. To compare both clots, their confocal images were obtained performing z-stacks, with 40 µm optical slice thickness, in the middle of the clot. The

number of RBCs was also the same (Figure 5 c,d). From these images, it was possible to measure the fibrin density of the clot. Results show that the fiber density increases for rhγ'γ' clots, when compared to those of rhγAγA (45.28 ± 0.15 *vs.* 35.72 ± 0.56 *per* 100 µm of clot) (Supplementary Figure 2).

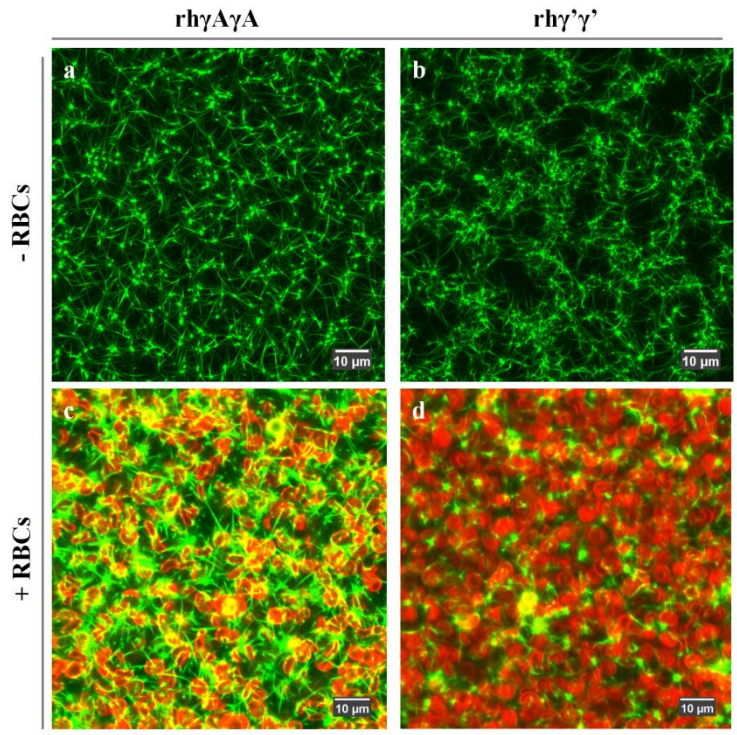

Figure 5 | Confocal micrographs of fibrin clots formed with fibers of rhγAγA or rhγ'γ' fibrinogen, in the absence or in the presence of RBCs. Laser scanning confocal microscopy images of fiber clots formed with rhγAγA and rhγ'γ' in the absence of RBCs (a,b) and in the presence of 2% RBCs (c,d). Both fibrinogen variants were at a concentration of 1 mg/mL. Alexa 488-labeled fibrin fibers are in green and Vibrant DiD-labeled RBCs in red. Images are at 63× magnification. Z-stacks of 41 (a,b) or 11 (c,d) slices.

Fibrinolysis experiments indicated that the fibrinolysis rate is higher for the rhγAγA clots, when compared to the rhγ'γ'clots (movement of the lysis front: 9.8 ± 1.0 µm/min *vs.* 6.6 ± 0.5 µm/min, respectively); however, this variation is not statistically significant (Figure 6a). Furthermore, it was possible to notice that the rhγ'γ' clot lysed in a less uniform manner, compared to those of rhγAγA (videos in Supplementary Information). The incorporation of RBCs lead to a decrease of the fibrinolysis rate of rhγ'γ' fibrin clots (6.6 ± 0.5 µm/min without RBCs *vs.* 2.5 ± 0.4 µm/min with RBCs; p=0.013; Figure 6a). In

clots with rhγAγA, the presence of RBCs did not lead to statistically significant changes on the fibrinolysis rate.

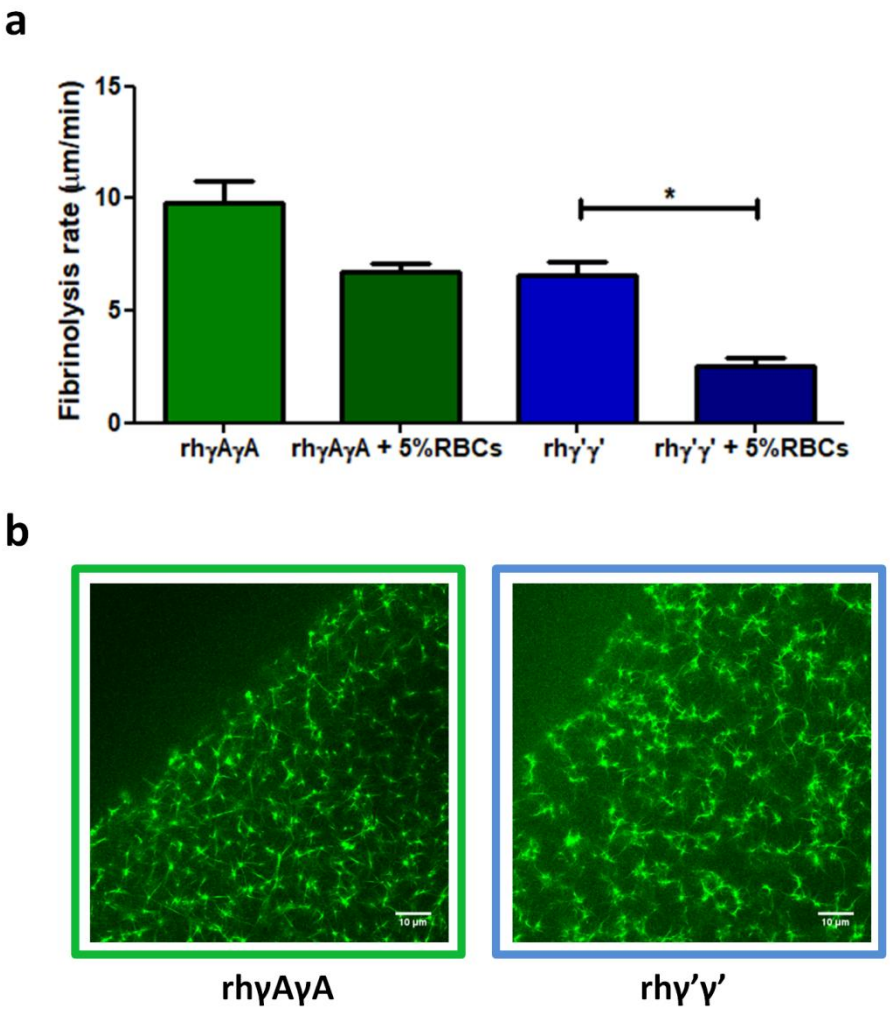

Figure 6 | **Fibrinolysis rate of rhγAγA or rhγ'γ' fibrin clots.** Clots lyses were measured in the absence or in the presence of 5% of RBCs, with 1 mg/mL of each fibrinogen variant (a). Examples of confocal microscopy images of rhγAγA or rhγ'γ' fibrin clots, under 40× magnification (b). Values are shown as mean ± SEM. * p=0.015.

Our experimental data showed an increased of the force and frequency of the binding between rhγ'γ' fibrinogen and RBCs and an increase of the fibrinolysis rate for rhγ'γ' fibrin clots. To complement these findings, computational predictions of fibrinogen γ chain structure were performed. The impact of the structural flexibility prediction of fibrinogen γ chain (γA compared to γ') on the interaction with RBCs and the correlation with the overall clot structure/function were studied. The experimentally determined

human fibrinogen structure (PDB ID 3GHG) [37] can reveal some insights into fibrinogen structure and function. However, in this experimental structure, the N- and C-terminal elements of the γ-chain are missing (in the N-terminus, from amino acids Y1 to E15, and in the C-terminus, from amino acids G395 to V411). As the key differences between γA and γ' are located precisely in the C-terminal region, we performed an *in silico* prediction of possible protein structures. Structural comparison and analysis of the *de novo* predicted protein structures indicated similar general conformations, fitting the former protein structure, both for the γA (Supplementary Figure 4a) and γ' (Supplementary Figure 4b) chains. The C-terminal predicted structure for γA missing in the experimental protein crystal structure is shown in Supplementary Figure 4a, highlighting the last 12 amino acid residues (H400-V411) with different color. Several alternative folds are suggested for this region, as expected for a dynamic region that is involved in the interaction with other molecules. The substitution of the last four residues of γA (AGDV) by the respective γ' chain 20 residues, as represented in Supplementary Figure 4b, does not change the overall structure of the γ-chain, as the globular D region (comprising the C-terminal domains of Bβ- and γ-chains) and the α-helical N-terminal sections superimposed perfectly well with the experimental former structure of γ-chain. Nevertheless, in the γ' C-terminal, the last 20 amino acid residues were predicted to acquire different folding, including α-helical structure, occupying a much wider surface. This may explain why the γ' chain binds RBCs more promptly than γA, as shown by our AFM data, or how it is more difficult for the fibrin clot to be dissolved by fibrinolytic agents, as shown in LSCM data. Furthermore, we superimposed the fibrinogen X-ray crystal structure (Supplementary Figure 3a) with the predicted γA and γ' structures (Supplementary Figure 4c). One may notice that the γ' chain displays a more bulky structure than γA.

For the sake of fibrin aggregation evaluation, we constructed the fibrin model through the superimposition of experimental structures 3GHG and 3H32 (fibrin D-dimer). This way, we predicted the structures of all variants (γAγA, γAγ' and γ'γ') during early stages of fibrin polymerization (Figure 7). Although the suggested arrangements produced within the context of the experimental fibrinogen structure do not fully correspond to the mature fibrin structure, it is already clear that the larger size and flexibility of the γ' chain is expected to allow it to interact more effectively with other molecules, including other γ

chains and RBCs. Complementing our experimental results, the γ'γ' fibrin model, when compared to γAγA, occupy a much wider surface but, at the same time, with a higher flexibility of movement.

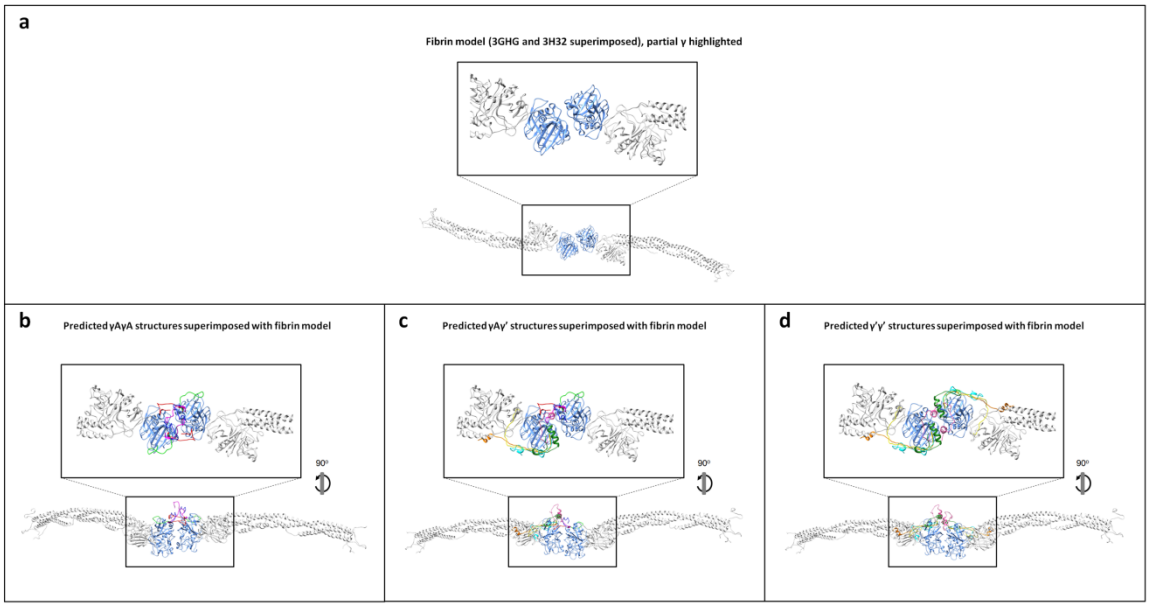

Figure 7 | Fibrin model with γ chain full-length predictions highlighted. Images display the fibrin model with the predicted γAγA (b), γAγ' (c) and γ'γ' (d) structures superimposed, respectively. (a) X-ray experimental structure of human fibrinogen (3GHG) superimposed with fibrin D-dimer X-ray structure (3H32), creating a fibrin model. The commonly structured C-terminal domain of the γ chain is colored in cyan from amino acid residue C153 to Q399 (b,c,d) Superimposition of the 3GHG and 3H32 molecules (fibrin model) with γ chain full-length predictions. Modeling based on the experimental partial structure of the γ chain resulted in 4 and 5 possible protein structures for the γA and γ' sequences, respectively. The γA predicted models are shown in: red (model 1), green (model 2), blue (model 3) and magenta (model 4). The γ' predicted models are colored in orange (model 1), green (model 2), yellow (model 3), cyan (model 4) and pink (model 5), showing conformational variations from residue H400 to L427, as expected for a flexible region involved in binding.

Discussion

In this study, different biophysical techniques in combination with microscopic techniques were used to understand the effect of the interaction between γ'γ' fibrinogen and RBCs on the structure and properties of the blood clot. For this, AFM-based force spectroscopy (using AFM tips functionalized with the fibrinogen variants γAγA and γ'γ') was applied as a nanotool for the functional evaluation of the γ'γ' fibrinogen-RBC interaction, at the single-molecule level. Changes on the fibrinogen-RBC binding force and frequency for both recombinant γAγA and γ'γ' were observed. When compared with the most abundant fibrinogen variant, rhγAγA fibrinogen, the binding between rhγ'/γ' fibrinogen and RBCs have a higher strength and is more likely to occur. Therefore, the γ' homodimer variant found *in vivo* could promote RBC aggregation. This is in agreement with the proposal of γ' fibrinogen as a novel biomarker of thrombosis, being up-regulated in patients with cardiovascular diseases [22].

Some studies have associated the increase of γ' fibrinogen with reduced risk for venous thrombosis [40-43], which have been attributed to the inhibitory effect of γ' fibrinogen on thrombin generation. Other studies have shown the association between increased γ' fibrinogen levels and increased risk for different cardiovascular diseases, namely arterial thrombosis, myocardial infarction and stroke [23, 44-46]. Both Alexander *et al.* and Pieters *et al.* reported γ' fibrinogen as a candidate for cardiovascular disease marker [47, 48], and demonstrated its effect on overall clot network and fibrinolysis. A recent prospective study showed that γ' fibrinogen concentrations associate with systemic inflammatory markers and may contribute to atherosclerotic cardiovascular diseases, instead of being a causal risk factor [25].

Clot viscoelastic properties showed that rhγ'γ' fibrin clots are more viscous (higher deformation) than rhγAγA fibrin clots, in the presence of RBCs. Thus, rhγ'γ' fibrin fibers attached more to RBCs and, under shear stress conditions, have higher deformability, which is characteristic of a high viscosity material. Collet *et al.* reported that the energy dissipated by viscous processes relative to the energy stored by elastic processes was decreased by 40% in γ'γ' fibrin, when compared with γAγA fibrin [16]. Our data reveal that there is no statistical significant changes between the values of the damping factor (Tan δ) of rhγAγA and rhγ'γ' fibrin clots in the absence of RBCs. This means that the

viscous and the elastic properties of the viscoelastic deformation of both fibrin clots are similar, which is not in agreement with the results from Collet *et al*. [16]. Possible differences in experimental set-up, magnetic tweezers (our study) *versus* torsion pendulum (Collet *et al.*) may explain some of these inconsistencies.

The hypothesis that γ' fibrinogen form fibrin blood clots with altered architecture was already proposed by others [22, 49]. The structure and function of the clot is a fundamental mechanism for thrombosis in a wide range of vascular diseases, including those affecting major vessels of the venous and arterial circulation and the microvasculature [50]. Different studies have demonstrated abnormal clot structure in patients with vascular diseases associated with increased risk of thrombosis, such as type 1 and type 2 diabetes [50, 51] and abdominal aortic aneurysm [52]. In this study, the characterization of fibrin clot structure was also performed, showing clear differences between both variants, being rhγ'γ' fibrin clots undoubtedly more heterogeneous constituted. From our data, rhγ'γ' fibrin clots are more branched, with a denser fiber network and larger pores, compared with rhγAγA fibrin clots. Fibrin fibers in the rhγ'γ' clots seem more loosely and heterogeneously packed. Furthermore, the γ' homodimer forms clots with fibers of smaller diameter than the common variant. The values obtained by SEM for the rhγAγA fibrin fiber diameter were approximately 3 times lower than those published by Collet *et al.* [53]. However, these authors prepared the fibrin clots with 1.5 mg/mL of fibrinogen and 0.9 U/mL of thrombin, instead of 1 mg/mL of fibrinogen and 1 U/mL of thrombin used in our experiments. As reported by Ryan *et al.* [54], fibrin fiber diameters decrease from 72 to 46 nm as the fibrinogen concentration increase from 0.5 to 6 mg/mL, and decrease from 108 to 44 nm as the thrombin concentration increase from 0.05 to 5 NIHU/mL (1NIHU/mL = [1.1 to 1.3] U/L[55]).

Using recombinant fibrinogen variants, some authors indicated that γ'γ' fibrinogen seems less compact, forming clots that are less dense (25% decrease) and have thicker fibers (7% increases) [16]. Gersh *et al*., studied the morphology of fibrin clots of all three variants of recombinant fibrinogen: γAγA, γAγ' and γ'γ' [19]. Contrary to the first authors and in accordance to our results, they observed that γ'γ' fibrin clots formed thinner fibers, with a high degree of fiber bundles and free fiber ends compared with γAγA fibrin clots. Our results demonstrate that the γ' homodimer directly alters fibrin formation and structure, which may help to explain the increase of thrombotic risk associated with this

variant, as reported by others [56]. Clinical studies have shown that abnormally dense fibrin structures are associated with thrombosis in patients with coronary artery disease [57], deep vein thrombosis [58] and stroke [59]. Confocal microscopy showed lower fiber density in rhγAγA clots, which is related to a less pro-thrombotic structure, when compared to rhγ'γ'. However, Collet *et al*. showed that γ'γ' fibrin displayed a slight decrease on the number of fibers per volume, relative to γAγA fibrin [16]. Denser fibrin networks are more resistant to degradation by plasmin [16], which slows down plasmin generation by plasminogen activators [60] and alters the mechanical properties by increasing clot stiffness [61-63]. To study fibrinolysis, dynamic and structural approaches with laser scanning confocal microscopy were performed. Our data show that, in the presence of RBCs, rhγ'γ' fibrin clots took more time to dissolve than rhγAγA fibrin clots, presenting a lower rate of fibrinolysis. A higher frequency of the binding between rhγ'γ' fibrinogen and RBCs could lead to higher resistance of rhγ'γ' fibrin clot to degradation, in the presence of fibrinolytic agents. The high frequency of rhγ'γ' fibrinogen-RBC binding can be responsible for the high number of arrested cells (visible on our confocal micrographs), blocking the fibrin clot interspaces. This could lead to slower rates of diffusion of fibrinolytic agents and increased resistance to fibrinolysis. Some studies have already reported rhγ'γ' fibrin clot resistance to fibrinolysis [16, 17]. A high density of thinner fibrin fibers becomes much more resistant to lysis than a low density of thicker fibrin fibers [16]. Thus, the potential use of γ'γ' fibrinogen as a biomarker of increased cardiovascular risk could be pointed out.

Our computational prediction of the full-length structure of the γ' and γA chains of fibrinogen supports our experimental findings and it is in agreement with our previous work [28, 32]. It shows the increased ability of γ' to interact with other molecules (namely, the receptors found on RBCs), even if the interaction is only transient (given its larger size and flexibility, as compared to γA). From our predicted models, γ'γ' fibrin occupies a large surface with greater flexibility than γAγA fibrin. This could justify a γ'γ' fibrin transient interaction with RBCs, forming a looser structure, as shown previously, that may culminate in *in vivo* clot emboli, more prompt to embolise. Clinical studies revealed the importance of γ' fibrinogen as a biomarker, with several findings reported [22, 23]. Although the γ'γ' homodimer is only found *in vivo* as less than 1% of total plasma fibrinogen [8], studying it provided us with a way to isolate the impact of the interaction

of γ’ chain with RBCs in a clot. It is important to notice that this study was performed at values of hematocrit below physiological (human hematocrit is in the 35-50% range). Due to technical limitations of the techniques used here, it is not possible to increase the number of RBCs to these levels.

In conclusion, this study shows that γ’γ’ fibrinogen alters the clot structure and fibrin polymerization in the presence of RBCs. The γ’γ’ fibrin clots are composed of thinner, shorter fibers, arranged heterogeneously, producing large open pores with areas of clustered fibers that extend throughout the clot. The production of a non-uniform fibrin clot, with bent fibers, may contribute to the association of γ’ fibrinogen with thrombosis and increased risk of embolism. Our results show that, in addition to the clinical assessment of the total plasma fibrinogen concentration itself, it will be important to quantify the levels of γ’ fibrinogen in plasma. A reduction in γ’ fibrinogen levels, leading to a decrease on RBCs aggregation, could be a good strategy to reduce the risk associated to cardiovascular diseases. However, a more detailed understanding of the molecular mechanisms involved on the dysfunction of the γ’ fibrinogen-RBC interaction on different cardiovascular diseases is essential to fully understand the contribution of the γ’ chains to the etiology of thrombotic diseases. The existence of a specific binding mechanism in fibrinogen-induced RBC hyperaggregation suggests the possibility of a drug therapy to decrease RBCs aggregation in different pathologies and, therefore, a decrease of the severity of cardiovascular pathologies.

Acknowledgements

Authors acknowledge Prof. Susan Lord from Department of Pathology and Laboratory Medicine, University of North Carolina, Chapel Hill, NC and Prof. David Farrell from Department of Surgery, Oregon Health and Science University, Portland, OR, USA, for the kind gift of the expression vectors to construct the fibrinogen variant.

Funding information

This work was funded by Fundação para a Ciência e a Tecnologia – Ministério da Ciência, Tecnologia e Ensino Superior (FCT-MCTES, Portugal) project PTDC/BBB-BMD/6307/2014 and Fundação Calouste Gulbenkian (Portugal). AFG also acknowledges FCT-MCTES PhD fellowship SFRH/BD/84414/2012. RASA is supported by the British Heart Foundation (RG/13/3/30104).

Conflict of interest disclosure

The authors declare no competing financial interests.

Authorship Contribution

A.F.G. performed the different types of experiment, analyzed the data, wrote and edited successive drafts of the manuscript and prepared it for submission; **F.A.C.** performed AFM experiments, analyzed force spectroscopy data, wrote and edited the drafts of the manuscript; **M.M.D.** performed magnetic tweezers experiments, analyzed data and edited the manuscript; **F.L.M.** assisted on SEM experiments and edited the manuscript; **H.R.M.** assisted on confocal microscopy experiments and edited the manuscript; **I.C.M.** performed the computational prediction analysis and wrote relevant manuscript sections; **C.D.** contributed to relevant methods and edited the manuscript drafts; **N.C.S.** conceived the idea, designed and directed the AFM experiments, analyzed the data, wrote part of the text and edited the successive drafts of the manuscript; and, **R.A.S.A.** conceived the idea, contributed to relevant methods and discussion sections, analyzed data, wrote part of the text and edited the successive drafts of the manuscript.

References of Chapter III

1. Wolberg AS. Determinants of fibrin formation, structure, and function. *Curr Opin Hematol.* 19(5), 349-356 (2012).

2. Delamaire M and Durand F. Erythrocyte aggregation and vascular pathology. *J Mol Vasc.* 15(4), 344-345 (1990).

3. Falcó C, Vaya A, Simo M, Contreras T, Santaolaria M, and Aznar J. Influence of fibrinogen levels on erythrocyte aggregation determined with the Myrenne aggregometer and the Sefam erythro-aggregometer. *Clin Hemorheol Microcirc.* 33(2), 145-151 (2005).

4. Hadengue AL, Del-Pino M, Simon A, and Levenson J. Erythrocyte disaggregation shear stress, sialic acid, and cell aging in humans. *Hypertension.* 32(2), 324-330 (1998).

5. Lominadze D, Dean WL, Tyagi SC, and Roberts AM. Mechanisms of fibrinogen-induced microvascular dysfunction during cardiovascular disease. *Acta Physiol.* 198(1), 1-13 (2010).

6. Henschen-Edman AH. Fibrinogen non-inherited heterogeneity and its relationship to function in health and disease. *Ann N Y Acad Sci.* 936(580-593 (2001).

7. Francis CW, Marder VJ, and Martin SE. Demonstration of a large molecular weight variant of the gamma chain of normal human plasma fibrinogen. *J Biol Chem.* 255(12), 5599-5604 (1980).

8. Wolfenstein-Todel C and Mosesson MW. Human plasma fibrinogen heterogeneity: evidence for an extended carboxyl-terminal sequence in a normal gamma chain variant (gamma'). *Proc Natl Acad Sci U S A.* 77(9), 5069-5073 (1980).

9. Chung DW and Davie EW. gamma and gamma' chains of human fibrinogen are produced by alternative mRNA processing. *Biochemistry.* 23(18), 4232-4236 (1984).

10. Fornace AJ, Cummings DE, Comeau CM, Kant JA, and Crabtree GR. *J Biol Chem.* 259(20), 12826-12830 (1984).

11. Meh DA, Siebenlist KR, and Mosesson MW. Identification and characterization of the thrombin binding sites on fibrin*. J Biol Chem.* 271(38), 23121-23125 (1996).

12. Uitte de Willige S, Standeven KF, Philippou H, and Ariëns RA. The pleiotropic role of the fibrinogen gamma' chain in hemostasis*. Blood.* 114(19), 3994-4001 (2009).

13. Lovely RS, Moaddel M, and Farrell DH. Fibrinogen gamma' chain binds thrombin exosite II*. J Thromb Haemost.* 1(1), 124-131 (2003).

14. Pospisil CH, Stafford AR, Fredenburgh JC, and Weitz JI. Evidence that both exosites on thrombin participate in its high affinity interaction with fibrin*. J Biol Chem.* 278(24), 21584-21591 (2003).

15. Macrae FL, Domingues MM, Casini A, and Ariëns RA. The (Patho)physiology of Fibrinogen gamma'*. Semin Thromb Hemost.* 42(4), 344-355 (2016).

16. Collet JP, Nagaswami C, Farrell DH, Montalescot G, and Weisel JW. Influence of gamma' fibrinogen splice variant on fibrin physical properties and fibrinolysis rate*. Arterioscler Thromb Vasc Biol.* 24(2), 382-386 (2004).

17. Falls LA and Farrell DH. Resistance of gammaA/gamma' fibrin clots to fibrinolysis*. J Biol Chem.* 272(22), 14251-14256 (1997).

18. Cooper AV, Standeven KF, and Ariëns RAS. Fibrinogen gamma-chain splice variant gamma' alters fibrin formation and structure*. Blood.* 102(2), 535-540 (2003).

19. Gersh KC, Nagaswami C, Weisel JW, and Lord ST. The presence of gamma' chain impairs fibrin polymerization*. Thromb Res.* 124(3), 356-363 (2009).

20. Domingues MM, Macrae FL, Duval C, McPherson HR, Bridge KI, Ajjan RA, Ridger VC, Connell SD, Philippou H, and Ariëns RA. Thrombin and fibrinogen gamma' impact clot structure by marked effects on intrafibrillar structure and protofibril packing*. Blood.* 127(4), 487-495 (2016).

21. Ariëns RA. Fibrin(ogen) and thrombotic disease. *J Thromb Haemost.* 11 (294-305 (2013).

22. Farrell DH. gamma' Fibrinogen as a novel marker of thrombotic disease. *Clin Chem Lab Med.* 50(11), 1903-1909 (2012).

23. Lovely RS, Falls LA, Al-Mondhiry HA, Chambers CE, Sexton GJ, Ni H, and Farrell DH. Association of gammaA/gamma' fibrinogen levels and coronary artery disease. *Thromb Haemost.* 88(1), 26-31 (2002).

24. Appiah D, Heckbert SR, Cushman M, Psaty BM, and Folsom AR. Lack of association of plasma gamma prime (gamma') fibrinogen with incident cardiovascular disease. *Thromb Res.* 143(50-52 (2016).

25. Appiah D, Schreiner PJ, MacLehose RF, and Folsom AR. Association of Plasma gamma' Fibrinogen With Incident Cardiovascular Disease: The Atherosclerosis Risk in Communities (ARIC) Study. *Arterioscler Thromb Vasc Biol.* 35(12), 2700-2706 (2015).

26. Siebenlist KR, Mosesson MW, Hernandez I, Bush LA, Di Cera E, Shainoff JR, Di Orio JP, and Stojanovic L. Studies on the basis for the properties of fibrin produced from fibrinogen-containing gamma' chains. *Blood.* 106(8), 2730-2736 (2005).

27. Guedes AF, Carvalho FA, Domingues MM, Macrae FL, McPherson HR, Santos NC, and Ariëns RA. Sensing adhesion forces between erythrocytes and gamma' fibrinogen, modulating fibrin clot architecture and function. *Nanomedicine.* 14(3), 909-918 (2018).

28. Guedes AF, Carvalho FA, Malho I, Lousada N, Sargento L, and Santos NC. Atomic force microscopy as a tool to evaluate the risk of cardiovascular diseases in patients. *Nat Nanotechnol.* 11(8), 687-692 (2016).

29. Duval C, Allan P, Connell SD, Ridger VC, Philippou H, and Ariëns RA. Roles of fibrin alpha- and gamma-chain specific cross-linking by FXIIIa in fibrin structure and function. *Thromb Haemost.* 111(5), 842-850 (2014).

30. Lord ST, Binnie CG, Hettasch JM, and Strickland E. Purification and characterization of recombinant human fibrinogen. *Blood Coagul Fibrinolysis.* 4(1), 55-59 (1993).

31. Standeven KF, Carter AM, Grant PJ, Weisel JW, Chernysh I, Masova L, Lord ST, and Ariens RA. Functional analysis of fibrin {gamma}-chain cross-linking by activated factor XIII: determination of a cross-linking pattern that maximizes clot stiffness. *Blood.* 110(3), 902-907 (2007).

32. Carvalho FA, Connell S, Miltenberger-Miltenyi G, Pereira SV, Tavares A, Ariëns RAS, and Santos NC. Atomic force microscopy-based molecular recognition of a fibrinogen receptor on human erythrocytes. *ACS Nano.* 4(8), 4609-4620 (2010).

33. Carvalho FA, de Oliveira S, Freitas T, Gonçalves S, and Santos NC. Variations on fibrinogen-erythrocyte interactions during cell aging. *PLoS One.* 6(3), e18167 (2011).

34. Hutter JB, J Bechhoefer. Calibration of atomic-force microscope tips. *Review of Scientific Instruments.* 64, 1868 (1993).

35. Ratto TV, Rudd RE, Langry KC, Balhorn RL, and McElfresh MW. Nonlinearly additive forces in multivalent ligand binding to a single protein revealed with force spectroscopy. *Langmuir.* 22(4), 1749-1757 (2006).

36. Evans RM, Tassieri M, Auhl D, and Waigh TA. Direct conversion of rheological compliance measurements into storage and loss moduli. *Phys Rev E Stat Nonlin Soft Matter Phys.* 80, 012501 (2009).

37. Kollman JM, Pandi L, Sawaya MR, Riley M, and Doolittle RF. Crystal structure of human fibrinogen. *Biochemistry.* 48(18), 3877-3886 (2009).

38. Pandi L, Kollman JM, Lopez-Lira F, Burrows JM, Riley M, and Doolittle RF. Two families of synthetic peptides that enhance fibrin turbidity and delay fibrinolysis by different mechanisms. *Biochemistry.* 48(30), 7201-7208 (2009).

39. Roy A, Kucukural A, and Zhang Y. I-TASSER: a unified platform for automated protein structure and function prediction. *Nat Protoc.* 5(4), 725-738 (2010).

40. Lovely RS, Rein CM, White TC, Jouihan SA, Boshkov LK, Bakke AC, McCarty OJ, and Farrell DH. gammaA/gamma' fibrinogen inhibits thrombin-induced platelet aggregation. *Thromb Haemost.* 100(5), 837-846 (2008).

41. Grunbacher G, Weger W, Marx-Neuhold E, Pilger E, Koppel H, Wascher T, Marz W, and Renner W. The fibrinogen gamma (FGG) 10034C>T polymorphism is associated with venous thrombosis. *Thromb Res.* 121(1), 33-36 (2007).

42. Nowak-Gottl U, Weiler H, Hernandez I, Thedieck S, Seehafer T, Schulte T, and Stoll M. Fibrinogen alpha and gamma genes and factor VLeiden in children with thromboembolism: results from 2 family-based association studies. *Blood.* 114(9), 1947-1953 (2009).

43. Uitte de Willige S, de Visser MC, Houwing-Duistermaat JJ, Rosendaal FR, Vos HL, and Bertina RM. Genetic variation in the fibrinogen gamma gene increases the risk for deep venous thrombosis by reducing plasma fibrinogen gamma' levels. *Blood.* 106(13), 4176-4183 (2005).

44. Cheung EY, Vos HL, Kruip MJ, den Hertog HM, Jukema JW, and de Maat MP. Elevated fibrinogen gamma' ratio is associated with cardiovascular diseases and acute phase reaction but not with clinical outcome. *Blood.* 114(20), 4603-4604 (2009).

45. Lovely RS, Yang Q, Massaro JM, Wang J, D'Agostino RB, O'Donnell CJ, Shannon J, and Farrell DH. Assessment of genetic determinants of the association of gamma' fibrinogen in relation to cardiovascular disease. *Arterioscler Thromb Vasc Biol.* 31(10), 2345-2352 (2011).

46. Mannila MN, Lovely RS, Kazmierczak SC, Eriksson P, Samnegard A, Farrell DH, Hamsten A, and Silveira A. Elevated plasma fibrinogen gamma' concentration is associated with myocardial infarction: effects of variation in fibrinogen genes and environmental factors. *J Thromb Haemost.* 5(4), 766-773 (2007).

47. Alexander KS, Madden TE, and Farrell DH. Association between gamma' fibrinogen levels and inflammation. *Thromb Haemost.* 105(4), 605-609 (2011).

48. Pieters M, Kotze RC, Jerling JC, Kruger A, and Ariëns RA. Evidence that fibrinogen gamma' regulates plasma clot structure and lysis and relationship to cardiovascular risk factors in black Africans. *Blood.* 121(16), 3254-3260 (2013).

49. Lovely RS, Kazmierczak SC, Massaro JM, D'Agostino R, O'Donnell CJ, and Farrell DH. Gamma' fibrinogen: evaluation of a new assay for study of associations with cardiovascular disease. *Clin Chem.* 56(5), 781-788 (2010).

50. Ariëns RA. Novel mechanisms that regulate clot structure/function. *Thromb Res.* 141, S25-27 (2016).

51. Dunn EJ, Ariëns RA, and Grant PJ. The influence of type 2 diabetes on fibrin structure and function. *Diabetologia.* 48(6), 1198-1206 (2005).

52. Scott DJ, Prasad P, Philippou H, Rashid ST, Sohrabi S, Whalley D, Kordowicz A, Tang Q, West RM, Johnson A, Woods J, Ajjan RA, and Ariëns RA. Clot architecture is altered in abdominal aortic aneurysms and correlates with aneurysm size. *Arterioscler Thromb Vasc Biol.* 31(12), 3004-3010 (2011).

53. Collet JP, Moen JL, Veklich YI, Gorkun OV, Lord ST, Montalescot G, and Weisel JW. The alphaC domains of fibrinogen affect the structure of the fibrin clot, its physical properties, and its susceptibility to fibrinolysis. *Blood.* 106(12), 3824-3830 (2005).

54. Ryan EA, Mockros LF, Weisel JW, and Lorand L. Structural origins of fibrin clot rheology. *Biophys J.* 77(5), 2813-2826 (1999).

55. Gaffney PJ and Edgell TA. The International and "NIH" units for thrombin--how do they compare? *Thromb Haemost.* 74(3), 900-903 (1995).

56. Allan P, Uitte de Willige S, Abou-Saleh RH, Connell SD, and Ariëns RA. Evidence that fibrinogen gamma' directly interferes with protofibril growth: implications for fibrin structure and clot stiffness. *J Thromb Haemost.* 10(6), 1072-1080 (2012).

57. Mills JD, Ariëns RA, Mansfield MW, and Grant PJ. Altered fibrin clot structure in the healthy relatives of patients with premature coronary artery disease. *Circulation.* 106(15), 1938-1942 (2002).

58. Undas A, Zawilska K, Ciesla-Dul M, Lehmann-Kopydlowska A, Skubiszak A, Ciepluch K, and Tracz W. Altered fibrin clot structure/function in patients with idiopathic venous thromboembolism and in their relatives. *Blood.* 114(19), 4272-4278 (2009).

59. Undas A, Slowik A, Wolkow P, Szczudlik A, and Tracz W. Fibrin clot properties in acute ischemic stroke: relation to neurological deficit. *Thromb Res.* 125(4), 357-361 (2010).

60. Mutch NJ, Engel R, Uitte de Willige S, Philippou H, and Ariëns RA. Polyphosphate modifies the fibrin network and down-regulates fibrinolysis by attenuating binding of tPA and plasminogen to fibrin. *Blood.* 115(19), 3980-3988 (2010).

61. Collet JP, Park D, Lesty C, Soria J, Soria C, Montalescot G, and Weisel JW. Influence of fibrin network conformation and fibrin fiber diameter on fibrinolysis speed: dynamic and structural approaches by confocal microscopy. *Arterioscler Thromb Vasc Biol.* 20(5), 1354-1361 (2000).

62. Konings J, Govers-Riemslag JW, Philippou H, Mutch NJ, Borissoff JI, Allan P, Mohan S, Tans G, Ten Cate H, and Ariëns RA. Factor XIIa regulates the structure of the fibrin clot independently of thrombin generation through direct interaction with fibrin. *Blood.* 118(14), 3942-3951 (2011).

63. Wolberg AS and Campbell RA. Thrombin generation, fibrin clot formation and hemostasis. *Transfus Apher Sci.* 38(1), 15-23 (2008).

Supplementary information of Chapter III

Impact of γ'γ' fibrinogen interaction with red blood cells on fibrin clots

Ana Filipa Guedes[1,2]; Filomena A. Carvalho[1]; Marco M. Domingues[1,2]; Fraser L. Macrae[2]; Helen R. McPherson[2]; Ivo C. Martins[1]; Cédric Duval[2]; Nuno C. Santos[1, *, #]; Robert A. S. Ariëns[2, *, #]

Fiber network structure without red blood cells

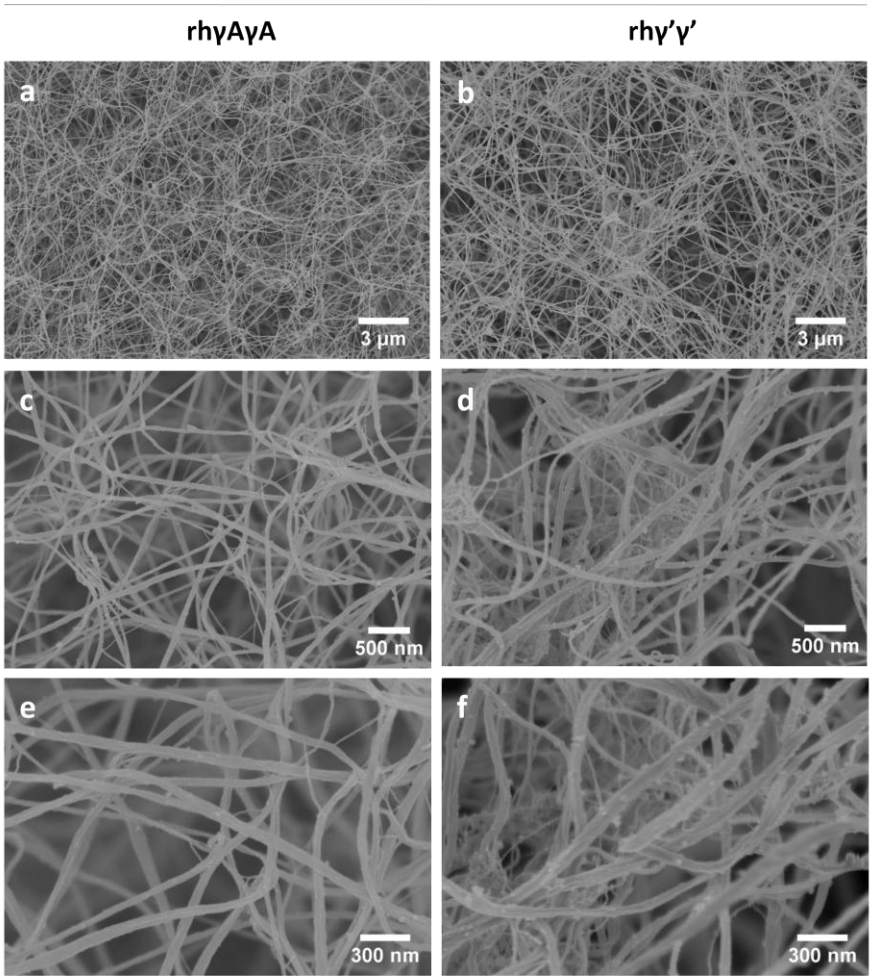

Supplementary Figure 1 | Scanning electron micrographs of fibers from recombinant rhγAγA (a, c, e) and rhγ'γ' (b, d, f) fibrin clots. Both fibrinogen variants were

at a concentration of 1 mg/mL. Images were obtained at 3 different magnifications (a, b – 5000×; c, d – 25000×; e, f – 50000×).

Regarding the spatial fiber distribution, it could be observed that rhγ'γ' fibers were less uniformly distributed than rhγAγA fibers (Supplementary Figure 1). The clots made with rhγ'γ' were arranged into tight interconnecting bundles, producing zones with large open pores and more branching. It was possible to observe regions with very compact fibers, connected and with small pores; but, at the same time, there were other regions with large pores between fibers.

Fibrin fiber density

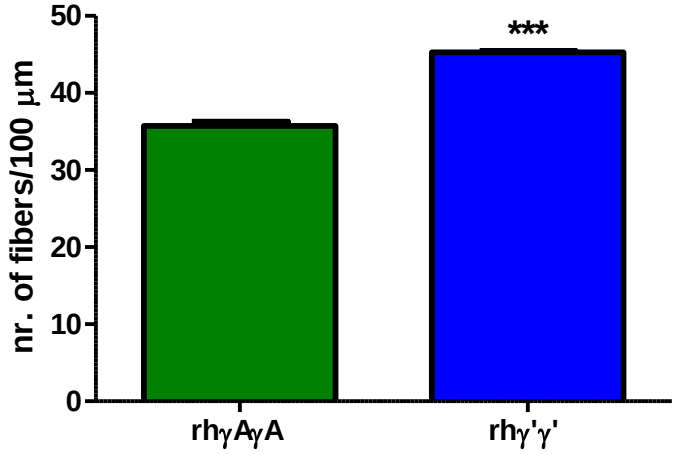

Supplementary Figure 2 | **Fibrin fiber density obtained from confocal image analysis of rhγAγA and rhγ'γ' fibrin clots.** Number of fibers measured by quantifying the fibers that crossed the manually disposed lines over 100 µm of clot image. Values are mean ± SEM. *** $p<0.0001$.

Confocal micrographs clearly show that rhγAγA clots are composed of longer and straighter fibers, when compared with rhγ'γ' clots, which are more bent and clustered (Figure 5 of the main document). Fibrin fiber density increases in rhγ'γ' clots compared to rhγAγA clots (45.28 ± 0.15 *vs.* 35.72 ± 0.56 fibers *per* 100 µm). Therefore, confocal

microscopy relates rhγAγA to a clot structure less pro-thrombotic, when compared to rhγ'γ' clots.

Fibrinolysis movies

Through laser scanning confocal microscopy we acquired movies depicting the fibrinolysis process on rhγAγA and rhγ'γ' fibrin clots, under 40× magnification. Fibrin was labeled with 5% AlexaFluor 488 (green). In these movies, it is possible to see the lysis front, digesting the clot. They clearly show that rhγ'γ' clots lysed in a less uniform way than the rhγAγA clots.

Computational analysis

The partial experimental X-ray structure coordinates of human fibrinogen, where not all the γ chain sequence is resolved (Supplementary Figure 3a), were obtained from the Protein Data Bank (PDB, www.pdb.org, file 3GHG) [1]. In this experimental structure, the N- and C-terminal elements of the γ-chain are missing (in the N-terminus, from residue Y1 to E15, and in the C-terminus, from residue G395 to V411). In order to build a model of fibrin aggregation, we used the experimental X-ray structure of the fibrin D-dimer (PDB, www.pdb.org, file 3H32) [2] for superimposing to the previously mentioned experimental X-ray structure of human fibrinogen (Supplementary Figure 3b). Molecules of 3GHG and 3H32 were superimposed through UCSF Chimera 1.6.2 software [3] MatchMaker tool [4]. Chain A corresponds to the Aα chain, B to Bβ chain and C to the γ chain of both molecules. Given our interest in the C-terminal section of γ chain (involved in blood clotting and fibrin formation), we superimposed the γ chains both from 3GHG and 3H32 molecules, using the γ chain (C chain) obtained from the PDB file 3GHG as a reference (Supplementary Figure 3c). All γ chain structures superimposed perfectly, especially in the C-terminal section (Supplementary Figure 3c).

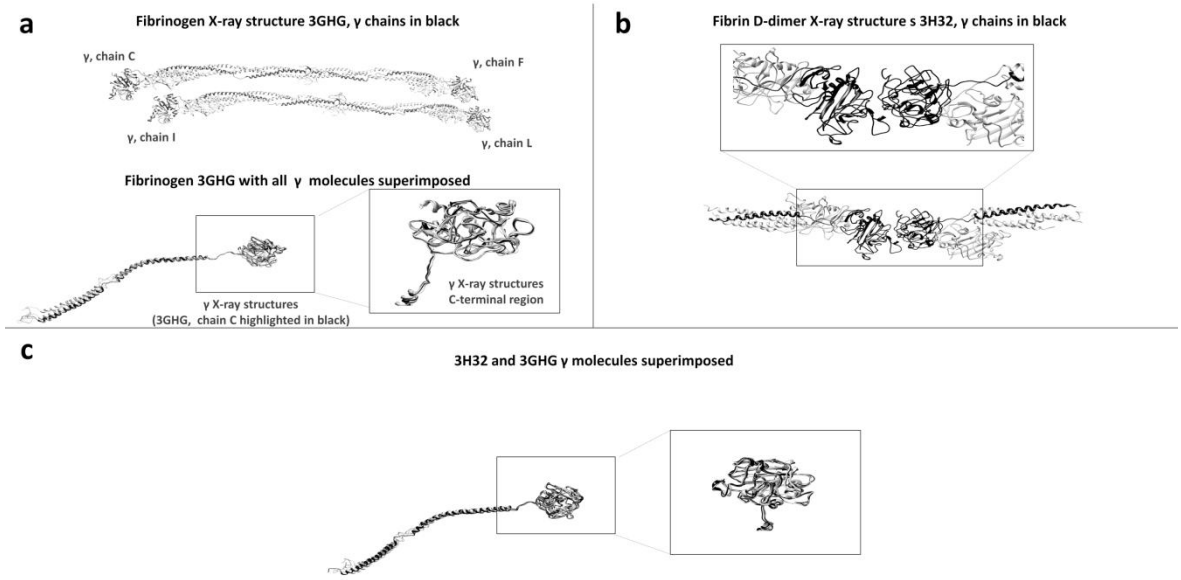

Supplementary Figure 3 | **The γ chains X-ray experimental structures of the human fibrinogen and of the fibrin D-dimer are highly superimposable and thus very similar.** (a) Human fibrinogen partial X-ray experimental structure (PDB ID 3GHG),[1] highlighting in black the partial γ chain structure. Superposition of all the experimental γ chain partial structures (PDB ID 3GHG), highlighting in black the γ molecule of chain C. Zooming shows that in the C-terminal all the partial experimental structures are completely superimposed. The chain C molecule of the experimental file was, for the sake of simplicity, used in all representations shown here. (b) The experimental X-ray structure of fibrin D-dimer (PDB ID 3H32) for superimposing the previously mentioned experimental X-ray structure of human fibrinogen, γ chains highlighting in black. (c) All γ-chains from both 3GHG and 3H32 superimposed, highlighting chain C.

In order to fully describe the γ-chain role, we performed an *in silico* prediction of possible protein structures of the full-length γA (Supplementary Figure 4a) and γ' (Supplementary Figure 4b) chains using I-TASSER (http://zhanglab.ccmb.med.umich.edu/I-TASSER/) [5], a *de novo* protein structure prediction algorithm. We used the γ chain (C chain) obtained from PDB file 3GHG as a reference for superimposition with predicted full length γA and γ' chains. The γ' sequence was generated via the substitution of the last four residues (^{408}AGDV^{411}) from γA chain by the extra C-terminal 20 residues of the γ' chain (^{408}VRPEHPAETEYDSLYPEDDL^{427}) [6].

Modeling based on the experimental partial structure of γ chain resulted in 4 and 5 possible protein structures for the γA and γ' full sequences, respectively. On Supplementary Figure 4c, it is possible to see the more bulky structure of the C-terminal of γ', when compared to γA.

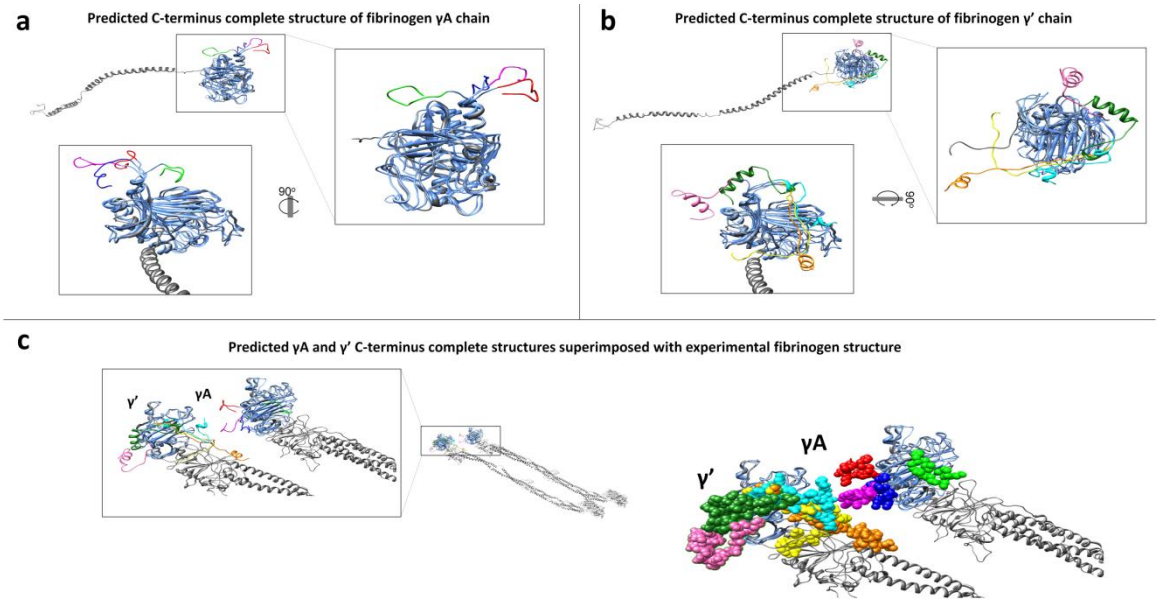

Supplementary Figure 4 | Predictions C-terminal structures of fibrinogen γ chains. (a) X-ray ribbon experimental partial structure of fibrinogen γ chain (PDB ID 3GHG, molecule C, colored gray) superimposed with the four fibrinogen γ predicted model structures. The commonly structured C-terminal domain of the γ chain of the four γA models is colored in light blue from amino acid C153 to Q399, to distinguish from the experimental structure, given the almost perfect superposition. The section corresponding to the last 12 amino acid residues (H400-V411), for which there is no experimental structure available, is highlighted in a different color for each of the four predicted models: red (model 1), green (model 2), blue (model 3) and magenta (model 4). (b) X-ray ribbon experimental partial structure of fibrinogen γ chain superimposed with the five fibrinogen γ' predicted model structures, color-coded as in (a), except for the five predicted γ' models. These models are colored in orange (model 1), green (model 2), yellow (model 3), cyan (model 4) and pink (model 5), showing conformational variation from residue H400 to L427, as expected for a flexible region involved in binding. (c) The experimental human fibrinogen structure (PDB ID 3GHG) with, respectively, the predicted γAγA and γAγ' structures close together superimposed, color-coded as in (a) and (b).

References

1. Kollman JM, Pandi L, Sawaya MR, Riley M, and Doolittle RF. Crystal structure of human fibrinogen. *Biochemistry.* 48(18), 3877-3886 (2009).
2. Pandi L, Kollman JM, Lopez-Lira F, Burrows JM, Riley M, and Doolittle RF. Two families of synthetic peptides that enhance fibrin turbidity and delay fibrinolysis by different mechanisms. *Biochemistry.* 48(30), 7201-7208 (2009).
3. Pettersen EF, Goddard TD, Huang CC, Couch GS, Greenblatt DM, Meng EC, and Ferrin TE. UCSF Chimera-a visualization system for exploratory research and analysis. *J Comput Chem.* 25(13), 1605-1612 (2004).
4. Meng EC, Pettersen EF, Couch GS, Huang CC, and Ferrin TE. Tools for integrated sequence-structure analysis with UCSF Chimera. *BMC Bioinformatics.* 7, 339 (2006).
5. Roy A, Kucukural A, and Zhang Y. I-TASSER: a unified platform for automated protein structure and function prediction. *Nat Protoc.* 5(4), 725-738 (2010).
6. Pineda AO, Chen ZW, Marino F, Mathews FS, Mosesson MW, and Di Cera E. Crystal structure of thrombin in complex with fibrinogen gamma' peptide. *Biophys Chem.* 125(2-3), 556-559 (2007).

Chapter IV ▫

Erythrocyte binding sites on the fibrinogen molecule

Overview

From previous studies, performed by our group it is known that there is a specific binding mechanism between fibrinogen and erythrocytes, which is not yet fully elucidated. Fibrinogen binds to the $\alpha_{IIb}\beta_3$ integrin on activated platelets, leading to the platelet aggregation necessary for blood coagulation. Two potential binding sites for this integrin on the fibrinogen molecule have been identified as the RGD (arginine-glycine-aspartate) sequences on each Aα chain (amino acid residues 572-575 and 95-98). However, it is not known which binding sites of the fibrinogen protein structure are involved on the interaction with its specific erythrocyte receptor, leading to erythrocyte aggregation.

In this Chapter, we evaluated the effect of different fibrinogen variants, specifically mutated in their putative integrin recognition sites on the Aα chain (mutants D97E, D574E and D97E/D574E), on the binding to its human erythrocyte receptor, in order to identify the interaction sites. Atomic force microscopy-based force spectroscopy measurements showed a significant decrease both on the fibrinogen-erythrocyte binding force and on its frequency for the proteins with the D97E mutation on the Aα chain, indicating that the corresponding RGD sequence (residues 95-97) is involved on this interaction. In order to overcome the risks of fibrinogen-driven erythrocyte hyperaggregation, new therapeutic approaches involving the fibrinogen Aα-RGD binding sites should be develop; however, further studies are still required.

Most of this work was done at Instituto de Medicina Molecular, Faculdade de Medicina, Universidade de Lisboa and the rest at the Leeds Institute of Cardiovascular and Metabolic Medicine and Multidisciplinary Cardiovascular Centre, Faculty of Medicine and Health, University of Leeds, United Kingdom, with the supervision of Prof. Robert Ariëns.

Declaration of authorship

I, Ana Filipa Guedes, declare that the laboratory work, namely AFM-based force spectroscopy experiments, data analysis and discussion was mainly done by Prof. Filomena A. Carvalho with my help, under the supervision of Prof. Nuno C. Santos. Fibrinogen mutants were produced by Dr. Cedric Duval and Luke Swithenbank, under the supervision of Prof. Robert A. S. Ariëns and Prof. David H. Farrell. The initial draft of the manuscript and scanning electron microscopy experiments were done by me. All authors revised and improved the manuscript.

I, Filomena A. Carvalho, as co-supervisor of Ana Filipa Guedes and co-author of the manuscript, hereby declare that the information above is correct.

I, Nuno C. Santos, as supervisor of Ana Filipa Guedes and corresponding author of the manuscript, hereby declare that the information above is correct.

Lisbon, April 6, 2018

Ana Filipa Guedes | Filomena Carvalho | Nuno C. Santos

Ana Filipa Guedes | Filomena A. Carvalho | Nuno C. Santos

Article information (annexes, article 2, start in page 371):

The $_{95}$RGD$_{97}$ sequence on the Aα chain of fibrinogen is essential for binding to its erythrocyte receptor

Filomena A. Carvalho[1,*], Ana Filipa Guedes[1,*], Cedric Duval[2], Fraser Macrae[2], Luke Swithenbank[2], David H. Farrell[3], Robert A.S. Ariëns[2], Nuno C. Santos[1,#]

Status: Published online on April 3, 2018

***Journal* (year) volume, pages:** *International Journal of Nanomedicine* (2018) 13, 1985-1992

DOI: 10.2147/IJN.S154523

JCR Impact factor 2016, quartile and field: 4.300, Q1 in Nanoscience and Nanotechnology and Biophysics

The $_{95}$RGD$_{97}$ sequence on the Aα chain of fibrinogen is essential for binding to its erythrocyte receptor

Filomena A. Carvalho[1,*], Ana Filipa Guedes[1,*], Cedric Duval[2], Fraser Macrae[2], Luke Swithenbank[2], David H. Farrell[3], Robert A.S. Ariëns[2], Nuno C. Santos[1,#]

[*] These authors contributed equally to this work.

[1]Instituto de Medicina Molecular, Faculdade de Medicina, Universidade de Lisboa, Lisboa, Portugal.

[2]Theme Thrombosis, Division of Cardiovascular and Diabetes Research, Leeds Institute for Genetics, Health and Therapeutics, University of Leeds, Leeds, UK.

[3]Department of Surgery, Oregon Health and Science University, Portland, OR, USA.

[#]To whom correspondence should be addressed: Nuno C. Santos, Instituto de Medicina Molecular, Faculdade de Medicina, Universidade de Lisboa, Av. Prof. Egas Moniz, 1649-028 Lisbon, Portugal; Tel.: +351-217999480; Fax: +351-217999477; E-mail: nsantos@fm.ul.pt.

Abstract

Erythrocyte aggregation, a cardiovascular risk factor, is increased by high plasma fibrinogen levels. Here, the effect of different fibrinogen mutations on the binding to its human erythrocyte receptor was assessed in order to identify the interaction sites. Three fibrinogen variants were tested, specifically mutated in their putative integrin recognition sites on the Aα chain (mutants D97E, D574E and D97E/D574E) and compared with wild-type fibrinogen. Atomic force microscopy-based force spectroscopy measurements showed a significant decrease both on the fibrinogen-erythrocyte binding force and on its frequency for fibrinogen with the D97E mutation, indicating that the corresponding arginine-glycine-aspartate sequence (residues 95-97) is involved in this interaction, and supporting that the fibrinogen receptor on erythrocytes has a β_3 subunit. Changes in the fibrin clot network obtained with the D97E mutant in presence of RBCs were observed by scanning electron microscopy. These findings may lead to innovative perspectives on the development of new therapeutic approaches to overcome the risks of fibrinogen-driven erythrocyte hyperaggregation.

Keywords: atomic force microscopy, fibrinogen, fibrin clot, erythrocyte aggregation, mutant protein.

Abbreviations: AFM – atomic force microscopy; APTES - aminopropyl-triethoxysilane; CHF – Chronic Heart Failure; RGD – arginine-glycine-aspartate amino acid residues sequence; SEM – scanning electron microscopy; WT – wild type.

Plain language summary

Currently, cardiovascular diseases are the leading cause of mortality worldwide, accounting for about one third of all deaths. Erythrocyte aggregation, which may lead to the formation of thrombus on the bloodstream, is associated with an increase in the concentration of fibrinogen. However, it is not known which binding sites on the fibrinogen protein structure are involved on the interaction with its specific receptor on the erythrocyte membrane, contributing to erythrocyte aggregation.

Here, the effect of different fibrinogen mutations on the binding to its human erythrocyte receptor was assessed in order to identify the interaction sites. Using atomic force microscopy (AFM), a nanotechnology technique, we were able to use mutated fibrinogen molecules as "bait" to "fish" its receptor on the surface of red blood cells. It was shown that the force required to break the binding between fibrinogen (the "bait") and red blood cell (the "fish"), as well as the frequency of this binding, were lower for the proteins with the D97E mutation on the Aα chain, indicating that the corresponding arginine-glycine-aspartate sequence is involved in this interaction. Changes on fibrin clot network for the D97E mutant in presence of RBCs were also observed.

This study opens new perspectives on the development of novel therapeutic approaches to overcome the risks of fibrinogen-driven erythrocyte hyperaggregation.

Introduction

Fibrinogen has a crucial role in blood clotting[1]. The increase in fibrinogen plasma concentration leads to increased erythrocyte aggregation, one of the most important factors affecting blood flow and a significant cardiovascular risk factor[2]. It has been reported that there is specific binding between fibrinogen and a previously unknown erythrocyte receptor[3].

The fibrinogen molecule contains multiple binding motifs for different cellular receptors, acting as a molecular link between coagulation, inflammation and immunity. Particularly, fibrinogen binds to the $\alpha_{IIb}\beta_3$ integrin on activated platelets, leading to the platelet aggregation necessary for blood coagulation[4, 5]. Three potential binding sites for this integrin on the fibrinogen molecule have been identified, which are structural RGD (arginine-glycine-aspartate) sequences on each Aα chain (amino acid residues 572-574 and 95-97) and one dodecapeptide sequence on the γ chain, yielding a total of six potential binding sites per fibrinogen molecule (formed by two Aα, two Bβ and two γ chains)[6].

Maeda *et al*. proposed a model for a possible location of the erythrocyte-binding regions of fibrinogen in its Aα chain, and tried to explain how it may affect erythrocyte aggregation and deformability[7]. The Aα 207-303 domain was found to include one of the possible erythrocyte-binding sites[7]. Using atomic force microscopy (AFM)-based force spectroscopy measurements, we demonstrated the existence of a single-molecule interaction between fibrinogen and a receptor on the erythrocyte membrane, with a lower but comparable affinity relative to platelet binding[8]. Fibrinogen binding to this receptor is inhibited by calcium depletion and by eptifibatide (an inhibitor considered to be specific for the receptor of fibrinogen on platelets, the glycoprotein $\alpha_{IIb}\beta_3$), but not as strongly as the platelet receptor. The results from a Glanzmann thrombasthenia (a rare hereditary bleeding disease caused by $\alpha_{IIb}\beta_3$ deficiency) patient showed an impaired fibrinogen-erythrocyte binding. Correlation with genetic sequencing data demonstrated that one of the units of the fibrinogen receptor on erythrocytes is a product of the expression of the β_3 gene[8, 9]. To further assess the specificity of the fibrinogen-erythrocyte binding, as well as to complete its identification, we recently measured the inhibition of

the fibrinogen-erythrocyte interaction using specific antibodies against integrins[10]. We also demonstrated that younger erythrocytes bind more fibrinogen than the older ones, being therefore the main cells responsible for the cardiovascular risk associated with an increase on the fibrinogen content in blood[11]. More recently, we showed that the interaction between fibrinogen and erythrocytes is modified in chronic heart failure (CHF) patients. The average force necessary to break the bond between fibrinogen and erythrocytes from CHF patients is higher than for erythrocytes from the control group[10]. Also using AFM, we showed that increasing fibrinogen levels lead to an increase in erythrocyte-erythrocyte adhesion in essential arterial hypertension patients[12]. Thus, AFM-based force spectroscopy is an approach with a high potential for applicability on biomedical research, inclusively on the study of cardiovascular diseases[10-14].

Here, three stable fibrinogen variants were obtained according to previously established procedures[4, 15], specifically altered in the described integrin binding sites on the Aα chain (D97E, D574E and the D97E/D574E double mutant). Using these variants, we conducted force spectroscopy measurements to determine the force necessary to break the bond between each fibrinogen variant (attached to the AFM tip) and erythrocytes. For the sake of comparison, identical measurements were conducted with wild-type (WT) fibrinogen. The analysis of the structure of the fibrin fibers in the blood clot was done using scanning electron microscopy (SEM). The results shed light on which integrin binding sites of the fibrinogen molecule are involved on the binding to the erythrocyte receptor. Knowledge of these aspects may lead to innovative perspectives on the development of new therapeutic drugs to overcome the risks of fibrinogen-driven erythrocyte hyperaggregation.

Methods

Fibrinogen mutants

The constructs for the fibrinogen variants were produced as previously described[4, 15]. We performed DNA sequence analysis, constructed the expression vectors and conducted site-directed mutagenesis according to established procedures. Briefly, baby hamster kidney cells (BHK), purchased from ATCC, were used to produce three stable fibrinogen mutants (Aα chain mutants D97E, D574E and the D97E/D574E double mutant) and the WT fibrinogen. Aα chain mutations have a single-nucleotide change, resulting in a codon for a different amino acid residue (aspartate changed to glutamate).

Erythrocyte isolation

Blood from adult healthy donors was collected into K_3EDTA anticoagulant tubes with their previous written informed consent, following a protocol with the Portuguese Blood Institute (Lisbon), approved by the joint Ethics Committee of the Faculty of Medicine of the University of Lisbon and the Santa Maria Hospital. The experimental work was carried out in accordance with the Declaration of Helsinki of the World Medical Association. Erythrocytes were isolated from the blood samples according to established procedures[8, 10, 11]. Briefly, erythrocytes were separated from the other blood components by centrifugation at 200 *g* for 10 min, at 10°C. Plasma and buffy-coat were removed, and the erythrocytes were washed three times with buffered saline glucose citrate (BSGC: 1.6 mM KH_2PO_4, 8.6 mM Na_2HPO_4, 120 mM NaCl, 13.6 mM sodium citrate, 11.1 mM glucose, pH 7.3) supplemented with 1 mM $CaCl_2$. Erythrocytes (0.1% hematocrit) were attached to a clean poly-L-lysine treated glass slide after 30 min of deposition, at room temperature. Non-adherent cells were removed by sequential washes with buffer. Samples were loaded into the AFM and allowed to equilibrate in buffer for 15 min before force spectroscopy measurements.

AFM tip functionalization

A previously optimized procedure was used for the covalent attachment of fibrinogen to the AFM tips (functionalization) and for blood cells deposition on a solid substrate[8, 10, 11]. Briefly, cleaned AFM silicon nitride tips were silanized with 3-aminopropyl-triethoxysilane (APTES). Then, the probes were treated with a glutaraldehyde solution 2.5% (v/v) and finally immersed in a 0.5 mg/mL final concentration of fibrinogen (WT or mutant).

AFM-based force spectroscopy

Force spectroscopy measurements were performed on a NanoWizard II atomic force microscope (JPK Instruments, Berlin, Germany), mounted on an Axiovert 200 inverted optical microscope (Zeiss, Jena, Germany), using fibrinogen functionalized OMCL TR-400-type silicon nitride AFM tips (Olympus, Tokyo, Japan), as previously described[8]. The spring constant of the tips was calibrated by the thermal fluctuation method, resulting in values of 19 ± 7 mN/m. The applied force was adjusted to 0.8 nN before retraction. Molecular recognition was searched by intermittently pressing the cantilevers on each erythrocyte adsorbed on the glass slide. Data collection for each force-distance cycle was performed at 2 µm/s, leading to a loading rate of 4 nN/s. Force curves were analyzed using the JPK image processing software v. 4.2.61. For any given experiment, approximately 5000 force-distance curves were collected, analyzed and adjusted by polynomial fit[16]. Each experiment was performed at least three times, each time on different blood samples and with different functionalized tips.

Scanning electron microscopy

SEM was used to investigate the differences on structure of clots formed from WT and D97E recombinant fibrinogen, especially in the presence of erythrocytes.

WT or D97E recombinant fibrinogen (0.5 mg/mL final concentration) and $CaCl_2$ (final concentration 10 mM) were diluted in TBS (50 mM Tris-HCl, 100 mM NaCl, pH 7.5) and premixed. Human thrombin (Calbiochem, Nottingham, UK; final concentration 1 U/mL) was then added to initiate clotting. The mixtures were immediately transferred to

Eppendorf lids, which were pierced with a syringe to assist solvent permeation. Clots were formed in a moist chamber, at room temperature, for 120 min. Clots were then washed with saline solution to remove excess salt, followed by fixation in 2% (v/v) glutaraldehyde (120 min). Clots were further washed extensively with sodium cacodylate buffer and dehydrated in a series of increasing acetone concentrations (30-100%). Clots were critical-point dried with CO_2, mounted onto stubs and sputter-coated with platinum, using a Cressington 208 HR (Watford, UK). Clots were also prepared with the appropriate amount of erythrocytes for a final hematocrit of 20%. They were observed and photographed digitally on at least 3 different areas *per* clot, using a scanning electron microscope Hitachi SU8230 FESEM (Tokyo, Japan), at 5 different magnifications (2500× (data not shown), 5000×, 10000× (data not shown), 25000× and 50000×). At least, duplicates of each type of clot were performed. Fiber diameters were measured from 20 random fibers of each image in high magnification (25000×), using ImageJ software (National Institutes of Health, Bethesda, MD, USA). Each cross-section measurement was performed over a single fibrin fiber and values of fiber diameter were extracted and averaged. All cross-section measurements were performed away from the branching points, in order to avoid biased results.

Statistical analysis

Unpaired samples Student's *t*-test was used for statistical analysis. Differences were considered statistically significant for $p < 0.05$. For atomic force microscopy, each experiment was performed at least three times, each time with different blood samples and with different functionalized tips. At least 15 erythrocytes were tested on each blood sample. For scanning electron microscopy, at least duplicates of each type of clot were performed. Average fiber diameters were measured from 20 random fibers of each image, at high magnification (25000 ×).

Results and discussion

AFM-based force spectroscopy studies, conducted at the single-molecule level, yielded force *vs*. distance curves, acquired after the binding of mutant or WT fibrinogen to the receptor on erythrocytes (Figure 1a). The repeated measurements of the adhesion events, as the one shown in Figure 1b, allowed us to build up rupture force histograms for each fibrinogen variant and cell population studied.

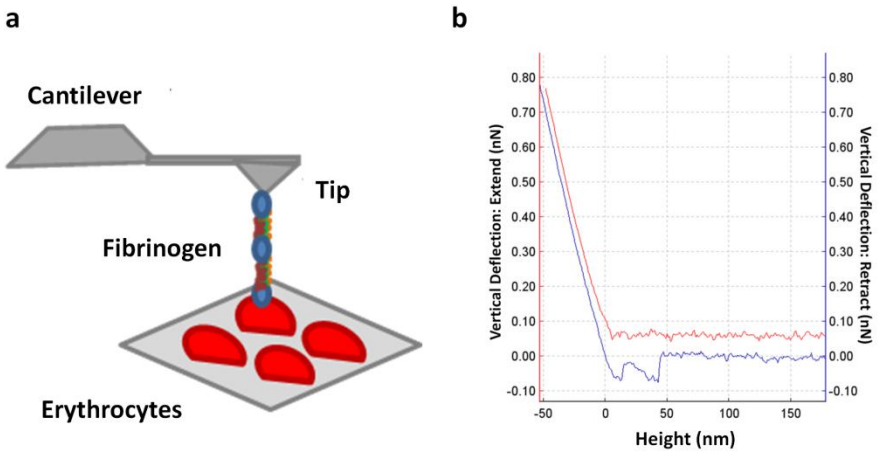

Figure 1 | **AFM-based force spectroscopy experiments and force-distance curve. a)** Schematic representation of the erythrocytes deposited on a poly-L-lysine-coated glass slide and an AFM tip chemically functionalized with different fibrinogen variants. The vertical movement approaching the tip to the sample until contact enables the binding of fibrinogen to the erythrocyte. The subsequent retraction progresses until a certain force (and distance) is reached and the fibrinogen molecule detaches from the erythrocyte surface. The (un)binding frequency corresponds to the fraction of these approach-retraction cycles in which binding and subsequent unbinding occur. **b)** Example of a force-distance curve. When approaching the tip to the sample (red line), the fibrinogen molecule may contact with cell receptor(s) and the binding between them can occur. By retracting the tip away from the sample (blue line), as the cantilever moves upward, the tip bends down to negative force values. In some surface distance point, the bond breaks and the cantilever jumps back to its neutral force position. At this point, the binding force necessary to break the bond, at the single-molecule level, can be measured.

Figure 2a shows the rupture force histograms for the three different fibrinogen mutants and WT fibrinogen. It can be noticed that, in the presence of the D97E or D97E/D574E mutant, the histogram is shifted to lower binding forces, when compared with those obtained for WT fibrinogen. The opposite variation trend was obtained for the rupture force histogram of D574E, which is shifted to higher and stronger binding forces.

As it can be observed in Figure 2b, the average force necessary to break the bond between the D97E fibrinogen mutant (43.2 ± 1.1 pN) or the D97E/D574E double mutant (49.2 ± 0.8 pN) and erythrocytes is significantly lower than for WT fibrinogen (58.8 ± 2.3 pN; $p < 0.0001$ for both pairs). On the other hand, the average force necessary to break the bond between erythrocytes and the D574E mutant (105.9 ± 1.7 pN) was significantly higher than for the WT ($p < 0.0001$).

Decreases on the frequency (probability) of fibrinogen-erythrocyte binding and subsequent unbinding for the D97E (11.4%), D574E (13.1%) or D97E/D574E (11.1%) mutants in comparison with the WT fibrinogen (15.9%) were observed. The variation of the binding frequency of the different mutants relative to the WT is presented in Figure 2c.

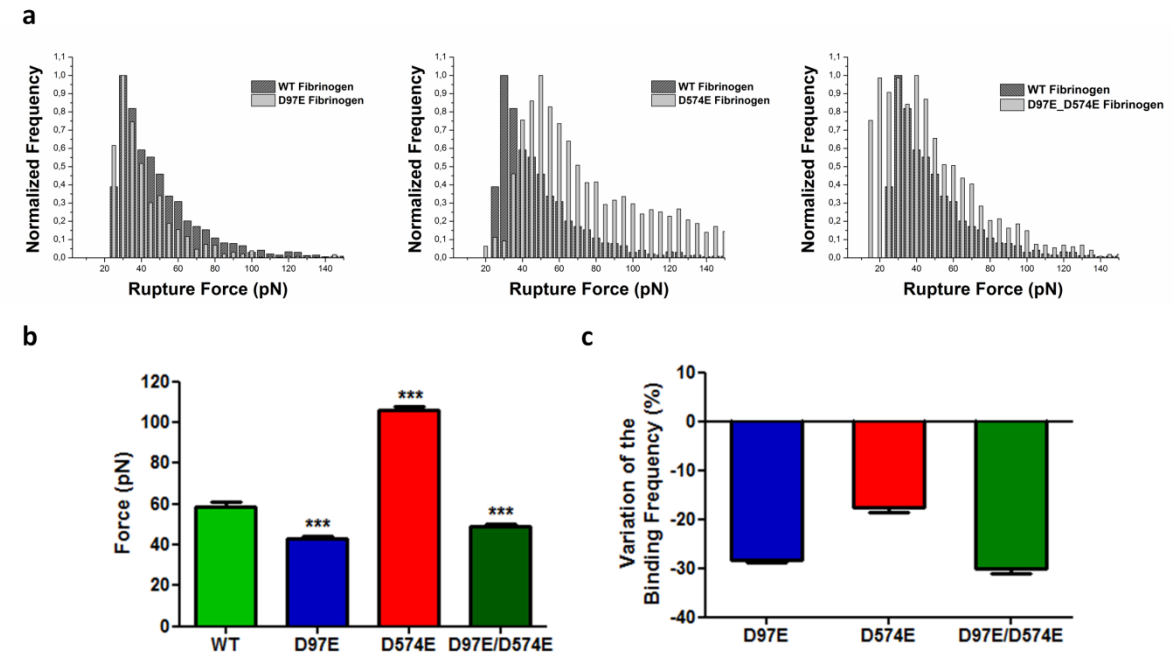

Figure 2 | AFM force spectroscopy data for the binding between different fibrinogen variants and erythrocytes. a) Rupture force histograms of the interactions

between the three different fibrinogen mutants (D97E, D574E and D97E/D574E: light grey) or wild-type fibrinogen (dark grey) and erythrocytes. On the rupture force histograms, each count represents a single molecule binding between one fibrinogen molecule and one of its cell receptors. **b)** Average (un)binding force of the interactions. Values are shown as mean ± standard error of mean (SEM). There were statistically significant variations (***, $p < 0.0001$) of the rupture forces between WT fibrinogen and the three fibrinogen variants with mutations on the Aα chain (D97E, D574E and D97E/D574E). **c)** Variation of the fibrinogen-erythrocyte (un)binding frequency of the different fibrinogen variants relative to WT fibrinogen. (Un)binding frequency variations were calculated based on the ratio between the frequency of (un)binding events determined for the mutants and the frequency of (un)binding events obtained for WT fibrinogen.

Our results indicate that the RGD sequence corresponding to amino acid residues 95 to 97 of the fibrinogen Aα chain is involved in the binding to the erythrocyte membrane receptor. It has previously been reported that this RGD sequence is also involved in the binding to the β_3 subunit of the $\alpha_V\beta_3$ receptor on endothelial cells[17]. These results further support our recent findings regarding the fibrinogen receptor on erythrocytes[8, 10].

The force necessary to break the bond between D574E fibrinogen and the erythrocyte membrane receptor was significantly higher than for WT fibrinogen, while the frequency of (un)binding events for this mutant was lower. These apparently opposite effects might be explained by the location of the specific binding site. As it is located close to the C-terminus of the α chain, the domain may eventually change conformation, leading to a stabilization of the complex formed upon binding to the erythrocyte receptor.

It is worth to mention that during the conversion of fibrinogen to fibrin, thrombin cleaves fibrinogen Aα chain at Arg-16 and the Bβ chain at Arg-14, releasing the fibrinopeptides A and B, respectively, and forming the so-called fibrin monomers[18, 19]. In the fibrinogen structure the thrombin cleavage regions are distant from the mutated regions of fibrinogen variants produced here. Therefore, these mutations on the

fibrinogen molecule do not interfere with the thrombin-induced conversion of fibrinogen to fibrin.

The existence of a specific binding mechanism in fibrinogen-induced erythrocyte hyperaggregation suggests the possibility of developing new treatments to decrease erythrocyte aggregation, therefore potentially decreasing cardiovascular risk. Fibrinogen is considered an independent risk factor on screening programs aimed at identifying individuals at high risk for cardiovascular diseases[20]. Our results shows that, in addition to the assessment of the plasma fibrinogen concentration itself, it may also be important to identify mutations in the fibrinogen molecules that may change the binding to erythrocytes as a risk assessment strategy.

Moreover, in order to see if this fibrinogen variant induces changes on the structure of the fibrin blood clot, a scanning electron microscopy assessment was also performed. From the micrographs obtained for the D97E and WT fibrin clots, we observed that there were no differences in fibrin clot structure (Figure 3).

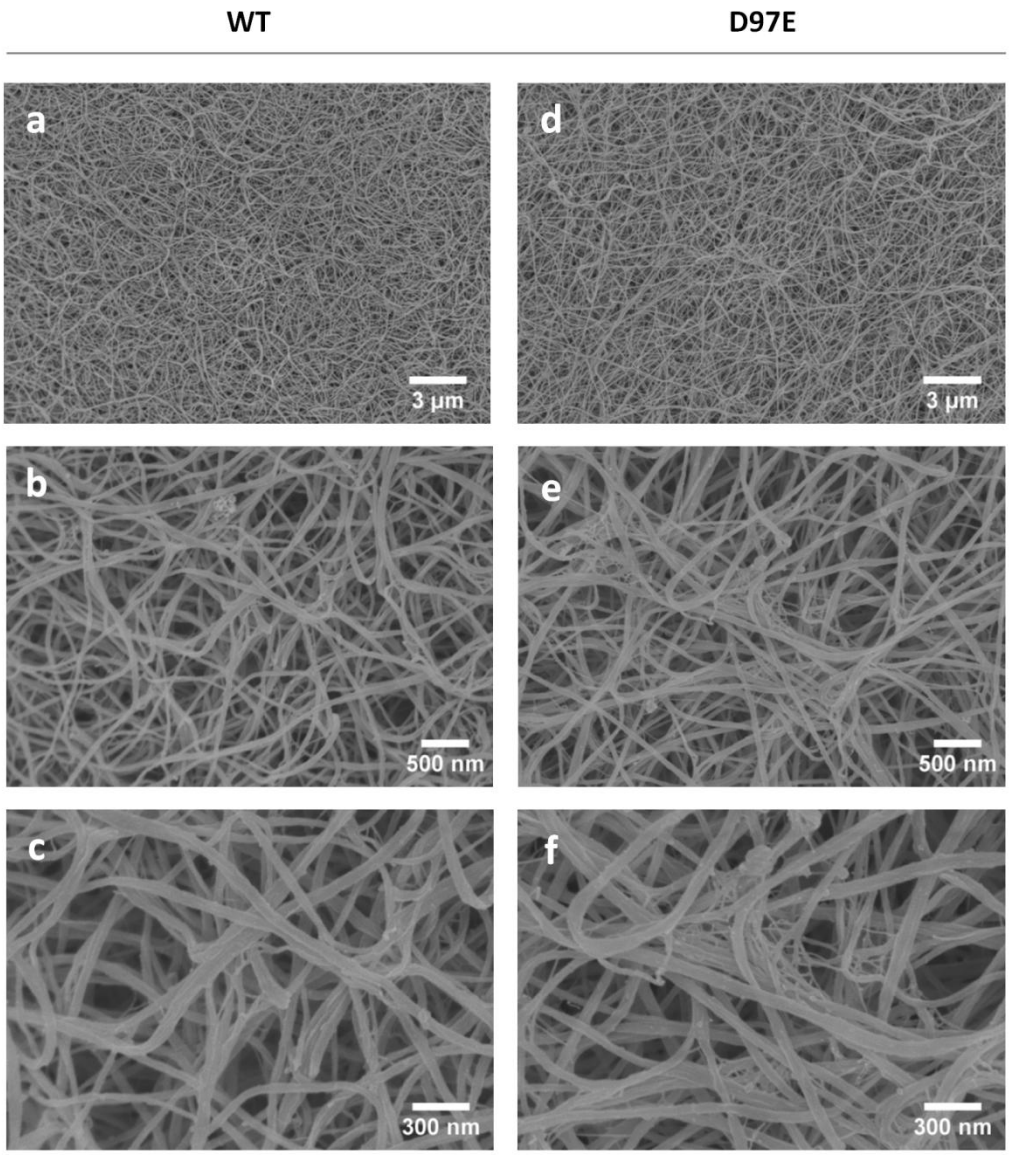

Figure 3 | **Clots made from WT (a-c) or D97E (d-f) fibrinogen (0.5 mg/mL), imaged by scanning electron microscopy.** Magnifications: a, c - 5000×; b, e - 25000×; c, f - 50000×.

Clots were also evaluated in the presence of 20% of erythrocytes (Figure 4). The clots formed with WT fibrin have a more homogeneous structure than those formed with the D97E mutant. The D97E fibrin clots seem to have a more disorganized structure, with higher number of clusters that entrap erythrocytes. The clots appear to be more loosely packed, eventually leading to a higher risk of embolism. SEM images correlate well with

the AFM data, where a decrease of both the binding force and the binding frequency were observed for this mutant, when compared with the WT fibrinogen.

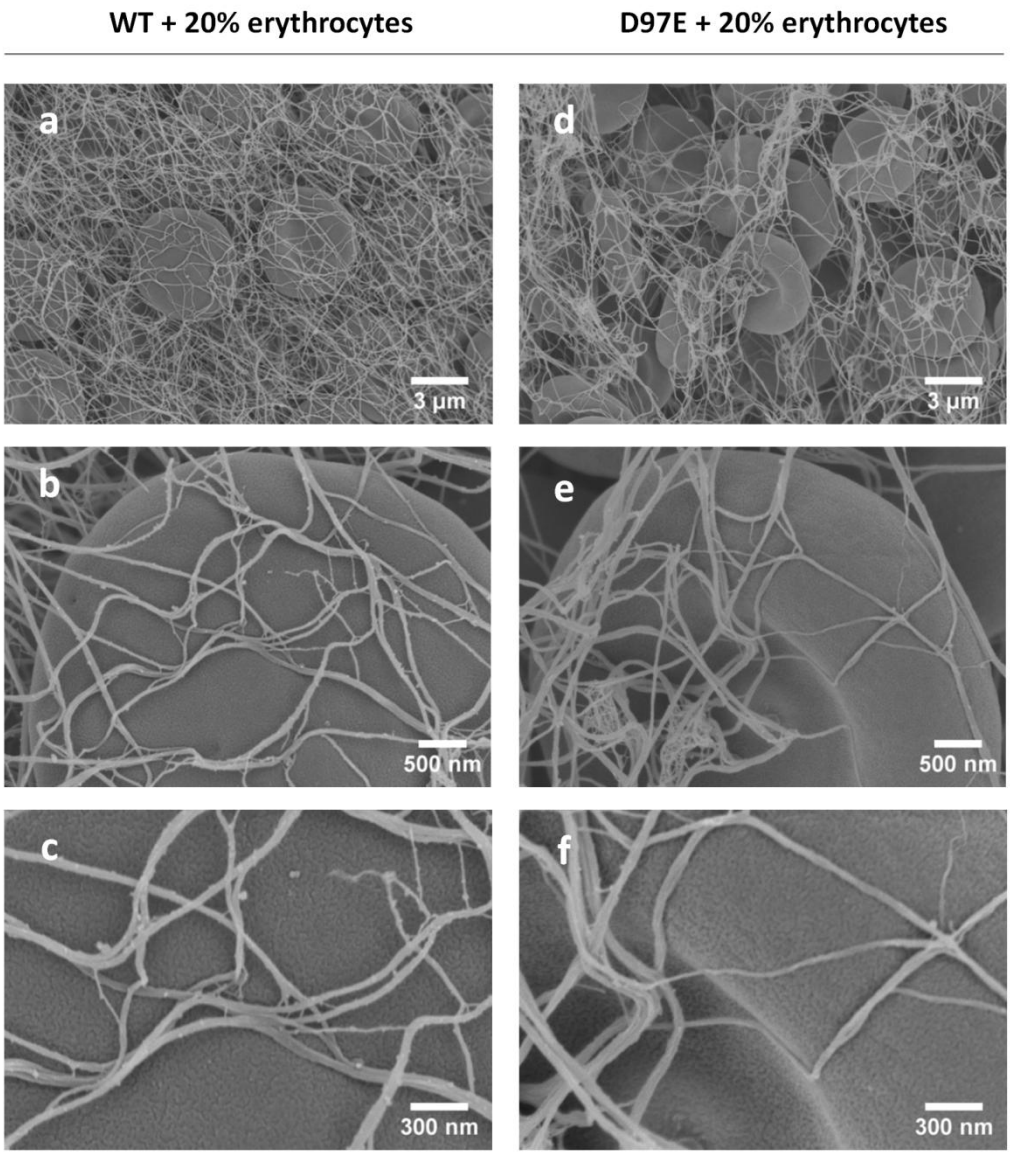

Figure 4 | **Fibrin clots formed in the presence of erythrocytes (20%), with WT (a-c) or D97E (d-f) fibrinogen, imaged by scanning electron microscopy.** Magnifications: a, d - 5000×; b, e- 25000×; c, f - 50000×.

After analyzing the SEM micrographs shown on Figures 3 and 4, the diameter of the fibers were calculated (Figure 5). No differences in fiber diameter between both fibrinogen variants were observed in the absence of erythrocytes, but statistically

significant differences were found in the presence of these cells. The addition of 20% of erythrocytes to the D97E fibrin clot caused a decrease in fiber thickness (37.7 ± 2.0 nm without erythrocytes *vs.* 18.9 ± 1.1 nm with erythrocytes; $p < 0.0001$) and led to an extensive network rearrangement. A statistically significant variation of the fibers' diameter was also observed between WT fibrin and D97E fibrin, both in the presence of erythrocytes (30.8 ± 1.8 nm *vs.* 18.9 ± 1.1 nm, respectively; $p < 0.0001$).

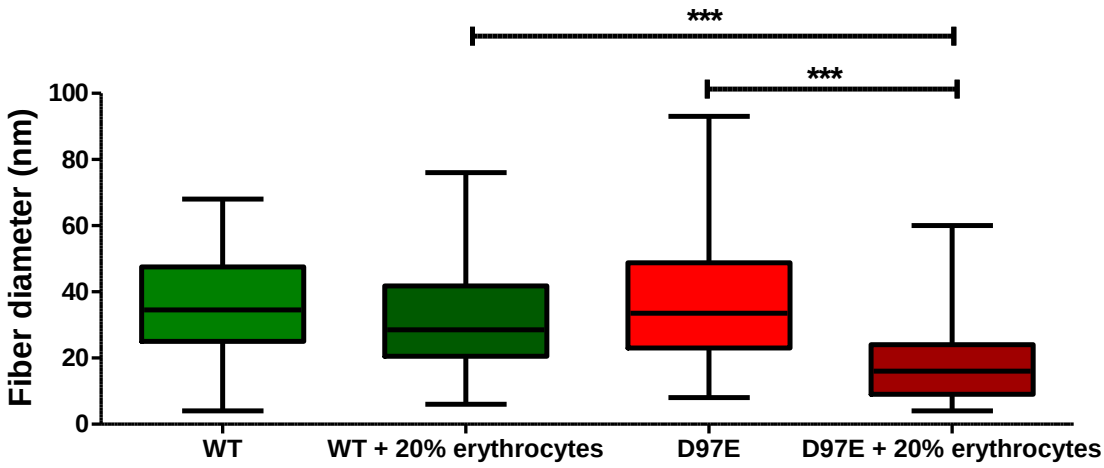

Figure 5 | **Diameter of fibers from WT or D97E fibrin clots, in the absence or presence of erythrocytes.** Data are presented as a box of whiskers plot. Fiber diameters were measured from 20 random fibers from each condition, imaged with 25000× magnification (***, $p < 0.0001$).

The difference in the D97E fibrin fibers' diameter in the presence of erythrocytes is clear. This should be due to the mutant fibrin(ogen) interaction with erythrocytes, and not to any difference in the polymerization of this fibrinogen variant itself, as the structure of the mutant fibrin without these cells seem the same as for the WT. Only when erythrocytes are present, the clot D97E fibrin structure becomes different.

The architecture of the clot may affect its stability, viscoelastic and mechanical properties, as well as its fibrinolytic characteristics[21, 22]. These characteristics may determine if a clot breaks down by fibrinolysis, or if it will lead to blood vessel occlusion or embolization[23]. Moreover, it has been previously reported that tightly packed and rigid clots, with thinner fibers and low porosity, are less susceptible to the action of thrombolytic agents[24, 25].

This work yields valuable new information on the identification of the fibrinogen domains that interact with its erythrocyte membrane receptor, contributing to the erythrocyte hyperaggregation in the bloodstream induced by increased levels of fibrinogen. Moreover, in this study, AFM-based force spectroscopy demonstrated its potential as an important nanotechnology approach for biomedical research application, important to measure the interaction forces between fibrinogen (or other plasma proteins) and human blood cells. Future studies using animal models would be important to test the binding between the fibrinogen variants and erythrocytes *in vivo*, in order to develop new therapeutic approaches to treat fibrinogen-driven erythrocyte hyperaggregation.

Acknowledgements

The authors thank Teresa Freitas (IMM, FM, UL) for excellent technical assistance. This work was supported by Fundação para a Ciência e a Tecnologia – Ministério da Ciência, Tecnologia e Ensino Superior (FCT-MCTES, Portugal) grants PTDC/QUI-BIQ/119509/2010 and PTDC/BBB-BMD/6307/2014, and by the Calouste Gulbenkian Foundation (Portugal). AFG also acknowledges FCT-MCTES PhD fellowship SFRH/BD/84414/2012. This work was also supported by LISBOA-01-0145-FEDER-007391, project cofunded by FEDER, through POR Lisboa 2020 - Programa Operacional Regional de Lisboa, PORTUGAL 2020, and Fundação para a Ciência e a Tecnologia. The authors declare no competing financial interests.

Authorship Contribution

F.A.C. performed AFM experiments, analyzed the force spectroscopy data, wrote and edited an initial draft and prepared the manuscript for submission; **A.F.G.** performed AFM experiments, analyzed force spectroscopy data, wrote and edited an initial draft of the manuscript; **C.D.** and **L.S.** constructed the fibrinogen mutants, contributed to relevant methods and edited the manuscript drafts; **F.M.** performed the acquisition and analysis of SEM micrographs; **D.H.F.** contributed to the construction of the fibrinogen mutants and to relevant discussions, and edited the manuscript drafts; **R.A.S.A.** contributed to the construction of the fibrinogen mutants and to relevant discussions, and edited the manuscript drafts; **N.C.S.** conceived the idea, designed and directed the AFM experiments, analyzed the data, wrote part of the text and edited the successive manuscript drafts.

Conflict of interest

Oregon Health and Science University (OHSU) and Dr. David Farrell have a significant interest in Gamma Therapeutics, a company that may have a commercial interest in the results of this research and technology this potential individual and institutional conflict of interest has been reviewed and managed by OHSU. The authors report no other conflict of interest in this work.

References of Chapter IV

1. Kamath, S. & Lip, G.Y. Fibrinogen: biochemistry, epidemiology and determinants. *QJM* **96**, 711-729 (2003).
2. Lominadze, D., Dean, W.L., Tyagi, S.C. & Roberts, A.M. Mechanisms of fibrinogen-induced microvascular dysfunction during cardiovascular disease. *Acta Physiol* **198**, 1-13 (2010).
3. Sokolova, I.A., Muravyov, A.V., Khokhlova, M.D., Rikova, S.Y., Lyubin, E.V., Gafarova, M.A., Skryabina, M.N., Fedyanin, A.A., Kryukova, D.V. & Shahnazarov, A.A. An effect of glycoprotein IIb/IIIa inhibitors on the kinetics of red blood cells aggregation. *Clin Hemorheol Microcirc* **57**, 291-302 (2014).
4. Farrell, D.H. & Thiagarajan, P. Binding of recombinant fibrinogen mutants to platelets. *J Biol Chem* **269**, 226-31 (1994).
5. Holmback, K., Danton, M.J., Suh, T.T., Daugherty, C.C. & Degen, J.L. Impaired platelet aggregation and sustained bleeding in mice lacking the fibrinogen motif bound by integrin alpha IIb beta 3. *EMBO J* **15**, 5760-71 (1996).
6. Salsmann, A., Schaffner-Reckinger, E. & Kieffer, N. RGD, the Rho'd to cell spreading. *Eur J Cell Biol* **85**, 249-54 (2006).
7. Maeda, N., Seike, M., Kume, S., Takaku, T. & Shiga, T. Fibrinogen-induced erythrocyte aggregation: erythrocyte-binding site in the fibrinogen molecule. *Biochim Biophys Acta* **904**, 81-91 (1987).
8. Carvalho, F.A., Connell, S., Miltenberger-Miltenyi, G., Pereira, S.V., Tavares, A., Ariëns, R.A.S. & Santos, N.C. Atomic force microscopy-based molecular recognition of a fibrinogen receptor on human erythrocytes. *ACS Nano* **4**, 4609-20 (2010).
9. Carvalho, F.A., Martins, I.C. & Santos, N.C. Atomic force microscopy and force spectroscopy on the assessment of protein folding and functionality. *Arch Biochem Biophys* **531**, 116-27 (2013).
10. Guedes, A.F., Carvalho, F.A., Malho, I., Lousada, N., Sargento, L. & Santos, N.C. Atomic force microscopy as a tool to evaluate the risk of cardiovascular diseases in patients. *Nat Nanotechnol* **11**, 687-92 (2016).
11. Carvalho, F.A., de Oliveira, S., Freitas, T., Goncalves, S. & Santos, N.C. Variations on fibrinogen-erythrocyte interactions during cell aging. *PLoS One* **6**, e18167 (2011).

12. Guedes, A.F., Carvalho, F.A., Moreira, C., Nogueira, J.B. & Santos, N.C. Essential arterial hypertension patients present higher cell adhesion forces, contributing to fibrinogen-dependent cardiovascular risk. *Nanoscale* **9**, 14897-14906 (2017).
13. Guedes, A.F., Carvalho, F.A., Domingues, M.M., Macrae, F.L., McPherson, H.R., Santos, N.C., Ariëns, R.A.S. Sensing adhesion forces between erythrocytes and γ' fibrinogen modulating fibrin clot architecture and function. *Nanomedicine* **14**, 909-918 (2018).
14. Carvalho, F.A. & Santos, N.C. Atomic force microscopy-based force spectroscopy--biological and biomedical applications. *IUBMB Life* **64**, 465-72 (2012).
15. Standeven, K.F., Carter, A.M., Grant, P.J., Weisel, J.W., Chernysh, I., Masova, L., Lord, S.T. & Ariens, R.A. Functional analysis of fibrin gamma-chain cross-linking by activated factor XIII: determination of a cross-linking pattern that maximizes clot stiffness. *Blood* **110**, 902-7 (2007).
16. Ratto, T.V., Rudd, R.E., Langry, K.C., Balhorn, R.L. & McElfresh, M.W. Nonlinearly additive forces in multivalent ligand binding to a single protein revealed with force spectroscopy. *Langmuir* **22**, 1749-57 (2006).
17. Thiagarajan, P., Rippon, A.J. & Farrell, D.H. Alternative adhesion sites in human fibrinogen for vascular endothelial cells. *Biochemistry* **35**, 4169-75 (1996).
18. Blomback, B., Hessel, B., Hogg, D. & Therkildsen, L. A two-step fibrinogen-fibrin transition in blood coagulation. *Nature* **275**, 501-5 (1978).
19. Hurlet-Jensen, A., Cummins, H.Z., Nossel, H.L. & Liu, C.Y. Fibrin polymerization and release of fibrinopeptide B by thrombin. *Thromb Res* **27**, 419-27 (1982).
20. Meade, T.W., North, W.R., Chakrabarti, R., Stirling, Y., Haines, A.P., Thompson, S.G. & Brozovie, M. Haemostatic function and cardiovascular death: early results of a prospective study. *Lancet* **1**, 1050-4 (1980).
21. Undas, A. & Ariëns, R.A. Fibrin clot structure and function: a role in the pathophysiology of arterial and venous thromboembolic diseases. *Arterioscler Thromb Vasc Biol* **31**, e88-99 (2011).
22. Weisel, J.W. Structure of fibrin: impact on clot stability. *J Thromb Haemost* **5**, 116-24 (2007).
23. Weisel, J.W. The mechanical properties of fibrin for basic scientists and clinicians. *Biophys Chem* **112**, 267-76 (2004).

24. Bridge, K.I., Philippou, H. & Ariëns, R. Clot properties and cardiovascular disease. *Thromb Haemost* **112**, 901-8 (2014).

25. Collet, J.P., Soria, J., Mirshahi, M., Hirsch, M., Dagonnet, F.B., Caen, J. & Soria, C. Dusart syndrome: a new concept of the relationship between fibrin clot architecture and fibrin clot degradability: hypofibrinolysis related to an abnormal clot structure. *Blood* **82**, 2462-9 (1993).

Chapter V ▫

Fibrinogen-erythrocyte binding in chronic heart failure

Overview

The main motivation for the work described in this Chapter came from the fact that it has been reported that increasing plasma fibrinogen levels have pathogenic implications in thrombus formation, due to the increase on erythrocyte aggregation. This Chapter had two main goals. Firstly, we wanted to evaluate the fibrinogen-erythrocyte interaction as a risk biomarker for a worse clinical prognosis in Chronic Heart Failure (CHF) patients. We showed that the interaction between fibrinogen and erythrocytes is modified in these patients, even in both etiologies of CHF (ischemic and non-ischemic). A 12-months clinical follow-up was performed, which allowed to observe that patients with higher fibrinogen-erythrocyte binding forces at the beginning of the study, had a significantly higher probability of being hospitalized due to cardiovascular complications during the subsequent year. We believe that a better understanding of the molecular mechanisms underlying the interaction between fibrinogen and erythrocytes in CHF patients may be important to reduce aggregation and enhance microcirculatory flow conditions. Patients' hemorheological profiles were also assessed and changes were observed.

Fibrinogen-induced erythrocyte aggregation has been considered to be caused by its non specific binding to erythrocyte membranes. In contrast, platelets are known to have a fibrinogen integrin receptor on their membrane, the glycoprotein complex $\alpha_{IIb}\beta_3$. The second main goal of this part of the study was to complete the identification of the erythrocyte receptor for fibrinogen. In order to identify a specific interaction between fibrinogen and an erythrocyte membrane receptor, we conducted AFM binding inhibition studies with specific antibodies against α_v and $\alpha_v\beta_3$ integrins to measure the inhibition of the fibrinogen-erythrocyte interaction. Further details are described in this Chapter, including the supplementary information of the article.

This work was performed at Instituto de Medicina Molecular, Faculdade de Medicina, Universidade de Lisboa but also at Hospital Pulido Valente, Centro Hospitalar Lisboa Norte.

Declaration of authorship

I, Ana Filipa Guedes, declare that the laboratory work, data analysis and writing of the manuscript initial draft were carried out by me. For hemorheological data experiments, I had also the help of Inês Malho, under supervision of Prof. Nuno C. Santos and Prof. Filomena A. Carvalho. Prof. Filomena A. Carvalho also wrote some parts of the manuscript and helped on data analysis and discussion. Dr. Nuno Lousada and Dr. Luís Sargento provided the samples and all clinical information, conducted the clinical follow-up and performed some statistical analysis. All authors revised and improved the manuscript.

I, Filomena A. Carvalho, as co-supervisor of Ana Filipa Guedes and co-corresponding author of the manuscript, hereby declare that the information above is correct.

I, Nuno C. Santos, as supervisor of Ana Filipa Guedes and co-corresponding author of the manuscript, hereby declare that the information above is correct.

Lisbon, April 6, 2018

Ana Filipa Guedes | Filomena A. Carvalho | Nuno C. Santos

Article information (annexes, article 3, start in page 381):

Atomic force microscopy as a tool to evaluate the risk of cardiovascular in patients

Ana Filipa Guedes[1]; Filomena A. Carvalho[1,*]; Inês Malho[1]; Nuno Lousada[2]; Luís Sargento[2]; Nuno C. Santos[1,*]

Status: Published online on May 16, 2016

***Journal* (year) volume, pages:** *Nature Nanotechnology* (2016) 11, 687-92

DOI: 10.1038/nnano.2016.52

JCR Impact factor 2016, quartile and field: 38.986, Q1 in Nanoscience and Nanotechnology

Atomic force microscopy as a tool to evaluate the risk of cardiovascular diseases in patients

Ana Filipa Guedes[1]; Filomena A. Carvalho[1,*]; Inês Malho[1]; Nuno Lousada[2]; Luís Sargento[2]; Nuno C. Santos[1,*]

[1]Instituto de Medicina Molecular, Faculdade de Medicina, Universidade de Lisboa, Lisboa, Portugal; [2]Heart Failure Unit, Cardiology Department, Hospital Pulido Valente, Centro Hospitalar Lisboa Norte, Lisbon, Portugal.

[*] To whom correspondence should be addressed:

Nuno C. Santos, Instituto de Medicina Molecular, Faculdade de Medicina, Universidade de Lisboa, Av. Prof. Egas Moniz, 1649-028 Lisbon, Portugal; E-mail: nsantos@fm.ul.pt; Tel.: +351 217999480; Fax: +351 217999477.

Filomena A. Carvalho, Instituto de Medicina Molecular, Faculdade de Medicina, Universidade de Lisboa, Av. Prof. Egas Moniz, 1649-028 Lisbon, Portugal; E-mail: filomenacarvalho@fm.ul.pt; Tel.: +351 217999476; Fax: +351 217999477.

Abstract

The availability of biomarkers to evaluate the risk of cardiovascular diseases is limited[1]. High fibrinogen levels have been identified as a relevant cardiovascular risk factor, but the biological mechanisms remain unclear[2, 3]. Increased aggregation of erythrocytes (red blood cells) has been linked to high plasma fibrinogen concentration[2, 4]. Here, we show using atomic force microscopy, that the interaction between fibrinogen and erythrocytes is modified in chronic heart failure patients. Ischemic patients showed increased fibrinogen-erythrocyte binding forces compared with non-ischemic patients. Cell stiffness in both patient groups was also altered. A 12-month follow-up shows that patients with higher fibrinogen-erythrocyte binding forces initially were subsequently hospitalized more frequently. Our results show that atomic force microscopy can be a promising tool to identify patients with increased risk for cardiovascular diseases.

Introduction

Cardiovascular diseases are the leading cause of death worldwide, being responsible for approximately 30% of the total number of human losses[5]. Chronic heart failure (CHF), a complex clinical cardiovascular syndrome, is characterized by the heart failing to pump enough blood with the right pressure[6, 7]. Ischemic cardiomyopathy is the most common cause of heart failure, and patients with this condition have poorer disease prognosis and response to treatment than non-ischemic patients[8].

Erythrocyte aggregation has pathogenic implications in thrombus formation[9, 10]. It is associated with an increase in the concentration of fibrinogen in blood plasma[2, 3], which is a significant risk factor for several cardiovascular disorders[11, 12]. A few studies have focused on a possible specific interaction between fibrinogen and erythrocytes[13, 14]. However, our recent finding indicated that an integrin receptor for fibrinogen, with a β_3 subunit, exists on the erythrocyte membrane[15, 16]. Establishing the diagnostic, extent, and severity of cardiovascular diseases, as well as determining the potential risk of cardiovascular events, are crucial steps towards improving patient outcomes. For information about non-invasive tests and procedures used to evaluate CHF patients, please see Supplementary Section “Biomedical Relevance”.

There are an increasing number of reports that utilize atomic force microscopy (AFM) as a nanodiagnostic tool for use with patient cells[17, 18, 19]. A better understanding of the molecular mechanisms underlying the interaction between fibrinogen and erythrocytes in CHF patients may be important for eventual future drug interventions to reduce aggregation and enhance microcirculatory flow conditions. Here, we evaluate the fibrinogen-erythrocyte interactions, in stable outpatients with systolic CHF, using AFM-based force spectroscopy. We examined (1) the fibrinogen-erythrocyte interaction as a risk biomarker for a worse clinical prognosis, leading to hospitalization; (2) the association of fibrinogen-erythrocyte interaction with CHF etiology (ischemic or non-ischemic); and (3) patients’ hemorheological profile.

Results and discussion

The baseline characteristics of the cohort CHF patients, their relevant clinical data and the list of drugs used in their therapy are presented in Table 1.

Table 1 | Clinical profile, concomitant diseases and therapeutics at baseline of all chronic heart failure patients studied and for non-ischemic CHF and ischemic CHF patient groups.

	CHF patients (all)	Non-ischemic CHF	Ischemic CHF
Demographics			
Number of patients	30	15	15
Age (mean ± SD)	63.8 ± 9.9	61.9 ± 10.8	65.6 ± 9.1
Male/Female (%)	90/10	85/15	92/8
Cardiac parameters			
NYHA, II/III (%)	57/43	33/67	80/20
LV ejection Fraction (%; mean ± SD)	30.3 ± 8.8	29.5 ± 10.0	31.01 ± 7.7
Fibrinogen (mg/dL; mean ± SD)	325 ± 85	355 ± 96	296 ± 62
NT-ProBNP (pg/ml; median)	1330	2683	744
Concomitant diseases			
Diabetes mellitus (%)	23	13	33
Hypertension (%)	87	80	93
Myocardial infarction (%)	50	0	100
Auricular fibrillation (%)	30	40	20
Chronic renal insufficiency (%)	50	60	40
Chronic obstructive pulmonary disease (%)	13	13	13

Therapeutics at inclusion			
Furosemide (%)	83	93	73
ACE inhibitor (%)	60	80	40
Angiotensin receptor blocker (%)	30	20	40
Beta-blocker (%)	83	93	73
Cardiac resynchronization therapy (%)	33	60	7
Anti-platelet aggregation (%)	80	60	100

Abbreviations: ACE, angiotensin-converting enzyme; LV, left ventricular; NT-ProBNP, N-terminal pro-brain natriuretic peptide; NYHA, New York Heart Association functional classification (II - symptomatically 'mild' CHF and III - symptomatically 'moderate' CHF).

Figure 1a presents a schematic illustration of the set-up, in which fibrinogen molecules attached to the AFM cantilever were allowed to bind to its specific erythrocyte membrane receptor. Force adhesion maps of erythrocytes were recorded to define the correct position of the cantilever on top of a single cell (Fig. 1b). With this AFM-based force spectroscopy methodology, fibrinogen-erythrocyte interactions were assessed at the single-molecule level using the adhesion profiles obtained on each force curve (Fig. 1c, d). It was possible to measure the fibrinogen-erythrocyte binding force, from the deflection of the AFM tip on the retraction curve (Fig. 1c).

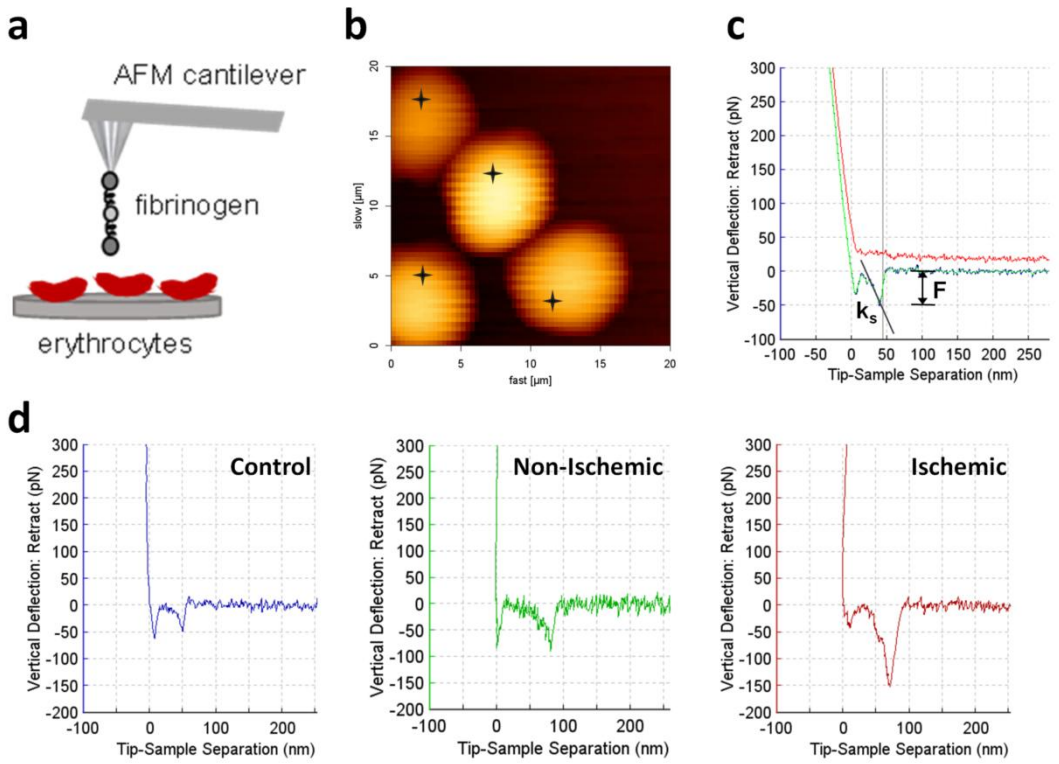

Figure 1 | **AFM-based force spectroscopy set-up and its crude data.** (**a**) Schematic representation of the erythrocytes deposited on a poly-L-lysine-coated glass slide and an AFM tip chemically functionalized with fibrinogen molecule(s). (**b**) Example of a force mapping height image of erythrocytes (image is 20 × 20 µm^2; height color scale was adjusted to 1.2 µm). The symbols indicate the surface locations chosen on each cell to perform the force spectroscopy measurements. (**c**) Example of a force-distance curve, showing a single adhesion event. When approaching the tip to the sample (red line), the fibrinogen molecule may contact with cell receptor(s), enabling binding. When retracting the tip away from the sample (blue line), as the cantilever moves upwards the tip bends down to negative force values. At a particular distance the bond breaks and the cantilever jumps back to its neutral force position. The force *F* necessary to break the bond at the single-molecule level can be obtained from this point, and the effective spring constant of the cantilever-cell system (k_s) can be calculated from the slope of the force-distance curve (black line). The green line, which is superimposed on the blue line, defines the fitting of the retraction curve. The grey vertical line indicates the recognition of an adhesion event between fibrinogen and its erythrocyte membrane receptor, with its force calculated after the polynomial fitting of the retraction curve. (**d**) Typical force-distance curves

obtained for the interaction of fibrinogen with erythrocytes from the three studied groups: control healthy donors (blue curve), non-ischemic CHF patients (green) and ischemic CHF patients (red). For simplicity, only the retraction curves are shown.

In a previous study, we showed that the interaction between fibrinogen and its integrin receptor on erythrocytes, assessed by AFM, is inhibited by the absence of calcium ions and by the presence of eptifibatide[15]. We have also reported the existence of a single-molecule interaction between fibrinogen and a $\alpha_{IIb}\beta_3$-related integrin receptor on the erythrocyte membrane[15]. It is known that an RGD (Agr-Gly-Asp) sequence at the Aα chain of the fibrinogen molecule is involved in binding to the β_3 subunit of the $\alpha_V\beta_3$ receptor on endothelial cells[20]. To further assess the specificity of the fibrinogen-erythrocyte binding, as well as to complete its identification, we measured the inhibition of the fibrinogen-erythrocyte interaction by specific antibodies against α_v and $\alpha_v\beta_3$ integrins (Supplementary Fig. 1), following an established procedure[21]. These results showed that the integrin $\alpha_V\beta_3$ is the receptor for fibrinogen on erythrocytes.

Changes in the fibrinogen-erythrocyte binding force and/or on its frequency could provide insights into the pathological condition at the microcirculatory level. Force histograms of the data obtained for the control group (healthy donors), non-ischemic and ischemic CHF patients are presented in Fig. 2a. The main differences were observed at the level of the stronger binding events (forces above 50 pN). The strongest fibrinogen-erythrocyte interactions were measured for ischemic CHF patients, followed by non-ischemic CHF patients and finally the group of healthy control subjects. The variations are clearer in Fig. 2b,d, which shows that the average force necessary to break the bond between fibrinogen and erythrocytes taken from CHF patients is higher than for erythrocytes taken from the control group (60.6 ± 6.6 pN versus 40.4 ± 3.0 pN; $p = 0.038$), despite the lower binding frequency in CHF patients (13.0 ± 2.4 % *vs.* 27.3 ± 4.2 %; $p = 0.003$). Looking into each CHF etiology, (Fig. 2c,e), ischemic patients presented a higher binding force than healthy donors (74.9 ± 10.7 pN *vs.* 40.4 ± 3.0 pN; $p = 0.004$), despite their lower binding frequency (11.7 ± 2.1 % *vs.* 27.3 ± 4.2 %; $p = 0.002$). Ischemic patients also presented higher binding forces than non-ischemic patients (74.9 ± 10.7 pN *vs.* 45.4 ± 5.6 pN; $p = 0.021$), and non-ischemic patients had a lower binding frequency than control donors (14.3 ± 4.3 % *vs.* 27.3 ± 4.2 %; $p = 0.040$).

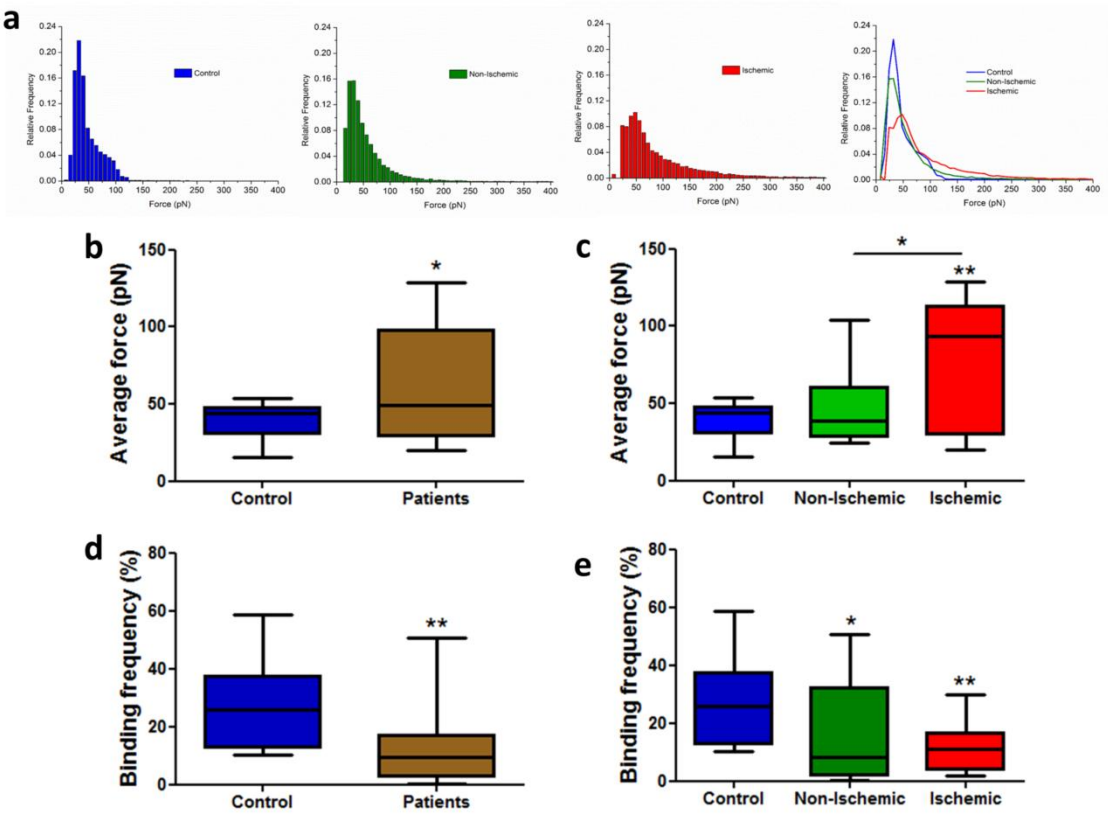

Figure 2 | **AFM-based force spectroscopy data of the interactions between fibrinogen and erythrocytes from heart failure patients and healthy blood donors.** (**a**) Rupture force histograms, showing the distribution of the values obtained for the interactions between fibrinogen and erythrocytes from healthy blood donors (control) and heart failure patients (non-ischemic and ischemic). A comparison of the rupture force profiles obtained for the three studied groups is also presented. The *y* axes of the histograms show the relative probability of the binding occurring. On the rupture force histograms, each count represents a single molecule binding (and subsequent unbinding) between one fibrinogen molecule and one of its specific erythrocyte receptors. Measurements were carried out with an applied force of 0.8 nN and a retraction speed of 2 μm/s. Average binding forces (**b**, **c**) and binding frequencies (**d**, **e**), for all patients versus control subjects (**b**, **d**), and with patients divided according to etiology (ischemic or non-ischemic) (**c**, **e**). The average force necessary to break the bond between fibrinogen and erythrocyte from CHF patients was higher than for the control group. Ischemic patients presented higher binding forces than the non-ischemic patients. Values are presented as mean ± SEM. Statistical significance values: (**b**) * $p = 0.038$; (**c**) * $p = 0.021$, ** $p = 0.004$;

(**d**) ** p = 0.003; and (**e**) * p = 0.040, ** p = 0.002. Error bars in **b-e** represent the minimum and maximum values for all data.

The stronger fibrinogen-erythrocyte binding in CHF patients, with the plasma protein eventually contributing to a transient bridging of two or more erythrocytes, may impair blood flow conditions and contribute to the higher thrombosis risk associated with this disease[3].

It has been reported that the erythrocyte membrane exhibit plastic changes under some pathological circumstances and can be permanently deformed by excessive shear forces[22]. Erythrocytes from the patients evaluated here may thus eventually have suffered changes at the membrane level leading to a lower binding frequency but, following binding, a stronger force is necessary to break the fibrinogen-erythrocyte interaction. Differences between CHF patients and healthy donors in terms of erythrocyte elasticity and AFM tip penetration depth into the cells were therefore assessed. Erythrocytes from non-ischemic patients presented higher average stiffness than those from the other two groups (Supplementary Fig. 2a). Nevertheless, a significantly higher cell penetration depth at the same applied force was observed for ischemic CHF patients (Supplementary Fig. 2b). Other studies performed with erythrocytes from patients with different diseases (*e.g.*, lupus erythematosus[23] and sickle cell disease[24]), have shown changes in these cell elastic properties. Young's modulus values for the erythrocytes from the control group in our study are in the same range as those reported by Maciaszek and Lykotrafitis for normal erythrocytes that have not been fixed[24].

The results obtained for whole blood viscosity (Fig. 3) show that the native (without hematocrit correction) whole blood viscosity, measured at two shear rates, was higher for non-ischemic patients than for ischemic patients (8.09 ± 0.42 mPa.s *vs.* 7.08 ± 0.24 mPa.s, p = 0.046, at a shear rate of 22.5 s^{-1}, and 4.70 ± 0.17 mPa.s *vs.* 4.23 ± 0.11 mPa.s, p = 0.028, at a shear rate of 225 s^{-1}). The data also show that, at low shear rate (22.5 s^{-1}), non-ischemic patients presented a higher native blood viscosity than the control group (8.09 ± 0.42 mPa.s versus 7.05 ± 0.08 mPa.s, p = 0.010). At 45% hematocrit, non-ischemic CHF patients presented whole blood viscosity values higher than the control group (7.63 ± 0.13 mPa.s versus 6.80 ± 0.11 mPa.s, $p < 0.0001$, at 22.5 s^{-1}, and 4.73 ± 0.07 mPa.s versus 4.18 ± 0.09 mPa.s, $p < 0.0001$, at 225 s^{-1}).

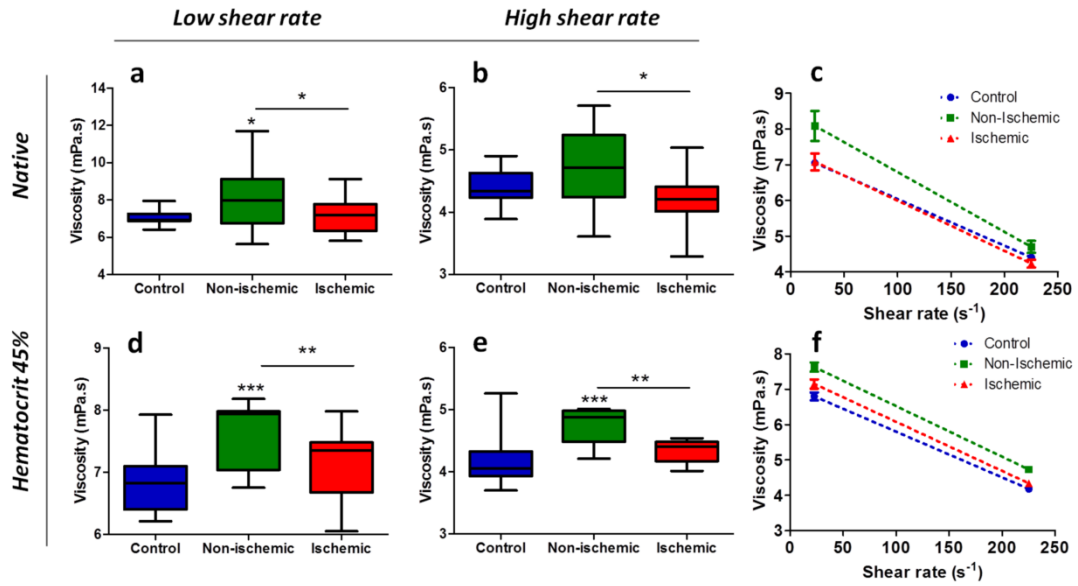

Figure 3 | **Changes in whole blood viscosity between ischemic and non-ischemic CHF patients and healthy donors.** Viscosities of native whole blood (**a**, **b**, **c**) or after hematocrit correction to 45% (**d**, **e**, **f**) were measured at low (22.5 s^{-1}**; a**, **d**) and high (225 s^{-1}**; b**, **e**) shear rate values. Plots of whole blood viscosity versus shear rate are also shown for each studied group (**c**, **f**; dashed lines are mere guides to the eye). At 45% hematocrit, non-ischemic CHF patients displayed higher whole blood viscosity than the control group. Non-ischemic patients showed higher whole blood viscosity than the ischemic patients. Values are presented as mean ± SEM. Statistical significance values: (**a**) * p = 0.010 (non-ischemic *vs.* control), * p = 0.046 (ischemic *vs.* non-ischemic); (**b**) * p = 0.028; (**d**) ** p = 0.014, *** p < 0.0001; and (**e**) ** p = 0.001, *** p < 0.0001. Error bars in **a**, **b**, **d**, **e** represent the minimum and maximum values for all data.

The whole blood viscosity was significantly higher in the non-ischemic group than for the ischemic patients (p = 0.014 at a shear rate of 22.5 s^{-1} and p = 0.001 at 225 s^{-1}). Ischemic patient results were similar to those obtained for the control group. This was an unexpected result because previous findings have indicated that ischemic patients present higher blood viscosities and this is associated with higher cardiovascular risk[8]. A statistically significant correlation (p = 0.042) between whole blood viscosity and fibrinogen-erythrocyte binding forces was observed only for non-ischemic CHF patients,

with a correlation coefficient of 0.53 (Supplementary Fig. 3). Baskurt and Meiselman considered that the apparent viscosity of blood depends on the existing shear forces and is determined by hematocrit, plasma viscosity, erythrocyte aggregation and their mechanical properties[22]. Erythrocytes aggregate under low blood flow, with a decrease in shear forces. Under these conditions, the viscosity of the blood becomes higher[25]. Under high shear forces, the apparent viscosity decreases and approaches a minimum value, as observed in our experiments (Fig. 3).

The erythrocyte deformability (assessed as elongation index) results obtained for all the experimental groups are presented in Fig. 4.

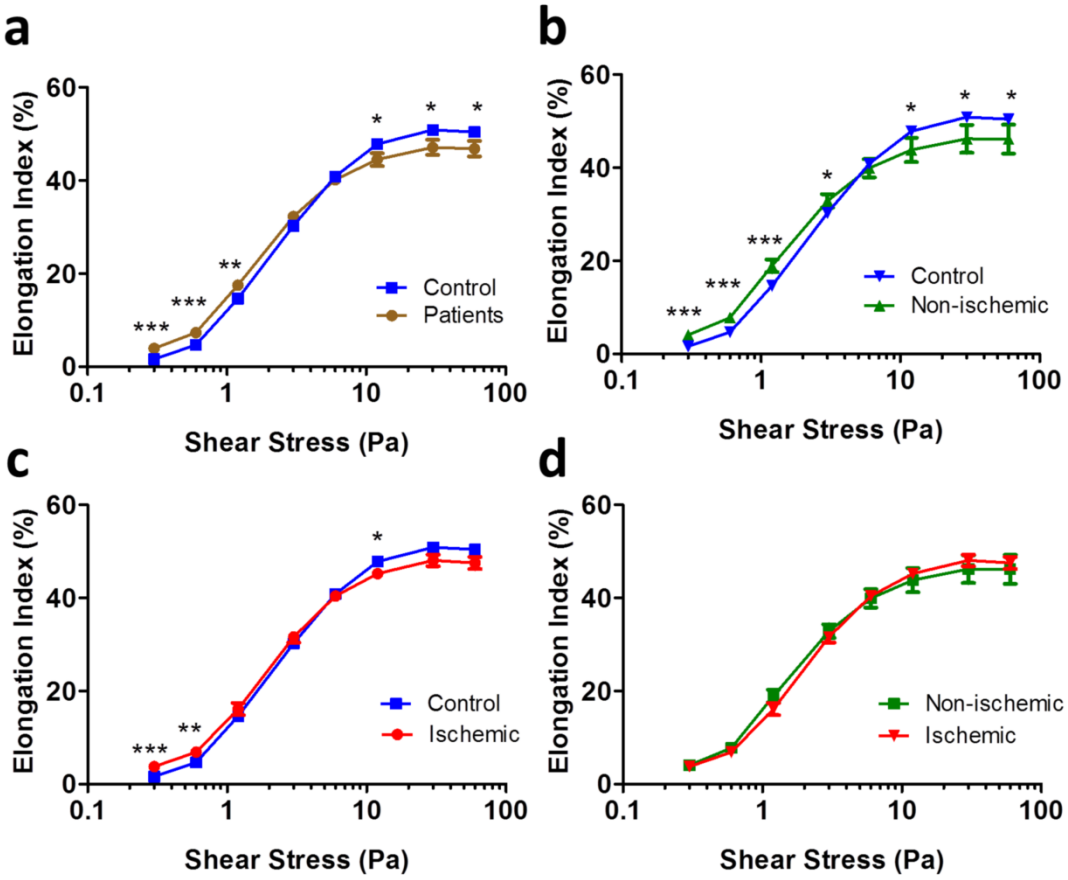

Figure 4 | Erythrocyte deformability measured at different shear stress values for all studied groups. Changes in erythrocyte deformability (assessed as elongation index) between CHF patients and healthy donors (**a**) and according to etiologies (**b**-**d**). Erythrocyte deformability was measured at shear stress values between 0.3 and 60 Pa, mimicking blood vessels of different diameters. Both patient groups showed higher deformability than the control group at low shear stresses, but lower deformability at

higher shear stresses. Values are presented as mean ± SEM. Statistical significance values: (**a**) * $p < 0.037$, ** $p = 0.0043$, *** $p < 0.0001$; (**b**) * $p < 0.046$, *** $p < 0.0003$; and (**c**) * $p = 0.032$, ** $p = 0.0056$, *** $p < 0.0001$.

Lower and higher shear stress values try to mimic the *in vivo* situation of erythrocyte flow along blood vessels with larger or smaller internal diameter, respectively[26]. The CHF patients presented higher erythrocyte deformability than the control group at lower shear stresses (0.3-1.2 Pa; $p < 0.0043$), and lower deformability at higher shear stresses (12-60 Pa; $p < 0.037$) (Fig. 4a). Both patient groups showed higher deformability than the control group at lower shear stresses ($p < 0.0056$ for ischemic and $p < 0.0003$ for non-ischemic patients), but lower deformability at higher shear stresses ($p = 0.032$ for ischemic and $p < 0.035$ for non-ischemic group). There were no statistically significant differences between the data obtained for the two groups of CHF patients. The deformability results indicate that CHF patients' erythrocytes are more deformable than those from healthy donors in vessels with larger internal diameters. However, in smaller-diameter vessels the opposite trend exists. Comparing these data with AFM results, we may hypothesize that patients' erythrocytes present alterations on the membrane-cytoskeleton complex, promoting an increased deformability in larger vessels and a lower frequency of fibrinogen-erythrocyte binding, but a higher binding force. In smaller vessels, erythrocyte deformability was lower for patients than for healthy donors. This result is extremely important because of the increased cardiovascular risk associated with such an alteration. Erythrocytes are highly deformable cells that tend to orient themselves with the blood flow streamlines, especially if shear forces are high enough to slightly deform these cells[27]. The transient interaction between fibrinogen and erythrocytes cannot lead to clot formation, but it is able to promote erythrocyte transient aggregation, increasing the cardiovascular risk associated with pathologic conditions.

Correlation analysis of the patient's clinical data (summarized in Table 1) with all the AFM and hemorheological data was performed. Fibrinogen plasma concentration was found to correlate positively and significantly with whole blood viscosity at high shear stress values (Supplementary Fig. 4).

Patients' annual hospitalization rate was 23.3%. Importantly, the 12-months clinical follow up showed that patients with higher fibrinogen-erythrocyte binding forces at the

beginning of the study had a higher probability of being hospitalized due to cardiovascular complications (103.8 pN, 95% confidence interval (CI) 55.1-112.9 *vs*. 36.9 pN, 95% CI 28.0-93.5; p = 0.033). The receiver operating characteristic (ROC) curve for hospitalization was associated with the AFM binding force (area under curve (AUC) = 0.770, 95% CI 0.598-0.902; p = 0.033) and the percentage of (un)binding events (AUC = 0.714, 95% CI 0.532-0.896; p = 0.091). Fibrinogen-erythrocyte binding forces above the median (52.37 pN) were associated with higher risk of hospitalization (hazard ratio, HR = 6.85, 95% CI 0.82-56.9; p = 0.075), as presented on the hospitalization curve (Fig. 5; p = 0.038).

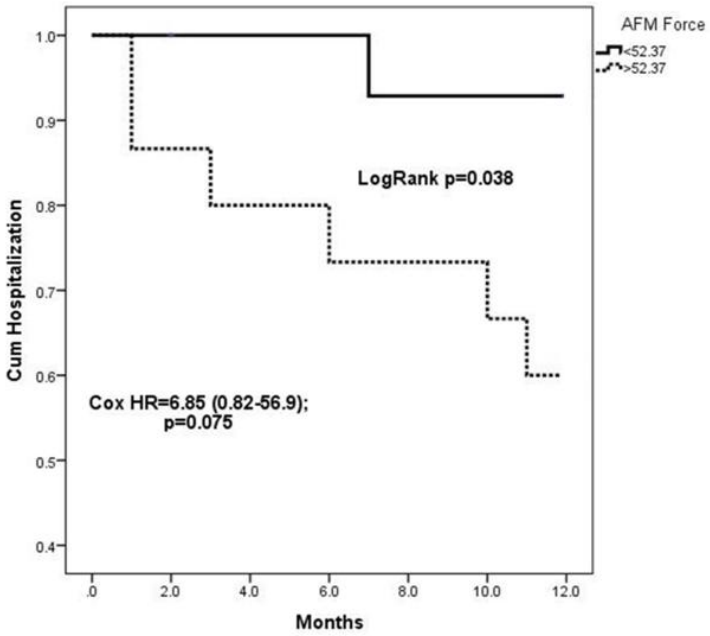

Figure 5 | **Hospitalization curve according to fibrinogen-erythrocyte (un)binding forces.** AFM-determined fibrinogen-erythrocyte (un)binding forces above the median (52.37 pN) were associated with the hospitalization curve (log rank p = 0.038) and tendency to higher risk of hospitalization (HR = 6.85; 95% CI 0.82-56.9; p = 0.075). The time-to-event data analyses included Kaplan-Meier representations with the log-rank test and the Cox regression for hazard risk determination.

We have shown that the fibrinogen-erythrocyte interaction, as characterized by AFM-based force spectroscopy, is modified in heart failure patients. Moreover, fibrinogen-erythrocyte binding forces have been shown to be associated with a patient's

clinical outcome: those with higher AFM-measured fibrinogen-erythrocyte binding forces presented a higher probability of cardiovascular disease-associated hospitalization during the subsequent 12-months clinical follow-up period. This result highlights the importance of the fibrinogen-erythrocyte interaction in CHF patients and identifies a possible subgroup of patients at higher risk. The AFM-based methodology presented here has proven to be a promising nanotool to evaluate changes in the interaction between fibrinogen and human blood cells, pinpointing patients with increased cardiovascular risk. Fibrinogen-erythrocyte binding forces, measured at the single-molecule level are thus a potential biomarker for CHF severity and may eventually be used also for the risk assessment of other cardiovascular diseases. However, this is a pilot study, with a relatively small number of patients. Studies with a larger number of patients should be encouraged to further confirm these findings before translating them for clinical application.

Methods

Study participants

Thirty patients with heart failure were enrolled in the study. Patients were in ambulatory care, with stable CHF, and were receiving optimized medical therapy according to the European Society of Cardiology (ESC) guidelines[28]. As interaction between heart failure etiology and the experimental variables under evaluation could be expected, an effort was made to include patients with ischemic and non-ischemic etiology in a 1:1 ratio. Inclusion criteria were CHF outpatients, systolic dysfunction (left ventricular ejection fraction ≤40%), functional classification according to the New York Heart Association (NHYA) on class II or III, and no recent hospitalization (>3 months). Additionally, a control group of 15 healthy donors was also included in the study, following a protocol with the Portuguese Blood Institute (IPS, Lisbon).

Clinical profiles were collected thoroughly. The clinical follow-up was 12 months-long. The evaluated outcome was cardiovascular-related hospitalization. A structured questionnaire for the description of events was used and the circumstances of the incident were determined from the hospital records and/or interviews with relatives.

Blood from healthy donors or CHF patients was obtained, with their previous written informed consent, at IPS or Hospital Pulido Valente (Lisbon), respectively. This study was approved by the joint Ethics Committee of Faculdade de Medicina da Universidade de Lisboa and Centro Hospitalar Lisboa Norte. All the study was conducted with double blinding between the clinicians and researchers conducting the laboratorial measurements.

Erythrocyte isolation and preparation for AFM measurements

For erythrocyte isolation, blood was centrifuged at 3000 rpm for 10 min at 10ºC. Plasma and buffy-coat were removed and the erythrocytes washed three times with buffered saline glucose citrate (BSGC: 1.6 mM KH_2PO_4, 8.6 mM Na_2HPO_4, 120 mM NaCl, 13.6 mM sodium citrate, 11.1 mM glucose) pH 7.3, supplemented with 1 mM calcium chloride. Erythrocytes were diluted to 0.1% hematocrit on the same buffer and placed on a clean poly-L-lysine-coated glass slide. Cells were firmly attached to poly-L-lysine coated

glass slide after 30 min of deposition, at room temperature. Non-adherent cells were removed by sequential washes with buffer, loaded into the atomic force microscope and allowed to equilibrate in this buffer for 15 min before force spectroscopy measurements. No cell fixation was involved in sample preparation.

AFM tip functionalization

For the covalent attachment of fibrinogen molecules to the AFM tips, we used our previously optimized procedure[15]. Briefly, UV light-cleaned OMCL TR-400-type silicon nitride tips (Olympus, Tokyo, Japan) were silanized in a vacuum chamber with 3-aminopropyl-triethoxysilane (APTES) for 1 h in an argon atmosphere. Then, the AFM tips were treated with a glutaraldehyde solution 2.5% (vol/vol) for 20 min. Finally, tips were placed in 1 mg/ml human purified fibrinogen (Sigma) for 30 min and immediately mounted on the AFM for the force spectroscopy experiments.

AFM-based force spectroscopy

AFM studies were conducted using a force spectroscopy methodology[15, 16, 17]. After covalently attaching fibrinogen molecules to the AFM tip (probe), we used it to tap on the surface of the erythrocytes (Fig. 1a), measuring the frequency or probability of binding, and the force necessary to break those bonds. AFM studies were performed on a NanoWizard II atomic force microscope (JPK Instruments, Berlin, Germany) mounted on an Axiovert 200 inverted optical microscope (Zeiss, Jena, Germany). The AFM head was equipped with a 15-µm z-range linearized piezoelectric scanner and an infrared laser. Force spectroscopy measurements were performed in liquid environment, using the softest triangular cantilevers, with a tip radius of 15 nm and a resonant frequency of 11 kHz in air, or approximately 3 kHz in solution. The spring constants of the cantilevers were calibrated by the thermal fluctuation method[29], yielding values of 21 ± 9 mN/m. The applied force was adjusted to maintain a force of 0.8 nN before retraction. Data was collected at 2 µm/s for each force-distance cycle. By measuring the average slope of the retraction traces of the force measurements (Fig. 1c), we determined the effective spring constant of the cell-cantilever system (k_s)[30, 31, 32, 33], yielding 2.9 ± 1.1 mN/m. Thus, by

multiplying the effective spring constant by the cantilever retraction rate we could obtain the loading rates for each force spectroscopy experiment, on each group. Thus, experiments were conducted at a loading rate of 3.96 ± 3.38 nN/s for the control group, 5.60 ± 4.24 nN/s for the non-ischemic group, and 5.36 ± 4.5 nN/s for the ischemic group (values in mean ± SD; see Supplementary Fig. 5, on the *Supplementary Information*). The differences between these ranges are not statistically significant. After positioning the cantilever on top of a single cell, with the help of a charge coupled device camera, AFM force mapping height images were recorded (Fig. 1b). Molecular recognition was searched by intermittently pressing the cantilevers on a point on the periphery of each cell adsorbed on the glass slide.

Force curves were analyzed using JPK image processing software v. 4.2.61. For each blood sample, approximately 3750 force *vs.* distance curves were collected, analyzed and adjusted by polynomial fit. Data were collected from 25 different erythrocytes on each sample and with different functionalized tips. All results from the patients were matched with those obtained with blood samples from healthy donors. Histograms of the unbinding forces for each studied group were constructed choosing the ideal bin size to achieve the best fitted Gaussian model peak forces. Binning size was fixed at 8 pN. Force rupture values up to 10 pN were considered to represent noise or artifacts. As we confirmed the specificity of the binding for force values above 25 pN (Supplementary Fig. 1), those between 10 and 25 pN were considered to be due to unspecific interactions. From each histogram, the single fibrinogen molecule rupture force can be determined by fitting the distributions of the rupture forces with the Gaussian model. In parallel, average rupture forces were also calculated from the binding data, obtained on the different cells tested for each patient or healthy donor. Rupture force values are defined as the force necessary to break the bond between a single molecule of fibrinogen and its cell receptor.

All the interactions between fibrinogen and erythrocytes were studied at room temperature in physiological buffer. The AFM laboratory was strictly maintained between 23 and 25ºC. Small variations in temperature on this range did not affect the force spectroscopy measurements, even after a long period of experiments. As controls for tip modification, measurements with tips at the different steps of their functionalization process (including non-functionalized tips) were conducted on glass slides, with and without poly-L-lysine, and on blood cells[15].

Following a previously established procedure[21], blocking experiments with antibodies against different integrins were performed in order to complement the identification of the fibrinogen receptor on erythrocytes and further confirm the specificity of the binding interactions between fibrinogen and its erythrocyte membrane receptor (Supplementary Fig. 1).

Cell elasticity analysis

Differences in erythrocyte elasticity between the studied patients (non-ischemic and ischemic) and control groups were evaluated by analyzing in parallel the approach curves of the previously described force spectroscopy measurements (Supplementary Fig.2). Data were analyzed to obtain the cells Young's modulus (E), using JPK Image Processing v. 4.2.53, by applying the Hertzian model, with a fixed tip-sample separation between -200 and 200 nm. Values of AFM tip penetration depth onto erythrocytes were also obtained (Supplementary Fig. 2).

Hematologic profile

Quantitative analysis of the hemogram of the blood samples of CHF patients and healthy donors were done by using a PocH-100iV equipment (Sysmex, Japan).

Whole blood viscosity

Whole blood viscosity was measured using a Brookfield DV-II viscometer (Brookfield Engineering Laboratories, MA, USA). Measurements were done both using native blood samples and samples with hematocrit adjusted to 45%, at 37°C, submitting the samples to both low (22.5 s^{-1}) and high (225 s^{-1}) shear rates.

Erythrocyte deformability

Erythrocyte deformability was assessed at 22ºC, using a Rheodyn SSD laser diffractometer (Myrenne, Roetgen, Germany), and presented as erythrocyte elongation indexes (EEIs). The diffraction pattern was analyzed at eight shear stress values, between

0.30 and 60.0 Pa. EEIs were calculated using the light intensities of the diffraction pattern[27].

Statistical Analysis

Descriptive statistics are given as mean ± standard error of mean (SEM), frequency and median (interquartile range, IQR). For every variable, all samples were tested against control group. Unpaired Student's *t*-test was used for statistical analysis of intergroup comparison. One-way analysis of vairance followed by a Dunnett post-test were used for multiple comparisons on data from CHF patients *versus* control. For non-Gaussian variables, the corresponding non-parametric methods were used, such as the Mann-Whitney U test when performing two group comparisons and the Spearman correlation test. Linear regression analyses to evaluate the relation between whole blood viscosity and AFM data (binding force or frequency) were also performed (Supplementary Fig. 3).

Categorical variables were compared using the χ^2 and Fisher's exact tests with the odds-ratio (OR) calculation. The accuracy for predicting the endpoint (hospitalization) was determined by the area under the receiver operating characteristic (ROC) curve, for the significant continuous variables. The optimal cutoff value used for AFM was the median. The time-to-event data analyses included Kaplan-Meier representations with the log-rank test and the Cox regression for hazard risk determination, with the calculation of hazard ratios (HRs) and 95% confidence intervals (CI). Statistical significance was set at $p<0.05$. Statistical analyses were performed using GraphPad Prism 5 and SPSS v. 22.0.

Acknowledgments

This work was supported by Fundação para a Ciência e Tecnologia – Ministério da Educação e Ciência (FCT-MCTES, Portugal) grants PTDC/QUI-BIQ/119509/2010 and PTDC/BBB-BMD/6307/2014, as well as fellowship SFRH/BD/84414/2012 to A.F.G. Authors thank Teresa Freitas (FMUL) for excellent technical assistance.

Author contributions

A.F.G. performed AFM experiments, analyzed force spectroscopy data, performed the statistical analysis, wrote and edited the draft and prepared the manuscript for submission; **F.A.C.** analyzed force spectroscopy data, wrote the manuscript and edited the successive drafts of the paper; **I.M.** performed some of the initial AFM experiments and analyzed their data; **L.S.** collected all clinical data, performed some statistical analysis, contributed to relevant discussion and edited the draft; **N.L.** contributed to the discussion section; and, **N.C.S.** conceived the idea, designed and directed the AFM experiments, analyzed the data, wrote the manuscript and edited the successive drafts of the paper.

Competing Financial Interests statement

The authors declare no competing financial interests.

References of Chapter V

1. Alexander, K.S., Kazmierczak, S.C., Snyder, C.K., Oberdorf, J.A. & Farrell, D.H. Prognostic utility of biochemical markers of cardiovascular risk: impact of biological variability. *Clin Chem Lab Med* **51**, 1875-82 (2013).
2. Lominadze, D., Dean, W.L., Tyagi, S.C. & Roberts, A.M. Mechanisms of fibrinogen-induced microvascular dysfunction during cardiovascular disease. *Acta Physiol* **198**, 1-13 (2010).
3. Reinhart, W.H. Fibrinogen-marker or mediator of vascular disease? *Vasc Med* **8**, 211-6 (2003).
4. Cecchi, E., Mannini, L. & Abbate, R. Role of hyperviscosity in cardiovascular and microvascular diseases. *G Ital Nefrol* **26**, 20-9 (2009).
5. WHO. Global status report on non-communicable diseases 2010. *Geneva: World Health Organization* (2011).
   http://www.who.int/nmh/publications/ncd_report2010/en/
6. Lillioja, S., Young, A.A., Culter, C.L., Ivy, J.L., Abbott, W.G., Zawadzki, J.K., Yki-Jarvinen, H., Christin, L., Secomb, T.W. & Bogardus, C. Skeletal muscle capillary density and fiber type are possible determinants of in vivo insulin resistance in man. *J Clin Invest* **80**, 415-24 (1987).
7. Mann, D.L. & Bristow, M.R. Mechanisms and models in heart failure: the biomechanical model and beyond. *Circulation* **111**, 2837-49 (2005).
8. Follath, F. Ischemic versus non-ischemic heart failure: should the etiology be determined? *Heart Fail Monit* **1**, 122-5 (2001).
9. Bishop, J.J., Nance, P.R., Popel, A.S., Intaglietta, M. & Johnson, P.C. Effect of erythrocyte aggregation on velocity profiles in venules. *Am J Physiol Heart Circ Physiol* **280**, H222-36 (2001).
10. Kim, S., Popel, A.S., Intaglietta, M. & Johnson, P.C. Aggregate formation of erythrocytes in postcapillary venules. *Am J Physiol Heart Circ Physiol* **288**, H584-90 (2005).
11. Delamaire, M. & Durand, F. Erythrocyte aggregation and vascular pathology. *J Mal Vasc* **15**, 344-5 (1990).

12. Falco, C., Vaya, A., Simo, M., Contreras, T., Santaolaria, M. & Aznar, J. Influence of fibrinogen levels on erythrocyte aggregation determined with the Myrenne aggregometer and the Sefam erythro-aggregometer. *Clin Hemorheol Microcirc* **33**, 145-51 (2005).
13. Maeda, N., Seike, M., Kume, S., Takaku, T. & Shiga, T. Fibrinogen-induced erythrocyte aggregation: erythrocyte-binding site in the fibrinogen molecule. *Biochim Biophys Acta* **904**, 81-91 (1987).
14. Lominadze, D. & Dean, W.L. Involvement of fibrinogen specific binding in erythrocyte aggregation. *FEBS Lett* **517**, 41-4 (2002).
15. Carvalho, F.A., Connell, S., Miltenberger-Miltenyi, G., Pereira, S.V., Tavares, A., Ariëns, R.A. & Santos, N.C. Atomic force microscopy-based molecular recognition of a fibrinogen receptor on human erythrocytes. *ACS Nano* **4**, 4609-20 (2010).
16. Carvalho, F.A., de Oliveira, S., Freitas, T., Goncalves, S. & Santos, N.C. Variations on fibrinogen-erythrocyte interactions during cell aging. *PLoS One* **6**, e18167 (2011).
17. Carvalho, F.A. & Santos, N.C. Atomic force microscopy-based force spectroscopy-biological and biomedical applications. *IUBMB Life* **64**, 465-72 (2012).
18. Choi, S., Jung, G.B., Kim, K.S., Lee, G.J. & Park, H.K. Medical applications of atomic force microscopy and Raman spectroscopy. *J Nanosci Nanotechnol* **14**, 71-97 (2014).
19. Pillet, F., Chopinet, L., Formosa, C. & Dague, E. Atomic Force Microscopy and pharmacology: from microbiology to cancerology. *Biochim Biophys Acta* **1840**, 1028-50 (2014).
20. Thiagarajan, P., Rippon, A.J. & Farrell, D.H. Alternative adhesion sites in human fibrinogen for vascular endothelial cells. *Biochemistry* **35**, 4169-75 (1996).
21. Carvalho, F.A., Carneiro, F.A., Martins, I.C., Assunção-Miranda, I., Faustino, A.F., Pereira, R.M., Bozza, P.T., Castanho, M.A., Mohana-Borges, R., Da Poian, A.T. & Santos, N.C. Dengue virus capsid protein binding to hepatic lipid droplets (LD) is potassium ion dependent and is mediated by LD surface proteins. *J. Virol.* **86**, 2096-108 (2012).
22. Baskurt, O.K. & Meiselman, H.J. Blood rheology and hemodynamics. *Semin Thromb Hemost* **29**, 435-50 (2003).

23. Ebner, A., Schillers, H. & Hinterdorfer, P. in Atomic Force Microscopy in Biomedical Research (eds. Braga, P.C. & Ricci, D.) *Humana Press* 736, 2011, 223-241.

24. Maciaszek, J.L. & Lykotrafitis, G. Sickle cell trait human erythrocytes are significantly stiffer than normal. *J Biomech* **44**, 657-61 (2011).

25. Rand, P.W., Lacombe, E., Hunt, H.E. & Austin, W.H. Viscosity of Normal Human Blood under Normothermic and Hypothermic Conditions. *J Appl Physiol* **19**, 117-22 (1964).

26. Papaioannou, T.G. & Stefanadis, C. Vascular wall shear stress: basic principles and methods. *Hellenic J Cardiol* **46**, 9-15 (2005).

27. Schmid-Schönbein, H., Wells, R.E. & Goldstone, J. Fluid drop-like behaviour of erythrocytes-disturbance in pathology and its quantification. *Biorheology* **7**, 227-34 (1971).

28. McMurray, J.J., Adamopoulos, S., Anker, S.D., Auricchio, A., Bohm, M., Dickstein, K., Falk, V., Filippatos, G., Fonseca, C., Gomez-Sanchez, M.A., Jaarsma, T., Køber, L., Lip, G.Y., Maggioni, A.P., Parkhomenko, A., Pieske, B.M., Popescu, B.A., Rønnevik, P.K., Rutten, F.H., Schwitter, J., Seferovic, P., Stepinska, J., Trindade, P.T., Voors, A.A., Zannad, F., Zeiher, A.; ESC Committee for Practice Guidelines. ESC Guidelines for the diagnosis and treatment of acute and chronic heart failure 2012: The Task Force for the Diagnosis and Treatment of Acute and Chronic Heart Failure 2012 of the European Society of Cardiology. Developed in collaboration with the Heart Failure Association (HFA) of the ESC. *Eur Heart J* **33**, 1787-1847 (2012).

29. Hutter, J.L., Bechhoefer, J. Calibration of atomic-force microscope tips. *Review of Scientific Instruments* **64**, 1868-1873 (1993).

30. Chen, A., Moy, V.T. Cross-linking of cell surface receptors enhances cooperativity of molecular adhesion. *Biophys J* **78**, 2814-2820 (2000).

31. Kienberger, F., Kada, G., Mueller, H., Hinterdorfer, P. Single molecule studies of antibody-antigen interaction strength versus intra-molecular antigen stability. *J Mol Biol* **347**, 597-606 (2005).

32. Neundlinger, I., Puntheeranurak, T., Wildling, L., Rankl, C., Wang, L.X., Gruber, H.J., Kinne, R.K, Hinterdorfer, P. Forces and dynamics of glucose and inhibitor binding

to sodium glucose co-transporter SGLT1 studied by single molecule force spectroscopy. *J Biol Chem* **289**, 21673-21683 (2014).

33. Zhang, X., Wojcikiewicz, E., Moy, V.T. Force spectroscopy of the leukocyte function-associated antigen-1/intercellular adhesion molecule-1 interaction. *Biophys J* **83**, 2270-2279 (2002).

Supplementary information of Chapter V

Atomic force microscopy as a tool to evaluate the risk for cardiovascular diseases in patients

Ana Filipa Guedes; Filomena A. Carvalho; Inês Malho; Nuno Lousada; Luís Sargento; Nuno C. Santos

Biomedical Relevance

Cardiovascular diseases are the leading cause of death worldwide, being responsible for approximately 30% of the total number of human losses[1]. Chronic heart failure (CHF), a complex clinical cardiovascular syndrome, is characterized by the heart failing to pump enough blood with the right pressure[2, 3]. Ischemic cardiomyopathy is the most common cause of heart failure in industrialized countries[4]. The prognosis and response to treatment of patients with ischemic heart failure are worse than in patients with a non-ischemic etiology[5]. The term "non-ischemic heart failure" includes different subgroups, such as hypertensive heart disease, myocarditis and cardiac dysfunction due to rapid atrial fibrillation, which may be reversible[5].

Establishing the diagnostic, extent, and severity of cardiovascular diseases, as well as determining the potential risk of cardiovascular events are crucial steps toward improving patient outcomes. The most common non-invasive tests and procedures used to evaluate CHF are reported on the *Guidelines for the Evaluation and Management of Heart Failure*[6], and include electrocardiogram, chest radiograph and transthoracic Doppler–two-dimensional echocardiogram, among others. Although these methods are well established within the daily clinical practice, none of them assesses changes at the cellular and molecular levels. The development of new methods to detect early molecular

changes in different tissues, or changes in normal blood flow before clinical symptoms appear, without invasive intervention, is therefore very important in clinical diagnosis and prognosis. Some methods proved to be effective in detecting local changes, by quantitatively evaluating them (*e.g.*, contrast-enhanced ultrasound) or imaging molecule-associated endothelial activation (*e.g.*, early detection of atherosclerotic lesions[7]). Other methods such as positron emission tomography imaging (PET), computer tomography, magnetic resonance imaging (MRI) or electron microscopy are extremely expensive and require complex sample preparation, modification and handling[8].

The development of new pharmacologic therapies, surgical cardiovascular procedures and mechanical circulatory support devices to treat heart failure has slowed down the increase in CHF-associated mortality[9]. However, the availability of biomarkers to evaluate risk in this disease is still limited[10]. A better understanding of the molecular mechanisms underlying the interaction between fibrinogen and erythrocytes in CHF patients may be important for eventual future drug interventions to reduce aggregation and enhance microcirculatory flow conditions.

Supplementary Methods

Fibrinogen-erythrocyte binding inhibition studies

As controls for this experimental approach, the interaction between fibrinogen and its integrin receptor on erythrocytes, assessed by AFM, was found to be inhibited by the absence of calcium ions (essential for the activity of the receptor), and by the presence of eptifibatide, a molecule used in hospital settings to inhibit fibrinogen-platelet binding, which we previously demonstrated to be also able to inhibit fibrinogen-erythrocyte binding[11].

Additionally, in order to further assess the specificity of the binding between fibrinogen and its erythrocyte membrane receptor, as well as to complete its identification, we measured the inhibition of the fibrinogen-erythrocyte interaction in the presence of two mouse anti-human antibodies: anti-α_v (clone NKI-M9; Biolegend, San Diego, CA, USA) and anti-$\alpha_v\beta_3$ integrins (clone 23C6; eBioscience Inc., San Diego, CA, USA), following a previously established procedure[12]. The effects of the two antibodies were evaluated by AFM-based force spectroscopy after incubating the erythrocytes at two different antibody concentrations (10 and 25 μg/ml), for 1 h, at room temperature. As a negative control for the antibodies blocking experiments, the effect of an isotype matched non-integrin antibody was also tested (normal mouse IgG serum, Santa Cruz Biotechnology, Santa Cruz, CA, USA).

Erythrocyte elasticity

Force spectroscopy data were analyzed to obtain the cells Young's modulus (E), using JPK Image Processing v. 4.2.53, by the application of the Hertzian model. The model was applied to all force curves obtained from non-ischemic and ischemic CHF patients and controls, with a fixed tip-sample separation between -200 and 200 nm. The probe was modeled as a quadratic pyramid, with a tip angle of 35° (half-angle to face) and a Poisson ration of 0.50. Young's modulus histograms were constructed for each experimental condition studied. The ideal histogram bin size was chosen in order to achieve the best fitted Gaussian model peak length, yielding a selected binning size of 0.1 kPa. The maximum values of the Gaussian peaks represent different statistical measure of the

Young's modulus of the cells. Values of the mean ± standard deviation and median of each group were also taken into consideration.

AFM tip penetration depth onto erythrocytes was also evaluated. This parameter is analyzed by the position of the maximal movement of the piezo sensor in the z-axis, which corresponds to the z-axis coordinate when the sensor reaches an indentation force of 800 pN, subtracting the z-axis position of the sensor when the tip begins the contact with the surface of the erythrocyte. Statistical significance was determined with pair-wise comparisons made with Student's *t*-test to compare the cells datasets, using a 5% confidence interval. Statistical analysis was carried out using the Graphpad Prism software v. 5.0.

Supplementary Results

Fibrinogen-erythrocyte binding inhibition studies

As shown in Supplementary Fig. 1, the percentage of inhibition of fibrinogen-erythrocyte binding induced by 10 μg/ml anti-α_v was 24.6%, a value higher than the percentage of inhibition achieved for the same concentration of anti-$\alpha_v\beta_3$ antibody. At higher antibody concentrations, the difference between the levels of inhibition of fibrinogen-erythrocyte binding observed for both antibodies becomes even more evident (54.4% *vs.* 13.9% for anti-α_v and anti-$\alpha_v\beta_3$, respectively). Inhibition is concomitant with a significant reduction of the stronger binding events, especially in the presence of the anti-$\alpha_v\beta_3$ integrin antibody, remaining mainly the interactions with lower (un)binding forces. No detectable binding inhibition or binding force reduction were observed in the presence of 25 μg/ml isotype-matched non-integrin antibody (negative control), further confirming the specificity of the interaction between fibrinogen and the erythrocyte membrane.

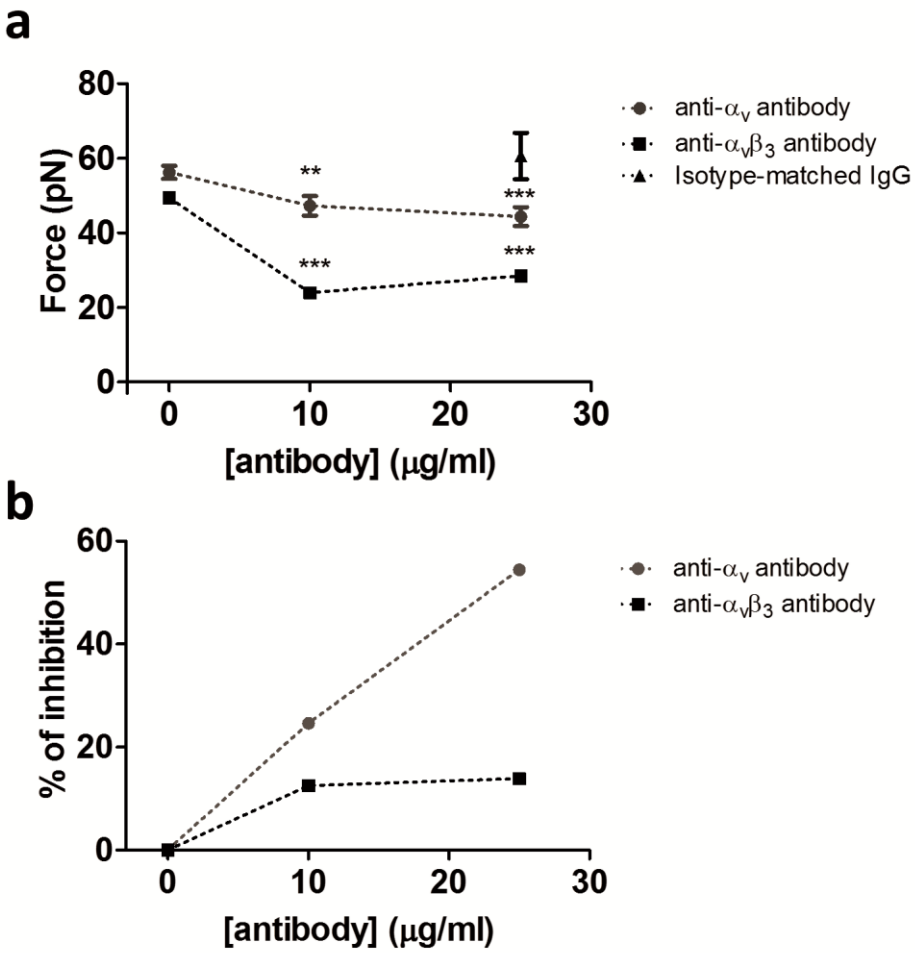

Supplementary Figure 1 | **Inhibition of the binding between the fibrinogen protein and erythrocyte receptor by antibodies against α_v and $\alpha_v\beta_3$ integrins.** (**a**) Average fibrinogen-erythrocyte binding rupture forces and (**b**) percentage of fibrinogen-erythrocyte binding inhibition (decrease on the binding frequency) in the presence of specific antibodies against α_v integrin (grey circles), $\alpha_v\beta_3$ integrin (black squares), and a negative control with an isotype-matched non-integrin antibody (black triangle). Antibody concentrations were 10 and 25 μg/mL, in BSGC buffer with $CaCl_2$ 1 mM.

Cell elasticity

In an effort to understand why the AFM data show that CHF patients (especially ischemic patients) have significantly increased fibrinogen-erythrocyte binding forces, we analyzed the erythrocyte elasticity parameters of the same samples. With this purpose, all force spectroscopy data were analyzed in order to determine the Young's modulus and

the penetration depth for each force-distance curve. The results obtained are presented in Supplementary Fig. 2. Young's modulus data of each group are presented in a relative frequency histogram (Supplementary Fig. 2a). Gaussian polynomial fit was applied, but the results could not be accurately compared between groups because the fitting does no converge for the control group. Comparing just the values of the mean ± SEM and median for each group, for the control group we obtained values of 1205 ± 14.2 Pa and 390.1 Pa, respectively. As for the non-ischemic CHF group, the values obtained were 1248 ± 10.8 Pa and 743.4 Pa. Finally, the results for ischemic CHF patients were 1142 ± 10.8 Pa and 568.5 Pa. These variations were only statistically significant for the median, in which we observed an increased cell stiffness (or decreased elasticity) on both groups of CHF patients, with the larger variation being observed for the non-ischemic patients.

On the assessment of erythrocyte stiffness variations between healthy and CHF patients, AFM tip penetration depth was also determined (Supplementary Fig. 2b). This parameter allows one to evaluate the capacity of the erythrocytes to deform. Data show that the mean penetration depth on erythrocytes from ischemic CHF patients was 323.6 nm, which is significantly higher than the mean penetration depth determined for the non-ischemic CHF patients (263.9 nm; $p < 0.001$) and control group (258.7 nm; $p < 0.001$). With these results we could conclude that CHF patients (mainly ischemic ones) have erythrocytes much more capable to deform than those from healthy donors.

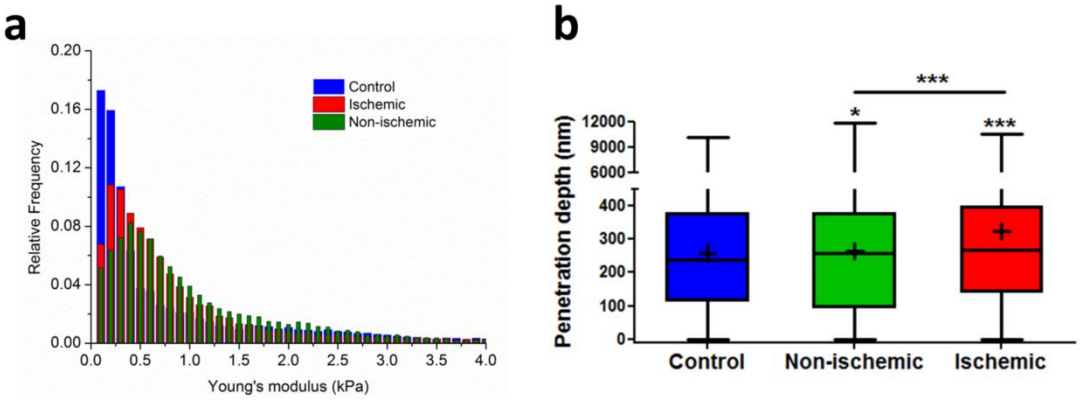

Supplementary Figure 2 | **Erythrocyte stiffness studies.** (**a**) Histograms of the distribution of the Young's modulus values obtained from the non-ischemic (green) and ischemic (red) CHF patients, and for the control group (blue). (**b**) AFM tip penetration

depth onto erythrocytes, for an applied force of 800 pN. The $^{+}$ symbol indicates the average value of penetration depth for each group. * $p = 0.022$; *** $p < 0.0001$.

Linear regression analysis between whole blood viscosity and AFM data

Trying to understand how the interactions between fibrinogen molecules and its erythrocyte membrane receptor could affect whole blood viscosity of each patients' group, data obtained for each parameter were compared. After performing linear regression analysis, we could only observe a statistically significant relation between blood viscosity and the average fibrinogen-erythrocyte (un)binding force for the non-ischemic group ($p = 0.042$; r = 0.53).

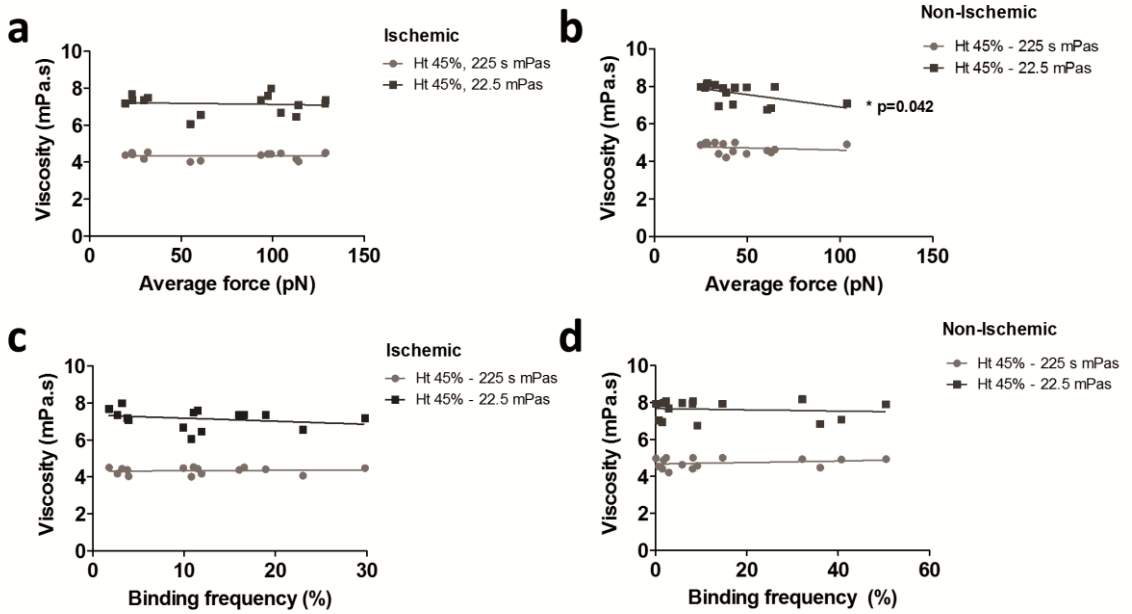

Supplementary Figure 3 | **Relation between AFM data and whole blood viscosity data.** Linear regression analysis between fibrinogen-erythrocyte average binding force (**a**, **b**) or binding frequency (**c**, **d**) and whole blood viscosity. Data shown are from ischemic (**a**, **c**) and non-ischemic (**b**, **d**) CHF patients. Linear regression was performed with a confidence interval of 95%. Only for non-ischemic CHF patients a statistically significant relation between whole blood viscosity and binding force was observed (* $p = 0.042$). No relation between whole blood viscosity and fibrinogen-erythrocyte binding frequency was observed.

Linear regression analysis between whole blood viscosity and total plasma fibrinogen

We performed a linear regression analysis in order to know the relation between whole blood viscosity and the total plasma fibrinogen levels. At hematocrit 45% and a high shear rate, a positive relation between the whole blood viscosity and fibrinogen data of CHF patients was observed (r = 0.428, *p* = 0.021).

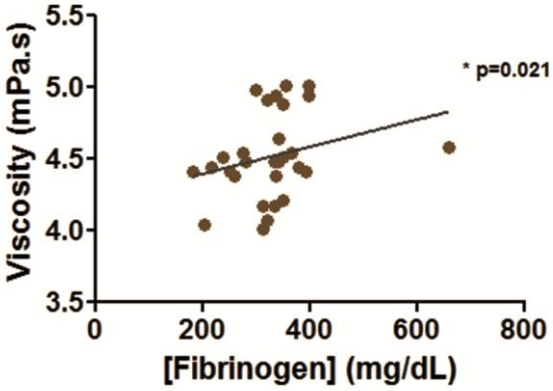

Supplementary Figure 4 | **Relation between whole blood viscosity data and total plasma fibrinogen.** Linear regression analysis was performed between whole blood viscosity (at 45% of hematocrit and at high shear rate) and plasma fibrinogen for CHF patients. Linear regression was done with a confidence interval of 95%. A statistically significant relation was observed (r = 0.428, *p* = 0.021).

Dynamic force spectroscopy analysis

Upon analyzing force spectroscopy data, beyond determining the values of the unbinding force and the frequency of the fibrinogen-erythrocyte interaction, it is important to evaluate the influence of the loading rate during experiments on each of the three studied groups. Supplementary Fig. 4a shows the variation of the loading rates determined for each group. The loading rates values (mean ± SD) were 3959 ± 3380 pN/s for the control group, 5604 ± 4239 pN/s for the non-ischemic group and 5358 ± 4515 pN/s for the ischemic group. These differences were not statistically significant, as determined by One-way ANOVA followed by a Dunnett's post-test.

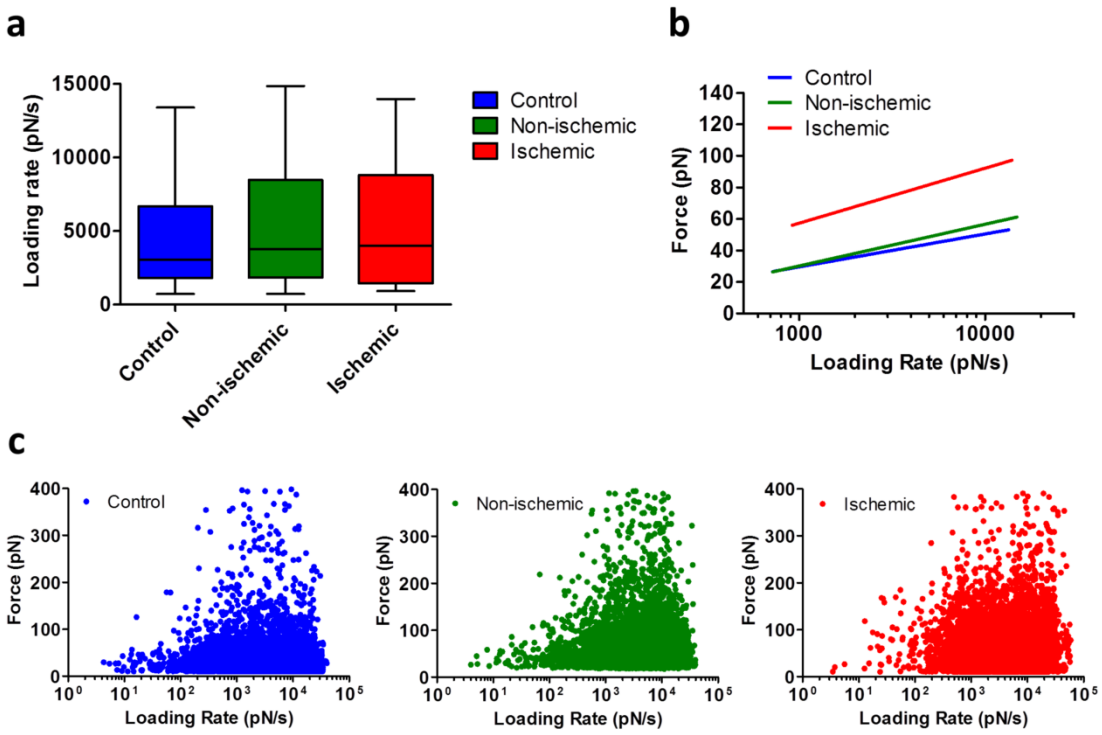

Supplementary Figure 5 | **Dynamic force spectroscopy analysis of the interaction between fibrinogen and erythrocytes from the control, non-ischemic and ischemic groups.** (**a**) Distribution of the loading rates of the three studied groups. Plots of box and whiskers indicating the mean values and distribution of the loading rate. The whiskers indicate the variation of the minimum to the maximum loading rate value. (**b**) The most probable unbinding forces were plotted against the logarithm of the loading rate of the control (blue line), non-ischemic (green line) and ischemic (red line) groups. Lines are the results of a non-linear least-squares regression fitting. (**c**) Distribution of all data of force *vs.* logarithm of the loading rate for the three studied groups.

We also looked at the unbinding force *vs.* loading rate pairs for each curve separately, for each sample on the control, non-ischemic CHF and ischemic CHF groups. The most probable unbinding forces were plotted against the logarithm of the loading rate (Supplementary Fig. 5b). It can be observed that the three groups have similar ranges of loading rates. The differences observed were at the level of the unbinding force. We performed a regression analysis for each set and obtained a slope of 20.9 $\pm$ 7.9 (r^2 = 0.366) for the control group, 26.4 $\pm$ 14.7 (r^2 = 0.212) for the non-ischemic CHF group, and

34.8 ± 27.4 ($r^2 = 0.119$) for the ischemic CHF group. Lines are almost parallel. There were no statistically significant differences on their slopes. Unbinding forces increase with the loading rate on each group, but the variations of the unbinding force between each group is not dependent on the loading rate. For this study we considered all the force curves, with values of loading rates between 1000 and 10 000 pN/s.

The distribution of the force *vs.* loading rate for the three studied groups is presented on Supplementary Fig. 5c. By the distribution of all points of unbinding force *vs.* logarithm of the loading rate, we could observe that increasing the loading rate leads to an increase of the unbinding force. The majority of the values are distributed between 20 and 200 pN of unbinding force and 10^3 to 10^4 pN/s of loading rate.

Supplementary references

1. WHO. Global status report on non-communicable diseases 2010. *Geneva: World Health Organization* (2011). http://www.who.int/nmh/publications/ncd_report2010/en/
2. Lillioja, S., Young, A.A., Culter, C.L., Ivy, J.L., Abbott, W.G., Zawadzki, J.K., Yki-Jarvinen, H., Christin, L., Secomb, T.W. & Bogardus, C. Skeletal muscle capillary density and fiber type are possible determinants of in vivo insulin resistance in man. *J Clin Invest* **80**, 415-24 (1987).
3. Mann, D.L. & Bristow, M.R. Mechanisms and models in heart failure: the biomechanical model and beyond. *Circulation* **111**, 2837-49 (2005).
4. Colluci, W.B., E. Textbook of cardiovascular Medicine. *Philadelphia, Pa: WB Saunders*, 394-420 (1997).
5. Follath, F. Ischemic versus non-ischemic heart failure: should the etiology be determined? *Heart Fail Monit* **1**, 122-5 (2001).
6. Guidelines for the evaluation and management of heart failure. Report of the American College of Cardiology/American Heart Association Task Force on Practice Guidelines (Committee on Evaluation and Management of Heart Failure). *Circulation* **92**, 2764-84 (1995).
7. Wu, Z., Curaj, A., Fokong, S., Liehn, E.A., Weber, C., Lammers, T., Kiessling, F. & Zandvoort van, M. Rhodamine-loaded intercellular adhesion molecule-1-targeted microbubbles for dual-modality imaging under controlled shear stresses. *Circ. Cardiovasc. Imaging* **6**, 974-81 (2013).
8. Rusu, M., Dulebo, A., Curaj, A. & Liehn, E.A. Ultra-rapid non-invasive clinical nano-diagnostic of inflammatory diseases. *Discoveries Reports* **1**, e2 (2014).
9. Hunt, S.A., Abraham, W.T., Chin, M.H., Feldman, A.M., Francis, G.S., Ganiats, T.G., Jessup, M., Konstam, M.A., Mancini, D.M., Michl, K., Oates, J.A., Rahko, P.S., Silver, M.A., Stevenson, L.W. & Yancy, C.W. 2009 focused update incorporated into the ACC/AHA 2005 Guidelines for the Diagnosis and Management of Heart Failure in Adults: a report of the American College of Cardiology Foundation/American Heart Association Task Force on Practice Guidelines: developed in collaboration with the

International Society for Heart and Lung Transplantation. *Circulation* **119**, e391-479 (2009).

10. Alexander, K.S., Kazmierczak, S.C., Snyder, C.K., Oberdorf, J.A. & Farrell, D.H. Prognostic utility of biochemical markers of cardiovascular risk: impact of biological variability. *Clin Chem Lab Med* **51**, 1875-82 (2013).
11. Carvalho, F.A., Connell, S., Miltenberger-Miltenyi, G., Pereira, S.V., Tavares, A., Ariens, R.A. & Santos, N.C. Atomic force microscopy-based molecular recognition of a fibrinogen receptor on human erythrocytes. *ACS Nano* **4**, 4609-20 (2010).
12. Carvalho, F.A., Carneiro, F.A., Martins, I.C., Assunção-Miranda, I., Faustino, A.F., Pereira, R.M., Bozza, P.T., Castanho, M.A., Mohana-Borges, R., Da Poian, A.T. & Santos, N.C. Dengue virus capsid protein binding to hepatic lipid droplets (LD) is potassium ion dependent and is mediated by LD surface proteins. *J Virol* **86**, 2096-108 (2012).

Chapter VI ▫

Fibrinogen-erythrocyte binding in essential arterial hypertension

Overview

In this Chapter, we tryed to understand how the interactions between fibrinogen and its specific erythrocyte membrane receptor are altered on patients with essential arterial hypertension (EAH). Hypertension is a very important public health challenge. Its complications include cardiovascular, cerebrovascular and renal diseases. All the clinical information and routine evaluation of the patients enrolled in this study was obtained and performed by clinicians from Serviço de Medicina I, Hospital de Santa Maria (Centro Hospitalar Lisboa Norte). Force spectroscopy measurements were complemented by hemorheological parameters assessement. Our findings evidenced that the interaction between fibrinogen and erythrocyte is increased on EAH patients, which could be an important cardiovascular risk factor to be considered in the future. Our data lead us to hypothesize that the increased fibrinogen adhesion to the erythrocytes from EAH patients and alterations on their cells elasticity may lead to changes on the whole blood flow. The changes revealed on the hemorheological parameters of these patients could also contribute for their blood flow perturbations.

Further details are described in the supplementary information of this manuscript.

This work was mainly done at Instituto de Medicina Molecular, Faculdade de Medicina, Universidade de Lisboa, but also at Hospital Santa Maria, Centro Hospitalar Lisboa Norte.

Declaration of authorship

I, Ana Filipa Guedes, declare that the laboratory work, data analysis and writing of the manuscript initial draft were carried by me, under the supervision of Prof. Filomena A. Carvalho and Prof. Nuno C. Santos. Prof. Filomena Carvalho also analyzed data and edited the initial draft of the manuscript. Prof. Carlos Moreira and Prof. José Braz Nogueira were the clinicians that provided us the samples, the clinical information of the patients and made the clinical routine evaluation by blood pressure monitoring, electrocardiography, echocardiography and blood measurements. All authors revised and improved the manuscript.

I, Filomena A. Carvalho, as co-supervisor of Ana Filipa Guedes and co-author of the manuscript, hereby declare that the information above is correct.

I, Nuno C. Santos, as supervisor of Ana Filipa Guedes and corresponding author of the manuscript, hereby declare that the information above is correct.

Lisbon, April 6, 2018

Ana Filipa Guedes | Filomena A. Carvalho | Nuno C. Santos

Manuscript:

Fibrinogen-erythrocyte binding and hemorheology measurements on the assessment of essential arterial hypertension patients

Ana Filipa Guedes[1], Carlos Moreira[2], José Braz Nogueira[2,] Nuno C. Santos[1,*], Filomena A. Carvalho[1,*]

- Submitted -

Fibrinogen-erythrocyte binding and hemorheology measurements on the assessment of essential arterial hypertension patients

Ana Filipa Guedes[1], Carlos Moreira[2], José Braz Nogueira[2], Nuno C. Santos[1,*], Filomena A. Carvalho[1,*]

[1]Instituto de Medicina Molecular, Faculdade de Medicina, Universidade de Lisboa, Lisboa, Portugal; [2]Hospital Santa Maria, Centro Hospitalar Lisboa Norte, Lisboa, Portugal.

[*] To whom correspondence should be addressed:

Nuno C. Santos, Instituto de Medicina Molecular, Faculdade de Medicina, Universidade de Lisboa, Av. Prof. Egas Moniz, 1649-028 Lisboa, Portugal; E-mail: nsantos@fm.ul.pt; Tel.: +351 217999480; Fax: +351 217999477.

Filomena A. Carvalho, Instituto de Medicina Molecular, Faculdade de Medicina, Universidade de Lisboa, Av. Prof. Egas Moniz, 1649-028 Lisboa, Portugal; E-mail: filomenacarvalho@fm.ul.pt; Tel.: +351 217999479; Fax: +351 217999477.

Abstract

Aims: Some studies have reported a positive association between plasma fibrinogen levels, erythrocyte aggregation and essential arterial hypertension (EAH). The aim of this study was to understand how the interaction between fibrinogen and its erythrocyte membrane receptor are altered on EAH.

Methods and Results: EAH patients (n = 31) and healthy blood donors (n = 65) were enrolled in the study. EAH patients, were therapeutically controlled for the disease, presenting systolic blood pressure between 108 and 180 mm Hg and diastolic blood pressure between 66 and 123 mm Hg, and. Clinical evaluation included blood pressure monitoring, electrocardiography, echocardiography and blood cell count. The hemorheological parameters, namely, erythrocyte aggregation, whole blood viscosity and erythrocyte deformability were also analyzed. Fibrinogen-erythrocyte binding force and frequency were evaluated quantitatively, at the single-molecule level, using atomic force microscopy (AFM)-based force spectroscopy. Changes on erythrocyte elasticity were also evaluated. Force spectroscopy data showed that the average fibrinogen-erythrocyte binding forces increase from 40.4 ± 3.0 pN in healthy donors to 73.8 ± 8.1 pN in patients with EAH, despite a lower binding frequency for patients, comparing to the control group (7.9 ± 1.6% *vs*. 27.6 ± 4.2%, respectively). Elasticity studies revealed an increase of erythrocyte stiffness on the patients.

Conclusions: The stronger fibrinogen binding to erythrocytes from EAH patients and alteration on cells elasticity may lead to changes on the whole blood flow. The patients' altered hemorheological parameters may also contribute for this blood flow perturbations. The transient bridging of two erythrocytes, by the simultaneous binding of fibrinogen to both of them, promoting erythrocyte aggregation, could represent an important cardiovascular risk factor.

Keywords: fibrinogen, erythrocyte, erythrocyte aggregation, cardiovascular risk, biomarker.

Introduction

Essential hypertension is the world's most prevalent cardiovascular disorder, affecting approximately 26% of the worldwide population and still rising [1]. From this prevalence, it is evident that hypertension is a very important public health challenge. Its complications, including cardiovascular, cerebrovascular and renal diseases are the major causes of morbidity and mortality [2, 3].

Hypertension, defined as a systolic blood pressure ≥140 mmHg and/or a diastolic pressure ≥90 mmHg, is due to specific causes in a small fraction of cases, but in the vast majority of individuals (>90%) its etiology cannot be determined. Therefore, the essential or primary hypertension term is used [1, 2, 4]. Essential hypertension is currently understood as a multifactorial disease arising from the combined action of many genetic, environmental and behavioral factors. It results from a failure on the compensatory mechanisms to counteract the perturbation of blood pressure homeostasis [5]. Clinical trials have demonstrated that lowering blood pressure reduces incidence of and death from cardiovascular diseases [6, 7].

Many pathophysiologic factors have been implicated in the genesis of essential hypertension [4, 8, 9], such as obesity, insulin resistance, high alcohol intake, high salt intake, sedentary lifestyle, stress, overproduction of sodium-retaining hormones and vasoconstrictors, increased vascular growth factors activity, dyslipidemia, alterations in adrenergic receptors that influence heart rate, and low potassium or calcium intake [4, 8]. Although several factors clearly contribute to the pathogenesis and maintenance of blood pressure elevation, our understanding of the underlying causal mechanism behind the pathology remains somewhat unclear.

Some studies reported that elevated plasma fibrinogen levels in patients with essential hypertension are related to vascular complications [10]. Moreover, the results of the Leigh study[11], in which hypertensive patients with plasma fibrinogen above 3.5 g/L had a 12-fold higher coronary risk than those with fibrinogen below 2.9 g/L, suggest that fibrinogen levels may affect the clinical prognosis in hypertension. Furthermore, high plasma fibrinogen concentrations have been shown to predict cardiovascular diseases,

incidence of cardiovascular events, and increased mortality from cardiovascular diseases [12, 13, 14].

The role of plasma fibrinogen, a key on inflammation processes, as a cardiovascular risk factor still remains controversial [15, 16, 17]. Erythrocytes were thought to be incorporated into venous thrombi via passive trapping in the growing fibrin network, culminating in the production of erythrocytes and fibrin-rich venous thrombus [18]. Little was known about mechanisms regulating the interaction between fibrinogen and erythrocytes, or how fibrinogen and these cells interact, contributing to venous thrombus size or resolution. Our group reported the existence of an interaction between fibrinogen and an erythrocyte receptor [19, 20], which binding was greater in cardiovascular patients, namely in chronic heart failure patients, than in healthy donors [21]. Using atomic force microscopy (AFM), we also showed that fibrinogen has an important role on erythrocyte aggregation, as increasing fibrinogen levels, erythrocyte-erythrocyte adhesion also increases [22]. The simultaneous binding of fibrinogen to receptors on two different erythrocytes may transiently bridge these cells, increasing blood viscosity at the microcirculatory level, impairing a proper blood flow and increasing cardiovascular risk [19, 20, 21].

Several studies have already addressed the correlation between cardiovascular and hemostatic balance [23, 24]; however, only a few of them were focused on hypertensive patients. Some hemorheological findings in essential hypertension are: increased hematocrit, plasma fibrinogen, plasma and whole blood viscosity, and erythrocyte aggregability, as well as impaired erythrocyte deformability [25], leading to impaired hemodynamic profiles both at the macro and microcirculation levels [26, 27], ultimately promoting inflammation and atherosclerotic plaque formation [28].

In recent years, essential arterial hypertension still presents a high mortality, associated with high risk of cardiovascular diseases. Therefore, early diagnosis and prognostic stratification seem to be of paramount importance in order to choose the best therapeutic strategies. Although much progress has been made for cardiovascular diseases in diagnosis, treatment and prognosis during the past two decades, there is still a clinical need for novel prognosis biomarkers and therapeutic interventions to decrease cardiovascular disease incidence. On this study, we evaluated the relevance of fibrinogen-

erythrocyte binding and hemorheological parameters on the risk assessment of essential arterial hypertension patients.

Methods

Study participants

A total of thirty-one patients with essential arterial hypertension (EAH) were included in the study. Patients were stable in ambulatory and with optimized standard medical therapy according to the European Society of Hypertension (ECS) guidelines [29]. The inclusion criteria were hypertensive patients consecutive examined on the Hypertension Centre of Hospital de Santa Maria (CHLN, Lisbon), taking calcium channels antagonists (ACC), angiotensin converting enzyme (ACE) inhibitors / angiotensin receptor antagonists (ARA), Beta-blockers (BB), aspirin or, in some cases, one statin. The patients included in the study were not taking any other antiaggregant drug beside aspirin. Exclusion criteria were: severe renal damage, defined as glomerular filtration rate (eGFR) below 30 ml/min, diabetes mellitus type I or II, heart failure NYHA (New York Heart Association functional classification) III or IV or left ventricular ejection fraction (LVEF) below 40%, liver failure, cancer or other systemic severe disease.

Clinical profiles were thoroughly collected. Each participant gave their previous informed consent and all clinical research has been conducted according to the principles expressed in the Declaration of Helsinki. This study was approved by the joint Ethics Committee of Centro Académico de Medicina de Lisboa (CAML, Faculdade de Medicina da Universidade de Lisboa and Centro Hospitalar Lisboa Norte).

A control group of 65 healthy donors was included in the study, following a protocol with the Portuguese Blood Institute (IPS, Lisbon). Controls did not have any known concomitant disease.

Measurements and definitions

Blood pressure (BP) was measured following indications of the European Society of Hypertension (ESH) and European Society of Cardiology (ESC) guidelines [30, 31], using validated mercury-free digital sphygmomanometers (OMRON 705CP-II, OMRON Healthcare, Lake Forest, IL, USA) with appropriate cuff size. The average of three consecutive measurements was used for the analysis. Controlled BP was defined as systolic BP (SBP) < 140 mmHg and diastolic BP (DBP) < 90 mmHg. In all patients, 24-hour

ambulatory blood pressure measurements (model 90207, Spacelabs Healthcare, Snoqualmie, WA, USA) were also taken and analysed as previously described [32]. The aortic central pressure and pulse wave velocity measurement by tomography were also performed.

Blood samples for measurements of plasma fasting glucose, total, LDL and HDL cholesterol, triglycerides and creatinine, as well as first morning urine specimens to determine albumin creatinine ratio (ACR) were obtained.

Ambulatory blood pressure monitoring

Ambulatory blood pressure monitoring (ABPM) was performed during 24 h on a day of standard activity, with an adequate cuff for the size of the patient's arm. A control system, validated according to the protocol of the British Hypertension Society, was used [33]. The records of readings considered to be valid were ≥ 80% of the total. The monitor was programmed for obtaining blood pressure measurements every 20 min during the waking period and every 30 min during the resting period. Individual correction was made for the waking and sleeping hours reported by the patient.

Echocardiography

Left ventricular dimensions were measured by echocardiography (model SSA - 370 A, Toshiba, Hyogo, Japan) following the American Society of Echocardiography recommendations [34]. For each patient, the following measurements were taken: end-diastolic and end-systolic interventricular septum thickness (IVSD and IVSS, respectively), posterior wall thickness (PWD and PWS, respectively), left ventricular diameters (LVDD and LVDS, respectively) and left atrial diameter (LAD). Left ventricular mass (LVM) was calculated (M-mode tracings under two-dimensional control, left parasternal short axis view, mean of three cardiac cycles) by using the Devereux's formula [35] and indexed by either body surface area (LVMi) [36] . In overweight or obese patients, LVH was defined according with recommendations [37]. Myocardial relative wall thickness (RWT) was also calculated [38], as well LVEF (LV end-diastolic area – LV end-systolic area)/ LV end-diastolic area (two dimensional apical four chambers view, mean of three cardiac cycles) [39].

Erythrocyte isolation and preparation for AFM measurements

Blood was centrifuged at 200 × *g* for 10 min. For erythrocyte isolation, plasma and buffy-coat were removed and the erythrocytes washed three times with buffered saline glucose citrate (BSGC: 1.6 mM KH_2PO_4, 8.6 mM Na_2HPO_4, 0.12 M NaCl, 13.6 mM sodium citrate, 11.1 mM glucose) pH 7.3, supplemented with 1 mM calcium chloride. Then, erythrocytes were diluted to 0.1% hematocrit on the same buffer and placed on a clean poly-L-lysine-coated glass slide.

AFM tip functionalization

For the covalent attachment of fibrinogen molecules to the AFM tips, we used our previously optimized procedure [19]. Briefly, AFM OMCL TR-400-type silicon nitride tips (Olympus, Tokyo, Japan) were cleaned with an intense ultraviolet light source and were silanized with 3-aminopropyl-triethoxysilane (APTES, 30 µl) and N,N-diisopropylethylamine (10 µl) to be coated with a self-assembly monolayer of amines. Then, the AFM tips were rinsed with fresh chloroform and dried under nitrogen gas. The probes were placed in a glutaraldehyde solution 2.5% (v/v). Finally, tips were placed in 1 mg/ml human fibrinogen (Sigma Aldrich, USA) to attach the fibrinogen molecules to the AFM tip.

AFM-based force spectroscopy

AFM studies were conducted using a force spectroscopy methodology previously described by us [19, 20, 40]. After covalently attaching fibrinogen molecules to the AFM tip (probe), we used it to tap on the surface of the erythrocytes, measuring the frequency or probability of binding and the force necessary to break those bonds. All the interactions between fibrinogen and erythrocytes were studied at room temperature, in physiological buffer (BSGC + $CaCl_2$). AFM studies were performed on a NanoWizard II atomic force microscope (JPK Instruments, Germany) mounted on an Axiovert 200 inverted optical microscope (Zeiss, Germany). Cantilevers with a nominal spring constant of approximately 0.02 N/m were used after their calibration using the thermal fluctuation method [41]. The applied force was adjusted to 0.8 nN, before retraction. Data collection for each force-distance cycle was performed at 3 µm/s, leading to an average loading rate of approximately 9 nN/s. Force-curves were analyzed using JPK image processing

software v. 4.2.61. For each blood sample, approximately 3750 force *vs.* distance curves were collected, analyzed and adjusted by polynomial fit.

All results from the patients were matched with those obtained with blood from healthy donors (n=15). Average rupture forces were calculated from the binding data, obtained on the different cells tested for each EAH patient (or healthy donor). Rupture force values were defined as the force necessary to break the bond between a single molecule of fibrinogen and its receptor.

Cell elasticity analysis

Differences on erythrocyte elasticity between EAH patients and control groups were evaluated by analyzing, in parallel, the approach curves of the previously described force spectroscopy measurements. Data were analyzed to obtain the cells Young's modulus (E), using JPK Image Processing v. 4.2.53, by applying the Hertzian model, with a fixed tip-sample separation between -200 and 200 nm. The probe was modeled as a quadratic pyramid, with a tip angle of 35° (half-angle to face) and a Poisson ration of 0.50. Young's modulus histograms were constructed for each experimental condition studied. The ideal histogram bin size was chosen in order to achieve the best fitted Gaussian model peak length, yielding a selected binning size of 0.1 kPa. The maximum values of the Gaussian peaks represent different statistical measure of the Young's modulus of the cells. Values of the mean ± standard deviation and median of each group were also taken into consideration.

AFM tip penetration depth onto erythrocytes was also evaluated. This parameter was analyzed by the position of the maximal movement of the piezo sensor in the z-axis, which corresponds to the z-axis coordinate when the sensor reaches an indentation force of 800 pN, subtracting the z-axis position of the sensor when the tip begins the contact with the surface of the erythrocyte.

Hematologic profile

Quantitative analysis of the hemogram of the human blood samples of essential arterial hypertension patients and healthy donors were also done by using PocH-100iV equipment (Sysmex, Kobe, Japan).

Whole blood viscosity

Whole blood viscosity was measured using a Brookfield DV-II viscometer (Brookfield Engineering Laboratories, MA, USA). Measurements were done at 37°C, both using native blood samples and samples with hematocrit adjusted to 45%, submitting them to low (22.5 s^{-1}) and high (225 s^{-1}) shear rates.

Erythrocyte deformability

Erythrocyte deformability was assessed at 22°C, using a Rheodyn SSD laser diffractometer (Myrenne, Roentgen, Germany). The diffraction pattern was analyzed at eight shear stress values, between 0.30 and 60.0 Pa. Erythrocyte elongation indexes (EEI) were calculated using the light intensities of the diffraction pattern [42].

Erythrocyte aggregation

Erythrocyte aggregation (EA) was measured in an erythrocyte aggregometer *(*Myrenne), at 22°C. The MA1 aggregometer consists of a rotative cone-plate aggregometer that disperses all pre-existing aggregates by high shear stress (600 Pa), and a photometer that determines the extent of aggregation. The intensity of light, exerted by a light emitting diode, is measured after transmission through the blood sample using a photodiode [43].

Erythrocyte aggregation was determined with 20 µl of blood sample, in stasis, after 5 or 10 s of integration time of dispersing the blood sample. To determine the effect of fibrinogen concentration on erythrocyte aggregation, measurements were also performed in the presence of different fibrinogen concentrations (0 to 80 mg/dl).

Statistical Analysis

Descriptive statistics are given as mean ± standard error of mean (SEM) and frequency. For every parameter studied, EAH patients group was tested against control group (healthy donors). Unpaired Student's *t*-test was used for statistical analysis of intergroup comparison. Statistical significance was set at $p<0.05$. Statistical analyses were performed using GraphPad Prism 5.

Results

The baseline characteristics of all randomized participants are summarized in Table 1. The group was comparable in their demographic, clinical and laboratorial characteristics. There was a good balance between women and men on each group. Essential arterial hypertension patients (N = 31) and healthy blood donors (N = 65) were engaged in the study. Treated EAH patients presented systolic blood pressure between 108 and 180 mm Hg and diastolic blood pressure between 66 and 123 mm Hg. They were overweight and presented high pulse wave velocity. Plasma lactate dehydrogenase (LDH) concentration was higher for these patients when compared to reference levels (up to 190 UI/l). The average of glycated hemoglobin (HbA1c) of the EAH patients population was in a range associated to a significant risk for *diabetes mellitus*.

Table 1 | Baseline characteristics of the essential arterial hypertension patients' cohort and relevant demographic, clinical and laboratory data. Values are in mean ± SEM, unless stated.

Demographics	
Number of EAH patients	31
Age (mean ± SD)	65.1 ± 12.9
Male/Female (%)	58 / 42
Height (mean ± SD, cm)	165.1 ± 9.0
Weight (mean ± SD, kg)	77.9 ± 14.0
Body mass index (mean ± SD, kg/m^2)	28.6 ± 4.4
Office Arterial Pressure	
*SBP (*mmHg)	138.7 ± 17.4
*DPB (*mmHg)	84.6 ± 10.6

Pulse (beats/minute)	54.2 ± 13.8
Mean arterial pressure *(*mmHg)	156.8 ± 21.2
ABPM parameters	
SBP ambulatory *(*mmHg)	129.8 ± 18.4
DBP ambulatory *(*mmHg)	73.5 ± 12.7
Mean blood pressure ambulatory *(*mmHg)	93.9 ± 13.6
Cardiac frequency ambulatory (beats/minute)	69.3 ± 12.7
Echocardiography parameters	
Endocardial fractional shortening (%)	43.4 ± 9.2
Septal thickness (mm)	10.9 ± 1.5
Left ventricular posterior wall thickness (mm)	11.1 ± 1.4
IVRT (ms)	93.9 ± 16.4
E/A ratio	1.1 ± 0.5
Pulse wave analysis	
Pulse wave velocity (m/s)	13.9 ± 4.3
SBP aortic (mmHg)	138.0 ± 27.1
DBP aortic (mmHg)	81.6 ± 13.8
Routine blood tests	
Hemoglobin (mg/dL)	13.9 ± 1.2
Creatinine (mg/dL)	0.97 ± 0.33
Sodium (mEq/L)	139.8 ± 2.2

Potassium (mEq/L)	4.3 ± 0.4
Glucose (mg/dL)	106.7 ± 21.5
HbA1c (%)	5.9 ± 0.7
ALT (U/L)	22.9 ± 12.5
γGT(U/L)	40.7 ± 47.3
Total protein (mg/dL)	7.1 ± 0.5
Albumin (%)	45.7 ± 24.0
Gamma globulins (%)	11.0 ± 6.3
LDH (U/L)	338.0 ± 78.4
Total Cholesterol (mg/dL)	176.4 ± 33.6
Triglycerides (mg/dL)	118.3 ± 48.9
HDL-cholesterol (mg/dL)	54.5 ± 12.4
LDL-cholesterol (mg/dL)	98.3 ± 29.1

Abbreviations: EAH - essential arterial hypertension; SBP - systolic blood pressure; DBP - diastolic blood pressure; IVRT - isovolumic relaxation time; HbA1c - glycated hemoglobin; ALT - alanine aminotransferase; LDH - lactate dehydrogenase; γGT - γ-glutamyl transpeptidase.

The fibrinogen-erythrocyte membrane receptor interaction was assessed by atomic force microscopy-based force spectroscopy. All the results were matched with those obtained for healthy donors (control group, n = 15). Well-defined and measurable adhesion forces curves were observed. The cells showed good adherence to poly-L-lysine treated glass slides and a typical morphology on the optical microscope images. AFM force spectroscopy data are shown in Figure 1. The average binding forces (Figure 1b) and frequencies (Figure 1c) were determined for the binding between fibrinogen and

erythrocytes from EAH patients and healthy blood donors. These results showed that the average force necessary to break the bond between fibrinogen and erythrocytes increases from 40.4 ± 3.0 pN on the control group to 73.8 ± 8.1 pN in EAH patients (p < 0.0061; Figure 1b). Moreover, we observed a lower binding frequency for EAH patients, comparing to the control group (27.6 ± 4.2 % *vs*. 7.9 ± 1.6 %; p < 0.0001; Figure 1c).

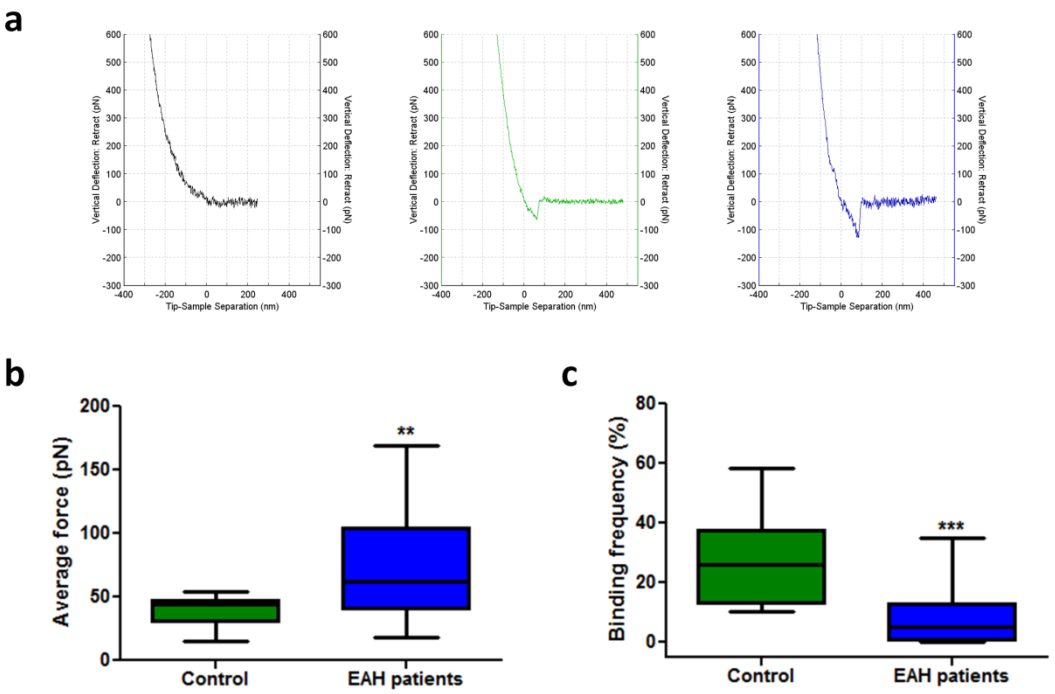

Figure 1 | Fibrinogen-erythrocyte interaction measured by atomic force microscopy-based force spectroscopy. Examples of retraction curves: Non-adhesion (black), healthy donor (green) and EAH patient (blue) AFM cantilever deflections *vs.* distance curves are represented **(a)**. Fibrinogen-erythrocyte binding force **(b)** and (un)binding frequency **(c)** determined for the control group (healthy donors) and EAH patients. ** p = 0.0061; *** p < 0.0001.

In parallel with the analysis of fibrinogen-erythrocyte binding by force spectroscopy data of EAH and control groups, we also analyzed the erythrocyte elasticity parameters of the same samples. All force spectroscopy data were analyzed in order to determine the Young's modulus and the penetration depth for each force-distance curve. The results obtained for Young's modulus data of both groups are presented in a relative frequency histogram (Figure 2a). Gaussian polynomial fit was applied, but the results could not be

accurately compared between groups because the fitting does not converge for the control group. Considering a stiffness cut-off of 4.0 kPa and the normal values for these cells [44, 45], we calculated the mean and median for both groups. Comparing just the values of the mean ± SEM and median for EAH patients, we obtained 0.83 ± 0.004 kPa and 0.54 kPa, respectively. For the control group, the values obtained were 0.77 ± 0.007 kPa and 0.32 kPa. EAH patients have a statistically significant ($p < 0.0001$) increase on erythrocyte stiffness (decreased elasticity).

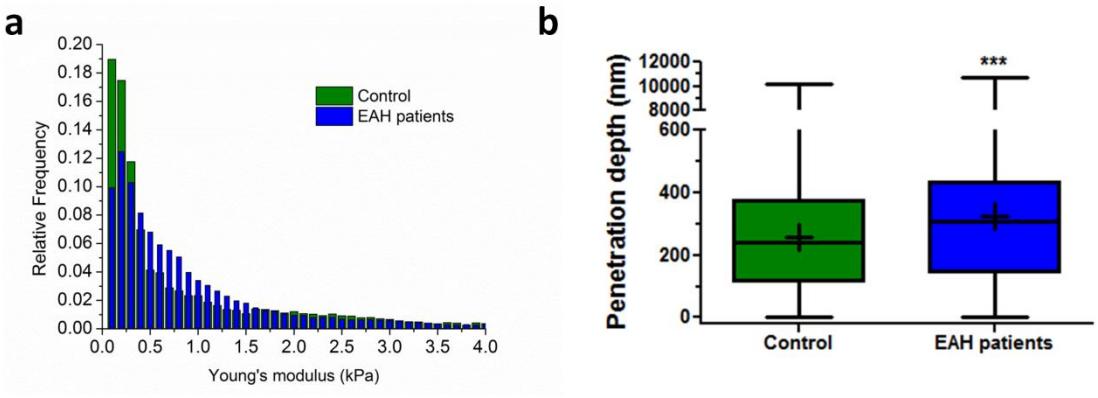

Figure 2 | **Erythrocyte stiffness studies. (a)** Histograms of the distribution of the Young's modulus (E, kPa) values obtained from EAH patients and for the control group. **(b)** AFM tip penetration depth onto erythrocytes for an applied force of 800 pN. The "+" symbol indicates the average value of penetration depth for each group. *** $p < 0.0001$.

To evaluate the ability of the erythrocytes to deform, AFM tip penetration depth was also determined (Figure 2b). Data show that the mean ± SEM penetration depth on erythrocytes from EAH patients was 322.2 ± 1.7 nm, which is significantly higher than the mean ± SEM penetration depth determined for the control group (258.7 ± 1.2 nm; $p < 0.0001$). With these results, we could conclude that EAH patients have erythrocytes with a higher penetration depth than those from healthy donors.

The analysis of the hemograms from EAH patients' blood samples revealed no significant differences from the control group. All hemogram parameters were within their normal ranges. Despite the large distribution range, EAH patients' plasma fibrinogen concentrations were significantly higher than those determined for the control group (301.6 ± 17.8 *vs.* 246.6 ± 11.0 mg/dl; $p = 0.0071$) (Figure 3).

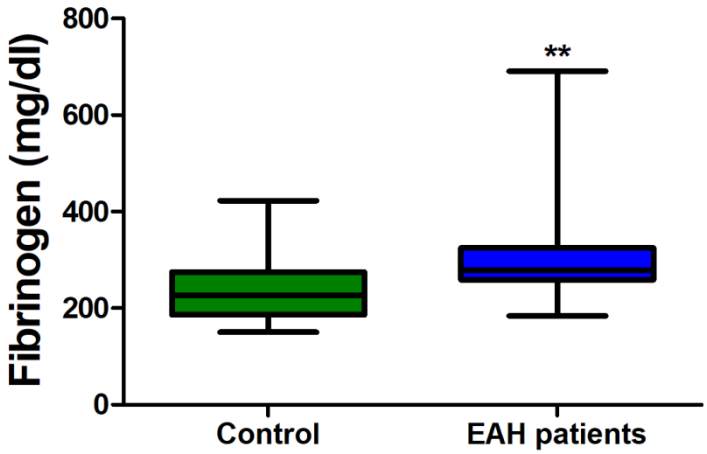

Figure 3 | **Fibrinogen levels.** Quantification of the blood plasma total fibrinogen concentration for control group (healthy donors) and essential arterial hypertension patients.

The clinical evaluation also included blood pressure monitoring, electrocardiography and echocardiography. We found that all hypertensive patients present sinus rhythm without electrocardiographic changes and, on the echocardiography, present several degrees of left ventricular hypertrophy. These techniques were very useful for assessing the heart function and for detecting cardiovascular complications.

Regarding the erythrocyte aggregation evaluation, we observed a significant increase of the erythrocyte aggregation index of EAH patients relative to the control group in the absence of added fibrinogen (Figure 4). This happened at both situations evaluated at stasis, during 5 s and 10 s after dispersion at 600 Pa, trying to mimic different hemorheologic blood flow conditions. Different concentrations of fibrinogen added to the blood samples were tested (0, 20, 40, 60 and 80 mg/dl), in order to evaluate the relation between erythrocyte aggregation and increasing fibrinogen blood levels. For all fibrinogen concentrations tested, the erythrocytes from EAH patients aggregate more than those from the control group. Statistically significant variations were observed between 0 and 80 mg/dl of fibrinogen added and at the time point analysis of 10 s and 5 s, comparing the control group with EAH patients (0 mg/dl, 10 s: 15.61 ± 0.39 *vs.* 20.09 ± 0.92, $p < 0.0001$; 0

mg/dl, 5 s: 5.40 ± 0.15 *vs.* 7.42 ± 0.33, $p < 0.0001$; 80 mg/dl, 10 s: 18.02 ± 0.47 *vs.* 21.50 ± 0.95, $p = 0.0004$; 80 mg/dl, 5 s: 6.46 ± 0.20 *vs.* 7.89 ± 0.36, $p = 0.0003$). For 60 mg/dl of added fibrinogen at 10 s, we did not observe a statistically significant variation, despite the maintenance of the same variation trend of the erythrocytes from EAH patients tending to aggregate more than those from the control (Figure 4).

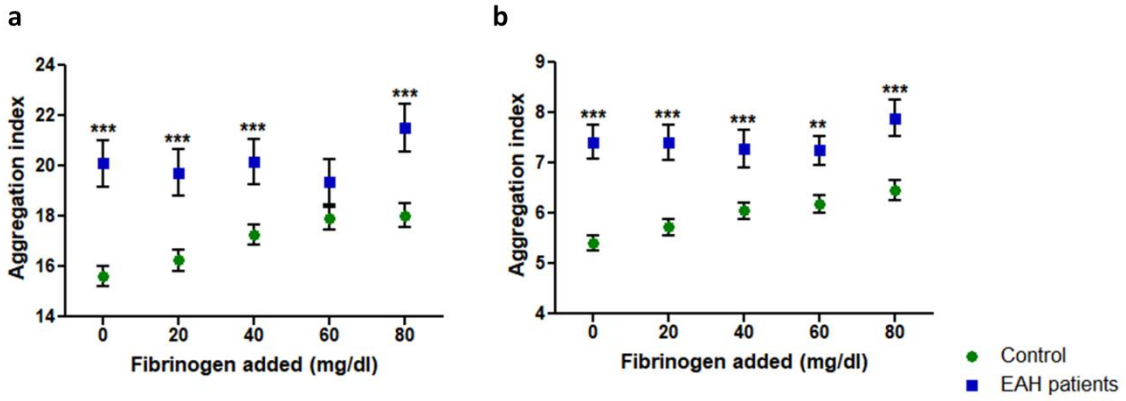

Figure 4 | **Erythrocyte aggregation as a function of the addition of fibrinogen to the blood samples.** Erythrocyte aggregation was measured during 10 s **(a)** or 5 s **(b)** after dispersion of the blood sample, at different concentrations of added fibrinogen (0 to 80 mg/dl). ** $p = 0.0013$; *** $p \leq 0.0008$.

The results obtained for whole blood viscosity of EAH patients and controls are shown in Figure 5. Our results show that native (without hematocrit correction) whole blood viscosity and hematocrit corrected whole blood viscosity were very similar between control and patients groups at both shear rates. No statistical significant differences were obtained.

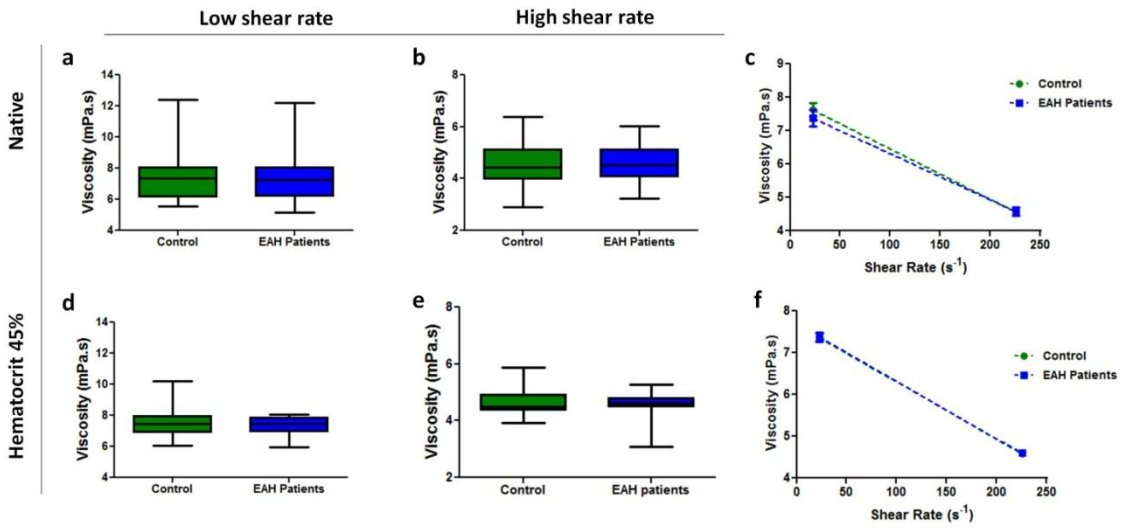

Figure 5 | **Changes on whole blood viscosity between essential arterial hypertension patients and healthy donors.** Values of blood viscosities of native whole blood **(a, b, c)** and after hematocrit correction to 45% **(d, e, f)** were measured at two shear rates: 22.5 s^{-1} **(a, d)** and 225 s^{-1} **(b, e)**. Plots of whole blood viscosity *vs.* shear rate for each studied group **(c, f)**. Dashed lines are mere guides to the eye.

Erythrocyte deformability was assessed as erythrocyte elongation index, at different shear stress values (Figure 6). Statistically significant differences in erythrocyte deformability between EAH patients and the control group were obtained for all shear stress values ($p \leq 0.0115$ from 0.6 to 60 Pa), except the lowest one tested (0.3 Pa). At these shear stress values, EAH patients presented higher deformability than the control group (0.6 Pa: 4.27 ± 0.25 *vs.* 5.36 ± 0.33, $p = 0.0115$; 60 Pa: 42.79 ± 0.54 *vs.* 55.79 ± 0.79, $p < 0.0001$).

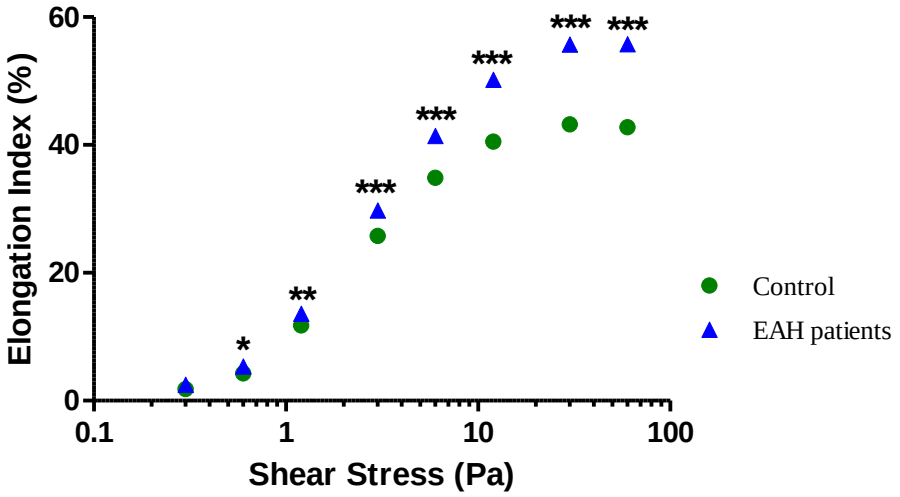

Figure 6 | Erythrocyte deformability measured at different shear stress values for both studied groups. Changes on erythrocyte deformability (assessed as erythrocyte elongation index) between EAH patients and healthy donors were measured at shear stress values between 0.3 and 60 Pa, mimicking blood vessels of different diameters. * p = 0.0115; ** $p \leq 0.0005$; *** $p \leq 0.0001$.

Correlations between AFM data, hemorheological, inflammatory and clinical parameters were tested. Statistically significant correlations were detected between fibrinogen-erythrocyte binding force and whole blood viscosity, fibrinogen or lactate dehydrogenase (LDH). All these data are described on the Supplementary information.

Discussion

Here we investigated the importance of the interactions between fibrinogen and erythrocytes and possible changes on hemorheological parameters on essential arterial hypertension disease.

The frequency of cardiovascular events is associated in a continuum manner with blood pressure [46]. In our study, blood pressure was measured as part of the initial evaluation of all EAH patients. However, this is not the only determinant of cardiovascular damage. The propensity of hypertensive patients to develop organ damage is markedly influenced by coexisting risk factors. Thus, others clinical tests were performed, helping to identify the causes of the disease, to characterize the patient, to facilitate the choice of therapy and to define prognosis [47].

Looking for new potential diagnostic and prognostic biomarkers is of paramount importance to enable a better characterization and assessment of EAH patients. The role that the binding between fibrinogen and erythrocyte plays in this disease has not yet received its due attention, despite its involvement on the increased erythrocyte-erythrocyte adhesion recently found for EAH patients[22]. Thus, on this study, we evaluated the importance of the binding between fibrinogen and erythrocytes as a cardiovascular risk factor on patients with essential arterial hypertension using a powerful nanotool for force spectroscopy measurements.

From the AFM-based force spectroscopy results, we can conclude that EAH patients have higher fibrinogen-erythrocyte binding forces than healthy donors, despite lower binding frequency. This may have an important role for the increase on erythrocyte aggregation in hypertension, and could be a predictor of cardiovascular risk to be evaluated in clinical practice. Furthermore, Lominadze *et al.* reported in a rat model of spontaneous hypertension that increased erythrocyte aggregation and plasma hyperviscosity were present not only during the established phase of hypertension, but also before blood pressure became elevated [48]. Thus, besides a diagnostic biomarker, this interaction could represent a powerful predictive biomarker to prevent cardiovascular events beforehand.

Several prospective studies have demonstrated a direct relationship between plasma fibrinogen levels and the risk of cardiovascular diseases [49, 50, 51]. Particularly, these

levels may affect prognosis in hypertension [11, 52]. Sechi *et al.* showed that high plasma concentrations of fibrinogen are associated with organ damage in essential hypertension [53]. However, Fassl *et al.* data indicate that perioperative administration of fibrinogen concentrate to bleeding patients undergoing cardiac surgery is not associated with increased incidence of major adverse cardiac or thromboembolic events and mortality after 30 days or 1 year [54].

Similarly, our recent results with heart failure patients also showed a significant increase of the binding force between fibrinogen and erythrocytes[21]. On this study, fibrinogen-erythrocyte binding forces determined by AFM were shown to be associated with the patient's clinical outcome: those with higher AFM-measured fibrinogen-erythrocyte binding forces presented a higher probability of cardiovascular disease-associated hospitalization during the subsequent 12-months clinical follow-up period. This result highlighted the importance of the fibrinogen-erythrocyte interaction in chronic heart failure patients and identified a subgroup of patients at higher risk [21].

Erythrocyte biomechanic properties associated to their elasticity (Young's modulus and AFM tip penetration depth upon pressing onto erythrocytes) were also analyzed. We found that erythrocytes from EAH patients were stiffer and had higher cell penetration depth than the control group.

It is possible that the stronger association between fibrinogen and erythrocyte can be promoted by the high blood pressure. Previous evidences have lead to the hypothesis that hypertension *per se* may confer to the patient a hypercoagulable state, as shown by Lip and Blann [55].

Hemorheological parameters have been associated with hypertension [52]. Therefore, erythrocyte aggregation, whole blood viscosity, erythrocyte deformability and fibrinogen levels were also analyzed on this study. Sloop *et al*. showed that blood viscosity contributed to hypertension by increasing systemic vascular resistance [47]. The Edinburgh Artery Study demonstrated the role of chronic hyperviscosity in atherosclerotic cardiovascular disease [56]. In a cohort study, patients sustaining a cardiovascular event had significantly higher blood viscosity values [56]. Our whole blood viscosity results revealed no differences on this parameter between EAH patients and healthy blood donors. This may be due to the pharmacologic therapy used by these patients (*e.g.*, aspirin), which is known to make the blood more fluid. Rosenson showed that aspirin/dipyridamole was

more effective than aspirin therapy in reducing blood viscosity at shear rates of 1 and 2 s^{-1}; however, there were no significant differences in blood viscosity at shear rates from 5 to 1000 s^{-1} [57].

Erythrocyte deformability data indicated that EAH patients' erythrocytes are more deformable than those from healthy donors at both shear stress values. This result is not in agreement with previous findings suggesting a decreased erythrocyte deformability in hypertensive patients, leading to an increased microvascular flow resistance [25]. Again, this difference may be related with patients' therapy. Furthermore, our erythrocyte deformability results are in agreement with the biomechanic data (erythrocyte penetration depth), indicating at the single-cell level that erythrocytes from these patients have a higher capacity to deform than those from healthy donors.

At high shear rates or blood flow, erythrocytes reversibly deform to minimize resistance to flow and viscosity. In addition, erythrocytes entrain or organize into columns, which minimizes potential collisions between cells caused by tumbling and orbiting motions, further decreasing viscosity[58]. In areas of slow blood flow or low shear, erythrocytes can aggregate and increase viscosity [58]. At this level, any molecule with a size large enough to simultaneously bind two erythrocytes, such as fibrinogen, can foster erythrocyte aggregation[22].

Concerning the erythrocyte aggregation data, we observed a significant increase of the erythrocyte aggregation from EAH patients, compared with the control group. In the presence of increasing fibrinogen concentrations, erythrocytes from EAH patients tend to increase their aggregation. This result corroborates the association of high plasma fibrinogen concentrations with increased erythrocyte aggregation, which could be a predictor of high cardiovascular risk.

The association between altered hemorheological parameters and hypertension should be considered with caution. Other hemostatic, clinical or therapeutic parameters may also be influencing the results. This may limit the generalizability of the conclusions to every EAH patients. Studies with a larger number of patients should be encouraged to further confirm these findings before translating these results for clinical application.

Correlation between parameters was tested trying to understand the interactions of binding force and different altered parameters in EAH patients (*vd.* Supplementary Information). We observed significant correlation between AFM binding force data and

whole blood viscosity, fibrinogen and LDH levels. These findings support the fact that EAH patients have a higher cardiovascular risk, associating all these altered parameters.

Our findings evidence that the binding between fibrinogen and erythrocyte is increased on EAH patients, which could be an important cardiovascular risk factor to be considered in the future. It is of paramount importance to develop a strategy to define the mechanisms involved on this binding and to prevent fibrinogen-erythrocyte interactions on those who developed or will develop the disease. Associated with this, hemorheological parameters were also altered on EAH disease. The pathophysiological mechanisms that lead to arterial hypertension are extremely complex, selective and variable between patients. With increased recognition of specific causes, it may be possible to select and develop therapies for each pathophysiologic mechanism, limitting adverse effects and leading to a more effective reduction of arterial hypertension.

Acknowledgments

This work was supported by Fundação para a Ciência e Tecnologia – Ministério da Educação e Ciência (FCT-MEC, Portugal) grant PTDC/QUI-BIQ/119509/2010 and PTDC/BBB-BMD/6307/2014, as well as, fellowship SFRH/BD/84414/2012 to AFG. Authors thank Teresa Freitas (FMUL) for excellent technical assistance.

Author contributions

A.F.G. performed AFM and hemorheological experiments, analyzed data, performed the statistical analysis, wrote and edited the draft and prepared the manuscript for submission; **F.A.C.** analyzed data and edited the initial draft of the manuscript; **C.S.M.** collected all clinical data, performed clinical evaluation and contributed to relevant discussion; **J.B.N.** contributed to the discussion section; and, **N.C.S.** conceived the idea, designed and directed the experiments, analyzed the data, wrote part of the text and edited the successive drafts of the paper.

Competing Financial Interests statement

The authors declare no competing financial interests.

References of Chapter VI

1. Kearney PM, Whelton M, Reynolds K, Muntner P, Whelton PK, He J. Global burden of hypertension: analysis of worldwide data. *Lancet* 2005; **365:** 217-223.

2. Messerli FH, Williams B, Ritz E. Essential hypertension. *Lancet* 2007; **370:** 591-603.

3. Staessen JA, Wang J, Bianchi G, Birkenhager WH. Essential hypertension. *Lancet* 2003; **361:** 1629-1641.

4. Carretero OA, Oparil S. Essential hypertension. Part I: definition and etiology. *Circulation* 2000; **101:** 329-335.

5. Mullins LJ, Bailey MA, Mullins JJ. Hypertension, kidney, and transgenics: a fresh perspective. *Physiol Rev* 2006; **86:** 709-746.

6. He J, Whelton PK. Elevated systolic blood pressure as a risk factor for cardiovascular and renal disease. *J Hypertens Suppl* 1999; **17:** S7-13.

7. Whelton PH, J. Blood Pressure Reduction. *In: Hennekens CH, Buring JE, Manson JE, Ridker PM, edsClinical trials in cardiovascular disease Philadelphia: WB Saunders;* 1999.

8. Calhoun DA, Bakin SE, Oparil, S. Etiology and pathogenesis of essential hypertension. *In: Crawford MH, DiMarco JP, eds Cardiology London: Mosby International* 2000**:** 3.1-3.10.

9. Oparil S, Zaman MA, Calhoun DA. Pathogenesis of hypertension. *Ann Intern Med* 2003; **139:** 761-776.

10. Lechi C, Gaino S, Zuliani V, Tommasoli RM, Faccini G, Fasson R, Arcaro G, Lechi A, Minuz P. Elevated plasma fibrinogen levels in patients with essential hypertension are related to vascular complications. *Int Angiol* 2003; **22:** 72-78.

11. Stone MC, Thorp JM. Plasma fibrinogen-a major coronary risk factor. *J R Coll Gen Pract* 1985; **35:** 565-569.

12. Danesh J, Lewington S, Thompson SG, Lowe GD, Collins R, Kostis JB, Wilson AC, Folsom AR, Wu K, Benderly M, Goldbourt U, Willeit J, Kiechl S, Yarnell JW, Sweetnam PM, Elwood PC, Cushman M, Psaty BM, Tracy RP, Tybjaerg-Hansen A, Haverkate F, de Maat MP, Fowkes FG, Lee AJ, Smith FB, Salomaa V, Harald K, Rasi R, Vahtera E, Jousilahti P, Pekkanen J, D'Agostino R, Kannel WB, Wilson PW, Tofler G, Arocha-Pinango CL, Rodriguez-Larralde A, Nagy E, Mijares M, Espinosa R, Rodriquez-Roa E, Ryder E, Diez-Ewald MP, Campos G, Fernandez V, Torres E, Marchioli R, Valagussa F, Rosengren A, Wilhelmsen L, Lappas G, Eriksson H, Cremer P, Nagel D, Curb JD, Rodriguez B, Yano K, Salonen JT, Nyyssonen K, Tuomainen TP, Hedblad B, Lind P, Loewel H, Koenig W, Meade TW, Cooper JA, De Stavola B, Knottenbelt C, Miller GJ, Cooper JA, Bauer KA, Rosenberg RD, Sato S, Kitamura A, Naito Y, Palosuo T, Ducimetiere P, Amouyel P, Arveiler D, Evans AE, Ferrieres J, Juhan-Vague I, Bingham A, Schulte H, Assmann G, Cantin B, Lamarche B, Despres JP, Dagenais GR, Tunstall-Pedoe H, Woodward M, Ben-Shlomo Y, Davey Smith G, Palmieri V, Yeh JL, Rudnicka A, Ridker P, Rodeghiero F, Tosetto A, Shepherd J, Ford I, Robertson M, Brunner E, Shipley M, Feskens EJ, Kromhout D, Dickinson A, Ireland B, Juzwishin K, Kaptoge S, Lewington S, Memon A, Sarwar N, Walker M, Wheeler J, White I, Wood A. Plasma fibrinogen level and the risk of major cardiovascular diseases and nonvascular mortality: an individual participant meta-analysis. *JAMA* 2005; **294:** 1799-1809.

13. Maple-Brown LJ, Cunningham J, Nandi N, Hodge A, O'Dea K. Fibrinogen and associated risk factors in a high-risk population: urban Indigenous Australians, the DRUID Study. *Cardiovasc Diabetol* 2010; **9:** 69.

14. Shi Y, Wu Y, Bian C, Zhang W, Yang J, Xu G. Predictive value of plasma fibrinogen levels in patients admitted for acute coronary syndrome. *Tex Heart Inst J* 2010; **37:** 178-183.

15. Onohara T, Komori K, Kume M, Ishida M, Ohta S, Takeuchi K, Matsumoto T, Sugimachi K. Increased plasma fibrinogen level and future risk of coronary artery disease after repair of abdominal aortic aneurysm. *J Am Coll Surg* 2000; **191:** 619-625.

16. Sato S, Kobayashi T, Iida M, Naito Y, Kiyama M, Kitamura A, Iso H, Komachi Y. A case-reference study on plasma fibrinogen concentrations and coronary atherosclerosis in Japanese. *J Epidemiol* 1996; **6:** 81-86.

17. Sweetnam PM, Thomas HF, Yarnell JW, Beswick AD, Baker IA, Elwood PC. Fibrinogen, viscosity and the 10-year incidence of ischaemic heart disease. *Eur Heart J* 1996; **17:** 1814-1820.

18. Aleman MM, Walton BL, Byrnes JR, Wolberg AS. Fibrinogen and red blood cells in venous thrombosis. *Thromb Res* 2014; **133:** S38-40.

19. Carvalho FA, Connell S, Miltenberger-Miltenyi G, Pereira SV, Tavares A, Ariëns RA, Santos NC. Atomic force microscopy-based molecular recognition of a fibrinogen receptor on human erythrocytes. *ACS nano* 2010; **4:** 4609-4620.

20. Carvalho FA, de Oliveira S, Freitas T, Gonçalves S, Santos NC. Variations on fibrinogen-erythrocyte interactions during cell aging. *PloS one* 2011; **6:** e18167.

21. Guedes AF, Carvalho FA, Malho I, Lousada N, Sargento L, Santos NC. Atomic force microscopy as a tool to evaluate the risk of cardiovascular diseases in patients. *Nat Nanotechnol* 2016; **11**: 687-692.

22. Guedes AF, Carvalho FA, Moreira C, Nogueira JB, Santos NC. Essential arterial hypertension patients present higher cell adhesion forces, contributing to fibrinogen-dependent cardiovascular risk. *Nanoscale* 2017; **9:** 14897-14906.

23. Wilhelmsen L, Svardsudd K, Korsan-Bengtsen K, Larsson B, Welin L, Tibblin G. Fibrinogen as a risk factor for stroke and myocardial infarction. *N Engl J Med* 1984; **311:** 501-505.

24. Hamsten A, de Faire U, Walldius G, Dahlen G, Szamosi A, Landou C, Blomback M, Wiman B. Plasminogen activator inhibitor in plasma: risk factor for recurrent myocardial infarction. *Lancet* 1987; **2:** 3-9.

25. Sandhagen B. Red cell fluidity in hypertension. *Clin Hemorheol Microcirc* 1999; **21:** 179-181.

26. Alexy T, Pais E, Wenby RB, Mack WJ, Hodis HN, Kono N, Wang J, Baskurt OK, Fisher TC, Meiselman HJ. Abnormal blood rheology and chronic low grade inflammation: Possible risk factors for accelerated atherosclerosis and coronary artery disease in Lewis negative subjects. *Atherosclerosis* 2015; **239:** 248-251.

27. Kesmarky G, Toth K, Habon L, Vajda G, Juricskay I. Hemorheological parameters in coronary artery disease. *Clin Hemorheol Microcirc* 1998; **18:** 245-251.

28. Ross R. Atherosclerosis-an inflammatory disease. *N Engl J Med* 1999; **340:** 115-126.

29. Mancia G, Fagard R, Narkiewicz K, Redon J, Zanchetti A, Bohm M, Christiaens T, Cifkova R, De Backer G, Dominiczak A, Galderisi M, Grobbee DE, Jaarsma T, Kirchhof P, Kjeldsen SE, Laurent S, Manolis AJ, Nilsson PM, Ruilope LM, Schmieder RE, Sirnes PA, Sleight P, Viigimaa M, Waeber B, Zannad F, Task Force for the Management of Arterial Hypertension of the European Society of H, the European

Society of C. 2013 ESH/ESC Practice Guidelines for the Management of Arterial Hypertension. *Blood Press* 2014; **23:** 3-16.

30. Chobanian AV, Bakris GL, Black HR, Cushman WC, Green LA, Izzo JL, Jr., Jones DW, Materson BJ, Oparil S, Wright JT, Jr., Roccella EJ, Joint National Committee on Prevention DE, Treatment of High Blood Pressure. National Heart L, Blood I, National High Blood Pressure Education Program Coordinating C. Seventh report of the Joint National Committee on Prevention, Detection, Evaluation, and Treatment of High Blood Pressure. *Hypertension* 2003; **42:** 1206-1252.

31. Mansia G, De Backer G, Dominiczak A, Cifkova R, Fagard R, Germano G, Grassi G, Heagerty AM, Kjeldsen SE, Laurent S, Narkiewicz K, Ruilope L, Rynkiewicz A, Schmieder RE, Struijker Boudier HA, Zanchetti A, European Society of H, European Society of C. 2007 ESH-ESC Guidelines for the management of arterial hypertension: the task force for the management of arterial hypertension of the European Society of Hypertension (ESH) and of the European Society of Cardiology (ESC). *Blood Press* 2007; **16:** 135-232.

32. Mancia G, Laurent S, Agabiti-Rosei E, Ambrosioni E, Burnier M, Caulfield MJ, Cifkova R, Clement D, Coca A, Dominiczak A, Erdine S, Fagard R, Farsang C, Grassi G, Haller H, Heagerty A, Kjeldsen SE, Kiowski W, Mallion JM, Manolis A, Narkiewicz K, Nilsson P, Olsen MH, Rahn KH, Redon J, Rodicio J, Ruilope L, Schmieder RE, Struijker-Boudier HA, van Zwieten PA, Viigimaa M, Zanchetti A, European Society of H. Reappraisal of European guidelines on hypertension management: a European Society of Hypertension Task Force document. *J Hypertens* 2009; **27:** 2121-2158.

33. O'Brien E, Petrie J, Littler W, de Swiet M, Padfield PL, O'Malley K, Jamieson M, Altman D, Bland M, Atkins N. The British Hypertension Society protocol for the evaluation of automated and semi-automated blood pressure measuring devices with special reference to ambulatory systems. *J Hypertens* 1990; **8:** 607-619.

34. Sahn DJ, DeMaria A, Kisslo J, Weyman A. Recommendations regarding quantitation in M-mode echocardiography: results of a survey of echocardiographic measurements. *Circulation* 1978; **58:** 1072-1083.

35. Devereux RB, Alonso DR, Lutas EM, Gottlieb GJ, Campo E, Sachs I, Reichek N. Echocardiographic assessment of left ventricular hypertrophy: comparison to necropsy findings. *Am J Cardiol* 1986; **57:** 450-458.

36. de Simone G, Devereux RB, Daniels SR, Koren MJ, Meyer RA, Laragh JH. Effect of growth on variability of left ventricular mass: assessment of allometric signals in adults and children and their capacity to predict cardiovascular risk. *J Am Coll Cardiol* 1995; **25:** 1056-1062.

37. Gerdts E, Okin PM, de Simone G, Cramariuc D, Wachtell K, Boman K, Devereux RB. Gender differences in left ventricular structure and function during antihypertensive treatment: the Losartan Intervention for Endpoint Reduction in Hypertension Study. *Hypertension* 2008; **51:** 1109-1114.

38. Savage DD, Garrison RJ, Kannel WB, Levy D, Anderson SJ, Stokes J, 3rd, Feinleib M, Castelli WP. The spectrum of left ventricular hypertrophy in a general population sample: the Framingham Study. *Circulation* 1987; **75:** I26-33.

39. Teichholz LE, Kreulen T, Herman MV, Gorlin R. Problems in echocardiographic volume determinations: echocardiographic-angiographic correlations in the presence of absence of asynergy. *Am J Cardiol* 1976; **37:** 7-11.

40. Carvalho FA, Santos NC. Atomic force microscopy-based force spectroscopy--biological and biomedical applications. *IUBMB Life* 2012; **64:** 465-472.

41. Hutter JL, Bechhoefer J. Calibration of atomic-force microscope tips. *Review of Scientific Instruments* 1993; **64:** 1868-1873.

42. Schmid-Schönbein H, Wells RE, Goldstone J. Fluid drop-like behaviour of erythrocytes--disturbance in pathology and its quantification. *Biorheology* 1971; **7:** 227-234.

43. Almeida JP, Carvalho FA, Freitas T, Saldanha C. Modulation of hemorheological parameters by the erythrocyte redox thiol status. *Clin Hemorheol Microcirc* 2008; **40:** 99-111.

44. Butcher DT, Alliston T, Weaver VM. A tense situation: forcing tumour progression. *Nature reviews Cancer* 2009; **9:** 108-122.

45. Cox TR, Erler JT. Remodeling and homeostasis of the extracellular matrix: implications for fibrotic diseases and cancer. *Disease models & mechanisms* 2011; **4:** 165-178.

46. MacMahon S, Peto R, Cutler J, Collins R, Sorlie P, Neaton J, Abbott R, Godwin J, Dyer A, Stamler J. Blood pressure, stroke, and coronary heart disease. Part 1, Prolonged differences in blood pressure: prospective observational studies corrected for the regression dilution bias. *Lancet* 1990; **335:** 765-774.

47. Sloop G, Holsworth RE, Weidman JJ, St Cyr JA. The role of chronic hyperviscosity in vascular disease. *Ther Adv Cardiovasc Dis* 2015; **9:** 19-25.

48. Lominadze D, Joshua IG, Schuschke DA. Increased erythrocyte aggregation in spontaneously hypertensive rats. *Am J Hypertens* 1998; **11:** 784-789.

49. Maeda N, Seike M, Kume S, Takaku T, Shiga T. Fibrinogen-induced erythrocyte aggregation: erythrocyte-binding site in the fibrinogen molecule. *Biochim Biophys Acta* 1987; **904:** 81-91.

50. Reinhart WH. Fibrinogen-marker or mediator of vascular disease? *Vasc Med* 2003; **8:** 211-216.

51. Lominadze D, Dean WL, Tyagi SC, Roberts AM. Mechanisms of fibrinogen-induced microvascular dysfunction during cardiovascular disease. *Acta Physiol (Oxf)* 2010; **198:** 1-13.

52. Poli KA, Tofler GH, Larson MG, Evans JC, Sutherland PA, Lipinska I, Mittleman MA, Muller JE, D'Agostino RB, Wilson PW, Levy D. Association of blood pressure with fibrinolytic potential in the Framingham offspring population. *Circulation* 2000; **101:** 264-269.

53. Sechi LA, Zingaro L, Catena C, Casaccio D, De Marchi S. Relationship of fibrinogen levels and hemostatic abnormalities with organ damage in hypertension. *Hypertension* 2000; **36:** 978-985.

54. Fassl J, Lurati Buse G, Filipovic M, Reuthebuch O, Hampl K, Seeberger MD, Bolliger D. Perioperative administration of fibrinogen does not increase adverse cardiac and thromboembolic events after cardiac surgery. *Br J Anaesth* 2015; **114:** 225-234.

55. Lip GY, Blann AD. Does hypertension confer a prothrombotic state? Virchow's triad revisited. *Circulation* 2000; **101:** 218-220.

56. Lowe GD, Lee AJ, Rumley A, Price JF, Fowkes FG. Blood viscosity and risk of cardiovascular events: the Edinburgh Artery Study. *Br J Haematol* 1997; **96:** 168-173.

57. Rosenson RS. Treatment with aspirin and dipyridamole is more effective than aspirin in reducing low shear blood viscosity. *Microcirculation* 2008; **15:** 615-620.

58. Schmid-Schönbein H, Wells R, Goldstone J. Influence of deformability of human red cells upon blood viscosity. *Circ Res* 1969; **25:** 131-143.

Supplementary information of Chapter VI

Fibrinogen-erythrocyte binding and hemorheology measurements on the assessment of essential arterial hypertension patients

Ana Filipa Guedes[1], Carlos Moreira[2], José Braz Nogueira[2], Nuno C. Santos[1,*], Filomena A. Carvalho[1,*]

Linear regression analysis between whole blood viscosity and AFM data

Trying to understand how the interactions between fibrinogen molecules and its erythrocyte membrane receptor could affect the whole blood viscosity of EAH patients' group, data obtained for each parameter were compared (Figure S1). After performing linear regression analysis, we could observe a significant relation between blood viscosity after the correction of hematocrit, at 225 s^{-1} shear rate, and the average fibrinogen-erythrocyte (un)binding force (p = 0.017; r^2 = 0.20). We also obtained significant relations for native blood viscosity at both shear rates (p = 0.0002 for 22.5 s^{-1}, r^2 = 0.40; p = 0.005 for 225 s^{-1}, r^2 = 0.25). This means that increasing the force of fibrinogen-erythrocyte binding, blood viscosity also increases.

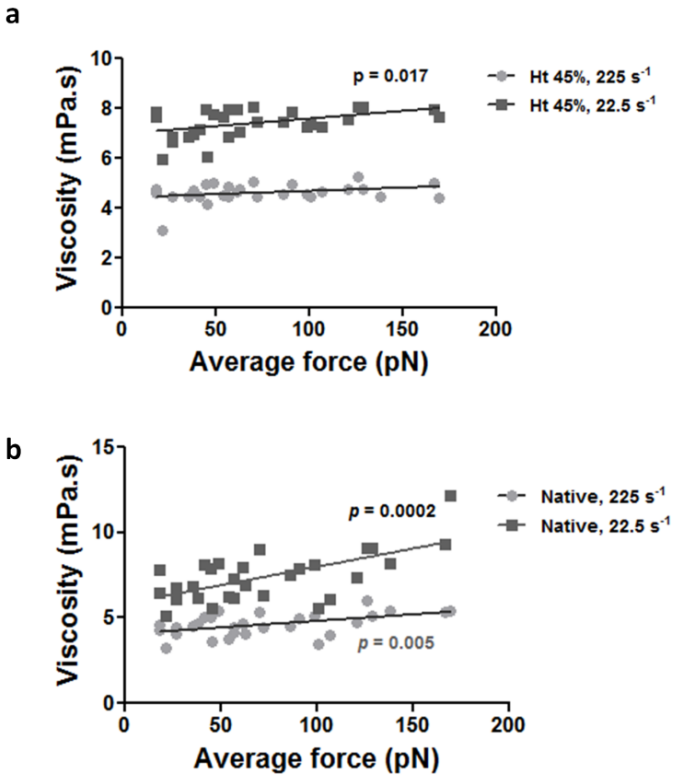

Figure S1 | **Relation between fibrinogen-erythrocyte binding force and whole blood viscosity for EAH patients.** Linear regression analysis between fibrinogen-erythrocyte average (un)binding force data and whole blood viscosity, for 45% hematocrit data **(a)** and native blood data **(b)**. Linear regression was performed with a confidence interval of 95%. We observed a significant relation between native whole blood viscosity at both shear rates and binding force, as well as between 45% hematocrit blood viscosity at 22.5 s^{-1} and binding force. Statistical significance values are shown.

Linear regression analysis between fibrinogen concentration and AFM data

In an effort to understand why the AFM data show that CHF patients have significantly increased fibrinogen-erythrocyte binding force, we evaluated the relationship between the fibrinogen levels in plasma from each EAH patient and binding force (Figure S2). We observed that increasing fibrinogen concentration, the average binding force (measured at the single-molecule level) also increases (p = 0.047, r^2 = 0.14). High fibrinogen plasma levels on EAH patients could lead to high binding strength between this protein and its erythrocyte membrane receptor. Thus, these findings support the idea

that fibrinogen has an important role on promoting erythrocyte aggregation, increasing the propensity for cardiovascular events.

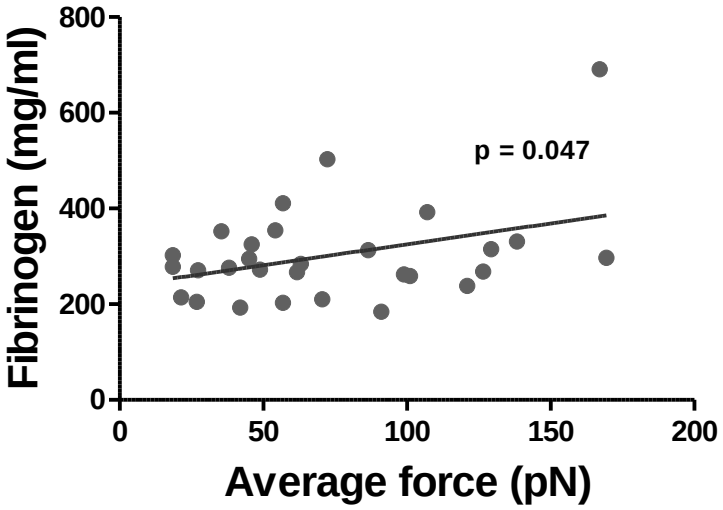

Figure S2 | Relation between fibrinogen-erythrocyte binding force and plasma fibrinogen concentration for EAH patients. Linear regression analysis showed a significant relation between fibrinogen-erythrocyte average (un)binding force data and plasma fibrinogen levels data. Linear regression was performed with a confidence interval of 95%. Statistical significance was $p = 0.047$.

Linear regression analysis between LDH and AFM data

Lactate dehydrogenase (LDH) blood levels are clinically used on the evaluation of a number of diseases and conditions. It is a general indicator of and cellular lysis, releasing the enzyme to the extracellular medium. Considering the tissue-specifity of the different isoforms of this enzyme, LDH is also used to help diagnose and monitor a heart attack. In our study, high LDH levels were observed for EAH group. To understand if there is any association between this parameter and the binding force between fibrinogen and erythrocytes, we performed a linear regression analysis (Figure S3). We observed a positive relation between fibrinogen-erythrocyte binding force and LDH data, showing

that in EAH patients, increasing the LDH circulating levels, also increases the binding force (p = 0.023, r^2 = 0.21).

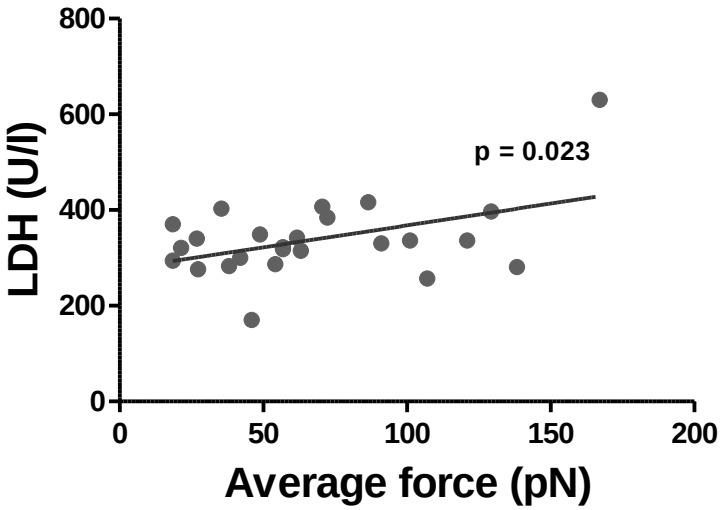

Figure S3 | **Linear regression shows the relation between fibrinogen-erythrocyte binding force and plasma LDH levels.** A significant relation was found between fibrinogen-erythrocyte average (un)binding force data and plasma LDH data. Linear regression was performed with a confidence interval of 95%. Statistical significance was p = 0.023.

Chapter VII ▫

Erythrocyte adhesion in healthy and pathological conditions

Overview

The work described in this Chapter has a close relation with the research conducted for the previous one (Chapter VI). Here, we wanted to evaluate how erythrocytes adhere to each other in the presence of increasing concentrations of fibrinogen molecules, in healthy subjects and in essential arterial hypertension patients. The rational for this study was to better understand, at the single molecule level, the role of blood plasma fibrinogen on erythrocyte aggregation, namely in patients with high cardiovascular risk (such as, essential arterial hypertension disease). Additionally, we wanted to know how the γ' fibrinogen variant levels are altered on these patients, in order to understand its influence on erythrocyte aggregation.

We found that erythrocytes from EAH patients adhere more to each other than the erythrocytes from healthy donors, with this cell-cell adhesion increasing in both populations when in the presence of higher fibrinogen levels. Higher levels of γ' fibrinogen were also found in EAH patients. Our data enabled us to hypothesize that the erythrocyte-erythrocyte binding and γ' fibrinogen variant levels could be promise markers of cardiovascular risk, as these parameters could lead to changes on microcirculation.

This work was done at Instituto de Medicina Molecular, Faculdade de Medicna, Universidade de Lisboa but also at Hospital Santa Maria, Centro Hospitalar Lisboa Norte.

Declaration of authorship

I, Ana Filipa Guedes, declare that most of the laboratory work, data analysis and writing of the manuscript initial draft were carried out by me, under the supervision of Prof. Filomena A. Carvalho and Prof. Nuno C. Santos. Prof. Filomena Carvalho also performed some experiments, wrote and edited the initial draft of the manuscript. Prof. Carlos Moreira and Prof. José Braz Nogueira provided the samples of essential arterial hypertension patients and all relevant clinical information. All authors revised and improved the manuscript.

I, Filomena A. Carvalho, as co-supervisor of Ana Filipa Guedes and co-corresponding author of the manuscript, hereby declare that the information above is correct.

I, Nuno C. Santos, as supervisor of Ana Filipa Guedes and co-corresponding author of the manuscript, hereby declare that the information above is correct.

Lisbon, April 6, 2018

Ana Filipa Guedes | Filomena A. Carvalho | Nuno C. Santos

Article information **(annexes, article 4, start in page 403)**:

Essential arterial hypertension patients present higher cell adhesion forces, contributing for fibrinogen-dependent cardiovascular risk

Ana F. Guedes[a,#], Filomena A. Carvalho[a,#,*], Carlos Moreira[b], José B. Nogueira[b], Nuno C. Santos[a,*]

Status: Published online on September 4, 2017

***Journal* (year) volume, pages:** *Nanoscale* (2017) 9, 14897-14906

DOI: 10.1039/C7NR03891G

JCR Impact factor 2016, quartile and field: 7.367, Q1 in Nanoscience and Nanotechnology

Essential arterial hypertension patients present higher cell adhesion forces, contributing for fibrinogen-dependent cardiovascular risk

Ana F. Guedes[a,#], Filomena A. Carvalho[a,#,*], Carlos Moreira[b], José B. Nogueira[b], Nuno C. Santos[a,*]

[a]Instituto de Medicina Molecular, Faculdade de Medicina, Universidade de Lisboa, Lisbon, Portugal

[b]Hospital de Santa Maria, Centro Hospitalar Lisboa Norte, Lisbon, Portugal

# - These authors contributed equally for the work.

* - Correspondence should be addressed to:

Filomena A. Carvalho, Instituto de Medicina Molecular, Faculdade de Medicina, Universidade de Lisboa, Av. Prof. Egas Moniz, 1649-028 Lisbon, Portugal; E-mail: filomenacarvalho@fm.ul.pt; Tel.: +351 217999476; Fax: +351 217999477.

Nuno C. Santos, Instituto de Medicina Molecular, Faculdade de Medicina, Universidade de Lisboa, Av. Prof. Egas Moniz, 1649-028 Lisbon, Portugal; E-mail: nsantos@fm.ul.pt; Tel.: +351 217999480; Fax: +351 217999477.

Abstract

The increase of erythrocyte aggregation by high fibrinogen levels may be an indicator of cardiovascular risk. γ' fibrinogen variant has been considered as a possible player on enhancing aggregation. Here, we assessed, at the single-cell level, the influence of fibrinogen on erythrocyte aggregation in essential arterial hypertension. We also aimed at understanding how γ' fibrinogen is altered in this disease. Using atomic force microscopy (AFM), we show that the work and force necessary for erythrocyte-erythrocyte detachment is higher for patients than for healthy donors, with these parameters further increasing in both groups when higher fibrinogen concentrations are present. This can be associated to changes in blood flow, due to transient bridging of two erythrocytes by fibrinogen, representing an important cardiovascular risk factor. γ' fibrinogen can influence the increased risk in essential arterial hypertension, as we demonstrate that its levels are significantly increased in these patients blood. Nevertheless, this cannot be the only cause for the changes observed in the AFM data.

Introduction

Erythrocytes play an important role in blood coagulation by increasing blood viscosity, which is associated with a propensity for clot formation.[1,2] In disease, this increase in viscosity leads to a greater risk of thrombosis.[3] Erythrocytes present surface adhesion receptors[4], contributing to thrombosis in different ways.[5,6] Several of these receptors mediate cell-cell adhesion, both on physiological and pathological conditions. Cell adhesion is involved in different processes such as tethering of a cell, cell-cell communication, tissue formation and aggregation.[7]

Erythrocyte-erythrocyte adhesion leads to erythrocyte aggregation and can cause a wide range of diseases. The established hypothesis for the increase on erythrocyte aggregation associated to cardiovascular pathologies is based on an increase on plasma adhesion proteins concentration, such as fibrinogen.[8,9] Fibrinogen-induced erythrocyte aggregation was often considered to be caused by its nonspecific binding to erythrocyte membrane.[9,10] It is known that platelets have an integrin receptor for fibrinogen in their membrane, the glycoprotein complex $\alpha_{IIb}\beta_3$.[11] Lominadze *et al.* suggested that fibrinogen can specifically interact with erythrocyte membranes.[12] In a previous study, we demonstrated the existence of single-molecule interactions between fibrinogen and a receptor on the erythrocyte membrane, with a relatively lower but comparable affinity relative to platelet binding.[13] The erythrocyte receptor was not as strongly influenced by calcium and eptifibatide (an $\alpha_{IIb}\beta_3$ specific inhibitor) as the platelet receptor.[13] By antibody-inhibition studies, we could identify the receptor on erythrocyte membrane as the $\alpha_v\beta_3$ integrin.[14] Moreover, we recently used atomic force microscopy as a nanotool to evaluate the risk of chronic heart failure (CHF).[14] In that work, we demonstrated that the force necessary to break the bond between fibrinogen and erythrocytes in ischemic CHF patients is stronger than in non-ischemic CHF patients and in healthy donors. Notably, our 12-month clinical follow-up has shown that the CHF patients that presented an higher fibrinogen-erythrocyte binding forces at the initial evaluation had a higher probability of being hospitalized due to cardiovascular disease-associated complications during the following year.[14] These results demonstrate the value of this nanotechnology-based approach for clinical prognosis, indicating the patients with higher risk.

Essential arterial hypertension (EAH) is a clinical complication considered as one of the major risk factors for cardiovascular and cerebrovascular diseases, such as heart failure, heart attack or stroke.[15] Worldwide, 7.6 million premature deaths (about 13.5% of the global total) were attributed to high blood pressure. About 54% of stroke events and 47% of ischemic heart disease were attributable to high blood pressure.[16] According to the European Hypertension Society, patients are considered hypertensive if their blood pressure reach or exceed 140 mmHg of systolic blood pressure (SBP) and/or 90 mmHg of diastolic blood pressure (DBP). The higher the pressure in blood vessels, the harder it is for the heart to properly pump the blood, leading to the increased cardiovascular risk.[17] Actuarial data demonstrated almost a century ago that elevated blood pressure shortened life expectancy[18], despite the rapid expansion of the efforts by the pharmaceutical industry to develop new therapies for hypertension.[17] New strategies to prevent or slow down the onset of hypertension should not be disregarded.[17] Moreover, if the hypertension is detected early, it will be possible to minimize the risk of other cardiovascular disorders.[15]

Elevated plasma fibrinogen level was positively associated with prevalent hypertension, both among men and women, and positively associated with 5-year incident hypertension among men, independently of several other cardiovascular risk factors.[10] It is also well established that total plasma fibrinogen concentration is elevated on patients with cardiovascular diseases.[8,9] In plasma, there is a fibrinogen variant, γ' fibrinogen, that arises from altered splicing of the fibrinogen γ-chain mRNA.[19] Recent studies suggest that γ' fibrinogen is a newly-emerging risk factor for cardiovascular disease.[20-25] Farrell and co-workers developed a new γ' fibrinogen enzyme immunoassay intended to be used as part of risk assessment in adults with suspected risk for cardiovascular diseases.[26,27]

Cell adhesion has been investigated using different techniques[28-30], despite some limitations, such as the absent or limited information on the adhesion strength between cells and substrate.[31-35] Force spectroscopy measurements using an atomic force microscope are capable of resolving individual cell-cell binding events, and have been applied on different cell systems.[36-38] AFM-based single cell force spectroscopy (SCFS) is an ultrasensitive method to quantify adhesion forces of individual cells under physiological conditions.[34,39] In SCFS adhesion measurements, a living cell is first attached

to the tipless AFM cantilever. To facilitate cell immobilization, cantilevers can be coated with different matrix proteins, such as fibronectin or laminin, or with sugar-binding lectins (e.g., concanavalin A (conA)), which provides gentle cell attachment via glycosylated cell surface proteins.[38-40] Then, a single cell is captured, converting this living cell into a probe. The cell attached to the cantilever is then brought into contact with cell attached to the surface and cell-cell contact is maintained under constant contact force for a certain defined dwell time. During subsequent cell retraction, cellular adhesion forces can be measured with high sensitivity from the degree of cantilever deflection, with single-molecule resolution. Force-distance curves are generated and could then provide quantitative information on overall cell adhesion, including the discrimination of a series of small rupture steps.[37,39,41]

To understand the differences between healthy and pathological conditions, it is important to recognize the molecular mechanisms underlying erythrocyte aggregation as a good indicator of cardiovascular risk. With this purpose, here we use AFM single-cell force spectroscopy to quantitatively evaluate erythrocyte adhesion and study the influence of fibrinogen molecules on this binding. We measured these interactions in samples from a group of healthy donors and from patients with EAH. In order to understand how γ' fibrinogen is altered in blood from EAH patients and whether this could be considered a new biomarker for cardiovascular risk, γ' fibrinogen concentration was also quantified.

Methods

Study participants

Twenty-one patients with essential arterial hypertension were enrolled in this study. Patients were stable in ambulatory and with optimized standard medical therapy according to the European Society of Hypertension (ESH) and the European Society of Cardiology (ECS) guidelines.[42] Inclusion criteria for the study were hypertensive patients consecutively examined in the Center of Hypertension of Hospital de Santa Maria (Lisbon, Portugal), medicated with calcium channel blockers (CCB), angiotensin converting enzyme (ACE) inhibitors, angiotensin II receptor blockers (ARB), beta blockers (BB), aspirin and/or statins. Exclusion criteria were severe renal damage (defined as glomerular filtration rate, eGFR, below 30 ml/min), diabetes mellitus type 1 or 2, heart failure with New York Heart Association (NYHA) Functional Classification III or IV, or left ventricular ejection fraction (LVEF) under 40%, liver failure, cancer or other systemic severe diseases. Clinical profiles were thoroughly collected.

A control group of healthy volunteers (n=8 for the AFM studies and n=44 for γ' fibrinogen determination) was also included in this study, following a protocol with Instituto Português do Sangue e Transplantação (IPST, Lisbon, Portugal). Control subjects did not present any known concomitant disease.

Each participant gave informed written consent and all clinical studies have been conducted according to the principles expressed in the Declaration of Helsinki. This study was approved by the joint Ethics Committee of Faculdade de Medicina da Universidade de Lisboa and Centro Hospitalar Lisboa Norte.

Erythrocyte isolation and preparation for AFM

Erythrocytes were isolated as previously described[13,14], using buffered saline glucose citrate (BSGC: 1.6 mM KH_2PO_4, 8.6 mM Na_2HPO_4, 0.12 M NaCl, 13.6 mM sodium citrate and 11.1 mM glucose), pH 7.3, supplemented with 1 mM $CaCl_2$. Erythrocytes (0.1% hematocrit) were attached on a clean poly-L-lysine-coated glass slide. Cells were attached to poly-L-lysine (PLL) treated glass slide after 30 min of deposition, at room temperature. Non-adherent cells were removed by sequential washes with buffer. Samples were

loaded into the AFM and allowed to equilibrate in buffer for 15 min before force spectroscopy measurements. No cell fixation was involved in sample preparation.

Cantilever functionalization

To conduct the AFM cell adhesion assays, tipless silicon nitride cantilevers (Arrow TL2, NanoWorld, Neuchâtel, Switzerland; thickness 1 µm, length 500 µm, width 100 µm and resonance frequency 6 kHz) were functionalized in order to attach one cell to the cantilever. The functionalization of the cantilever is a multi-step procedure. First, the cantilever was activated by UV treatment, for 15 min. Then, the cantilever was immersed in a 0.5 mg/mL biotinylated albumin solution (at 37ºC, overnight), then in 0.5 mg/mL streptavidin (30 min, at room temperature) and, finally, in 0.4 mg/mL biotin-concanavalin A (30 min, at room temperature).[43] Cantilevers were washed with phosphate buffer saline (PBS) between each step of the functionalization process. The cantilevers were kept in PBS to ensure the integrity of the surface treatment until usage. All reagents were purchase from Sigma Aldrich (St. Louis, MO, USA).

AFM measurements of cell-cell adhesion

Experiments were performed on a NanoWizard II atomic force microscope (JPK Instruments, Berlin, Germany) mounted on an Axiovert 200 inverted optical microscope (Zeiss, Jena, Germany). Long range force-spectroscopy was made possible by using the CellHesion module (JPK instruments), with a 100-µm z-range piezoelectric scanner. The objective was mounted with a PIFOC to enable concurrent movement of the objective with the sample holder during force spectroscopy measurements. Concanavalin A-functionalized cantilevers were mounted on the microscope, erythrocytes were injected, and one erythrocyte was captured by positioning the cantilever above the cell center and gently lowering onto the cell for approximately 30 s. The applied force was adjusted to 300 pN before retraction. Data collection for each force-distance cycle was performed at 2 µm/s, with a z-length of 30 µm. Retraction and extension time delays of 5 s were applied.[44] Erythrocyte-erythrocyte adhesion was measured in the presence of different human fibrinogen (Sigma Aldrich) concentrations, up to 1.0 mg/mL (Figure 1). Fibrinogen solutions were allowed to incubate for 15 min before erythrocyte adhesion

measurements. Five force-distance curves were recorded for each erythrocyte on the substrate, and a maximum of 8 different adherent cells on the substrate were tested with the same erythrocyte attached to the AFM cantilever. A total of 40 cells were tested for each experimental condition. Force-distance curves were analyzed using JPK image processing software v. 4.2.61 (JPK Instruments). The values of work correspond to the area under the retraction curve obtained on a force-distance plot. Values of the initial maximum detachment force (by the minimum value of adhesion force) and of two types of events (jumps and membrane tethers) were also obtained after analyzing the cell-cell adhesion retraction curves. We considered a membrane tether as a step in force detected after a force plateau of more than 0.25 µm in distance. Jump events (force plateau of less than 0.25 µm in distance) could be attributed to the breaking of cell-cell interactions without a preceding membrane deformation. Membrane tethers events corresponded to situations where a membrane tether was extruded before the breaking of a connection between surface components of two interacting cells.[44] Work and detachment force data histograms are presented in Supplementary Figures S1 and S2, respectively.

γ' fibrinogen quantification

γ' fibrinogen concentration in human plasma was quantified using a specific two-site sandwich enzyme linked immunosorbent assay immunoassay kit (Gamma Couer ELISA kit, Gamma Therapeutics, Portland, OR, USA). First, a monoclonal anti-γ' fibrinogen antibody, clone 2.G2.H9, specific for the unique carboxyl terminal peptide of the γ' fibrinogen chain, was used as capture antibody. Secondly, an enzyme-labeled polyclonal anti-fibrinogen detection antibody was added, which binds to the captured γ' fibrinogen, forming a detection antibody sandwich. Absorbance of the colored end-product was read at 450 nm on an Infinite M200 microplate reader (Tecan, Männedorf, Switzerland). Plasma samples from EAH patients (n=31) and healthy donors (n=44) were analyzed. Values that fall above the cut-off (>30 mg/dL) were considered as indicative of increased risk of cardiovascular disease and may require further testing for cardiovascular diseases.[26,27]

Statistical analysis

Descriptive statistics were given as mean ± standard error of mean (SEM). For every parameter, all samples were tested against control group. Unpaired Student's *t*-test was used for statistical analysis of intergroup comparison. The nonparametric Mann-Whitney test was used when data do not have a normal distribution. Statistical significance was set at $p<0.05$. Statistical analyses were performed using GraphPad Prism 5.

Results

Cell adhesion experiments

A schematic representation of AFM cell-cell adhesion experiments performed using erythrocyte-functionalized probes and erythrocyte on the substrate is shown in Figure 1. Erythrocytes isolated from blood samples of the patients with essential arterial hypertension and healthy volunteers (control) were tested in the presence of fibrinogen concentrations up to 1.0 mg/mL.

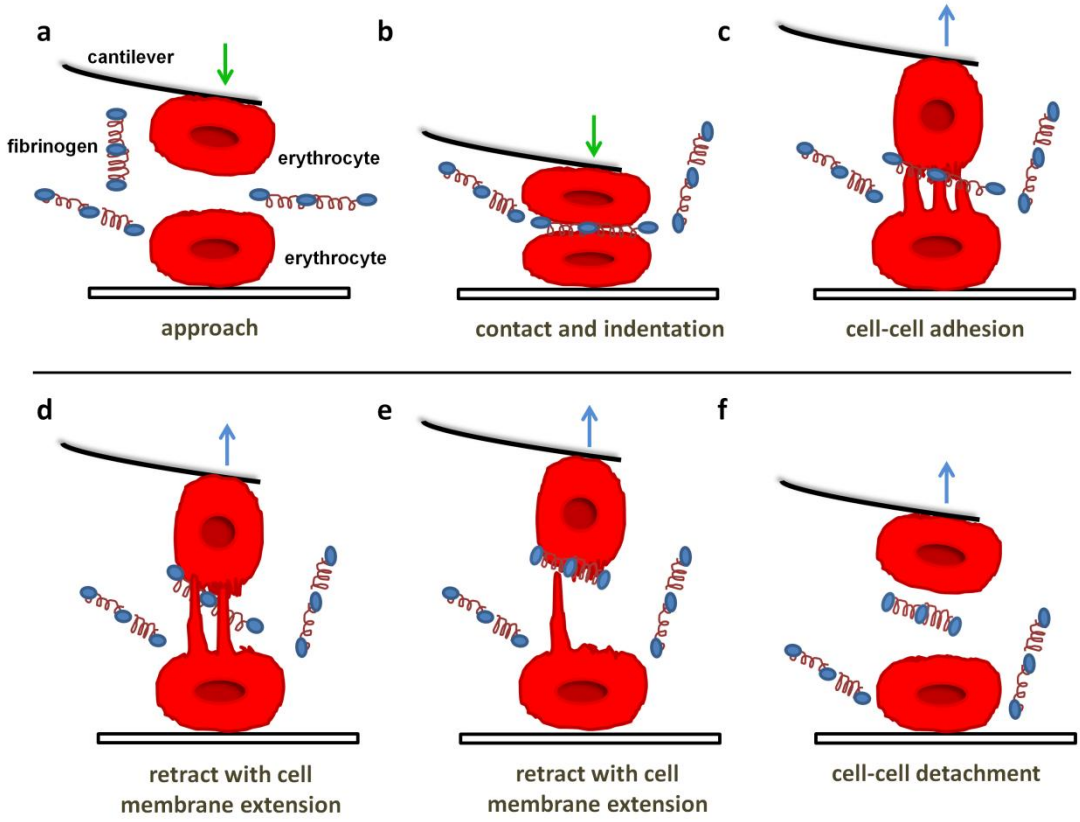

Figure 1 | Schematic representation of the erythrocyte-erythrocyte adhesion experiments using atomic force microscope, done in the presence of fibrinogen. First, the cantilever with an attached erythrocyte is brought into contact with another erythrocyte on the substrate (a), until a certain contact force is reached (b). Afterwards, during retraction, cell-cell adhesion may occur causing the cantilever to adhere to the sample up to a distance beyond the initial contact point (c). When the spring force overcomes the interaction forces, the cantilever pulls of sharply, and different types of

adhesion between both cell surfaces could occur (d and e), before totally breaking contact and completing erythrocyte-erythrocyte detachment (f).

During AFM experiments, it was possible to perform several approach/retract cycles between the erythrocyte attached on the cantilever and erythrocytes on the glass slide. These cycles generate different cell-cell adhesion curves. Two examples of these curves can be seen in Figure 2. Without the presence of fibrinogen, unspecific adhesion between erythrocytes could be observed (Figure 2a). Erythrocytes are non-adherent and very soft cells, with an extremely high capacity to deform. In the cell-cell adhesion experiments, a low retraction velocity of 2 µm/s and a cell-cell contact time of 5 s were used. This constant time is associated with an elastic deformation regime, exponentially increasing viscous creep[45]. As so, in the absence of fibrinogen, cells experienced a viscous drag effect of the aqueous working conditions. If a strong adhesion between both erythrocytes was observed, it would be possible to visualize a step in the force profile of the retraction curve, as those observed in Figure 2b. In Figure 2a, only a slow continuous decrease of the deflection of the cantilever was observed, without any detectable jump in force, until the cantilever reach the zero value of force. The total separation of both erythrocytes occurs at a tip-sample distance of approximately 20 µm. These results may be due to the combination of different forces exerted on the cell: the viscous dragging force, the pulling off of the erythrocyte and the elastic deformation of both erythrocytes.

In the presence of 1 mg/mL fibrinogen, it was possible to observe strong and specific cell-cell interactions (Figure 2b). Different parameters could be extracted by analyzing the retraction curves: the work necessary to detach cells, the maximum detachment force and also two different types of events: jumps and membrane tethers (Figure 2b). Upon closer examination of the cell-cell adhesion curves, it became evident that in the presence of fibrinogen (1 mg/mL), erythrocyte-erythrocyte detachment occurs *via* several rupture events that were not observed in the absence of this plasma protein (Figure 2).

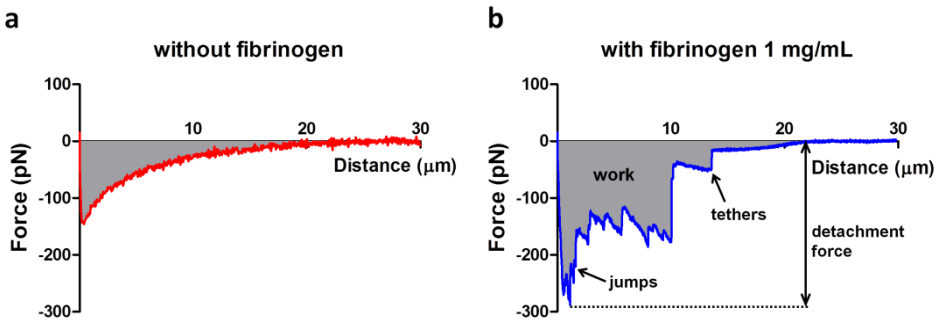

Figure 2 | **Examples of retraction curves acquired during AFM cell-cell adhesion experiments.** Erythrocyte-erythrocyte adhesion without fibrinogen (a) and in the presence of 1 mg/mL fibrinogen (b).

Erythrocytes adhesion is mediated by fibrinogen

To prove the specificity of the binding between two erythrocytes mediated by fibrinogen molecules, three different control experiments were performed: *i)* interaction between tipless cantilever without an erythrocyte attached and an erythrocyte on the substrate; *ii)* interaction between an erythrocyte attached to the cantilever and the poly-L-lysine glass slide (without erythrocytes); and, *iii)* erythrocyte-erythrocyte interaction in the presence of both 1 mg/mL fibrinogen and 4 mM EDTA (as a chelating agent of calcium ions, to inhibit the fibrinogen receptor on erythrocytes[13]). The results extracted from the AFM adhesion data after performing these control experiments are shown in Figure 3.

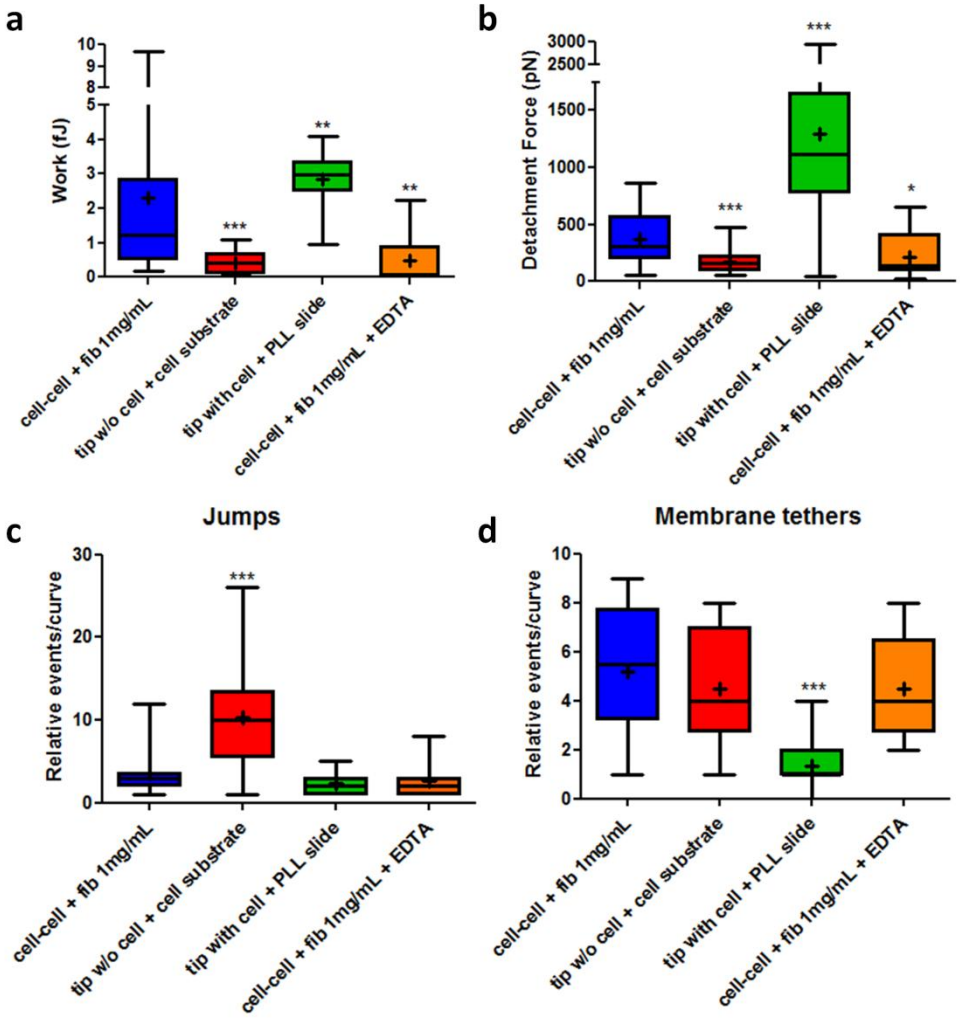

Figure 3 | **AFM data of work (a), detachment force (b), jumps events (c) and membrane tethers (d) of samples and controls.** Comparison of AFM data achieved from the interaction of two erythrocytes in the presence of fibrinogen 1 mg/mL (blue) and 3 different control systems, for the interaction between: *i)* tipless cantilever without an erythrocyte attached and an erythrocyte on the substrate (red); *ii)* an erythrocyte attached on the cantilever and the PLL glass slide without erythrocytes (green); and, *iii)* erythrocyte-erythrocyte interaction in the presence of 1 mg/mL fibrinogen and 4 mM EDTA (orange). Values are presented as box with median value and 1st and 3rd quartiles, and whiskers with maximum and minimum values. The mean value is presented as '+'. The relative events/curve are given by the ratio between the total number of jump (c) or membrane tether (d) events per the total number of force-adhesion curves. Statistical values: (a) *** p<0.0001, ** $p \leq 0.0038$; (b) *** p<0.0002, * p=0.0407; (c) *** p<0.0001; (d) *** p<0.0001.

Analyzing the results achieved with control experiments, a decrease in the work and maximum force necessary to detach the cantilever-substrate system was observed. This situation occurred when the experiments were performed with a cantilever without an erythrocyte (p<0.0001) and for the erythrocyte-erythrocyte interaction in the presence of EDTA (p=0.002). As expected, the force necessary to overcome the binding between an erythrocyte attached to the cantilever and PLL glass slide is higher than for the erythrocyte-erythrocyte interaction in the presence of fibrinogen (p=0.0038). PLL is usually used to facilitate the attachment of cells and proteins to solid surfaces in biological applications. This cationic substrate strongly interacts with the negatively charged surface of the erythrocytes.[46] These strong erythrocyte-PLL interactions were observed also by detachment force data (Figure 3b, p<0.0001). As all experiments were conducted in an AFM coupled with an inverted fluorescence microscope connected to a CCD camera, interactions between the cell attached to the cantilever and the PLL substrate were avoided on all cell-cell interaction experiments. To guarantee this, the cantilever (with an erythrocyte) was mechanically and optically placed on top of an erythrocyte on the substrate each measurement. After performing these three types of control experiments, we could demonstrate the specificity of the interaction between two erythrocytes in the presence of fibrinogen molecules and apply the same procedure to blood samples from EAH patients.

EAH patients present stronger erythrocyte-erythrocyte adhesion

Figure 4a shows that the work necessary to detach two erythrocytes, either from healthy donors or EAH patients, was significantly higher in the presence of increasing fibrinogen concentrations (from 0.4 to 1 mg/mL) than on its absence (p<0.0001). Moreover, in the absence of fibrinogen, the work necessary to detach two erythrocytes from EAH patients was significantly higher than for erythrocytes isolated from healthy donors (1.45 ± 0.06 fJ for EAH patients *vs.* 0.48 ± 0.04 fJ for healthy donors; p<0.0001). In all fibrinogen concentrations tested, higher forces (and work) were needed to overcome erythrocyte-erythrocyte adhesion for EAH patients than for healthy donors (Figure 4a), although statistically significant differences were only observed in the presence of 0.7

mg/mL fibrinogen (3.13 ± 0.16 fJ for EAH patients *vs.* 2.10 ± 0.31 fJ for healthy donors; *p*=0.022).

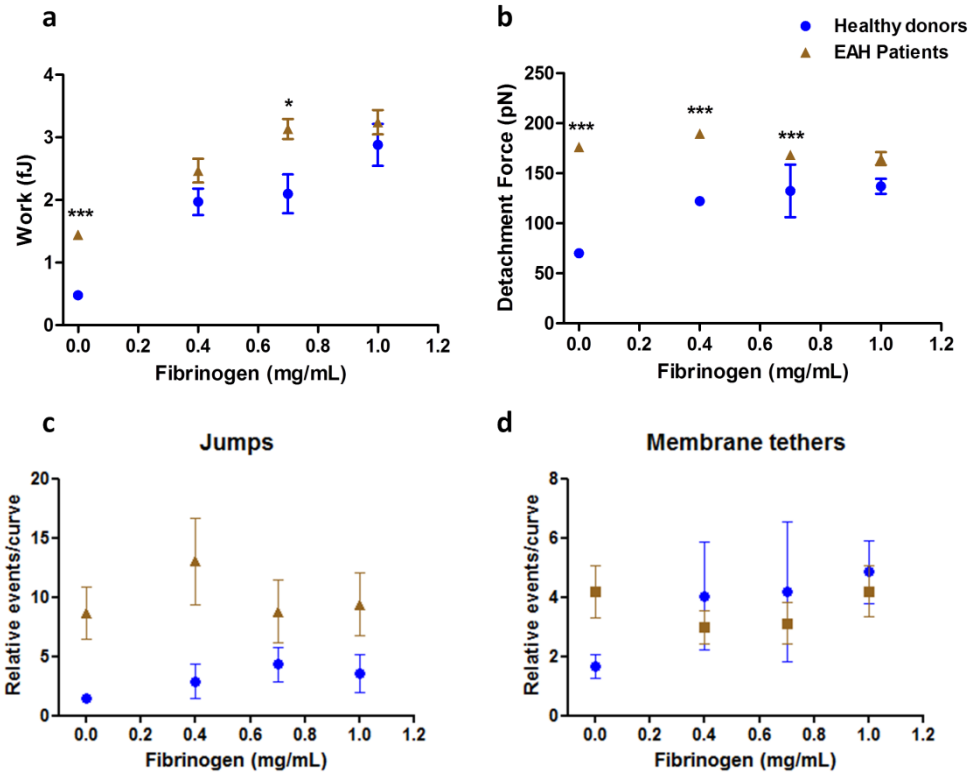

Figure 4 | AFM data of work (a), detachment force (b), jumps events (c) and membrane tethers (d) from blood samples of healthy donors (n=8) and EAH patients (n=21). Comparison of AFM data achieved from the interaction of two erythrocytes in the absence or in the presence of increasing fibrinogen concentrations (from 0.4 to 1 mg/mL), for healthy donors (blue) and EAH patients (brown). Values are presented as mean ± SEM. Histograms are presented on Supplementary Figures S1 and S2. The relative events/curve is given by the ratio between the total number of jump (c) or membrane tether (d) events per the total number of force-adhesion curves. (a) *** $p<0.0001$, * $p=0.022$; (b) *** $p\leq0.0007$.

The maximum detachment force required to separate the cantilever-bound erythrocyte from the erythrocyte at the surface of the glass slide was also determined directly from each force-distance curve (Figure 2b). Similarly to the values of work, the maximum detachment force necessary to detach two erythrocytes in the absence of

fibrinogen is higher for EAH patients than for healthy donors (p<0.0001). Higher detachment forces data for EAH patients were also observed in the presence of 0.4 mg/mL (p<0.0001) and 0.7 mg/mL (p=0.0007) fibrinogen (Figure 4b).

For healthy donors, upon increasing fibrinogen concentrations, the erythrocyte-erythrocyte binding force also increased. These variations were statistically significant for all fibrinogen concentrations tested (p<0.0001 at 0.4 and 1.0 mg/mL; p=0.0002 at 0.7 mg/mL). Regarding EAH patients, the same fibrinogen concentration dependence of erythrocyte-erythrocyte binding forces did not occur. Despite the statistically significant differences between detachment forces of EAH patients erythrocytes in the presence of fibrinogen 0.4 and 0.7 mg/mL and in their absence, only small differences were observed (Figure 4b).

Looking at the force retract curve (Figure 2b), an initial unbinding event is followed by a number of smaller force steps, which could be distinguished and analyzed as jumps events and membrane tethers. Comparing jumps events for both study groups (Figure 4c), one may notice that EAH patients present more frequent events per curve than healthy donors, either in the absence or in the presence of fibrinogen. A 2 to 5-fold increase in the number of jump events was observed for erythrocytes from EAH patients. Regarding membrane tethers (Figure 4d), the same difference could not be observed. Only in the absence of fibrinogen, a 2.5-fold increase in the number of membrane tethers/curve could be seen for the erythrocytes from EAH patients. When fibrinogen was added, approximately the same number of membrane tethers/curve was detectable in erythrocytes from EAH patients and healthy donors.

EAH patients have higher levels of γ' fibrinogen

In parallel with the AFM experiments, the levels of total fibrinogen and γ' fibrinogen variant were quantified in plasma from EAH patients (Figure 5). EAH patients presented higher total plasma fibrinogen (3.02 ± 0.18 mg/mL *vs.* 2.43 ± 0.11 mg/mL; p=0.0034) and γ' fibrinogen levels (0.43 ± 0.02 mg/mL *vs.* 0.33 ± 0.02 mg/mL; p=0.0003) than healthy donors. Despite the fact that the total fibrinogen concentrations determined for the patients are significantly higher than those from healthy donors, both groups presented values within the normal range for this parameter (1.5-3.5 g/L[47]). As for γ' fibrinogen

concentration, values above a cut-off of approximately 0.3 mg/mL have been referred as indicative of increased risk of cardiovascular diseases.[27] Our results show that EAH patients present γ' fibrinogen concentrations above this cut-off, and that those concentrations are significantly higher than those determined for the healthy donors. However, the ratio between γ' fibrinogen and the total plasma fibrinogen was not statistically different among EAH patients and healthy donors.

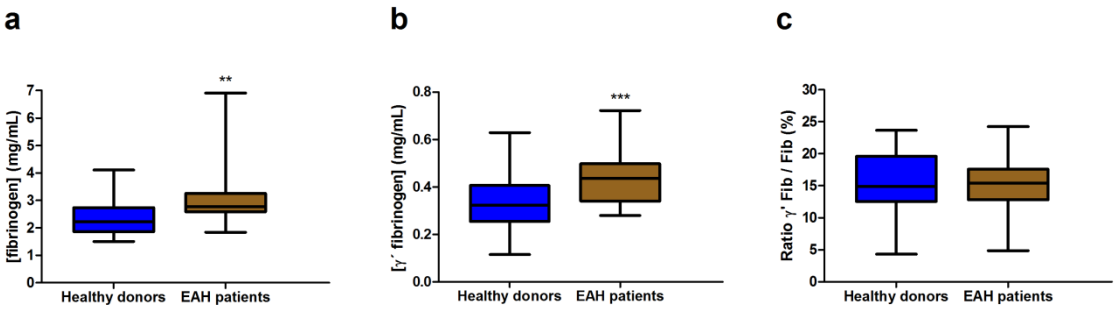

Figure 5 | Total plasma fibrinogen (a) and γ' fibrinogen (b) concentrations, as well as the ratio between both parameters (c), for EAH patients (n=31) and healthy blood donors (n=44). Values are presented as box with median value and 1st and 3rd quartiles, and whiskers with maximum and minimum values. (a) ** p=0.0034; (b) *** p=0.0003.

Discussion

The present work shows for the first time that the erythrocyte-erythrocyte interaction in the presence of fibrinogen, characterized here by AFM-based force spectroscopy, is modified in essential arterial hypertension patients. AFM cell-cell adhesion measurements were used to assess the interactions between an erythrocyte attached to the AFM cantilever and erythrocytes on the substrate. This is also a good example of application of AFM as a versatile tool to quantify cell adhesion under near-physiological conditions, from the cellular level down to the contribution of single molecules, opening new possibilities in terms of nanodiagnostics and optimized therapeutics. In previous studies, Puech *et al*. also showed that an atomic force microscope with an extended pulling range is a powerful tool to study multiple features of melanoma disease progression.[38] Friedrichs *et al*. considered that this technique allows to obtain a large amount of essential cell biological and biophysical information that will contribute to different biomedical and material applications.[34] We previously reported the use of AFM to study the broad effect of azurin at the cancer cell surface level.[48] In another study, using different AFM modes, we showed that P-cadherin and Src family kinase signaling induce changes in the morphological and viscoelastic properties of breast cancer cells. These cells also revealed differences on their biomechanical cell-cell adhesion, which are associated with a more invasive breast cancer cell phenotype.[44]

In order to prove the specificity of the erythrocyte-fibrinogen-erythrocyte binding under evaluation, different control experiments were performed. From these experiments (Figure 3), we could conclude that the interaction between two erythrocytes in the presence of fibrinogen molecules is specific, validating the subsequent measurements. The analysis of the unbinding events from the cell-cell force-distance curves helped us to characterize the strength of single bonds, as well as other erythrocyte properties. The extended effective pulling range of the instrument enabled the detection of unbinding forces associated with short-range unspecific interactions, up to specific jumps and membrane tethers associated interactions.

AFM data showed that higher work and forces had to be applied to completely detach two erythrocytes from EAH patients, when compared with cells from healthy

donors, both in the absence or in the presence of fibrinogen molecules in solution. With the increasing of fibrinogen levels, the work and the maximum force necessary to detach two erythrocytes increased in both groups.

The differences obtained between the values of work necessary to detach two erythrocytes from EAH patients, or from healthy donors, in the absence of fibrinogen should not be due to the presence of fibrinogen molecules coming from the plasma. Several centrifugation and washing cycles were performed before the use of the erythrocytes on the experiments. Some fibrinogen molecules may be attached to the erythrocytes surface even at 0 mg/mL of fibrinogen, but their amount should be considered as neglectable. The stronger erythrocyte-erythrocyte adhesion observed may be due to changes in the EAH erythrocytes' membrane lipid composition and/or its membrane charge associated to the pathological condition, which could facilitate erythrocyte-erythrocyte adhesion.

AFM also provided quantitative information on a series of small rupture steps, namely, jumps and membrane tethers. From the results it is clear that the relative events per curve for jumps and membrane tethers were higher in EAH patients compared to healthy volunteers. This fact is more pronounced for the number of jump events and not for membrane tethers. Thus, it seems that the main contributor for the increase of the binding between two erythrocytes from EAH patients is the interactions between fibrinogen molecules and its specific $\alpha_v\beta_3$ integrin membrane receptor. This conclusion could be extracted from the number of jumps events on the force-distance retract curves (Figure 2b).

In our previous work, using also AFM but not at the level of the evaluation of cell-cell interactions, we measured the binding between fibrinogen molecules covalently attached to the AFM tip and erythrocytes from heart failure patients.[14] We demonstrated that the interaction between fibrinogen and erythrocytes is strong in these patients. Importantly, based on a 12-month clinical follow-up, we have shown that patients with higher fibrinogen-erythrocyte (un)binding forces at the initial AFM evaluation had a higher probability of being hospitalized due to cardiovascular complications in the following year.

In the present study, the fact that erythrocytes from EAH patients presented higher cell-cell adhesion in the presence of fibrinogen than those from healthy donors could be

associated with an increase of erythrocyte aggregation in these patients. Considering that erythrocyte aggregation is an important cardiovascular risk factor associated to the pathological condition[49], fibrinogen "bridging" between two erythrocytes may be considered as a key aspect for this aggregation and, therefore, to the higher cardiovascular risk in EAH patients. Moreover, and having in mind our previous results[14], AFM could be an important technique to better define the cardiovascular risk and facilitate the clinical prognosis for patients with cardiovascular diseases.

Different studies reported that elevated plasma fibrin(ogen) levels significantly increases the cardiovascular risk.[50-52] For this reason, simultaneously with the AFM studies, we quantified the levels of total fibrinogen and of the γ' fibrinogen variant in the plasma from EAH patients. This quantification was performed to understand how and what type of fibrinogen molecules may lead to an increase of erythrocyte-erythrocyte binding in EAH patients. From the results, it was found that γ' fibrinogen levels were higher in EAH patients than in healthy donors. The values obtained for EAH patients were above the cut-off value of 0.3 mg/mL, considered to be indicative of an increased cardiovascular risk.[26,27] Moreover the increase of γ' fibrinogen concentration was not dependent of the total plasma fibrinogen levels. Our results are in accordance with those of Lovely *et al*., who indicated that a raise in γ' fibrinogen concentration was associated with an increased risk of coronary artery disease, independently of the total plasma fibrinogen concentration.[23] On the other hand, Mannila *et al*. showed that plasma γ' fibrinogen concentration influences the risk of myocardial infarction, and this relationship seems to be strengthened by the presence of an elevated total plasma fibrinogen concentration.[25] The ratio between γ' fibrinogen (γA/γ' and γ'/γ') concentrations has been associated to atherothrombotic disease.[23,25] We expect that our present results may help to clarify and move further on the impact of γ' fibrinogen on cardiovascular diseases, contributing to establish it as a new biomarker for cardiovascular risk. It should be highlighted that an accurate evaluation of the clinical prognosis of EAH patients should not depend only on the quantification of γ' fibrinogen and/or of the characterization of erythrocyte-erythrocyte interactions. This information should be considered together with current state-of-the-art tests and clinical information available, in order to pinpoint patients at higher risk, enabling therapy optimization in order to prevent serious cardiovascular events.

The fact that erythrocytes from EAH patients in the presence of fibrinogen adhere more than those from healthy blood donors may be expected to lead to changes in the whole blood flow. At the cellular level, this could be due to the formation of a bridge of fibrinogen molecule(s) in between two erythrocytes, forming an erythrocyte-fibrinogen-erythrocyte transient complex. This could lead to higher erythrocyte aggregation, which could represent an important risk factor for developing cardiovascular pathologies. A continued research into the erythrocyte aggregation as a determinant for cardiovascular risk is still necessary, with a particular emphasis on the discovery strategies to condition the fibrinogen-erythrocyte interactions, especially those evolving γ' fibrinogen, or on the development of therapeutic strategies to specifically decrease the levels of this fibrinogen variant. These strategies could have a high impact on the reduction or prevention of cardiovascular pathologies.

Acknowledgments

This work was supported by Fundação para a Ciência e a Tecnologia – Ministério da Ciência, Tecnologia e Ensino Superior (FCT-MCTES, Portugal) grants PTDC/QUI-BIQ/119509/2010 and PTDC/BBB-BMD/6307/2014, as well as the fellowship SFRH/BD/84414/2012 to AFG.

Author contributions

A.F.G. performed part of the experiments, analyzed the data, performed the statistical analysis, wrote and edited the draft of the manuscript and prepared it for submission; **F.A.C.** performed part of the experiments, analyzed the data, wrote and edited the manuscript; **C.S.M.** collected all clinical data, performed clinical evaluation, contributed to relevant discussion and participated on the writing of the manuscript; **J.B.N.** contributed to the discussion section and participated on the writing of the manuscript; and, **N.C.S.** conceived the idea, designed and directed the experiments and participated on the writing of the manuscript.

Competing Financial Interests statement

Authors declare no competing financial interests.

References of Chapter VII

1. Wohner, N. Role of cellular elements in thrombus formation and dissolution. *Cardiovasc Hematol Agents Med Chem* **6**, 224-8 (2008).
2. Zannad, F. & Stoltz, J.F. Blood rheology in arterial hypertension. *J Hypertens Suppl* **10**, S69-78 (1992).
3. Landolfi, R., Rocca, B. & Patrono, C. Bleeding and thrombosis in myeloproliferative disorders: mechanisms and treatment. *Crit Rev Oncol Hematol* **20**, 203-22 (1995).
4. Telen, M.J. Red blood cell surface adhesion molecules: their possible roles in normal human physiology and disease. *Semin Hematol* **37**, 130-42 (2000).
5. Peyrou, V., Lormeau, J.C., Herault, J.P., Gaich, C., Pfliegger, A.M. & Herbert, J.M. Contribution of erythrocytes to thrombin generation in whole blood. *Thromb Haemost* **81**, 400-6 (1999).
6. Whelihan, M.F., Zachary, V., Orfeo, T. & Mann, K.G. Prothrombin activation in blood coagulation: the erythrocyte contribution to thrombin generation. *Blood* **120**, 3837-45 (2012).
7. Juliano, R.L. Signal transduction by cell adhesion receptors and the cytoskeleton: functions of integrins, cadherins, selectins, and immunoglobulin-superfamily members. *Annu Rev Pharmacol Toxicol* **42**, 283-323 (2002).
8. Lominadze, D. & Dean, W.L. Involvement of fibrinogen specific binding in erythrocyte aggregation. *FEBS Lett* **517**, 41-4 (2002).
9. Maeda, N., Seike, M., Kume, S., Takaku, T. & Shiga, T. Fibrinogen-induced erythrocyte aggregation: erythrocyte-binding site in the fibrinogen molecule. *Biochim Biophys Acta* **904**, 81-91 (1987).
10. Shankar, A., Wang, J.J., Rochtchina, E. & Mitchell, P. Positive association between plasma fibrinogen level and incident hypertension among men: population-based cohort study. *Hypertension* **48**, 1043-9 (2006).
11. Jennings, L.K. & Phillips, D.R. Purification of glycoproteins IIb and III from human platelet plasma membranes and characterization of a calcium-dependent glycoprotein IIb-III complex. *J Biol Chem* **257**, 10458-66 (1982).

12. Lominadze, D., Schuschke, D.A., Joshua, I.G. & Dean, W.L. Increased ability of erythrocytes to aggregate in spontaneously hypertensive rats. *Clin Exp Hypertens* **24**, 397-406 (2002).
13. Carvalho, F.A., Connell, S., Miltenberger-Miltenyi, G., Pereira, S.V., Tavares, A., Ariëns, R.A. & Santos, N.C. Atomic force microscopy-based molecular recognition of a fibrinogen receptor on human erythrocytes. *ACS Nano* **4**, 4609-20 (2010).
14. Guedes, A.F., Carvalho, F.A., Malho, I., Lousada, N., Sargento, L. & Santos, N.C. Atomic force microscopy as a tool to evaluate the risk of cardiovascular diseases in patients. *Nat Nanotechnol* **11**, 687-92 (2016).
15. WHO. Global brief on hypertension (2013). http://www.who.int/cardiovascular_diseases/publications/global_brief_hypertension/en/
16. Lawes, C.M., Vander Hoorn, S., Rodgers, A. & International Society of, H. Global burden of blood-pressure-related disease, 2001. *Lancet* **371**, 1513-8 (2008).
17. Chobanian, A.V. Guidelines for the Management of Hypertension. *Med Clin North Am* **101**, 219-227 (2017).
18. Hunter, A. Mortality study of impaired lives. *Actuarial Soc* **24**, 338 (1923).
19. Chung, D.W. & Davie, E.W. gamma and gamma' chains of human fibrinogen are produced by alternative mRNA processing. *Biochemistry* **23**, 4232-6 (1984).
20. Cheung, E.Y., Uitte de Willige, S., Vos, H.L., Leebeek, F.W., Dippel, D.W., Bertina, R.M. & de Maat, M.P. Fibrinogen gamma' in ischemic stroke: a case-control study. *Stroke* **39**, 1033-5 (2008).
21. Cheung, E.Y., Vos, H.L., Kruip, M.J., den Hertog, H.M., Jukema, J.W. & de Maat, M.P. Elevated fibrinogen gamma' ratio is associated with cardiovascular diseases and acute phase reaction but not with clinical outcome. *Blood* **114**, 4603-4 (2009).
22. Drouet, L., Paolucci, F., Pasqualini, N., Laprade, M., Ripoll, L., Mazoyer, E., Bal dit Sollier, C. & Vanhove, N. Plasma gamma'/gamma fibrinogen ratio, a marker of arterial thrombotic activity: a new potential cardiovascular risk factor? *Blood Coagul Fibrinolysis* **10**, S35-9 (1999).
23. Lovely, R.S., Falls, L.A., Al-Mondhiry, H.A., Chambers, C.E., Sexton, G.J., Ni, H. & Farrell, D.H. Association of gammaA/gamma' fibrinogen levels and coronary artery disease. *Thromb Haemost* **88**, 26-31 (2002).

24. Macrae, F.L., Domingues, M.M., Casini, A. & Ariëns, R.A. The (Patho)physiology of Fibrinogen gamma'. *Semin Thromb Hemost* **42**, 344-55 (2016).
25. Mannila, M.N., Lovely, R.S., Kazmierczak, S.C., Eriksson, P., Samnegard, A., Farrell, D.H., Hamsten, A. & Silveira, A. Elevated plasma fibrinogen gamma' concentration is associated with myocardial infarction: effects of variation in fibrinogen genes and environmental factors. *J Thromb Haemost* **5**, 766-73 (2007).
26. Alexander, K.S., Madden, T.E. & Farrell, D.H. Association between gamma' fibrinogen levels and inflammation. *Thromb Haemost* **105**, 605-9 (2011).
27. Lovely, R.S., Kazmierczak, S.C., Massaro, J.M., D'Agostino, R.B., O'Donnell, C.J. & Farrell, D.H. Gamma' fibrinogen: evaluation of a new assay for study of associations with cardiovascular disease. *Clin Chem* **56**, 781-8 (2010).
28. Dai, J. & Sheetz, M.P. Mechanical properties of neuronal growth cone membranes studied by tether formation with laser optical tweezers. *Biophys J* **68**, 988-96 (1995).
29. Kuo, S.C., Hammer, D.A. & Lauffenburger, D.A. Simulation of detachment of specifically bound particles from surfaces by shear flow. *Biophys J* **73**, 517-31 (1997).
30. Thie, M., Harrach-Ruprecht, B., Sauer, H., Fuchs, P., Albers, A. & Denker, H.W. Cell adhesion to the apical pole of epithelium: a function of cell polarity. *Eur J Cell Biol* **66**, 180-91 (1995).
31. Burton, K. & Taylor, D.L. Traction forces of cytokinesis measured with optically modified elastic substrata. *Nature* **385**, 450-4 (1997).
32. Lee, J., Leonard, M., Oliver, T., Ishihara, A. & Jacobson, K. Traction forces generated by locomoting keratocytes. *J Cell Biol* **127**, 1957-64 (1994).
33. Oliver, T., Jacobson, K. & Dembo, M. Design and use of substrata to measure traction forces exerted by cultured cells. *Methods Enzymol* **298**, 497-521 (1998).
34. Friedrichs, J., Legate, K.R., Schubert, R., Bharadwaj, M., Werner, C., Muller, D.J. & Benoit, M. A practical guide to quantify cell adhesion using single-cell force spectroscopy. *Methods* **60**, 169-78 (2013).
35. Taubenberger, A., Cisneros, D.A., Friedrichs, J., Puech, P.H., Muller, D.J. & Franz, C.M. Revealing early steps of alpha2beta1 integrin-mediated adhesion to collagen type I by using single-cell force spectroscopy. *Mol Biol Cell* **18**, 1634-44 (2007).

36. Clausen-Schaumann, H., Seitz, M., Krautbauer, R. & Gaub, H.E. Force spectroscopy with single bio-molecules. *Curr Opin Chem Biol* **4**, 524-30 (2000).

37. Kashef, J. & Franz, C.M. Quantitative methods for analyzing cell-cell adhesion in development. *Dev Biol* **401**, 165-74 (2015).

38. Puech, P.H., Poole, K., Knebel, D. & Muller, D.J. A new technical approach to quantify cell-cell adhesion forces by AFM. *Ultramicroscopy* **106**, 637-44 (2006).

39. Benoit, M., Gabriel, D., Gerisch, G. & Gaub, H.E. Discrete interactions in cell adhesion measured by single-molecule force spectroscopy. *Nat Cell Biol* **2**, 313-7 (2000).

40. Helenius, J., Heisenberg, C.P., Gaub, H.E. & Muller, D.J. Single-cell force spectroscopy. *J Cell Sci* **121**, 1785-91 (2008).

41. Panorchan, P., Thompson, M.S., Davis, K.J., Tseng, Y., Konstantopoulos, K. & Wirtz, D. Single-molecule analysis of cadherin-mediated cell-cell adhesion. *J Cell Sci* **119**, 66-74 (2006).

42. Mancia, G., Fagard, R., Narkiewicz, K., Redon, J., Zanchetti, A., Bohm, M., Christiaens, T., Cifkova, R., De Backer, G., Dominiczak, A., Galderisi, M., Grobbee, D.E., Jaarsma, T., Kirchhof, P., Kjeldsen, S.E., Laurent, S., Manolis, A.J., Nilsson, P.M., Ruilope, L.M., Schmieder, R.E., Sirnes, P.A., Sleight, P., Viigimaa, M., Waeber, B. & Zannad, F. 2013 ESH/ESC Practice Guidelines for the Management of Arterial Hypertension. *Blood Press* **23**, 3-16 (2014).

43. Friedrichs, J., Helenius, J. & Muller, D.J. Quantifying cellular adhesion to extracellular matrix components by single-cell force spectroscopy. *Nat Protoc* **5**, 1353-61 (2010).

44. Ribeiro, A.S., Carvalho, F.A., Figueiredo, J., Carvalho, R., Mestre, T., Monteiro, J., Guedes, A.F., Fonseca, M., Sanches, J., Seruca, R., Santos, N.C. & Paredes, J. Atomic force microscopy and graph analysis to study the P-cadherin/SFK mechanotransduction signalling in breast cancer cells. *Nanoscale* **8**, 19390-19401 (2016).

45. Haase, K. & Pelling, A.E. Investigating cell mechanics with atomic force microscopy. *J R Soc Interface* **12**, 20140970 (2015).

46. Carvalho, F.A., de Oliveira, S., Freitas, T., Gonçalves, S. & Santos, N.C. Variations on fibrinogen-erythrocyte interactions during cell aging. *PLoS One* **6**, e18167 (2011).

47. Oswald, M.W., Hunt, H.H. & Lazarchick, J. Normal range of plasma fibrinogen. *Am J Med Technol* **49**, 57-9 (1983).

48. Bernardes, N., Abreu, S., Carvalho, F.A., Fernandes, F., Santos, N.C. & Fialho, A.M. Modulation of membrane properties of lung cancer cells by azurin enhances the sensitivity to EGFR-targeted therapy and decreased beta1 integrin-mediated adhesion. *Cell Cycle* **15**, 1415-24 (2016).

49. Sloop, G.D., Bialczak, J.K., Weidman, J.J. & St Cyr, J.A. Uric acid increases erythrocyte aggregation: Implications for cardiovascular disease. *Clin Hemorheol Microcirc* **63** 349-359 (2015).

50. Aleman, M.M., Walton, B.L., Byrnes, J.R. & Wolberg, A.S. Fibrinogen and red blood cells in venous thrombosis. *Thromb Res* **133**, S38-40 (2014).

51. van Hylckama Vlieg, A. & Rosendaal, F.R. High levels of fibrinogen are associated with the risk of deep venous thrombosis mainly in the elderly. *J Thromb Haemost* **1**, 2677-8 (2003).

52. Machlus, K.R., Cardenas, J.C., Church, F.C. & Wolberg, A.S. Causal relationship between hyperfibrinogenemia, thrombosis, and resistance to thrombolysis in mice. *Blood* **117**, 4953-63 (2011).

Supplementary information of Chapter VII

Essential arterial hypertension patients present higher cell adhesion forces, contributing for fibrinogen-dependent cardiovascular risk

Ana F. Guedes[a,#], Filomena A. Carvalho[a,#,*], Carlos Moreira[b], José B. Nogueira[b], Nuno C. Santos[a,*]

[a]Instituto de Medicina Molecular, Faculdade de Medicina, Universidade de Lisboa, Lisboa, Portugal

[b]Hospital de Santa Maria, Centro Hospitalar Lisboa Norte, Lisboa, Portugal

Supplementary Results

AFM cell-cell adhesion

To better understand the shape of the distribution of the values of work and detachment force of the adhesion between two erythrocytes, histograms of both parameters were build up (Supplementary Figures S1 and S2). Comparisons between the histograms of the adhesion of erythrocytes from EAH patients *vs.* healthy donors, in the absence or in the presence of fibrinogen, were performed. The work and maximum force required to detach two erythrocytes from essential arterial hypertension (EAH) patients were higher than for healthy donors, at each fibrinogen concentration (from 0 to 1 mg/mL).

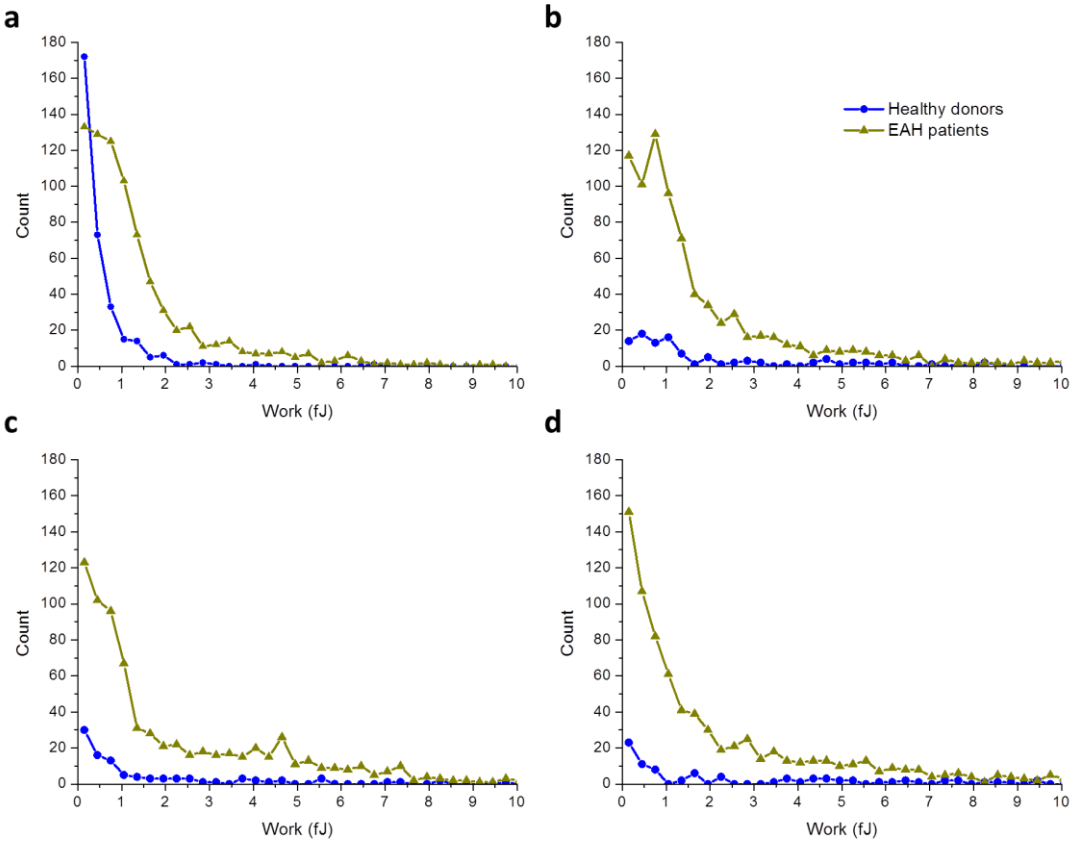

Supplementary Figure S1 | Histograms of the work necessary to detach two erythrocytes on AFM cell-cell adhesion measurements. Data obtained with erythrocytes isolated from healthy donors (blue) and EAH patients (olive) for each studied condition:

(a) without fibrinogen; (b) with 0.4 mg/mL fibrinogen; (c) with 0.7 mg/mL fibrinogen; and, (d) with 1 mg/mL fibrinogen.

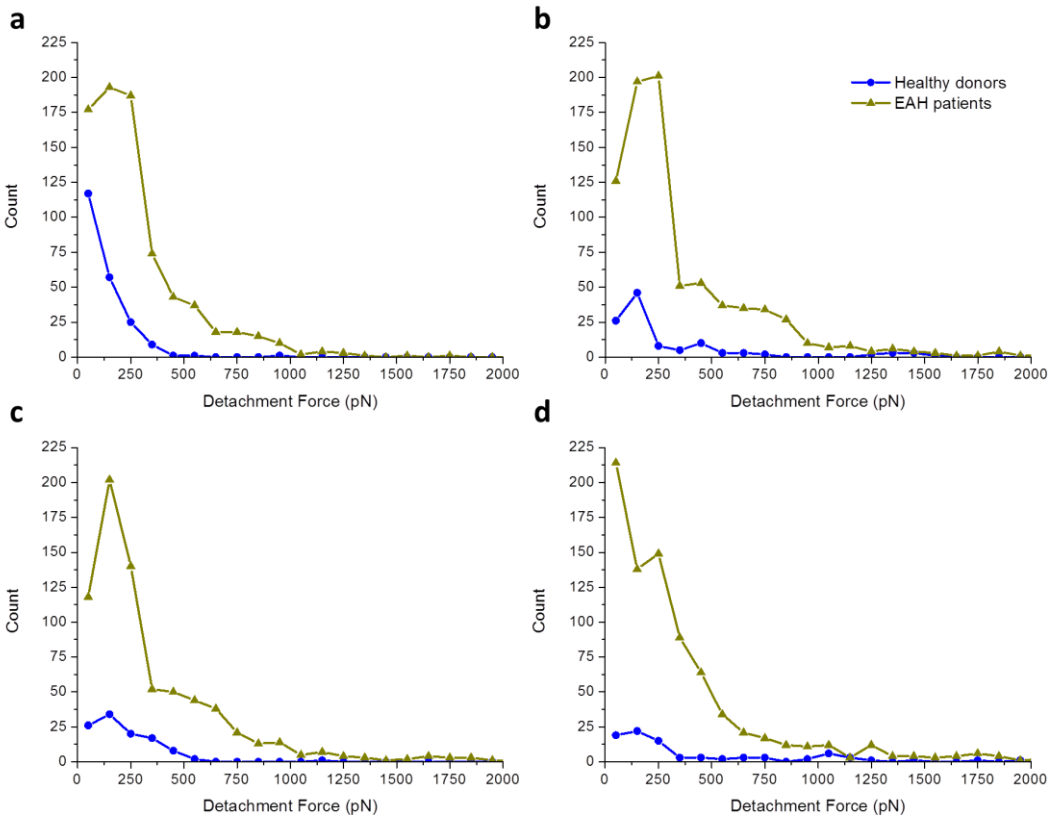

Supplementary Figure S2 | **Histograms of the maximum force necessary to detach two erythrocytes on AFM cell-cell adhesion measurements.** Data obtained with erythrocytes isolated from healthy donors (blue) and EAH patients (olive) for each studied condition: (a) without fibrinogen; (b) with 0.4 mg/mL fibrinogen; (c) with 0.7 mg/mL fibrinogen; and, (d) with 1 mg/mL fibrinogen.

Chapter VIII ▫

Adhesion of erythrocytes in stroke disease

Preliminary results

Overview

This Chapter encompasses mainly the investigating of the adhesion of erythrocytes in the presence of fibrinogen molecules in a cerebrovascular pathology. After the previous studies in other cardiovascular diseases, we proposed to study the fibrinogen-erythrocyte interactions and the cell-cell adhesion in stroke patients. Hemoreological parameters evaluation and γ' fibrinogen quantification were also conducted for these patients. As one of the most common causes of death, stroke has been considered to have different risks factors, including the high levels of fibrinogen in plasma. For this reason, we wanted to understand the influence of fibrinogen on erythrocytes adhesion in stroke patients, trying to reveal how this interaction could be an important risk factor of a worse clinical prognosis and to be considered in future clinical routine. This work is ongoing in the Lab in collaboration with Prof. Ana Catarina Fonseca, from Department of Neurology, Hospital de Santa Maria, Centro Hospitalar Lisboa Norte. At the time of the writing of this Thesis, a low number of samples has already been analyzed. It is our priority to enlarge the number of patients analyzed to be more confident on the results and conclusions before submitting the work for publication. Nevertheless, some important results were already obtained. The preliminary results showed that fibrinogen-erythrocyte binding seems to be stronger in stroke patients than in healthy donors, pointing to this protein-cell interaction to be a new cerebrovascular risk factor for the disease. Even without circulating fibrinogen molecules, the erythrocytes from patients adhere more to each other than those from healthy donors.

This work has been performed in Instituto de Medicina Molecular, Faculdade de Medicina, Universidade de Lisboa but also at Hospital Santa Maria, Centro Hospitalar Lisboa Norte.

Erythrocyte-erythrocyte adhesion in the of presence of fibrinogen on stroke

Introduction

The world is facing a stroke epidemic [1]. Globally, stroke has been identified as the second main cause of death above the age of 60 years, and the fifth leading cause of death in people aged 15 to 59 years old [2]. This debilitating event is increasingly becoming a major public health problem, leading to nearly double death by 2030 [3]. In the past decade, the definition of stroke has been revised and major advances have been made for its treatment and prevention [1]. An updated definition of this disease is an acute episode of focal dysfunction of the brain, retina or spinal cord lasting longer than 24 h, or of any duration if imaging or autopsy show focal infarction or hemorrhage relevant to the symptoms [4]. Typical symptoms include sudden unilateral weakness, numbness, visual loss, diplopia, altered speech, ataxia and non-orthostatic vertigo [5].

The major risk factors for brain stroke have been categorized as immutable factors such as age, gender, race and heredity [6-8]. Hypertension, hypercholesterolemia, carotid stenosis and atrial fibrillation are also known to be causal risk factors for stroke. Clinical trials have shown that treatment of these conditions reduces the incidence of stroke [9]. However, many other factors have been associated, such as current smoking or alcohol consumption [10, 11]. After the stroke event, about 40% of survivors are disabled between 1 month and 5 years [12]. The case fatality rates after a stroke event are about 15% at 1 month, 25% at 1 year, and 50% at 5 years. Moreover, after an ischemic stroke, the risk of recurrent stroke without treatment is about 10% at 1 week, 15% at 1 month, and 18% at 3 months [13]. Neurological and medical complications after stroke are a major cause of morbidity and mortality. Thus, it is urgent to anticipate, prevent and manage appropriately these events on patients.

The evaluation of novel risk factors can help to identify individuals at higher cerebrovascular or cardiovascular risk. The prevention of these events focuses on

identifying and managing risk factors, both on all the population and at individual levels, through primordial, primary and secondary prevention.

Some studies associated high levels of fibrinogen in blood plasma with a wide variety of thrombotic diseases, including stroke [14]. Fibrinogen has been identified as a major independent risk factor for cardiovascular disease [15] and should be consider for screening programs, identifying individuals at high risk for cardiovascular diseases [16, 17]. High fibrinogen levels promote fibrin formation, which is a major contributor to plasma viscosity [18]. Thus, increased levels of plasma fibrinogen result in changes on blood rheological properties, and these alterations intensify the complications in peripheral blood circulation during cardiovascular pathologies [19]. Erythrocyte aggregation is also important to understand the risk of primary and secondary cardiovascular events. Therefore, the interaction between fibrinogen and erythrocytes could be an important indicator of cardiovascular risk.

Our previous studies presented atomic force microscopy as a tool to evaluate cardiovascular risk in patients. We observed that the average force necessary to break the bond between fibrinogen and erythrocytes from chronic heart failure (CHF) patients was higher than for erythrocytes from healthy donors [20]. In more detail, we studied two different etiologies of CHF patients (ischemic and non-ischemic) and the strongest fibrinogen-erythrocyte interactions were measured for ischemic CHF patients, followed by non-ischemic CHF patients and finally by healthy control subjects [20]. After these findings, we proposed to do similar studies on the context of cerebrovascular pathologies, namely stroke.

In this study, an extensive clinical and hemorheological evaluation of stroke patients will be performed and the results combined with those achieved by AFM-based force spectroscopy (both fibrinogen-erythrocyte interaction and erythrocyte-erythrocyte adhesion measurements). The results obtained from these patients will be also matched with those obtained for healthy blood donors, to evaluate pathology-associated differences, and trying to assess the erythrocyte hyperaggregation induced by increased plasma fibrinogen. In more detail, it will be checked *in vitro* if these patients have increased fibrinogen-erythrocyte and erythrocyte-erythrocyte adhesion, relative to healthy donors, in the absence or in the presence of the same concentration of fibrinogen. The results obtained for these patients may be relevant to conclude on the

degree of pathophysiological relevance of fibrinogen on erythrocyte aggregation, since an increment on both is expected to induce changes on normal blood flow. Additionally, they will help us to understand the impact of this interaction as a cerebrovascular risk factor. As fibrinogen is an essential protein on this mechanism, it may become an important therapeutic target for cerebro/cardiovascular diseases.

On the following pages, there is a detailed description of the methods and the preliminary results achieved so far on this new project. Six stroke patients were assessed. This number is currently being increased. Our objective is to reach a group of at least 30 stroke patients.

Methods

The methods performed for this section were optimized and described in the previous Chapters. Namely, the protein-cell interactions procedure is in Chapters V and VI, the cell-cell adhesion protocol can be found in Chapter VII, the hemorheological parameters determination procedures are explained in Chapters V and VI, and for the quantification of γ' fibrinogen we used the protocol described in Chapter VII.

Preliminary results

At the time of the writing of this Thesis, we still had not received from our clinical collaborators from Hospital Santa Maria, Prof. Carlos Moreira, Prof. Ana Catarina Fonseca and Prof. José Ferro (Department of Neurology) the clinical data of each stroke patient included on the study. Presently, this work is ongoing and, in collaboration with the participating clinicians, we will study a larger number of patients, trying to prove our hypothesis. Until now, different techniques were performed for each patient, evaluated less than 48 h after an ischemic stroke.

From AFM-based force spectroscopy experiments to assess fibrinogen-erythrocyte binding, it could be observed that stroke patients tend to have higher (un)binding forces than the control group (67.5 ± 20.3 pN *vs.* 40.4 ± 3.0 pN; Figure 1a), despite lower binding frequency (9.2 ± 2.8 % *vs.* 27.3 ± 4.2 %; p = 0.017; Figure 1b). It means that, on stroke patients, the erythrocytes seem to bind to fibrinogen molecules with higher strength, but with a lower probability for the binding to occur, when compared to healthy donors.

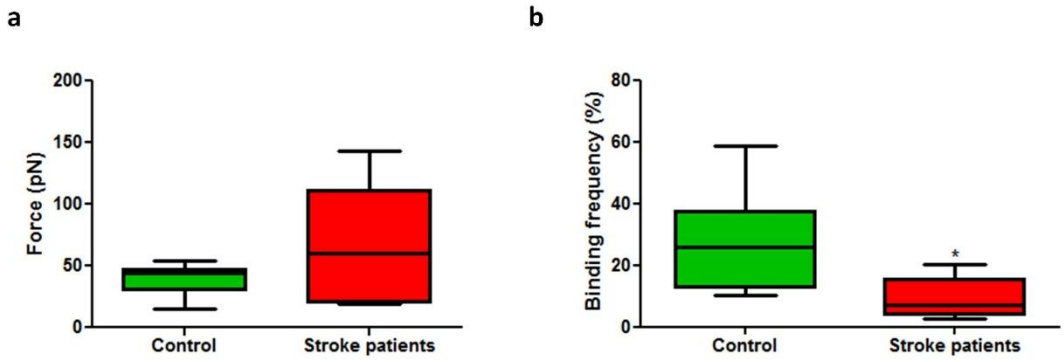

Figure 1 | **AFM-based force spectroscopy data for the fibrinogen-erythrocyte interactions.** Fibrinogen-erythrocyte binding force (a) and frequency (b) on erythrocytes from stroke patients (n=6) and healthy donors control group (n=15). Data are represented as box and whiskers plots, with median, maximum and minimum values. Statistical values: *, *p*=0.017.

From the cell-cell adhesion data, it was possible to observe that the work necessary to detach one erythrocyte from another was higher for stroke patients than for the

control group, without fibrinogen addition (2.86 ± 0.29 fJ *vs.* 0.48 ± 0.04 fJ; p<0.0001; Figure 2a).

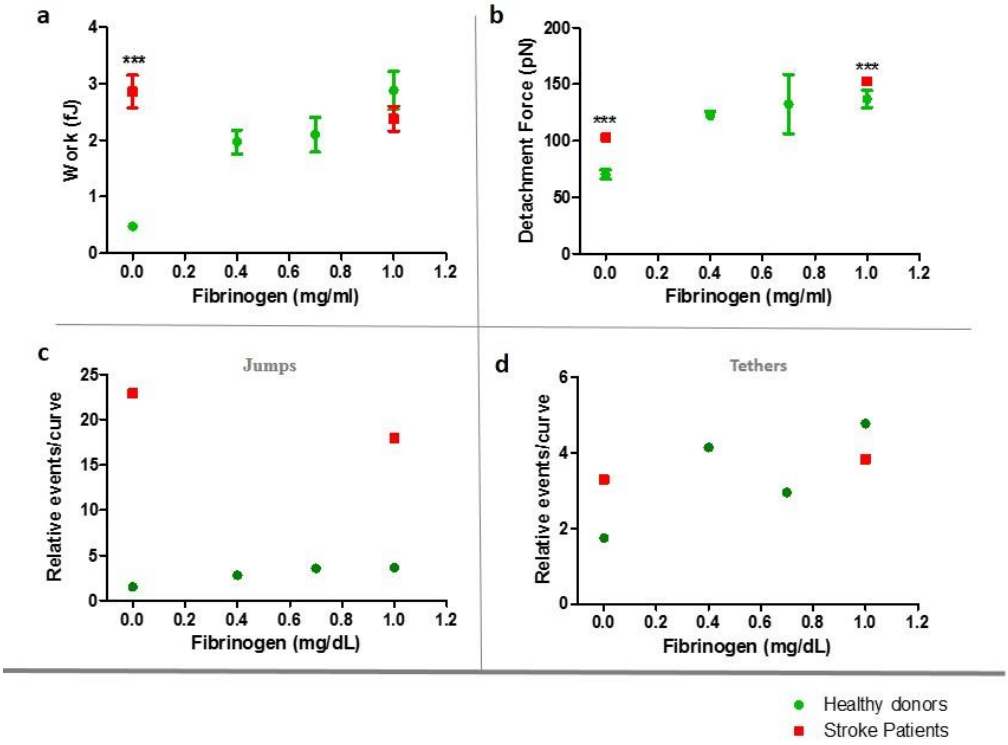

Figure 2 | **AFM-based force spectroscopy erythrocyte-erythrocyte adhesion data measured with increasing fibrinogen concentrations.** Work (a) and detachment force (b) necessary to break the adhesion between two erythrocytes from stroke patients (n=6) and from healthy donors (n=15). Small events of force: relative events of jumps (c) and of membrane tethers (d) formed after the binding between two erythrocytes from stroke patients and from control. Values are in mean ± SEM. Statistical values: ***, p<0.0001.

For healthy donors, when increasing fibrinogen concentrations, the work necessary to detach two cells increased. This increment in erythrocyte-erythrocyte adhesion was not observed for stroke patients. The maximal force was also determined by the difference between the baseline and the point of the minimum negative deflection of the cantilever on a force-distance curve. Values of erythrocyte-erythrocyte maximum detachment force were also higher for stroke patients, when compared to healthy donors, both in the absence of added fibrinogen and in the presence of 1 mg/mL of fibrinogen (103.0 ± 0.03 pN *vs.* 70.20 ± 0.23 pN without fibrinogen, p<0.0001; and, 152.4 ± 0.24 pN *vs.* 137.0 ± 0.89 pN with 1 mg/mL of fibrinogen, p<0.0001; Figure 2b).

Identically to the work values, looking at the detachment force, it can be noticed that when fibrinogen concentration increases, there is a concomitant increase on erythrocyte-erythrocyte adhesion, being this effect more pronounced on the control group. From the force-distance curve, it was also possible to quantitatively evaluate small events of forces (jumps and membrane tethers), which are important to understand the cell-cell adhesion process. The erythrocytes from stroke patients have more relative events of jumps/curve than the control, both in the absence and presence of fibrinogen (Figure 2c). In addition, the number of membrane tethers formed during erythrocyte-erythrocyte detachment in the absence of added fibrinogen is higher on stroke patients than for the control group (Figure 2d). However, in the presence of 1.0 mg/mL of fibrinogen the results revealed the opposite trend.

Knowing that increasing fibrinogen levels can result in changes in blood rheological properties and this could complicate the normal blood flow, we quantified the fibrinogen levels in both groups. Regarding plasma total fibrinogen concentration, both groups were within the normal range of 180 to 350 mg/dL [21]. Despite this fact, fibrinogen levels on stroke patients were higher than in healthy donors (290.7 ± 19.3 mg/dL *vs*. 246.6 ± 11.0 mg/dL), but the difference was not statistically significant (Figure 3a).

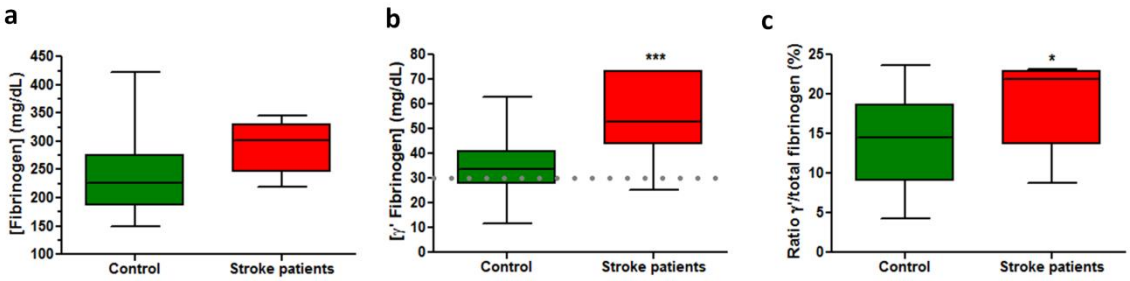

Figure 3 | **Fibrinogen quantification on each studies group.** Total plasma fibrinogen concentration (a), γ' fibrinogen variant concentration (b), and ratio between γ' fibrinogen and total fibrinogen concentrations (c) quantified for stroke patients (n=6) and healthy control group (n=47). Values are presented as box and whiskers plots, including median, maximum and minimum values. Statistical values: ***, p=0.0004; * p=0.410.

Using an ELISA kit (Gamma Couer ELISA kit, Gamma Therapeutics, Portland, OR, USA), it was possible to quantify the γ' fibrinogen variant concentration in the blood

plasmas from both groups (Figure 3b). Values above the cut off value (>30 mg/dL, represented by grey dashed line, Figure 3b) may be indicative of increased risk of cardiovascular disease. It can be noticed that stroke patients have higher concentration of γ' fibrinogen in plasma than the control group, with values well above the cut off value (54.6 ± 7.3 mg/dL *vs*. 34.4 ± 1.7 mg/dL, respectively; ***, p=0.0004). The ratio between γ' fibrinogen and total fibrinogen concentrations (Figure 3c) of stroke patients was significant higher than for the control group (18.95 ± 2.37% *vs*. 14.10 ± 0.78%; *, p=0.0410). The normal percentage of γ' fibrinogen in human plasma is approximately 15% [22], which is similar to the values obtained for the healthy donors. The increased γ' fibrinogen levels may therefore be associated with the increased cardiovascular risk of these patients.

In parallel with the analysis of force spectroscopy data and fibrinogen quantification, the evaluation of hemorheologic parameters (namely, erythrocyte deformability, erythrocyte aggregation and whole blood viscosity) was performed for both groups. Erythrocyte deformability was determined by exposing the cell to different values of shear stress, varying between 0.3 and 60.0 Pa. When compared with the control group, stroke patients had higher erythrocyte deformability at lower shear stress values (0.3 to 1.2 Pa; p<0.02), but lower deformability at higher shear stress (12 to 60 Pa; p≤0.0233; Figure 4a).

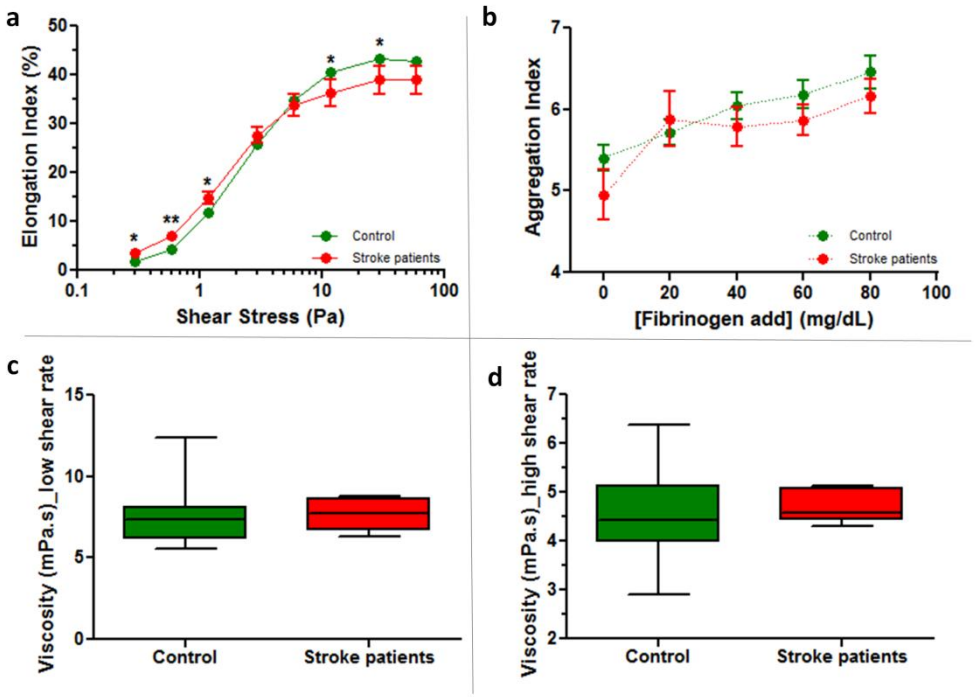

Figure 4 | **Hemorheologic parameters determined for stroke patients (n=6) and healthy control donors (n=65).** (a) Erythrocyte deformability, assessed as erythrocyte elongation index, at different shear stress values. Values are presented as mean ± SEM. (b) Erythrocyte aggregation, measured during 5 s, as a function of the addition of different fibrinogen concentrations. Values are presented as mean ± SEM. (c, d) Native whole blood viscosity at low (22.5 s^{-1}, c) and high (225 s^{-1}, d) shear rates. Values are presented as box and whiskers plots, including median, maximum and minimum values. Statistical values: **, p=0.0017; *, p≤0.0233.

Erythrocyte aggregation was measured by the infrared light transmission through a whole blood suspension, at stasis during 5 s (Figure 4b) and 10 s (data not shown), in the absence of added fibrinogen and after the addition of different fibrinogen concentrations, up to 80.0 mg/dL. There were no statistically significant changes on erythrocyte aggregation between these groups.

Whole blood viscosity was measured in blood from stroke patients and control group at low (22.5 s^{-1}) and high (225 s^{-1}) shear rates, both at native hematocrit conditions (Figure 4c and 4d) and after correction of the hematocrit to 45% (data not shown), at 37°C. Stroke patients seem to have a tendency for higher whole blood viscosity (at native

conditions) than the control group, both at low and high shear rates (Figure 4c and 4d); however, the variations were not statistically significant.

As previously indicated, these preliminary results were obtained for a small group of stroke patients (n = 6). This project is currently ongoing, enlarging the number of enrolled patients.

Discussion

The aggregation/adhesion of erythrocytes is a reversible phenomenon that occurs with macromolecules bridging the surfaces of adjacent cells. It is influenced by the shearing force of blood, the properties of erythrocytes (hematocrit, deformability, surface charge and shape) and the bridging force of high molecular weight plasma proteins. The presence of increased concentrations of acute phase proteins, particularly fibrinogen, leads to enhanced erythrocyte aggregation by such bridging [23, 24]. The major achievement of this work was to study erythrocyte aggregation and its interactions with fibrinogen molecules, in one of the most prevalent cerebrovascular disease, stroke.

Atomic force microscopy was used to measure fibrinogen-erythrocyte interactions and erythrocyte-erythrocyte adhesion, in the presence of different fibrinogen concentrations. Hemorheologic parameters and fibrinogen concentration were also quantified.

AFM force measurements of ligand-receptor interaction can be used to determine the dynamic strength of a complex [25]. In this study, we examined the interaction between the erythrocyte presenting a particular receptor and fibrinogen. Fibrinogen-erythrocyte interactions are modified in stroke patients. Atomic force microscopy-based force spectroscopy measurements, at the single-molecule level, showed that there is a strongest fibrinogen-erythrocyte binding in stroke patients than in the control, despite its lower binding frequency, as we reported for other cardiovascular pathology [20]. Furthermore, AFM can also be used to study erythrocyte's adhesion properties [26]. Cell adhesion experiments allowed the acquisition of both single-molecule measurements, like in above-mentioned studies, as well as multiple-bond interactions. These data provided information about the individual bonds as well as the force and work required to break apart the entire complex. Thus, combining single-molecule and multiple-bond data allows us to describe the thermodynamic model of the separation of a particular complex in addition to the mechanism of its action on the cellular scale [25, 27]. The adhesion between erythrocytes was also increased on these patients. It was also clear that in healthy donors, increasing fibrinogen concentrations, the work necessary to detach one erythrocyte from another increases, highlighting the important role of

fibrinogen on erythrocyte aggregation. Erythrocyte-erythrocyte adhesion data showed that, with increasing fibrinogen concentrations, the maximum force necessary to detach two erythrocytes was increased. Thus, erythrocytes from stroke patients have higher tendency to aggregate.

The hemorheologic parameters of stoke patients seem to be altered, potentially promoting changes on blood flow. Specifically, we observed statistically significant changes on erythrocyte deformability. We observed an increased deformability in larger vessels, while for smaller vessels the erythrocyte deformability was lower for patients than for healthy donors, as we previously reported for chronic heart failure patients [20]. Additionally, these patients had an increase of the plasma γ' fibrinogen concentrations. γ' fibrinogen has been studied as a possible risk factor for thrombosis [28, 29]. γ' fibrinogen levels had been linked with cardiovascular diseases, such as coronary heart disease [30], heart attack [31] and stroke [32]. All these alterations lead us to conclude that the blood samples from stroke patients tested are associated to significant risk factors for a bad clinical prognosis. It should also be taken into consideration that the binding between fibrinogen and erythrocyte may be used as a new cerebrovascular risk factor for stroke. The results obtained might be relevant to conclude on the degree of pathophysiological relevance of fibrinogen and erythrocyte aggregation, since an increment on both might induce a state of hyperviscosity and a reduction of the microcirculatory blood flow. As fibrinogen is an essential protein for this mechanism, it might become an important therapeutic target for the reduction of stroke events. However, it is crucial to enlarge the number of patients engaged on this study to further support our conclusions.

References of Chapter VIII

1. Hankey GJ. Stroke. *Lancet.* 389, 641-654 (2017).
2. World Heart Federation. Stroke. (2017).
3. Tran J, Mirzaei M, Anderson L, and Leeder SR. The epidemiology of stroke in the Middle East and North Africa. *J Neurol Sci.* 295(1-2), 38-40 (2010).
4. Sacco RL, Kasner SE, Broderick JP, Caplan LR, Connors JJ, Culebras A, Elkind MS, George MG, Hamdan AD, Higashida RT, Hoh BL, Janis LS, Kase CS, Kleindorfer DO, Lee JM, Moseley ME, Peterson ED, Turan TN, Valderrama AL, Vinters HV, American Heart Association Stroke Council CoCS, Anesthesia, Council on Cardiovascular R, Intervention, Council on C, Stroke N, Council on E, Prevention, Council on Peripheral Vascular D, Council on Nutrition PA, and Metabolism. An updated definition of stroke for the 21st century: a statement for healthcare professionals from the American Heart Association/American Stroke Association. *Stroke.* 44(7), 2064-2089 (2013).
5. Hankey GJ and Blacker DJ. Is it a stroke? *BMJ.* 350, h56 (2015).
6. Lai SM, Alter M, Friday G, and Sobel E. A multifactorial analysis of risk factors for recurrence of ischemic stroke. *Stroke.* 25(5), 958-962 (1994).
7. Sacco RL. Risk factors and outcomes for ischemic stroke. *Neurology.* 45, S10-14 (1995).
8. Xu G, Liu X, Wu W, Zhang R, and Yin Q. Recurrence after ischemic stroke in chinese patients: impact of uncontrolled modifiable risk factors. *Cerebrovasc Dis.* 23(2-3), 117-120 (2007).
9. Collins R, Reith C, Emberson J, Armitage J, Baigent C, Blackwell L, Blumenthal R, Danesh J, Smith GD, DeMets D, Evans S, Law M, MacMahon S, Martin S, Neal B, Poulter N, Preiss D, Ridker P, Roberts I, Rodgers A, Sandercock P, Schulz K, Sever P, Simes J, Smeeth L, Wald N, Yusuf S, and Peto R. Interpretation of the evidence for the efficacy and safety of statin therapy. *Lancet.* 388(10059), 2532-2561 (2016).
10. Global Burden of Disease Pediatrics C, Kyu HH, Pinho C, Wagner JA, Brown JC, Bertozzi-Villa A, Charlson FJ, Coffeng LE, Dandona L, Erskine HE, Ferrari AJ, Fitzmaurice C, Fleming TD, Forouzanfar MH, Graetz N, Guinovart C, Haagsma J,

Higashi H, Kassebaum NJ, Larson HJ, Lim SS, Mokdad AH, Moradi-Lakeh M, Odell SV, Roth GA, Serina PT, Stanaway JD, Misganaw A, Whiteford HA, Wolock TM, Wulf Hanson S, Abd-Allah F, Abera SF, Abu-Raddad LJ, AlBuhairan FS, Amare AT, Antonio CA, Artaman A, Barker-Collo SL, Barrero LH, Benjet C, Bensenor IM, Bhutta ZA, Bikbov B, Brazinova A, Campos-Nonato I, Castaneda-Orjuela CA, Catala-Lopez F, Chowdhury R, Cooper C, Crump JA, Dandona R, Degenhardt L, Dellavalle RP, Dharmaratne SD, Faraon EJ, Feigin VL, Furst T, Geleijnse JM, Gessner BD, Gibney KB, Goto A, Gunnell D, Hankey GJ, Hay RJ, Hornberger JC, Hosgood HD, Hu G, Jacobsen KH, Jayaraman SP, Jeemon P, Jonas JB, Karch A, Kim D, Kim S, Kokubo Y, Kuate Defo B, Kucuk Bicer B, Kumar GA, Larsson A, Leasher JL, Leung R, Li Y, Lipshultz SE, Lopez AD, Lotufo PA, Lunevicius R, Lyons RA, Majdan M, Malekzadeh R, Mashal T, Mason-Jones AJ, Melaku YA, Memish ZA, Mendoza W, Miller TR, Mock CN, Murray J, Nolte S, Oh IH, Olusanya BO, Ortblad KF, Park EK, Paternina Caicedo AJ, Patten SB, Patton GC, Pereira DM, Perico N, Piel FB, Polinder S, Popova S, Pourmalek F, Quistberg DA, Remuzzi G, Rodriguez A, Rojas-Rueda D, Rothenbacher D, Rothstein DH, Sanabria J, Santos IS, Schwebel DC, Sepanlou SG, Shaheen A, Shiri R, Shiue I, Skirbekk V, Sliwa K, Sreeramareddy CT, Stein DJ, Steiner TJ, Stovner LJ, Sykes BL, Tabb KM, Terkawi AS, Thomson AJ, Thorne-Lyman AL, Towbin JA, Ukwaja KN, Vasankari T, Venketasubramanian N, Vlassov VV, Vollset SE, Weiderpass E, Weintraub RG, Werdecker A, Wilkinson JD, Woldeyohannes SM, Wolfe CD, Yano Y, Yip P, Yonemoto N, Yoon SJ, Younis MZ, Yu C, El Sayed Zaki M, Naghavi M, Murray CJ and Vos T. Global and National Burden of Diseases and Injuries Among Children and Adolescents Between 1990 and 2013: Findings From the Global Burden of Disease 2013 Study. *JAMA Pediatr.* 170(3), 267-287 (2016).

11. O'Donnell MJ, Chin SL, Rangarajan S, Xavier D, Liu L, Zhang H, Rao-Melacini P, Zhang X, Pais P, Agapay S, Lopez-Jaramillo P, Damasceno A, Langhorne P, McQueen MJ, Rosengren A, Dehghan M, Hankey GJ, Dans AL, Elsayed A, Avezum A, Mondo C, Diener HC, Ryglewicz D, Czlonkowska A, Pogosova N, Weimar C, Iqbal R, Diaz R, Yusoff K, Yusufali A, Oguz A, Wang X, Penaherrera E, Lanas F, Ogah OS, Ogunniyi A, Iversen HK, Malaga G, Rumboldt Z, Oveisgharan S, Al Hussain F, Magazi D, Nilanont Y, Ferguson J, Pare G, Yusuf S, and investigators I. Global and regional effects of potentially modifiable risk factors associated with acute stroke

in 32 countries (INTERSTROKE): a case-control study. *Lancet.* 388(10046), 761-775 (2016).

12. Luengo-Fernandez R, Paul NL, Gray AM, Pendlebury ST, Bull LM, Welch SJ, Cuthbertson FC, Rothwell PM, and Oxford Vascular S. Population-based study of disability and institutionalization after transient ischemic attack and stroke: 10-year results of the Oxford Vascular Study. *Stroke.* 44(10), 2854-2861 (2013).
13. Coull AJ, Lovett JK, Rothwell PM, and Oxford Vascular S. Population based study of early risk of stroke after transient ischaemic attack or minor stroke: implications for public education and organisation of services. *BMJ.* 328(7435), 326 (2004).
14. Rothwell PM, Howard SC, Power DA, Gutnikov SA, Algra A, van Gijn J, Clark TG, Murphy MF, and Warlow CP. Fibrinogen concentration and risk of ischemic stroke and acute coronary events in 5113 patients with transient ischemic attack and minor ischemic stroke. *Stroke.* 35(10), 2300-2305 (2004).
15. Lominadze D, Dean WL, Tyagi SC, and Roberts AM. Mechanisms of fibrinogen-induced microvascular dysfunction during cardiovascular disease. *Acta Physiol.* 198(1), 1-13
16. Ernst E and Koenig W. Fibrinogen and cardiovascular risk. *Vasc Med.* 2(2), 115-125 (1997).
17. Steinvil A, Berliner S, Shapira I, Rogowski O, Justo D, George J, Halkin A, Keren G, Finkelstein A, Banai S, and Arbel Y. Time to rheology in acute myocardial infarction: inflammation and erythrocyte aggregation as a consequence and not necessarily as precursors of the disease. *Clin Res Cardiol.* 99(10), 651-656 (2010).
18. Stec JJ, Silbershatz H, Tofler GH, Matheney TH, Sutherland P, Lipinska I, Massaro JM, Wilson PF, Muller JE, and D'Agostino RB. Association of fibrinogen with cardiovascular risk factors and cardiovascular disease in the Framingham Offspring Population. *Circulation.* 102(14), 1634-1638 (2000).
19. Lominadze D, Dean WL, Tyagi SC, and Roberts AM. Mechanisms of fibrinogen-induced microvascular dysfunction during cardiovascular disease. *Acta Physiol.* 198(1), 1-13 (2010).
20. Guedes AF, Carvalho FA, Malho I, Lousada N, Sargento L, and Santos NC. Atomic force microscopy as a tool to evaluate the risk of cardiovascular diseases in patients. *Nat Nanotechnol.* 11(8), 687-692 (2016).

21. Taira C, Matsuda K, Arai S, Sugano M, Uehara T, and Okumura N. A Novel Mutation in the Fibrinogen Bbeta Chain (c.490G>A; End of Exon 3) Causes a Splicing Abnormality and Ultimately Leads to Congenital Hypofibrinogenemia. *Int J Mol Sci.* 18(11), (2017).
22. Wolfenstein-Todel C and Mosesson MW. Human plasma fibrinogen heterogeneity: evidence for an extended carboxyl-terminal sequence in a normal gamma chain variant (gamma'). *Proc Natl Acad Sci USA.* 77(9), 5069-5073 (1980).
23. Lominadze D, Schuschke DA, Joshua IG, and Dean WL. Increased ability of erythrocytes to aggregate in spontaneously hypertensive rats. *Clin Exp Hypertens.* 24(5), 397-406 (2002).
24. Maeda N, Seike M, Kume S, Takaku T, and Shiga T. Fibrinogen-induced erythrocyte aggregation: erythrocyte-binding site in the fibrinogen molecule. *Biochim Biophys Acta.* 904(1), 81-91 (1987).
25. Wojcikiewicz EP, Zhang X, and Moy VT. Force and Compliance Measurements on Living Cells Using Atomic Force Microscopy (AFM). *Biol Proced Online.* 6(1-9 (2004).
26. Mukherjee R, Saha M, Routray A, and Chakraborty C. Nanoscale Surface Characterization of Human Erythrocytes by Atomic Force Microscopy: A Critical Review. *IEEE Trans Nanobioscience.* 14(6), 625-633 (2015).
27. Zhang X, Wojcikiewicz E, and Moy VT. Force spectroscopy of the leukocyte function-associated antigen-1/intercellular adhesion molecule-1 interaction. *Biophys J.* 83(4), 2270-2279 (2002).
28. Uitte de Willige S, Standeven KF, Philippou H, and Ariens RA. The pleiotropic role of the fibrinogen gamma' chain in hemostasis. *Blood.* 114(19), 3994-4001 (2009).
29. Farrell DH. gamma' Fibrinogen as a novel marker of thrombotic disease. *Clin Chem Lab Med.* 50(11), 1903-1909 (2012).
30. Lovely RS, Falls LA, Al-Mondhiry HA, Chambers CE, Sexton GJ, Ni H, and Farrell DH. Association of gammaA/gamma' fibrinogen levels and coronary artery disease. *Thromb Haemost.* 88(1), 26-31 (2002).
31. Mannila MN, Lovely RS, Kazmierczak SC, Eriksson P, Samnegard A, Farrell DH, Hamsten A, and Silveira A. Elevated plasma fibrinogen gamma' concentration is

associated with myocardial infarction: effects of variation in fibrinogen genes and environmental factors. *J Thromb Haemost.* 5(4), 766-773 (2007).

32. Cheung EY, Uitte de Willige S, Vos HL, Leebeek FW, Dippel DW, Bertina RM, and de Maat MP. Fibrinogen gamma' in ischemic stroke: a case-control study. *Stroke.* 39(3), 1033-1035 (2008).

Chapter IX ▫

Integrated discussion and final remarks

Integrated discussion

The main goal of this discussion is to integrate all background knowledge and the most recent findings (highlighted on Chapter I) with all the work obtained during my PhD and presented in this Thesis. The preceding knowledge and the work previous done in the group originated new and pertinent questions and hypothesis to be tested, many of which constituting the purpose of my PhD Thesis research. The main aims that we proposed to investigate (*vd.* "Aims of the project" in Chapter I) were: **i)** to understand the effect of human plasma fibrinogen variants and erythrocytes on *in vivo* fibrin clots; **ii)** to characterize the fibrinogen binding sites for its receptor on erythrocytes **iii)** to complete the identification of the fibrinogen receptor on erythrocytes; **iv)** to understand the influence of fibrinogen on erythrocyte-erythrocyte adhesion; and, the major goal and the main focus of this Thesis, **v)** to evaluate the interaction between fibrinogen and erythrocytes in healthy and pathological conditions, pinpointing patients with increased cardiovascular or cerebrovascular risk.

The identification of clinically applicable new biomarkers would help to screen for and to diagnose cardiovascular diseases, monitor disease severity and its progression, and to evaluate the response to therapy[1]. Based on the results presented on this Thesis, the obvious association between erythrocyte and fibrinogen is compelling, and certainly warrants further investigation as a clinical prognosis biomarker. Certainly, the pharmacological therapies to inhibit this binding will aim at both the treatment and prophylaxis of CVD improving cardiovascular risk prevention and also assisting Clinician in making decisions concerning patients at higher risk for specific diseases.

In each Chapter, the results obtained and a detailed discussion were presented according to the proposed goals. In this Chapter, the discussion of all the subjects was integrated and the main conclusions presented.

Erythrocytes and γ' fibrinogen change the structure as well as the behavior of fibrin clots

Although recent data demonstrate that there is a close association between high fibrinogen levels and cardiovascular diseases[2-6], further studies must be carried out taking

into account the different fibrinogen variants in each individual. Human plasma fibrinogen includes an alternatively spliced variant (γ' fibrinogen) which mainly exist as a heterodimer[7, 8] and it has been associated with cardiovascular diseases[9-11]. As the direct effect of γ' fibrinogen on fibrin formation and structure has so far been unknown or not totally clarified, especially in the presence of the most common cells in the blood (erythrocytes), from a clinical perspective, the study of the properties of *in vivo* blood clots is an extremely important area.

To conduct these studies, we used commercial but also recombinant plasma protein once it was not possible to isolate the γ'/γ' variant from commercial fibrinogen due to the low amount available (~1%). Using these isolated proteins, we were able to compare molecules that differed only by the presence or absence of the γ' chain in one or both half-molecules. One of the aims of this study was to study properties of the clots formed with purified γAγ' and γAγA fibrinogen to understand the effect of γ' chain on hemostasis or thrombosis, according to the work described in the Chapter II. Using anion-exchange chromatography, these fibrinogen variants were purified. This work used multiple complementary techniques in order to study structural, viscoelastic and biophysical properties of the clots. The binding between fibrinogen and erythrocytes was also evaluated using AFM. Our observations have provided evidence that erythrocytes are important players in hemostasis and thrombosis, in accordance with the studies from other groups[12, 13]. Clearly, our results showed that erythrocytes promote variability in the fibrin network structure and in overall clot properties. In the presence of the γ' chain of fibrinogen, the erythrocyte-erythrocyte detachment was higher at low concentrations of γAγ' fibrinogen, leading to changes on the function and properties of the clots. The presence of erythrocytes also increased the stiffness of γAγ' fibrin clots, which are less permeable and more resistant to lysis than γAγA fibrin clots. Thus, clots with γAγ' fibrinogen seem to interact differently with erythrocytes and, eventually alter the risk of thrombotic diseases.

After that, we went a step further in order to understand the impact of γ'γ' homodimer fibrinogen on the structure and on the properties of the fibrin clots in the presence of erythrocytes, compared to the common variant γAγA fibrinogen (Chapter III). Prior to proceeding onto a comprehensive study of the behavior of these fibrin clots and, in order to achieve our goals, we produced the recombinant homodimer γ'γ' fibrinogen.

Using this fibrinogen variant, an increase of the binding force and of the frequency of the binding to erythrocytes were reported, which could promote cell aggregation. Still in the fibrin clot structure, we observed alterations in the presence of γ'γ' fibrinogen, compared to the recombinant common variant, γAγA, such as more branching, larger porosity and less dense fibers, displaying a non-uniform fibrin network. In the presence of erythrocytes, γ'γ' fibrin clots were more viscous than with γAγA. Moreover, the fibrinolysis of γ'γ' fibrin clots with erythocytes took longer than without these cells. Computational analyses of both fibrin models reinforce these findings. The full length of the γ' chain structure occupies a much wider surface and is more flexible when compared to the γA chain prediction. Thus, it allows an increase of the binding between γ' fibers (and, eventually their binding to erythrocytes), possibly in a context of a transient interaction due to the high flexibility of the γ' chain C-terminal. All data combined show the impact of γ' fibrinogen on the binding to erythrocytes, leading to an altered fibrin clot and the importance of erythrocytes as complements of the complex reactions of clot formation.

Fibrinogen $\alpha_{94}RGD_{97}$ sequence is involved on erythrocyte binding

The fibrinogen molecule has three potential integrin binding sites: two RGD (arginine-glycine-aspartic acid) amino acid residues sequences within the Aα chain and a 12 amino acids (dodecapetide) sequence on the γ chain but can also interact with cells through nonintegrin receptors[14]. In order to identify the interaction sites of fibrinogen with the human erythrocyte receptor, different fibrinogen mutations were produced, specifically altered on the described integrin binding sites of the Aα chain (D97E, D574E and D97E/D574E double mutant), produced according to established procedures[15, 16]. Thus, besides using wild-type fibrinogen, we conducted force spectroscopy measurements using AFM to determine the force necessary to break the bond between each fibrinogen mutant (attached to the AFM tip) and erythrocytes (adhered to poly-L-lysine treated glass slides). According to the data reported in Chapter IV, we observed a significant decrease on fibrinogen-erythrocyte binding force and on its frequency in the presence of fibrinogen with an Aα chain mutation on residue 97 from aspartic acid to glutamic acid, D97E, indicating that the corresponding RGD sequence (residues 95-97)

may be involved on this interaction. On the scanning electron microscopy micrographs obtained in the presence of D97E fibrin clots, we did not find significant differences, compared to the common variant. However, the addition of erythrocytes promoted highly structurally arranged clots. This indicates that the main effect is due to the binding to the erythrocytes and it is not caused by differences on fibrin polymerization of this variant. These results allowed us to understand a little better the fibrinogen domains involved on its interaction with the receptor on the erythrocytes. However, further studies are required to fully understand the specific fibrinogen binding sites involved on its interaction with erythrocytes. During my visit to the University of Leeds, we started to produce other fibrinogen variants with three different mutations in and near the RGD sequence: mutation from arginine to glutamamine R95Q, aspartate to asparagine D97N and phenylalanine to isoleucine F98I. We hope that these new fibrinogen variants will help to clarify, using different approaches, which sequences of the fibrinogen molecule interact with the erythrocyte membrane and the impact of the mutations on the fibrin clot.

$\alpha_V\beta_3$ integrin is the receptor for fibrinogen on the erythrocyte membrane

Fibrinogen-induced erythrocyte hyperaggregation has previously been associated to a nonspecific binding mechanism[17, 18]. However, the published data on the changes in erythrocyte aggregation during hypertension points to the possible existence of other mechanisms[19]. In a previous study, we reported the existence of a specific binding between fibrinogen and an unknown receptor on the human erythrocyte membrane with a lower but comparable affinity relative to platelet binding, which interaction seemed to be calcium ion dependent and inhibited by the eptifibatide (an inhibitor of the $\alpha_{IIb}\beta_3$ integrin)[20]. As a negative control for this study, cells from a patient with Glanzmann thrombastenia (a rare hereditary bleeding disease caused by $\alpha_{IIb}\beta_3$ deficiency) were collected. This patient presented a pathogenic mutation in the *ITGB3* gene, which was previously described as causing this disease, due to a nonfunctional expression of the glycoprotein $\alpha_{IIb}\beta_3$. Results obtained for Glanzmann Thombastenia patient showed an impaired fibrinogen-erythrocyte binding. It was demonstrated, correlating these data with genetic sequencing, that one of the units of the fibrinogen receptor on erythrocytes

is also a product of the expression of the β_3 gene, found to be mutated in this patient. After these experiments, we concluded that the β_3 chain is part of the receptor for fibrinogen on the erythrocyte membrane[20]. In our recent data reported in Chapter V, antibody inhibition studies, lead to a decrease of the binding force, particularly with the antibody against $\alpha_V\beta_3$ integrin. Combining these data with our previous results, we proposed that the receptor for fibrinogen on erythrocyte membrane is the integrin $\alpha_V\beta_3$. The same receptor for fibrinogen was identified on endothelial cells[21, 22]. The knowledge of the receptor may open important doors to innovative therapeutic drugs to inhibit this binding, in order to decrease erythrocyte hyperaggregation and improve blood flow conditions. For instance, eptifibatide, the inhibitor of $\alpha_{IIb}\beta_3$ integrin is already used in hospital settings to reduce platelet hyperaggregation[23, 24].

Fibrinogen-erythrocyte interaction as a cardiovascular risk factor

After the characterization of the fibrinogen-erythrocyte binding and the adhesion between these cells, we wanted to know more about this interaction in cardiovascular patients.

Atomic force microscopy-based force spectroscopy measurements showed, at the single molecule level, that fibrinogen-erythrocyte binding forces were increased in patients with chronic heart failure (Chapter V), essential arterial hypertension (Chapter VI) and preliminary results displayed higher binding forces also in patients who suffered a stroke (Chapter VIII). Despite a higher binding force observed, data displayed lower binding frequency. The reasons for this observation are still not clear and further studies will be necessary.

In the chronic heart failure study, we found that patients who presented higher binding forces at the beginning of the study had higher probability of being hospitalized in the following year due to cardiovascular complications. This shows the value of this approach as a potential clinical prognosis biomarker. Thus, the results presented through this Thesis, along with some other published work[20] showed that the fibrinogen-erythrocyte interaction appears to have an important prognostic value in patients with chronic heart failure[25] and may be useful in the prognosis of other cardiovascular and cerebrovascular diseases. Clearly, continued research into the prothrombotic nature of

both erythrocytes and fibrin(ogen) is necessary, with a particular emphasis on the physical and biochemical interactions between erythrocytes and fibrin(ogen). Disrupting the interaction between fibrin(ogen) and erythrocytes in venous thrombi, knowing its membrane receptor has a high potentially therapeutic value for reducing cardiovascular diseases-related squeals. To evaluate this binding in other pathologies may also have an great impact in clinical routine prognosis, both for clinicians and patients.

Adhesion between erythrocytes is influenced by fibrinogen levels

Increased fibrinogen concentrations[18] and erythrocyte aggregation[26] have been considered as factors that significantly increase the risk of cardiovascular and cerebrovascular diseases. Erythrocyte aggregation has become an issue of increasing interest due to its pathogenic implications on thrombus formation, both at venous and arterial levels. This parameter is used especially to assess the risk of primary or secondary cardiovascular events[27]. Here, we showed, at the single cell level and using a powerful new accessory of the AFM (CellHesion module), that the increase of erythrocyte adhesion is partially due to an increase of the plasma concentration of fibrinogen (Chapter VII). Arterial essential hypertension patients presented higher adhesion forces compared to healthy donors, even without fibrinogen. This may be due to changes on its membrane composition and/or charge, which could facilitate erythrocyte-erythrocyte adhesion. This fact is worth of being addressed in the near future. The higher adhesion forces promoted by circulating fibrinogen levels could be an important factor for increased erythrocyte aggregation and consequently, impairment of the microcirculation.

γ' fibrinogen levels are increased in cardiovascular and cerebrovascular diseases

Many epidemiological studies have shown the association between total fibrinogen levels and cardiovascular diseases[28-30]. Studies have shown that a first-order relationship exists between fibrinogen concentration and fibrinolysis rate[31], suggesting that elevated fibrinogen levels may actually cause thrombosis by slowing fibrinolysis[32]. However, possible mechanisms by which fibrinogen may contribute to cardiovascular diseases

continue to be a subject of controversy. Higher levels of γ' fibrinogen have also been found among individuals with some pathological conditions[9, 11, 33-35]. Notwithstanding, this association is not clear, as some studies showed an inverse association with γ' fibrinogen levels and the development of the disease[36]. In our study, high concentrations of this fibrinogen variant (γA/γ' and γ'/γ') were found in plasma from essential arterial hypertension (Chapter VII) and stroke patients (Chapter VIII), when compared to healthy blood donors. We hypothesize that increasing γ' fibrinogen levels in plasma from EAH and stroke patients could influence the adhesion between erythrocytes, increasing their aggregation. Cell-cell adhesion experiments were performed with wild-type plasma fibrinogen, and even so, higher cell-cell adhesion of erythrocytes from EAH patients was observed. It is expected that in a pathological condition, with high levels of γ' fibrinogen variant circulating in the plasma of the patient, the adhesion between erythrocytes could increase. These aspects will be the matter of study in the close future. γ' fibrinogen could be an effective newly-emerging cardiovascular disease risk factor that seems to have an association with CVD independent from that of total fibrinogen. This variant has several biochemical and biophysical features that distinguish it from γAγA fibrinogen and these properties, such as, highly resistance to fibrinolysis and altered clot structure may actually contribute to thrombosis[32].

Clinical and hemorheological parameters altered in the disease

Patients attending to the hospital regularly and the close collaboration with clinicians allow us to evaluate patients at different levels and at different times, trying to correlate all clinical information with our data whenever possible.

In order to evaluate the unfavorable hemorheological factors in our population, we analyzed different parameters in patients and healthy individuals. Changes on whole blood viscosity, erythrocyte aggregation and erythrocyte deformability were observed in all patients (Chapters V, VI and VIII). The results obtained for chronic heart failure patients showed that, at 45% hematocrit, patients as a whole presented higher whole blood viscosity, mainly the non-ischemic ones. Both patient groups (ischemic and non-ischemic etiology) displayed higher deformability than the control group at low shear stress, but lower deformability at higher shear stress, which could eventually contribute to the

blocking of an artery or vein downstream, compromising the circulation. These results are detailed in Chapter V. We also observed differences on elasticity or stiffness (Young's modulus) of the erythrocytes isolated from each patient (Chapter V, VI and VIII). For instance, we observed an increased cell stiffness (or decreased elasticity) on both groups of CHF patients, with the larger variation being observed, for the non-ischemic patients. For EAH patients, a decreased elasticity of the erythrocytes was observed compared to the healthy donors.

AFM as a powerful nanomedicine tool

The use of nanotechnologies for medical applications raises high expectations. Particularly, there is an increasing number of reports using AFM as a nanomedicine tool [20, 37-39]. AFM-based force spectroscopy measurements are becoming increasingly common and easier to handle, which also allows for their wider use in several areas. This is of special importance for biomedical studies, since a detailed understanding of the molecular mechanisms involved in health and disease are crucial for the future development of novel protein-targeted drugs and treatments. Protein-cell interaction and cell-cell adhesion measurements seem to have huge medical applications, besides the applicability reported for basic research [40, 41].

Using this methodology, we studied the interaction between fibrinogen molecules and erythrocytes in order to understand the observed increase of erythrocyte aggregation on the patients with some cardiovascular risk factors. Thus, we showed the immense potential of AFM as a bench-top technique of undeniable value for the study of biologically relevant samples, such as blood samples. Its ability to early detect such alteration on the binding between fibrinogen and erythrocytes in healthy and disease conditions has opened up the exciting prospective of using a simple nanodevice as a clinical screening tool. As we previously showed, AFM-based force spectroscopy is highly sensitive, rapid and low operation cost nanotool [20]. Moreover, a great advantage of AFM is that only small amount of biological sample (~ 1 µl of erythrocytes) is required. This has allowed methodologies to be readily applied to biological systems, such as single molecules and living cells. Moreover, AFM measurements can also be performed in physiological environments. Further research is warranted to develop a user-friendly *in*

situ AFM setup that will allow a direct and more precise prognosis and screening of cardiovascular patients.

Final remarks and future directions

At the end, with the major results described on the manuscripts included on this Thesis, we concluded that the main goals were successfully achieved (please consult "Aims of the project", in Chapter I). In the present Thesis we have demonstrated, for the first time, the increase of fibrinogen-erythrocyte binding forces in patients with cardiovascular diseases and the potential of this approach as a clinical prognosis biomarker. Future directions are already designed in close collaboration with clinicians from Centro Hospitalar Lisboa Norte and from other hospitals. First of all, we will go further in our study with patients who suffered a stroke, enlarging our population, in order to increase the confidence on our results. Other pathologies, such as myocardial infarction will be studied, involving as many patients as possible, in order to optimize and validate the force spectroscopy method. In those cases, the fibrinogen-erythrocyte binding will be evaluated, but also erythrocyte adhesion by cell-cell interaction studies. All patients will be clinically evaluated in close collaboration with specialized cardiologists. Clinical follow-up studies will be also conducted and all results will be matched with those obtained for healthy donors.

At this stage, we identified new approaches we would like to conduct and new exciting ways to explore them. Thus, several questions to address emerged.

Recent data suggest a new role for erythrocytes in hemostasis and thrombosis, driven through interactions of erythrocytes with fibrin(ogen). A better understanding of the fibrin(ogen)-erythrocyte binding sites could give us new insights to overcome this binding. On the University of Leeds, in collaboration with Prof. Robert Ariëns, we started to produce new fibrinogen variants, with different mutations on the Aα-chain to conclude the characterization of the fibrinogen binding sites to its erythrocyte receptor. Our goal is to investigate the role of the fibrinogen Aα-chain $_{95}$RGD$_{97}$ sequence, which is located in the coiled coil region of the protein, in the binding of fibrinogen to its erythrocyte membrane receptor. For that, three different mutations on the fibrinogen protein are being produced, in or near the RGD sequence: R95Q, D97N and F98I. At this level, the recombinant proteins have already been analyzed by SDS-PAGE, circular dichroism (CD) and turbidity, for their basic structure/function and comparison to the wild type. An

fibrinogen-erythrocyte binding assay (ELISA) with a specific α_V antibody was also developed to study the binding between fibrinogen and erythrocytes. Some preliminary results have already been obtained. The SDS-PAGE analysis showed high integrity and purity of the proteins, but the mobility of the Aα-chains appeared slightly affected, indicating some differences in polypeptide folding for all mutations. CD spectra confirmed minor differences on the α-helical content for each mutation. Turbidity analysis showed reduced maximum absorbency for each fibrinogen mutant compared to the wild type, which is indicative of thinner fibers. Erythrocyte binding was increased in the presence of the F98I fibrinogen mutation, and reduced on the D97N fibrinogen variant, but not on the R95Q. Erythocyte binding was inhibited by an anti-α_V antibody, but not by an non-immune IgG. The results indicate a role for the fibrinogen $\alpha_{95}RGD_{97}$ sequence in erythrocyte binding, and that the binding is medidated by the $\alpha_V\beta_3$ receptor as we already proposed[25]. However, we would also like to understand the impact of these mutations on a fibrin clot in the presence and in the absence of erythrocytes. Hence, new experimental approaches will be performed, such as magnetic tweezers, permeability studies, confocal and scanning electron microscopy.

Another question emerged from the results of this Thesis: atherosclerotic plaques can cause stenosis, embolization and thrombosis and have been associated with increased serum levels of fibrinogen[42-44]. Peripheral vascular disease (PVD) affects 3 to 10% of the Portuguese population[45]. It is an abnormal condition of the blood vessels, which become completely or partially blocked as a result of atherosclerosis. Establishing the diagnostic, extent and severity of vascular diseases, as well as determining the mechanisms underlying the potential risk of recurrence of thromboembolic events, are crucial steps toward improving patient clinical diagnosis and prognosis. New methods to detect early molecular changes in tissues or changes in normal blood flow before clinical symptoms of vascular disease appear, without invasive interventions, are of paramount importance. Fibrinogen and erythrocyte aggregation may have a central role on the mechanism of thrombosis and coagulation. As increased levels of plasma fibrinogen results in changes in blood rheological properties, such as increased erythrocyte aggregation, the role of fibrinogen on increasing erythrocyte aggregation may be a good candidate as a biomarker of assessment of the risk of thromboembolic events. Thus, in the future, we intend to study the molecular interactions of fibrinogen with erythrocytes

in vascular thromboembolic diseases as a new approach for early identifying patients with higher risk of development of the disease. We will do this by taking advantage of the acquired knowledge and the results previously obtained by us [20, 25, 46], mainly using AFM-based force spectroscopy. A more specific goal is to conduct follow-up studies of patients with deep vein thrombosis (DVT), focusing on the changes on erythrocyte-erythrocyte adhesion and on the fibrinogen-erythrocyte interactions. Additionally, we want to quantify the plasma γ' fibrinogen levels on DVT patients. Other goal will be to perform functional cell-based assays to mimic the *in vivo* blood flow in healthy and vascular disease.

Finally, our promising aim is to identify which drug(s) may be successfully used to overcome the risks of fibrinogen-driven erythrocyte hyperaggregation associated to the inhibition of the fibrinogen-erythrocyte binding, preventing cardiovascular diseases.

A new area of therapeutics is emerging right now, with the promise and ambitious goal of modulating the fibrinogen-erythrocyte binding. Altogether, the knowledge gathered and the hypothesis formulated on this Thesis are certainly of great interest, not only for a better understanding the fibrinogen-erythrocyte interaction, but also for future drug developments strategies in order to overcome erythrocyte hyperaggregation, a cardiovascular risk factor for different pathologies.

References of Chapter IX

1. Shaw, J.G., Vaughan, A., Dent, A.G., O'Hare, P.E., Goh, F., Bowman, R.V., Fong, K.M. & Yang, I.A. Biomarkers of progression of chronic obstructive pulmonary disease (COPD). *J Thorac Dis* **6**, 1532-47 (2014).
2. Chandy, S., Joseph, K., Sankaranarayanan, A., Issac, A., Babu, G., Wilson, B. & Joseph, J. Evaluation of C-Reactive Protein and Fibrinogen in Patients with Chronic and Aggressive Periodontitis: A Clinico-Biochemical Study. *J Clin Diagn Res* **11**, ZC41-45 (2017).
3. Gupta, S., Gudapati, R., Gaurav, K. & Bhise, M. Emerging risk factors for cardiovascular diseases: Indian context. *Indian J Endocrinol Metab* **17**, 806-14 (2013).
4. Kalaria, V.G., Zareba, W., Moss, A.J., Pancio, G., Marder, V.J., Morrissey, J.H., Weiss, H.J., Sparks, C.E., Greenberg, H., Dwyer, E., Goldstein, R. & Watelet, L.F. Gender-related differences in thrombogenic factors predicting recurrent cardiac events in patients after acute myocardial infarction. The THROMBO Investigators. *Am J Cardiol* **85**, 1401-8 (2000).
5. Ndrepepa, G., Braun, S., King, L., Fusaro, M., Keta, D., Cassese, S., Tada, T., Schomig, A. & Kastrati, A. Relation of fibrinogen level with cardiovascular events in patients with coronary artery disease. *Am J Cardiol* **111**, 804-10 (2013).
6. van Holten, T.C., Waanders, L.F., de Groot, P.G., Vissers, J., Hoefer, I.E., Pasterkamp, G., Prins, M.W. & Roest, M. Circulating biomarkers for predicting cardiovascular disease risk; a systematic review and comprehensive overview of meta-analyses. *PLoS One* **8**, e62080 (2013).
7. Chung, D.W. & Davie, E.W. gamma and gamma' chains of human fibrinogen are produced by alternative mRNA processing. *Biochemistry* **23**, 4232-6 (1984).
8. Mosesson, M.W., Finlayson, J.S. & Umfleet, R.A. Human fibrinogen heterogeneities. 3. Identification of chain variants. *J Biol Chem* **247**, 5223-7 (1972).
9. Cheung, E.Y., Uitte de Willige, S., Vos, H.L., Leebeek, F.W., Dippel, D.W., Bertina, R.M. & de Maat, M.P. Fibrinogen gamma' in ischemic stroke: a case-control study. *Stroke* **39**, 1033-5 (2008).

10. Lovely, R.S., Falls, L.A., Al-Mondhiry, H.A., Chambers, C.E., Sexton, G.J., Ni, H. & Farrell, D.H. Association of gammaA/gamma' fibrinogen levels and coronary artery disease. *Thromb Haemost* **88**, 26-31 (2002).
11. Mannila, M.N., Lovely, R.S., Kazmierczak, S.C., Eriksson, P., Samnegard, A., Farrell, D.H., Hamsten, A. & Silveira, A. Elevated plasma fibrinogen gamma' concentration is associated with myocardial infarction: effects of variation in fibrinogen genes and environmental factors. *J Thromb Haemost* **5**, 766-73 (2007).
12. Litvinov, R.I. & Weisel, J.W. Role of red blood cells in haemostasis and thrombosis. *ISBT Sci Ser* **12**, 176-183 (2017).
13. Tombak, A. Red blood cells and relation to thrombosis. *Intech* **3**, 43-52 (2017).
14. Herrick, S., Blanc-Brude, O., Gray, A. & Laurent, G. Fibrinogen. *Int J Biochem Cell Biol* **31**, 741-6 (1999).
15. Farrell, D.H. & Thiagarajan, P. Binding of recombinant fibrinogen mutants to platelets. *J Biol Chem* **269**, 226-31 (1994).
16. Standeven, K.F., Carter, A.M., Grant, P.J., Weisel, J.W., Chernysh, I., Masova, L., Lord, S.T. & Ariëns, R.A. Functional analysis of fibrin {gamma}-chain cross-linking by activated factor XIII: determination of a cross-linking pattern that maximizes clot stiffness. *Blood* **110**, 902-7 (2007).
17. Chien, S. & Jan, K. Ultrastructural basis of the mechanism of rouleaux formation. *Microvasc Res* **5**, 155-66 (1973).
18. Maeda, N., Seike, M., Kume, S., Takaku, T. & Shiga, T. Fibrinogen-induced erythrocyte aggregation: erythrocyte-binding site in the fibrinogen molecule. *Biochim Biophys Acta* **904**, 81-91 (1987).
19. Lominadze, D., Schuschke, D.A., Joshua, I.G. & Dean, W.L. Increased ability of erythrocytes to aggregate in spontaneously hypertensive rats. *Clin Exp Hypertens* **24**, 397-406 (2002).
20. Carvalho, F.A., Connell, S., Miltenberger-Miltenyi, G., Pereira, S.V., Tavares, A., Ariëns, R.A. & Santos, N.C. Atomic force microscopy-based molecular recognition of a fibrinogen receptor on human erythrocytes. *ACS Nano* **4**, 4609-20 (2010).
21. Cheresh, D.A., Berliner, S.A., Vicente, V. & Ruggeri, Z.M. Recognition of distinct adhesive sites on fibrinogen by related integrins on platelets and endothelial cells. *Cell* **58**, 945-53 (1989).

22. Thiagarajan, P., Rippon, A.J. & Farrell, D.H. Alternative adhesion sites in human fibrinogen for vascular endothelial cells. *Biochemistry* **35**, 4169-75 (1996).
23. Galli, M., Maggioni, A.P., Vassanelli, C. & Tavazzi, L. The clinical use of the GPIIb/IIIa inhibitors eptifibatide and tirofiban in the treatment of acute coronary syndromes of the "non-ST elevation" type. *Ital Heart J Suppl* **1**, 202-11 (2000).
24. Zeymer, U. & Wienbergen, H. A review of clinical trials with eptifibatide in cardiology. *Cardiovasc Drug Rev* **25**, 301-15 (2007).
25. Guedes, A.F., Carvalho, F.A., Malho, I., Lousada, N., Sargento, L. & Santos, N.C. Atomic force microscopy as a tool to evaluate the risk of cardiovascular diseases in patients. *Nat Nanotechnol* **11**, 687-92 (2016).
26. Delamaire, M. & Durand, F. Erythrocyte aggregation and vascular pathology. *J Mal Vasc* **15**, 344-5 (1990).
27. Falco, C., Vaya, A., Simo, M., Contreras, T., Santaolaria, M. & Aznar, J. Influence of fibrinogen levels on erythrocyte aggregation determined with the Myrenne aggregometer and the Sefam erythro-aggregometer. *Clin Hemorheol Microcirc* **33**, 145-51 (2005).
28. Danesh, J., Lewington, S., Thompson, S.G., Lowe, G.D., Collins, R., Kostis, J.B., Wilson, A.C., Folsom, A.R., Wu, K., Benderly, M., Goldbourt, U., Willeit, J., Kiechl, S., Yarnell, J.W., Sweetnam, P.M., Elwood, P.C., Cushman, M., Psaty, B.M., Tracy, R.P., Tybjaerg-Hansen, A., Haverkate, F., de Maat, M.P., Fowkes, F.G., Lee, A.J., Smith, F.B., Salomaa, V., Harald, K., Rasi, R., Vahtera, E., Jousilahti, P., Pekkanen, J., D'Agostino, R., Kannel, W.B., Wilson, P.W., Tofler, G., Arocha-Pinango, C.L., Rodriguez-Larralde, A., Nagy, E., Mijares, M., Espinosa, R., Rodriquez-Roa, E., Ryder, E., Diez-Ewald, M.P., Campos, G., Fernandez, V., Torres, E., Marchioli, R., Valagussa, F., Rosengren, A., Wilhelmsen, L., Lappas, G., Eriksson, H., Cremer, P., Nagel, D., Curb, J.D., Rodriguez, B., Yano, K., Salonen, J.T., Nyyssonen, K., Tuomainen, T.P., Hedblad, B., Lind, P., Loewel, H., Koenig, W., Meade, T.W., Cooper, J.A., De Stavola, B., Knottenbelt, C., Miller, G.J., Cooper, J.A., Bauer, K.A., Rosenberg, R.D., Sato, S., Kitamura, A., Naito, Y., Palosuo, T., Ducimetiere, P., Amouyel, P., Arveiler, D., Evans, A.E., Ferrieres, J., Juhan-Vague, I., Bingham, A., Schulte, H., Assmann, G., Cantin, B., Lamarche, B., Despres, J.P., Dagenais, G.R., Tunstall-Pedoe, H., Woodward, M., Ben-Shlomo, Y., Davey Smith, G., Palmieri, V.,

Yeh, J.L., Rudnicka, A., Ridker, P., Rodeghiero, F., Tosetto, A., Shepherd, J., Ford, I., Robertson, M., Brunner, E., Shipley, M., Feskens, E.J., Kromhout, D., Dickinson, A., Ireland, B., Juzwishin, K., Kaptoge, S., Lewington, S., Memon, A., Sarwar, N., Walker, M., Wheeler, J., White, I. & Wood, A. Plasma fibrinogen level and the risk of major cardiovascular diseases and nonvascular mortality: an individual participant meta-analysis. *JAMA* **294**, 1799-809 (2005).

29. de Moerloose, P., Boehlen, F. & Neerman-Arbez, M. Fibrinogen and the risk of thrombosis. *Semin Thromb Hemost* **36**, 7-17 (2010).
30. Kaptoge, S., White, I.R., Thompson, S.G., Wood, A.M., Lewington, S., Lowe, G.D. & Danesh, J. Associations of plasma fibrinogen levels with established cardiovascular disease risk factors, inflammatory markers, and other characteristics: individual participant meta-analysis of 154,211 adults in 31 prospective studies: the fibrinogen studies collaboration. *Am J Epidemiol* **166**, 867-79 (2007).
31. Kim, P.Y., Stewart, R.J., Lipson, S.M. & Nesheim, M.E. The relative kinetics of clotting and lysis provide a biochemical rationale for the correlation between elevated fibrinogen and cardiovascular disease. *J Thromb Haemost* **5**, 1250-6 (2007).
32. Falls, L.A. & Farrell, D.H. Resistance of gammaA/gamma' fibrin clots to fibrinolysis. *J Biol Chem* **272**, 14251-6 (1997).
33. Farrell, D.H. Gamma' fibrinogen as a novel marker of thrombotic disease. . *Clinical chemistry and laboratory medicine: CCLM/FESCC* **50**, 1903-1909 (2012).
34. Cheung, E.Y., Vos, H.L., Kruip, M.J., den Hertog, H.M., Jukema, J.W. & de Maat, M.P. Elevated fibrinogen gamma' ratio is associated with cardiovascular diseases and acute phase reaction but not with clinical outcome. *Blood* **114**, 4603-4; author reply 4604-5 (2009).
35. Lovely, R.S., Yang, Q., Massaro, J.M., Wang, J., D'Agostino, R.B., O'Donnell, C.J., Shannon, J. & Farrell, D.H. Assessment of genetic determinants of the association of gamma' fibrinogen in relation to cardiovascular disease. *Arterioscler Thromb Vasc Biol* **31**, 2345-52 (2011).
36. Appiah, D., Heckbert, S.R., Cushman, M., Psaty, B.M. & Folsom, A.R. Lack of association of plasma gamma prime (gamma') fibrinogen with incident cardiovascular disease. *Thromb Res* **143**, 50-2 (2016).

37. Aigner, T., Schmitz, N. & Haag, J. Nanomedicine: AFM tackles osteoarthritis. *Nat Nanotechnol* **4**, 144-5 (2009).

38. Carvalho, F.A. & Santos, N.C. Atomic force microscopy-based force spectroscopy--biological and biomedical applications. *IUBMB Life* **64**, 465-72 (2012).

39. Cross, S.E., Jin, Y.S., Rao, J. & Gimzewski, J.K. Nanomechanical analysis of cells from cancer patients. *Nat Nanotechnol* **2**, 780-3 (2007).

40. Chen, Y., Gao, T., Wang, Y. & Yang, G. Investigating the Influence of Magnesium Ions on p53-DNA Binding Using Atomic Force Microscopy. *Int J Mol Sci* **18** (2017).

41. Koo H, P.I., Lee Y, Kim HJ, Jung JH, Lee JH, Kim Y, Kim JH, Park JW. Visualization and Quantification of MicroRNA in a Single Cell Using Atomic Force Microscopy. *J Am Chem Soc* **138**, 11664-11671 (2016).

42. Assayag EB, B.I., Kesler A, Berliner S, Shapira I, Bornstein NM. Erythrocyte aggregation as an early biomarker in patients with asymptomatic carotid stenosis. *Dis Markers* **24**, 33-39 (2008).

43. Sabeti, S., Exner, M., Mlekusch, W., Amighi, J., Quehenberger, P., Rumpold, H., Maurer, G., Minar, E., Wagner, O. & Schillinger, M. Prognostic impact of fibrinogen in carotid atherosclerosis: nonspecific indicator of inflammation or independent predictor of disease progression? *Stroke* **36**, 1400-4 (2005).

44. Fatah, K., Hamsten, A., Blomback, B. & Blomback, M. Fibrin gel network characteristics and coronary heart disease: relations to plasma fibrinogen concentration, acute phase protein, serum lipoproteins and coronary atherosclerosis. *Thromb Haemost* **68**, 130-5 (1992).

45. Norgren, L., Hiatt, W.R., Dormandy, J.A., Nehler, M.R., Harris, K.A., Fowkes, F.G., Group, T.I.W., Bell, K., Caporusso, J., Durand-Zaleski, I., Komori, K., Lammer, J., Liapis, C., Novo, S., Razavi, M., Robbs, J., Schaper, N., Shigematsu, H., Sapoval, M., White, C., White, J., Clement, D., Creager, M., Jaff, M., Mohler, E., 3rd, Rutherford, R.B., Sheehan, P., Sillesen, H. & Rosenfield, K. Inter-Society Consensus for the Management of Peripheral Arterial Disease (TASC II). *Eur J Vasc Endovasc Surg* **33**, S1-75 (2007).

46. Carvalho, F.A., de Oliveira, S., Freitas, T., Gonçalves, S. & Santos, N.C. Variations on fibrinogen-erythrocyte interactions during cell aging. *PLoS One* **6**, e18167 (2011).

Annexes ▫

Published articles

Article 1

Nanomedicine: Nanotechnology, Biology, and Medicine
14 (2018) 909–918

nanomedicine
Nanotechnology, Biology, and Medicine

nanomedjournal.com

Sensing adhesion forces between erythrocytes and γ' fibrinogen, modulating fibrin clot architecture and function

Ana Filipa Guedes[a,b], Filomena A. Carvalho[a], Marco M. Domingues[a,b], Fraser L. Macrae[b], Helen R. McPherson[b], Nuno C. Santos[a,*,1], Robert A.S. Ariëns[b,**,1]

[a]*Instituto de Medicina Molecular, Faculdade de Medicina, Universidade de Lisboa, Lisboa, Portugal*

[b]*Thrombosis and Tissue Repair Group, Division of Cardiovascular and Diabetes Research, Leeds Institute of Cardiovascular and Metabolic Medicine and Multidisciplinary Cardiovascular Centre, Faculty of Medicine and Health, University of Leeds, Leeds, United Kingdom*

Received 11 April 2017; accepted 11 January 2018

Abstract

Plasma fibrinogen includes an alternatively spliced γ-chain variant (γ'), which mainly exists as a heterodimer (γAγ') and has been associated with thrombosis. We tested γAγ' fibrinogen-red blood cells (RBCs) interaction using atomic force microscopy-based force spectroscopy, magnetic tweezers, fibrin clot permeability, scanning electron microscopy and laser scanning confocal microscopy. Data reveal higher work necessary for RBC-RBC detachment in the presence of γAγ' rather than γAγA fibrinogen. γAγ' fibrinogen–RBCs interaction is followed by changes in fibrin network structure, which forms an heterogeneous clot structure with areas of denser and highly branched fibrin fibers. The presence of RBCs also increased the stiffness of γAγ' fibrin clots, which are less permeable and more resistant to lysis than γAγA clots. The modifications on clots promoted by RBCs-γAγ' fibrinogen interaction could alter the risk of thrombotic disorders.

© 2018 Elsevier Inc. All rights reserved.

Key words: Cell adhesion; Atomic force microscopy; Magnetic tweezers; Fibrin clot; γ' fibrinogen

Fibrinogen is a 340 kDa homodimeric plasma glycoprotein, composed of three pairs of polypeptide chains, denoted Aα, Bβ and γ, linked together by 29 disulphide bonds.[1] A common variant of the fibrinogen is produced by alternative splicing of mRNA of the γ-chain, called γ' fibrinogen.[2] The γ' isoform has a substitution of the final 4 carboxyl-terminal amino acid residues (AGDV) of the prevalent γA-chain with a different 20-amino acid residue sequence (VRPEHPAETEYDSLYPEDDL), which includes a high proportion of negatively charged residues and two sulfated tyrosines. This variant accounts for 8%-15% of all plasma fibrinogen, largely in the form of the heterodimer γAγ', while the homodimer γ'γ' accounts for less than 1% of total plasma fibrinogen.[3] γ' fibrinogen has distinct biochemical and biophysical properties that distinguish it from the more common γA isoform.[4–6] Studies have highlighted that abnormal plasma levels of γAγ' fibrinogen are associated with thrombotic diseases, such as coronary artery disease,[7] myocardial infarction[8] and stroke.[9] Elevated levels of γ' fibrinogen in patients with

Abbreviations: γ', gamma prime fibrinogen; AFM, atomic force microscopy; γA, the most common fibrinogen variant; RBCs, red blood cells; CVD, cardiovascular diseases; FXIII, factor XIII; SEM, scanning electron microscopy; LSCM, laser scanning confocal microscopy

Funding: This work was supported by Fundação para a Ciência e a Tecnologia–Ministério da Ciência, Tecnologia e Ensino Superior (FCT-MCTES, Portugal; PTDC/QUI-BIQ/119509/2010, PTDC/BBB-BMD/6307/2014 and SFRH/BD/84414/2012), the British Heart Foundation (RG/13/3/30104) and the Garfield Weston Trust.

Conflicts of interest: The authors have no conflicts of interest to disclose.

*Correspondence to: N.C. Santos, Instituto de Medicina Molecular, Faculdade de Medicina, Universidade de Lisboa, Av. Prof. Egas Moniz, 1649-028 Lisboa, Portugal.

**Correspondence to: R. Ariëns, Thrombosis and Tissue Repair Group, Division of Cardiovascular and Diabetes Research, Leeds Institute of Cardiovascular and Metabolic Medicine and Multidisciplinary Cardiovascular Centre, Faculty of Medicine and Health, University of Leeds, Leeds, Clarendon Way, Leeds LS2 9JT, United Kingdom.

E-mail addresses: nsantos@fm.ul.pt (N.C. Santos), r.a.s.ariens@leeds.ac.uk (R.A.S. Ariëns).

[1] Equal contribution.

https://doi.org/10.1016/j.nano.2018.01.006
1549-9634/© 2018 Elsevier Inc. All rights reserved.

cardiovascular disease (CVD) were independent of the total plasma fibrinogen concentration.[7] This could indicate that the proportion of γ' variant in plasma may be a risk factor for cardiovascular pathologies. However, reduced concentrations have been associated with microangiopathy syndrome[10] and deep vein thrombosis.[11] Studies by Appiah *et al* did not support the hypothesis that γ' fibrinogen influences CVD events through its prothrombotic properties. Rather, γ' fibrinogen concentrations seem to reflect general inflammation that accompanies and may contribute to atherosclerotic CVD, instead of γ' fibrinogen being a causal risk factor.[12] In addition to this, Walton *et al* found that elevated levels of γAγA fibrinogen promoted arterial thrombosis *in vivo*, whereas γAγ' fibrinogen did not.[13] Nevertheless, as γ' chain modulates clot formation *in vitro*, further studies are required to elucidate its functional properties and its possible relationship with bleeding disorders or thrombosis.

The formation of a thrombus and subsequent impairment of blood flow to vital organs are the immediate cause of CVD events.[14] The architecture of the clot network affects clot stability, particularly its viscoelastic or mechanical properties and fibrinolytic characteristics.[15,16] These aspects can determine if the clot is broken down by fibrinolysis or if it will lead to occlusion or embolization.[17] Other studies have indicated the clinical relevance of fibrin clot structure. It has been shown that tightly packed and rigid clots with thinner fibers and low porosity are less susceptible to the action of thrombolytic agents,[18,19] and a prolonged clot lysis time has been associated with CVD events.[20] Several studies have shown that clots produced from γAγ' fibrinogen have a different structure and behave differently from γAγA clots.[4–6] Fibrin clots formed in the presence of the fibrinogen γ' variant are more resistant to fibrinolysis, due to reduced binding of plasminogen and tissue plasminogen activator, leading to reduced plasmin generation.[21] Fibrinogen γ' variant is associated with a heterogeneous, non-uniform clot structure, with more branch points than clots formed by γA chains.[6,22,23] In addition, γ' fibrinogen binds to thrombin exosite II.[24] The binding of thrombin to the γ' chain has been reported to modulate thrombin activity, particularly towards substrates that require exosite II interaction such as coagulation factors FV and FVIII (but not those dependent on exosite I interactions, e.g. fibrinogen and factor FXIII), which may influence clot structure.[6] However, some of the effects of γ' fibrinogen on clot structure have been shown to be independent of thrombin, as clots produced with snake venom enzyme ancrod, which cleaves fibrinopeptide A from fibrinogen but not fibrinopeptide B, show similar structural abnormalities as those produced with thrombin.[22] On the other hand, it has been shown that the high affinity binding of thrombin to γAγ' fibrin protects thrombin from inhibition by antithrombin, raising the possibility that γAγ' fibrin serves as a scavenger and reservoir for thrombin in the clot.[25]

Fibrinogen is thought to contribute to CVD, not only through altering the fibrin network structure, but also through several other mechanisms, such as promoting red blood cell (RBC) aggregation.[26] Although several studies on isolated fibrin clots have been performed, *in vitro* experiments using fibrin blood clots containing RBCs are scarce in the literature. RBCs play a role in blood coagulation by increasing blood viscosity, which is associated with propensity for clot formation.[27] RBCs have been shown to interact specifically with fibrinogen, with *ca.* 20,000 binding sites *per* RBC and a dissociation constant, K_d, of approximately 1.3 μM.[28] We have identified a specific receptor for fibrinogen on the surface of RBCs.[29–31]

Despite their significance in thrombosis and hemostasis, relatively few studies have been conducted to describe the effects of RBCs on blood clot structure, particularly with different fibrinogen variants. One complication of studying RBC-rich thrombi is that incorporation of RBCs into a thrombus seems uncontrolled and variable. This scarcity may also be, in part, due to the fact that the presence of RBCs in a clot often interferes with the techniques available to monitor clot structure.[32]

The present study aimed to investigate, through atomic force microscopy-based force spectroscopy, the adhesion of RBCs in the presence of γAγA or γAγ' fibrinogen variants. Moreover, we aimed to understand the effect of RBC-γAγ' fibrinogen interactions on fibrin clot structure, properties and function through scanning electron microscopy, laser scanning confocal microscopy, magnetic tweezers and permeability studies.

Methods

Purification of γAγA and γAγ' fibrinogen

The γAγA and γAγ' fibrinogen variants were purified from human plasminogen-depleted fibrinogen using anion-exchange chromatography (Millipore, Billerica, MA) as previously described.[22,23] Detailed description of the method can be found in Supplementary Material.

Human RBCs isolation

Blood from healthy donors was obtained, with written informed consent, at the Instituto Português do Sangue e da Transplantação (IPST, Lisbon) and at the University of Leeds. This study was approved by the joint Ethics Committee of Faculdade de Medicina da Universidade de Lisboa and Centro Hospitalar Lisboa Norte, and by the University of Leeds Medical School Ethical Committee. RBCs were isolated through standard procedures.[29–31]

Atomic force microscopy (AFM): cell–cell adhesion

AFM studies were performed on a NanoWizard II atomic force microscope with a CellHesion 200 module (JPK Instruments, Berlin, Germany), mounted on an Axiovert200 inverted optical microscope (Zeiss, Jena, Germany). RBCs were attached to tipless cantilevers through the functionalization with concanavalin A (for details see Supplementary Material). RBCs on the substrate were adhered to poly-L-lysine coated glass slides. RBC–RBC adhesion was measured in the presence of different fibrinogen variant concentrations, from 0 to 1.0 mg/ml. Detailed description of the method can be found in Supplementary Material.

Magnetic tweezers

To examine the viscoelastic properties of the fibrin clots, magnetic tweezers were used. The magnetic microrheometer operates by applying a force of 40 pN to a 4.5 μm super-paramagnetic bead (Dynabeads M-450 Epoxy, Invitrogen, Paisley, UK) using a magnetic field gradient generated by four

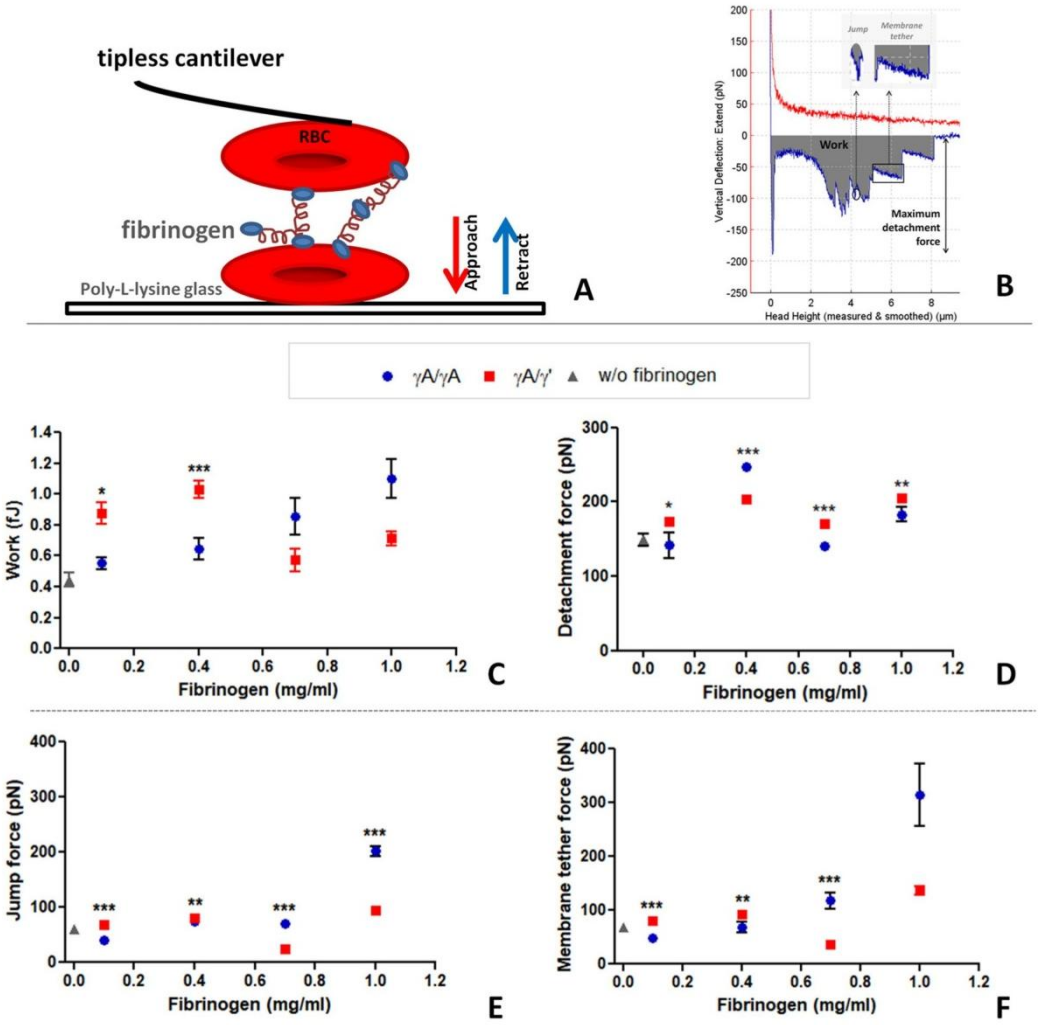

Figure 1. AFM cell–cell adhesion data. **(A)** Schematic representation of the adhesion between two RBCs (one chemically attached to the cantilever and the other on the poly-L-lysine-treated substrate) in the presence of fibrinogen variants. **(B)** Representative force–distance curve with the relevant analyzed parameters, namely, work of cell–cell detachment (grey area), maximum detachment force, jumps and membrane tethers (insets magnify examples of a jump and a membrane tether event on the force–distance curve). **(C)** Work necessary to overcome RBC-RBC adhesion in the presence of different concentrations of γAγA or γAγ' fibrinogen (*, $P = 0.0275$; ***, $P < 0.0001$). **(D)** Maximum detachment force to detach two RBCs (*, $P = 0.0279$; **, $P = 0.0054$; ***, $P < 0.0001$). **(E)** Jumps and **(F)** membrane tethers force data (**, $P \leq 0.0069$; ***, $P < 0.0001$) in the presence of each fibrinogen variant or in their absence. Values are presented as mean ± standard error of mean (SEM).

electromagnets in 2D directions. The device was used coupled with an Olympus IX71 inverted microscope (Olympus, UK) incorporating an ultralong working objective (40× magnification) and a CCD camera. Particle tracking, electromagnet control and image analysis were performed in real time using custom written Labview 7.1 software (National Instruments, Newbury, UK). Fibrin clots were formed with and without RBCs. The viscoelastic properties were measured using the procedure of Evans *et al.*[33] The parameters G', G" and Tan δ were calculated at a frequency of 0.1 Hz. The displacement of 8 random magnetic beads was measured *per* sample, and each sample was studied at least in triplicate. Please find detailed description in Supplementary Material.

Fibrin clot permeability

To study the clot permeability, samples were prepared in triplicate, according to the standardized protocol published by the Fibrinogen and FXIII Subcommittee of the International Society on Thrombosis and Hemostasis (ISTH).[34] Purified

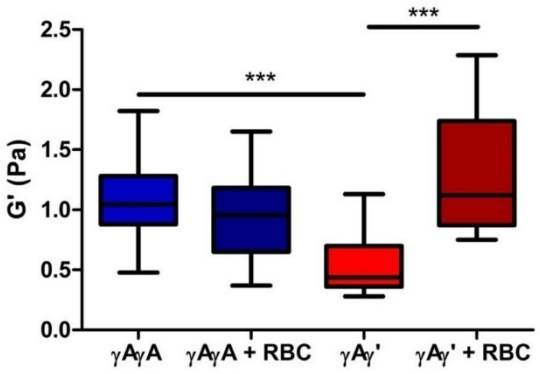

Figure 2. Viscoelastic properties of the purified γAγA and γAγ' fibrinogen clots. Storage modulus G' (elastic modulus) data are presented in the presence of 0.5% RBCs and in the absence of RBCs (***, $P < 0.0001$ for γAγA *vs.* γAγ' and for γAγ' *vs.* γAγ' + RBC). Fibrinogen concentration was 0.5 mg/ml. Values are presented as mean ± SEM.

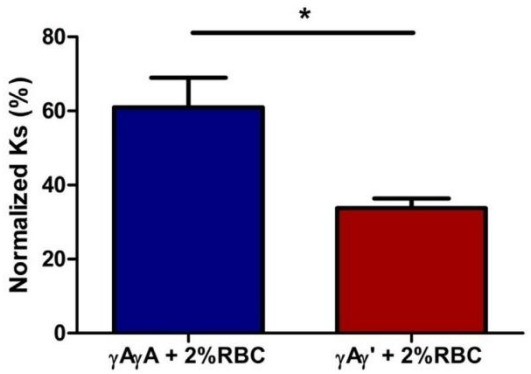

Figure 3. Normalized permeability data (normalized in percentage against K_s of each variant without RBCs) in the presence of RBCs for fibrin clots formed with purified γAγA or γAγ' fibrinogen. Darcy constant, K_s, represents the average size of the pores within the clot (*, $P = 0.0319$). Values are presented as mean ± SEM.

fibrinogen samples (final concentration of 1 mg/ml) were incubated with 1 U/ml human thrombin (Calbiochem, Nottingham, UK) and 2.5 mM $CaCl_2$. Samples were placed in mechanically scratched open clotting tips for 120 min, at room temperature, in a humidity chamber. A detailed description of the method can be seen in Supplementary Material.

Scanning electron microscopy

Scanning electron microscopy (SEM) was used to further investigate the structure of clots formed with γAγA and γAγ′ fibrinogen in the presence or in the absence of RBCs.

Clots were generated by adding 100 μl of γAγA or γAγ' fibrinogen variants (final concentration of 1 mg/ml) to 10 μl of activation mixture (human thrombin 1 U/ml and 10 mM $CaCl_2$, final concentrations, in TBS (50 mM Tris, 100 mM NaCl, pH 7.5)). All details of the procedure are described in Supplementary Material.

Laser scanning confocal microscopy

Fibrin clots were prepared according to the procedure described in Supplementary Material. Three random areas of the clot were visualized under higher magnification. 20 μm optical z-stacks were obtained and projected into 2D images. In order to obtain 3D images of the fibrin clots, 40 μm z-stacks were also performed. Confocal microscopy was also used to assess, in real time, the rate of fibrinolysis following the procedure also described in Supplementary Material.

Statistical analysis

Descriptive statistics are given as mean ± standard error of mean (SEM). Unpaired Student's *t*-test was used for statistical analysis of comparisons between two groups. Non-parametric analysis was also performed in cell–cell adhesion data, applying the Mann Whitney U test. *P* values below 0.05 were considered to indicate statistical significance. Statistical analyses were performed using GraphPad Prism 5 (La Jolla, CA, USA).

Results

RBC–RBC adhesion is altered in the presence of fibrinogen variants

Atomic force microscopy experiments were performed to investigate RBC cell–cell adhesion and the influence of γAγ' and γAγA fibrinogen variants in the cells adhesion. We evaluated the interaction between RBCs, in the presence of different concentrations of γAγA and γAγ' fibrinogen variants, up to 1.0 mg/ml, by force–distance retract curves (Figure 1).

Force spectroscopy data showed that, in the presence of low concentrations of γAγ' fibrinogen, the work (thermodynamic parameter corresponding to the area under the curve on a force × distance plot, Figure 1, *B*) required to detach one RBC from another was higher than in the presence of the same concentration of γAγA fibrinogen (0.87 ± 0.07 fJ *vs.* 0.55 ± 0.04 fJ, $P = 0.0275$, for 0.1 mg/ml fibrinogen, and 1.03 ± 0.06 fJ *vs.* 0.65 ± 0.07 fJ, $P < 0.0001$, for 0.4 mg/ml fibrinogen) (Figure 1, *C*). At higher concentrations of fibrinogen variants, statistically significant differences between both variants were not observed (for 1.0 mg/ml fibrinogen, 0.71 ± 0.05 fJ for γAγ' *vs.* 1.10 ± 0.13 fJ for γAγA, $P = 0.144$; for 0.7 mg/ml fibrinogen, 0.57 ± 0.07 fJ for γAγ' *vs.* 0.86 ± 0.04 fJ for γAγA, $P = 0.248$). γAγA fibrinogen concentrations showed a clear dose–response for interactions with RBCs, whereas γAγ' had a dual effect at low and high concentrations (Figure 1, *C*). Values of the maximum detachment force (schematically explained in Figure 1, *B*) were also calculated. As shown on Figure 1, *D*, statistically significant differences between the values of maximum RBC-RBC detachment force in the presence of γAγ' or γAγA fibrinogen were found at all fibrinogen concentrations: for 0.1 mg/ml fibrinogen, 141.8 ± 17.2 pN for γAγA *vs.* 173.6 ± 0.85 pN for γAγ', $P = 0.0279$; for 0.4 mg/ml fibrinogen, 246.3 ± 5.64 pN for γAγA *vs.* 203.7 ± 0.70 pN for γAγ', $P < 0.0001$; for 0.7 mg/ml fibrinogen, 141.2 ± 5.35 pN for γAγA *vs.* 170.3 ± 0.95 pN for γAγ', $P < 0.0001$; and, for 1 mg/ml fibrinogen, 182.9 ± 9.80 pN for γAγA *vs.* 205.5 ± 1.90 pN for γAγ', $P = 0.0054$). With the exception of the data obtained for 0.4 mg/ml fibrinogen, the values of maximum

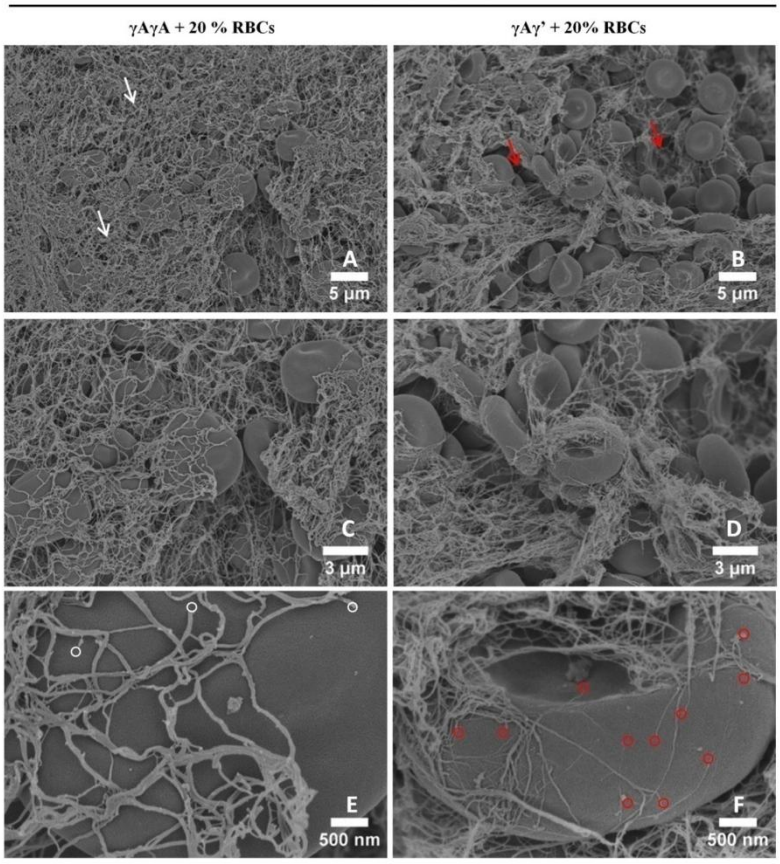

Figure 4. Scanning electron micrographs of fibrin fiber clots with 20% of RBCs. Fibers were formed from 1.0 mg/ml fibrinogen variants γAγA **(A, C** and **E)** and γAγ' **(B, D** and **F)**. White arrows in **A** indicate the more homogeneous structure in the γAγA clot network, when compared with the areas of small and large holes, pinpointed by red arrows in **B**, associating a more heterogeneous structure to the γAγ' clots. The free fiber ends and the fiber-to-RBC points of connections are represented as small circles, being more frequent for γAγ' (red circles in **F**) than for γAγA (white circles in **E**). Magnifications: **A** and **B**, 2500×; **C** and **D**, 5000×; **E** and **F**, 25,000×.

detachment force obtained for γAγA fibrinogen were always lower than those of γAγ' fibrinogen.

After the initial maximum detachment force, two types of jumps could be observed on the force curves (Figure 1, *B*): jumps preceded by a ramp of force or jumps preceded by a force plateau. We considered a membrane tether as a step in force detected after a force plateau of 0.25 µm in distance. Jump events were assigned to the unbinding of membrane ligand–receptor interactions without a preceding membrane deformation, while membrane tether events corresponded to situations where a membrane tether was extruded before the unbinding of the ligand–receptor complex (Figure 1, *B*).[35] A combination of each of the parameters extracted from the force–distance curves (maximum detachment force, number of jumps events/curve × mean force of jumps and number of membrane tethers events × mean force of tethers) could be considered as the value of the work needed to detach one cell from another. Similarly to the values of work (Figure 1, *C*), the same profile is observed for the values of force of jumps and membrane tethers events with increasing fibrinogen concentrations when comparing both fibrinogen variants. As depicted in Figure 1, *E*, *F*, at lower fibrinogen concentrations, jumps and membrane tethers displayed higher forces for γAγ' fibrinogen, when compared to γAγA variant, both for 0.1 mg/ml fibrinogen (jumps, 68.52 ± 2.42 pN *vs.* 40.40 ± 0.80 pN, $P < 0.0001$; membrane tethers, 79.80 ± 7.06 pN *vs.* 47.56 ± 3.37 pN, $P < 0.0001$) and 0.4 mg/ml fibrinogen (jumps, 80.82 ± 3.45 pN *vs.* 74.94 ± 3.31 pN, $P = 0.0061$; membrane tethers, 91.91 ± 6.32 pN *vs.* 68.08 ± 9.69 pN, $P = 0.0069$). Figure 1, *E*, *F* also shows that, at higher fibrinogen concentrations, similarly to the values of work, higher forces of jumps and membrane tethers were measured for γAγA fibrinogen, when compared to the γAγ' variant. This becomes evident at 0.7 mg/ml of fibrinogen (jumps, 70.94 ± 4.36 pN *vs.* 24.01 ± 0.77 pN, $P < 0.0001$; membrane tethers, 117.75 ± 14.64 pN *vs.* 36.47 ± 5.13 pN, $P < 0.0001$) and at 1.0 mg/ml of fibrinogen (jumps, 201.51 ± 8.54 pN *vs.* 93.41 ± 2.85 pN, $P < 0.0001$; membrane tethers, 313.95 ± 58.05 pN *vs.* 135.51 ± 7.98 pN, $p > 0.05$).

RBCs influence γAγ' fibrin clot mechanical properties

The viscoelastic properties of γAγA and γAγ' fibrin clots were examined using a magnetic microrheometer and the

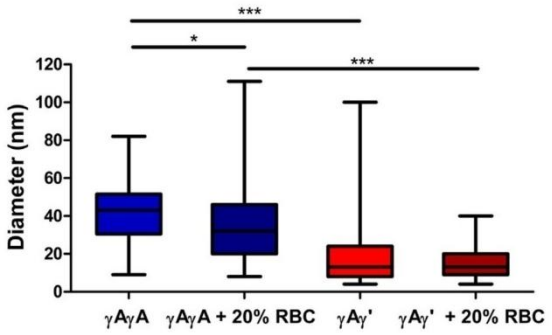

Figure 5. Diameters of purified γAγA and γAγ' fibrin fibers in the absence or in the presence of 20% of RBCs. Fiber diameters were measured from 20 random fibers of each image using a 50,000× magnification (*, $P = 0.0439$; ***, $P < 0.0001$).

influence of RBCs was studied. In agreement with previous findings,[22] we observed that γAγA clots were stiffer than γAγ' clots (storage modulus, G', 1.076 ± 0.065 Pa *vs.* 0.512 ± 0.051 Pa, respectively; $P < 0.0001$; Figure 2). The presence of RBCs in the γAγA fibrin clots did not statistically change their stiffness. On the other hand, a significant increase in the stiffness of γAγ' clots was observed in clots with RBCs, when compared to those without RBCs (1.220 ± 0.104 Pa *vs.* 0.512 ± 0.051 Pa, respectively; $P < 0.0001$). There were no significant differences on storage modulus G' between γAγA and γAγ' clots in the presence of RBCs; however, there was a trend for the γAγ' clots to be stiffer than γAγA clots (Figure 2).

In addition, we observed a statistically significant change on loss tangent (Tan δ) comparing γAγA clots with RBCs and without RBCs (0.460 ± 0.066 *vs.* 1.013 ± 0.126, respectively; $P = 0.0008$), but only a trend for higher Tan δ in γAγ' with RBCs than for this variant in the absence of RBCs (data not shown).

RBCs reduce γAγ' fibrin clot permeability

To characterize the fibrin network of γAγA and γAγ' fibrin with and without RBCs, permeability experiments were performed. The results for the Darcy constant (K_s), which represents the pore size of the fibrin clot, are shown in Figure 3.

Importantly, in the presence of RBCs, normalized K_s was higher for γAγA fibrin clots with RBCs ($(2.44 \pm 0.31) \times 10^{-9}$ cm^2) than for γAγ' fibrin clot with RBCs ($(1.40 \pm 0.10) \times 10^{-9}$ cm^2) ($P = 0.0001$). Thus, when comparing clots of both fibrinogen variants with RBCs, the γAγ' clots were less porous.

RBCs influence γAγA and γAγ' fibrin clot structure

Scanning electron microscopy data showed differences between the structures of the fibers formed by γAγA or γAγ' fibrinogen (different magnification micrographs from each sample are shown in Figure S1 in the supplementary information).

We next investigated the structure of clots formed *in vitro* in the presence of RBCs to determine the effect that these cells might have on clot structure *in vivo*. RBCs tended to be heterogeneously spread throughout the sample, particularly in clots produced with γAγ' fibrin (Figure 4). Upon the addition of 20% RBCs, the structure of the γAγ' clot became more heterogeneous, with densely packed fiber regions, as well as, large holes where more RBCs were located (Figure 4, *B*, *D*, *F*). γAγ' fibrin fibers were thinner and the network of the clot showed more interconnections with RBCs compared to γAγA fibers. On the micrographs of Figure 4, *B*, *D* and *F*, it can be noticed that γAγ' fibrin clots contained more free fiber ends and there were more fiber-to-RBC points of connections, when compared to γAγA fibrin clots (Figure 4, *A*, *C*, *E*), resulting in "clustered" cell arrangements.

In order to measure the diameter of the fibers, twenty fibers from 50,000× magnification images were assessed on 2 different clots from each condition and in 3 different zones of the clot. Average fiber diameters were smaller in γAγ' fibrin compared to the γAγA variant (18.29 ± 1.32 nm *vs.* 41.10 ± 1.58 nm, $P < 0.0001$; Figure 5). The presence of RBCs in the fibrin clot caused a decrease of the γAγA fibers diameters compared to the clot without RBCs (41.10 ± 1.58 nm in the absence of RBCs *vs.* 35.39 ± 2.46 nm in their presence, $P = 0.044$) (Figure 5). The presence of RBCs on clots with γAγ' fibers did not statistically change the diameter of the fibers compared to the clots without cells. However, clots with RBCs and prepared with γAγ' fibrinogen led to thinner fibers than those produced with γAγA fibrinogen and RBCs (35.39 ± 2.46 nm for γAγA *vs.* 15.23 ± 0.98 nm for γAγ', $P < 0.0001$; Figure 5).

Increased fibrinolytic resistance of γAγ' fibrin clots in the presence of RBCs

We used laser scanning confocal microscopy LSCM to study clot structure and resistance to fibrinolysis in the presence and absence of RBCs for each fibrin variant.

Figure 6 shows representative examples of the confocal micrographs obtained for fiber clots made with γAγA and γAγ' purified fibrinogen variants. In clots formed with γAγA fibrinogen, the area occupied by the fibers seems to be larger (Figure 6, *A*) than for the clots with γAγ' fibrinogen (Figure 6, *B*). However, these differences were not statistically significant. In agreement with SEM imaging and with previous studies,[22] there was a clear difference between the structures of γAγA and γAγ' fibrin. The γAγA fibrin clots were composed of longer and straighter fibers than γAγ' fibrin clots. The later showed fibers that were shorter and clustered, producing larger pores. However, we did not find differences regarding the fiber density comparing γAγA with γAγ' fibrin clots (Figure S2).

Relevant was to study the micrographs of fibrin clots from γAγA and γAγ' fibrinogen variants in the presence of 2% of RBCs, as shown on Figure 6, *C*, *D*. In the presence of γAγA fibrinogen, the network of the fibers seemed straighter and denser. In clots with γAγ' fibers, we observed that the fibers were more clustered and the RBCs were more visible. We also studied fibrin clots in the presence of 5% and 10% of RBCs by LSCM; however, the high number of RBCs did not allow clearly differentiating fibrin fibers from RBCs. Thus, technical limitations restricted us to increase the amount of RBCs closer to the physiological range (the normal hematocrit is ~40%RBCs).

Finally, we studied fibrinolysis of clots made with both fibrinogen variants (Figure 7). In line with previous studies,[21] a significant increase in lysis time was observed for γAγ' compared with γAγA fibrin clots (15.82 ± 1.48 min *vs.* 10.54 ±

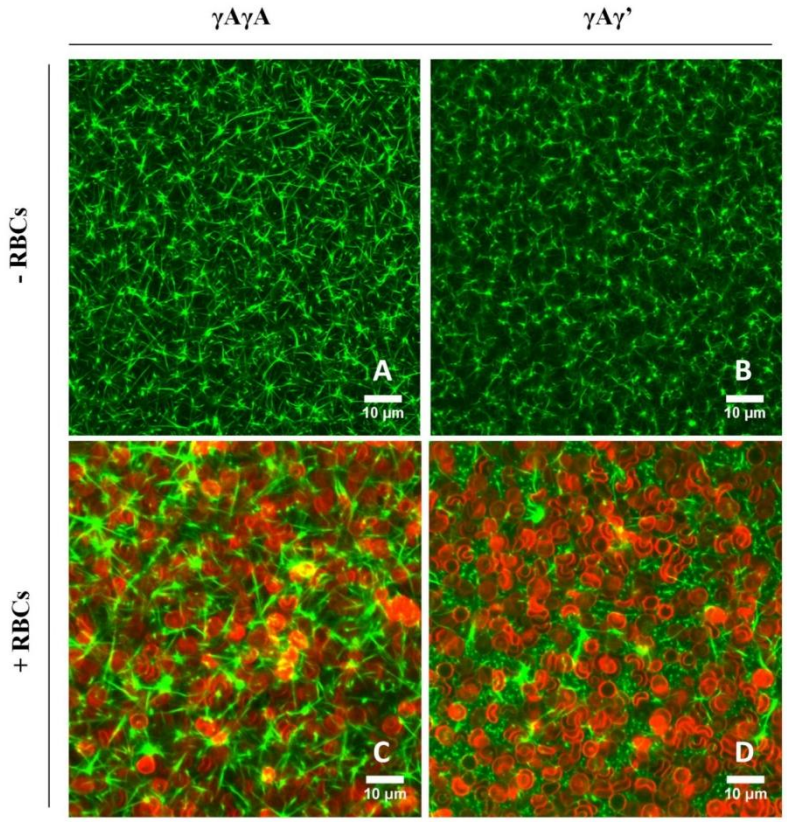

Figure 6. Laser scanning confocal microscopy images of fiber clots formed with purified γAγA **(A and C)** and γAγ' **(B and D)** fibrinogen, at 1.0 mg/ml fibrinogen concentration. Alexa 488-labeled fibrin fibers are shown in green. Confocal micrographs of fiber clots with 2% of RBCs formed with 1.0 mg/ml of purified γAγA **(C)** and γAγ' fibrinogen **(D)**. RBCs were labeled with Vibrant DiD cell-labeling solution (red). Z-stack images at 40 μm and 63× magnification are shown in **A** and **B** and Z-stacks images at 20 μm, also with 63× magnification are shown in panels **C** and **D**.

0.44 min, respectively; $P = 0.0267$). During the experiment, we observed a non-uniform lysis of the γAγ' fibrin clot, taking more time to achieve complete lysis than the γAγA clot (videos in Supplementary information).

We measured the lysis time for γAγA and γAγ' clots in the presence of 5% (data not shown) and 10% of RBCs. Under these conditions, there were no significant differences in fibrinolysis times in the presence of RBCs, when compared to the clots without RBCs. Statistical significance was observed in fibrinolysis times for γAγA *vs.* γAγ' fibrin clots in the presence of RBCs (12.03 ± 0.49 min *vs.* 18.30 ± 1.47 min; $P = 0.0476$).

Discussion

In this study, we evaluated the interaction of purified γAγ' and γAγA fibrinogen with RBCs, as well as their influence on the structure and function of clots formed with both variants. They show a discernible effect of the presence of RBCs on fibrin clot structure and function. To pursue this study further, we purified the main component of plasma fibrinogen, γAγA, and its splice-variant, γAγ'. Cell–cell adhesion studies were performed to evaluate the relative roles of both fibrinogen variants on the interaction between RBCs. We also evaluated the changes of biophysical properties of the clots, by studying their permeability and viscoelastic properties. By laser scanning confocal microscopy and scanning electron microscopy, we directly observed the effects of RBCs on the architecture of clots formed from γAγ' and γAγA fibrinogens.

AFM data showed that in the presence of low concentrations of γAγ' fibrinogen (≤ 0.4 mg/ml), the force of the binding between two RBCs was higher than with γAγA fibrinogen. Statistically significant differences between both fibrinogen variants at all fibrinogen concentrations were obtained for the values of force for the maximum cell–cell detachment, jumps and membrane tether events. Although these three parameters contribute to the values of the work necessary to completely detach two RBCs, no statistically significant variations were obtained for this parameter at fibrinogen concentrations ≥ 0.7 mg/ml.

Thus, at lower fibrinogen concentrations, γAγ' fibrinogen binds more promptly to RBCs, inducing higher RBC-RBC adhesion than γAγA fibrinogen. RBCs adhesion has a clear

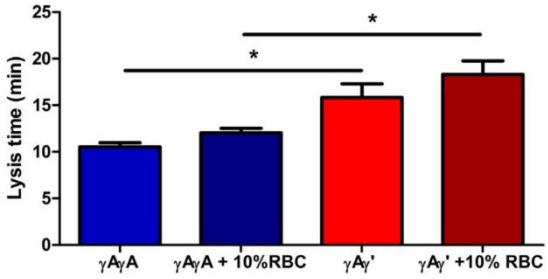

Figure 7. Fibrinolysis time were assessed by laser scanning confocal microscopy from clots formed with purified γAγA and γAγ' fibrinogen, in the absence and presence of RBCs (10%). The serial time scans were taken with 40× magnification. Values are shown as mean ± SEM (*, $P \leq 0.0476$).

γAγA fibrinogen dose response curve, whereas γAγ' did not. This could be due to differences in fibrinogen variant molecular conformations and net protein electrostatic charge, which could lead to different binding affinities at different fibrinogen concentrations. It is known that RBCs present sialic acid residues on their surface, contributing to their negative surface charge, which induces repulsive electrostatic forces that minimize RBC aggregation under blood flow conditions.[36] The binding of the more negatively charged γ' fibrinogen to RBCs may increase the overall negative cell surface charge. This may overcome the strong RBC–RBC interactions observed at lower γAγ' fibrinogen concentration, by lowering cell–cell adhesion forces, due to increased electrostatic repulsion. On the other hand, γAγA fibrinogen lacks the negatively charged sequence of the γ' chain, leading to an increase of RBC-RBC adhesion upon increasing its concentration.

Previous studies have shown that RBCs influence the viscoelastic properties of the clot.[32,37] Our evaluation of the viscoelastic properties of the clots revealed that γAγA fibrin clots are stiffer than γAγ' fibrin clots in the absence of RBCs, in agreement with previous studies on the effect of γAγ' on clot stiffness.[22] Our data show that γAγ' clots are inherently weaker. This is likely due to differences in fibrin fiber structure. We recently demonstrated that fibrinogen γ' influences intrafibrillar structure of fibrin and significantly reduces the average number of protofibrils packed within the fibrin fiber, thereby influencing clot stiffness.[38] In γAγA fibrin clots, more protofibrils are packed within fibrin fibers, which increase the rigidity and the viscosity of the clot, when compared to γAγ' fibrin clots. In this study, the presence of RBCs did not influence the stiffness of the γAγA fibrin clots. In γAγ' fibrin clots, the presence of RBCs resulted in a significant increase in stiffness. This indicates that the combination of γAγ' fibrinogen variant and RBCs may affect clot structure and mechanical properties. The stiffening of the γAγ' fibrin clots in the presence of RBCs may be related to rearrangements of protofibril packing or significant modifications in clot structure. The imaging by SEM of the clot structure in the presence of RBCs, compared to its absence, showed a looser structure in clots produced with γAγ' fibrinogen, which may be more prone to creep, as well as more fiber interconnections, which turn the clot more rigid. Our data indicate that RBCs are not a mere bystander in blood clot formation. Indeed, other studies have shown that RBCs influence fibrin network structure and pore size.[39,40] A decrease in the permeability of fibrin clots after the addition of RBCs was shown to be proportional to the total RBC surface area and their total concentration.[40] Here, we show that the addition of RBCs promotes the decrease of permeability. Importantly, we show that the γAγ' clots with RBCs were less porous than γAγA clots with RBCs. This could potentially lead to pro-thrombotic clots, due to a higher resistance to fibrinolysis.[41] In agreement with this, we also found an increase in the lysis time of γAγ' clots with RBCs, when compared to γAγA clots with RBCs.

According with previous studies,[22,23] SEM and confocal microcopy showed that the clots formed by γAγA and γAγ' fibers have a different structure. The incorporation of RBCs has an important impact on fibrin fiber size and on its network structure. Regions of higher and lower RBC density were clearly visible in the clots made with γ' fibrinogen. In the presence of RBCs, the γ' fibrin clots were more heterogeneous, seeming to form a looser structure when compared with the clots of γA fibrinogen. These findings are supported by our AFM data. At high γAγ' fibrinogen concentrations, the work necessary to detach two RBCs was the same that the one achieved in the presence of γAγA fibrinogen. In agreement with this, the clot might become looser, with a higher ability to deform and embolize, eventually blocking a downstream blood capillary.

The γAγ' fibrin clots contain a large number of free fiber ends. Fiber ends are normally found at low levels in scanning electron micrographs of fibrin clots, and have been suggested to arise from early truncation of protofibril formation or lateral aggregation.[42,43] It was previously proposed that the negative charge of γAγ' fibrinogen on the D-D interface may disrupt oligomerization and, therefore, interrupt the continuous growth of the protofibril, leading to highly branched fibers.[44,45]

This study has shown that the incorporation of RBCs into the clot affects fibrin fiber formation. RBCs induced thinning of fibers in fibrin clots formed with γAγA, but not with γAγ' fibrinogen. However, in the presence of RBCs, γAγA fibers remained significantly thicker than γAγ' fibers. Here, we could conclude that thinner fibrin fibers (such as γAγ' fibrin fibers) form highly branched networks. We propose that growing fibers surround RBCs, interacting with them through an RBC surface receptor. We have already reported the existence of a receptor for fibrinogen on RBCs.[29–31] RBCs specifically bind fibrin(ogen) via an integrin receptor with a β_3 subunit,[29] possibly $\alpha_v\beta_3$.[31]

Previous studies indicated that fibrin clots with increased fiber branching and resistance to fibrinolysis are a risk factor for thrombosis.[15] Fibrinolysis data showed that the lysis time of a γAγ' fibrin clot is longer than for a γAγA clot, as already reported.[4,5] The presence of RBCs seems to increase the lysis time. However these studies were conducted with a 10% hematocrit, due to technical limitations, considerably below the normal hematocrit of ~40% RBCs. Aleman *et al* and Tutwiler *et al* suggested that RBCs cause direct and complex effects on clot structure and stability.[46,47] Furthermore, RBCs can support thrombin generation and decrease fibrinolysis, suggesting that RBCs may promote fibrin deposition during venous thrombosis.[46] Other authors reported the role of RBCs on stabilizing clots based on suppressed tissue plasminogen activator (tPA)-induced fibrinolysis

in RBC-modified fibrin structures. They also observed, using eptifibatide inhibition, that RBCs modulate fibrinolysis through a specific fibrinogen receptor.[41] Collet *et al* demonstrated that fibrin clots with a tight fibrin conformation made of thinner fibers were lysed at a slower rate than those with a loose fibrin conformation made of thicker fibers, although the overall fibrin content remained constant.[48] The γAγ' clot is more heterogeneous than the γAγA clot. The densely packed areas with fibers and RBCs may impair the diffusion of fibrinolytic agents. However, at the same time, there are areas with large holes, where their diffusion may be increased. It was suggested that the slower lysis of γ' clots is due to delayed fibrinopeptide B release, leading to a delay of plasminogen binding and activation.[21]

Some of these findings may provide a mechanism underpinning the epidemiological data suggesting that a high ratio between γAγ' and γAγA fibrinogen variants may be a risk factor for thrombotic disease.[7–9] Further studies on the prothrombotic nature of RBCs and on fibrinogen variants are necessary to fully understand the contribution of the γ' chain and RBCs to different etiologies of thrombotic diseases.

In conclusion, the incorporation of RBCs into a fibrin clot significantly affects the clot structure and its mechanical properties. RBCs interact differently with clots made with γ-chain fibrinogen splice variants, which may explain some of the cardiovascular clinical associations that have been reported with these fibrinogen variants.

Appendix A. Supplementary data

Supplementary data to this article can be found online at https://doi.org/10.1016/j.nano.2018.01.006.

References

1. Brown JH, Volkmann N, Jun G, Henschen-Edman AH, Cohen C. The crystal structure of modified bovine fibrinogen. *Proc Natl Acad Sci U S A* 2000;**97**:85-90.
2. Chung DW, Davie EW, et al. *Biochemistry* 1984;**23**:4232-6.
3. Mosesson MW, Finlayson JS, Umfleet RA. Human fibrinogen heterogeneities. 3. Identification of chain variants. *J Biol Chem* 1972;**247**:5223-7.
4. Collet JP, Nagaswami C, Farrell DH, Montalescot G, Weisel JW. Influence of gamma' fibrinogen splice variant on fibrin physical properties and fibrinolysis rate. *Arterioscler Thromb Vasc Biol* 2004;**24**:382-6.
5. Falls LA, Farrell DH. Resistance of gammaA/gamma' fibrin clots to fibrinolysis. *J Biol Chem* 1997;**272**:14251-6.
6. Siebenlist KR, et al. Studies on the basis for the properties of fibrin produced from fibrinogen-containing gamma' chains. *Blood* 2005;**106**:2730-6.
7. Lovely RS, et al. Association of gammaA/gamma' fibrinogen levels and coronary artery disease. *Thromb Haemost* 2002;**88**:26-31.
8. Mannila MN, et al. Elevated plasma fibrinogen gamma' concentration is associated with myocardial infarction: effects of variation in fibrinogen genes and environmental factors. *J Thromb Haemost* 2007;**5**:766-73.
9. Cheung EY, et al. Fibrinogen gamma' in ischemic stroke: a case-control study. *Stroke* 2008;**39**:1033-5.
10. Mosesson MW, et al. Plasma fibrinogen gamma' chain content in the thrombotic microangiopathy syndrome. *J Thromb Haemost* 2007;**5**:62-9.
11. Uitte de Willige S, de Visser MC, Houwing-Duistermaat JJ, Rosendaal FR, Vos HL, Bertina RM. Genetic variation in the fibrinogen gamma gene increases the risk for deep venous thrombosis by reducing plasma fibrinogen gamma' levels. *Blood* 2005;**106**:4176-83.
12. Appiah D, Schreiner PJ, MacLehose RF, Folsom AR. Association of plasma gamma' fibrinogen with incident cardiovascular disease: the Atherosclerosis Risk in Communities (ARIC) study. *Arterioscler Thromb Vasc Biol* 2015;**35**:2700-6.
13. Walton BL, Getz TM, Bergmeier W, Lin FC, Uitte de Willige S, Wolberg AS. The fibrinogen gammaA/gamma' isoform does not promote acute arterial thrombosis in mice. *J Thromb Haemost* 2014;**12**:680-9.
14. Fuster V, Moreno PR, Fayad ZA, Corti R, Badimon JJ. Atherothrombosis and high-risk plaque: part I: evolving concepts. *J Am Coll Cardiol* 2005;**46**:937-54.
15. Undas A, Ariëns RA. Fibrin clot structure and function: a role in the pathophysiology of arterial and venous thromboembolic diseases. *Arterioscler Thromb Vasc Biol* 2011;**31**:e88-99.
16. Weisel JW. Structure of fibrin: impact on clot stability. *J Thromb Haemost* 2007;**5**(Suppl 1):116-24.
17. Weisel JW. The mechanical properties of fibrin for basic scientists and clinicians. *Biophys Chem* 2004;**112**:267-76.
18. Collet JP, et al. Dusart syndrome: a new concept of the relationship between fibrin clot architecture and fibrin clot degradability: hypofibrinolysis related to an abnormal clot structure. *Blood* 1993;**82**: 2462-2469.
19. Bridge KI, Philippou H, Ariëns R. Clot properties and cardiovascular disease. *Thromb Haemost* 2014;**112**:901-8.
20. Carter AM, Cymbalista CM, Spector TD, Grant PJ. Heritability of clot formation, morphology, and lysis: the EuroCLOT study. *Arterioscler Thromb Vasc Biol* 2007;**27**:2783-9.
21. Kim PY, Vu TT, Leslie BA, Stafford AR, Fredenburgh JC, Weitz JI. Reduced plasminogen binding and delayed activation render gamma'-fibrin more resistant to lysis than gammaA-fibrin. *J Biol Chem* 2014;**289**:27494-503.
22. Allan P, Uitte de Willige S, Abou-Saleh RH, Connell SD, Ariëns RA. Evidence that fibrinogen gamma' directly interferes with protofibril growth: implications for fibrin structure and clot stiffness. *J Thromb Haemost* 2012;**10**:1072-80.
23. Cooper AV, Standeven KF, Ariëns RA. Fibrinogen gamma-chain splice variant gamma' alters fibrin formation and structure. *Blood* 2003;**102**:535-40.
24. Lovely RS, Moaddel M, Farrell DH. Fibrinogen gamma' chain binds thrombin exosite II. *J Thromb Haemost* 2003;**1**:124-31.
25. Fredenburgh JC, Stafford AR, Leslie BA, Weitz JI. Bivalent binding to gammaA/gamma'-fibrin engages both exosites of thrombin and protects it from inhibition by the antithrombin-heparin complex. *J Biol Chem* 2008;**283**:2470-7.
26. de Moerloose P, Boehlen F, Neerman-Arbez M. Fibrinogen and the risk of thrombosis. *Semin Thromb Hemost* 2010;**36**:7-17.
27. Schmid-Schonbein H, Wells R, Goldstone J. Influence of deformability of human red cells upon blood viscosity. *Circ Res* 1969;**25**:131-43.
28. Lominadze D, Dean WL, Tyagi SC, Roberts AM. Mechanisms of fibrinogen-induced microvascular dysfunction during cardiovascular disease. *Acta Physiol (Oxf)* 2010;**198**:1-13.
29. Carvalho FA, et al. Atomic force microscopy-based molecular recognition of a fibrinogen receptor on human erythrocytes. *ACS Nano* 2010;**4**:4609-20.
30. Carvalho FA, de Oliveira S, Freitas T, Gonçalves S, Santos NC. Variations on fibrinogen-erythrocyte interactions during cell aging. *PLoS One* 2011;**6** e18167.
31. Guedes AF, Carvalho FA, Malho I, Lousada N, Sargento L, Santos NC. Atomic force microscopy as a tool to evaluate the risk of cardiovascular diseases in patients. *Nat Nanotechnol* 2016;**11**:687-92.
32. Gersh KC, Nagaswami C, Weisel JW. Fibrin network structure and clot mechanical properties are altered by incorporation of erythrocytes. *Thromb Haemost* 2009;**102**:1169-75.
33. Evans RM, Tassieri M, Auhl D, Waigh TA. Direct conversion of rheological compliance measurements into storage and loss moduli. *Phys Rev E Stat Nonlin Soft Matter Phys* 2009;**80** 012501.

34. Pieters M, Undas A, Marchi R, De Maat MP, Weisel J, Ariëns RA. An international study on the standardization of fibrin clot permeability measurement: methodological considerations and implications for healthy control values. *J Thromb Haemost* 2012;**10**:2179-81.
35. Ribeiro AS, et al. Atomic force microscopy and graph analysis to study the P-cadherin/SFK mechanotransduction signalling in breast cancer cells. *Nanoscale* 2016;**8**:19390-401.
36. Fernandes HP, Cesar CL, Barjas-Castro Mde L. Electrical properties of the red blood cell membrane and immunohematological investigation. *Rev Bras Hematol Hemoter* 2011;**33**:297-301.
37. Carr Jr ME, Hardin CL. Fibrin has larger pores when formed in the presence of erythrocytes. *Am J Physiol* 1987;**253**:H1069-73.
38. Domingues MM, et al. Thrombin and fibrinogen gamma' impact clot structure by marked effects on intrafibrillar structure and protofibril packing. *Blood* 2016;**127**:487-95.
39. Cines DB, et al. Clot contraction: compression of erythrocytes into tightly packed polyhedra and redistribution of platelets and fibrin. *Blood* 2014;**123**:1596-603.
40. van Gelder JM, Nair CH, Dhall DP. The significance of red cell surface area to the permeability of fibrin network. *Biorheology* 1994;**31**:259-75.
41. Wohner N, et al. Lytic resistance of fibrin containing red blood cells. *Arterioscler Thromb Vasc Biol* 2011;**31**:2306-13.
42. Woodhead JL, Nagaswami C, Matsuda M, Arocha-Pinango CL, Weisel JW. The ultrastructure of fibrinogen Caracas II molecules, fibers, and clots. *J Biol Chem* 1996;**271**:4946-53.
43. Hamano A, et al. Thrombophilic dysfibrinogen Tokyo V with the amino acid substitution of gammaAla327Thr: formation of fragile but fibrinolysis-resistant fibrin clots and its relevance to arterial thrombo-embolism. *Blood* 2004;**103**:3045-50.
44. Macrae FL, Domingues MM, Casini A, Ariëns RA. The (patho)physiology of fibrinogen gamma'. *Semin Thromb Hemost* 2016;**42**:344-55.
45. Gersh KC, Nagaswami C, Weisel JW, Lord ST. The presence of gamma' chain impairs fibrin polymerization. *Thromb Res* 2009;**124**:356-63.
46. Aleman MM, Walton BL, Byrnes JR, Wolberg AS. Fibrinogen and red blood cells in venous thrombosis. *Thromb Res* 2014;**133**(Suppl 1):S38-40.
47. Tutwiler V, et al. Kinetics and mechanics of clot contraction are governed by the molecular and cellular composition of the blood. *Blood* 2016;**127**:149-59.
48. Collet JP, et al. Influence of fibrin network conformation and fibrin fiber diameter on fibrinolysis speed: dynamic and structural approaches by confocal microscopy. *Arterioscler Thromb Vasc Biol* 2000;**20**:1354-61.

Supplementary Material

Sensing adhesion forces between erythrocytes and γ' fibrinogen, modulating fibrin clot architecture and function

Ana Filipa Guedes[1,2], Filomena A. Carvalho[1], Marco M. Domingues[1,2], Fraser L. Macrae[2], Helen R. McPherson[2], Nuno C. Santos[1,*#], Robert A. S. Ariëns[2,*#]

Supplementary methods

Purification of γAγA and γAγ' fibrinogen

The variants were separated by chromatography on DE-52 resin using an AKTA Avant 25. Before chromatography, fibrinogen was dissolved in equilibration buffer (39 mM Tris, 5 mM H_3PO_4, 0.5 mM phenylmethylsulfonyl fluoride (PMSF), 1 mM benzamidine and 5 mM ε-aminocaproic acid, pH 8.6). Elution of the fibrinogen variants was established by a concave gradient from equilibration buffer toelution buffer (0.5 M Tris, 0.65 M H_3PO_4, 0.5 mM PMSF, 1 mM benzamidine and 5 mM ε-aminocaproic acid, pH 4.2). Fractions containing γAγA and γAγ' were concentrated using a Vivaspin centrifugal concentrator (Sartorius, Germany). Protein peaks were analyzed by 8%-12%SDS-PAGE electrophoresisand protein concentration was determined by spectrophotometry, using a molar extinction coefficient at 280 nm of 1.51 mg^{-1}.ml.cm^{-1}.

Atomic Force Microscopy (AFM) – Cell-Cell adhesion

For the cell-cell adhesion studies, RBCs were diluted to 0.1% hematocrit on BSGC with $CaCl_2$ and placed on a clean poly-L-lysinecoated glass slide. Cells were firmly attached to poly-L-lysine according to our previous procedures[1,2,3].

RBCs were attached to tipless cantilevers (Arrow TL2, NanoWorld AG, Switzerland) using the lectin concanavalin A. Initially, the cantilever was UV-light treated and then subsequently coated with biotinylated BSA (0.5 mg/ml, at 37ºC, overnight), streptavidin (0.5 mg/ml, for 30 min) and finally biotinylated concanavalin A (0.4 mg/ml, for 30 min). This way, the cell could be attached to the flexible cantilever and brought into contact

with the second cell, attached to poly-L-lysine coated glass slide (substrate). The applied force was adjusted to 300 pN before retraction. Data collection for each force-distance cycle was performed at 2 µm/s, with a z-length of 30 µm. Retraction and extension delays were set to 5 s. Force curves were analyzed using JPK image processing software v. 4.2.61 (JPK Instruments, Berlin, Germany).

Fibrinogen was added, at different concentrations, to BSCG with $CaCl_2$ and allowed to incubate for 15 min before starting the measurements. For each cell attached to the cantilever, approximately 40 force *vs.* distance curves were performed for each fibrinogen concentration (5 curves per RBC on the substrate). At least 3 cantilevers, with 6 different cells attached (2 cells/cantilever) were tested on each condition.

Magnetic tweezers

The fibrin clots were prepared using fibrinogen variants at 0.5 mg/ml, $CaCl_2$ at 5.0 mM and thrombin at 1 U/ml. Magnetic beads were added at 1:250 (v:v), just before the addition of $CaCl_2$ and thrombin. Immediately after thrombin addition, the mixture was transferred to a small capillary tube, which was sealed with vaseline on both ends to avoid sample dehydration. The magnetic beads are trapped within the polymerizing fibrin clot network. Viscoelastic properties of the blood clots after the addition of RBCs were also evaluated. For these experiments, 0.5% of RBCs were added for each condition. In each experiment, an isolated magnetic bead was selected (away from capillary walls) and tested.

The viscoelastic properties were measured, calculating the parameters of G', G'' and Tan δ. The storage modulus, G' (elastic modulus), is a measure of the elastic energy stored during deformation and relates to clot stiffness. The loss modulus G'' (viscous modulus), is a measure of the energy dissipated during deformation and relates to clot viscosity. The loss tangent (Tan δ) or damping factor (G''/G'), indicates the physical behavior of a system, thus showing the ratio of the viscous and the elastic portion of the viscoelastic deformation. For a viscous material, Tan $\delta >> 1$, *i.e.*, G''>>G', whereas for an elastic solid, Tan $\delta << 1$, *i.e.*, G''<<G'. For a viscoelastic material with Tan$\delta \approx 1$, the amounts of energy dissipated and stored are similar.

Fibrin clot permeability

To study clot permeability, samples were prepared in triplicate, according to the standardized protocol published by the Fibrinogen and FXIII Subcommittee of the International Society on Thrombosis and Hemostasis (ISTH).

Briefly, purified fibrinogen samples (final concentration of 1 mg/ml) were incubated with 1 U/ml human thrombin (Calbiochem, Nottingham, UK) and 2.5 mM $CaCl_2$. Samples were incubated in mechanically scratched open clotting tips for 120 min, at room temperature, in a humidity chamber. The tubes with the fibrin clots were connected via a silicone tube to a reservoir containing TBS buffer (50 mM Tris, 100 mM NaCl, pH 7.5), with 4 cm of pressure drop. After the clot had been washed for 120 min, flow rates of buffer through the fibrin clots were calculated every 30 min for 120 min on each tube. For each 30 min time point, the eluted buffer solution was collected and the volume was analyzed by weight measurements using an analytical balance. The fibrin clot permeability was also evaluated with 2% of RBCs. From the extracted data, the Darcy constant, K_s, which represent the average pore size within the clot, was calculated as previously described, using the equation:

$$K_s = \frac{Q \cdot L \cdot \eta}{t \cdot A \cdot \Delta P} \quad (1)$$

where Q is the volume of liquid (ml), with viscosity η (10^{-2} poise), flowing through a clot with length L (1.3 cm) and a cross-sectional area A (0.049 cm^2), in time t (s), under a pressure ΔP (dyn/cm^2). The unit of the resulting Darcy constant is cm^2. The mean value of K_s was calculated from triplicates for each sample.

Scanning electron microscopy

To prepare the clots of γAγA and γAγ' fibrinogen variants (100 µl, final concentration of 1 mg/ml) were added to the activation mixture (10 µl, human thrombin 1 U/ml and $CaCl_2$ 10 mM, final concentrations, in TBS). The mixtures were immediately transferred to pierced Eppendorf lids. Clots were formed in a humidity chamber at room temperature for 120 min. Clots were washed with saline solution to remove excess salt and prepared for microscopy by fixation in 2% glutaraldehyde solution for at least 120 min. Clots were further washed with sodium cacodylate buffer and dehydrated in a series of increasing concentrations of acetone (30–100%). Clots were critical-point dried with CO_2, mounted

onto stubs and sputter-coated with platinum using a Cressington 208 HR (Cressington Scientific Instruments, Watford, UK). Clots were also prepared in the presence of 20% RBCs. They were observed and photographed digitally in at least 3 different areas *per* clot, using a scanning electron microscope Hitachi SU8230 FE-SEM (Hitachi, Tokyo. Japan), at 5 different magnifications (2500×, 5000×, 10000× (data not shown), 25000× and 50000×). Clots were also formed in duplicate. Average fiber diameters were measured from 20 random fibers of each image in high magnification (25000×) using ImageJ software (National Institutes of Health, Bethesda, MD, USA). Each cross-section measurement was performed over a single fibrin fiber and values of the fibrin diameter were extracted and averaged. All cross-section measurements were performed away from the branching points, in order to avoid biased results.

Laser scanning electron microscopy

Fibrin clots were prepared by mixing purified fibrinogen variants (1.0 mg/ml) with $CaCl_2$ (5 mM), 5% AlexaFluor 488 fibrinogen (Invitrogen, Paisley, UK) and TBS buffer. RBCs were labeled with Vibrant DiD cell-labeling solution (Molecular Probes, Leiden, Netherlands) and washed with HEPES buffer (HEPES 10 mM, NaCl 150 mM, pH 7.4) supplemented with 0.05% Pluronic F-127 (Sigma, Saint Louis, MO, USA). Clots with labeled RBCs were performed at a final RBCs concentration (hematocrit) of 2% (just for images), 5% and 10%. After the addition of human thrombin (0.1 U/ml; Calbiochem, Nottingham, UK), the reaction components were gently mixed and immediately transferred into slides (µ-slide $VI^{0.4}$, Ibidi GmbH, Munich, Germany). Clots were incubated for 120 min in a humidity chamber, at room temperature, protected from the light. Laser scanning confocal microscopy (LSCM) was performed using an upright Zeiss LSM510 META (Axioplan 2 stand) microscope (Carl Zeiss, Welwyn Garden City, UK), with a 63× oil immersion objective, using a 488 nm Argon laser and 633 nm HeNe laser.

Confocal microscopy was also used to assess, in real time, the rate of fibrinolysis. Lysis of the fibrin clots was initiated by loading a mixture containing tissue-type plasminogen activator (tPA) at 5 ng/ml (Technoclone, Vienna, Austria) and 1.1 µM Glu-Plasminogen (Enzyme Research, Swansea, UK) in TBS buffer, to the edge of the thrombus in a uniform manner after which the slides were held in a vertical position for 1 min. The slide was next incubated in a flat position for 4 min before starting a time series of imaging under

40× magnification. The visual field was set and real time serial scans (every 1 s) were taken as the front of fibrinolysis proceeded across the visual field digesting the edge of the clot. The time of fibrin clot lysis was monitored. Fibrinolysis experiments were performed, at least, in triplicate.

Supplementary results

γAγ***A and*** γAγ***' fibrin clot structure***

It could be observed that γAγA fibers (Figure S1, left column) were more uniformly spatially distributed than γAγ' fibers (Figure S1, right column). Fibers produced with γAγA fibrinogen were also straighter and showed less bending. Clots from γAγ' fibers were structured into tight interconnecting bundles, producing zones with more branches and larger pores. It is possible to observe areas with fibers that were very compacted, highly connected and with small pores (Figure S1, right column). Furthermore, γAγ' fibrin clots showed more branching than γAγA fibrin clots.

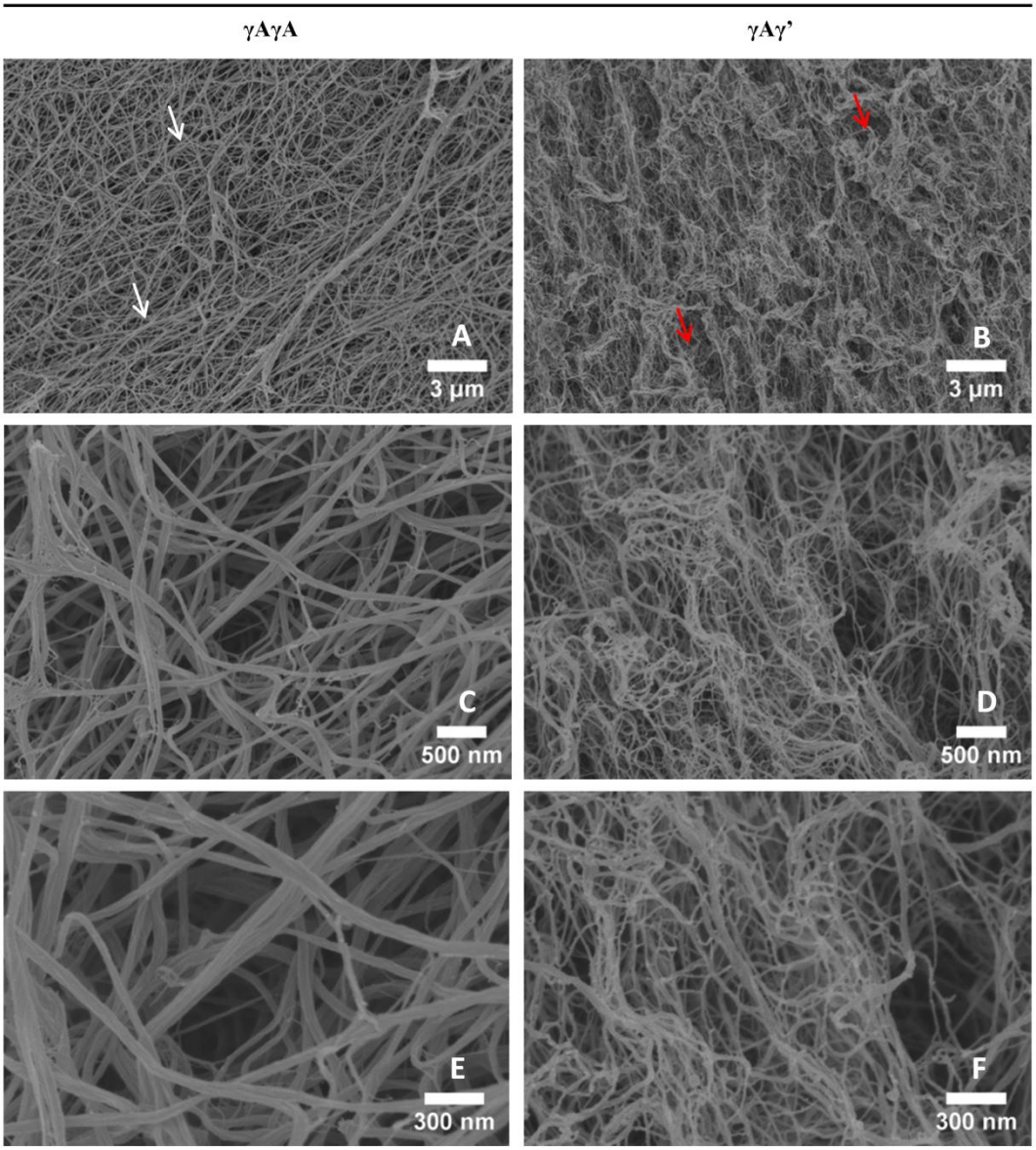

Figure S1 | Scanning electron micrographs of fibrin fiber clots (without RBCs) formed with 1.0 mg/ml of γAγA (A, C and E) or γAγ' (B, D and F) fibrinogen variants. White arrows in A highlight the more homogeneous structure of the γAγA clot network, while the red arrows in B indicate the areas with small or large holes, associating a more heterogeneous structure to the γAγ' clots. Images were obtained with a Cold Field Emission SEM, as detailed in the Methods section. Magnifications: A and B, 5000×; C and D, 25000×; E and F, 50000×.

Laser scanning confocal microscopy image analysis

Confocal microscopy images, shown on Figure 6 of the main manuscript, were analyzed to determine the fibrin fiber density (Figure S2). Fiber density was determined by counting the number of fibers crossing three arbitrary horizontal and vertical lines of 100 µm through each image. The analysis was done in three different micrographs per sample. The fiber density of the sample was taken as the average number of fibers per 100 µm of length. There were no statistical differences between fibrinogen variants regarding the number of fibers that cross the horizontal or vertical lines.

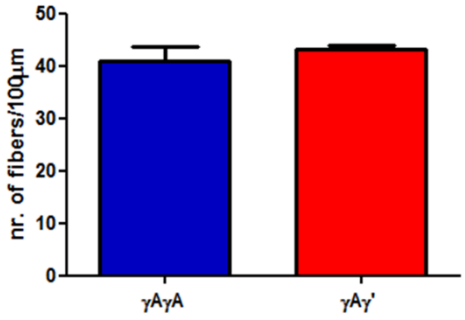

Figure S2 | **Fibrin fiber density analysis.** Data obtained from confocal images of γAγA and γAγ' fibrin clots. Values are presented as mean ± SEM.

It could be observed from confocal microscopy images that γAγ' fibrin clots have lower fiber density. This could be explained by the fact that γAγ' fibers are more compacted in some areas, producing large pores and not by the increase on the number of fibers (Figure S2)

Fibrinolysis data for fibrinogen variants

Fibrinolysis movies for γAγA (A) and γAγ' (B) fibrinogen variants were obtained, in real time by laser scanning confocal microscopy. The time serial scans were taken under 40× magnification. Clots were produced with 1.0 mg/ml fibrinogen, 5 mM $CaCl_2$ and 0.1 U/ml human thrombinfinal concentrations.

References

1. Carvalho FA*, et al.* Atomic force microscopy-based molecular recognition of a fibrinogen receptor on human erythrocytes. *ACS Nano* 2010; **4:** 4609-20.

2. Carvalho FA, de Oliveira S, Freitas T, Gonçalves S, Santos NC. Variations on fibrinogen-erythrocyte interactions during cell aging. *PLoS One* 2011; **6:** e18167.

3. Guedes AF, Carvalho FA, Malho I, Lousada N, Sargento L, Santos NC. Atomic force microscopy as a tool to evaluate the risk of cardiovascular diseases in patients. *Nat Nanotechnol* 2016; **11:** 687-92.

4. Pieters M, Undas A, Marchi R, De Maat MP, Weisel J, Ariëns RA. An international study on the standardization of fibrin clot permeability measurement: methodological considerations and implications for healthy control values. *J Thromb Haemost* 2012; **10:** 2179-81.

5. Ariëns RA, Philippou H, Nagaswami C, Weisel JW, Lane DA, Grant PJ. The factor XIII V34L polymorphism accelerates thrombin activation of factor XIII and affects cross-linked fibrin structure. *Blood* 2000; **96**: 988-95.

Article 2

International Journal of Nanomedicine

Dovepress
open access to scientific and medical research

Open Access Full Text Article

ORIGINAL RESEARCH

The $_{95}$RGD$_{97}$ sequence on the Aα chain of fibrinogen is essential for binding to its erythrocyte receptor

This article was published in the following Dove Press journal:
International Journal of Nanomedicine

International Journal of Nanomedicine downloaded from https://www.dovepress.com/ by 194.117.10.254 on 05-Apr-2018
For personal use only.

Filomena A Carvalho[1,*]
Ana Filipa Guedes[1,*]
Cedric Duval[2]
Fraser L Macrae[2]
Luke Swithenbank[2]
David H Farrell[3]
Robert AS Ariëns[2]
Nuno C Santos[1]

[1]Instituto de Medicina Molecular, Faculdade de Medicina, Universidade de Lisboa, Lisbon, Portugal; [2]Theme Thrombosis, Division of Cardiovascular and Diabetes Research, Leeds Institute for Genetics, Health and Therapeutics, University of Leeds, Leeds, UK; [3]Department of Surgery, Oregon Health and Science University, Portland, OR, USA

*These authors contributed equally to this work

Background: Erythrocyte aggregation, a cardiovascular risk factor, is increased by high plasma fibrinogen levels. Here, the effect of different fibrinogen mutations on binding to its human erythrocyte receptor was assessed in order to identify the interaction sites.

Methods: Three fibrinogen variants were tested, specifically mutated in their putative integrin recognition sites on the Aα chain (mutants D97E, D574E and D97E/D574E) and compared with wild-type fibrinogen.

Results: Atomic force microscopy-based force spectroscopy measurements showed a significant decrease both on the fibrinogen–erythrocyte binding force and on its frequency for fibrinogen with the D97E mutation, indicating that the corresponding arginine–glycine–aspartate sequence (residues 95–97) is involved in this interaction, and supporting that the fibrinogen receptor on erythrocytes has a β_3 subunit. Changes in the fibrin clot network structure obtained with the D97E mutant were observed by scanning electron microscopy.

Conclusion: These findings may lead to innovative perspectives on the development of new therapeutic approaches to overcome the risks of fibrinogen-driven erythrocyte hyperaggregation.

Keywords: atomic force microscopy, fibrinogen, fibrin clot, erythrocyte aggregation, mutant protein

Plain language summary

Currently, cardiovascular diseases are the leading cause of mortality worldwide, accounting for about one third of all deaths. Erythrocyte aggregation, which may lead to the formation of thrombus on the bloodstream, is associated with an increase in the concentration of fibrinogen. However, it is not known which binding sites on the fibrinogen protein structure are involved on the interaction with its specific receptor on the erythrocyte membrane, contributing to erythrocyte aggregation.

Here, the effect of different fibrinogen mutations on binding to its human erythrocyte receptor was assessed in order to identify the interaction sites. Using atomic force microscopy, a nanotechnology technique, we were able to use mutated fibrinogen molecules as "bait" to "fish" its receptor on the surface of red blood cells. It was shown that the force required to break the binding between fibrinogen (the "bait") and red blood cell (the "fish"), as well as the frequency of this binding, were lower for the proteins with the D97E mutation on the Aα chain, indicating that the corresponding arginine–glycine–aspartate sequence is involved in this interaction. Changes on fibrin clot network for the D97E mutant were also observed.

This study opens new perspectives on the development of novel therapeutic approaches to overcome the risks of fibrinogen-driven erythrocyte hyperaggregation.

Correspondence: Nuno C Santos
Instituto de Medicina Molecular, Faculdade de Medicina, Universidade de Lisboa, Avenida Professor Egas Moniz, 1649-028 Lisbon, Portugal
Tel +351 21 799 9480
Fax +351 21 799 9477
Email nsantos@fm.ul.pt

submit your manuscript | www.dovepress.com
Dovepress

http://dx.doi.org/10.2147/IJN.S154823

© 2018 Carvalho et al. This work is published and licensed by Dove Medical Press Limited. The full terms of this license are available at https://www.dovepress.com/terms.php and incorporate the Creative Commons Attribution – Non Commercial (unported, v3.0) License (http://creativecommons.org/licenses/by-nc/3.0/). By accessing the work you hereby accept the Terms. Non-commercial uses of the work are permitted without any further permission from Dove Medical Press Limited, provided the work is properly attributed. For permission for commercial use of this work, please see paragraphs 4.2 and 5 of our Terms (https://www.dovepress.com/terms.php).

International Journal of Nanomedicine downloaded from https://www.dovepress.com/ by 194.117.10.254 on 05-Apr-2018
For personal use only.

Introduction

Fibrinogen has a crucial role in blood clotting.[1] The increase in fibrinogen plasma concentration leads to increased erythrocyte aggregation, one of the most important factors affecting blood flow and a significant cardiovascular risk factor.[2] It has been reported that there is specific binding between fibrinogen and a previously unknown erythrocyte receptor.[3]

The fibrinogen molecule contains multiple binding motifs for different cellular receptors, acting as a molecular link between coagulation, inflammation and immunity. Particularly, fibrinogen binds to the $\alpha_{IIb}\beta_3$ integrin on activated platelets, leading to the platelet aggregation necessary for blood coagulation.[4,5] Three potential binding sites for this integrin on the fibrinogen molecule have been identified, which are structural RGD (arginine–glycine–aspartate) sequences on each Aα chain (amino acid residues 572–574 and 95–97) and one dodecapeptide sequence on the γ chain, yielding a total of six potential binding sites per fibrinogen molecule (formed by two Aα, two Bβ and two γ chains).[6]

Maeda et al proposed a model for a possible location of the erythrocyte-binding regions of fibrinogen in its Aα chain and tried to explain how it may affect erythrocyte aggregation and deformability.[7] The Aα 207–303 domain was found to include one of the possible erythrocyte-binding sites.[7] Using atomic force microscopy (AFM)-based force spectroscopy measurements, we demonstrated the existence of a single-molecule interaction between fibrinogen and a receptor on the erythrocyte membrane, with a lower but comparable affinity relative to platelet binding.[8] Fibrinogen binding to this receptor is inhibited by calcium depletion and by eptifibatide (an inhibitor considered to be specific for the receptor of fibrinogen on platelets, the glycoprotein $\alpha_{IIb}\beta_3$), but not as strongly as the platelet receptor. The results from a Glanzmann thrombasthenia (a rare hereditary bleeding disease caused by $\alpha_{IIb}\beta_3$ deficiency) patient showed an impaired fibrinogen–erythrocyte binding. Correlation with genetic sequencing data demonstrated that one of the units of the fibrinogen receptor on erythrocytes is a product of the expression of the β_3 gene.[8,9] To further assess the specificity of the fibrinogen–erythrocyte binding, as well as to complete its identification, we recently measured the inhibition of the fibrinogen–erythrocyte interaction using specific antibodies against integrins.[10] We also demonstrated that younger erythrocytes bind more fibrinogen than the older ones, being therefore the main cells responsible for the cardiovascular risk associated with an increase in the fibrinogen content in blood.[11] More recently, we showed that the interaction between fibrinogen and erythrocytes is modified in chronic heart failure (CHF) patients. The average force necessary to break the bond between fibrinogen and erythrocytes from CHF patients is higher than for erythrocytes from the control group.[10] Also using AFM, we showed that increasing fibrinogen levels lead to an increase in erythrocyte–erythrocyte adhesion in essential arterial hypertension patients.[12] Thus, AFM-based force spectroscopy is an approach with a high potential for applicability on biomedical research, inclusively on the study of cardiovascular diseases.[10–14]

Here, three stable fibrinogen variants were obtained according to previously established procedures,[4,15] specifically altered in the described integrin binding sites on the Aα chain (D97E, D574E and the D97E/D574E double mutant). Using these variants, we conducted force spectroscopy measurements to determine the force necessary to break the bond between each fibrinogen variant (attached to the AFM tip) and erythrocytes. For the sake of comparison, identical measurements were conducted with wild-type (WT) fibrinogen. The analysis of the structure of the fibrin fibers in the blood clot was done using scanning electron microscopy (SEM). The results shed light on which integrin binding sites of the fibrinogen molecule are involved on the binding to the erythrocyte receptor. Knowledge of these aspects may lead to innovative perspectives on the development of new therapeutic drugs to overcome the risks of fibrinogen-driven erythrocyte hyperaggregation.

Methods

Fibrinogen mutants

The constructs for the fibrinogen variants were produced as previously described.[4,15] We performed DNA sequence analysis, constructed the expression vectors and conducted site-directed mutagenesis according to established procedures. Briefly, baby hamster kidney cells, purchased from ATCC, were used to produce three stable fibrinogen mutants (Aα chain mutants D97E, D574E and the D97E/D574E double mutant) and the WT fibrinogen. Aα chain mutations have a single-nucleotide change, resulting in a codon for a different amino acid residue (aspartate changed to glutamate).

Erythrocyte isolation

Blood from adult healthy donors was collected into K_3EDTA anticoagulant tubes with their previous written informed consent, following a protocol with the Portuguese Blood Institute (Lisbon), approved by the joint Ethics Committee of the Faculty of Medicine of the University of Lisbon and the Santa Maria Hospital. The experimental work was carried out in accordance with the Declaration of Helsinki of the World Medical Association. Erythrocytes were isolated from the blood samples according to established

International Journal of Nanomedicine downloaded from https://www.dovepress.com/ by 194.117.10.254 on 05-Apr-2018
For personal use only.

procedures.[8,10,11] Briefly, erythrocytes were separated from the other blood components by centrifugation at 200 *g* for 10 min, at 10°C. Plasma and buffy-coat were removed, and the erythrocytes were washed three times with buffered saline glucose citrate (1.6 mM KH_2PO_4, 8.6 mM Na_2HPO_4, 120 mM NaCl, 13.6 mM sodium citrate, 11.1 mM glucose, pH 7.3) supplemented with 1 mM $CaCl_2$. Erythrocytes (0.1% hematocrit) were attached to a clean poly-L-lysine-treated glass slide after 30 min of deposition, at room temperature. Nonadherent cells were removed by sequential washes with buffer. Samples were loaded into the AFM and allowed to equilibrate in buffer for 15 min before force spectroscopy measurements.

AFM tip functionalization

A previously optimized procedure was used for the covalent attachment of fibrinogen to the AFM tips (functionalization) and for blood cells deposition on a solid substrate.[8,10,11] Briefly, cleaned AFM silicon nitride tips were silanized with 3-aminopropyl-triethoxysilane. Then, the probes were treated with a glutaraldehyde solution 2.5% (v/v) and finally immersed in a 0.5 mg/mL final concentration of fibrinogen (WT or mutant).

AFM-based force spectroscopy

Force spectroscopy measurements were performed on a NanoWizard II atomic force microscope (JPK Instruments, Berlin, Germany), mounted on an Axiovert 200 inverted optical microscope (Zeiss, Jena, Germany), using fibrinogen functionalized OMCL TR-400-type silicon nitride AFM tips (Olympus, Tokyo, Japan), as previously described.[8] The spring constant of the tips was calibrated by the thermal fluctuation method, resulting in values of 19±7 mN/m. The applied force was adjusted to 0.8 nN before retraction. Molecular recognition was searched by intermittently pressing the cantilevers on each erythrocyte adsorbed on the glass slide. Data collection for each force–distance cycle was performed at 2 µm/s, leading to a loading rate of 4 nN/s. Force curves were analyzed using the JPK image processing software v. 4.2.61. For any given experiment, ~5,000 force–distance curves were collected, analyzed and adjusted by polynomial fit.[16] Each experiment was performed at least three times, each time on different blood samples and with different functionalized tips.

SEM

SEM was used to investigate the differences on structure of clots formed from WT and D97E recombinant fibrinogen, especially in the presence of erythrocytes.

WT or D97E recombinant fibrinogen (0.5 mg/mL final concentration) and $CaCl_2$ (final concentration 10 mM) were diluted in TBS (50 mM Tris–HCl, 100 mM NaCl, pH 7.5) and premixed. Human thrombin (Calbiochem, Nottingham, UK; final concentration 1 U/mL) was then added to initiate clotting. The mixtures were immediately transferred to Eppendorf lids, which were pierced with a syringe to assist solvent permeation. Clots were formed in a moist chamber, at room temperature, for 120 min. Clots were then washed with saline solution to remove excess salt, followed by fixation in 2% (v/v) glutaraldehyde (120 min). Clots were further washed extensively with sodium cacodylate buffer and dehydrated in a series of increasing acetone concentrations (30%–100%). Clots were critical-point dried with CO_2, mounted onto stubs and sputter-coated with platinum, using a Cressington 208 HR (Watford, UK). Clots were also prepared with the appropriate amount of erythrocytes for a final hematocrit of 20%. They were observed and photographed digitally on at least three different areas per clot, using a scanning electron microscope Hitachi SU8230 FESEM (Tokyo, Japan), at five different magnifications (2,500× [data not shown], 5,000×, 10,000× [data not shown], 25,000× and 50,000×). At least, duplicates of each type of clot were performed. Fiber diameters were measured from 20 random fibers of each image in high magnification (25,000×), using ImageJ software (National Institutes of Health, Bethesda, MD, USA). Each cross-section measurement was performed over a single fibrin fiber and values of fiber diameter were extracted and averaged. All cross-section analysis were performed away from the branching points, in order to avoid biased results.

Statistical analysis

Unpaired samples Student's *t*-test was used for statistical analysis. Differences were considered statistically significant for $p<0.05$. For AFM, each experiment was performed at least three times, each time with different blood samples and with different functionalized tips. At least 15 erythrocytes were tested on each blood sample. For SEM, at least duplicates of each type of clot were performed. Average fiber diameters were measured from 20 random fibers of each image, at high magnification (25,000×).

Results and discussion

AFM-based force spectroscopy studies, conducted at the single-molecule level, yielded force vs distance curves, acquired after the binding of mutant or WT fibrinogen to the receptor on erythrocytes (Figure 1A). The repeated

International Journal of Nanomedicine downloaded from https://www.dovepress.com/ by 194.117.10.254 on 05-Apr-2018
For personal use only.

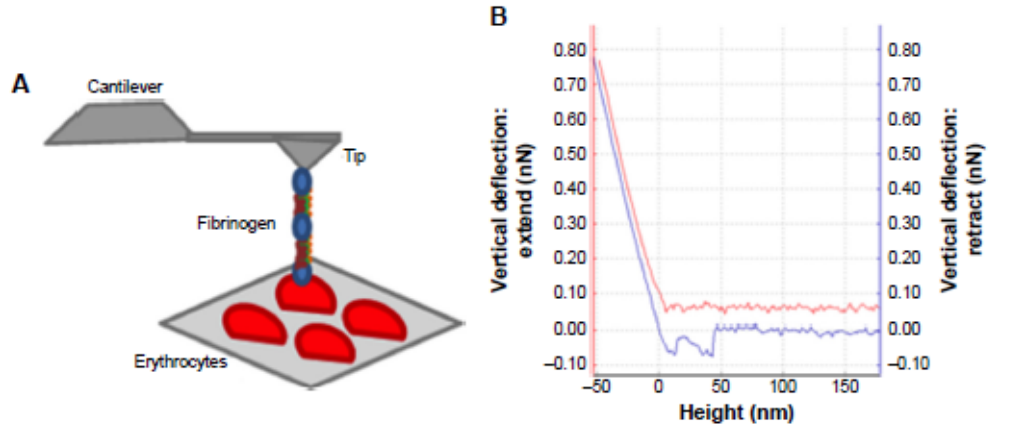

Figure 1 AFM-based force spectroscopy experiments and force–distance curve.
Notes: (**A**) Schematic representation of the erythrocytes deposited on a poly-L-lysine-coated glass slide and an AFM tip chemically functionalized with different fibrinogen variants. The vertical movement approaching the tip to the sample until contact enables the binding of fibrinogen to the erythrocyte. The subsequent retraction progresses until a certain force (and distance) is reached and the fibrinogen molecule detaches from the erythrocyte surface. The (un)binding frequency corresponds to the fraction of these approach–retraction cycles in which binding and subsequent unbinding occur. (**B**) Example of a force–distance curve. When approaching the tip to the sample (red line), the fibrinogen molecule may contact with cell receptor(s) and the binding between them can occur. By retracting the tip away from the sample (blue line), as the cantilever moves upward, the tip bends down to negative force values. In some surface distance point, the bond breaks and the cantilever jumps back to its neutral force position. At this point, the binding force necessary to break the bond, at the fibrinogen single-molecule level, can be measured.
Abbreviation: AFM, atomic force microscopy.

measurements of the adhesion events, as the one shown in Figure 1B, allowed us to build up rupture force histograms for each fibrinogen variant and cell population studied.

Figure 2A shows the rupture force histograms for the three different fibrinogen mutants and WT fibrinogen. It can be noticed that, in the presence of the D97E or D97E/D574E mutant, the histogram is shifted to lower binding forces, when compared with those obtained for WT fibrinogen. The opposite variation trend was obtained for the rupture force histogram of D574E, which is shifted to higher and stronger binding forces.

As it can be observed in Figure 2B, the average force necessary to break the bond between the D97E fibrinogen mutant (43.2±1.1 pN) or the D97E/D574E double mutant (49.2±0.8 pN) and erythrocytes is significantly lower than for WT fibrinogen (58.8±2.3 pN; $p<0.0001$ for both pairs). On the other hand, the average force necessary to break the bond between erythrocytes and the D574E mutant (105.9±1.7 pN) was significantly higher than for the WT ($p<0.0001$).

Decreases on the frequency (probability) of fibrinogen–erythrocyte binding and subsequent unbinding for the D97E (11.4%), D574E (13.1%) or D97E/D574E (11.1%) mutants in comparison with the WT fibrinogen (15.9%) were observed. The variation of the binding frequency of the different mutants relative to the WT is presented in Figure 2C.

Our results indicate that the RGD sequence corresponding to amino acid residues 95–97 of the fibrinogen Aα chain is involved in the binding to the erythrocyte membrane receptor. It has previously been reported that this RGD sequence is also involved in the binding to the β_3 subunit of the $\alpha_V\beta_3$ receptor in endothelial cells.[17] These results further support our recent findings regarding the fibrinogen receptor on erythrocytes.[8,10]

The force necessary to break the bond between D574E fibrinogen and the erythrocyte membrane receptor was significantly higher than for WT fibrinogen, while the frequency of (un)binding events for this mutant was lower. These apparently opposite effects might be explained by the location of the specific binding site. As it is located close to the C-terminus of the α chain, the domain may eventually change conformation, leading to a stabilization of the complex formed upon binding to the erythrocyte receptor.

It is worth to mention that during the conversion of fibrinogen to fibrin, thrombin cleaves fibrinogen Aα chain at Arg-16 and the Bβ chain at Arg-14, releasing the fibrinopeptides A and B, respectively, and forming the so-called fibrin monomers.[18,19] In the fibrinogen structure, the thrombin

International Journal of Nanomedicine downloaded from https://www.dovepress.com/ by 194.117.10.254 on 05-Apr-2018
For personal use only.

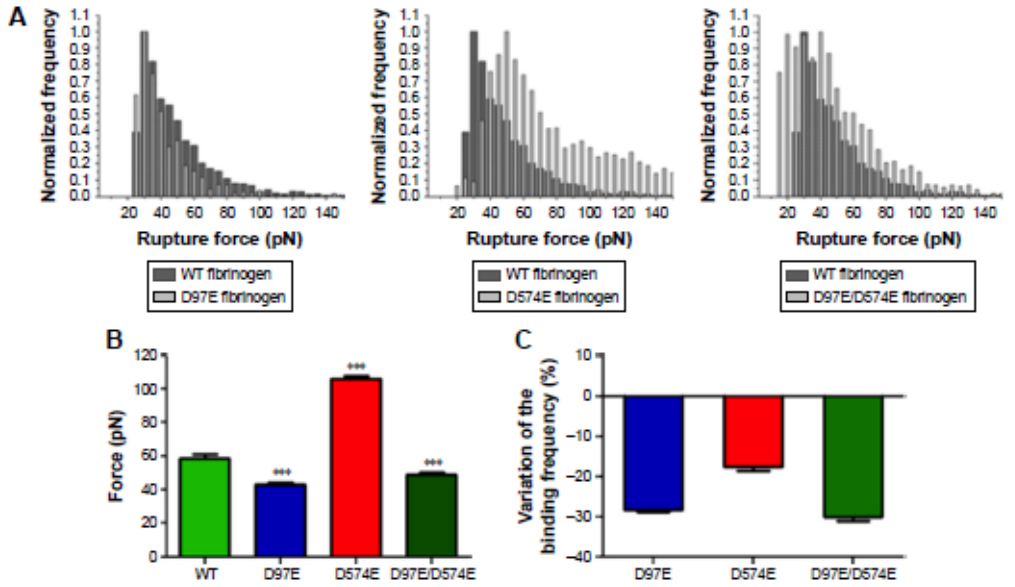

Figure 2 AFM force spectroscopy data for the binding between different fibrinogen variants and erythrocytes.
Notes: (A) Rupture force histograms of the interactions between the three different fibrinogen mutants (D97E, D574E and D97E/D574E: light gray) or WT fibrinogen (dark gray) and erythrocytes. On the rupture force histograms, each count represents a single-molecule binding between one fibrinogen molecule and one of its cell receptors. (B) Average (un)binding force of the interactions. Values are shown as mean ± standard error of mean (SEM). There were statistically significant variations (***$p<0.0001$) of the rupture forces between WT fibrinogen and the three fibrinogen variants with mutations on the Aα chain (D97E, D574E and D97E/D574E). (C) Variation of the fibrinogen–erythrocyte (un)binding frequency of the different fibrinogen variants relative to WT fibrinogen. (Un)binding frequency variations were calculated based on the ratio between the frequency of (un)binding events determined for the fibrinogen mutants and the frequency of (un)binding events obtained for WT fibrinogen.
Abbreviations: AFM, atomic force microscopy; WT, wild-type.

cleavage regions are distant from the mutated regions of fibrinogen variants produced here. Therefore, these mutations on the fibrinogen molecule do not interfere with the thrombin-induced conversion of fibrinogen to fibrin.

The existence of a specific binding mechanism in fibrinogen-induced erythrocyte hyperaggregation suggests the possibility of developing new treatments to decrease erythrocyte aggregation, therefore potentially decreasing cardiovascular risk. Fibrinogen is considered an independent risk factor on screening programs aimed at identifying individuals at high risk for cardiovascular diseases.[20] Our results show that, in addition to the assessment of the plasma fibrinogen concentration itself, it may also be important to identify mutations in the fibrinogen molecules that may change the binding to erythrocytes as a risk assessment strategy.

Moreover, in order to see if this fibrinogen variant induces changes on the structure of the fibrin blood clot, SEM analysis was also performed. From the micrographs obtained for the D97E and WT fibrin clots, we observed that there were no differences in fibrin clot structure (Figure 3). Clots were also evaluated in the presence of 20% of erythrocytes (Figure 4). The clots formed with WT fibrin have a more homogeneous structure than those formed with the D97E mutant. The D97E fibrin clots seem to have a more disorganized structure, with higher number of clusters that entrap erythrocytes. The clots appear to be more loosely packed, eventually leading to a higher risk of embolism. SEM images correlate well with the AFM data, where a decrease in both the binding force and the binding frequency were observed for this mutant, when compared with the WT fibrinogen.

After analyzing the SEM micrographs shown in Figures 3 and 4, the diameters of the fibers were calculated (Figure 5). No differences in fiber diameter between both fibrinogen variants were observed in the absence of erythrocytes, but statistically significant differences were found in the presence of these cells. The addition of 20% of erythrocytes to the D97E fibrin clot caused a decrease in fiber thickness (37.7±2.0 nm without erythrocytes vs 18.9±1.1 nm with erythrocytes; $p<0.0001$) and led to an extensive network rearrangement.

International Journal of Nanomedicine downloaded from https://www.dovepress.com/ by 194.117.10.254 on 05-Apr-2018
For personal use only.

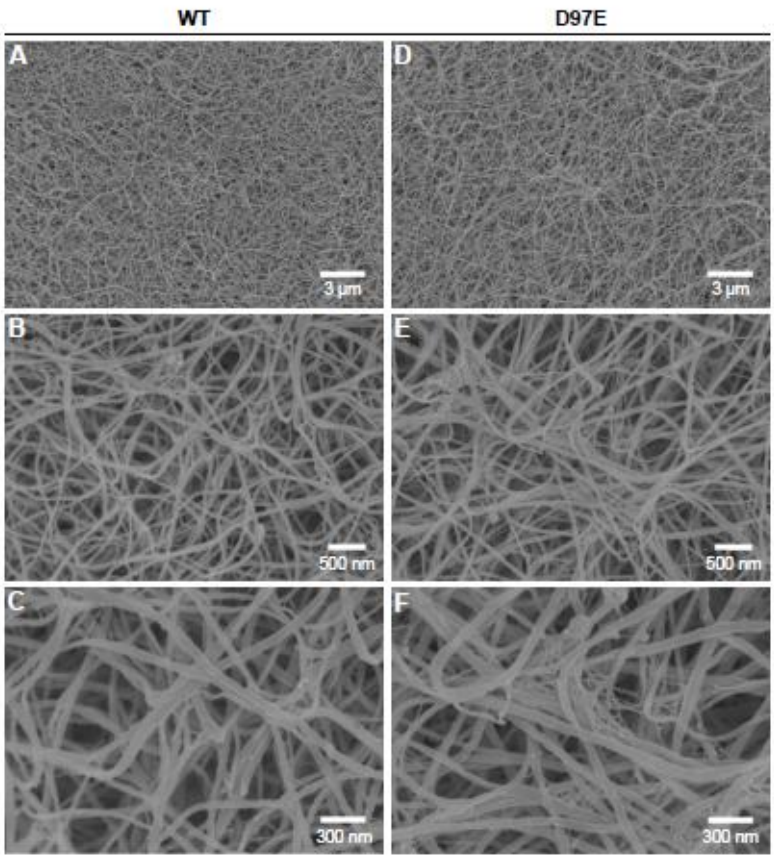

Figure 3 Clots made from WT (A–C) or D97E (D–F) fibrinogen (0.5 mg/mL), imaged by scanning electron microscopy.
Notes: Magnifications: A, D, 5,000×; B, E, 25,000×; C, F, 50,000×.
Abbreviation: WT, wild-type.

A statistically significant variation of the fibers' diameters was also observed between WT fibrin and D97E fibrin, both in the presence of erythrocytes (30.8±1.8 nm vs 18.9±1.1 nm, respectively; $p<0.0001$).

The difference in the D97E fibrin fibers' diameter in the presence of erythrocytes is clear. This should be due to the mutant fibrin(ogen) interaction with erythrocytes, and not due to any difference in the polymerization of this fibrinogen variant itself, as the structure of the mutant fibrin without these cells seems the same as for the WT. Only when erythrocytes are present, the clot D97E fibrin structure becomes different.

The architecture of the clot may affect its stability, viscoelastic and mechanical properties, as well as its fibrinolytic characteristics.[21,22] These characteristics may determine if a clot breaks down by fibrinolysis, or if it will lead to blood vessel occlusion or embolization.[23] Moreover, it has been previously reported that tightly packed and rigid clots, with thinner fibers and low porosity, are less susceptible to the action of thrombolytic agents.[24,25]

This work yields valuable new information on the identification of the fibrinogen domains that interact with its erythrocyte membrane receptor, contributing to the erythrocyte hyperaggregation in the bloodstream induced by increased levels of fibrinogen. Moreover, in this study, AFM-based force spectroscopy demonstrated its potential as an important nanotechnology approach for biomedical research application, important to measure the interaction forces between fibrinogen (or other plasma proteins) and human blood cells. Future studies using animal models

International Journal of Nanomedicine downloaded from https://www.dovepress.com/ by 194.117.10.254 on 05-Apr-2018
For personal use only.

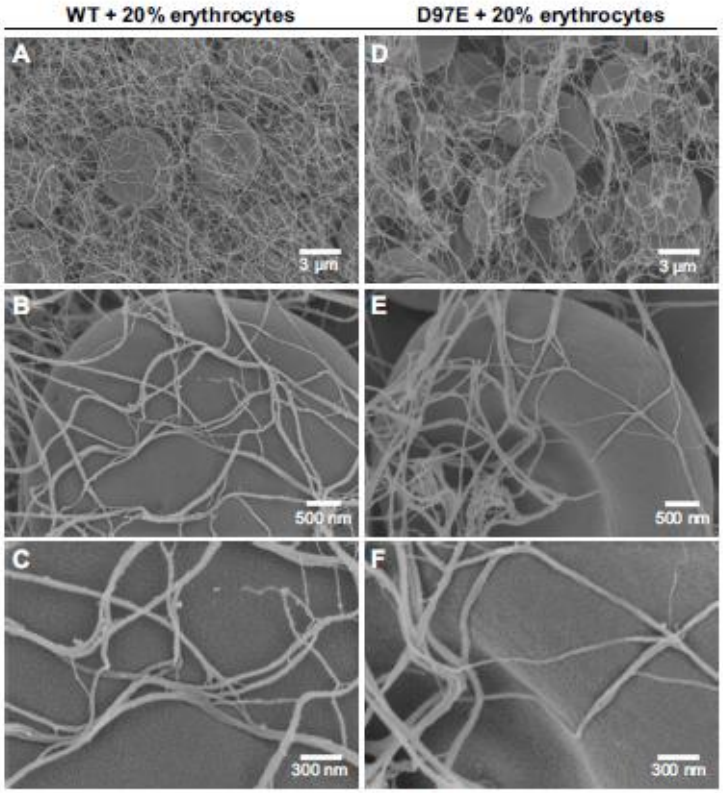

Figure 4 Fibrin clots formed in the presence of erythrocytes (20%), with WT (A–C) or D97E (D–F) fibrinogen, imaged by scanning electron microscopy.
Notes: Magnifications: A, D, 5,000×; B, E, 25,000×; C, F, 50,000×.
Abbreviation: WT, wild-type.

would be important to test the binding between the fibrinogen variants and erythrocytes in vivo, in order to develop new therapeutic approaches to treat fibrinogen-driven erythrocyte hyperaggregation.

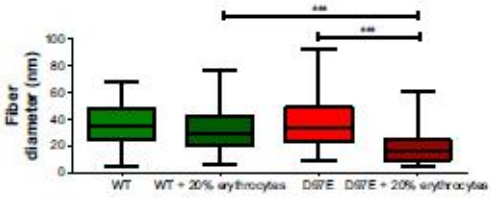

Figure 5 Diameter of fibers from WT or D97E fibrin clots, in the absence or presence of erythrocytes.
Notes: Data are presented as a box-and-whiskers plot. Fiber diameters were measured from 20 random fibers from each condition, imaged with 25,000× magnification (**** $p<0.0001$).
Abbreviation: WT, wild-type.

Acknowledgments

The authors thank Teresa Freitas (IMM, FM, UL) for excellent technical assistance. This work was supported by Fundação para a Ciência e a Tecnologia – Ministério da Ciência, Tecnologia e Ensino Superior (FCT-MCTES, Portugal) grants PTDC/QUI-BIQ/119509/2010 and PTDC/BBB-BMD/6307/2014, FEDER, through POR Lisboa 2020 - Programa Operacional Regional de Lisboa, PORTUGAL 2020 and FCT-MCTES (LISBOA-01-0145-FEDER-007391), and by the Calouste Gulbenkian Foundation (Portugal). AFG also acknowledges FCT-MCTES PhD fellowship SFRH/BD/84414/2012.

Disclosure

Oregon Health and Science University (OHSU) and Dr David Farrell have a significant interest in Gamma Therapeutics, a company that may have a commercial interest in the results

of this research and technology. This potential individual and institutional conflict of interest has been reviewed and managed by OHSU. The authors report no other conflicts of interest in this work.

References

1. Kamath S, Lip GY. Fibrinogen: biochemistry, epidemiology and determinants. *QJM*. 2003;96(10):711–729.
2. Lominadze D, Dean WL, Tyagi SC, Roberts AM. Mechanisms of fibrinogen-induced microvascular dysfunction during cardiovascular disease. *Acta Physiol (Oxf)*. 2010;198(1):1–13.
3. Sokolova IA, Muravyov AV, Khokhlova MD, et al. An effect of glycoprotein IIb/IIIa inhibitors on the kinetics of red blood cells aggregation. *Clin Hemorheol Microcirc*. 2014;57(3):291–302.
4. Farrell DH, Thiagarajan P. Binding of recombinant fibrinogen mutants to platelets. *J Biol Chem*. 1994;269(1):226–231.
5. Holmback K, Danton MJ, Suh TT, Daugherty CC, Degen JL. Impaired platelet aggregation and sustained bleeding in mice lacking the fibrinogen motif bound by integrin alpha IIb beta 3. *EMBO J*. 1996;15(21):5760–5771.
6. Salsmann A, Schaffner-Reckinger E, Kieffer N. RGD, the Rho'd to cell spreading. *Eur J Cell Biol*. 2006;85(3–4):249–254.
7. Maeda N, Seike M, Kume S, Takaku T, Shiga T. Fibrinogen-induced erythrocyte aggregation: erythrocyte-binding site in the fibrinogen molecule. *Biochim Biophys Acta*. 1987;904(1):81–91.
8. Carvalho FA, Connell S, Miltenberger-Miltenyi G, et al. Atomic force microscopy-based molecular recognition of a fibrinogen receptor on human erythrocytes. *ACS Nano*. 2010;4(8):4609–4620.
9. Carvalho FA, Martins IC, Santos NC. Atomic force microscopy and force spectroscopy on the assessment of protein folding and functionality. *Arch Biochem Biophys*. 2013;531(1–2):116–127.
10. Guedes AF, Carvalho FA, Malho I, Lousada, Sargento L, Santos NC. Atomic force microscopy as a tool to evaluate the risk of cardiovascular diseases in patients. *Nat Nanotechnol*. 2016;11(8):687–692.
11. Carvalho FA, de Oliveira S, Freitas T, Gonçalves S, Santos NC. Variations on fibrinogen-erythrocyte interactions during cell aging. *PLoS One*. 2011;6(3):e18167.
12. Guedes AF, Carvalho FA, Moreira C, Nogueira JB, Santos NC. Essential arterial hypertension patients present higher cell adhesion forces, contributing to fibrinogen-dependent cardiovascular risk. *Nanoscale*. 2017;9(39):14897–14906.
13. Guedes AF, Carvalho FA, Domingues MM, Macrae FL, McPherson HR, Santos NC, Ariëns RAS. Sensing adhesion forces between erythrocytes and γ′ fibrinogen, modulating fibrin clot architecture and function. *Nanomedicine*. 2018;14(3):909–918.
14. Carvalho FA, Santos NC. Atomic force microscopy-based force spectroscopy – biological and biomedical applications. *IUBMB Life*. 2012;64(6):465–472.
15. Standeven KF, Carter AM, Grant PJ, et al. Functional analysis of fibrin gamma-chain cross-linking by activated factor XIII: determination of a cross-linking pattern that maximizes clot stiffness. *Blood*. 2007;110(3):902–907.
16. Ratto TV, Rudd RE, Langry KC, Balhorn RL, McElfresh MW. Nonlinearly additive forces in multivalent ligand binding to a single protein revealed with force spectroscopy. *Langmuir*. 2006;22(4):1749–1757.
17. Thiagarajan P, Rippon AJ, Farrell DH. Alternative adhesion sites in human fibrinogen for vascular endothelial cells. *Biochemistry*. 1996;35(13):4169–4175.
18. Blomback B, Hessel B, Hogg D, Therkildsen L. A two-step fibrinogen – fibrin transition in blood coagulation. *Nature*. 1978;275(5680):501–505.
19. Hurlet-Jensen A, Cummins HZ, Nossel HL, Liu CY. Fibrin polymerization and release of fibrinopeptide B by thrombin. *Thromb Res*. 1982;27(4):419–427.
20. Meade TW, North WR, Chakrabarti R, et al. Haemostatic function and cardiovascular death: early results of a prospective study. *Lancet*. 1980;1(8177):1050–1054.
21. Undas A, Ariens RA. Fibrin clot structure and function: a role in the pathophysiology of arterial and venous thromboembolic diseases. *Arterioscler Thromb Vasc Biol*. 2011;31(12):e88–e99.
22. Weisel JW. Structure of fibrin: impact on clot stability. *J Thromb Haemost*. 2007;5(Suppl 1):116–124.
23. Weisel JW. The mechanical properties of fibrin for basic scientists and clinicians. *Biophys Chem*. 2004;112(2–3):267–276.
24. Bridge KI, Philippou H, Ariens R. Clot properties and cardiovascular disease. *Thromb Haemost*. 2014;112(5):901–908.
25. Collet JP, Soria J, Mirshahi M, et al. Dusart syndrome: a new concept of the relationship between fibrin clot architecture and fibrin clot degradability: hypofibrinolysis related to an abnormal clot structure. *Blood*. 1993;82(8):2462–2469.

International Journal of Nanomedicine Dovepress

Publish your work in this journal

The International Journal of Nanomedicine is an international, peer-reviewed journal focusing on the application of nanotechnology in diagnostics, therapeutics, and drug delivery systems throughout the biomedical field. This journal is indexed on PubMed Central, MedLine, CAS, SciSearch®, Current Contents®/Clinical Medicine, Journal Citation Reports/Science Edition, EMBase, Scopus and the Elsevier Bibliographic databases. The manuscript management system is completely online and includes a very quick and fair peer-review system, which is all easy to use. Visit http://www.dovepress.com/testimonials.php to read real quotes from published authors.

Submit your manuscript here: http://www.dovepress.com/international-journal-of-nanomedicine-journal

International Journal of Nanomedicine downloaded from https://www.dovepress.com/ by 194.117.10.254 on 05-Apr-2018
For personal use only.

Article 3

nature nanotechnology

LETTERS

PUBLISHED ONLINE: 16 MAY 2016 | DOI: 10.1038/NNANO.2016.52

Atomic force microscopy as a tool to evaluate the risk of cardiovascular diseases in patients

Ana Filipa Guedes[1], Filomena A. Carvalho[1]*, Inês Malho[1], Nuno Lousada[2], Luís Sargento[2] and Nuno C. Santos[1]*

The availability of biomarkers to evaluate the risk of cardiovascular diseases is limited[1]. High fibrinogen levels have been identified as a relevant cardiovascular risk factor, but the biological mechanisms remain unclear[2,3]. Increased aggregation of erythrocytes (red blood cells) has been linked to high plasma fibrinogen concentration[2,4]. Here, we show, using atomic force microscopy, that the interaction between fibrinogen and erythrocytes is modified in chronic heart failure patients. Ischaemic patients showed increased fibrinogen–erythrocyte binding forces compared with non-ischaemic patients. Cell stiffness in both patient groups was also altered. A 12-month follow-up shows that patients with higher fibrinogen–erythrocyte binding forces initially were subsequently hospitalized more frequently. Our results show that atomic force microscopy can be a promising tool to identify patients with increased risk for cardiovascular diseases.

Cardiovascular diseases are the leading cause of death worldwide, being responsible for approximately 30% of the total number of human losses[5]. Chronic heart failure (CHF), a complex clinical cardiovascular syndrome, is characterized by the heart failing to pump enough blood with the right pressure[6,7]. Ischaemic cardiomyopathy is the most common cause of heart failure, and patients with this condition have poorer disease prognosis and response to treatment than non-ischaemic patients[8].

Erythrocyte aggregation has pathogenic implications in thrombus formation[9,10]. It is associated with an increase in the concentration of fibrinogen in blood plasma[2,3], which is a significant risk factor for several cardiovascular disorders[11,12]. A few studies have focused on a possible specific interaction between fibrinogen and erythrocytes[13,14]. However, our recent finding indicated that an integrin receptor for fibrinogen, with a β_3 subunit, exists on the erythrocyte membrane[15,16]. Establishing the diagnosis, extent and severity of cardiovascular diseases, as well as determining the potential risk of cardiovascular events, are crucial steps towards improving patient outcomes. For information about non-invasive tests and procedures used to evaluate CHF patients, see Supplementary Section 'Biomedical relevance'.

There are an increasing number of reports that utilize atomic force microscopy (AFM) as a nanodiagnostic tool for use with patient cells[17–19]. A better understanding of the molecular mechanisms underlying the interaction between fibrinogen and erythrocytes in CHF patients may be important for eventual future drug interventions to reduce aggregation and enhance microcirculatory flow conditions. Here, we evaluate the fibrinogen–erythrocyte interactions in stable outpatients with systolic CHF, using AFM-based force spectroscopy. We examine (1) the fibrinogen–erythrocyte interaction as a risk biomarker for a worse clinical prognosis, leading to hospitalization; (2) the association of the fibrinogen–erythrocyte interaction with CHF aetiology (ischaemic or non-ischaemic); and (3) patients' haemorrheological profiles.

The baseline characteristics of the cohort of CHF patients, their relevant clinical data and the list of drugs used in their therapy are listed in Table 1. Figure 1a presents a schematic illustration of the set-up, in which fibrinogen molecules attached to the AFM cantilever were allowed to bind to its specific erythrocyte membrane receptor. Force adhesion maps of erythrocytes were recorded to define the correct position of the cantilever on top of a single cell (Fig. 1b). With this AFM-based force spectroscopy methodology, fibrinogen–erythrocyte interactions were assessed at the single-molecule level using the adhesion profiles obtained on each force curve (Fig. 1c,d). It was possible to measure the fibrinogen–erythrocyte binding force from the deflection of the AFM tip on the retraction curve (Fig. 1c). In a previous study, we showed that the interaction between fibrinogen and its integrin receptor on erythrocytes, assessed by AFM, is inhibited by the absence of calcium ions and by the presence of eptifibatide[15]. We have also reported the existence of a single-molecule interaction between fibrinogen and a $\alpha_{IIb}\beta_3$-related integrin receptor on the erythrocyte membrane[15]. It is known that an RGD (Arg-Gly-Asp) sequence at the Aα chain of the fibrinogen molecule is involved in binding to the β_3 subunit of the $\alpha_V\beta_3$ receptor on endothelial cells[20]. To further assess the specificity of the fibrinogen–erythrocyte binding, as well as to complete its identification, we measured the inhibition of the fibrinogen–erythrocyte interaction by specific antibodies against α_V and $\alpha_V\beta_3$ integrins (Supplementary Fig. 1), following an established procedure[21]. These results showed that integrin $\alpha_V\beta_3$ is the receptor for fibrinogen on erythrocytes.

Changes in the fibrinogen–erythrocyte binding force and/or its frequency could provide insights into the pathological condition at the microcirculatory level. Force histograms of the data obtained for the control group (healthy donors), non-ischaemic and ischaemic CHF patients are presented in Fig. 2a. The main differences were observed at the level of the stronger binding events (forces above 50 pN). The strongest fibrinogen–erythrocyte interactions were measured for ischaemic CHF patients, followed by non-ischaemic CHF patients and finally the group of healthy control subjects. The variations are clearer in Fig. 2b,d, which shows that the average force necessary to break the bond between fibrinogen and erythrocytes taken from CHF patients is higher than for erythrocytes taken from the control group (60.6 ± 6.6 pN versus 40.4 ± 3.0 pN; $P = 0.038$), despite the lower binding frequency in CHF patients ($13.0 \pm 2.4\%$ versus $27.3 \pm 4.2\%$; $P = 0.003$). Looking into each CHF aetiology (Fig. 2c,e), ischaemic patients presented a higher binding force than healthy donors (74.9 ± 10.7 pN versus 40.4 ± 3.0 pN; $P = 0.004$), despite their lower binding frequency ($11.7 \pm 2.1\%$ versus $27.3 \pm 4.2\%$; $P = 0.002$). Ischaemic patients also presented

[1]Instituto de Medicina Molecular, Faculdade de Medicina, Universidade de Lisboa, Av. Prof. Egas Moniz, 1649-028 Lisbon, Portugal. [2]Heart Failure Unit, Cardiology Department, Hospital Pulido Valente, Centro Hospitalar Lisboa Norte, Lisbon, Portugal. *e-mail: filomenacarvalho@fm.ul.pt; nsantos@fm.ul.pt

© 2016 Macmillan Publishers Limited. All rights reserved

higher binding forces than non-ischaemic patients (74.9 ± 10.7 pN versus 45.4 ± 5.6 pN; $P = 0.021$), and non-ischaemic patients had a lower binding frequency than control donors (14.3 ± 4.3% versus 27.3 ± 4.2%; $P = 0.040$). The stronger fibrinogen–erythrocyte binding in CHF patients, with the plasma protein eventually contributing to a transient bridging of two or more erythrocytes, may impair blood flow conditions and contribute to the higher thrombosis risk associated with this disease[3].

It has been reported that the erythrocyte membrane exhibits plastic changes under some pathological circumstances and can be permanently deformed by excessive shear forces[22]. Erythrocytes from the patients evaluated here may thus eventually have suffered changes at the membrane level, leading to a lower binding frequency, but, following binding, a stronger force is necessary to break the fibrinogen–erythrocyte interaction. Differences between CHF patients and healthy donors in terms of erythrocyte elasticity and AFM tip penetration depth into the cells were therefore assessed. Erythrocytes from non-ischaemic patients presented a higher average stiffness than those from the other two groups (Supplementary Fig. 2a). Nevertheless, a significantly higher cell penetration depth at the same applied force was observed for ischaemic CHF patients (Supplementary Fig. 2b). Other studies performed with erythrocytes from patients with different diseases (for example, lupus erythematosus[23] and sickle cell disease[24]) have shown changes in these cell elastic properties. Young's modulus values for erythrocytes from the control group in our study are in the same range as those reported by Maciaszek and Lykotrafitis for normal erythrocytes that have not been fixed[24].

The results obtained for whole blood viscosity (Fig. 3) show that the native (without haematocrit correction) whole blood viscosity, measured at two shear rates, was higher for non-ischaemic patients than for ischaemic patients (8.09 ± 0.42 mPa s versus 7.08 ± 0.24 mPa s, $P = 0.046$, at a shear rate of 22.5 s^{-1}; 4.70 ± 0.17 mPa s versus 4.23 ± 0.11 mPa s, $P = 0.028$, at a shear rate of 225 s^{-1}). The data also show that, at a low shear rate (22.5 s^{-1}), non-ischaemic patients presented a higher native blood viscosity than the control group (8.09 ± 0.42 mPa s versus 7.05 ± 0.08 mPa s, $P = 0.010$). At 45% haematocrit, non-ischaemic CHF patients presented whole blood viscosity values higher than the control group (7.63 ± 0.13 mPa s versus 6.80 ± 0.11 mPa s, $P < 0.0001$, at 22.5 s^{-1}; 4.73 ± 0.07 mPa s versus 4.18 ± 0.09 mPa s, $P < 0.0001$, at 225 s^{-1}). The whole blood viscosity was significantly higher in the non-ischaemic group than for ischaemic patients ($P = 0.014$ at a shear rate of 22.5 s^{-1} and $P = 0.001$ at 225 s^{-1}). Ischaemic patient results were similar to those obtained for the control group. This was an unexpected result because previous findings have indicated that ischaemic patients present higher blood viscosities and this is associated with higher cardiovascular risk[8]. A statistically significant correlation ($P = 0.042$) between whole blood viscosity and fibrinogen–erythrocyte binding forces was observed only for non-ischaemic CHF patients, with a correlation coefficient of 0.53 (Supplementary Fig. 3). Baskurt and Meiselman considered that the apparent viscosity of blood depends on the existing shear forces and is determined by haematocrit, plasma viscosity, erythrocyte aggregation and their mechanical properties[22]. Erythrocytes aggregate under low blood flow, with a decrease in shear forces. Under these conditions, the viscosity of the blood becomes higher[25]. Under high shear forces, the apparent viscosity decreases and approaches a minimum value, as observed in our experiments (Fig. 3).

The erythrocyte deformability (assessed as elongation index) results obtained for all experimental groups are presented in Fig. 4. Lower and higher shear stress values try to mimic the *in vivo* situations of erythrocyte flow along blood vessels with larger or smaller internal diameter, respectively[26]. The CHF patients presented higher erythrocyte deformability than the control group at lower shear stresses (0.3–1.2 Pa; $P < 0.0043$), and lower deformability at higher shear stresses (12–60 Pa; $P < 0.037$) (Fig. 4a). Both patient groups showed higher deformability than the control group at lower shear stresses ($P < 0.0056$ for ischaemic and $P < 0.0003$ for non-ischaemic patients), but lower deformability at higher shear stresses ($P = 0.032$ for ischaemic and $P < 0.035$ for non-ischaemic group). There were no statistically significant differences between the data obtained for the two groups of CHF patients. The deformability results indicate that CHF patients' erythrocytes are more deformable than those from healthy donors in vessels with larger internal diameters. However, in smaller-diameter vessels the opposite trend exists. Comparing these data with AFM results, we may hypothesize that patients' erythrocytes present alterations on the membrane–cytoskeleton complex, promoting an increased deformability in larger vessels and a lower frequency of fibrinogen–erythrocyte binding, but a higher binding force. In smaller vessels, erythrocyte deformability was lower for patients than for healthy donors. This result is extremely important because of the increased cardiovascular risk associated with such an alteration. Erythrocytes are highly deformable cells that tend to orient themselves with the blood flow streamline, especially if shear forces are high enough to slightly deform these cells[27]. The transient interaction between fibrinogen and erythrocytes cannot lead to clot formation, but it is able to promote erythrocyte transient aggregation, increasing the cardiovascular risk associated with pathological conditions.

Correlation analysis of the patients' clinical data (summarized in Table 1) with all the AFM and haemorrheological data was

Table 1 | Clinical profile, concomitant diseases and therapeutics at baseline of all CHF patients studied and for non-ischaemic and ischaemic CHF patient groups.

	CHF patients (all)	Non-ischaemic CHF	Ischaemic CHF
Demographics			
No. of patients	30	15	15
Age (mean ± s.d.)	63.8 ± 9.9	61.9 ± 10.8	65.6 ± 9.1
Male/female (%)	90/10	85/15	92/8
Cardiac parameters			
NYHA, II/III (%)	57/43	33/67	80/20
LV ejection fraction (%; mean ± s.d.)	30.3 ± 8.8	29.5 ± 10.0	31.01 ± 7.7
Fibrinogen (mg dl^{-1}; mean ± s.d.)	325 ± 85	355 ± 96	296 ± 62
NT-ProBNP (pg ml^{-1}; median)	1,330	2,683	744
Concomitant diseases			
Diabetes mellitus (%)	23	13	33
Hypertension (%)	87	80	93
Myocardial infarction (%)	50	0	100
Auricular fibrillation (%)	30	40	20
Chronic renal insufficiency (%)	50	60	40
Chronic obstructive pulmonary disease (%)	13	13	13
Therapeutics at inclusion			
Furosemide (%)	83	93	73
ACE inhibitor (%)	60	80	40
Angiotensin receptor blocker (%)	30	20	40
Beta-blocker (%)	83	93	73
Cardiac resynchronization therapy (%)	33	60	7
Anti-platelet aggregation (%)	80	60	100

ACE, angiotensin-converting enzyme; LV, left ventricular; NT-ProBNP, N-terminal pro-brain natriuretic peptide; NYHA, New York Heart Association functional classification (II, symptomatically 'mild' CHF; III, symptomatically 'moderate' CHF); s.d., standard deviation.

© 2016 Macmillan Publishers Limited. All rights reserved

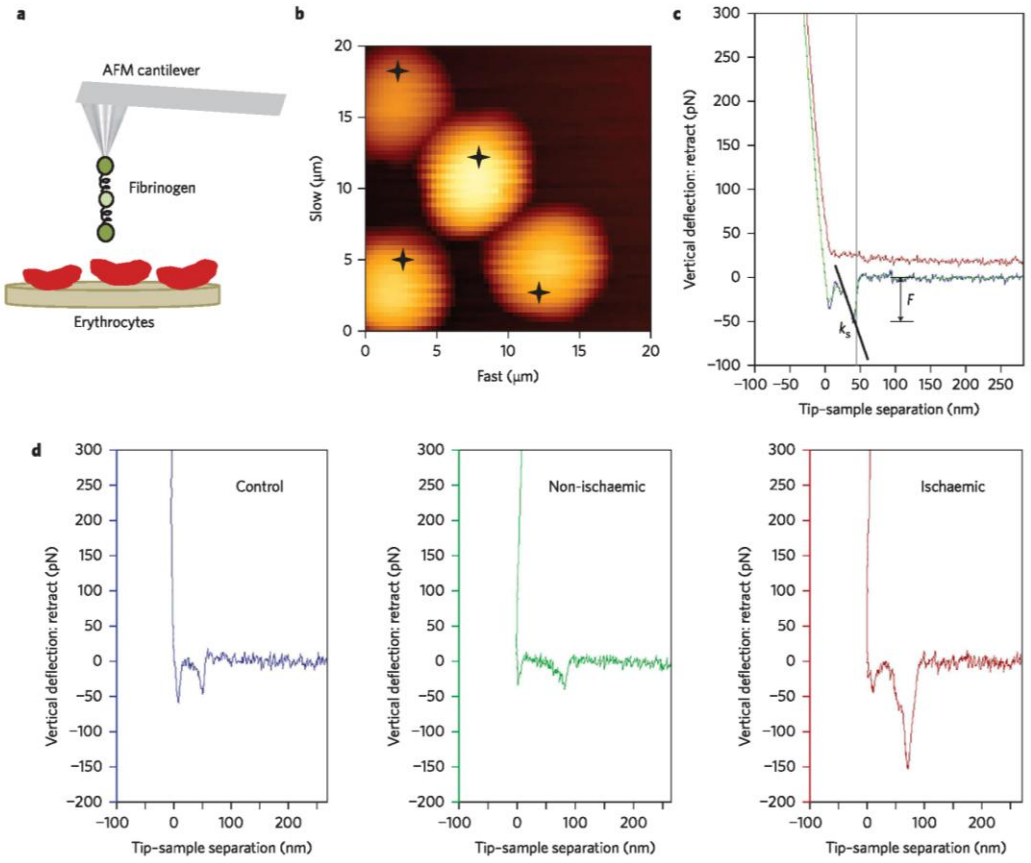

Figure 1 | AFM-based force spectroscopy set-up and its crude data. a, Schematic representation of erythrocytes deposited on a poly-L-lysine-coated glass slide and an AFM tip chemically functionalized with fibrinogen molecule(s). **b**, Example of a force mapping height image of erythrocytes (image is 20 × 20 μm^2; height colour scale adjusted to 1.2 μm). The symbols indicate the surface locations chosen on each cell to perform force spectroscopy measurements. **c**, Example of a force–distance curve, showing a single adhesion event. When approaching the tip to the sample (red line), the fibrinogen molecule may contact cell receptor(s), enabling binding. When retracting the tip away from the sample (blue line), as the cantilever moves upwards the tip bends down to negative force values. At a particular distance the bond breaks, and the cantilever jumps back to its neutral force position. The force *F* necessary to break the bond at the single-molecule level can be determined from this point, and the effective spring constant of the cantilever–cell system (k_s) can be calculated from the slope of the force–distance curve (black line). The green line, which is superimposed on the blue line, defines the fitting of the retraction curve. The grey vertical line indicates the recognition of an adhesion event between fibrinogen and its erythrocyte membrane receptor, with its force calculated after polynomial fitting of the retraction curve. **d**, Typical force–distance curves obtained for the interaction of fibrinogen with erythrocytes from the three studied groups: control healthy donors (blue curve), non-ischaemic CHF patients (green) and ischaemic CHF patients (red). For simplicity, only the retraction curves are shown.

performed. Fibrinogen plasma concentration was found to correlate positively and significantly with whole blood viscosity at high shear rate values (Supplementary Fig. 4).

Patients' annual hospitalization rate was 23.3%. Importantly, the 12-month clinical follow-up showed that patients with higher fibrinogen–erythrocyte binding forces at the beginning of the study had a higher probability of being hospitalized due to cardiovascular complications (103.8 pN, 95% confidence interval (CI) 55.1–112.9 versus 36.9 pN, 95% CI 28.0–93.5; $P = 0.033$). The receiver operating characteristic (ROC) curve for hospitalization was associated with the AFM binding force (area under curve (AUC) = 0.770, 95% CI 0.598–0.902; $P = 0.033$) and the percentage of (un)binding events (AUC = 0.714, 95% CI 0.532–0.896; $P = 0.091$). Fibrinogen–erythrocyte binding forces above the median (52.37 pN) were associated with higher risk of hospitalization (hazard ratio, HR = 6.85, 95% CI 0.82–56.9; $P = 0.075$), as presented on the hospitalization curve (Fig. 5; $P = 0.038$).

We have shown that the fibrinogen–erythrocyte interaction, as characterized by AFM-based force spectroscopy, is modified in heart failure patients. Moreover, fibrinogen–erythrocyte binding forces have been shown to be associated with a patient's clinical outcome: those with higher AFM-measured fibrinogen–erythrocyte binding forces presented a higher probability of cardiovascular disease-associated hospitalization during the subsequent 12-month clinical follow-up period. This result highlights the importance of the fibrinogen–erythrocyte interaction in CHF patients and identifies a possible subgroup of patients at higher risk. The AFM-based methodology presented here has proven to be a promising nanotool to evaluate changes in the interaction

© 2016 Macmillan Publishers Limited. All rights reserved

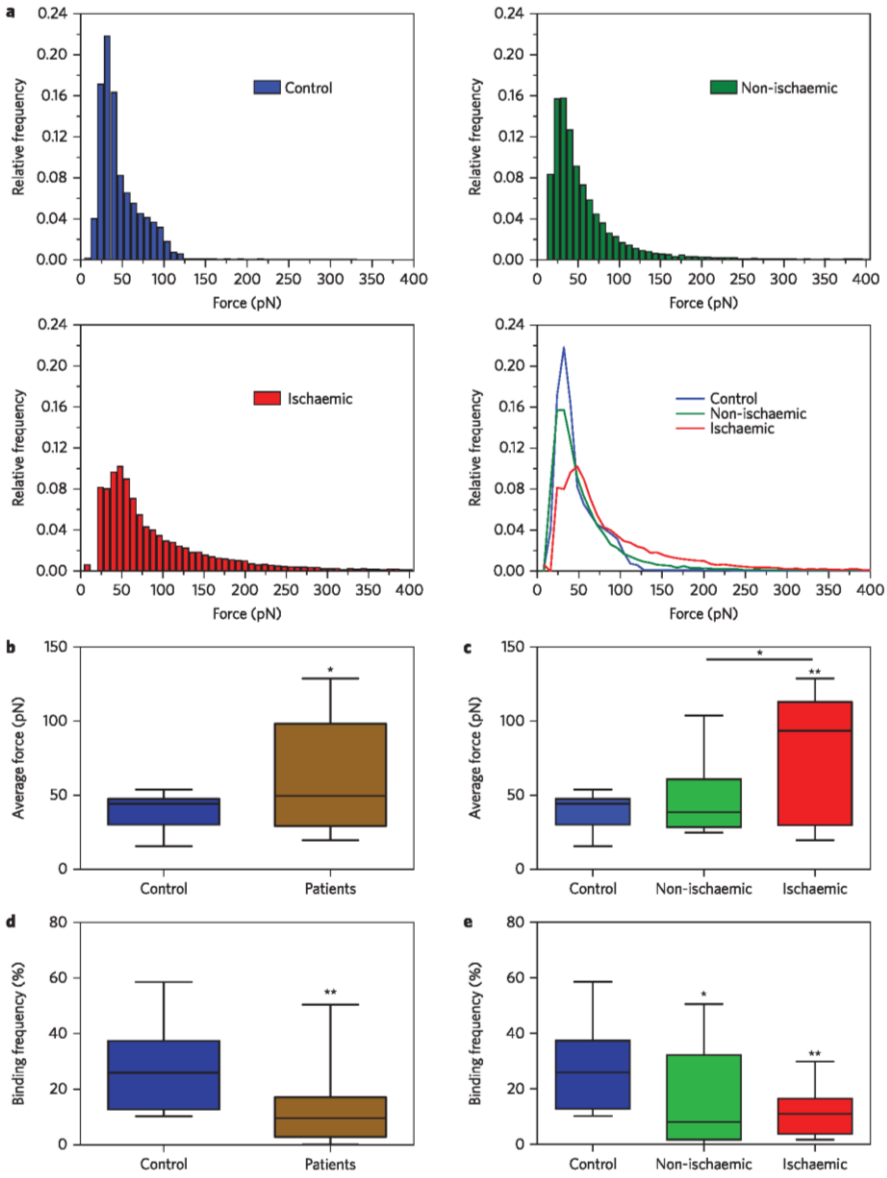

Figure 2 | AFM-based force spectroscopy data for the interactions between fibrinogen and erythrocytes from heart failure patients and healthy blood donors. **a**, Rupture force histograms, showing the distributions of the values for the interactions between fibrinogen and erythrocytes from healthy blood donors (control) and heart failure patients (non-ischaemic and ischaemic). A comparison of the rupture force profiles obtained for the three studied groups is also presented. The *y* axes of the histograms show the relative probability of the binding occurring. On the rupture force histograms, each count represents single-molecule binding (and subsequent unbinding) between one fibrinogen molecule and one of its specific erythrocyte receptors. Measurements were carried out with an applied force of 0.8 nN and a retraction speed of 2 μm s^{-1}. **b–e**, Average binding forces (**b**,**c**) and binding frequencies (**d**,**e**) for all patients versus control subjects (**b**,**d**) and with patients divided according to aetiology (ischaemic or non-ischaemic) (**c**,**e**). The average force necessary to break the bond between fibrinogen and erythrocytes from CHF patients was higher than for the control group. Ischaemic patients presented higher binding forces than non-ischaemic patients. Values are presented as mean ± s.e.m. Statistical significance values: $^{*}P = 0.038$ (**b**); $^{*}P = 0.021$ and $^{**}P = 0.004$ (**c**); $^{**}P = 0.003$ (**d**); $^{*}P = 0.040$ and $^{**}P = 0.002$ (**e**). Error bars in **b–e** represent the minimum and maximum values for all data.

between fibrinogen and human blood cells, pinpointing patients with increased cardiovascular risk. Fibrinogen–erythrocyte binding forces, measured at the single-molecule level, are thus a potential biomarker for CHF severity and may eventually be used also for the risk assessment of other cardiovascular diseases. However, this is a pilot study, with a relatively small number of

© 2016 Macmillan Publishers Limited. All rights reserved

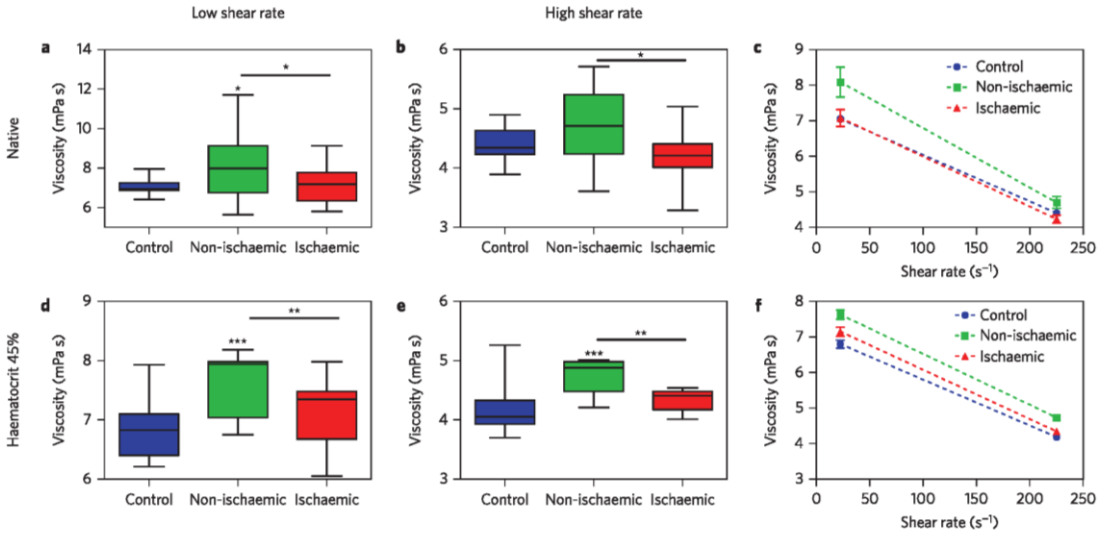

Figure 3 | Changes in whole blood viscosity between ischaemic and non-ischaemic CHF patients and healthy donors. a–f, Viscosities of native whole blood (**a–c**) or after haematocrit correction to 45% (**d–f**) were measured at low (22.5 s^{-1}; **a,d**) and high (225 s^{-1}; **b,e**) shear rate values. Plots of whole blood viscosity versus shear rate are also shown for each studied group (**c,f**; dashed lines are guides to the eye). At 45% haematocrit, non-ischaemic CHF patients displayed higher whole blood viscosity than the control group. Non-ischaemic patients showed higher whole blood viscosity than ischaemic patients. Values are presented as mean ± s.e.m. Statistical significance values: $*P = 0.010$ (non-ischaemic versus control) and $*P = 0.046$ (**a**, ischaemic versus non-ischaemic); $*P = 0.028$ (**b**); $**P = 0.014$ and $***P < 0.0001$ (**d**); $**P = 0.001$ and $***P < 0.0001$ (**e**). Error bars in **a,b,d,e** represent the minimum and maximum values for all data.

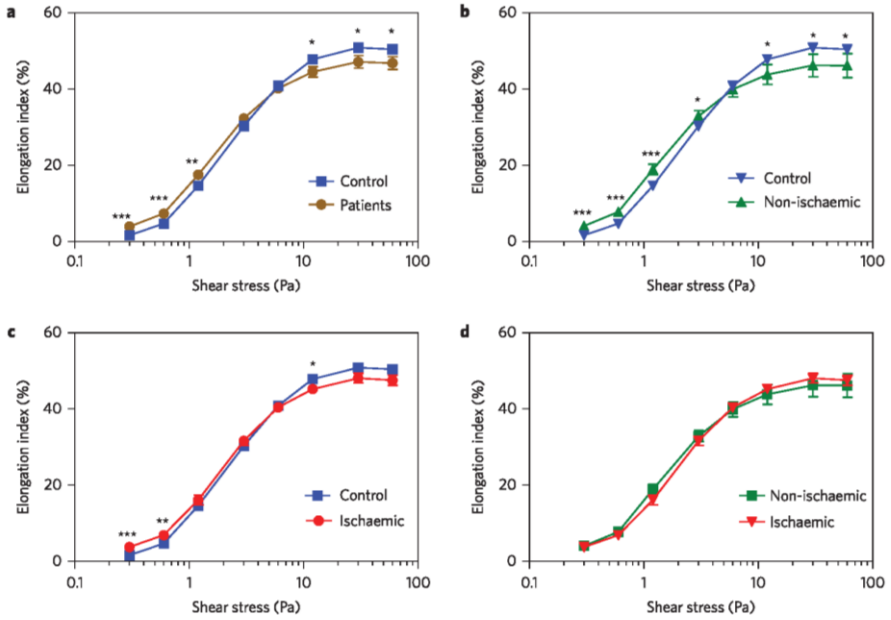

Figure 4 | Erythrocyte deformability measured at different shear stress values for all studied groups. a–d, Changes in erythrocyte deformability (assessed as elongation index) between CHF patients and healthy donors (**a**) and according to aetiologies (**b–d**). Erythrocyte deformability was measured at shear stress values between 0.3 and 60 Pa, mimicking blood vessels of different diameters. Both patient groups showed higher deformability than the control group at low shear stresses, but lower deformability at higher shear stresses. Values are presented as mean ± s.e.m. Statistical significance values: $*P < 0.037$, $**P = 0.0043$ and $***P < 0.0001$ (**a**); $*P < 0.046$ and $***P < 0.0003$ (**b**); $*P = 0.032$, $**P = 0.0056$ and $***P < 0.0001$ (**c**).

© 2016 Macmillan Publishers Limited. All rights reserved

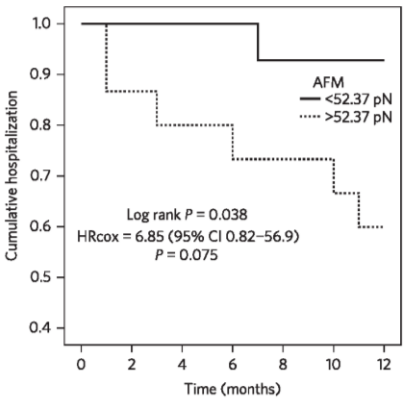

Figure 5 | Hospitalization curve according to fibrinogen–erythrocyte (un)binding forces. AFM-determined fibrinogen–erythrocyte (un)binding forces above the median (52.37 pN) are associated with the hospitalization curve (log rank $P = 0.038$) and tendency to a higher risk of hospitalization (HR = 6.85; 95% CI 0.82–56.9; $P = 0.075$). The time-to-event data analyses include Kaplan–Meier representations with the log-rank test and the Cox regression for hazard risk determination.

patients. Studies with a larger number of patients should be encouraged to further confirm these findings before translating them for clinical application.

Methods

Methods and any associated references are available in the online version of the paper.

Received 5 October 2015; accepted 3 March 2016; published online 16 May 2016

References

1. Alexander, K. S., Kazmierczak, S. C., Snyder, C. K., Oberdorf, J. A. & Farrell, D. H. Prognostic utility of biochemical markers of cardiovascular risk: impact of biological variability. *Clin. Chem. Lab. Med.* **51,** 1875–1882 (2013).
2. Lominadze, D., Dean, W. L., Tyagi, S. C. & Roberts, A. M. Mechanisms of fibrinogen-induced microvascular dysfunction during cardiovascular disease. *Acta Physiol. (Oxf.)* **198,** 1–13 (2010).
3. Reinhart, W. H. Fibrinogen—marker or mediator of vascular disease? *Vasc. Med.* **8,** 211–216 (2003).
4. Cecchi, E., Mannini, L. & Abbate, R. Role of hyperviscosity in cardiovascular and microvascular diseases. *G. Ital. Nefrol.* **26,** 20–29 (2009).
5. WHO. *Global Status Report on Non-Communicable Diseases 2010* (World Health Organization, 2011).
6. Lillioja, S. *et al.* Skeletal muscle capillary density and fiber type are possible determinants of *in vivo* insulin resistance in man. *J. Clin. Invest.* **80,** 415–424 (1987).
7. Mann, D. L. & Bristow, M. R. Mechanisms and models in heart failure: the biomechanical model and beyond. *Circulation* **111,** 2837–2849 (2005).
8. Follath, F. Ischemic versus non-ischemic heart failure: should the etiology be determined? *Heart Fail. Monit.* **1,** 122–125 (2001).
9. Bishop, J. J., Nance, P. R., Popel, A. S., Intaglietta, M. & Johnson, P. C. Effect of erythrocyte aggregation on velocity profiles in venules. *Am. J. Physiol. Heart. Circ. Physiol.* **280,** H222–H236 (2001).
10. Kim, S., Popel, A. S., Intaglietta, M. & Johnson, P. C. Aggregate formation of erythrocytes in postcapillary venules. *Am. J. Physiol. Heart Circ. Physiol.* **288,** H584–H590 (2005).
11. Delamaire, M. & Durand, F. Erythrocyte aggregation and vascular pathology. *J. Mal. Vasc.* **15,** 344–346 (1990).
12. Falcó, C. *et al.* Influence of fibrinogen levels on erythrocyte aggregation determined with the Myrenne aggregometer and the Sefam erythro-aggregometer. *Clin. Hemorheol. Microcirc.* **33,** 145–151 (2005).
13. Maeda, N., Seike, M., Kume, S., Takaku, T. & Shiga, T. Fibrinogen-induced erythrocyte aggregation: erythrocyte-binding site in the fibrinogen molecule. *Biochim. Biophys. Acta* **904,** 81–91 (1987).
14. Lominadze, D. & Dean, W. L. Involvement of fibrinogen specific binding in erythrocyte aggregation. *FEBS Lett.* **517,** 41–44 (2002).
15. Carvalho, F. A. *et al.* Atomic force microscopy-based molecular recognition of a fibrinogen receptor on human erythrocytes. *ACS Nano* **4,** 4609–4620 (2010).
16. Carvalho, F. A., de Oliveira, S., Freitas, T., Gonçalves, S. & Santos, N. C. Variations on fibrinogen-erythrocyte interactions during cell aging. *PLoS ONE* **6,** e18167 (2011).
17. Carvalho, F. A. & Santos, N. C. Atomic force microscopy-based force spectroscopy—biological and biomedical applications. *IUBMB Life* **64,** 465–472 (2012).
18. Choi, S., Jung, G. B., Kim, K. S., Lee, G. J. & Park, H. K. Medical applications of atomic force microscopy and Raman spectroscopy. *J. Nanosci. Nanotechnol.* **14,** 71–97 (2014).
19. Pillet, F., Chopinet, L., Formosa, C. & Dague, E. Atomic force microscopy and pharmacology: from microbiology to cancerology. *Biochim. Biophys. Acta* **1840,** 1028–1050 (2014).
20. Thiagarajan, P., Rippon, A. J. & Farrell, D. H. Alternative adhesion sites in human fibrinogen for vascular endothelial cells. *Biochemistry* **35,** 4169–4175 (1996).
21. Carvalho, F. A. *et al.* Dengue virus capsid protein binding to hepatic lipid droplets (LD) is potassium ion dependent and is mediated by LD surface proteins. *J. Virol.* **86,** 2096–2108 (2012).
22. Baskurt, O. K. & Meiselman, H. J. Blood rheology and hemodynamics. *Semin. Thromb. Hemost.* **29,** 435–450 (2003).
23. Ebner, A., Schillers, H. & Hinterdorfer, P. in *Atomic Force Microscopy in Biomedical Research* Vol. 736 (eds Braga, P. C. & Ricci, D.) 223–241 (Humana, 2011).
24. Maciaszek, J. L. & Lykotrafitis, G. Sickle cell trait human erythrocytes are significantly stiffer than normal. *J. Biomech.* **44,** 657–661 (2011).
25. Rand, P. W., Lacombe, E., Hunt, H. E. & Austin, W. H. Viscosity of normal human blood under normothermic and hypothermic conditions. *J. Appl. Phys.* **19,** 117–122 (1964).
26. Papaioannou, T. G. & Stefanadis, C. Vascular wall shear stress: basic principles and methods. *Hellenic J. Cardiol.* **46,** 9–15 (2005).
27. Schmid-Schonbein, H., Wells, R. E. & Goldstone, J. Fluid drop-like behaviour of erythrocytes—disturbance in pathology and its quantification. *Biorheology* **7,** 227–234 (1971).

Acknowledgements

This work was supported by Fundação para a Ciência e a Tecnologia – Ministério da Ciência, Tecnologia e Ensino Superior (FCT-MCTES, Portugal) grants PTDC/QUI-BIQ/119509/2010 and PTDC/BBB-BMD/6307/2014, as well as fellowship SFRH/BD/84414/2012 to A.F.G. The authors thank T. Freitas (FMUL) for technical assistance.

Author contributions

A.F.G. performed AFM experiments, analysed force spectroscopy data, performed the statistical analysis, wrote and edited the draft and prepared the manuscript for submission. F.A.C. analysed the force spectroscopy data, wrote the manuscript and edited successive drafts of the paper. I.M. performed some of the initial AFM experiments and analysed their data. L.S. collected all clinical data, performed some statistical analysis, contributed to relevant discussions and edited the draft. N.L. contributed to the discussion section and N.C.S. conceived the idea, designed and directed the AFM experiments, analysed the data, wrote the manuscript and edited successive drafts of the paper.

Additional information

Supplementary information is available in the online version of the paper. Reprints and permissions information is available online at www.nature.com/reprints. Correspondence and requests for materials should be addressed to F.A.C. and N.C.S.

Competing financial interests

The authors declare no competing financial interests.

© 2016 Macmillan Publishers Limited. All rights reserved

Methods

Study participants. Thirty patients with heart failure were enrolled in the study. Patients were in ambulatory care, with stable CHF, and were receiving optimized medical therapy according to the European Society of Cardiology (ESC) guidelines[28]. As the interaction between heart failure aetiology and the experimental variables under evaluation could be expected, an effort was made to include patients with ischaemic and non-ischaemic aetiologies in a 1:1 ratio. Inclusion criteria were CHF outpatients, systolic dysfunction (left ventricular ejection fraction ≤40%), functional classification according to the New York Heart Association (NHYA) on class II or III, and no recent hospitalization (>3 months). Additionally, a control group of 15 healthy donors was also included in the study, following a protocol with the Portuguese Blood Institute (IPS, Lisbon).

Clinical profiles were collected thoroughly. The clinical follow-up was 12 months long. The evaluated outcome was cardiovascular-related hospitalization. A structured questionnaire for the description of events was used and the circumstances of the incident were determined from the hospital records and/or interviews with relatives.

Blood from healthy donors or CHF patients was obtained, with their previous written informed consent, at IPS or Hospital Pulido Valente (Lisbon). The study was approved by the joint Ethics Committee of Faculdade de Medicina da Universidade de Lisboa and Centro Hospitalar Lisboa Norte. All the study was conducted with double blinding between the clinicians and researchers conducting the laboratory measurements.

Erythrocyte isolation and preparation for AFM measurements. For erythrocyte isolation, blood was centrifuged at 220*g* for 10 min at 10 °C. Plasma and buffy coat were removed, and the erythrocytes were washed three times with buffered saline glucose citrate (BSGC: 1.6 mM KH_2PO_4, 8.6 mM Na_2HPO_4, 120 mM NaCl, 13.6 mM sodium citrate, 11.1 mM glucose) pH 7.3, supplemented with 1 mM calcium chloride. Erythrocytes were diluted to 0.1% haematocrit on the same buffer and placed on a clean poly-L-lysine-coated glass slide. Cells were firmly attached to the glass slide after 30 min of deposition, at room temperature. Non-adherent cells were removed by sequential washes with buffer, loaded into the atomic force microscope and allowed to equilibrate in this buffer for 15 min before force spectroscopy measurements. No cell fixation was involved in sample preparation.

AFM tip functionalization. For the covalent attachment of fibrinogen molecules to the AFM tips, we used our previously optimized procedure[15]. Briefly, ultraviolet-light-cleaned OMCL TR-400-type silicon nitride tips (Olympus) were silanized in a vacuum chamber with 3-aminopropyl-triethoxysilane (APTES) for 1 h in an argon atmosphere. The AFM tips were then treated with a glutaraldehyde solution (2.5% vol/vol) for 20 min. Finally, the tips were placed in 1 mg ml^{-1} human purified fibrinogen (Sigma) for 30 min and immediately mounted on the AFM for the force spectroscopy experiments.

AFM-based force spectroscopy. AFM studies were conducted using a force spectroscopy methodology[15–17]. After covalently attaching fibrinogen molecules to the AFM tip (probe), we used it to tap on the surface of the erythrocytes (Fig. 1a), measuring the frequency or probability of binding and the force necessary to break those bonds. AFM studies were performed on a NanoWizard II atomic force microscope (JPK Instruments) mounted on an Axiovert 200 inverted optical microscope (Zeiss). The AFM head was equipped with a 15 μm *z*-range linearized piezoelectric scanner and an infrared laser. Force spectroscopy measurements were performed in a liquid environment, using the softest triangular cantilevers, with a tip radius of 15 nm and a resonant frequency of 11 kHz in air, or ~3 kHz in solution. The spring constants of the cantilevers were calibrated by the thermal fluctuation method[29], yielding values of 21 ± 9 mN m. The applied force was adjusted to maintain a force of 0.8 nN before retraction. Data were collected at 2 μm s^{-1} for each force–distance cycle. By measuring the average slope of the retraction traces of the force measurements (Fig. 1c), we determined the effective spring constant of the cell–cantilever system (k_s)[30–33] as 2.9 ± 1.1 mN m^{-1}. Thus, by multiplying the effective spring constant by the cantilever retraction rate we could obtain the loading rates for each force spectroscopy experiment, for each group. Thus, experiments were conducted at a loading rate of 3.96 ± 3.38 nN s^{-1} for the control group, 5.60 ± 4.24 nN s^{-1} for the non-ischaemic group and 5.36 ± 4.5 nN s^{-1} for the ischaemic group (values in mean ± s.d.; Supplementary Fig. 5). The differences between these ranges are not statistically significant. After positioning the cantilever on top of a single cell, with the help of a charge-coupled device camera, AFM force mapping height images were recorded (Fig. 1b). Molecular recognition was searched by intermittently pressing the cantilevers on a point on the periphery of each cell adsorbed on the glass slide.

Force curves were analysed using JPK image processing software v. 4.2.61. For each blood sample, approximately 3,750 force versus distance curves were collected, analysed and adjusted by polynomial fit. Data were collected from 25 different erythrocytes on each sample and with different functionalized tips. All results from the patients were matched with those obtained with blood samples from healthy donors. Histograms of the unbinding forces for each studied group were constructed by choosing the ideal bin size to achieve the best fitted Gaussian model peak forces. Binning size was fixed at 8 pN. Force rupture values up to 10 pN were considered to represent noise or artefacts. As we confirmed the specificity of the binding for force values above 25 pN (Supplementary Fig. 1), those between10 and 25 pN were considered to be due to unspecific interactions. From each histogram, the single fibrinogen molecule rupture force can be determined by fitting the distributions of the rupture forces with the Gaussian model. In parallel, average rupture forces were also calculated from the binding data, obtained on the different cells tested for each patient or healthy donor. Rupture force values are defined as the force necessary to break the bond between a single molecule of fibrinogen and its cell receptor.

All the interactions between fibrinogen and erythrocytes were studied at room temperature in physiological buffer. The AFM laboratory was strictly maintained between 23 and 25 °C. Small variations in temperature within this range did not affect the force spectroscopy measurements, even after a long period of experiments. As controls for tip modification, measurements with tips at different steps of their functionalization process (including non-functionalized tips) were conducted on glass slides, with and without poly-L-lysine, and on blood cells[15].

Following a previously established procedure[21], blocking experiments with antibodies against different integrins were performed to complement the identification of the fibrinogen receptor on erythrocytes and further confirm the specificity of the binding interactions between fibrinogen and its erythrocyte membrane receptor (Supplementary Fig. 1).

Cell elasticity analysis. Differences in erythrocyte elasticity between the studied patients (non-ischaemic and ischaemic) and control groups were evaluated by analysing in parallel the approach curves of the previously described force spectroscopy measurements (Supplementary Fig. 2). Data were analysed to obtain the cells' Young's modulus *E*, using JPK Image Processing v. 4.2.53, by applying the Hertzian model, with a fixed tip–sample separation of between −200 and 200 nm. Values of AFM tip penetration depth into the erythrocytes were also obtained (Supplementary Fig. 2).

Haematological profile. Quantitative analyses of the haemogram of the blood samples of CHF patients and healthy donors were performed using PocH-100iV equipment (Sysmex).

Whole blood viscosity. Whole blood viscosity was measured with a Brookfield DV-II viscometer (Brookfield Engineering Laboratories). Measurements were performed both using native blood samples and samples with haematocrit adjusted to 45%, at 37 °C, while submitting the samples to both low (22.5 s^{-1}) and high (225 s^{-1}) shear rates.

Erythrocyte deformability. Erythrocyte deformability was assessed at 22 °C using a Rheodyn SSD laser diffractometer (Myrenne) and presented as erythrocyte elongation indexes (EEIs). The diffraction pattern was analysed at eight shear stress values, between 0.30 and 60.0 Pa. EEIs were calculated using the light intensities of the diffraction pattern[27].

Statistical analysis. Descriptive statistics are given as mean ± standard error of the mean (s.e.m.), frequency and median (interquartile range). For every variable, all samples were tested against the control group. The unpaired Student's *t*-test was used for statistical analysis of the intergroup comparison. One-way analysis of variance followed by a Dunnett post-test were used for multiple comparisons of data from CHF patients versus control. For non-Gaussian variables, the corresponding non-parametric methods were used, such as the Mann–Whitney U test when performing two group comparisons and the Spearman correlation test. Linear regression analyses to evaluate the relation between whole blood viscosity and AFM data (binding force or frequency) were also performed (Supplementary Fig. 3).

Categorical variables were compared using the χ^2 and Fisher's exact tests with the odds-ratio calculation. The accuracy of predicting the endpoint (hospitalization) was determined by the area under the ROC curve, for significant continuous variables. The optimal cutoff value used for AFM was the median. The time-to-event data analyses included Kaplan–Meier representations with the log-rank test and the Cox regression for hazard risk determination, with the calculation of hazard ratios (HRs) and 95% CIs. Statistical significance was set at $P < 0.05$. Statistical analyses were performed using GraphPad Prism 5 and SPSS v. 22.0.

References

28. McMurray, J. J. *et al.* ESC guidelines for the diagnosis and treatment of acute and chronic heart failure 2012: The Task Force for the Diagnosis and Treatment of Acute and Chronic Heart Failure 2012 of the European Society of Cardiology. Developed in collaboration with the Heart Failure Association (HFA) of the ESC. *Eur. Heart J.* **33,** 1787–1847 (2012).
29. Hutter, J. L. & Bechhoefer, J. Calibration of atomic-force microscope tips. *Rev. Sci. Instrum.* **64,** 1868–1873 (1993).
30. Chen, A. & Moy, V. T. Cross-linking of cell surface receptors enhances cooperativity of molecular adhesion. *Biophys. J.* **78,** 2814–2820 (2000).
31. Kienberger, F., Kada, G., Mueller, H. & Hinterdorfer, P. Single molecule studies of antibody–antigen interaction strength versus intra-molecular antigen stability. *J. Mol. Biol.* **347,** 597–606 (2005).
32. Neundlinger, I. *et al.* Forces and dynamics of glucose and inhibitor binding to sodium glucose co-transporter SGLT1 studied by single molecule force spectroscopy. *J. Biol. Chem.* **289,** 21673–21683 (2014).
33. Zhang, X., Wojcikiewicz, E. & Moy, V. T. Force spectroscopy of the leukocyte function-associated antigen-1/intercellular adhesion molecule-1 interaction. *Biophys. J.* **83,** 2270–2279 (2002).

© 2016 Macmillan Publishers Limited. All rights reserved

SUPPLEMENTARY INFORMATION
DOI: 10.1038/NNANO.2016.52

Atomic force microscopy as a tool to evaluate the risk of cardiovascular diseases in patients

Ana Filipa Guedes; Filomena A. Carvalho; Inês Malho; Nuno Lousada; Luís Sargento; Nuno C. Santos

Biomedical Relevance

Cardiovascular diseases are the leading cause of death worldwide, being responsible for approximately 30% of the total number of human losses[1]. Chronic heart failure (CHF), a complex clinical cardiovascular syndrome, is characterized by the heart failing to pump enough blood with the right pressure[2, 3]. Ischemic cardiomyopathy is the most common cause of heart failure in industrialized countries[4]. The prognosis and response to treatment of patients with ischemic heart failure are worse than in patients with a non-ischemic etiology[5]. The term "non-ischemic heart failure" includes different subgroups, such as hypertensive heart disease, myocarditis and cardiac dysfunction due to rapid atrial fibrillation, which may be reversible[5].

Establishing the diagnostic, extent, and severity of cardiovascular diseases, as well as determining the potential risk of cardiovascular events are crucial steps toward improving patient outcomes. The most common non-invasive tests and procedures used to evaluate CHF are reported on the *Guidelines for the Evaluation and Management of Heart Failure*[6], and include electrocardiogram, chest radiograph and transthoracic Doppler–two-dimensional echocardiogram, among others. Although these methods are well established within the daily clinical practice, none of them assesses changes at the cellular and molecular levels. The development of new methods to detect early molecular changes in different tissues, or changes in normal blood flow before clinical symptoms appear, without invasive intervention, is therefore very important in clinical diagnosis and prognosis. Some methods proved to be

© 2016 Macmillan Publishers Limited. All rights reserved.

DOI: 10.1038/NNANO.2016.52

effective in detecting local changes, by quantitatively evaluating them (*e.g.*, contrast-enhanced ultrasound) or imaging molecule-associated endothelial activation (*e.g.*, early detection of atherosclerotic lesions[7]). Other methods such as positron emission tomography imaging (PET), computer tomography, magnetic resonance imaging (MRI) or electron microscopy are extremely expensive and require complex sample preparation, modification and handling[8].

The development of new pharmacologic therapies, surgical cardiovascular procedures and mechanical circulatory support devices to treat heart failure has slowed down the increase in CHF-associated mortality[9]. However, the availability of biomarkers to evaluate risk in this disease is still limited[10]. A better understanding of the molecular mechanisms underlying the interaction between fibrinogen and erythrocytes in CHF patients may be important for eventual future drug interventions to reduce aggregation and enhance microcirculatory flow conditions.

Supplementary Methods

Fibrinogen-erythrocyte binding inhibition studies

As controls for this experimental approach, the interaction between fibrinogen and its integrin receptor on erythrocytes, assessed by AFM, was found to be inhibited by the absence of calcium ions (essential for the activity of the receptor), and by the presence of eptifibatide, a molecule used in hospital settings to inhibit fibrinogen-platelet binding, which we previously demonstrated to be also able to inhibit fibrinogen-erythrocyte binding[11].

Additionally, in order to further assess the specificity of the binding between fibrinogen and its erythrocyte membrane receptor, as well as to complete its identification, we measured the inhibition of the fibrinogen-erythrocyte interaction in the presence of two mouse anti-human antibodies: anti-α_v (clone NKI-M9; Biolegend, San Diego, CA, USA) and anti-$\alpha_v\beta_3$ integrins (clone 23C6; eBioscience Inc., San Diego, CA, USA), following a previously established procedure[12]. The effects of the two antibodies were evaluated by AFM-based force spectroscopy after incubating the erythrocytes at two different antibody concentrations (10 and 25 μg/mL),

© 2016 Macmillan Publishers Limited. All rights reserved.

for 1 h, at room temperature. As a negative control for the antibodies blocking experiments, the effect of an isotype matched non-integrin antibody was also tested (normal mouse IgG serum, Santa Cruz Biotechnology, Santa Cruz, CA, USA).

Erythrocyte elasticity

Force spectroscopy data were analyzed to obtain the cells Young's modulus (E), using JPK Image Processing v. 4.2.53, by the application of the Hertzian model. The model was applied to all force curves obtained from non-ischemic and ischemic CHF patients and controls, with a fixed tip-sample separation between -200 and 200 nm. The probe was modeled as a quadratic pyramid, with a tip angle of 35° (half-angle to face) and a Poisson ration of 0.50. Young's modulus histograms were constructed for each experimental condition studied. The ideal histogram bin size was chosen in order to achieve the best fitted Gaussian model peak length, yielding a selected binning size of 0.1 kPa. The maximum values of the Gaussian peaks represent different statistical measure of the Young's modulus of the cells. Values of the mean ± standard deviation and median of each group were also taken into consideration.

AFM tip penetration depth onto erythrocytes was also evaluated. This parameter is analyzed by the position of the maximal movement of the piezo sensor in the z-axis, which corresponds to the z-axis coordinate when the sensor reaches an indentation force of 800 pN, subtracting the z-axis position of the sensor when the tip begins the contact with the surface of the erythrocyte. Statistical significance was determined with pair-wise comparisons made with Student's *t*-test to compare the cells datasets, using a 5% confidence interval. Statistical analysis was carried out using the Graphpad Prism software v. 5.0.

© 2016 Macmillan Publishers Limited. All rights reserved.

DOI: 10.1038/NNANO.2016.50

Supplementary Results

Fibrinogen-erythrocyte binding inhibition studies

As shown in Supplementary Fig. 1, the percentage of inhibition of fibrinogen-erythrocyte binding induced by 10 μg/mL anti-α_v was 24.6%, a value higher than the percentage of inhibition achieved for the same concentration of anti-$\alpha_v\beta_3$ antibody. At higher antibody concentrations, the difference between the levels of inhibition of fibrinogen-erythrocyte binding observed for both antibodies becomes even more evident (54.4% *vs.* 13.9% for anti-α_v and anti-$\alpha_v\beta_3$, respectively). Inhibition is concomitant with a significant reduction of the stronger binding events, especially in the presence of the anti-$\alpha_v\beta_3$ integrin antibody, remaining mainly the interactions with lower (un)binding forces. No detectable binding inhibition or binding force reduction were observed in the presence of 25 μg/mL isotype-matched non-integrin antibody (negative control), further confirming the specificity of the interaction between fibrinogen and the erythrocyte membrane.

© 2016 Macmillan Publishers Limited. All rights reserved.

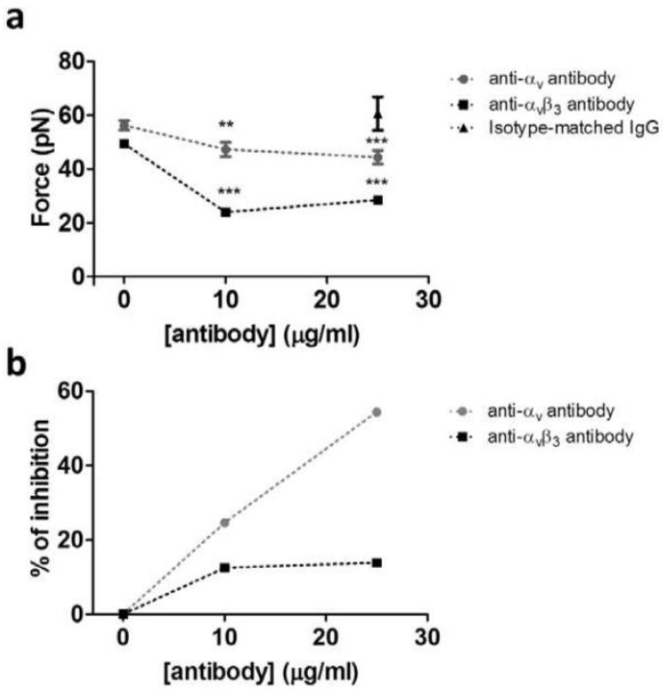

Supplementary Figure 1 | Inhibition of the binding between the fibrinogen protein and erythrocyte receptor by antibodies against α_v and $\alpha_v\beta_3$ integrins. (**a**) Average fibrinogen-erythrocyte binding rupture forces and (**b**) percentage of fibrinogen-erythrocyte binding inhibition (decrease on the binding frequency) in the presence of specific antibodies against α_v integrin (grey circles), $\alpha_v\beta_3$ integrin (black squares), and a negative control with an isotype-matched non-integrin antibody (black triangle). Antibody concentrations were 10 and 25 μg/mL, in BSGC buffer with $CaCl_2$ 1 mM.

© 2016 Macmillan Publishers Limited. All rights reserved.

DOI: 10.1038/NNANO.2016.50

Cell elasticity

In an effort to understand why the AFM data show that CHF patients (especially ischemic patients) have significantly increased fibrinogen-erythrocyte binding forces, we analyzed the erythrocyte elasticity parameters of the same samples. With this purpose, all force spectroscopy data were analyzed in order to determine the Young's modulus and the penetration depth for each force-distance curve. The results obtained are presented in Supplementary Fig. 2. Young's modulus data of each group are presented in a relative frequency histogram (Supplementary Fig. 2a). Gaussian polynomial fit was applied, but the results could not be accurately compared between groups because the fitting does no converge for the control group. Comparing just the values of the mean ± SEM and median for each group, for the control group we obtained values of 1205 ± 14.2 Pa and 390.1 Pa, respectively. As for the non-ischemic CHF group, the values obtained were 1248 ± 10.8 Pa and 743.4 Pa. Finally, the results for ischemic CHF patients were 1142 ± 10.8 Pa and 568.5 Pa. These variations were only statistically significant for the median, in which we observed an increased cell stiffness (or decreased elasticity) on both groups of CHF patients, with the larger variation being observed for the non-ischemic patients.

On the assessment of erythrocyte stiffness variations between healthy and CHF patients, AFM tip penetration depth was also determined (Supplementary Fig. 2b). This parameter allows one to evaluate the capacity of the erythrocytes to deform. Data show that the mean penetration depth on erythrocytes from ischemic CHF patients was 323.6 nm, which is significantly higher than the mean penetration depth determined for the non-ischemic CHF patients (263.9 nm; $p < 0.001$) and control group (258.7 nm; $p < 0.001$). With these results we could conclude that CHF patients (mainly ischemic ones) have erythrocytes much more capable to deform than those from healthy donors.

© 2016 Macmillan Publishers Limited. All rights reserved.

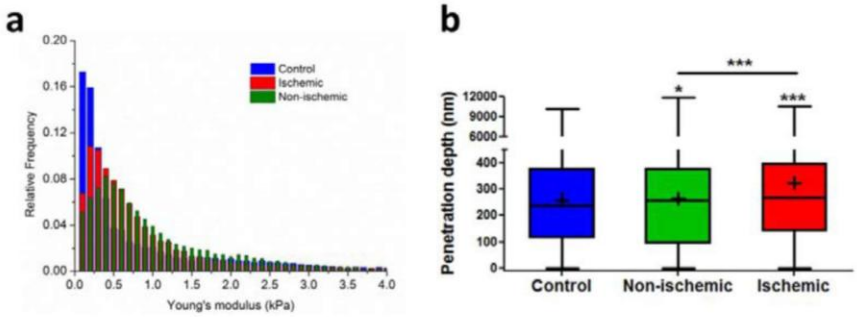

Supplementary Figure 2 | Erythrocyte stiffness studies. (**a**) Histograms of the distribution of the Young's modulus values obtained from the non-ischemic (green) and ischemic (red) CHF patients, and for the control group (blue). (**b**) AFM tip penetration depth onto erythrocytes, for an applied force of 800 pN. The $^{+}$ symbol indicates the average value of penetration depth for each group. * $p = 0.022$; *** $p < 0.0001$.

Linear regression analysis between whole blood viscosity and AFM data

Trying to understand how the interactions between fibrinogen molecules and its erythrocyte membrane receptor could affect whole blood viscosity of each patients' group, data obtained for each parameter were compared. After performing linear regression analysis, we could only observe a statistically significant relation between blood viscosity and the average fibrinogen-erythrocyte (un)binding force for the non-ischemic group ($p = 0.042$; $r = 0.53$).

© 2016 Macmillan Publishers Limited. All rights reserved.

DOI: 10.1038/NNANO.2016.50

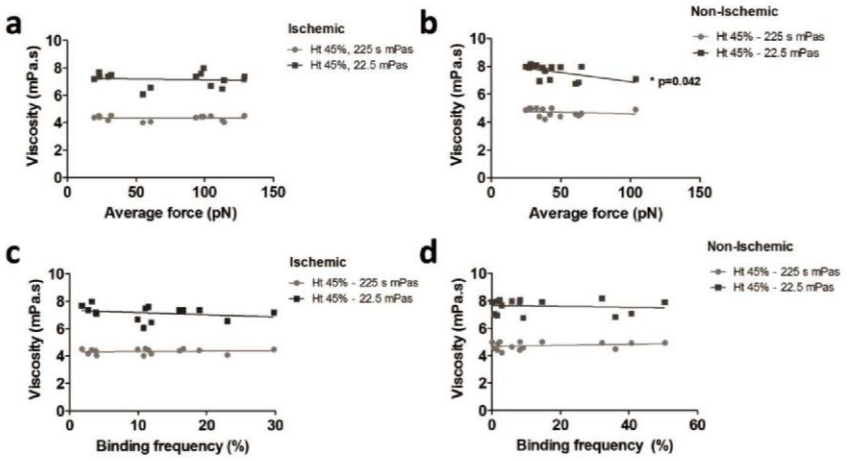

Supplementary Figure 3 | Relation between AFM data and whole blood viscosity data. Linear regression analysis between fibrinogen-erythrocyte average binding force (**a**, **b**) or binding frequency (**c**, **d**) and whole blood viscosity. Data shown are from ischemic (**a**, **c**) and non-ischemic (**b**, **d**) CHF patients. Linear regression was performed with a confidence interval of 95%. Only for non-ischemic CHF patients a statistically significant relation between whole blood viscosity and binding force was observed (* $p = 0.042$). No relation between whole blood viscosity and fibrinogen-erythrocyte binding frequency was observed.

Linear regression analysis between whole blood viscosity and total plasma fibrinogen

We performed a linear regression analysis in order to know the relation between whole blood viscosity and the total plasma fibrinogen levels. At hematocrit 45% and high shear rate, a positive relation between whole blood viscosity and fibrinogen data of CHF patients was observed ($r = 0.428$; $p = 0.021$).

© 2016 Macmillan Publishers Limited. All rights reserved.

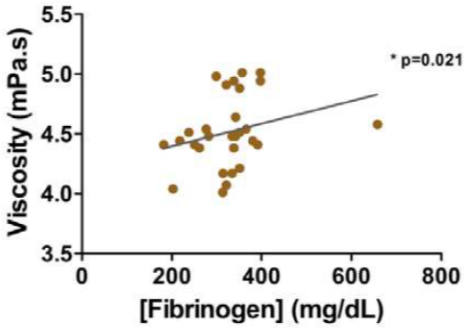

Supplementary Figure 4 | Relation between whole blood viscosity data and total plasma fibrinogen. Linear regression analysis was performed between whole blood viscosity (at 45% of hematocrit and at high shear rate) and plasma fibrinogen for CHF patients. Linear regression was done for a confidence interval of 95%. A statistically significant relation was observed ($r = 0.428$; $p = 0.021$).

Dynamic force spectroscopy analysis

Upon analyzing force spectroscopy data, beyond determining the values of the unbinding force and the frequency of the fibrinogen-erythrocyte interaction, it is important to evaluate the influence of the loading rate during experiments on each of the three studied groups. Supplementary Fig. 4a shows the variation of the loading rates determined for each group. The loading rates values (mean ± SD) were 3959 ± 3380 pN/s for the control group, 5604 ± 4239 pN/s for the non-ischemic group and 5358 ± 4515 pN/s for the ischemic group. These differences were not statistically significant, as determined by One-way ANOVA followed by a Dunnett's post-test.

© 2016 Macmillan Publishers Limited. All rights reserved.

DOI: 10.1038/NNANO.2016.50

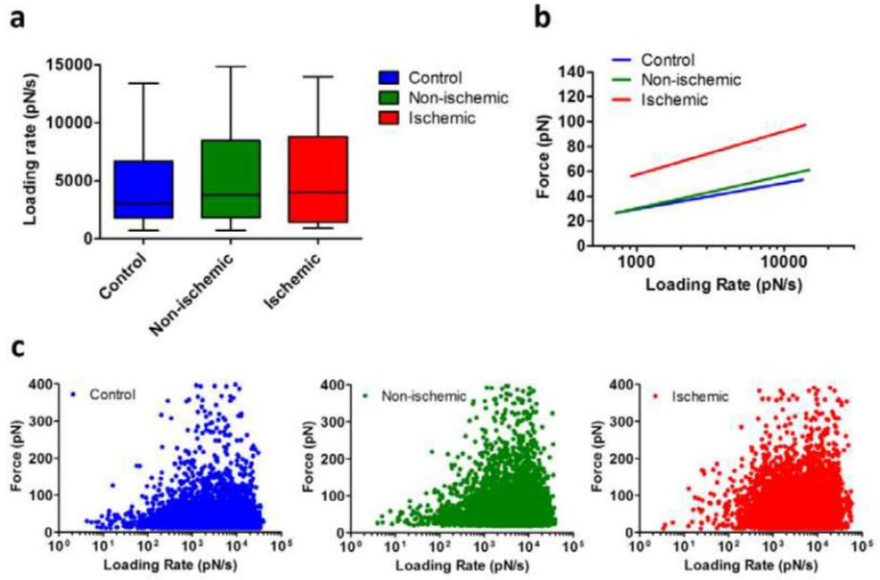

Supplementary Figure 5 | Dynamic force spectroscopy analysis of the interaction between fibrinogen and erythrocytes from the control, non-ischemic and ischemic groups. (**a**) Distribution of the loading rates of the three studied groups. Plots of box and whiskers indicate the mean values and distribution of the loading rate. The whiskers indicate the variation of the minimum to the maximum loading rate value. (**b**) The most probable unbinding forces were plotted against the logarithm of the loading rate of the control (blue line), non-ischemic (green line) and ischemic (red line) groups. Lines are the results of a non-linear least-squares regression fitting. (**c**) Distribution of all data of force *vs.* logarithm of the loading rate for the three studied groups.

We also looked at the unbinding force *vs.* loading rate pairs for each curve separately, for each sample on the control, non-ischemic CHF and ischemic CHF groups. The most probable unbinding forces were plotted against the logarithm of the loading rate (Supplementary Fig. 5b). It can be observed that the three groups have similar ranges of loading rates. The differences observed were at the level of the unbinding force. We performed a regression analysis for each set and obtained a slope of 20.9 ± 7.9 ($r^2 = 0.366$) for the control group, 26.4 ± 14.7 ($r^2 = 0.212$) for the non-ischemic CHF group, and 34.8 ± 27.4 ($r^2 = 0.119$) for the ischemic CHF group.

© 2016 Macmillan Publishers Limited. All rights reserved.

Lines are almost parallel. There were no statistically significant differences on their slopes. Unbinding forces increase with the loading rate on each group, but the variations of the unbinding force between each group is not dependent on the loading rate. For this study we considered all the force curves, with values of loading rates between 1000 and 10 000 pN/s.

The distribution of the force *vs.* loading rate for the three studied groups is presented on Supplementary Fig. 5c. By the distribution of all points of unbinding force *vs.* logarithm of the loading rate, we could observe that increasing the loading rate leads to an increase of the unbinding force. The majority of the values are distributed between 20 and 200 pN of unbinding force and 10^3 to 10^4 pN/s of loading rate.

Supplementary References

1. WHO. Global status report on non-communicable diseases 2010. *Geneva: World Health Organization* (2011).

2. Lillioja, S., Young, A.A., Culter, C.L., Ivy, J.L., Abbott, W.G., *et al.* Skeletal muscle capillary density and fiber type are possible determinants of in vivo insulin resistance in man. *J. Clin. Invest.* **80**, 415-424 (1987).

3. Mann, D.L., Bristow, M.R. Mechanisms and models in heart failure: the biomechanical model and beyond. *Circulation* **111**, 2837-2849 (2005).

4. Colluci, W.B., E. Textbook of cardiovascular Medicine. *Philadelphia, Pa: WB Saunders* 394-420 (1997).

5. Follath, F. Ischemic versus non-ischemic heart failure: should the etiology be determined? *Heart Fail. Monit.* **1**, 122-125 (2001).

6. Guidelines for the evaluation and management of heart failure. Report of the American College of Cardiology/American Heart Association Task Force on Practice Guidelines (Committee on Evaluation and Management of Heart Failure). *Circulation* **92**, 2764-2784 (1995).

7. Wu, Z., Curaj, A., Fokong, S., Liehn, E.A., Weber, C., *et al.* Rhodamine-loaded intercellular adhesion molecule-1-targeted microbubbles for dual-modality imaging under controlled shear stresses. *Circ. Cardiovasc. Imaging* **6**, 974-981 (2013).

8. Rusu, M., Dulebo, A., Curaj, A., Liehn, E.A. Ultra-rapid non-invasive clinical nano-diagnostic of inflammatory diseases. *DISCOVERIES REPORTS* **1**, e2 (2014).

9. Hunt, S.A., Abraham, W.T., Chin, M.H., Feldman, A.M., Francis, G.S., *et al.* 2009 focused update incorporated into the ACC/AHA 2005 Guidelines for the Diagnosis and Management of Heart Failure in Adults: a report of the American College of Cardiology

© 2016 Macmillan Publishers Limited. All rights reserved.

DOI: 10.1038/NNANO.2016.50

Foundation/American Heart Association Task Force on Practice Guidelines: developed in collaboration with the International Society for Heart and Lung Transplantation. *Circulation* **119**, e391-479 (2009).

10. Alexander, K.S., Kazmierczak, S.C., Snyder, C.K., Oberdorf, J.A., Farrell, D.H. Prognostic utility of biochemical markers of cardiovascular risk: impact of biological variability. *Clin. Chem. Lab. Med.* **51**, 1875-1882 (2013).

11. Carvalho, F.A., Connell, S., Miltenberger-Miltenyi, G., Pereira, S.V., Tavares, A., *et al.* Atomic force microscopy-based molecular recognition of a fibrinogen receptor on human erythrocytes. *ACS Nano* **4**, 4609-4620 (2010).

12. Carvalho, F.A., Carneiro, F.A., Martins, I.C., Assunção-Miranda, I., Faustino, A.F., *et al.* Dengue virus capsid protein binding to hepatic lipid droplets (LD) is potassium ion dependent and is mediated by LD surface proteins. *J. Virol.* **86**, 2096-2108 (2012).

© 2016 Macmillan Publishers Limited. All rights reserved.

Article 4

Nanoscale

PAPER

View Article Online
View Journal | View Issue

Check for updates

Cite this: *Nanoscale*, 2017, **9**, 14897

Essential arterial hypertension patients present higher cell adhesion forces, contributing to fibrinogen-dependent cardiovascular risk†

Ana F. Guedes, ‡[a] Filomena A. Carvalho, *‡[a] Carlos Moreira,[b] José B. Nogueira[b] and Nuno C. Santos *[a]

The increase of erythrocyte aggregation by high fibrinogen levels may be an indicator of cardiovascular risk. γ′ fibrinogen variant has been considered as a possible player in enhancing aggregation. Here, we assessed, at the single-cell level, the influence of fibrinogen on erythrocyte aggregation in essential arterial hypertension. We also aimed at understanding how γ′ fibrinogen is altered in this disease. Using atomic force microscopy (AFM), we show that the work and force necessary for erythrocyte–erythrocyte detachment is higher for patients than for healthy donors, with these parameters further increasing in both groups when higher fibrinogen concentrations are present. This can be associated with changes in blood flow, due to transient bridging of two erythrocytes by fibrinogen, representing an important cardiovascular risk factor. γ′ fibrinogen can influence the increased risk in essential arterial hypertension, as we demonstrate that its levels are significantly increased in these patients' blood. Nevertheless, this cannot be the only cause for the changes observed in the AFM data.

Received 1st June 2017,
Accepted 1st September 2017

DOI: 10.1039/c7nr03891g

rsc.li/nanoscale

Introduction

Erythrocytes play an important role in blood coagulation by increasing blood viscosity, which is associated with a propensity for clot formation.[1,2] In disease, this increase in viscosity leads to a greater risk of thrombosis.[3] Erythrocytes present surface adhesion receptors,[4] contributing to thrombosis in several ways.[5,6] Several of these receptors mediate cell–cell adhesion, both under physiological and pathological conditions. Cell adhesion is involved in different processes such as tethering of a cell, cell–cell communication, tissue formation and aggregation.[7]

Erythrocyte–erythrocyte adhesion leads to erythrocyte aggregation and can cause a wide range of diseases. The established hypothesis for the increase in erythrocyte aggregation associated with cardiovascular pathologies is based on an increase in plasma adhesion protein concentration, such as fibrinogen.[8,9] Fibrinogen-induced erythrocyte aggregation was often considered to be caused by its nonspecific binding to erythrocyte membrane.[9,10] It is known that platelets have an integrin receptor for fibrinogen in their membrane, the glycoprotein complex $\alpha_{IIb}\beta_3$.[11] Lominadze *et al.* suggested that fibrinogen can specifically interact with erythrocyte membranes.[12] In a previous study, we demonstrated the existence of single-molecule interactions between fibrinogen and a receptor on the erythrocyte membrane, with a relatively lower but comparable affinity to platelet binding.[13] The erythrocyte receptor was not as strongly influenced by calcium and eptifibatide (an $\alpha_{IIb}\beta_3$ specific inhibitor) as the platelet receptor.[13] By antibody-inhibition studies, we could identify the receptor on the erythrocyte membrane as the $\alpha_v\beta_3$ integrin.[14] Moreover, we recently used atomic force microscopy as a nanotool to evaluate the risk of chronic heart failure (CHF).[14] In that work, we demonstrated that the force necessary to break the bond between fibrinogen and erythrocytes in ischemic CHF patients is stronger than in non-ischemic CHF patients and in healthy donors. Notably, our 12-month clinical follow-up has shown that the CHF patients with higher fibrinogen–erythrocyte binding forces at the initial evaluation had a higher probability of being hospitalized due to cardiovascular disease-associated complications in the following year.[14] These results demonstrate the value of this nanotechnology-based approach for clinical prognosis, indicating the patients with a higher risk.

Essential arterial hypertension (EAH) is a clinical complication considered as one of the major risk factors for cardiovascular and cerebrovascular diseases, such as heart failure,

[a]*Instituto de Medicina Molecular, Faculdade de Medicina, Universidade de Lisboa, Lisbon, Portugal. E-mail: filomenacarvalho@fm.ul.pt, nsantos@fm.ul.pt; Fax: +351 217999477; Tel: +351 217999476, +351 217999480*

[b]*Hospital de Santa Maria, Centro Hospitalar Lisboa Norte, Lisbon, Portugal*

†Electronic supplementary information (ESI) available. See DOI: 10.1039/c7nr03891g

‡These authors contributed equally to this work.

This journal is © The Royal Society of Chemistry 2017

heart attack or stroke.[15] Worldwide 7.6 million premature deaths (about 13.5% of the global total) were attributed to high blood pressure. About 54% of stroke events and 47% of ischemic heart disease were attributable to high blood pressure.[16] According to the European Hypertension Society, patients are considered hypertensive if their blood pressure reach or exceed 140 mmHg of systolic blood pressure (SBP) and/or 90 mmHg of diastolic blood pressure (DBP). The higher the pressure in blood vessels, the harder it is for the heart to properly pump the blood, leading to the increased cardiovascular risk.[17] Actuarial data demonstrated almost a century ago that elevated blood pressure shortened life expectancy,[18] despite the rapid expansion of the efforts by the pharmaceutical industry to develop new therapies for hypertension.[17] New strategies to prevent or slow down the onset of hypertension should not be disregarded.[17] Moreover if hypertension is detected early, it will be possible to minimize the risk of other cardiovascular disorders.[15]

The elevated plasma fibrinogen level was positively associated with prevalent hypertension, both among men and women, and positively associated with 5-year incident hypertension among men, independently of several other cardiovascular risk factors.[10] It is also well established that total plasma fibrinogen concentration is elevated in patients with cardiovascular diseases.[8,9] In plasma, there is a fibrinogen variant, γ′ fibrinogen, that arises from altered splicing of the fibrinogen γ-chain mRNA.[19] Recent studies suggest that γ′ fibrinogen is a newly-emerging risk factor for cardiovascular disease.[20–25] Farrell and co-workers developed a new γ′ fibrinogen enzyme immunoassay intended to be used as part of risk assessment in adults with suspected risk for cardiovascular diseases.[26,27]

Cell adhesion has been investigated using different techniques,[28–30] despite some limitations, such as the absent or limited information on the adhesion strength between the cells and substrate.[31–35] Force spectroscopy measurements using an atomic force microscope are capable of resolving individual cell–cell binding events, and have been applied on different cell systems.[36–38] AFM-based single cell force spectroscopy (SCFS) is an ultrasensitive method to quantify adhesion forces of individual cells under physiological conditions.[34,39] In SCFS adhesion measurements, a living cell is first attached to a tipless AFM cantilever. To facilitate cell immobilization, cantilevers can be coated with different matrix proteins, such as fibronectin or laminin, or with sugar-binding lectins (*e.g.*, concanavalin A), which provide gentle cell attachment *via* glycosylated cell surface proteins.[38–40] Then, a single cell is captured, converting this living cell into a probe. The cell attached to the cantilever is then brought into contact with a cell attached to the surface and cell–cell contact is maintained under a constant contact force for a certain defined dwell time. During subsequent cell retraction, cellular adhesion forces can be measured with high sensitivity from the degree of cantilever deflection, with single-molecule resolution. Force–distance curves are generated and could then provide quantitative information on overall cell adhesion, including the discrimination of a series of small rupture steps.[37,39,41]

To understand the differences between healthy and pathological conditions, it is important to recognize the molecular mechanisms underlying erythrocyte aggregation as a good indicator of cardiovascular risk. With this purpose, here we use AFM single-cell force spectroscopy to quantitatively evaluate erythrocyte adhesion and study the influence of fibrinogen molecules on this binding. We measured these interactions in samples from a group of healthy donors and from patients with EAH. In order to understand how γ′ fibrinogen is altered in blood from EAH patients and whether this could be considered a new biomarker for cardiovascular risk, γ′ fibrinogen concentration was also quantified.

Methods

Study participants

Twenty-one patients with essential arterial hypertension were enrolled in this study. Patients were stable in ambulatory and with optimized standard medical therapy according to the European Society of Hypertension (ESH) and the European Society of Cardiology (ECS) guidelines.[42] Inclusion criteria for the study were hypertensive patients consecutively examined in the Center of Hypertension of Hospital de Santa Maria (Lisbon, Portugal), medicated with calcium channel blockers (CCB), angiotensin converting enzyme (ACE) inhibitors, angiotensin II receptor blockers (ARB), beta blockers (BB), aspirin and/or statins. Exclusion criteria were severe renal damage (defined as glomerular filtration rate, eGFR, below 30 ml min^{-1}), diabetes mellitus type 1 or 2, heart failure with New York Heart Association (NYHA) Functional Classification III or IV, or left ventricular ejection fraction (LVEF) under 40%, liver failure, cancer or other systemic severe diseases. Clinical profiles were thoroughly collected.

A control group of healthy volunteers (n = 8 for the AFM studies and n = 44 for γ′ fibrinogen determination) was also included in this study, following a protocol with Instituto Português do Sangue e Transplantação (IPST, Lisbon, Portugal). Control subjects did not present any known concomitant disease.

Each participant gave informed written consent and all clinical studies have been conducted according to the principles expressed in the Declaration of Helsinki. This study was approved by the joint Ethics Committee of Faculdade de Medicina da Universidade de Lisboa and Centro Hospitalar Lisboa Norte.

Erythrocyte isolation and preparation for AFM

Erythrocytes were isolated as previously described,[13,14] using buffered saline glucose citrate (BSGC: 1.6 mM KH_2PO_4, 8.6 mM Na_2HPO_4, 0.12 M NaCl, 13.6 mM sodium citrate and 11.1 mM glucose), pH 7.3, supplemented with 1 mM $CaCl_2$. Erythrocytes (0.1% hematocrit) were attached to a clean poly-

This journal is © The Royal Society of Chemistry 2017

L-lysine (PLL) treated glass slide after 30 min of deposition, at room temperature. Non-adherent cells were removed by sequential washes with buffer. Samples were loaded into the AFM and allowed to equilibrate in buffer for 15 min before force spectroscopy measurements. No cell fixation was involved in sample preparation.

Cantilever functionalization

To conduct the AFM cell adhesion assays, tipless silicon nitride cantilevers (Arrow TL2, NanoWorld, Neuchâtel, Switzerland; thickness 1 μm, length 500 μm, width 100 μm and resonance frequency 6 kHz) were functionalized in order to attach one cell to the cantilever. The functionalization of the cantilever is a multi-step procedure. First, the cantilever was activated by UV treatment for 15 min. Then, the cantilever was immersed in a 0.5 mg mL^{-1} biotinylated albumin solution (at 37 °C, overnight), then in 0.5 mg mL^{-1} streptavidin (30 min, at room temperature) and, finally, in 0.4 mg mL^{-1} biotin-concanavalin A (30 min, at room temperature).[43] Cantilevers were washed with phosphate buffer saline (PBS) between each step of the functionalization process. The cantilevers were kept in PBS to ensure the integrity of the surface treatment until usage. All reagents were purchased from Sigma Aldrich (St Louis, MO, USA).

AFM measurements of cell–cell adhesion

Experiments were performed on a NanoWizard II atomic force microscope (JPK Instruments, Berlin, Germany) mounted on an Axiovert 200 inverted optical microscope (Zeiss, Jena, Germany). Long range force spectroscopy was made possible by using the CellHesion module (JPK Instruments) with a 100 μm *z*-range piezoelectric scanner. The objective was mounted with a PIFOC to enable concurrent movement of the objective with the sample holder during force spectroscopy measurements. Concanavalin A-functionalized cantilevers were mounted on the microscope, erythrocytes were injected, and one erythrocyte was captured by positioning the cantilever above the cell center and gently lowering onto the cell for approximately 30 s. The applied force was adjusted to 300 pN before retraction. Data collection for each force–distance cycle was performed at 2 μm s^{-1}, with a *z*-length of 30 μm. Retraction and extension time delays of 5 s were applied.[44] Erythrocyte–erythrocyte adhesion was measured in the presence of different human fibrinogen (Sigma Aldrich) concentrations, up to 1.0 mg mL^{-1} (Fig. 1). Fibrinogen solutions were allowed to incubate for 15 min before erythrocyte adhesion measurements. Five force–distance curves were recorded for each erythrocyte on the substrate, and a maximum of 8 different adherent cells on the substrate were tested with the same erythrocyte attached to the AFM cantilever. A total of 40 cells were tested for each experimental condition. Force–

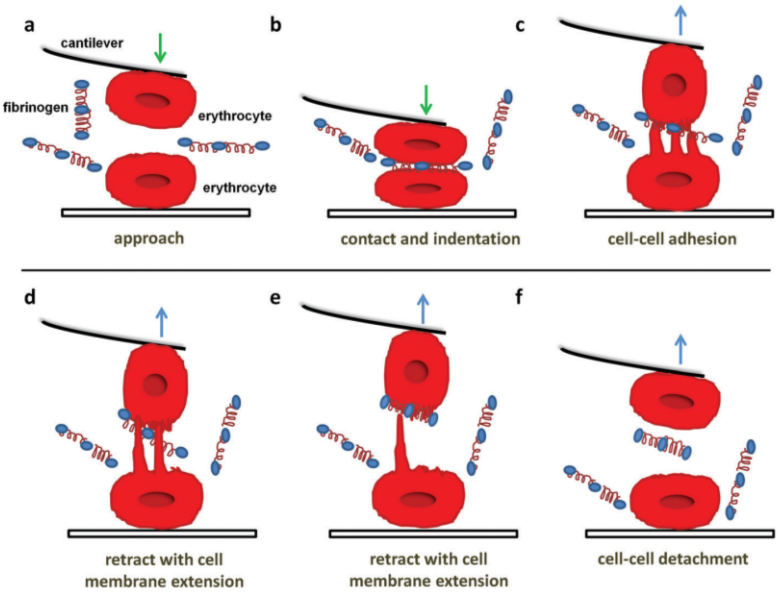

Fig. 1 Schematic representation of the erythrocyte–erythrocyte adhesion experiments using atomic force microscopy, done in the presence of fibrinogen. First, the cantilever with an attached erythrocyte is brought into contact with another erythrocyte on the substrate (a), until a certain contact force is reached (b). Afterwards, during retraction, cell–cell adhesion may occur causing the cantilever to adhere to the sample up to a distance beyond the initial contact point (c). When the spring force overcomes the interaction forces, the cantilever pulls of sharply, and different types of adhesion between both cell surfaces may occur (d and e), before totally breaking contact and completing the erythrocyte–erythrocyte detachment (f).

distance curves were analyzed using JPK image processing software v. 4.2.61 (JPK Instruments). The values of work correspond to the area under the retraction curve obtained on a force–distance plot. Values of the initial maximum detachment force (by the minimum value of adhesion force) and of two types of events (jumps and membrane tethers) were also obtained after analyzing the cell–cell adhesion retraction curves. We considered a membrane tether as a step in force detected after a force plateau of more than 0.25 μm in distance. Jump events (force plateau of less than 0.25 μm in distance) could be attributed to the breaking of cell–cell interactions without a preceding membrane deformation. Membrane tether events corresponded to situations where a membrane tether was extruded before the breaking of a connection between surface components of two interacting cells.[44] Work and detachment force data histograms are presented in ESI Fig. S1 and S2,† respectively.

γ′ fibrinogen quantification

γ′ fibrinogen concentration in human plasma was quantified using a specific two-site sandwich enzyme linked immunosorbent assay kit (Gamma Couer ELISA kit, Gamma Therapeutics, Portland, OR, USA). First, a monoclonal anti-γ′ fibrinogen antibody, clone 2.G2.H9, specific for the unique carboxyl terminal peptide of the γ′ fibrinogen chain, was used as a capture antibody. Secondly, an enzyme-labeled polyclonal anti-fibrinogen detection antibody was added, which binds to the captured γ′ fibrinogen, forming a detection antibody sandwich. Absorbance of the colored end-product was read at 450 nm on an Infinite M200 microplate reader (Tecan, Männedorf, Switzerland). Plasma samples from EAH patients (n = 31) and healthy donors (n = 44) were analyzed. Values that fall above the cut-off (>30 mg dL^{-1}) were considered as indicative of increased risk of cardiovascular disease and may require further testing for cardiovascular diseases.[26,27]

Statistical analysis

Descriptive statistics were given as mean ± standard error of mean (SEM). For every parameter, all samples were tested against the control group. An unpaired Student's t-test was used for statistical analysis of intergroup comparison. The nonparametric Mann–Whitney test was used when data do not have a normal distribution. Statistical significance was set at $p < 0.05$. Statistical analyses were performed using GraphPad Prism 5.

Results

Cell adhesion experiments

A schematic representation of AFM cell–cell adhesion experiments performed using erythrocyte-functionalized probes and erythrocyte on the substrate is shown in Fig. 1. Erythrocytes isolated from blood samples from patients with essential arterial hypertension and healthy volunteers (control) were tested in the presence of fibrinogen concentrations up to 1.0 mg mL^{-1}.

During AFM experiments, it was possible to perform several approach/retract cycles between the erythrocyte attached on the cantilever and erythrocytes on the glass slide. These cycles generate different cell–cell adhesion curves. Two examples of these curves can be seen in Fig. 2. Without the presence of fibrinogen, unspecific adhesion between erythrocytes could be observed (Fig. 2a). Erythrocytes are non-adherent and very soft cells, with an extremely high capacity to deform. In the cell–cell adhesion experiments, a low retraction velocity of 2 μm s^{-1} and a cell–cell contact time of 5 s were used. This constant time is associated with an elastic deformation regime, exponentially increasing viscous creep.[45] As so, in the absence of fibrinogen, cells experienced a viscous drag effect of the aqueous working conditions. If a strong adhesion between both erythrocytes was observed, it would be possible to visualize a step in the force profile of the retraction curve, as those observed in Fig. 2b. In Fig. 2a, only a slow continuous decrease of the deflection of the cantilever was observed, without any detectable jump in force, until the cantilever reached the zero value of force. The total separation of both erythrocytes occurs at a tip–sample distance of approximately 20 μm. These results may be due to the combination of different forces exerted on the cell: the viscous dragging force, the pulling off of the erythrocyte and the elastic deformation of both erythrocytes.

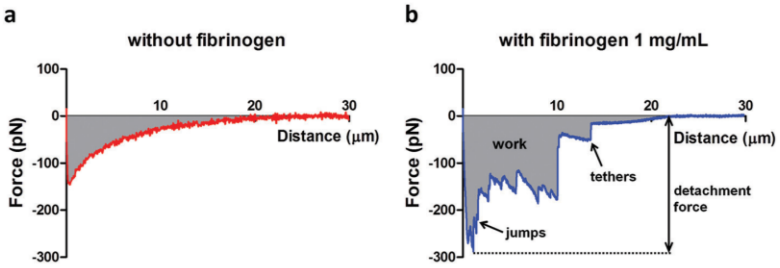

Fig. 2 Examples of retraction curves acquired during AFM cell–cell adhesion experiments. Erythrocyte–erythrocyte adhesion without fibrinogen (a) and in the presence of 1 mg mL^{-1} fibrinogen (b).

This journal is © The Royal Society of Chemistry 2017

In the presence of 1 mg mL^{-1} fibrinogen, it was possible to observe strong and specific cell–cell interactions (Fig. 2b). Different parameters could be extracted by analyzing the retraction curves: the work necessary to detach cells, the maximum detachment force and also two different types of events: jumps and membrane tethers (Fig. 2b). Upon closer examination of the cell–cell adhesion curves, it became evident that in the presence of fibrinogen (1 mg mL^{-1}), erythrocyte–erythrocyte detachment occurs *via* several rupture events that were not observed in the absence of this plasma protein (Fig. 2).

Erythrocyte adhesion is mediated by fibrinogen

To prove the specificity of the binding between two erythrocytes mediated by fibrinogen molecules, three different control experiments were performed: (i) interaction between tipless cantilever without an erythrocyte attached and an erythrocyte on the substrate; (ii) interaction between an erythrocyte attached to the cantilever and the poly-L-lysine glass slide (without erythrocytes); and, (iii) erythrocyte–erythrocyte interaction in the presence of both 1 mg mL^{-1} fibrinogen and 4 mM EDTA (as a chelating agent of calcium ions, to inhibit the fibrinogen receptor on erythrocytes[13]). The results extracted from the AFM adhesion data after performing these control experiments are shown in Fig. 3.

Analyzing the results achieved from control experiments, a decrease in the work and maximum force necessary to detach the cantilever–substrate system was observed. This situation occurred when the experiments were performed with a cantilever without an erythrocyte ($p < 0.0001$) and for the erythrocyte–erythrocyte interaction in the presence of EDTA ($p = 0.002$). As expected, the force necessary to overcome the binding

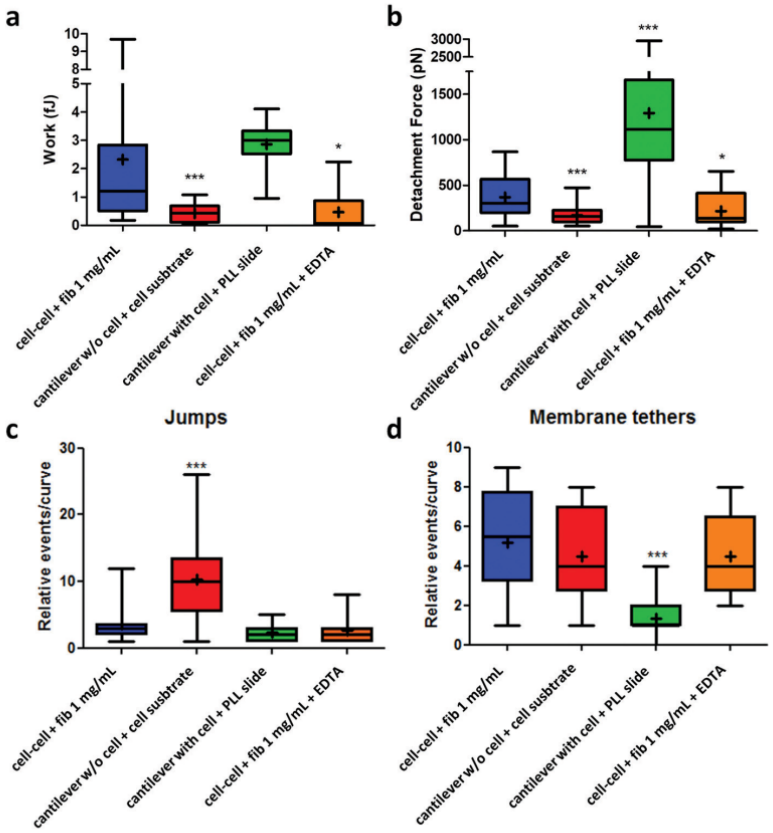

Fig. 3 AFM data of work (a), detachment force (b), jump events (c) and membrane tethers (d) of samples and controls. Comparison of AFM data achieved from the interaction of two erythrocytes in the presence of fibrinogen 1 mg mL^{-1} (blue) and 3 different control systems, for the interaction between: (i) tipless cantilever without an erythrocyte attached and an erythrocyte on the substrate (red); (ii) an erythrocyte attached on the cantilever and the PLL glass slide without erythrocytes (green); and, (iii) erythrocyte–erythrocyte interaction in the presence of 1 mg mL^{-1} fibrinogen and 4 mM EDTA (orange). Values are presented as box with median value and 1st and 3rd quartiles, and whiskers with maximum and minimum values. The mean value is presented as '+'. The relative events/curve are given by the ratio between the total number of jump (c) or membrane tether (d) events per total number of force–adhesion curves. Statistical values: (a) ***$p < 0.0001$, **$p < 0.0038$; (b) ***$p < 0.0002$, *$p = 0.0407$; (c) ***$p < 0.0001$; (d) ***$p < 0.0001$.

between an erythrocyte attached to the cantilever and PLL glass slide is higher than for the erythrocyte–erythrocyte interaction in the presence of fibrinogen (p = 0.0038). PLL is usually used to facilitate the attachment of cells and proteins to solid surfaces in biological applications. This cationic substrate strongly interacts with the negatively charged surface of the erythrocytes.[46] These strong erythrocyte–PLL interactions were observed also by detachment force data (Fig. 3b, $p < 0.0001$). As all experiments were conducted in an AFM coupled with an inverted fluorescence microscope connected to a CCD camera, interactions between the cell attached to the cantilever and the PLL substrate were avoided in all cell–cell interaction experiments. To guarantee this, the cantilever (with an erythrocyte) was mechanically and optically placed on top of an erythrocyte on the substrate for each measurement. After performing these three types of control experiments, we could demonstrate the specificity of the interaction between two erythrocytes in the presence of fibrinogen molecules and apply the same procedure to blood samples from EAH patients.

EAH patients present stronger erythrocyte–erythrocyte adhesion

Fig. 4a shows that the work necessary to detach two erythrocytes, either from healthy donors or EAH patients, was significantly higher in the presence of increasing fibrinogen concentrations (from 0.4 to 1 mg mL^{-1}) than in its absence ($p < 0.0001$). Moreover, in the absence of fibrinogen, the work necessary to detach two erythrocytes from EAH patients was significantly higher than for erythrocytes isolated from healthy donors (1.45 ± 0.06 fJ for EAH patients *vs.* 0.48 ± 0.04 fJ for healthy donors; $p < 0.0001$). In all fibrinogen concentrations tested, higher forces (and work) were needed to overcome erythrocyte–erythrocyte adhesion for EAH patients than for healthy donors (Fig. 4a), although statistically significant differences were only observed in the presence of 0.7 mg mL^{-1} fibrinogen (3.13 ± 0.16 fJ for EAH patients *vs.* 2.10 ± 0.31 fJ for healthy donors; $p = 0.022$).

The maximum detachment force required to separate the cantilever-bound erythrocyte from the erythrocyte at the surface of the glass slide was also determined directly from each force–distance curve (Fig. 2b). Similarly to the values of work, the maximum detachment force necessary to detach two erythrocytes in the absence of fibrinogen is higher for EAH patients than for healthy donors ($p < 0.0001$). Higher detachment force data for EAH patients were also observed in the presence of 0.4 mg mL^{-1} ($p < 0.0001$) and 0.7 mg mL^{-1} ($p = 0.0007$) fibrinogen (Fig. 4b).

For healthy donors, upon increasing fibrinogen concentrations, the erythrocyte–erythrocyte binding force also increased. These variations were statistically significant for all fibrinogen concentrations tested ($p < 0.0001$ at 0.4 and 1.0 mg mL^{-1}; $p = 0.0002$ at 0.7 mg mL^{-1}). Regarding EAH patients,

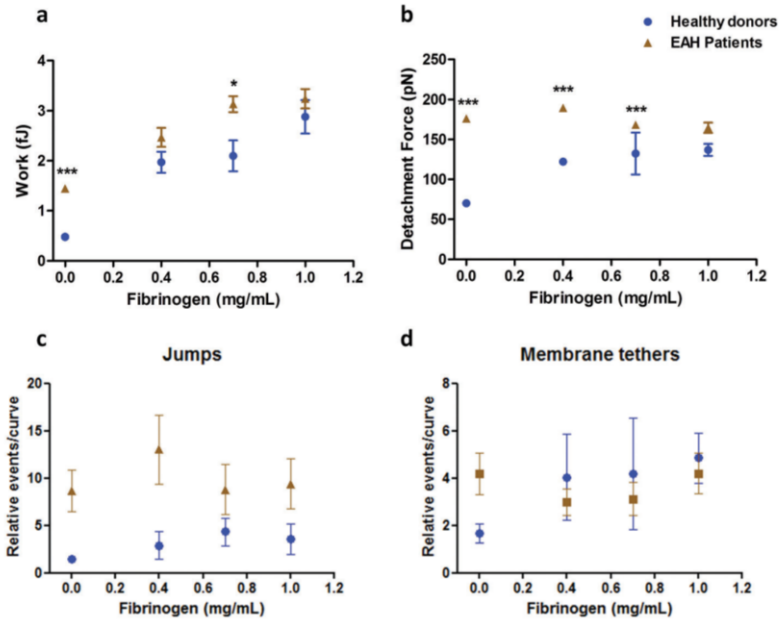

Fig. 4 AFM data of work (a), detachment force (b), jump events (c) and membrane tethers (d) from blood samples of healthy donors (n = 8) and EAH patients (n = 21). Comparison of AFM data achieved from the interaction of two erythrocytes in the absence or in the presence of increasing fibrinogen concentrations (from 0.4 to 1 mg mL^{-1}), for healthy donors (blue) and EAH patients (brown). Values are presented as mean ± SEM. Histograms are presented in ESI Fig. S1 and S2.† The relative events/curve is given by the ratio between the total number of jump (c) or membrane tether (d) events per total number of force–adhesion curves. (a) ***$p < 0.0001$, *$p = 0.022$; (b) ***$p \leq 0.0007$.

This journal is © The Royal Society of Chemistry 2017

the same fibrinogen concentration dependence of erythrocyte–erythrocyte binding forces did not occur. Despite the statistically significant differences between detachment forces of EAH patient erythrocytes in the presence of fibrinogen 0.4 and 0.7 mg mL^{-1} and in their absence only small differences were observed (Fig. 4b).

Looking at the force retract curve (Fig. 2b), an initial unbinding event is followed by a number of smaller force steps, which could be distinguished and analyzed as jump events and membrane tethers. Comparing jump events for both study groups (Fig. 4c), one may notice that EAH patients present more frequent events per curve than healthy donors, either in the absence or in the presence of fibrinogen. A 2 to 5-fold increase in the number of jump events was observed for erythrocytes from EAH patients. Regarding membrane tethers (Fig. 4d), the same difference could not be observed. Only in the absence of fibrinogen, a 2.5-fold increase in the number of membrane tethers/curve could be seen for the erythrocytes from EAH patients. When fibrinogen was added, approximately the same number of membrane tethers/curve was detectable in erythrocytes from EAH patients and healthy donors.

EAH patients have higher levels of γ′ fibrinogen

In parallel with the AFM experiments, the levels of total fibrinogen and γ′ fibrinogen variant were quantified in plasma from EAH patients (Fig. 5). EAH patients presented higher total plasma fibrinogen (3.02 ± 0.18 mg mL^{-1} *vs.* 2.43 ± 0.11 mg mL^{-1}; $p = 0.0034$) and γ′ fibrinogen levels (0.43 ± 0.02 mg mL^{-1} *vs.* 0.33 ± 0.02 mg mL^{-1}; $p = 0.0003$) than healthy donors. Despite the fact that the total fibrinogen concentrations determined for the patients are significantly higher than those from healthy donors, both groups presented values within the normal range for this parameter (1.5–3.5 mg mL^{-1}).[47] As for γ′ fibrinogen concentration, values above a cut-off of approximately 0.3 mg mL^{-1} have been referred to as indicative of increased risk of cardiovascular diseases.[27] Our results show that EAH patients present γ′ fibrinogen concentrations above this cut-off, and that those concentrations are significantly higher than those determined for the healthy donors. However, the ratio between γ′ fibrinogen and the total plasma fibrinogen was not statistically different among EAH patients and healthy donors.

Discussion

The present work shows for the first time that the erythrocyte–erythrocyte interaction in the presence of fibrinogen, characterized here by AFM-based force spectroscopy, is modified in essential arterial hypertension patients. AFM cell–cell adhesion measurements were used to assess the interactions between an erythrocyte attached to the AFM cantilever and erythrocytes on the substrate. This is also a good example of application of AFM as a versatile tool to quantify cell adhesion under near-physiological conditions, from the cellular level down to the contribution of single molecules, opening new possibilities in terms of nanodiagnostics and optimized therapeutics. In previous studies, Puech *et al.* also showed that an atomic force microscope with an extended pulling range is a powerful tool to study multiple features of melanoma disease progression.[38] Friedrichs *et al.* considered that this technique allows one to obtain a large amount of essential cell biological and biophysical information that will contribute to different biomedical and material applications.[34] We previously reported the use of AFM to study the broad effect of azurin at the cancer cell surface level.[48] In another study, using different AFM modes, we showed that P-cadherin and Src family kinase signaling induce changes in the morphological and viscoelastic properties of breast cancer cells. These cells also revealed differences in their biomechanical cell–cell adhesion, which are associated with a more invasive breast cancer cell phenotype.[44]

In order to prove the specificity of the erythrocyte–fibrinogen–erythrocyte binding under evaluation, different control experiments were performed. From these experiments (Fig. 3), we could conclude that the interaction between two erythrocytes in the presence of fibrinogen molecules is specific, validating the subsequent measurements. The analysis of the

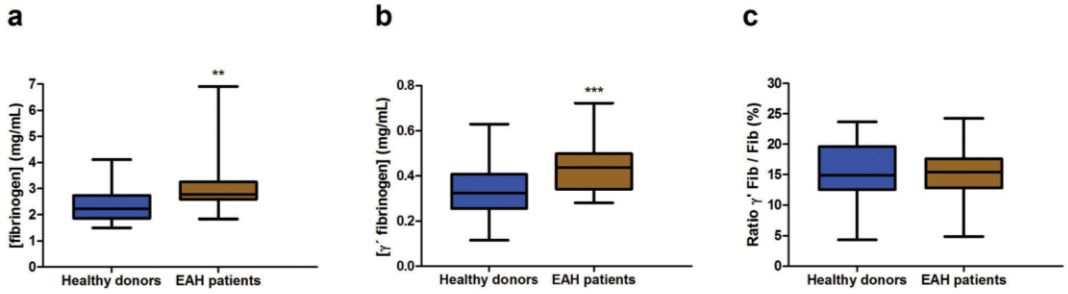

Fig. 5 Total plasma fibrinogen (a) and γ′ fibrinogen (b) concentrations, as well as the ratio between both parameters (c), for EAH patients ($n = 31$) and healthy blood donors ($n = 44$). Values are presented as box with median value and 1st and 3rd quartiles, and whiskers with maximum and minimum values. (a) $^{**}p = 0.0034$; (b) $^{***}p = 0.0003$.

unbinding events from the cell–cell force–distance curves helped us to characterize the strength of single bonds, as well as other erythrocyte properties. The extended effective pulling range of the instrument enabled the detection of unbinding forces associated with short-range unspecific interactions, up to specific jump and membrane tether associated interactions.

AFM data showed that higher work and forces had to be applied to completely detach two erythrocytes from EAH patients, when compared with cells from healthy donors, both in the absence or in the presence of fibrinogen molecules in solution. With the increasing of fibrinogen levels, the work and the maximum force necessary to detach two erythrocytes increased in both groups.

The differences obtained between the values of work necessary to detach two erythrocytes from EAH patients, or from healthy donors, in the absence of fibrinogen should not be due to the presence of fibrinogen molecules coming from the plasma. Several centrifugation and washing cycles were performed before the use of the erythrocytes in the experiments. Some fibrinogen molecules may be attached to the erythrocyte surface even at 0 mg mL^{-1} of fibrinogen, but their amount should be considered as negligible. The stronger erythrocyte–erythrocyte adhesion observed may be due to changes in the EAH erythrocytes' membrane lipid composition and/or its membrane charge associated with the pathological conditions, which could facilitate erythrocyte–erythrocyte adhesion.

AFM also provided quantitative information on a series of small rupture steps, namely, jumps and membrane tethers. From the results it is clear that the relative events per curve for jumps and membrane tethers were higher in EAH patients compared to healthy volunteers. This fact is more pronounced for the number of jump events and not for membrane tethers. Thus, it seems that the main contributor for the increase of the binding between two erythrocytes from EAH patients is the interaction between fibrinogen molecules and its specific $\alpha_v\beta_3$ integrin membrane receptor. This conclusion could be extracted from the number of jump events on the force–distance retract curves (Fig. 2b).

In our previous work, using also AFM but not at the level of the evaluation of cell–cell interactions, we measured the binding between fibrinogen molecules covalently attached to the AFM tip and erythrocytes from heart failure patients.[14] We demonstrated that the interaction between fibrinogen and erythrocytes is strong in these patients. Importantly, based on a 12-month clinical follow-up, we have shown that patients with higher fibrinogen–erythrocyte (un)binding forces at the initial AFM evaluation had a higher probability of being hospitalized due to cardiovascular complications in the following year.

In the present study, the fact that erythrocytes from EAH patients presented higher cell–cell adhesion in the presence of fibrinogen than those from healthy donors could be associated with an increase of erythrocyte aggregation in these patients. Considering that erythrocyte aggregation is an important cardiovascular risk factor associated with pathological conditions,[49] fibrinogen "bridging" between two erythrocytes may be considered as a key aspect for this aggregation and, therefore, to the higher cardiovascular risk in EAH patients. Moreover, and having in mind our previous results,[14] AFM could be an important technique to better define the cardiovascular risk and facilitate the clinical prognosis for patients with cardiovascular diseases.

Different studies reported that elevated plasma fibrin(ogen) levels significantly increases the cardiovascular risk.[50–52] For this reason, simultaneously with the AFM studies, we quantified the levels of total fibrinogen and of the γ′ fibrinogen variant in the plasma from EAH patients. This quantification was performed to understand how and what type of fibrinogen molecules may lead to an increase of erythrocyte–erythrocyte binding in EAH patients. From the results it was found that γ′ fibrinogen levels were higher in EAH patients than in healthy donors. The values obtained for EAH patients were above the cut-off value of 0.3 mg mL^{-1}, considered to be indicative of an increased cardiovascular risk.[26,27] Moreover the increase of γ′ fibrinogen concentration was not dependent on the total plasma fibrinogen levels. Our results are in accordance with those of Lovely *et al.*, who indicated that a raise in γ′ fibrinogen concentration was associated with an increased risk of coronary artery disease, independently of the total plasma fibrinogen concentration.[23] On the other hand, Mannila *et al.* showed that plasma γ′ fibrinogen concentration influences the risk of myocardial infarction, and this relationship seems to be strengthened by the presence of an elevated total plasma fibrinogen concentration.[25] The ratio between γ′ fibrinogen (γA/γ′ and γ′/γ′) concentrations has been associated with atherothrombotic disease.[23,25] We expect that our present results may help to clarify and move further on the impact of γ′ fibrinogen on cardiovascular diseases, contributing to establish it as a new biomarker for cardiovascular risk. It should be highlighted that an accurate evaluation of the clinical prognosis of EAH patients should not depend only on the quantification of γ′ fibrinogen and/or of the characterization of erythrocyte–erythrocyte interactions. This information should be considered together with current state-of-the-art tests and clinical information available, in order to pinpoint patients at higher risk, enabling therapy optimization to prevent serious cardiovascular events.

The fact that erythrocytes from EAH patients in the presence of fibrinogen adhere more than those from healthy blood donors may be expected to lead to changes in the whole blood flow. At the cellular level, this could be due to the formation of a bridge of fibrinogen molecule(s) in between two erythrocytes, forming an erythrocyte–fibrinogen–erythrocyte transient complex. This could lead to higher erythrocyte aggregation, which could represent an important risk factor for developing cardiovascular pathologies. A continued research into the erythrocyte aggregation as a determinant for cardiovascular risk is still necessary, with a particular emphasis on the discovery strategies to condition the fibrinogen–erythrocyte interactions, especially those evolving γ′ fibrinogen, or on the development of therapeutic strategies to specifically decrease the

This journal is © The Royal Society of Chemistry 2017

levels of this fibrinogen variant. These strategies could have a high impact on the reduction or prevention of cardiovascular pathologies.

Author contributions

A. F. G. performed part of the experiments, analyzed the data, performed the statistical analysis, wrote and edited the draft of the manuscript and prepared it for submission; F. A. C. performed part of the experiments, analyzed the data, wrote and edited the manuscript; C. S. M. collected all clinical data, performed clinical evaluation, contributed to relevant discussion and participated in the writing of the manuscript; J. B. N. contributed to the discussion section and participated in the writing of the manuscript; and, N. C. S. conceived the idea, designed and directed the experiments and participated in the writing of the manuscript.

Conflicts of interest

Authors declare no competing financial interest.

Acknowledgements

This work was supported by Fundação para a Ciência e a Tecnologia – Ministério da Ciência, Tecnologia e Ensino Superior (FCT-MCTES, Portugal) grants PTDC/QUI-BIQ/119509/2010 and PTDC/BBB-BMD/6307/2014, as well as the fellowship SFRH/BD/84414/2012 to AFG.

References

1 N. Wohner, *Cardiovasc. Hematol. Agents Med. Chem.*, 2008, **6**, 224–228.
2 F. Zannad and J. F. Stoltz, *J. Hypertens. Suppl.*, 1992, **10**, S69–S78.
3 R. Landolfi, B. Rocca and C. Patrono, *Crit. Rev. Oncol. Hematol.*, 1995, **20**, 203–222.
4 M. J. Telen, *Semin. Hematol.*, 2000, **37**, 130–142.
5 V. Peyrou, J. C. Lormeau, J. P. Herault, C. Gaich, A. M. Pfliegger and J. M. Herbert, *Thromb. Haemostasis*, 1999, **81**, 400–406.
6 M. F. Whelihan, V. Zachary, T. Orfeo and K. G. Mann, *Blood*, 2012, **120**, 3837–3845.
7 R. L. Juliano, *Annu. Rev. Pharmacol. Toxicol.*, 2002, **42**, 283–323.
8 D. Lominadze and W. L. Dean, *FEBS Lett.*, 2002, **517**, 41–44.
9 N. Maeda, M. Seike, S. Kume, T. Takaku and T. Shiga, *Biochim. Biophys. Acta*, 1987, **904**, 81–91.
10 A. Shankar, J. J. Wang, E. Rochtchina and P. Mitchell, *Hypertension*, 2006, **48**, 1043–1049.
11 L. K. Jennings and D. R. Phillips, *J. Biol. Chem.*, 1982, **257**, 10458–10466.
12 D. Lominadze, D. A. Schuschke, I. G. Joshua and W. L. Dean, *Clin. Exp. Hypertens.*, 2002, **24**, 397–406.
13 F. A. Carvalho, S. Connell, G. Miltenberger-Miltenyi, S. V. Pereira, A. Tavares, R. A. Ariens, *et al.*, *ACS Nano*, 2010, **4**, 4609–4620.
14 A. F. Guedes, F. A. Carvalho, I. Malho, N. Lousada, L. Sargento and N. C. Santos, *Nat. Nanotechnol.*, 2016, **11**, 687–692.
15 WHO, *Cardiovascular diseases (CVDs)*, World Health Organization, 2013.
16 C. M. Lawes, S. Vander Hoorn, A. Rodgers and International Society of Hypertension, *Lancet*, 2008, **371**, 1513–1518.
17 A. V. Chobanian, *Med. Clin. North Am.*, 2017, **101**, 219–227.
18 R. O. H. Hunter A., *Actuarial Soc.*, 1923, **24**, 338.
19 D. W. Chung and E. W. Davie, *Biochemistry*, 1984, **23**, 4232–4236.
20 E. Y. Cheung, S. Uitte de Willige, H. L. Vos, F. W. Leebeek, D. W. Dippel, R. M. Bertina, *et al.*, *Stroke*, 2008, **39**, 1033–1035.
21 E. Y. Cheung, H. L. Vos, M. J. Kruip, H. M. den Hertog, J. W. Jukema and M. P. de Maat, *Blood*, 2009, **114**, 4603–4604; author reply 4604–4605.
22 L. Drouet, F. Paolucci, N. Pasqualini, M. Laprade, L. Ripoll, E. Mazoyer, *et al.*, *Blood Coagulation Fibrinolysis*, 1999, **10**(Suppl. 1), S35–S39.
23 R. S. Lovely, L. A. Falls, H. A. Al-Mondhiry, C. E. Chambers, G. J. Sexton, H. Ni, *et al.*, *Thromb. Haemostasis*, 2002, **88**, 26–31.
24 F. L. Macrae, M. M. Domingues, A. Casini and R. A. Ariens, *Semin. Thromb. Hemostasis*, 2016, **42**, 344–355.
25 M. N. Mannila, R. S. Lovely, S. C. Kazmierczak, P. Eriksson, A. Samnegard, D. H. Farrell, *et al.*, *J. Thromb. Haemostasis*, 2007, **5**, 766–773.
26 K. S. Alexander, T. E. Madden and D. H. Farrell, *Thromb. Haemostasis*, 2011, **105**, 605–609.
27 R. S. Lovely, S. C. Kazmierczak, J. M. Massaro, R. B. D'Agostino Sr., C. J. O'Donnell and D. H. Farrell, *Clin. Chem.*, 2010, **56**, 781–788.
28 J. Dai and M. P. Sheetz, *Biophys. J.*, 1995, **68**, 988–996.
29 S. C. Kuo, D. A. Hammer and D. A. Lauffenburger, *Biophys. J.*, 1997, **73**, 517–531.
30 M. Thie, B. Harrach-Ruprecht, H. Sauer, P. Fuchs, A. Albers and H. W. Denker, *Eur. J. Cell Biol.*, 1995, **66**, 180–191.
31 K. Burton and D. L. Taylor, *Nature*, 1997, **385**, 450–454.
32 J. Lee, M. Leonard, T. Oliver, A. Ishihara and K. Jacobson, *J. Cell Biol.*, 1994, **127**, 1957–1964.
33 T. Oliver, K. Jacobson and M. Dembo, *Methods Enzymol.*, 1998, **298**, 497–521.
34 J. Friedrichs, K. R. Legate, R. Schubert, M. Bharadwaj, C. Werner, D. J. Muller, *et al.*, *Methods*, 2013, **60**, 169–178.
35 A. Taubenberger, D. A. Cisneros, J. Friedrichs, P. H. Puech, D. J. Muller and C. M. Franz, *Mol. Biol. Cell*, 2007, **18**, 1634–1644.
36 H. Clausen-Schaumann, M. Seitz, R. Krautbauer and H. E. Gaub, *Curr. Opin. Chem. Biol.*, 2000, **4**, 524–530.
37 J. Kashef and C. M. Franz, *Dev. Biol.*, 2015, **401**, 165–174.
38 P. H. Puech, K. Poole, D. Knebel and D. J. Muller, *Ultramicroscopy*, 2006, **106**, 637–644.

This journal is © The Royal Society of Chemistry 2017

39 M. Benoit, D. Gabriel, G. Gerisch and H. E. Gaub, *Nat. Cell Biol.*, 2000, **2**, 313–317.
40 J. Helenius, C. P. Heisenberg, H. E. Gaub and D. J. Muller, *J. Cell Sci.*, 2008, **121**, 1785–1791.
41 P. Panorchan, M. S. Thompson, K. J. Davis, Y. Tseng, K. Konstantopoulos and D. Wirtz, *J. Cell Sci.*, 2006, **119**, 66–74.
42 G. Mancia, R. Fagard, K. Narkiewicz, J. Redon, A. Zanchetti, M. Bohm, *et al.*, *Blood Pressure*, 2014, **23**, 3–16.
43 J. Friedrichs, J. Helenius and D. J. Muller, *Nat. Protoc.*, 2010, **5**, 1353–1361.
44 A. S. Ribeiro, F. A. Carvalho, J. Figueiredo, R. Carvalho, T. Mestre, J. Monteiro, *et al.*, *Nanoscale*, 2016, **8**, 19390–19401.
45 K. Haase and A. E. Pelling, *J. R. Soc., Interface*, 2015, **12**, 20140970.
46 F. A. Carvalho, S. de Oliveira, T. Freitas, S. Gonçalves and N. C. Santos, *PLoS One*, 2011, **6**, e18167.
47 M. W. Oswald, H. H. Hunt and J. Lazarchick, *Am. J. Med. Technol.*, 1983, **49**, 57–59.
48 N. Bernardes, S. Abreu, F. A. Carvalho, F. Fernandes, N. C. Santos and A. M. Fialho, *Cell Cycle*, 2016, **15**, 1415–1424.
49 G. D. Sloop, J. K. Bialczak, J. J. Weidman and J. A. St Cyr, *Clin. Hemorheol. Microcirc.*, 2016, **63**, 349–359.
50 M. M. Aleman, B. L. Walton, J. R. Byrnes and A. S. Wolberg, *Thromb. Res.*, 2014, **133**(Suppl. 1), S38–S40.
51 A. van Hylckama Vlieg and F. R. Rosendaal, *J. Thromb. Haemostasis*, 2003, **1**, 2677–2678.
52 K. R. Machlus, J. C. Cardenas, F. C. Church and A. S. Wolberg, *Blood*, 2011, **117**, 4953–4963.

This journal is © The Royal Society of Chemistry 2017

Electronic Supplementary Material (ESI) for Nanoscale.
This journal is © The Royal Society of Chemistry 2017

Supplementary Information

Essential arterial hypertension patients present higher cell adhesion forces, contributing for fibrinogen-dependent cardiovascular risk

Ana F. Guedes[a,#], Filomena A. Carvalho[a,#,*], Carlos Moreira[b], José B. Nogueira[b], Nuno C. Santos[a,*]

[a]Instituto de Medicina Molecular, Faculdade de Medicina, Universidade de Lisboa, Lisbon, Portugal

[b]Hospital de Santa Maria, Centro Hospitalar Lisboa Norte, Lisbon, Portugal

Supplementary Results

AFM cell-cell adhesion

To better understand the shape of the distribution of the values of work and detachment force of the adhesion between two erythrocytes, histograms of both parameters were build up (Supplementary Figures S1 and S2). Comparisons between the histograms of the adhesion of erythrocytes from EAH patients *vs.* healthy donors, in the absence or in the presence of fibrinogen, were performed. The work and maximum force required to detach two erythrocytes from essential arterial hypertension (EAH) patients were higher than for healthy donors, at each fibrinogen concentration (from 0 to 1 mg/mL).

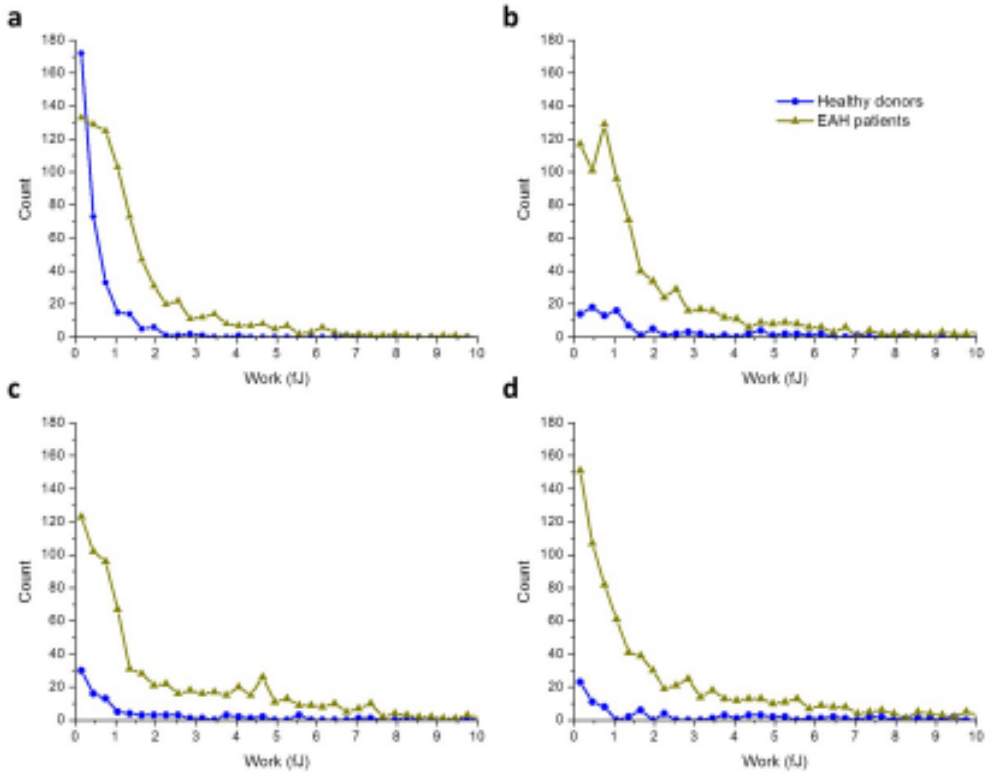

Supplementary Figure S1 | Histograms of the work necessary to detach two erythrocytes on AFM cell-cell adhesion measurements. Data obtained with erythrocytes isolated from healthy donors (blue) and EAH patients (olive) for each studied condition: (A) without fibrinogen; (B) with 0.4 mg/mL fibrinogen; (C) with 0.7 mg/mL fibrinogen; and, (D) with 1 mg/mL fibrinogen.

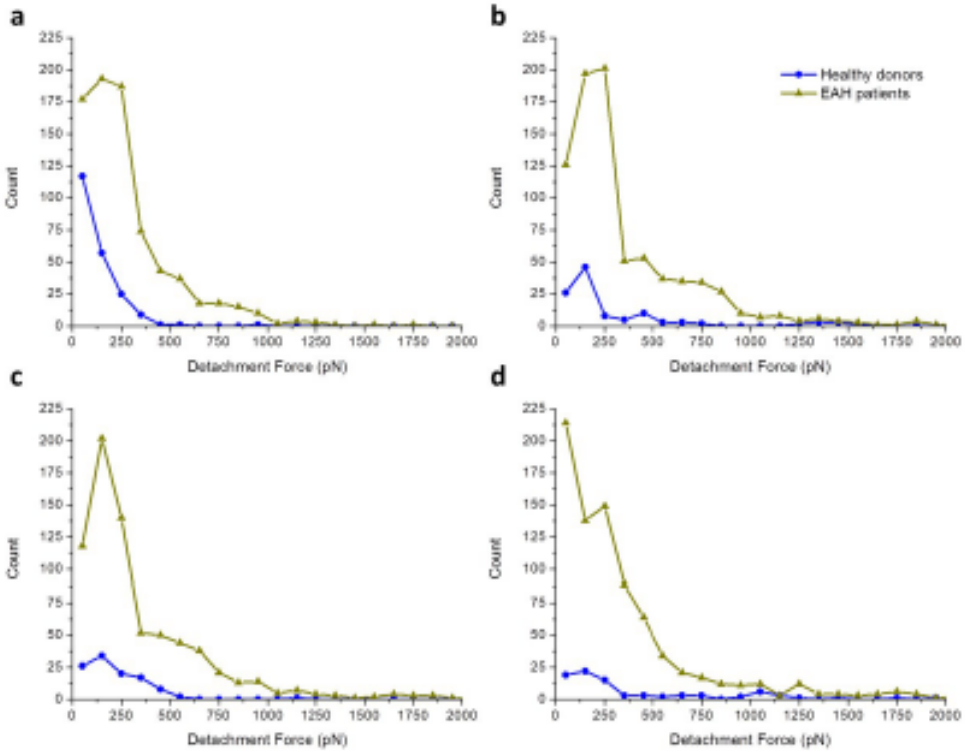

Supplementary Figure S2 | Histograms of the maximum force necessary to detach two erythrocytes on AFM cell-cell adhesion measurements. Data obtained with erythrocytes isolated from healthy donors (blue) and EAH patients (olive) for each studied condition: (A) without fibrinogen; (B) with 0.4 mg/mL fibrinogen; (C) with 0.7 mg/mL fibrinogen; and, (D) with 1 mg/mL fibrinogen.